University of Southampton

Faculty of Engineering, Science and Mathematics

School of Geography

Tracking Holocene Climate Change using Peat Bog Stable Isotopes

by

Timothy James Daley

Thesis for the degree of Doctor of Philosophy

June 2007

BEST COPY

AVAILABLE

Variable print quality

UNIVERSITY OF SOUTHAMPTON

ABSTRACT

FACULTY OF ENGINEERING, SCIENCE & MATHEMATICS

SCHOOL OF GEOGRAPHY

Doctor of Philosophy

TRACKING HOLOCENE CLIMATE CHANGE USING PEAT BOG STABLE ISOTOPES

By Timothy James Daley

Stable isotopic analyses of *Sphagnum* cellulose from four raised peat bog cores in the North Atlantic region are used to reconstruct past variation in the isotopic composition of precipitation. These records are then calibrated using modern relationships for each site between the isotopic composition of precipitation and temperature to derive palaeotemperature estimates through the mid- to late Holocene in Europe and during the widespread cold event ~8200 BP in Newfoundland. The data indicate that through the mid- to late Holocene in Europe, regional scale precipitation-isotopic gradients were generally similar to the present day, although during periods of climatic instability, the amplitude of change increased with distance from the Atlantic Ocean. During the ~8200 BP event in Newfoundland, it is estimated that surface air temperatures decreased by 8.9 ± 3.5 °C between ~8450 and 8360 BP. It is demonstrated that the link between the isotopic composition of precipitation and the signal recorded in *Sphagnum* moss involves limited isotopic fractionation. The link to palaeotemperature is made difficult for sites in Europe by uncertainty in the relationship between the isotopic composition of precipitation and temperature in the modern day. Variation in Bog Surface Wetness records is highly correlated with variation in the isotopic signal from *Sphagnum* cellulose, suggesting a common primary driver.

Table of Contents

ABSTRACT *ii*

Table of Contents *iii*

List of Figures *vi*

List of Plates *xix*

List of Equations *xx*

List of Tables *xx*

Declaration of Authorship *xxiii*

Acknowledgements *xxiv*

1 Introduction *1*

1.1 Project rationale and aims **1**

1.2 Thesis structure **3**

2 Background and context *5*

2.1 Reconstructing Holocene climate from raised peat **5**
2.1.1 Searching for the causes of abrupt and millennial scale change 5
2.1.2 Millennial and abrupt changes in peat 10
2.1.3 The climate record from peat 11
2.1.4 Identifying the key drivers of water table change 16
2.1.5 A role for stable isotopic investigation 19

2.2 Water isotopes and their link to climate **20**
2.2.1 Isotopes in water 20
2.2.2 Fractionation as a climatic encoder 21
2.2.3 Distribution of water isotopes in time and space 26
2.2.4 Maintenance of the temperature-dominant signal over time 32
2.2.5 Tracking the source of moisture in air 33

2.3 The incorporation of water isotopes in plant cellulose **34**
2.3.1 Towards mechanistic understanding 34
2.3.2 Advantages of non-vascular plants in climate reconstruction 35
2.3.3 Different pathways for oxygen and hydrogen 37

2.4 Advances in isotopic techniques **42**
2.4.1 Taxonomic variation in isotope values 42
2.4.2 Oxygen and hydrogen analytical techniques 44
2.4.3 The need for alpha-cellulose as a precise recorder 49

3 Site selection and description *52*

3.1 Site selection criteria **52**
3.1.1 Wide geographical area 52
3.1.2 Site characteristics: *Sphagnum* depth maximisation 52

3.2 Walton Moss, northern England **55**

3.3 Dosenmoor, northern Germany **67**

3.4 Raheenmore, midland Ireland **79**

3.5 Nordans Pond Bog, Newfoundland **90**

3.6 Comparison of site climatologies 97

4 Methods *102*

4.1 Introduction 102

4.2 Core location selection, retrieval and storage 102

4.3 Isotopic methods 104
4.3.1 Development of an isotopic preparation method 104
4.3.1.1 Isolation of *Sphagnum* from the peat matrix 104
4.3.1.1 Preparation test results and discussion 108
4.3.1.2 Quantifying *Sphagnum* concentrate measurement error 118
4.3.1.3 Alpha-cellulose extraction 119
4.3.2 Oxygen isotopic analysis 121
4.3.3 Hydrogen isotopic analysis 121
4.3.4 Modern sampling for isotopic calibration 122

4.4 Palaeoecological methods 126
4.4.1 Palaeoecological proxy selection 126
4.4.2 Plant macrofossil preparation 127
4.4.3 Humification Preparation 128
4.4.4 Testate Amoebae Preparation 129
4.4.5 Data Analysis methods: condensation of multivariate data 130
4.4.5.1 Critical comparison of DCA ordination versus Dupont for plant macrofossil data 130
4.4.5.2 Dupont hydroclimatic index 134

4.5 Dating Methods 136
4.5.1 Chronological methodology 136
4.5.2 Age depth modelling 138

5 Chronological results and age-depth modelling *139*

5.1 Introduction 139

5.2 Walton Moss 139
5.2.1 ^{14}C dating 139
5.2.2 Age-depth modelling 141

5.3 Dosenmoor 142
5.3.1 ^{14}C dating 142
5.3.2 Age-depth modelling 144

5.4 Raheenmore 146
5.4.1 ^{14}C dating 146
5.4.2 Age-depth modelling. 148

5.5 Nordans Pond Bog 150
5.5.1 ^{14}C dating 150
5.5.2 Age-depth modelling 152

6 Palaeoecological results and analysis *154*

6.1 Introduction 154

6.2 Walton Moss 154
6.2.1 WLM22 plant macrofossil data 154
6.2.2 WLM22 testate amoebae data 160
6.2.3 WLM22 humification data 168
6.2.4 Multiproxy comparison for WLM22 172

6.3 Dosenmoor 178
6.3.1 DSM3 plant macrofossil data 178

6.3.2 DSM3 humification data 182
6.3.3 Multi-proxy comparison for DSM3 185

6.4 Raheenmore 189
6.4.1 RHM2 plant macrofossil data 189
6.4.2 RHM2 humification data 193
6.4.3 Multi-proxy comparison for RHM2 195

7 Isotopic results and analysis *199*

7.1 Introduction 199

7.2 Modern monitoring results 200
7.2.1 Introduction 200
7.2.2 $\delta^{18}O$ and δD in precipitation and bog water 200
7.2.3 $\delta^{18}O_{Sphagnum}$ values 214
7.2.4 $\delta D_{Sphagnum}$ values 221

7.3 Sphagnum cellulose palaeo-isotopic results 226
7.3.1 WLM22 $\delta^{18}O_{Sphagnum}$ record 226
7.3.2 WLM22 $\delta D_{Sphagnum}$ record 228
7.3.3 DSM3 $\delta^{18}O_{Sphagnum}$ record 230
7.3.4 RHM2 $\delta^{18}O_{Sphagnum}$ record 232
7.3.5 NDN02/1 $\delta^{18}O_{Sphagnum}$ record 235
7.3.6 NDN02/1 $\delta D_{Sphagnum}$ record 238

8 Discussion *245*

8.1 Introduction 245

8.2 Validation of the climatic driver of BSW 247

8.3 BSW-isotopic variability comparison 254

8.4 What drives the isotopic signal in cellulose? 258

8.5 Estimation of isotopic values of Palaeo-precipitation 267

8.6 Improved understanding of change through the mid- to late Holocene 278

8.7 Palaeotemperature reconstruction 284

8.8 Modelling the 8200 BP cold event 289
8.8.1 Newfoundland 289
8.8.2 Europe 296

8.9 Is BSW forced by temperature? 297

9 Conclusions and future research *299*

9.1 Specific conclusions from the research 299

9.2 Methodological appraisal and future directions 301

References *303*

List of Figures

Figure 2.1 The effect of hydrological processes on the isotopic composition of water (Clark and Fritz, 1997).....28

Figure 2.2 Geographical distribution of $\delta^{18}O$ in precipitation from the 508 stations (black dots) included in the GNIP database (Araguas-Araguas *et al.*, 2000).....29

Figure 2.3 A simplified representation of the pathways involved in the metabolism leading to the synthesis of cellulose in C3 plants under photoheterotrophic (F3) or heterotrophic (F1) conditions or a combination of the two (autotrophic; F2) (Yakir and DeNiro, 1990).....40

Figure 2.4 Schematic of the cellulose molecule (source: http://en.wikipedia.org/wiki/Cellulose) 46

Figure 2.5 Schematic of the molecular structure of cellulose nitrate (source: http://en.wikipedia.org/wiki/Nitrocellulose).....47

Figure 2.6 Schematic of the new equilibration chamber interfaced with an online pyrolysis IRMS system (Filot *et al.*, 2006). 49

Figure 3.1 Location of study sites (red dots) in relation to meteorological (open dots) and Global Network for Isotopes in Precipitation (GNIP) stations (blue diamonds) for NW Europe 54

Figure 3.2 Location of Nordans Pond Bog (red dot) in relation to meteorological station at Musgrave Harbour (open circle) and GNIP stations at Goose Bay, Labrador and Truro, Nova Scotia (blue diamonds) 54

Figure 3.3 Aerial photo of Walton Moss (Getmapping.com, 2007).....56

Figure 3.4. Monthly mean maximum and minimum temperature (red and blue dots) and precipitation (grey bars) (1961-1990) for Aspatria, northern England (54.761°N, 3.329°W; 62 m altitude).....57

Figure 3.5 Comparison of mean monthly precipitation totals for Aspatria (1971-2000), Walton (1971-2000) and Brampton (1999-2007).....58

Figure 3.6 Bi-plot of mean monthly δD and $\delta^{18}O$ values in precipitation for Wallingford (1981-2002) (IAEA/WMO, 2004).....60

Figure 3.7 Relationship between mean monthly $\delta^{18}O$ values in precipitation and surface air temperature for Wallingford (1981-2002) (IAEA/WMO, 2004) (linear regression in solid line, 95% confidence limits in dashed lines).....61

Figure 3.8 Relationship between mean monthly $\delta^{18}O$ values in precipitation and precipitation amount for Wallingford (1981-2002) (IAEA/WMO, 2004) (linear regression in solid line, 95% confidence limits in dashed lines).....62

Figure 3.9 Bi-plot of mean monthly isotopic values in precipitation by season for Wallingford (1981-2002) (IAEA/WMO, 2004).....64

Figure 3.10 Relationship between long-term monthly means of $\delta^{18}O_{precipitaiton}$ and surface air temperature for Wallingford (1981-2002) (linear regression in solid line, 95% confidence limits in dashed lines).....65

Figure 3.11 Relationship between long-term monthly means of $\delta^{18}O_{precipitaiton}$ and precipitation amount for Wallingford (1981-2002) by season (summer = red dots; winter = black dots)....66

Figure 3.12 Mean monthly temperature (dots) and precipitation (grey bars) (1961-1990) for Neumunster, Schleswig-Holstein, Germany (54.067N, 9.983E; 13 km south of Dosenmoor)69

Figure 3.13 Bi-plot of mean monthly δD and $\delta^{18}O$ values in precipitation for Cuxhaven (1978-2001) (IAEA/WMO, 2004).....70

Figure 3.14 Relationship between mean monthly $\delta^{18}O$ values in precipitation and surface air temperature for Cuxhaven (1984-2001) (IAEA/WMO, 2004) (linear regression in solid line, 95% confidence limits in dashed lines).....71

Figure 3.15 Relationship between mean monthly $\delta^{18}O$ values in precipitation and precipitation amount for Cuxhaven (1984-2001) (IAEA/WMO, 2004) (linear regression in solid line, 95% confidence limits in dashed lines).....72

Figure 3.16 Bi-plot of mean monthly isotopic values in precipitation by season for Cuxhaven (1978-2001) (IAEA/WMO, 2004).....73

Figure 3.17 Relationship between long-term monthly means of $\delta^{18}O_{precipitaiton}$ and surface air temperature for Cuxhaven (1978-2001) (IAEA/WMO, 2004) (linear regression in solid line, 95% confidence limits in dashed lines).....74

Figure 3.18 Relationship between long-term monthly means of $\delta^{18}O_{precipitaiton}$ and precipitation amount for Cuxhaven (1978-2001) (IAEA/WMO, 2004) (linear regression in solid line, 95% confidence limits in dashed lines).....75

Figure 3.19 Transects used for stratigraphical analysis superimposed on a map of the surface area of Dosenmoor (adapted from Irmler *et al.*, 1998). Transect labels refer to stratigraphical cores used in analysis (Figure 3.21, Figure 3.22).....76

Figure 3.20 Geological cross-section of Dosenmoor along a north-south transect. Top three layers refer to peat deposits. Brighter colours refer to riverine and lacustrine deposits. Cut sections of the bog surface are clearly represented. Red box indicates bog region from which additional stratigraphical survey work was undertaken (adapted from Irmler *et al.*, 1998).....77

Figure 3.21 Stratigraphical summary for West-East transect of Dosenmoor. Symbol notation follows Troels-Smith (1955).....78

Figure 3.22 Stratigraphical summary for North-South transect of Dosenmoor. Symbol notation follows Troels-Smith (1955).....78

Figure 3.23 Surface level contour map of Raheenmore Bog with stratigraphical transect locations (black cross), former (now ingrown) drainage system in northeast corner and Irish co-ordinate system overlaid (van der Schaaf, 1999).....80

Figure 3.24 Mean monthly maximum and minimum temperature (dots) and precipitation (grey bars) (1961-1990) for Birr, midland Ireland (53.08°N, 7.88°W; 73 m altitude).....81

Figure 3.25 Bi-plot of mean monthly δD and $\delta^{18}O$ values in precipitation for Valentia (1960-2002) (IAEA/WMO, 2004).....82

Figure 3.26 Relationship between mean monthly $\delta^{18}O$ values in precipitation and surface air temperature for Valentia (1960-2002) (IAEA/WMO, 2004) (linear regression in solid line, 95% confidence limits in dashed lines) 83

Figure 3.27 Relationship between mean monthly $\delta^{18}O$ values in precipitation and precipitation amount for Valentia (1960-2002) (IAEA/WMO, 2004) (linear regression in solid line, 95% confidence limits in dashed lines).....84

Figure 3.28 Bi-plot of mean monthly isotopic values in precipitation by season for Valentia (1960-2002) (IAEA/WMO, 2004).....85

Figure 3.29 Relationship between long-term monthly means of $\delta^{18}O_{precipitation}$ and surface air temperature for Valentia (1960-2002) (IAEA/WMO, 2004) (linear regression in solid line, 95% confidence limits in dashed lines) 87

Figure 3.30 Relationship between long-term monthly means of $\delta^{18}O_{precipitaiton}$ and precipitation amount for Valentia (1960-2002) (IAEA/WMO, 2004) (linear regression in solid line, 95% confidence limits in dashed lines).....88

Figure 3.31 Stratigraphical summary for west-east transect of Raheenmore bog. Symbol notation follows Troels-Smith (1955).....89

Figure 3.32 Stratigraphical summary for south-north transect of Raheenmore bog. Symbol notation follows Troels-Smith (1955).....89

Figure 3.33 Mean monthly maximum and minimum temperature (dots) and precipitation (grey bars) (1971-2000) for Musgrave Harbour (49.450°N, 53.967°W; 43 km NW of Nordans Pond bog).....91

Figure 3.34 Bi-plot of mean monthly δD and $\delta^{18}O$ values in precipitation for Truro, Nova Scotia (1975-1983) and Goose Bay, Labrador (1961-1965) (IAEA/WMO, 2004).....93

Figure 3.35 Relationship between mean monthly $\delta^{18}O$ values in precipitation and surface air temperature for Truro, NS (1975-1983; red dots) and Goose Bay, Labrador (1961-1965; blue dots) (IAEA/WMO, 2004).....94

Figure 3.36 Relationship between mean monthly $\delta^{18}O$ values in precipitation and precipitation amount for Truro, NS (1975-1983; red dots) and Goose Bay, Labrador (1961-1965; blue dots) (IAEA/WMO, 2004).....95

Figure 3.37 Bi-plot of mean monthly isotopic values of precipitation by season for Truro, Nova Scotia (1975-1983) and Goose Bay, Labrador (1961-1965) (IAEA/WMO, 2004).....96

Figure 3.38 Bi-plot of mean monthly δD and $\delta^{18}O$ values in precipitation for all GNIP stations (IAEA/WMO, 2004).....97

Figure 3.39 Monthly time-series of $\delta^{18}O_{precipitation}$ values for data from all five GNIP stations used in this study (IAEA/WMO, 2004) (dark gray = Goose Bay, light green = Truro, black = Valentia, blue = Wallingford, red = Cuxhaven).....99

Figure 4.1 Photographic results of the elutriation process at Petri-dish scale and at 10x magnification (before and after). Absence of heavy dicot remains and reduction in fine ericaceous rootlets and sedge roots is observed.....107

Figure 4.2 $\delta^{18}O_{bulk\ raw}$ (brown line) versus $\delta^{18}O_{bulk\ \alpha\text{-cell}}$ values (grey line). 2σ range on duplicate measurements is given (vertical bars).....109

Figure 4.3 $\delta^{18}O_{Sphag\text{-pure}}$ (blue line) versus $\delta^{18}O_{bulk\ \alpha\text{-cell}}$ values (grey line). 2σ range on duplicate measurements is given (vertical bars).....111

Figure 4.4 $\delta^{18}O_{Sphag\text{-pure}}$ (blue line) versus $\delta^{18}O_{Sphag\text{-conc}}$ values (red line). 2σ range on duplicate measurements is given (vertical bars).....113

Figure 4.5 Bi-plot of $\delta^{18}O_{Sphag\text{-}pure}$ and $\delta^{18}O_{bulk\ \alpha\text{-}cell}$ values for sample levels in the preparation test.....115

Figure 4.6 Bi-plot of $\delta^{18}O_{Sphag\text{-}pure}$ and $\delta^{18}O_{Sphag\text{-}conc}$ values for sample levels in the preparation test.....116

Figure 4.7 $\delta^{18}O$ residuals from the arithmetic difference between $\delta^{18}O_{Sphag\text{-}pure}$ and $\delta^{18}O_{Sphag\text{-}conc}$ values plotted against the degree of species mixture. Group means (red dots) and 2σ range (vertical blue bars) are shown with individual sample values (hollow circles).....118

Figure 4.8 New chemical extraction glassware 120

Figure 4.9 Bi-plot of DCA ordination results for WLM22 plant macrofossil data 133

Figure 4.10 WLM22 DCA axis one sample scores with depth 134

Figure 5.1 Calibrated ^{14}C dates with calibration range from 2σ error on conventional radiocarbon age for WLM22 141

Figure 5.2 Calibrated ^{14}C dates for core WLM22 (red dots) with calibration range from 2σ error on conventional radiocarbon age. Linear regression age depth model (Age = 10.24 x depth – 54) is shown (bold black line).....142

Figure 5.3 Calibrated ^{14}C dates with calibration range from 2σ error on conventional radiocarbon age for DSM3.....144

Figure 5.4 Calibrated ^{14}C dates for DSM3 (red dots) with calibration range from 2σ error on conventional radiocarbon age (black bars). A 4th order polynomial age-depth model (Age = k + ax + bx^2 + cx^3 + dx^4) (bold black line) is given as an approximation of accumulation rate with depth.....146

Figure 5.5 Calibrated ^{14}C dates with calibration range from 2σ error on conventional radiocarbon age for RHM2 148

Figure 5.6 Calibrated ^{14}C dates for core RHM2 (red dots) with calibration range from 2σ error on conventional radiocarbon age (black bars). A 4th order polynomial is used as an age-depth model of the accumulation rate (bold black line). 150

Figure 5.7 Calibrated ^{14}C dates with calibration range from 2σ error on conventional radiocarbon age for NDN02/1 152

Figure 5.8 Calibrated ^{14}C dates for NDN02/1 (red dots) with calibration range from 2σ error on conventional radiocarbon age (black bars). Cubic regression age-depth model ($y = -156.6 + 4.46x + 0.03617x^2 - 0.000035x^3$) is given as approximation of accumulation rate change (bold black line) 153

Figure 6.1 WLM22 plant macrofossil diagram (896 - 0 cm; 9120 BP - present).....155

Figure 6.2 WLM22 Dupont wetness index reconstruction for plant macrofossil data; raw values on secondary y-axis, σ anomlies from the mean on primary y-axis.....159

Figure 6.3 WLM22 testate amoebae diagram (676 – 0 cm; 6660 BP to present).....161

Figure 6.4 Bi-plot of species scores for DCA ordination of WLM22 testate amoebae data (32 - 656 cm) 163

Figure 6.5 Bi-plot of species and sample scores for DCA ordination of WLM22 testate amoebae data.....166

Figure 6.6 WLM22 testate amoebae DCA axis 1 sample scores and transfer function results with depth (32 – 656 cm); dotted lines represent root mean squared error for the transfer function reconstruction. 167

Figure 6.7 WLM22 peat humification data; A) raw transmission values and demonstration of artificial freshening at depth with whole core detrending, B) detrended (16 - 504 cm) and normalised transmission values presented as σ anomalies from the mean 171

Figure 6.8 WLM22 multi-proxy comparison comprising plant macrofossil data (black line; 4 - 832 cm), testate amoebae transfer function data (red line; 0 - 656 cm) and peat humification data (blue line; 12 - 700 cm) 172

Figure 6.9 WLM22 stacked record of inferred Bog Surface Wetness change using all available data 175

Figure 6.10 WLM22 stacked record of inferred Bog Surface Wetness (BSW) using all samples with ≥ 2 proxies available 176

Figure 6.11 WLM22 multi-proxy climatic time-series; A) using all available data, B) using all samples with ≥ 2 proxies available 177

Figure 6.12 DSM3 plant macrofossil diagram (672 – 0 cm; 5830 BP to present) 179

Figure 6.13 DSM3 Dupont wetness index reconstruction using plant macrofossil data; raw values on primary y-axis, σ anomalies from the mean on secondary y-axis 182

Figure 6.14 DSM3 peat humification data; A) raw transmission values, B) detrended (448 – 0 cm) and normalised transmission values presented as σ anomalies from the mean 184

Figure 6.15 DSM3 multi-proxy comparison comprising plant macrofossil data (blue line) and peat humification data (red line) 185

Figure 6.16 DSM3 stacked record of inferred Bog Surface Wetness change using all available data 187

Figure 6.17 DSM3 stacked record of inferred Bog Surface Wetness (BSW) using all samples with 2 proxies 187

Figure 6.18 DSM3 multi-proxy climatic time-series A) using all available data, B) using samples with 2 proxies available 188

Figure 6.19 RHM2 plant macrofossil diagram (1112 – 888 cm; 10030 – 7460 BP) 190

Figure 6.20 RHM2 Dupont wetness index reconstruction for plant macrofossil data; raw values on primary y-axis, σ anomalies from the mean on secondary y-axis 193

Figure 6.21 RHM2 peat humification data; A) raw transmission values; B) detrended (600 – 0 cm) and normalised transmission values presented as σ anomalies from the mean 194

Figure 6.22 RHM2 multi-proxy comparison comprising plant macrofossil data (1112 – 888 cm; black line) and peat humification data (1112 cm – surface; red line).....196

Figure 6.23 RHM2 stacked record of inferred Bog Surface Wetness (BSW).....197

Figure 6.24 RHM2 multi-proxy climatic time-series (10030 – 7460 BP; blue line) and full core peat humification time-series (10030 BP – present; red line).....198

Figure 7.1 $\delta^{18}O_{precipitation}$ values for all sites for the period November 2003 – December 2005; Brampton weather station 3 km south of Walton Moss (red dots), Dosenmoor centre of bog surface (blue dots) and Raheenmore centre of bog surface (green dots).....201

Figure 7.2 $\delta D_{precipitation}$ values for all sites for the period November 2003 – December 2005; Brampton weather station 3 km south of Walton Moss (red dots), Dosenmoor centre of bog surface (blue dots) and Raheenmore centre of bog surface (green dots).....202

Figure 7.3 $\delta^{18}O_{bog\ water}$ values for all sites for the period November 2003 – December 2005; replicate measurements are indicated by different symbols (Walton Moss, red symbols; Dosenmoor, blue dots; Raheenmore, green symbols; Nordans Pond Bog, yellow dots) 203

Figure 7.4 $\delta D_{bog\ water}$ values for all sites for the period November 2003 – December 2005; replicate measurements are indicated by different symbols (Walton Moss, red symbols; Dosenmoor, blue symbols; Raheenmore, green symbols; Nordans Pond Bog, yellow dots).204

Figure 7.5 Bi-plot of mean monthly δD and $\delta^{18}O$ values in precipitation (black dots; from Brampton weather station 3 km south of Walton Moss) and bog water (green dots) from the surface of Walton Moss 205

Figure 7.6 Bi-plot of mean monthly δD and $\delta^{18}O$ values in precipitation (black dots) and bog water (green dots) from the surface of Dosenmoor 206

Figure 7.7 Bi-plot of mean monthly δD and $\delta^{18}O$ values in precipitation (black dots) and bog water (green dots) from the surface of Raheenmore.....207

Figure 7.8 Bi-plot of mean monthly δD and $\delta^{18}O$ values in precipitation (black dots; from Brampton weather station 3 km south of Walton Moss) and bog water separated by season (blue dots = September to February, red dots = March to August) from the surface of Walton Moss.....208

Figure 7.9 Bi-plot of mean monthly δD and $\delta^{18}O$ values in precipitation (black dots) and bog water separated by season (blue dots = September to February, red dots = March to August) from the surface of Dosenmoor 209

Figure 7.10 Bi-plot of mean monthly δD and $\delta^{18}O$ values in precipitation (black dots) and bog water separated by season (blue dots = September to February, red dots = March to August) from the surface of Raheenmore.....210

Figure 7.11 Bi-plot of mean monthly δD and $\delta^{18}O$ values in precipitation from Wallingford (GNIP; 1981-2002) (black dots) compared against precipitation at Brampton weather station 3 km south of Walton Moss (blue dots) and bog water (green dots) from the surface of Walton Moss (November 2003 – December 2005).....211

Figure 7.12 Bi-plot of mean monthly δD and $\delta^{18}O$ values in precipitation from Cuxhaven (GNIP; 1978-2001) (black dots) compared against precipitation (blue dots) and bog water (green dots) from the surface of Dosenmoor (June 2004 – December 2005).....212

Figure 7.13 Bi-plot of mean monthly δD and $\delta^{18}O$ values in precipitation from Valentia (GNIP; 1960-2002) (black dots) compared against precipitation (blue dots) and bog water (green dots) from the surface of Raheenmore (December 2004 – November 2005).....213

Figure 7.14 Bi-plot of δD and $\delta^{18}O$ values in bog water from the surface of Nordans Pond Bog (green dots; June 2004) compared against mean monthly precipitation from Goose Bay (light blue dots; GNIP, 1961-1965) and Truro (dark blue dots; GNIP, 1975-1983).....214

Figure 7.15 Species mean $\delta^{18}O_{Sphagnum}$ values (dots) and 2σ range (bars) for modern surface samples from Walton Moss (April 2004 – July 2005).....215

Figure 7.16 Species mean $\delta^{18}O_{Sphagnum}$ values (dots) and 2σ range (bars) for modern surface samples from Dosenmoor (September 2004 – August 2005).....218

Figure 7.17 Species mean $\delta^{18}O_{Sphagnum}$ values (dots) and σ range (bars) for modern surface samples from Raheenmore (December 2004 – November 2005).....219

Figure 7.18 Species mean $\delta^{18}O_{Sphagnum}$ values (solid dots) and 2σ range (bars) for modern surface samples from Nordans Pond Bog (June 2004). Individual samples are shown in open circles. 221

Figure 7.19 Bi-plot of δD and $\delta^{18}O$ values in *Sphagnum* cellulose from the surface of Dosenmoor (September 2004 – August 2005).....223

Figure 7.20 Bi-plot of δD and $\delta^{18}O$ values in *Sphagnum* cellulose from the surface of Dosenmoor (September 2004 – August 2005) by taxon (*S. cuspidatum*, blue dots; *S. magellanicum*, red dots; *S. papillosum*, green dots) 224

Figure 7.21 Bi-plot of δD and $\delta^{18}O$ values in *Sphagnum* cellulose from the surface of Dosenmoor (September 2004 – August 2005) by month of sampling 225

Figure 7.22 WLM22 $\delta^{18}O_{Sphagnum}$ record 227

Figure 7.23 WLM22 $\delta^{18}O_{Sphagnum}$ time-series 228

Figure 7.24 Comparison of $\delta D_{Sphagnum}$ values (red line) and $\delta^{18}O_{Sphagnum}$ values (blue line) from WLM22 (160 – 110 cm; ~1580 – 1090 BP) 229

Figure 7.25 WLM22 δD - $\delta^{18}O$ palaeo-cellulose bi-plot; linear regression (solid line) and 95% confidence limits (dashed lines) are shown 230

Figure 7.26 DSM3 $\delta^{18}O_{Sphagnum}$ record 231

Figure 7.27 DSM3 $\delta^{18}O_{Sphagnum}$ timeseries 232

Figure 7.28 RHM2 $\delta^{18}O_{Sphagnum}$ record 233

Figure 7.29 RHM2 $\delta^{18}O_{Sphagnum}$ time-series.....235

Figure 7.30 NDN02/1 $\delta^{18}O_{Sphagnum}$ record 236

Figure 7.31 NDN02/1 $\delta^{18}O_{Sphagnum}$ time-series 237

Figure 7.32 NDN02/1 $\delta^{18}O_{Sphagnum}$ time-series (8750 – 7720 BP) 238

Figure 7.33 NDN02/1 $\delta D_{Sphagnum}$ record 239

Figure 7.34 NDN02/1 $\delta D_{Sphagnum}$ time-series.....240

Figure 7.35 NDN02/1 $\delta D_{Sphagnum}$ time-series (8750 – 7720 BP) 240

Figure 7.36 Comparison of records of δD values (red line) and $\delta^{18}O$ values (blue line) from NDN02/1.....242

Figure 7.37 Comparison of records of δD values (red line) and $\delta^{18}O$ values (blue line) from NDN02/1 (8750 – 7720 BP) 242

Figure 7.38 NDN02/1 palaeo-cellulose bi-plot; linear regression (solid line) and 95% confidence limits (dashed lines) are shown 244

Figure 8.1 Comparison of BSW records from the three NW European raised bog sites investigated in this project: A) Raheenmore B) Walton Moss C) Dosenmoor. Dating control points and calibrated ranges (from ^{14}C 2σ error) are shown beneath each record. Grey bars represent periods of regionally identified wet shifts (Barber, 2006). 251

Figure 8.2 Comparison of BSW records (blue lines) and $\delta^{18}O_{Sphagnum}$ values (red lines) from A) Walton Moss B) Dosenmoor C) Raheenmore 255

Figure 8.3 Monthly α coefficients for the three European study sites modelled using precipitation as source water (grey bars) and bog water as source water (black bars).....264

Figure 8.4 Monthly alpha coefficients for each European site where $\delta_{sw} = \delta_{bw}$.....266

Figure 8.5 WLM22 palaeo- $\delta^{18}O_{precipitation}$ estimate using $\alpha = 1.0274 \pm 0.0010$ (1σ). 269

Figure 8.6 DSM3 palaeo- $\delta^{18}O_{precipitation}$ estimate using $\alpha = 1.0274 \pm 0.0010$ (1σ). Dotted lines refer to 2σ error range on biochemical enrichment estimate. 269

Figure 8.7 RHM2 palaeo- $\delta^{18}O_{precipitation}$ estimate using $\alpha = 1.0274 \pm 0.0010$ (1σ). Dotted lines refer to 2σ error range on biochemical enrichment estimate. 270

Figure 8.8 Nordans bog water values compared with GNIP precipitation data by season. Closed symbols = Truro. Open symbols = Goose Bay. Bog waters = black dots. 271

Figure 8.9 Source water estimates for modern *Sphagnum* cellulose from Nordans Pond Bog (red dots). Yellow dots are bog waters used for calibration. Blue dots are GNIP precipitation data from Truro, NS (1975-1983; dark blue dots) and Goose Bay, Labrador (1961-1965; light blue dots) (IAEA/WMO, 2004). 273

Figure 8.10 Comparison of Holocene *Sphagnum* source water reconstruction from NDN02/1 with modern GNIP precipitation data (IAEA/WMO, 2004). GNIP variation in the isotopic composition of meteoric waters is given by season. Closed symbols = Truro. Open symbols = Goose Bay. Bog water used for calibration = black dots. NDN02/1 cellulose palaeo-source water estimates = bold blue dots. 274

Figure 8.11 Comparison of Holocene *Sphagnum* source water reconstruction from NDN02/1 with modern GNIP precipitation data (IAEA/WMO, 2004) *using* $\alpha = 1.0274$ *for* $\delta^{18}O$ *cellulose-water enrichment.* GNIP variation in the isotopic composition of meteoric waters is given by season. Closed symbols = Truro. Open symbols = Goose Bay. Bog water used for calibration = black dots. Cellulose palaeo-source water estimates = bold blue dots. 277

Figure 8.12 $\delta^{18}O$ precipitation estimates for four study sites (Red line = Dosenmoor; Blue line = Walton Moss; Black line = Raheenmore; Green line = Nordans Pond Bog). Error bars refer to the upper and lower calibrated ranges from the 2σ error on AMS ^{14}C dates 279

Figure 8.13 Reconstructed surface air temperature anomalies for each of the European sites using *decadal scale* $\delta^{18}O_{precipitation}$ -temperature coefficients derived from modern GNIP data (chapter 3) (Walton Moss = A, Dosenmoor = B, Raheenmore = C) 285

Figure 8.14 Reconstructed surface air temperature anomalies for each of the European sites using $\delta^{18}O_{precipitation}$ -temperature coefficients derived from *raw monthly resolution* modern GNIP data (Chapter 3) (Walton Moss = A, Dosenmoor = B, Raheenmore = C) 288

Figure 8.15 Map of the Northwest Atlantic showing modern ocean-surface currents, Glacial Lake Agassiz outflow and site locations. Shown are the core locations (solid circles), GNIP monitoring stations at Goose Bay, Labrador and Truro, Nova Scotia (open circles), modern ocean-surface currents (red lines = warm currents; blue lines = cold currents; L.C. = Labrador Current, G.S. = Gulf Stream, N.A.D. = North Atlantic Drift, E.G.C = East Greenland Current, I.C. = Irminger Current) and routing of the final drainage from Glacial Lake Agassiz ~8450 years ago (Barber *et al.*, 1999) (bold blue arrow).....291

Figure 8.16 Atmospheric response over Newfoundland (A) compared with North Atlantic seawater freshening (Ellison *et al.*, 2006) offset by minus 100 years (B) and two recently synchronised isotope records (C) from Greenland ice cores (Vinther *et al.*, 2006; Rasmussen *et al.*, 2006) covering the period 9000 to 7600 BP. Chronological uncertainty in (C) assumes a layer-counting error of 47 yr throughout this time period (Vinther *et al.*, 2006). 292

List of Plates

Plate 3.1 Aerial photo of Dosenmoor from the south indicating substantial surface disturbance through peat cutting and drainage (photo: K. Müller) 67

Plate 3.2 Bog pool development and survival of typical ombrotophic species in restored areas at Dosenmoor (photo: T. Daley) 68

Plate 4.1 Capitulum of *Sphagnum cuspidatum* (photo: T. Daley) 125

List of Equations

Equation 1) $\delta = [(R_{sample} - R_{standard})/ R_{standard}] \times 1000$ 21

Equation 2) $\alpha = ((R_1 / 1000) +1) / ((R_2 / 1000) + 1)$ 22

Equation 3) $\delta D = 8 \times \delta^{18}O + 10$.....26

Equation 4) $\delta_{cell} = \delta_{sw} + \varepsilon_b + (\varepsilon_e + \varepsilon_k)(1-h)$ 35

Equation 5) $\alpha = ((\delta_{cellulose} / 1000) +1) / ((\delta_{source\ water} / 1000) + 1)$.....41

Equation 6) $\Delta T = 3.64(\Delta\delta^{18}O)$.....63

Equation 7) $\Delta T = 5.93(\Delta\delta^{18}O)$.....74

Equation 8) $\Delta T = 3.83(\Delta\delta^{18}O)$.....86

Equation 9) $\Delta T = 2.28(\Delta\delta^{18}O)$.....92

Equation 10) $Age = k + ax + bx^2 + cx^3 + dx^4$ 144

Equation 11) $\delta_{cell} = \delta_{sw} + \Delta$.....259

Equation 12) $\delta_{cell} = \delta_{sw} + \varepsilon_b$ 259

List of Tables

Table 2.1 Natural relative abundance of stable isotopes of water (Walker *et al.*, 1989).....20

Table 2.2 Physical characteristics of three main types of water molecules (Hoefs, 1997; Criss, 1999) 20

Table 2.3 VSMOW standard values for $^{2}H/^{1}H$ (De Witt *et al.*, 1980) and $^{18}O/^{16}O$ (Baertschi, 1976) 21

Table 3.1 Seasonal means of monthly mean isotopic data for Wallingford (1981-2002) (IAEA/WMO, 2004) 64

Table 3.2 Seasonal means of monthly isotopic data for Cuxhaven (1978-2001) (IAEA/WMO, 2004) 73

Table 3.3 Seasonal means of monthly isotopic data for Valentia (1960-2002).....85

Table 3.4 Seasonal means of monthly isotopic data for Goose Bay (1961-1965) and Truro (1975-1983) (IAEA/WMO, 2004) 96

Table 3.5 Summary of seasonal means from all GNIP stations (IAEA/WMO, 2004).....98

Table 4.1 $\delta^{18}O$ values for all preparations from WLM22 including the difference between $\delta^{18}O_{Sphag\text{-}pure}$ and $\delta^{18}O_{Sphag\text{-}conc}$ values ($\delta^{18}O_{Sphag\text{-}conc}$ residuals) and species mixture ranking .109

Table 4.2 Pearson correlation and r^2 for data from three preparation procedures with $\delta^{18}O_{Sphag\text{-}pure}$ values.....114

Table 4.3 $\delta^{18}O$ values for replicate measurement data from *Sphagnum* preparation error test (IAEA cellulose: Vienna, IAEA C3 cellulose; Sigma cellulose: Batch No 92F0243, 99.5% α-cellulose) 119

Table 4.4 Key to species labels in Figure 4.9 133

Table 4.5 Species weightings for the Dupont Hydroclimatic index reconstruction 135

Table 5.1 Walton Moss Radiocarbon Measurements and Calibration 140

Table 5.2 Dosenmoor Radiocarbon Measurements and Calibration 143

Table 5.3 Raheenmore Radiocarbon Measurements and Calibration.....147

Table 5.4 Nordans Pond Bog Radiocarbon Measurements and Calibration 151

Table 6.1 Assemblage zones and environmental interpretation for WLM22 plant macrofossils 156

Table 6.2 Assemblage zones and environmental interpretations for WLM22 Testate Amoebae data.....162

Table 6.3 Species legend for WLM22 Testate Amoebae DCA ordination 164

Table 6.4 Assemblage zones for core DSM3 from Dosenmoor 180

Table 6.5 Assemblage description and interpretation for RHM2 plant macrofossil data.....191

Table 7.1 $\delta^{18}O_{Sphagnum}$ species means and σ range for Walton Moss (April 2004 – July 2005) 216

Table 7.2 $\delta^{18}O_{Sphagnum}$ species means and σ range for Dosenmoor (September 2004 – August 2005) 218

Table 7.3 $\delta^{18}O_{Sphagnum}$ species means and σ range for Raheenmore (December 2004 – November 2005) 220

Table 7.4 Summary of Nordans Pond Bog surface cellulose and bog water isotopic data 226

Table 8.1 Climatic fluctuation dates for European raised and blanket peat proxy data. Adapted from Barber (2006). For full references see Barber et al. (2004). All ages are given in calendar years before present (BP) and represent the onset of a shift in proxy-records towards increased BSW.....250

Table 8.2 Mean biochemical enrichment coefficients for species and sites.....261

Table 8.3 Monthly mean $\alpha_{cellulose\text{-}bog\ water}$ (bw) coefficients.....263

Table 8.4 Monthly mean $\alpha_{cellulose\text{-}precipitation}$ coefficients 263

Declaration of Authorship

I, Timothy James Daley,

declare that the thesis entitled

Tracking Holocene Climate Change using Peat Bog Stable Isotopes

and the work presented in it are my own. I confirm that:

- this work was done wholly or mainly while in candidature for a research degree at this University;
- where any part of this thesis has previously been submitted for a degree or any other qualification at this University or any other institution, this has been clearly stated;
- where I have consulted the published work of others, this is always clearly attributed;
- where I have quoted from the work of others, the source is always given. With the exception of such quotations, this thesis is entirely my own work;
- I have acknowledged all main sources of help;
- where the thesis is based on work done by myself jointly with others, I have made clear exactly what was done by others and what I have contributed myself;

none of this work has been published before submission,

Signed: .....[redacted].....

Date: 27/6/2007

Acknowledgements

This research was part of a nested project, ISOMAP-UK, funded by the Natural Environment Research Council (NERC) within the RAPID thematic programme. Overall project guidance was given by Dr. Jonathan Holmes and thanks go to him and all the ISOMAP-UK members for advice throughout the duration of the project.

Analyses of water samples used in this project were undertaken in collaboration with ISOMAP-UK members Dr. Elizabeth Fisher and Prof. Jim Marshall and thanks are due here for the free use of these data.

Analyses of cellulose samples for hydrogen stable isotope ratios were undertaken in collaboration with Prof. Marcus Leuenberger, Dr. Marc Filot and Sarah Hangartner. Special thanks go to Sarah for her assistance in the laboratory and for her ever friendly approach to problem solving.

^{14}C AMS radiocarbon dating was provided by the NERC Radiocarbon Laboratory, Beta-Analytic Inc. and Gröningen Radiocarbon Laboratory.

Collection of samples from a wide area of northern Europe and Newfoundland involved extensive fieldwork. Thanks must go to Dr. Al Brown, Dr. Mike Grant, Dr. Leanne Franklin-Smith, Matt Amesbury, Sarah Lomas-Clarke, Sue Way and Sam Rogers for their able assistance during coring operations. For the regular collection of moss and water samples extra thanks must go to Dr Frank McDermott and Dr. Michael Trepel. Access to land was granted by Friedwart Pütz (Untere Naturschutzbehörde, Dosenmoor), Jim Moore (Duchas, Raheenmore) and Major Johnson, (Owner, Walton Moss).

Heartfelt thanks are given to the team at Swansea University Dendrochronology group. Special mention must be given to my supervisor Dr. Neil Loader, who tirelessly supported this research, beyond the call of duty, in the process of 'feeding' the mass-spectrometer. Thanks also to Jonathan Woodman-Ralfe for laboratory assistance and for his motivational speeches and to Paula Stanillo and Dr. Iain Robertson for advice and assistance.

It is clear that special thanks must be reserved for my supervisors: Prof. Keith Barber, Prof. Alayne Street-Perrott and Dr. Neil Loader for their wise guidance and constant encouragement throughout the course of this project. Their unwavering support and challenging insight continually energised my interest in finding out more. Without obligation to supervise, Dr. Paul Hughes was also kind enough to offer much support both intellectually and through donation of a core from Newfoundland, from which some of the most interesting data have been derived and for which I am most grateful.

On a more personal note, I would wish to thank my parents for avoiding the temptation to enquire as to when I would be finishing and dear Sam for her ever special and unorthodox means of motivating me to complete this thesis!

1 Introduction

1.1 *Project rationale and aims*

Accelerated melting of Greenland ice (Chen *et al.*, 2006) has raised concern over the future impact of enhanced freshwater discharge on regional climate through its effect on ocean circulation. Changes in the rate of meridional overturning circulation (MOC) in the North Atlantic (Marchitto *et al.*, 1998; Bianchi and McCave, 1999; Chapman and Shackleton, 2000; Oppo *et al.*, 2003) have been associated with multiple climate changes during the Holocene with a quasi-periodicity of ~1500 years for which the triggering mechanisms are unclear (O'Brien *et al.*, 1995; Bond *et al.*, 2001) and also with abrupt change due to meltwater release from decaying continental ice sheets (Broecker, 1994; Barber *et al.*, 1999). The largest climatic change in the last 10,000 years occurred ~8200 BP and is believed to have been caused by the release of 5.2 sverdrups (1 Sv = 10^6 m^3s^{-1}) of meltwater from Glacial Lake Agassiz ~8450 BP over the period of one year (Barber *et al.*, 1999; Teller *et al.*, 2002).

Improved characterisation of change ~8200 BP has become a focus of research both for interest in the impact of meltwater discharge on climate and also for its role in testing numerical climate models (Alley and Agustsdottir, 2005). Ombrotrophic (rain-fed) peatlands have the potential to provide high quality data on both effective precipitation (precipitation minus evaporation) and variability in the isotopic composition of precipitation over Holocene timescales from mid-latitude locations in the North Atlantic region. This makes them ideal climatic archives for tracking the atmospheric response over land to changes associated with the North Atlantic over these timescales.

There has been rapid progress in the reconstruction of Holocene climate using raised bogs in the last decade. Multi-proxy analyses are now routinely applied to fossil remains preserved in the peat archive to define climatic signals and allow proxy cross-validation (Charman *et al.*, 1999; Chiverrell, 2001; Langdon *et al.*, 2003; Blundell and Barber, 2005). Those climatic signals are presently provided in the format of a palaeohydrological reconstruction based on the determination of Bog Surface Wetness (BSW) by the interaction of precipitation amount and temperature-controlled evaporation rates (Barber and Charman, 2003). The primary

driver of BSW response remains a contentious issue in the literature. Results from studies investigating the primary driver continue to provide mixed conclusions over the relative dominance of temperature and precipitation over Holocene timescales (Hendon and Charman, 2004; Schoning *et al.*, 2005; Charman, 2007). Despite improvements towards more quantitative methods with the use of testate amoebae transfer functions (Woodland *et al.*, 1998; Charman *et al.*, 2007), there remains a need for a technique that generates quantitative estimates of meteorological variables that can be directly compared with estimates from other palaeo-archives and used to validate General Circulation Model (GCM) estimates.

Isotopic analysis of the cellulose in *Sphagnum* moss has the potential to provide these quantitative estimates. Variation in the isotopic composition of precipitation is related to climate (Craig, 1961a; Dansgaard, 1964; Gat, 1980; Rozanski *et al.*, 1992; Rozanski *et al.*, 1993). The cellulose of plant remains contains information on the isotopic composition of the water that was used in its synthesis (Roden *et al.*, 2000; Waterhouse *et al.*, 2002). In the case of ombrotrophic peat bogs, that plant source water is derived entirely from precipitation. *Sphagnum* moss is particularly well suited to isotopic analysis owing to the simple pathways that lead to cellulose synthesis in this genus (Ménot-Combes *et al.*, 2002; Zanazzi and Mora, 2005). Early studies of the isotopic composition of peat (Schiegl, 1972; Brenninkmeijer *et al.*, 1982; Dupont and Brenninkmeijer, 1984; Dupont, 1986; Dupont and Mook, 1987) found that the mixture of plant species in peat stratigraphy produced variations in isotopic character that amplified the signal beyond the range of source water variability. It has been hypothesised that a temperature signal could be isolated from peat if it was possible to perform analyses on only a single genus (van Geel and Middeldorp, 1988). Advances in isotopic techniques have led to the ability to derive data from only a few mg of material, offering the opportunity to test this hypothesis (McCarroll and Loader, 2004; Filot *et al.*, 2006).

The derivation of a temperature signal from isotopic analysis of *Sphagnum* cellulose offers two major advances. Firstly, it allows for independent testing of the primary driver of change in BSW records from the peat archive. Crucially, however, the derivation of isotopic records from an array of sites in the North Atlantic region will provide new information on the magnitude of Holocene climate change with distance from the North Atlantic Ocean and hence insight into the mechanisms responsible for those changes.

Whilst considerable knowledge has been gained on the link between the stable isotopic composition of precipitation and climate (Dansgaard, 1964; Rozanski *et al.*, 1992; Rozanski *et al.*, 1993) and furthermore on how that signal is captured in the cellulose of plants (Sternberg *et al.*, 1986; Yakir and DeNiro, 1990), use of the technique in peatlands remains to be established. For isotopic variability in *Sphagnum* to be linked to climate or indeed temperature, mechanistic investigation is required to determine the nature of the signal.

This research therefore targets the following questions:

1) How does the isotopic composition of *Sphagnum* cellulose relate to the isotopic composition of precipitation?
2) How does variability in the isotopic composition of palaeo-*Sphagnum* cellulose relate to variation in past bog surface wetness?
3) How have spatial isotopic gradients varied in the past and what information do these provide on the mechanisms of change throughout the Holocene?
4) How have palaeotemperatures varied during key Holocene climatic changes?
5) Is temperature the primary driver of BSW?

The answers to these questions enable testing of the hypothesis that a temperature signal is contained in *Sphagnum* cellulose stable isotopic composition. If a signal does exist, this allows for direct testing of the hypothesis that variability in the bog surface wetness of temperate peatlands during the Holocene was primarily driven by variation in temperature.

1.2 *Thesis structure*

The research questions stated above are addressed through the chapters that follow. In Chapter 2, the role for stable isotope analysis as a tracer of Holocene climate change in raised peat bogs is developed through review of the mechanisms thought to be responsible for centennial and millennial scale climate change and the need for quantitative estimates of those changes. Background in understanding how isotopic variability provides information on climate, how this information is captured and archived in organic sediments and how methods

have developed to make modern use of this tracer in peat more successful are provided subsequently.

Four raised bog study sites were selected for this research. Three are in northern Europe and one in Newfoundland. The reasons for their selection and their physical characteristics along with their modern climatology and isotope climatology are described in Chapter 3. Empirical relationships are then derived that link the modern isotopic composition of precipitation to temperature and precipitation amount, for use in later calibration of peat core isotopic data with modern climate.

From each site, data were collected on isotopic variability in the modern environment and from core stratigraphy. Samples for ^{14}C AMS dating were collected to estimate the age of the peat stratigraphy. Data on palaeoecological change were collected from the European bogs only, the reasons for which are explained in Chapter 4. The methods used to collect these data are described and justified in Chapter 4. Prior to reconstruction of the palaeo-sequences, development of a new preparation procedure was required for separation of *Sphagnum* remains from the peat matrix. Four procedures were tested. The results of this preparation testing are presented and discussed prior to application of the chosen procedure later in the study. The results from the chronological, palaeoecological and isotopic analyses are presented in Chapters 5-7, respectively.

In Chapter 8, the questions listed above provide a structure for discussion. This includes analysis of how the isotopic composition of *Sphagnum* relates to precipitation, how isotopic variation through time compares with Bog Surface Wetness records and estimation of palaeotemperature change from each of the study sites. The isotopic data are then used in consideration of the postulated mechanisms of Holocene climate change over millennial time scales and the 8200 BP event. These findings are summarised with recommendations for future work in Chapter 9.

2 Background and context

2.1 *Reconstructing Holocene climate from raised peat*

2.1.1 Searching for the causes of abrupt and millennial scale change

Compared to the Pleistocene, the Holocene is considered to be a period of relative climatic stability (Dansgaard *et al.*, 1993). But this is an oversimplification (Oldfield, 2003). The view of stability has been progressively overturned by the discovery of clear cyclical changes in tracers from Greenland (O'Brien *et al.*, 1995) and the North Atlantic (Bond *et al.*, 1997; Bond *et al.*, 2001; Oppo *et al.*, 2003), coupled with dramatic changes in African lake levels (Faure *et al.*, 1963; Street and Grove, 1979; Street-Perrott and Perrott, 1990), lake productivity and level in Europe (Magny *et al.*, 2003a; Magny *et al.*, 2003b; Nesje *et al.*, 2004; Velle *et al.*, 2005; Nesje *et al.*, 2006), glacial fluctuations (Glasser *et al.*, 2004; Clague *et al.*, 2004), variability in temperate peatland surface wetness (Barber, 1981; Barber *et al.*, 1994; Hughes *et al.*, 2000; Langdon *et al.*, 2003; Langdon and Barber, 2005; Charman *et al.*, 2006) and tree-ring width and isotopic composition in the last millennium (McCarroll and Loader, 2004; Briffa *et al.*, 2004).

The North Atlantic region holds particular importance for understanding Holocene climate because of 1) the role that North Atlantic Ocean circulation has on influencing Northern Hemisphere (NH) climate[1] and 2) the existence of both regular cycles of climate change and abrupt events in the region reflected in both oceanic and atmospheric proxies during this period for which understanding remains limited.

Holocene climate in the North Atlantic region is characterised by variability over a range of timescales. The climate in any one location in time is a result of the interaction of these

[1] Heat transport of up to 1 PW (1 PW = 10^{15} W) has been calculated to account for a ~5°C SST difference between the Pacific and Atlantic Oceans north of 24°N (Rahmstorf, 2006). Modelled shutdown of overturning circulation leads to cooling of up to 10°C over the Nordic Seas (Rahmstorf, 2000; LeGrande *et al.*, 2006).

influences. Two modes of variability at the centennial to millennial timescales are focussed on here as they are readily detectable with the temporal range and resolution of the peatland archive.

Millennial scale cycles with a quasi-periodicity of ~1500 years and rapid events (10-100 years) have been evidenced from a variety of archives and are superimposed on variation induced by changes in the precession of Earth's orbit. Precession is understood to have contributed to an early-Holocene Thermal Maximum (HTM) characterised by greater Northern Hemisphere (NH) temperature seasonality and warm NH summer temperatures, followed by a mid-late Holocene general cooling trend (Marchal *et al.*, 2002). .

Millennial scale cycles are a major feature of North Atlantic oceanic and atmospheric climate. Originally recognised in spectral analysis of sediments from the late Pleistocene through to the Holocene (Pisias *et al.*, 1973), renewed attention was raised after both ice core and ocean core data revealed cycles at similar (1500 ± 500 yr) spacing which appeared to extend from cyclical behaviour occurring during the Pleistocene associated with Dansgaard-Oeschger events (Maslin *et al.*, 2003). In the Holocene, these cycles were most readily recognised by shifts towards cooler conditions.

The cause of the millennial cycles remains under debate although records indicate oceanic involvement (Bianchi and McCave, 1999; Oppo *et al.*, 2003). Change in deep ocean circulation is an attractive candidate for modulation of millennial cyclicity because the rate of overturning is commensurate with millennial timescales and because the magnitude of change occurring over these timescales is comparable to variation in oceanic heat transport in the present day (Rahmstorf, 2006). Solar variability over the period of the Holocene is estimated to have varied by only 2.4 % (Beer *et al.*, 2000; Bradley, 2003). The timescales of atmospheric circulation change are typically very rapid in comparison to the observed millennial cycles. Oceanic circulation has therefore been suggested as the only mechanism capable of sustaining the cycles observed (Maslin *et al.*, 2003).

Meridional overturning circulation (MOC) in the modern day is maintained by the sinking of North Atlantic Deep Water (NADW) in the Nordic and Labrador Seas. Radiative cooling of

warm, salty water advected from the Gulf of Mexico produces a water mass of high relative density in the Nordic and Labrador Seas. The sinking of this water drives deep ocean circulation in the North Atlantic and maintains the surface flow of water from lower latitudes to higher latitudes through the conservation of mass. The formation of NADW can be weakened either by atmospheric circulation changes or through the input of water of lower density, creating stable stratification and thereby inhibiting deep convection (Clark *et al.*, 2002). Weakening of the rate of MOC results in reduced latitudinal heat transport expressed as cool, dry conditions in the North Atlantic region (Maslin *et al.*, 2003).

Evidence for variation in the rate of MOC in the North Atlantic on the timescales of millennial cyclicity has been observed (Marchitto *et al.*, 1998; Bianchi and McCave, 1999; Chapman and Shackleton, 2000; Oppo *et al.*, 2003; Hall *et al.*, 2004; Lund *et al.*, 2006). Analysis of the grain size fraction of bottom sediments beneath modern conduits of deep water flow provides a proxy of deep water flow strength. These analyses reveal cycles in NADW production that have a quasi-periodicity of ~1500 years (Bianchi and McCave, 1999; Chapman and Shackleton, 2000; Oppo *et al.*, 2003). The reliability of these data hinges on the lack of any spatial alias due to shifting location of the current either horizontally or through shoaling that might result in an ambiguous signal in the bottom sediments. The regular nature of these inferred weakenings in current strength and their correspondence with atmospheric impact in Greenland and the wider North Atlantic region support the interpretation of regular variation in THC strength and corresponding climatic effects.

Whilst the involvement of ocean circulation in Holocene climate change is well demonstrated, the cause of the changes in NADW production remains uncertain. Three mechanisms have been proposed related to 1) the internal dynamics of continental and sea ice, 2) a self-sustaining bi-polar mechanism and 3) amplification of solar variability (Maslin *et al.*, 2003). Both the first and second mechanisms affect NADW production through regulation of the delivery of freshwater to sites of deep convection. In the model of ice sheet regulation, rates of waxing and waning of ice are controlled by internal processes. Periods of waning are represented by increased melt-water flux leading to reduced NADW production. The bi-polar regulation model (Maslin *et al.*, 2001; Stocker and Johnsen, 2003) is derived from the observation that heat piracy is observed between the hemispheres during glacial millennial

scale events (Blunier *et al.*, 1998; Barbante *et al.*, 2006) and is suggested as an extension of these glacial events into the Holocene (Maslin *et al.*, 2001). As conditions become colder in the northern hemisphere, reduced heat transport to northern latitudes results in warming of the southern latitudes: the so-called bi-polar seesaw (Broecker, 1998; Seidov and Maslin, 2001; Lynch-Stieglitz, 2004). The model is suggested to be self-sustaining through meltwater release in one hemisphere initiating a sequence of events that leads to meltwater release in the opposite hemisphere and a switching of the direction of heat piracy (Maslin *et al.*, 2001). The tools used for this switching are variations in the relative strengths of NADW and Antarctic Bottom Water (AABW). If this mechanism was responsible for Holocene millennial cyclicity, changes in AABW strength or latitudinal penetration would be expected in addition to evidence for changes in NADW. Data are, however, very limited on AABW change in the Holocene (Jones and Johnson, 1984; Broecker *et al.*, 1999) and typically limited to glacial timescales (Sarnthein *et al.*, 1994; Beveridge *et al.*, 1995).

The third mechanism is driven by changes in atmospheric circulation linked to solar variability rather than meltwater input (Bond *et al.*, 1997; Bond *et al.*, 2001; Sarnthein *et al.*, 2003; Alley *et al.*, 2003). Changes in solar output are reflected in fluctuations in the temperature gradient between low and high latitudes resulting in alteration of atmospheric circulation patterns. NADW production is weakened by alteration of surface winds and hydrography rather than by the input of freshwater, leading to reduced northward advection of warm, salty waters and a consequent freshening of the Nordic and Labrador Seas (Bond *et al.*, 2001). Solar variability is therefore the trigger but its effect is amplified through changing deep ocean convection. Support for this theory resides in correspondence in both frequency and time domains of variations in radionuclide tracers of solar output and in the latitudinal extent of polar waters inferred from Ice Rafted Debris (IRD) and sea surface temperatures (SSTs)(Bond *et al.*, 1997; Bond *et al.*, 2001; Sarnthein *et al.*, 2003; Muscheler *et al.*, 2004). Limitations of the theory arise from the link between atmospheric concentrations of radionuclides and ocean circulation (Beck *et al.*, 2001; Richards and Beck, 2001) and from variable deposition with changing precipitation patterns (Meese *et al.*, 1994; Finkel and Nishiizumi, 1997).

Rapid Holocene climate changes are considered to occur when "the climate system is forced to cross some threshold, triggering a transition to a new state at a rate determined by the climate system itself and faster than the cause" (Alley *et al.*, 2003)(p. 2006). Abrupt change in any system requires a trigger, an amplifier and resistance to an immediate return to the original state (Alley *et al.*, 2003). Whilst millennial cycles were pervasive throughout the Holocene and Pleistocene, abrupt centennial scale changes were prevalent in the early-Holocene and exhibit a structure that is not explained by millennial cyclicity (Rohling and Pälike, 2005). A crucial difference in the understanding of millennial change and key abrupt early Holocene changes ~8200 BP, 9300 BP and 10,300 BP is that the cause of the abrupt events is believed to be known. Change is thought to be associated with rapid responses of the THC to meltwater perturbation (Broecker, 1994; Barber *et al.*, 1999; Clark *et al.*, 2001).

The 8200 BP event was the largest climatic perturbation in the Holocene (Alley *et al.*, 1997). It is thought to have been caused by the influx of 163,000 km^3 of meltwater from Glacial Lake Agassiz ~8450 BP (Barber *et al.*, 1999; Teller *et al.*, 2002; Clarke *et al.*, 2004). This influx of water is believed to have produced a freshwater anomaly in the North Atlantic of sufficient amplitude to disrupt NADW formation and weaken the MOC resulting in a circum-North Atlantic cold event of ~150 years duration (Rohling and Pälike, 2005; Wiersma and Renssen, 2006; LeGrande *et al.*, 2006). Evidence for the 8200 BP event was first observed in records from Greenland ice cores (Alley *et al.*, 1997). It has since been observed in marine cores from the North Sea (Klitgaard-Kristensen *et al.*, 1998), European lake response (von Grafenstein *et al.*, 1998; Heiri *et al.*, 2003; Magny *et al.*, 2003b; Magny and Begeot, 2004; Heiri *et al.*, 2004; Nesje *et al.*, 2006), European vegetation response (Tinner and Lotter, 2001), lake productivity in northeast North America (Spooner *et al.*, 2002; Kurek *et al.*, 2004) and with tropical teleconnection (Street-Perrott and Perrott, 1990; Hughen *et al.*, 1996; Lachniet *et al.*, 2004). Studies from outside the North Atlantic region have attempted to link anomalies observed over longer timescales to the causes of the 8200 BP event. Whilst there remains the possibility of association through global teleconnection, it has been argued that incorporation of these events stretches the definition of "the event" beyond the short, sharp character observed in the North Atlantic region (Rohling and Pälike, 2005). Linkage of the rapid 8200 BP event with changes in sea surface temperatures and with changes in the flux of NADW has recently been demonstrated (Ellison *et al.*, 2006).

Increased emphasis on the testing of palaeoclimatic hypotheses by data-model comparison has led to a strong focus of research on the 8200 BP event from both palaeo-data and modelling communities. 8200 BP provides the ideal model testing ground where strong evidence exists for both cause and effect (Alley and Agustsdottir, 2005). Data-model comparison has become important because it allows for assessment of the performance of GCMs in reconstructing observed climate. That in turn permits improved estimation of confidence limits of those same models in predicting future climate change. The development of datasets from the early-Holocene period that can be used for data-model comparison is one of the key objectives of ISOMAP-UK. ISOMAP-UK is a nested project within a UK government research council (NERC) funded thematic programme called RAPID. The research conducted here forms the peat-based contribution to ISOMAP-UK. Necessarily then, a major aim of the research has been the derivation of palaeo-data from the early-Holocene period for the North Atlantic region.

2.1.2 Millennial and abrupt changes in peat

Atmospheric response at Holocene millennial periodicity is readily detected in raised peat bogs, the most recent fluctuations being the Medieval Warm Period and Little Ice Age, which are expressed strongly in bogs across the North Atlantic region (Barber *et al.*, 1994; Blackford and Chambers, 1995; Hughes *et al.*, 2000; Langdon *et al.*, 2003; Barber *et al.*, 2004; Blundell and Barber, 2005). These are detected as changes in BSW both through time domain comparison and in spectral analysis. Comparison of records in the time domain has revealed the coherent responses of bogs across Europe to the millennial scale oscillations. Successive regional syntheses have been constructed in publications over the past decade, each updating the previous, in which the ages of major climatic deteriorations are grouped into broad periods (Hughes *et al.*, 2000; Barber and Charman, 2003; Barber, 2007). The advantage of this approach is that variability in the quality of dating control can be minimised for increased regional perspective. In the most part, these "wet shifts" correspond well with the ages of millennial scale climatic change recorded in the ocean and other proxy archives from the North Atlantic region. Not all sites register change within the broad periods identified and

some register higher frequency oscillations. Whilst these may reflect real climatic differences they may also reflect locally variable conditions. A review of the ability of a single core to represent all regional changes is given in Barber *et al.* (1998).

Recent spectral analysis of the frequency of climatic changes has revealed that the ~1500 year period observed in Greenland (O'Brien *et al.*, 1995) is composed of two main harmonics in the rate of thermohaline circulation (THC) through Iceland-Scotland Overflow Water (ISOW) at 1000 yr and 550 yr frequencies (Chapman and Shackleton, 2000). In European peat bogs, cycles at 600 and 1100 yr are observed in a record from Walton Moss (Hughes *et al.*, 2000) and cycles at 1100 years in records from Scotland (Langdon *et al.*, 2003), suggesting a clear commonality of driver for both millennial ocean circulation change and atmospheric response over Greenland and the British Isles through the mid-to late Holocene.

Few peat records have been analysed that extend back far enough to capture changes at 8200 BP. A recently published record from Newfoundland, however, has provided the first peat-based evidence for a clear signal at this time (Hughes *et al.*, 2006) and demonstrated that the event was within the temporal detection range of peat-based proxy reconstruction. In northern England, records from Walton Moss and Bolton Fell Moss exhibit fluctuations in this early-Holocene period of approximately 200 years in duration (Hughes *et al.*, 2000; Barber *et al.*, 2003).

2.1.3 The climate record from peat

Peat is an excellent archive for providing terrestrial data to help resolve climate change questions in the Holocene. Sediments are deposited continuously and *in situ*, offer decadal resolution and are easily datable (Barber and Charman, 2003; Chambers and Charman, 2004). Continuing debate over the meteorological inference that can be derived from a composite proxy-hydrological reconstruction and limited information on magnitude, however, result in problems of comparison with other proxy archives limiting the wider use of peat climate data in data-model comparison for example.

As recently as thirty years ago, the link between peat bog stratigraphy and climate change was still conjecture. It was believed that variations in peat stratigraphy from taxa indicative of modern wet conditions to taxa typically inhabiting relatively dry positions in the modern day related to the autogenic infilling of hollows with little or no relationship with climate (Osvald, 1923). In the early 1980s, this cyclic regeneration model was formally falsified (Barber, 1981) when clear correspondence was demonstrated between changes in stratigraphy and climate indices of winter severity and summer wetness (Lamb, 1977). Since that time, understanding of the link between BSW and climate has been progressively strengthened with quantification of the extent of biological-induced noise (Barber *et al.*, 1998; Woodland *et al.*, 1998) and improved understanding of the climatic parameters involved in determining the water balance signal (Schoning *et al.*, 2005; Charman, 2007).

The climate record from peat is based on biological and chemical responses to changing conditions of BSW over time. In ombrotrophic (rain-fed) systems, all moisture and nutrients are received solely from atmospheric deposition. Consequently, the hydrology of the mire is directly related to climate. Bog hydrology is therefore controlled by a balance between the amount of input by precipitation (P) and the amount of evaporation (E), controlled largely by relative humidity and temperature. In northwest Europe, for much of the year, $P > E$. Excess precipitation is shed from the bog surface by saturation excess runoff (Ingram, 1983). The duration of the summer water deficit, when $E > P$, has a critical role in determining the mean annual hydrological conditions (Charman, 2007). How this relationship is manifest over Holocene timescales remains contentious.

Analyses of plant macrofossils, testate amoebae and the degree of humification are three proxy-indicator techniques commonly used to establish palaeohydrological change. Plant macrofossil analysis has been the proxy-indicator most commonly used, in part, by virtue of its position as the founding technique. The technique relies on the premise that surface wetness is the main control on the composition of plant communities. Assuming that the ecological preferences of individual taxa have not changed over time, fossil distributions can therefore be related to moisture controlled distributions observed in the modern day. Evidence from numerous studies strongly supports this uniformitarian ecology although exceptions are noted in one particular species (Stoneman *et al.*, 1993). The technique benefits from the

sensitivity of *Sphagnum* species to changes in water table where a strong gradient is observed between xerophilic to hygrophilic taxa (Barber and Charman, 2003). Since early inception the technique has undergone evolution from a qualitative indicator into what is now a reliable and objective semi-quantitative measure of past BSW using ordination techniques (Hughes *et al.*, 2000; Langdon *et al.*, 2003; Blundell and Barber, 2005).

As with all techniques, plant macrofossil analysis has limitations. The technique necessarily relies on a sensitive response of taxa to changing hydrological conditions. Whilst it has been shown to have excellent application in northwest European raised bogs, single species dominance of stratigraphy has been observed in sites from the southern hemisphere (Pendall *et al.*, 2001; Mauquoy *et al.*, 2004) and Newfoundland (Hughes *et al.*, 2006) and in reduced sensitivity in *Sphagnum* species to moisture gradients in continental settings (Haslam, 1987). Relatively low species diversity with wide hydrological tolerances prevents the use of transfer functions for the quantitative estimation of hydrological change. The dominant peat-former of northwest European peat bogs in the mid-late Holocene is *S. imbricatum*. In the modern day, this species is restricted to high hummocks in most northwest European bogs, apart from in highly oceanic sites (Slater and Slater, 1978). Evidence suggests that the species may have inhabited wetter conditions throughout much of the mid-late Holocene (Stoneman *et al.*, 1993). Consequently, interpretation of these extended sections is complicated (Barber and Charman, 2003; Barber, 2007).

Testate amoebae are unicellular organisms that inhabit the moist pore spaces near the bog surface and which secrete a shell (or test) for protection (Bobrov *et al.*, 1999; Charman, 2001). Extensive research in the 1990s revealed a dominant moisture control on the ecological distribution of testate species (Charman and Warner, 1992; Warner and Charman, 1994; Charman and Warner, 1997; Woodland *et al.*, 1998). Tests preserved posthumously therefore provide a fossil archive of relative species abundance that can be isolated and analysed for reconstruction of past moisture conditions (Charman, 2001). Given the large species diversity in relation to moss species, it has been possible to determine hydrological optima and ranges for each species assuming a Gaussian distribution in relation to hydrological factors (Woodland *et al.*, 1998; Charman *et al.*, 2007). These variables have been used as training data for transfer functions based on weighted averaging that allow quantitative estimates of

the depth to water table to be reconstructed from fossil testate assemblage data (Woodland *et al.*, 1998; Charman *et al.*, 2007).

Limitations of the technique relate to differential preservation and a lack of modern analogues for fossil species (Charman, 2001; Charman *et al.*, 2007). *Difflugia pulex* tests are abundant in many European and North American raised peat bogs, yet the species is rarely found on modern surfaces. Consequently, precise identification of the optima and range for *D. pulex* has been difficult to obtain. There is some evidence for a relationship between its abundance and that of *S. imbricatum* where both are observed to decline at a similar time in the fossil record, suggesting a possible host species status (Langdon *et al.*, 2003). The absence of certain species from records below surface layers in which they are readily abundant is suggestive of differential preservation. This factor can be easily accounted for in hydrological reconstruction, however, by omission of those species from the transfer function. Additionally, recent evidence points towards differences in the hydrological ranking of species optima in relation to different forms of hydrological measure (Charman *et al.*, 2007). Whilst depth to water table remains the dominant control on testate assemblage (Woodland *et al.*, 1998; Charman *et al.*, 2007), greater sensitivity to changes in either water tables or percentage moisture indicate that the hydrological relationship is complex.

Humification analysis exploits control on the rate of biological decay by the degree of surface wetness to derive a climate signal. Decomposition primarily takes place in the well-aerated, highly-porous surface zone, or acrotelm (Rochefort *et al.*, 1990; Johnson and Damman, 1991). The acrotelm is underlain by the slowly permeable water saturated catotelm (Gore, 1983; Charman, 2002). During phases of dry bog surface conditions, typically inferred to represent warm conditions, water tables are lower and so the depth of the aerated zone is greatest. These conditions maximise the duration of acrotelmic decomposition before the plants are buried in the catotelmic zone of permanent saturation. Plants are therefore subject to greater decay during low water tables. During phases of high bog water tables this zone is shallow, offering less time for aerobic decomposition to take place prior to incorporation in permanently saturated sediments. Decay is thus low during high water tables. A variety of methods exists for measurement. The most common technique involves measurement of the percentage transmission of 540nm light through an alkaline extract of the humic acids (Blackford and

Chambers, 1993b). The technique has many benefits. Firstly it allows the rapid processing of large volumes of data. Secondly, it is an ideal indicator for cores in which plant macrofossil data are dominated by a single taxon for extended periods (Hughes *et al.*, 2006). Thirdly, and related to the second, it offers a useful proxy where the extent of decay is high resulting in limited preservation of biological fossil remains (Blackford and Chambers, 1991; Blackford and Chambers, 1995; Yeloff and Mauquoy, 2006).

Limitations of the technique are primarily related to differential rates of decay among different species (Chiverrell, 2001; Blundell and Barber, 2005; Yeloff and Mauquoy, 2006). Variation in fossil plant assemblages is inferred to represent changes in climate through knowledge of their present ecological distribution. So at the periods in which a change in the humification signal may be expected, the change in plant species may also introduce non-climatic variation due to changes in the decay rate of individual taxa. In the acrotelm, *Sphagnum* litter decomposes more slowly than the leaves of vascular plants (Coulson and Butterfield, 1978), due to chemical protection of cell wall polysaccharides by polyphenolic compounds and lipid coatings (Karunen and Ekman, 1982; Ekman and Karunen, 1982). The proportion of humic acids derived from *Sphagnum* for a given aerobic depth of acrotelm is unlikely therefore to be equivalent to that derived from vascular species resulting in some species distortion of the climate signal (Yeloff and Mauquoy, 2006). Further limitation is related to uncertainty over the source of the signal from the procedure of alkali extraction. Luminescence spectroscopy has demonstrated that alkali extraction converts high-molecular weight humic acids into compounds of lower molecular weight fulvic and amino acids and polysaccarides (Caseldine *et al.*, 2000). Percentage transmission is dependent upon the luminescence wavelength and the molecular weight of the compounds present. Differing tendencies towards molecular decomposition by the action of alkali extraction on the differing species will be reflected in species-dependent variation in the humification signal (Caseldine *et al.*, 2000).

Recent studies have sought to combine these techniques in multi-proxy investigation where co-registration of wetness signals allows for cross-validation of the climate reconstruction. Whilst the number of multi-proxy investigations using more than two proxies remains relatively few, published studies reveal good coherence between the proxies (Chiverrell,

2001; Langdon *et al.*, 2003; Blundell and Barber, 2005; Hughes *et al.*, 2006; Chambers *et al.*, 2007). Where one proxy indicator is observed to disagree with the direction of change of the other two, the causes of this disagreement can be assessed and where necessary the proxy least representative of water table change can be omitted (Hughes *et al.*, 2006). Multi-proxy investigation has substantially enhanced the reliability of the reconstruction of direction of change in bog water tables. Magnitudes of change remain difficult to quantify given the derivation of variability on potentially non-linear scales. Greater sensitivity may be observed within certain water table ranges that differ between the techniques. Normalisation of inferred BSW from each of the techniques has allowed relative magnitude to be compared in terms of standard deviations (σ) from the mean (Blundell and Barber, 2005; Hughes *et al.*, 2006; Charman *et al.*, 2006). Similarity in the σ anomaly in the independent proxy reconstructions has validated the construction of composite inferred wetness curves from the mean of the sigma anomalies in each indicator. Whilst these mean sigma anomalies must inevitably be interpreted with caution given the potential for non-linear influence from the scales of measurement, correspondence on a regional scale has demonstrated the effectiveness of the data transformation (Blundell and Barber, 2005; Charman *et al.*, 2006).

2.1.4 Identifying the key drivers of water table change

Determination of the main control of hydrological change over Holocene timescales has become a vigorous area of research in peatland palaeoclimatology (Hendon and Charman, 2004; Schoning *et al.*, 2005; Charman, 2007). The question over the relative influences of precipitation and temperature was addressed in the investigation of BSW response from two bogs, 300 km apart horizontally and 900 m altitudinally from Fallahogy, N. Ireland and Moine Mhor in the Cairngorms, Scotland (Barber *et al.*, 2000). In view of its greater spatial and temporal coherence, temperature was considered to provide a better explanation for the observed regional climatic teleconnection than the comparatively heterogenous precipitation signal. The literature since then has provided conflicting examples.

Methods employed to investigate the competing roles of temperature and precipitation have been innovative. These have included:

1) Comparison over short times scales between bog records and instrumental records of climate change.
2) Comparison with independently derived summer temperature reconstructions from nearby lakes.
3) Regional syntheses incorporating areas of differing precipitation regimes

Comparison over the short (~125-200 year) timescales of instrumental records is inevitably problematic due to the necessity for accurate chronological constraint. Results from these investigations have been mixed, further energising the debate on the principal climatic control on BSW. Evidence exists for a link between both mean annual and summer temperatures and BSW over the past 200 years. Hydrological changes over the last 200 years in the Border mires of northern England were primarily driven by summer temperature changes (Hendon and Charman, 2004). Similarly, a statistically significant correlation ($P<0.05$) between mean annual temperature and decadal means of BSW has been observed from two ombrotrophic mires in central Sweden (Schoning *et al.*, 2005). Other studies, however, have placed greater emphasis on the influence of precipitation amount on forcing BSW. It has been suggested that precipitation exerts a strong influence over short (50 year) timescales with increased influence of temperature over longer time-scales (Charman *et al.*, 2004). More recent work suggests that the response to either precipitation or temperature may be controlled by location of the bog site. Temperature is observed to have greater influence with increased continentality (Charman, 2007). Whilst this is unlikely to have changed greatly in the mid-late Holocene, sea level changes in the early Holocene may have influenced this parameter over time.

The derivation of an independent proxy-temperature indicator, proximal to the bog site, over Holocene timescales, offers an alternative approach to determination of the climatic driver of BSW. Chironomid-inferred temperature (CI-T) reconstruction is based on the observation that modern chironomid distributions are driven primarily by summer temperatures (Brooks, 1996; Brooks and Birks, 2001). Reconstruction of summer temperatures is therefore obtained by analysis of the relative abundances of fossil larval remains preserved in lakes. Close

correspondence was observed between the independent CI-T reconstruction of Talkin Tarn, Cumbria with BSW changes in nearby Walton Moss over a 6000 year period, supporting the hypothesis that longer term changes in BSW were driven primarily by changes in summer temperatures (Langdon *et al.*, 2004). To date this represents the only published CI-T reconstruction from Britain for the period of the mid-late Holocene.

The moisture holding capacity of an air mass is directly proportional to its temperature. There is therefore significant potential for correlation between the two variables. Analysis of temperature and precipitation data from the first half of the twentieth century indicates significant correlation between the variables in Europe and the United States (Madden and Williams, 1978). This correlation is temporally variable, however, with switching exhibited between periods when the measures are in phase and out of phase. Comparisons between the Central England Temperature series (Parker *et al.*, 1992) and the England and Wales Precipitation series (Wigley *et al.*, 1984; Jones and Conway, 1997) over slightly longer timescales indicate that the two varied independently.

In addition to the possibility of correlation, changes in both temperature and precipitation are likely to have occurred in the North Atlantic region as a result of atmospheric circulation changes during the Holocene. Evidence exists for significant changes in atmospheric circulation during this period (Mayewski *et al.*, 2004) operating over a variety of timescales. Evidence from European Holocene lake level reconstructions suggest that changes in the latitudinal position of westerly storm-tracks were associated with variation in the temperature gradient between low and high latitudes (Magny *et al.*, 2003b; Magny *et al.*, 2006). Further evidence for changes in the atmospheric circulation over Europe is found in inferred storm intensity, tree-line variations, pollen stratigraphy and lake-carbonate isotope records (Seppa and Birks, 2001; Hammarlund *et al.*, 2002; Veski *et al.*, 2004; De Jong *et al.*, 2006). Significant changes in atmospheric circulation have also been reported from Holocene palaeo-archives in the North American continental interior (Edwards *et al.*, 1996; Dean *et al.*, 2002) and in the southern mid-latitudes (van Geel *et al.*, 2000; Chambers *et al.*, 2007). Shorter term variability in the isotopic composition of precipitation has been shown to relate to atmospheric circulation changes associated with the NAO (White *et al.*, 1997) and reduced

deep convection in the Labrador Sea during the Great Salinity Anomaly (1968-1971) (Serreze *et al.*, 1992; Curry *et al.*, 1998; Curry and Mauritzen, 2005).

2.1.5 A role for stable isotopic investigation

Key questions surrounding understanding of Holocene climate on centennial and millennial time scales are well suited to investigation by the peatland archive. Yet it is evident that there is a need for data which provide magnitude information on a linear scale in a format that is directly comparable between various palaeo-archives and which can be used to test theories of Holocene climate change mechanisms through data-model comparison. There is also the need for a tracer that has the potential to isolate a climate signal from peat that is independent of changes in bog hydrology and can be related to meteorological variables.

Data on the stable isotopic composition of cellulose archived in peat stratigraphy may hold the key to resolving both issues. Firstly, reconstruction of the isotopic composition of precipitation allows for direct comparison of the signal from peat with palaeo-isotopic data from other archives such as lake sediments, ice cores, speleothems and tree-rings in which the use of isotopic tracers is already well established. Secondly, isotopic data allow the opportunity to test the relationship between BSW records and the primary driver of moisture balance through established relationships between isotope data and meteorological variables in the modern day (Dansgaard, 1964; Rozanski *et al.*, 1992).

There are therefore two clear purposes to this research. The first is the derivation of isotopic data, with a particular focus on the early-Holocene, which may be used for tracking the magnitudes of climate change and hypothesis testing by data-model validation within ISOMAP-UK. The second is to derive isotopic records that can be used to test the role of temperature or precipitation in forcing BSW. The link between the stable isotopic composition of precipitation and climate and the incorporation of that signal in the cellulose preserved in peat is reviewed in the following sections.

2.2 *Water isotopes and their link to climate*

2.2.1 Isotopes in water

Oxygen has three stable isotopes, ^{16}O, ^{17}O, and ^{18}O; hydrogen has two stable isotopes, ^{1}H and ^{2}H (deuterium; D), and one radioactive isotope, ^{3}H (tritium). There are therefore nine possible configurations of these isotopes of which only three that occur in nature are easily measurable (Clark and Fritz, 1997; Araguas-Araguas *et al.*, 2000). These measurable configurations are $H_2{}^{18}O$, $HD^{16}O$ and $H_2{}^{16}O$, and their atomic weights are 20, 19 and 18, respectively. Given that oxygen and hydrogen combine to form water their isotopic composition can be used as a powerful tracer of the hydrosphere.

Table 2.1 Natural relative abundance of stable isotopes of water (Walker *et al.*, 1989)

Isotope	Relative abundance (%)
^{16}O	99.76
^{17}O	0.04
^{18}O	0.2
^{1}H	99.985
^{2}H	0.015

Table 2.2 Physical characteristics of three main types of water molecules (Hoefs, 1997; Criss, 1999)

	$H_2{}^{16}O$	$D_2{}^{16}O$	$H_2{}^{18}O$
Density @ 25°C	0.997	1.1051	1.1106
Boiling Point	100	101.42	100.14
Vapour pressure @ 100°C	760	721.6	?

Variations in the stable isotopes of water are typically expressed in delta notation (δ per mille deviation) relative to a standard (Vienna Standard Mean Ocean Water, V-SMOW) that is representative of the mean isotopic composition of the ocean (Equation 1)(Craig, 1961b; Coplen, 1995).

Equation 1) $$\delta = [(R_{sample} - R_{standard})/ R_{standard}] \times 1000$$

where R_{sample} and $R_{standard}$ are the isotopic ratios of either hydrogen or oxygen in the sample and standard respectively.

Delta notation is used given the low relative abundance of the heavier isotopes in the water molecule (Table 2.1) and relatively small variations in the isotopic composition throughout the hydrological cycle (Araguas-Araguas *et al.*, 2000). The isotopic ratios $^{2}H/^{1}H$ and $^{18}O/^{16}O$ of V-SMOW are given in Table 2.3.

Table 2.3 VSMOW standard values for $^{2}H/^{1}H$ (De Witt *et al.*, 1980) and $^{18}O/^{16}O$ (Baertschi, 1976)

Ratio	Value
$^{2}H/^{1}H$	$(155.95 \pm 0.08) \times 10^{-6}$
$^{18}O/^{16}O$	$(2005.20 \pm 0.45) \times 10^{-6}$

2.2.2 Fractionation as a climatic encoder

Isotopic fractionation is the partial separation of light from heavier isotopes due to differences in reaction rates as a result of differences in mass (Criss, 1999). It is because of fractionation, which arises as a result of the differing responses of isotopes to thermo-dynamic conditions, that waters develop unique isotopic compositions that can be indicative of their source or the processes that formed them (Gat, 1980; Clark and Fritz, 1997). Consequently the tracers can be used to infer climate (Rozanski *et al.*, 1992). Isotopic composition differs for sea water, polar ice, atmospheric water vapour, and meteoric water (Dansgaard, 1954; Craig, 1961a; Yurtsever and Gat, 1981; Darling *et al.*, 2003). Observed variations in the isotopic composition of meteoric waters arise from fractionation occurring during phase change (evaporation and condensation). More energy is required to excite water molecules composed of heavier isotopes than those composed of lighter isotopes resulting in separation and concentration of heavy and light isotopes in the lower and higher energy phases respectively (Criss, 1999). A fractionation factor is commonly used to describe isotopic differentiation and

is defined by the isotopic ratio between two phases (e.g. water and vapour, or precipitation and cellulose) given by the equation:

Equation 2) $$\alpha = ((R_1 / 1000) + 1) / ((R_2 / 1000) + 1)$$

where R_1 and R_2 are the isotopic ratios of the two phases respectively (Criss, 1999).

Fractionation can occur either in equilibrium, where mass is conserved, or in unidirectional (kinetic) processes that result from differences in molecular diffusivity. Equilibrium fractionation results from differences in the thermodynamic properties of the isotopes. Kinetic fractionation results from differences in the reaction rates of the isotopes. Both forms are considered below.

Isotopic exchange reactions that occur between two different phases of a compound at a rate that maintains equilibrium of mass represent equilibrium fractionation. The following description is adapted from the excellent summaries by Clark and Fritz (1997) and Hoefs (1997). Equilibrium fractionation between two phases of the same compound (in this case water) in a closed system can be expressed as:

$$H_2O_{(v)} \underset{c_2}{\overset{c_1}{\Leftrightarrow}} H_2O_{(l)}$$

H_2O *(v)* is the water in vapour phase; H_2O *(l)* is the water in liquid phase. The rate of exchange between the two phases is constant ($c_1 = c_2$). In order to maintain equilibrium, the rate of exchange must remain constant, although it varies for different isotopic compositions. Consequently, with ^{18}O, for example, $c_1 = c_2$:

$$H_2{}^{18}O_{(v)} \underset{c_2{}^{18}}{\overset{c_1{}^{18}}{\Leftrightarrow}} H_2{}^{18}O_{(l)}$$

Similarly, with ^{16}O:

$$H_2{}^{16}O_{(v)} \underset{c_2{}^{16}}{\overset{c_1{}^{16}}{\Leftrightarrow}} H_2{}^{16}O_{(l)}$$

and again $c_1 = c_2$.

The rate of exchange for ^{16}O is not the same as that for ^{18}O. Instead, $c_1{}^{18} < c_1{}^{16}$ leading to the more rapid exchange of ^{16}O. ^{18}O becomes relatively enriched in the liquid and ^{16}O becomes relatively enriched in water vapour. The process is in equilibrium in both instances, but the rate of these exchanges is different, so that enrichment of one of the isotopes results.

Equilibrium fractionation (α_e) for both ^{2}H and ^{18}O is temperature dependent. Fractionation is greater at lower temperatures than higher temperatures and the ratio of the fractionation factors for hydrogen to oxygen declines with increasing temperature until a critical point (C.P., 374°C) (Majoube, 1971a; Majoube, 1971b; Horita and Wesolowski, 1994).

Under natural conditions, it is rare for thermodynamic equilibrium to be reached. Where relative humidity < 100%, mass transfer in the form of evaporation takes place between the liquid and vapour phases of water with net transfer towards the vapour phase. Differences in the rate of transfer of heavy and light water molecules through viscous boundary layers between water and air (Merlivat and Coantic, 1975; Merlivat, 1978; Merlivat and Jouzel, 1979) produce an additional source of fractionation. This is kinetic fractionation (α_k) and is controlled by three factors:

1) the vapour pressure deficit
2) the molecular diffusivity of the different molecular species in air
3) the temperature of the evaporating surface.

This last factor is of lesser importance than factors (1) and (2) (Merlivat and Coantic, 1975; Merlivat and Jouzel, 1979). Total isotopic fractionation of water can therefore be expressed as $\alpha = \alpha_e\alpha_k$.

Critically, the rates of kinetic fractionation are different for the three measurable combinations of water isotopomers related to differences in their molecular diffusivities (factor 2 above). The extent of equilibrium and kinetic fractionation therefore imprints a characteristic labelling on water vapour. The processes responsible for isotopic evolution can then be inferred from the measured isotopic composition of the water.

The isotopic character of precipitation reflects that of the water vapour over the area of precipitation (Sonntag *et al.*, 1983; Jacob and Sonntag, 1991). The isotopic character of the water vapour is subject to four major sources of fractionation:

1) during the evaporation of surface source water
2) during condensation in cloud formation without precipitation
3) during rainout by a Rayleigh distillation process
4) as adiabatic cooling occurs in rising air parcels.

The net evaporation flux (δ_E) from the surface source water has been quantified as a function of the ambient conditions of temperature and humidity and the isotopic composition of the evaporating surface and free atmospheric vapour (Craig and Gordon, 1965). Whilst δ_E cannot be measured directly, if the hydrological cycle is assumed to be in isotopic steady state on the global scale, the isotopic composition of water vapour over the ocean will equal that of the net evaporative flux (Merlivat and Jouzel, 1979). The process of evaporation leads to depletion in the water vapour relative to the surface water source given the preferential evaporation of the lighter water molecules.

During condensation in the formation of clouds by adiabatic cooling, heavier water molecules preferentially convert to liquid droplets or ice crystals (Criss, 1999). This leads to further isotopic depletion of the remaining water vapour with respect to the original source water composition. The extent of this fractionation has been quantified previously using a simple isotope mass balance model (Liljequist and Cehak, 1979).

With the addition of further moist adiabatic cooling by advection either latitudinally or with increasing altitude, the residual vapour becomes progressively depleted by preferential loss of

the heavier isotopes through precipitation. This is known as rainout and is primarily controlled by the ambient temperature and humidity of the moist air mass. The isotopic depletion of the water vapour can be described by a Rayleigh distillation process if it is assumed that the air mass is isolated from additional moisture input during advection. Rayleigh distillation describes the progressive removal of a fractional increment of a trace substance from a larger reservoir. Once formed, each increment is removed and isolated from the system (Criss, 1999). Whilst the Rayleigh model cannot account for evaporative input during advection and turbulent mixing with other air masses during global circulation, it offers a useful mechanistic understanding of changes in the isotopic composition of the air mass with precipitation.

The Rayleigh model can also be used to estimate isotopic depletion with increasing altitude in the troposphere (Sonntag *et al.*, 1983). The decrease is exponential with a reduction in δD of -40‰ km^{-1} and -5‰ km^{-1} in $\delta^{18}O$. Above the troposphere, progressive enrichment is observed which has been attributed to the sourcing of stratospheric water from methane oxidation (Taylor, 1972; Ehhalt, 1974; Rozanski and Sonntag, 1982; Gedzelman, 1988).

The extent of fractionation between precipitation at the cloud base and the ground surface is important for two reasons. Firstly, it is necessary to understand whether the isotopic composition of precipitation is representative of ground or tropospheric conditions. Secondly, near-ground atmospheric water vapour is persistently influencing surface hydrology. Precipitation is spatially and temporally constrained. Modification of the isotopic composition of surface waters will be strongly influenced by both the saturation of the air at the air-water interface and by the isotopic composition of that vapour.

The isotopic composition should theoretically be more depleted at the cloud base than at ground level (Rozanski and Sonntag, 1982; Aravena *et al.*, 1999; Gonfiantini *et al.*, 2001). Measurements of the isotopic composition of local water vapour and precipitation at ground level, however, demonstrate that equilibrium is maintained between vapour and rain (Sonntag *et al.*, 1983; Jacob and Sonntag, 1991). The difference between cloud base and ground level is reduced by two processes: 1) the higher equilibrium fractionation factors at lower temperature (see above) and 2) fractionation of raindrops during descent to the ground. Comparison of the

temperature dependence of the isotopic composition of precipitation with that of water vapour (Jacob and Sonntag, 1991) demonstrated close similarity indicating that samples of rainfall, in the mid-latitudes at least, reflect isotopic variation in near-ground water vapour.

The sources of fractionation described above give rise to what are known as the fractionation "effects" in precipitation (Dansgaard, 1964; Yurtsever and Gat, 1981; Rozanski *et al.*, 1993). These have been termed rainout effect, amount effect, continentality effect, temperature effect and altitude effect. The isotopic composition of precipitation is determined by the interaction between these fractionation effects. Spatial and temporal variation in the relative magnitudes of these effects gives rise to variations in the isotopic composition of precipitation over these scales and provides a tracer of climate. The distribution of $\delta_{precipitation}$ produced by these interactions is considered in the following section.

2.2.3 Distribution of water isotopes in time and space

The relationship between isotopic composition of precipitation and climate variables is highly dependent on location. The location will influence the relative magnitude of the fractionation "effects". Climate change is likely to alter the relative importance of these effects.

Following the discovery of a rough linear correlation between δD and $\delta^{18}O$ in nine non-marine meteoric waters (Epstein and Mayeda, 1953), analysis of ~ 400 samples of freshwaters from a wide range of global locations revealed that meteoric waters exhibited a linear relationship between δD and $\delta^{18}O$ (Craig, 1961a) with the following form:

Equation 3) $$\delta D = 8 \times \delta^{18}O + 10$$

This relationship has been termed the Global Meteoric Water Line (GMWL) (Craig, 1961a). Craig (1961a) demonstrated that precipitation in tropical areas showed the least isotopic depletion with respect to SMOW. With increasing latitude, depletion increased linearly in both isotopes in line with a progressive reduction in total precipitable moisture by Rayleigh condensation. The slope and intercept of the GMWL are primarily a reflection of differences

in the equilibrium fractionation factors for hydrogen and oxygen (Majoube, 1971a; Majoube, 1971b; Horita and Wesolowski, 1994). The temperature dependence of this fractionation was described in the previous section. Hence the GMWL represents an average of variation in the isotopic composition of precipitation on a global scale.

The GMWL has since been validated using data collected on the isotopic composition of precipitation by the Global Network for Isotopes in Precipitation (GNIP) (Rozanski *et al.*, 1993). GNIP is a joint venture of the International Atomic Energy Agency (IAEA) and the World Meteorological Organisation (WMO), operational since 1961, with the primary aim of providing information at the global scale on the spatial and temporal distribution of environmental isotopes in precipitation. Since 1961, more than 800 meteorological stations in 101 countries have collected monthly precipitation samples. Figure 2.2 shows the location of all stations included in the GNIP database. It is evident that there is spatial heterogeneity of coverage with many stations concentrated in Europe and the mid-latitudes (50% between 30-60°N), few (9%) in the very high latitudes and most at low altitudes (80% <250 m a.s.l) (Araguas-Araguas *et al.*, 2000). The paucity of high latitude data has been supplemented by the analysis of fresh snow collected in Greenland and Antarctica (Morgan, 1982; Ciais *et al.*, 1995) and more recently by analysis of data from Russia (Kurita *et al.*, 2004). Perhaps most significant has been the length of coverage made available by the GNIP data. Two hundred and seven stations have records extending back at least five years and in 2000, seven stations had records covering twenty-five years (Araguas-Araguas *et al.*, 2000).

There are, however, deviations from the slope and intercept of the GMWL in particular regions relating to local or regional factors. These include the relative humidity of the prevailing source region, the proportion of moisture derived from continental interiors and processes occurring during fractionation of falling precipitation (Figure 2.1). Slopes < 8 are typically observed in precipitation in areas characterised by seasonal aridity due to partial evaporation of falling raindrops in the relatively dry atmosphere between cloud base and ground surface (Worden *et al.*, 2007). Seasonal variation in atmospheric circulation also has the effect of modifying the slope and/or absolute values of δD and $\delta^{18}O$ by altering the prevailing moisture source from which precipitation is derived (Sengupta and Sarkar, 2006; Rhodes *et al.*, 2006). Slopes > 8 are associated with areas in which a humid vapour source

supplies winter precipitation and increasing aridity characterises the summer precipitation regime (Araguas-Araguas *et al.*, 1998; Garcia *et al.*, 1998; Araguas-Araguas *et al.*, 2000).

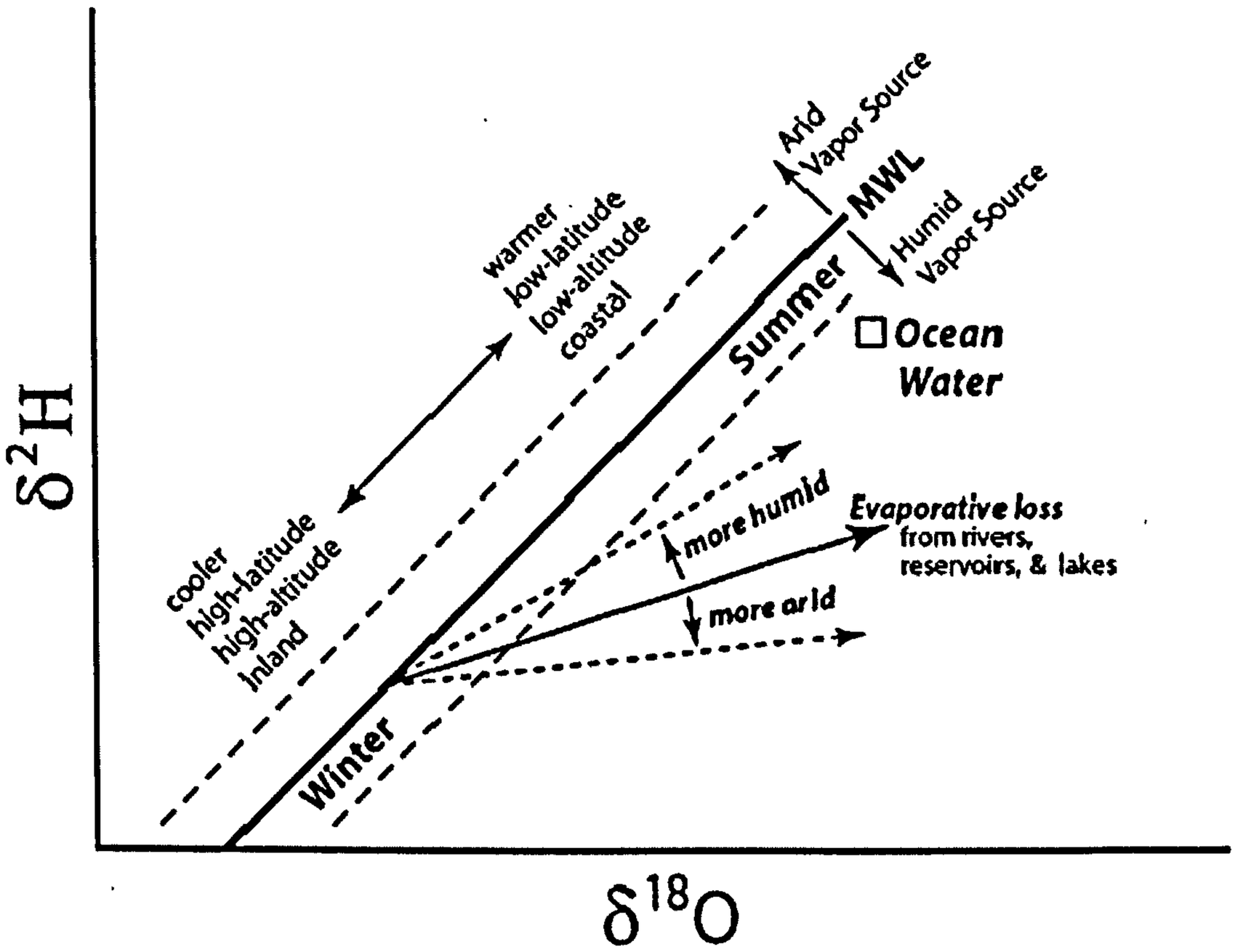

Figure 2.1 The effect of hydrological processes on the isotopic composition of water (Clark and Fritz, 1997)

Analyses of the spatial distribution of variability in meteoric isotopic composition in the GNIP dataset (Dansgaard, 1964; Yurtsever and Gat, 1981; Rozanski *et al.*, 1993) has greatly added detail but largely confirmed findings of the first global freshwater survey (Dansgaard, 1954). It was from these initial spatial surveys that relationships were derived between temperature, altitude, continentality and the amount of precipitation which are known now as the fractionation "effects" (section 2.2.2)(Dansgaard, 1964). Essentially, however, all of these effects relate to the rainout history of the moist air mass (Garcia *et al.*, 1998; Araguas-Araguas *et al.*, 2000). $\delta_{precipitation}$ is therefore a tracer of atmospheric circulation and meteorological conditions between the moisture source and site of final precipitation (Cole *et al.*, 1999).

The global pattern of spatial variation in $\delta_{precipitation}$ exhibits values similar to SMOW in the low latitudes with increasing depletion towards higher latitudes associated with the progressive removal of moisture from moist air masses transported from the low latitudes towards the poles (Dansgaard, 1954; Dansgaard, 1964; Yurtsever and Gat, 1981; Rozanski *et al.*, 1993)(Figure 2.2). On low latitude islands and coasts, $\delta_{precipitation}$ values for both oxygen and hydrogen are ~2 to 3 ‰ and hence very similar to ocean water. This is due to the local origin of the moisture for precipitation and reflects limited advection of air masses either latitudinally or vertically. Figure 2.2 shows the distribution of $\delta^{18}O_{precipitation}$ values (Araguas-Araguas *et al.*, 2000). In the mid-high latitudes depletion progressively increases to values -10‰ to -15‰ in coastal Antarctica, -20‰ in northern Canada and -50‰ at the South Pole (Ciais *et al.*, 1995). Two major conclusions are drawn from these early works: moisture is predominantly sourced from low latitudes and delivered progressively polewards and the depletion of precipitation reflects the water retention capacity of the moist air mass which is controlled primarily by the amount of cooling of the air mass during advection.

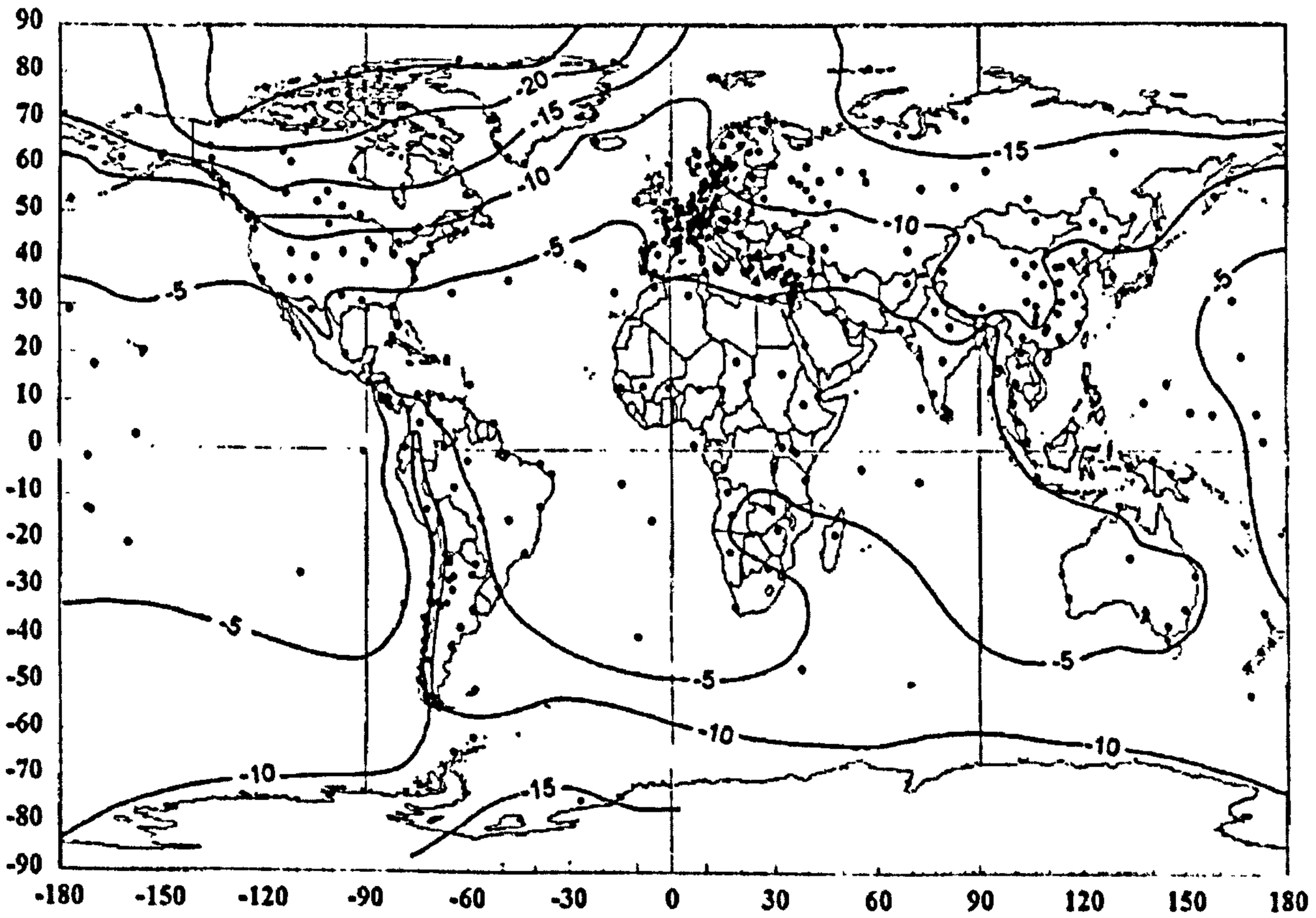

Figure 2.2 Geographical distribution of $\delta^{18}O$ in precipitation from the 508 stations (black dots) included in the GNIP database (Araguas-Araguas *et al.*, 2000).

This simple thermal latitudinal gradient is modified by ocean and atmospheric circulation patterns and by interaction with the surface. In the North Atlantic region, advection of warm surface waters by the North Atlantic current has a significant effect on modifying the latitudinal gradient (Figure 2.2). Moderation of the extent of latitudinal cooling results in the extention of isotopically enriched precipitation towards NW Europe in a lobe structure overlying the warm surface waters. Modification by the land surface is represented by the altitude and continentality effects. Both represent enhanced depletion in heavy isotopes in precipitation and relate to processes of increased rainout and reduction in the total precipitable water of the moist air mass.

Zones of increased depletion of rainfall are observed in mountainous areas due to the altitude effect. Decreasing temperatures with increasing altitude produce enhanced rainout for a given latitude. Enhanced condensation and rainout lead to highly depleted isotopic values. On the lee side of the mountainous formation, rain shadows are also expressed as significant isotopic shadows of strongly depleted precipitation (Stern and Blisniuk, 2002). This relationship with altitude is well documented (Siegenthaler and Oeschger, 1980; Aravena *et al.*, 1999; Gonfiantini *et al.*, 2001; Stern and Blisniuk, 2002). δD values vary by -1 to -4 ‰ 100 m^{-1} (Holdsworth *et al.*, 1991) and $\delta^{18}O$ values vary by -0.15 to -0.5 ‰ 100 m^{-1} (Siegenthaler and Oeschger, 1980).

Progressive isotopic depletion of precipitation is observed with distance from the coast in mid-latitudes as a result of progressive rainout of the air masses entering a continent (Ingraham and Taylor, 1986; Rozanski *et al.*, 1993; Stern and Blisniuk, 2002). In Europe, the modern continental isotope gradient is -2‰ $\delta^{18}O$ per 1000 km. Lower gradients are observed in tropical areas, in particular the Amazon basin, and have been attributed to the vigorous recycling of moisture (Salati *et al.*, 1979; Gat and Matsui, 1991; Victoria *et al.*, 1991; Garcia *et al.*, 1998). The steepest continental gradients in $\delta_{precipitation}$ values are observed in those areas in which moisture is predominantly transported inland and in which the coastal zone is mountainous. The altitude effect and the continentality effect are hence combined (Ingraham and Taylor, 1986; Yonge *et al.*, 1989; Stern and Blisniuk, 2002).

Depleted values of $\delta_{precipitation}$ are observed in tropical areas due to the "amount effect" and can relate to the location of the ITCZ. The amount effect occurs due to the enhanced rainout of total precipitable water over an area during the rainy season(s). Where temperature variation is minimal, a large amount of precipitation is therefore reflected in more depleted isotopic values. The effect is detected most readily in parts of southeast Asia affected by monsoonal rains and inter-tropical Pacific islands (Rozanski *et al.*, 1993; Pang *et al.*, 2006; Mayr *et al.*, 2007).

Seasonal variation in tropical regions is primarily driven by changes in the amount of precipitation. The effect is quite different in this instance to the amount effect just described. Seasonal displacement of the ITCZ not only controls the amount of precipitation falling on a particular area but regularly alters the origin of the vapour source from which the precipitation is derived which has a different rainout history. Variations in isotopic composition have been observed that are far greater than could have been forced by either temperature or the amount of precipitation. These have accordingly been attributed to the influence of alternate moisture source regions from which precipitation is derived (Araguas-Araguas *et al.*, 1998; Garcia *et al.*, 1998; Sengupta and Sarkar, 2006; Pang *et al.*, 2006; Mayr *et al.*, 2007).

Seasonal variation in the mid- to high latitudes is often pronounced and is a reflection of temperature seasonality (Rozanski *et al.*, 1992; Jouzel *et al.*, 2000; Yamanaka *et al.*, 2007). Araguas-Araguas *et al.* (2000) identify three factors that can produce the observed isotopic seasonality:

1) changes in temperature at the site of precipitation
2) changes in the evaporation flux on the continents
3) changes in the moisture source.

Essentially, factor (1) relates to the general increased cooling of the moist air mass during transport from source area to site of precipitation and occurs due to the increased latitudinal temperature gradient that exists during winter season. The more rapid cooling of poleward moisture bearing air masses produces earlier rainout of heavier isotopes. Precipitation in winter months consequently exhibits depleted values compared to the annual average. Factor

(2) acts to amplify the seasonal differences in total precipitable water through reduction in the recycling of moisture. It is highly likely that this is not simply constrained to continental areas but is also a factor of importance in the evaporation of moisture over the oceans as the air mass is advected towards the site of precipitation. Factor (3) is of high importance as it has the potential to weaken considerably any linear association between temperature and the isotopic composition of precipitation in the mid- to high latitudes (Jouzel *et al.*, 2000). Conceivably a fourth factor may also affect temporal variation in isotopic composition in the mid- to high latitudes and that is any seasonal variation in the amount of precipitation. The magnitude of change due to variation in precipitation amount is negligible, however, in comparison to that induced by temperature seasonality in the mid-high latitudes.

2.2.4 Maintenance of the temperature-dominant signal over time

It has been demonstrated that for sites in mid- to high latitudes linear relationships exist between surface air temperature and isotopic composition of precipitation (Dansgaard, 1964; Rozanski *et al.*, 1992; Jouzel *et al.*, 1997; Yamanaka *et al.*, 2007). Accordingly these relationships have been used to infer palaeotemperatures from isotope palaeodata. Whilst this relationship can be well defined in the present day, in order to predict past temperatures from mid-high latitude archives of palaeoprecipitation, it is necessarily assumed that the relationship holds true at a particularly location throughout time and throughout any climate change within that time. Consequently, atmospheric circulation is assumed to have had an insignificant impact on the isotopic composition of precipitation over the period of interest. The validity of this assumption has recently been tested (Jouzel *et al.*, 1997; Jouzel *et al.*, 2000) where numerical modeling results were found to support the dominating influence of local temperature changes on the palaeoisotope signal in most regions.

Evidence for significant variation in atmospheric circulation over the Holocene is, however, quite considerable (section 2.1.4). Whilst the coefficients of seasonal and longer-term decadal relationships between temperature and isotopic composition are similar, Rozanski *et al.*, (1993) found that increased scatter in the longer-term data substantially reduced the strength

of the relationship. With knowledge of the importance of moisture trajectory on $\delta_{precipitation}$ (section 2.2.3)(Cole *et al.*, 1999) and knowledge of the variability of atmospheric circulation during the Holocene (section 2.1.4) it is possible that any simple linear relationship with temperature for a site in the modern day may have been subject to modification and hence may not have prevailed in the past (Araguas-Araguas *et al.*, 2000).

In the absence of atmospheric circulation change, the magnitude of temperature change estimated from isotopic data at a sample site can also be distorted by changes in the temperature of the oceanic moisture source. Isotopic composition of precipitation at a given location depends on the difference in temperature between moisture source area and that location (Darling and Talbot, 2003) (section 2.2.2). Consequently, an increase in SST in the vapour source region is reflected as enrichment in the stable isotopic composition of precipitation at a sample site if all other factors remain constant.

This has important implications for the work undertaken in this study. It implies that even if a relationship is demonstrated in the modern day between the isotopic composition of precipitation and surface air temperature for each of the sites it does not necessarily follow that the relationship holds over time (Darling and Talbot, 2003). Relationships between isotopic composition of precipitation and meteorological variables for the study sites used in this project in the present day are explored in Chapter 3.

2.2.5 Tracking the source of moisture in air

Deuterium excess is defined as $d = \delta D - (8 \times \delta^{18}O)$ (Dansgaard, 1964). It is based on the equation for the GMWL and is a measure of deviation in the y-axis of a single data point from the GMWL. It is heavily dependent on meteorological conditions in the source region of the water vapour, principally surface temperature, wind speed and relative humidity (Merlivat and Jouzel, 1979). In the average, as represented by the GMWL, d = 10‰ (Darling and Talbot, 2003). For an individual location, however, this value varies seasonally such that during winter months in the Northern Hemisphere d = ~10‰ whereas during summer months, d falls to values < 10‰. High d values are indicative of moisture derived from regions of low

relative humidity such as the Mediterranean (Gat and Carmi, 1970) and regions where moisture is sourced from continental interiors (Gat *et al.*, 1994). Lower values of d are typically observed in the summer months due to the secondary evaporation of falling precipitation through a warm, dry atmosphere. The measure has become used as a tool for characterising the temporal evolution of an air mass (Merlivat and Jouzel, 1979; Jouzel *et al.*, 1991; Gat and Matsui, 1991) and for identifying the source region of precipitation (Petit *et al.*, 1991; Ciais *et al.*, 1995).

2.3 *The incorporation of water isotopes in plant cellulose*

2.3.1 Towards mechanistic understanding

An inevitable consequence of the discovery of a climatic signal in the isotopic composition of meteoric waters was the isotopic analysis of plant tissues to search for records of past variations in meteoric waters in their tissues. Facilitated by known processes for the extraction of cellulose (Green, 1963) and mass-spectrometric techniques for the measurement of organics, a series of high profile papers in the late 1970s and early 1980s demonstrated links between the isotopic composition of cellulose and environmental parameters (Libby and Pandolfi, 1974; Gray and Thompson, 1976; Libby *et al.*, 1976; Epstein and Yapp, 1977; Burk and Stuiver, 1981; Yapp and Epstein, 1982b). Investigation in the late 1970s and 1980s was focussed on developing mechanistic understanding of fractionation of D/H and $^{18}O/^{16}O$ through biochemical processes (Epstein *et al.*, 1977; DeNiro and Epstein, 1979; Estep and Hoering, 1980; DeNiro and Epstein, 1981; Estep and Hoering, 1981; Sternberg and Deniro, 1983; Sternberg *et al.*, 1986; Yakir and DeNiro, 1990). In the 1990s, mixed results in the identification of a dominant environmental variable responsible for observed cellulose values (Yapp and Epstein, 1982a; Edwards and Fritz, 1986; DeNiro and Cooper, 1989; White *et al.*, 1994; Feng and Epstein, 1994) led research to focus on the development of universal mechanistic models for the prediction of the source water isotopic composition (White *et al.*, 1994; Roden *et al.*, 2000). Much of this model development was undertaken with a view to

understanding the fractionation occurring in the synthesis of tree-ring cellulose (Roden *et al.*, 2000; Waterhouse *et al.*, 2002; Anderson *et al.*, 2002).

2.3.2 Advantages of non-vascular plants in climate reconstruction

Once water derived from meteoric sources arrives in the leaf of a photosynthetic plant there are two major sources of fractionation that will alter the isotopic composition of the cellulose from that of the meteoric water (Brenninkmeijer *et al.*, 1982; Zanazzi and Mora, 2005). Firstly, there is fractionation of the leaf water due to evaporation. Secondly, there is biochemical fractionation i) of the intermediates of cellulose synthesis and ii) due to re-exchange of intermediates with surrounding metabolic water.

Various models have been developed that relate cellulose isotopic composition to that of the source water and a series of thermo- and fluid dynamic properties (Dongmann *et al.*, 1974; White *et al.*, 1994; Roden *et al.*, 2000; Pendall *et al.*, 2001; Waterhouse *et al.*, 2002; Ménot-Combes *et al.*, 2002; Anderson *et al.*, 2002). These are typically based on modification of a model for steady state evaporation from a closed basin (Craig and Gordon, 1965). These models have become progressively more advanced incorporating terms to account for only a fraction of the leaf water being subject to evaporation (Buhay *et al.*, 1996; Wang *et al.*, 1998), fractionation during carbohydrate transfer along vascular tissues (Roden *et al.*, 2000), and exchange with xylem water (Waterhouse *et al.*, 2002). Whilst these models differ in terms of their complexity, the terms of each fall within the summary:

Equation 4) $$\delta_{cell} = \delta_{sw} + \varepsilon_b + (\varepsilon_e + \varepsilon_k)(1\text{-}h)$$

where δ_{cell} = isotopic composition of cellulose,

δ_{sw} = isotopic composition of the source water,

ε_b = the biochemical enrichment factor

ε_e = the liquid vapour equilibrium enrichment factor

ε_k = the liquid - vapour kinetic enrichment factor due to evaporation

h = relative humidity (value from 0 to 1)

Significant differences exist between the water sourcing strategies of vascular and non-vascular plants which are reflected in the complexity of the isotopic fractionation occurring in these modes. In vascular plants, whilst no fractionation of source water occurs in water uptake (Wershaw *et al.*, 1966), several fractionation opportunities exist prior to cellulose synthesis (Darling, 2004). Water is sourced from the ground. Evaporation of soil water has the potential to directly alter the source water isotopic composition close to the surface (Darling, 2004; McCarroll and Loader, 2004). Soil water residence time affects both the amount of evaporation that takes place and also the seasonal composition and age of the water that is used by the vascular plant (Dawson, 1993; Buhay and Edwards, 1995; Dawson and Pate, 1996). Water sourced from depth may represent older or more homogenised water than that sourced from shallow roots. Once water has entered the vascular plant it is transported to the leaf where it is subjected to fractionation prior to photosynthesis. Leaf water fractionation is controlled both environmentally through the isotopic composition of atmospheric vapour and the vapour pressure difference between the leaf and the atmosphere, and physiologically by water loss regulation (McCarroll and Loader, 2004). Large isotopic differences exist along vascular leaves due to the increased influence of evaporation near stomata (Wang and Yakir, 1995; Helliker and Ehleringer, 2002; Farquhar and Gan, 2003). This spatial heterogeneity of leaf water is reflected in the cellulose synthesized in these sections of leaf and in the sugars transported to other parts of the plant (Wang and Yakir, 1995; Helliker and Ehleringer, 2002). Evaporation from stomata drives a convective flow of plant water towards the sites of evaporation. This Péclet effect partly mitigates the diffusion of isotopically enriched source water away from the sites of evaporation (Barbour *et al.*, 2004; Barbour, 2007). Enrichment along a single sedge leaf, however, can be greater than isotopic variation observed in source water (Helliker and Ehleringer, 2002).

Non-vascular *Sphagnum* is equipped with no vascular apparatus for water transport and an inability to control water loss. This simpler physiology offers benefits for the modelling of fractionation of source water. Limited work has been undertaken in the modelling of fractionation of source water in *Sphagnum* cellulose (Brenninkmeijer *et al.*, 1982; Pendall *et al.*, 2001; Ménot-Combes *et al.*, 2002; Zanazzi and Mora, 2005). Previous mechanistic modelling efforts have incorporated leaf water fractionation and achieved good

correspondence with observations. Zanazzi and Mora (2005) demonstrate that because *Sphagnum* inhabits areas of relative humidity close to 100% (Vitt *et al.*, 1975; Clymo and Hayward, 1982), the relationship with source water can be simplified. In Equation 4 above, relative humidity is close to 1. Therefore, leaf water fractionation,

$$(\varepsilon_e + \varepsilon_k)(1\text{-}h) = 0.$$

The difference between $\delta_{source\ water}$ and $\delta_{cellulose}$ should therefore be related to fractionation occurring during biochemical enrichment only.

Relative humidity is not always 100%. Under conditions of high vapour pressure deficit and strong evaporation, the leaf water within the moss dries out. It is argued that under these conditions, *Sphagnum* suspends photosynthetic production until moisture levels recover (Williams, 1996). This would not occur to the same degree in trees as functioning guard cells in stomata are able to regulate water loss and facilitate continued photosynthetic production under conditions of strong leaf water enrichment due to evaporation.

2.3.3 Different pathways for oxygen and hydrogen

Biochemical fractionation affects oxygen and hydrogen to different extents due to the different pathways followed during cellulose synthesis (Estep and Hoering, 1981; Sternberg and DeNiro, 1983; Sternberg *et al.*, 1986; Yakir and DeNiro, 1990). For both elements, the cellulose synthesis process involves reactions that take place in light conditions (photosynthesis) and those that occur during biosynthesis later on in the pathway (Yakir and DeNiro, 1990).

Cellulose synthesis of oxygen atoms exhibits a nearly constant enrichment of ~27‰ relative to source water in plants from all photosynthetic modes and under a range of environmental conditions (DeNiro and Epstein, 1979; DeNiro and Epstein, 1981; Sternberg *et al.*, 1986; Yakir and DeNiro, 1990). Initially it was proposed that this enrichment related to the relative proportions of oxygen derived from CO_2 and H_2O (Epstein *et al.*, 1977; DeNiro and Epstein,

1979) entering the Calvin cycle. It was suggested that 2/3 of the oxygen entering the cycle was derived from CO_2 in isotopic equilibrium with the leaf water and 1/3 from the leaf water itself. Two problems existed with this model. Firstly, the model could not explain why tunicates (sea squirts, the only animals able to create cellulose), which do not fix CO_2, exhibited the same $\delta^{18}O$ values as cellulose. Secondly, it was observed that the enrichment was not temperature dependent, while the equilibration of CO_2 with water is temperature dependent (Sternberg *et al.*, 1986).

A second model was forwarded to explain the 27 ± 3‰ enrichment observed in oxygen in both terrestrial and aquatic plants. It was suggested that the enrichment may be due to isotopic fractionation during hydration of carbonyl groups of the intermediates of cellulose synthesis (DeNiro and Epstein, 1981). According to this model, $\delta^{18}O$ values of carbonyl oxygen should be $27‰ > \delta^{18}O_{source\ water}$ and should not be affected by subsequent reactions leading to cellulose synthesis. This was tested on acetone as a model compound where the $\delta^{18}O$ of the carbonyl group was found to equal 27‰ with no temperature dependent effect, consistent with the absence of temperature dependence in observations of $\delta^{18}O$ cellulose-water fractionation (Sternberg and Deniro, 1983). This second model was further tested using carrot tissue cultures and a cellulose producing bacterium (Sternberg *et al.*, 1986). It was demonstrated that the percentage of oxygen that exchanged with water agreed with the percentages expected based on the number of carbonyl groups in a substrate and subsequent intermediates for cellulose synthesis. The rapidity of the exchangeability depended on the substrate. Carbonyl oxygens that exchanged rapidly with water, such as those in the intermediates found in the pathway from glycerol, had a fractionation factor necessary to make $\delta^{18}O_{cellulose}$ values 27‰ more enriched than those of water at the site of synthesis (Sternberg *et al.*, 1986). It was noted that plants of all photosynthetic modes have a stage in which oxygen passes through a carbonyl stage which explained the occurrence of 27‰ in all plant types (Sternberg *et al.*, 1984a; Sternberg *et al.*, 1984b; Yakir and DeNiro, 1990).

Hydrogen fixation, on the other hand, is not the same for all plants. This difference results partly from the variable extent of biochemical fractionation occurring in different biosynthetic pathways (Estep and Hoering, 1980; Estep and Hoering, 1981; Yakir and DeNiro, 1990). Hydrogen in cellulose is derived entirely from hydrogen in leaf water. Consequently,

understanding the fractionation involved in hydrogen biosynthesis has great importance in reconstruction of source water (Yapp and Epstein, 1982b). Whilst oxygen exhibited a temperature insensitive constant fractionation factor of 27‰, it was demonstrated that much higher variability existed in δD values that was suggested to be temperature dependent (DeNiro and Epstein, 1981). Mechanistic investigation revealed that fractionation was regulated both by processes occurring in the leaf during photosynthesis (leading to strong depletion in the cellulose) and subsequent processes of cellulose synthesis from the intermediates (leading to enrichment) (Estep and Hoering, 1981; Yakir and DeNiro, 1990; Luo and Sternberg, 1991). Differences in the δD values of cellulose cultured in light and dark conditions and differences in the rate of uptake of water enriched in deuterium (^2H) compared to that that of organic substrates led to the proposition that the photosynthetic depletion relates to preferential hydration of nicotinamide adenine dinucleotide phosphate (NADP) with protium rather than deuterium to form NADPH. Subsequent enrichment occurs during exchange with hydrogen in heterotrophic cellulose synthesis (Estep and Hoering, 1981; Yakir and DeNiro, 1990; Luo and Sternberg, 1991).

During photosynthesis, light energy initiates elevation of electrons in chloroplasts to higher excitation states. These then begin a cascade reaction along a redox potential leading to the formation of NADP. To sustain the process, the transferred electron must be replaced. Leaf water is used to provide the replacement electrons. It is at this stage that the photosynthetic depletion occurs (Yakir and DeNiro, 1990). Leaf water molecules composed of lighter protium (^1H) are preferentially used in the donation of electrons. This is due to the reduced dissociation of HDO than H_2O (Luo *et al.*, 1991). Photosynthetic electron transfer therefore produces a pool of hydrogen ions dominated by protium as a reductant. NADP is subsequently reduced by these hydrogen ions into NADPH which is then used to energise the RPP pathway for the production of sugars. This is achieved by donation of the acquired hydrogen atom returning NADPH to NADP whereupon the cycle is continued for as long as photosynthetic production progresses. This NADP – NADPH cycle (Figure 2.3) operates as the pump for delivering depleted hydrogen into the sugars used for cellulose synthesis.

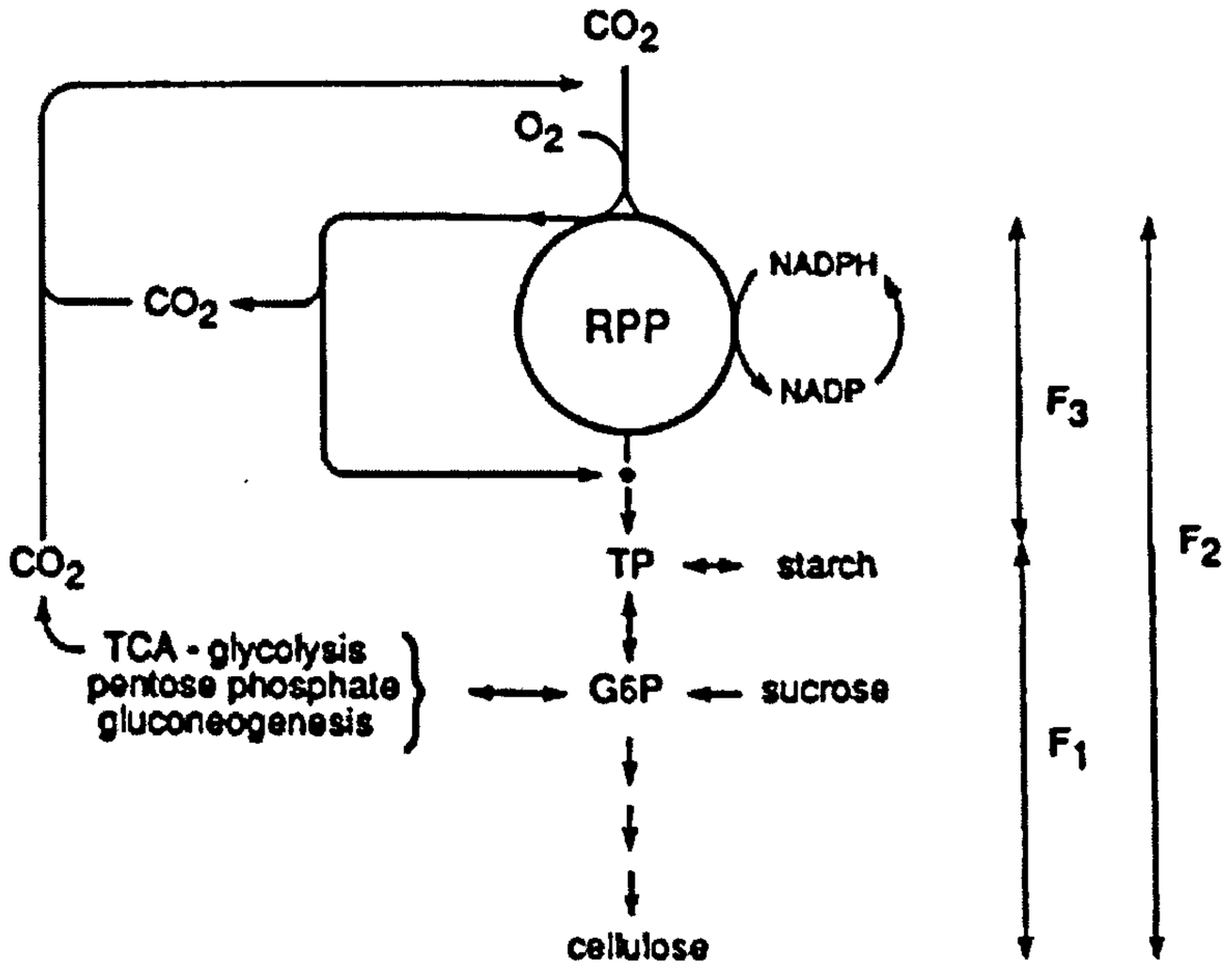

Figure 2.3 A simplified representation of the pathways involved in the metabolism leading to the synthesis of cellulose in C3 plants under photoheterotrophic (F3) or heterotrophic (F1) conditions or a combination of the two (autotrophic; F2) (Yakir and DeNiro, 1990).

Greater depletion in cellulose was observed to occur under autotrophic conditions than photoheterotrophic conditions (Estep and Hoering, 1981; Yakir and DeNiro, 1990). Under photoheterotrophic conditions, CO_2 is limited and only available through re-fixation of plant respired CO_2. Consequently, flux through the RPP photosynthetic pathway is reduced. During photorespiratory activity, NADPH has increased opportunity to exchange H with leaf water. It has been suggested that the greater depletion observed in autotrophic conditions may be due to increased flux through the RPP pathway relative to an unchanged photorespiratory flux when CO_2 and water are abundant. The NADPH "effect" is therefore preserved in the cellulose product to a greater degree (Yakir and DeNiro, 1990).

Hydrogen isotope fractionation associated with heterotrophic carbohydrate metabolism (ε_{HH}), by contrast, produces deuterium enrichment (Yakir and DeNiro, 1990; Luo and Sternberg, 1991; Luo and Sternberg, 1992). Reported values for this enrichment are relatively consistent. ε_{HH} for *Hordeum*, *Triticum* and *Ricinus* are +144 to +166‰ (Luo and Sternberg, 1992). ε_{HH} for *Lemna* is +158‰ (Yakir and DeNiro, 1990). In *Lemna*, the depletion due to NADPH

discrimination (-171‰) is greater than enrichment due to heterotrophic metabolism (+158‰) leading to net biochemical depletion in $\delta D_{cellulose}$ values relative to $\delta D_{source\ water}$.

The fractionation factor that describes the isotopic discrimination in the formation of cellulose from water is defined as:

Equation 5) $$\alpha = ((\delta_{cellulose} / 1000) + 1) / ((\delta_{source\ water} / 1000) + 1)$$

The biological fractionation factor for oxygen (α_{18}) due to the hydration of carbonyl groups has been experimentally determined to be $\alpha_{18} = 1.027$ (Sternberg and DeNiro, 1983; Sternberg *et al.*, 1986). Field experiments on *Sphagnum* have reported $\alpha_{18} = 1.0253$ with respect to surface waters which may have been evaporatively enriched (Aucour *et al.*, 1996). For the case of *Lemna* above, the net depletion in deuterium (α_D) is reflected in a fractionation factor of $\alpha_D = 0.977$ under autotrophic conditions. In Patagonian *Sphagnum*, α_D has been determined as 0.922 and reflects a greater net depletion of *Sphagnum* tissues with respect to source waters than that observed in *Lemna* (Pendall *et al.*, 2001). Strong depletion of *Sphagnum* δD relative to vascular plants has also been reported from sites in Europe (Brenninkmeijer *et al.*, 1982). Investigation of the fractionation of hydrogen in *Sphagnum* cellulose is limited, although the studies above indicate that a strong depletion signal may be present in the genus. Considering the discussion above, it is possible that this may reflect the simple physiology of *Sphagnum*. Enrichment has been identified as occurring during heterotrophic metabolism where sugars are generated from components sourced from the substrate in which the organism is growing (Luo and Sternberg, 1991). Raised bog *Sphagnum* moss grows in highly nutrient depleted conditions and instead relies on nutrients delivered by precipitation to sustain growth. It is possible therefore that a strongly depleted deuterium value in cellulose relative to the source water reflects limited post-photosynthetic exchange of intermediates used in cellulose synthesis.

2.4 *Advances in isotopic techniques*

2.4.1 Taxonomic variation in isotope values

Previous research on the reconstruction of water isotopic composition from peat cellulose has been limited. Much of the work was undertaken during the 1980s by teams working in the Universities of Amsterdam and Gröningen. The conclusions from all of these works were that the isotopic signal in peat was dominated by changes in the botanical composition of the peat rather than by changes in the isotopic composition of cellulose source water (Brenninkmeijer *et al.*, 1982; Dupont and Brenninkmeijer, 1984; van Geel and Middeldorp, 1988). This species effect was first identified by evidence of a strong correlation between isotopic ratio and floral composition but more importantly by the magnitude of variability exceeding that expected due to changes in precipitation alone (Brenninkmeijer *et al.*, 1982; Brenninkmeijer, 1983; Dupont and Brenninkmeijer, 1984; Dupont, 1986; Dupont and Mook, 1987; van Geel and Middeldorp, 1988). This large variability was attributed to differences in the relative proportions of vascular and non-vascular plants in the peat sample. A statistically significant difference exists between the isotopic compositions of vascular plants versus non-vascular plants by up to 25‰ and 5‰ in deuterium and oxygen-18, respectively (Brenninkmeijer *et al.*, 1982; Ménot-Combes *et al.*, 2002). Annual seasonal variation in precipitation in NW Europe in the present day is ~ 2-4‰ in oxygen (Rozanski *et al.*, 1993). The strong enrichment seen in vascular plants results from fractionation occurring during evaporation from leaves (section 2.3.2). Fluctuations in the botanical composition of the core from dominance by non-vascular plants to vascular plants were therefore reflected in large variations in isotopic value which exceeded that due to precipitation. It was argued that the isotopic composition still reflected a temperature signal, however, as botanical composition would switch to vascular plants during periods of warm/dry conditions. Hence, the isotopic composition of precipitation would become more enriched due to temperature increase and also be amplified by vegetation change (Schiegl, 1972; van Geel and Middeldorp, 1988).

In the late 1980s, workers attempted to isolate the climate signal from the botanical signal by correcting δD for taxon dependence (Dupont and Mook, 1987; van Geel and Middeldorp,

1988). The method used was a series of multiple linear regressions where δD was considered the dependent variable and the volume percentages of a particular taxon the independent variable. Floral composition was necessarily simplified to the most substantial peat-forming taxa and the remaining signal termed the Isotope Climatic Index (ICI) (Dupont and Mook, 1987). Coefficients were obtained between temperature and predicted source water that were three to four times larger than the precipitation-temperature coefficients identified by other workers (Dansgaard, 1964; Libby and Pandolfi, 1974; Gray and Thompson, 1976; Yapp and Epstein, 1982b). The same procedure was used later on data from Carbury Bog, Ireland and compared against the climatological indices for the last 1000 years (van Geel and Middeldorp, 1988). The authors were obliged to conclude that no evidence for a direct climate signal existed in the peat isotope data.

The principal limiting factor stemmed from the need for large sample sizes (5g of dry peat) for analysis by mass spectrometry. It was suggested that if individual taxa could be analysed, a much closer link to source water would be observed, but that the requirement of 5g of material from each taxon was prohibitive (van Geel and Middeldorp, 1988). Recent technological advances now allow for the analysis of organic samples of 0.3-0.35mg for oxygen (Werner *et al.*, 1996; Saurer *et al.*, 1998) and 0.5-0.7mg for hydrogen (Filot *et al.*, 2006)(section 2.4.2 below). This radical reduction in the amount of material necessary for analysis provides the opportunity to employ a genus-specific approach to peat-based palaeo-isotopic research.

The applicability of any genus-specific approach relies on the absence of any statistically significant difference in fractionation between the species of that genus. The occurrence of higher levels of isotopic enrichment in *Sphagnum* species with height above the water table has been observed (Brenninkmeijer *et al.*, 1982; Aravena and Warner, 1992). These studies were conducted during single sample periods in summer months when evaporative enrichment of the *Sphagnum* leaf water is likely to have been strongest. Consequently, the enrichment observed during these months may not be representative of the decadally averaged signal preserved in the stratigraphical archive. More recent investigation has revealed that this difference is not statistically significant and does not relate to variability in the isotopic

composition of bog surface water (Ménot-Combes *et al.*, 2002). The discovery of limited within-genus variability supports the use of *Sphagnum*-specific investigation.

Whilst *Sphagnum*-specific analysis has been employed recently for analysis of δD values on a raised bog in Patagonia yielding results that appear to relate strongly to climate variability (Pendall *et al.*, 2001), there is clearly a need for improvement in the understanding of the source of the isotopic signal in *Sphagnum* and its relationship with precipitation. To the best of my knowledge, no study has yet been conducted on past variations in the *oxygen* isotopic composition of *Sphagnum*-specific cellulose.

2.4.2 Oxygen and hydrogen analytical techniques

The reduction in sample size is, at least in part, the result of the development of techniques that allow measurement of stable isotope ratios "on-line" (Werner *et al.*, 1996; Saurer *et al.*, 1998; Filot *et al.*, 2006). Isotope ratios of an organic sample are measured either "on-line" or "off-line", defined by the manner in which a measurable gas is generated from the organic sample. In both cases, the organic sample must be transformed into a gas suitable for mass spectrometry by pyrolysis (Saurer and Siegwolf, 2004). On-line preparation involves the coupling of a pyrolysis reactor with a mass spectrometer allowing continuous transport of the pyrolysis products through to the mass spectrometer by means of a helium carrier gas stream. Off-line preparation involves gas generation in a separate process to that of the later measurement.

Following pyrolysis, the gas produced from the organic sample is directed into a mass spectrometer (MS). Inside the MS, the sample gas is ionised then accelerated by high voltage through a magnetic field where the difference in mass of the isotopes is reflected in differences in deflection due to the magnetic field. The ions are collected in a sequence of Faraday cups and "counted" by means of the detection of an electrical signal. The trajectories of the separated isotopes are tuned against the accelerating voltage to maximise capture of the

deflected ions (McCarroll and Loader, 2004). These counts are then compared against standards to yield δ values.

In general, off-line techniques are very precise but highly time-consuming. Oxygen off-line preparation is undertaken either by mercury chloride pyrolysis or nickel tube pyrolysis (Saurer *et al.*, 1998; McCarroll and Loader, 2004). The former is time-consuming and involves exposure to toxic chemicals. The latter has the advantage that both CO_2 and H_2 can be captured for analysis but suffers from the potential for oxidation of the nickel tubes used for pyrolysis and cannot be used with compounds containing nitrogen. Hydrogen pyrolysis can also be undertaken using the nickel tube method or through *in vacuo* combustion of the organic sample in the presence of excess copper oxide to form water that is then reacted with zinc to yield hydrogen gas.

The time-consuming and costly nature of these off-line methods has encouraged the development of more rapid "on-line" techniques. On-line (or continuous flow) methods were originally pioneered for the analysis of carbon stable isotope ratios and developed from the integration of an Elemental Analyser with a Mass Spectrometer (Preston and Owens, 1983; Preston and Owens, 1985). Sample throughput was enabled by a continuous flow of a helium carrier gas stream that carried the sample gas through pyrolysis, purification and measurement. There are some limitations to the use of on-line techniques. Unlike dual-inlet (off-line) techniques, the pressure of the reference gas and gas derived from the sample are not balanced prior to analysis. Changes in the mass and hence pressure of the sample gas are produced through small variations in the size of the organic sample. Limits to sample sizes have been investigated and set, however, yielding precision within these ranges of ~0.3‰ for oxygen analysis for example (Saurer *et al.*, 1998; Saurer and Siegwolf, 2004). Throughput of large numbers of samples in an on-line "run" increases the potential for variation in carrier gas flow and combustion pyrolysis efficiency between samples, leading to a drift in isotope measurement. This drift can, however, be corrected by the regular incorporation of reference samples of known isotopic composition.

Continuous flow systems for analysis of the stable isotopic composition of oxygen remain under development (McCarroll and Loader, 2004). Despite differences, most involve a

procedure that leads to total pyrolysis of the organic sample by high temperature to yield carbon monoxide which is then measured (Werner *et al.*, 1996; Farquhar *et al.*, 1997; Saurer *et al.*, 1998; Saurer and Siegwolf, 2004).

Until recently, the on-line analysis of hydrogen isotopes was complicated by the difficulty in differentiating deuterium from the helium carrier gas of identical mass, separation of the isotopes in the MS and amount effects in the detector (McCarroll and Loader, 2004). It is further complicated by the need to account for the potential exchangeability of up to 30% of the hydrogen atoms in the cellulose (Schimmelmann, 1991).

Cellulose molecules are made up of chains of β–glucose units joined by glycosidic bonds in a condensation reaction. Approximately 70% of the hydrogen atoms that form the polymer are bound to carbon atoms (Figure 2.4) (Schimmelmann, 1991) whilst the remaining ~30% are bound to oxygen in hydroxyl groups (OH, Figure 2.4).

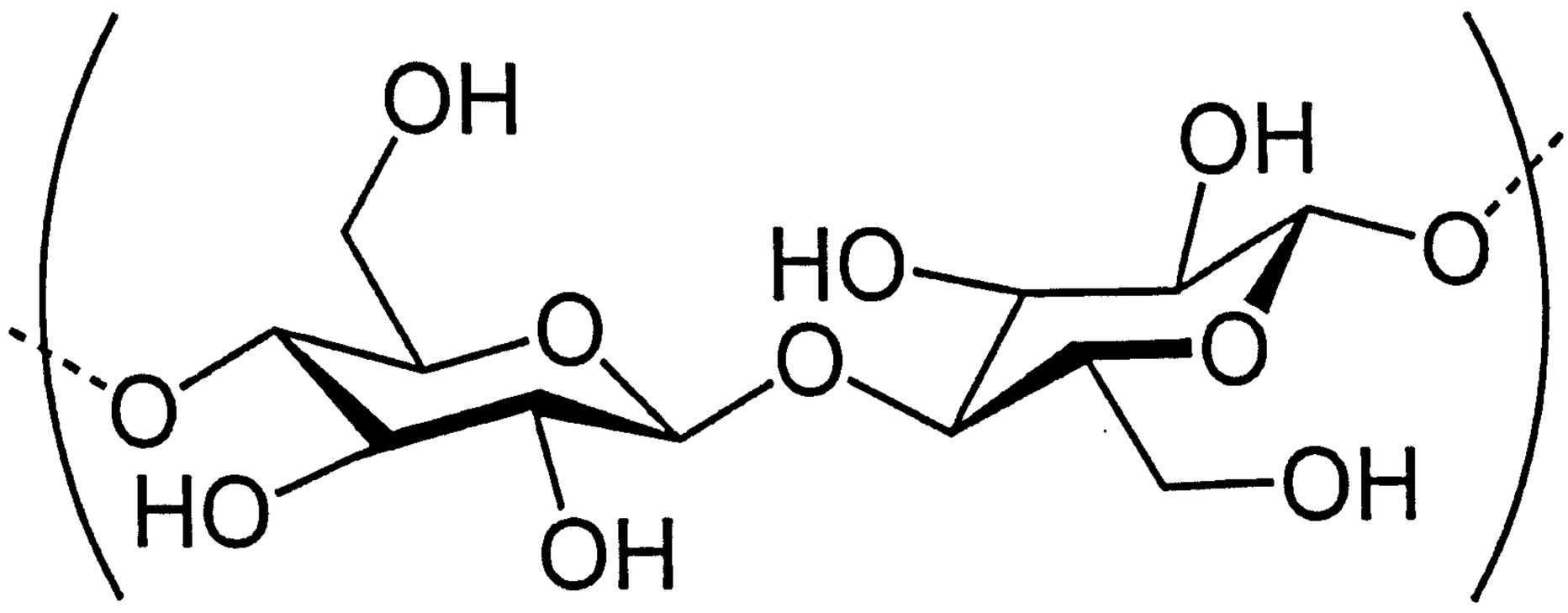

Figure 2.4 Schematic of the cellulose molecule (source: http://en.wikipedia.org/wiki/Cellulose)

These oxygen-bound hydrogen atoms are exchangeable with those of surrounding environmental waters and the solutions used for cellulose extraction. Therefore only the non-exchangable carbon-bound hydrogen atoms can be used to derive information on the isotopic composition of the source water used during cellulose synthesis. For meaningful analysis of

hydrogen data, it is necessary to either control the isotopic composition of these exchangeable hydrogen atoms by equilibration with water of known isotopic composition or replace the hydroxyl hydrogen with other functional groups that do not contain hydrogen.

Two methods are available. The most common technique involves the replacement of the hydroxyl hydrogens with NO_2 (Figure 2.5) (Bennett and Timmell, 1955; Green, 1963; Luo and Sternberg, 1991; White *et al.*, 1994; Buhay and Edwards, 1995). This nitration procedure produces the explosive product cellulose-nitrate (Guncotton) but permits analysis of the carbon-bound hydrogen atoms. Whilst cellulose nitrate can be analysed on-line, the limitations of the technique are that the substance has the potential to degrade, altering the isotopic composition between construction and measurement and the sample sizes required are relatively large (~2-12 mg) (Luo and Sternberg, 1991; White *et al.*, 1994; Kelly *et al.*, 1998).

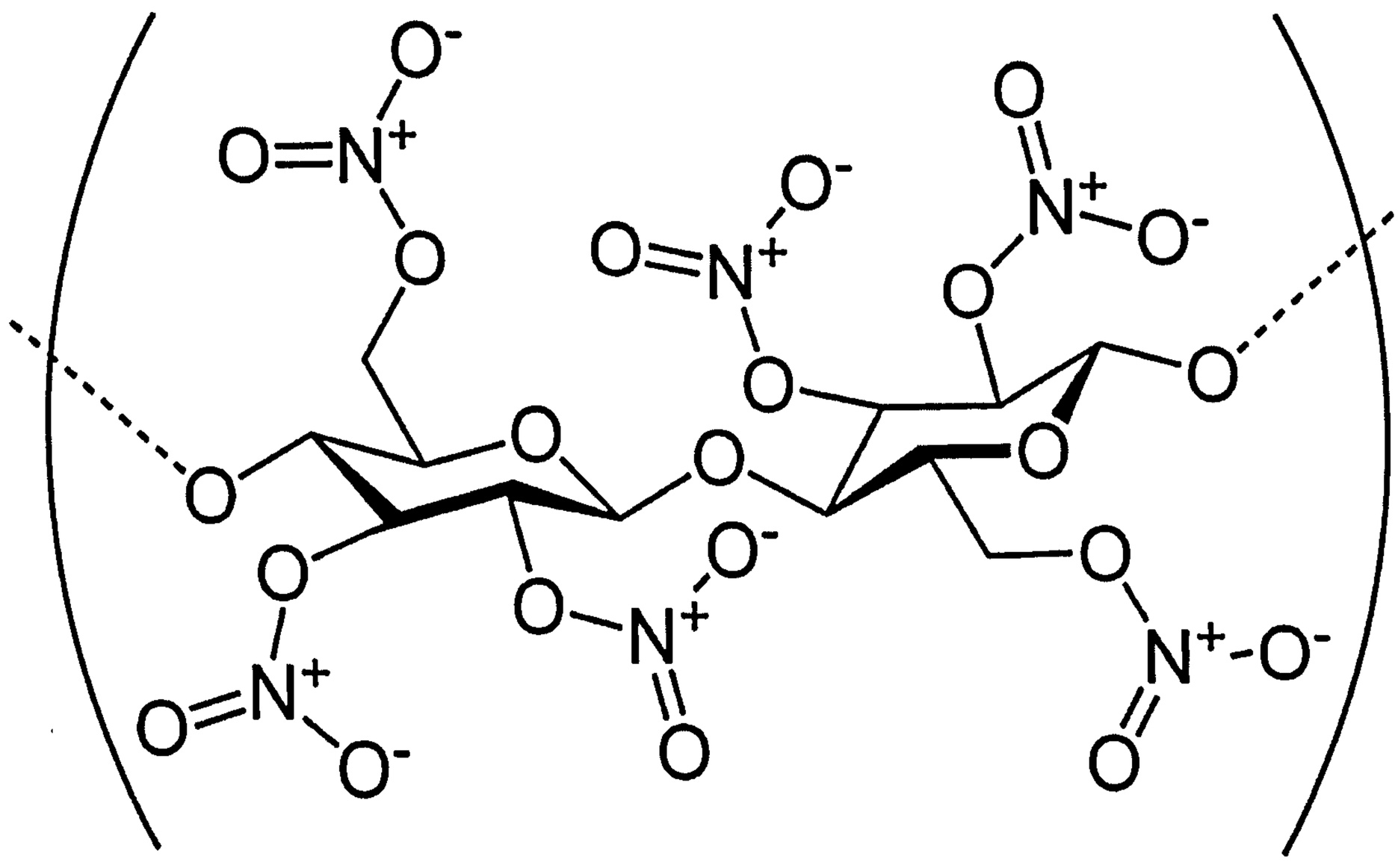

Figure 2.5 Schematic of the molecular structure of cellulose nitrate (source: http://en.wikipedia.org/wiki/Nitrocellulose)

The second method involves the replacement of the exchangeable hydrogen atoms with others of known isotopic composition and is called equilibration (Schimmelmann, 1991; Feng *et al.*, 1993; Filot *et al.*, 2006). Until recently, this method had to be carried out in a static off-line

procedure (Feng *et al.*, 1993). The disadvantages of this procedure are that it is very slow (>34 hours per sample), that a large sample size is required and that there is the potential for fractionation effects through the different stages of the method.

In 2006 a new online method for equilibration was published that allowed for a 100-fold reduction in the duration of the procedure, a > 50-fold reduction in sample sizes, reduced potential for fractionation and which avoided the use of hazardous chemicals used in nitration, whilst maintaining an uncertainty of only ± 4‰ (Filot *et al.*, 2006). The method, developed at the Institute for Climate and Environmental Physics in Berne, Switzerland, couples a novel on-line equilibration chamber with a pyrolysis reactor and continuous flow isotope ratio mass spectrometry (CF-IRMS) instrument (Figure 2.6). Prior to pyrolysis, cellulose samples are equilibrated with a continuous flow of water vapour at 110°C for 600 seconds in a helium carrier gas stream. The sample is delivered to an autosampler immediately after equilibration and enters the pyrolysis oven within a few seconds. The helium carrier gas prevents air and moisture entering the chamber so that the only source of hydrogen for equilibration is the supplied water vapour. Samples of alpha cellulose as small as 0.5-0.7 mg are processed every ten minutes. This radical reduction in processing time with reliable results is ideally suited to the analysis of palaeo-*Sphagnum* cellulose samples which are necessarily low in volume by virtue of the need to isolate a *Sphagnum*-specific component from the peat matrix. For further details on experimental procedure the reader is referred to Filot *et al.* (2006) and section 4.3.3.

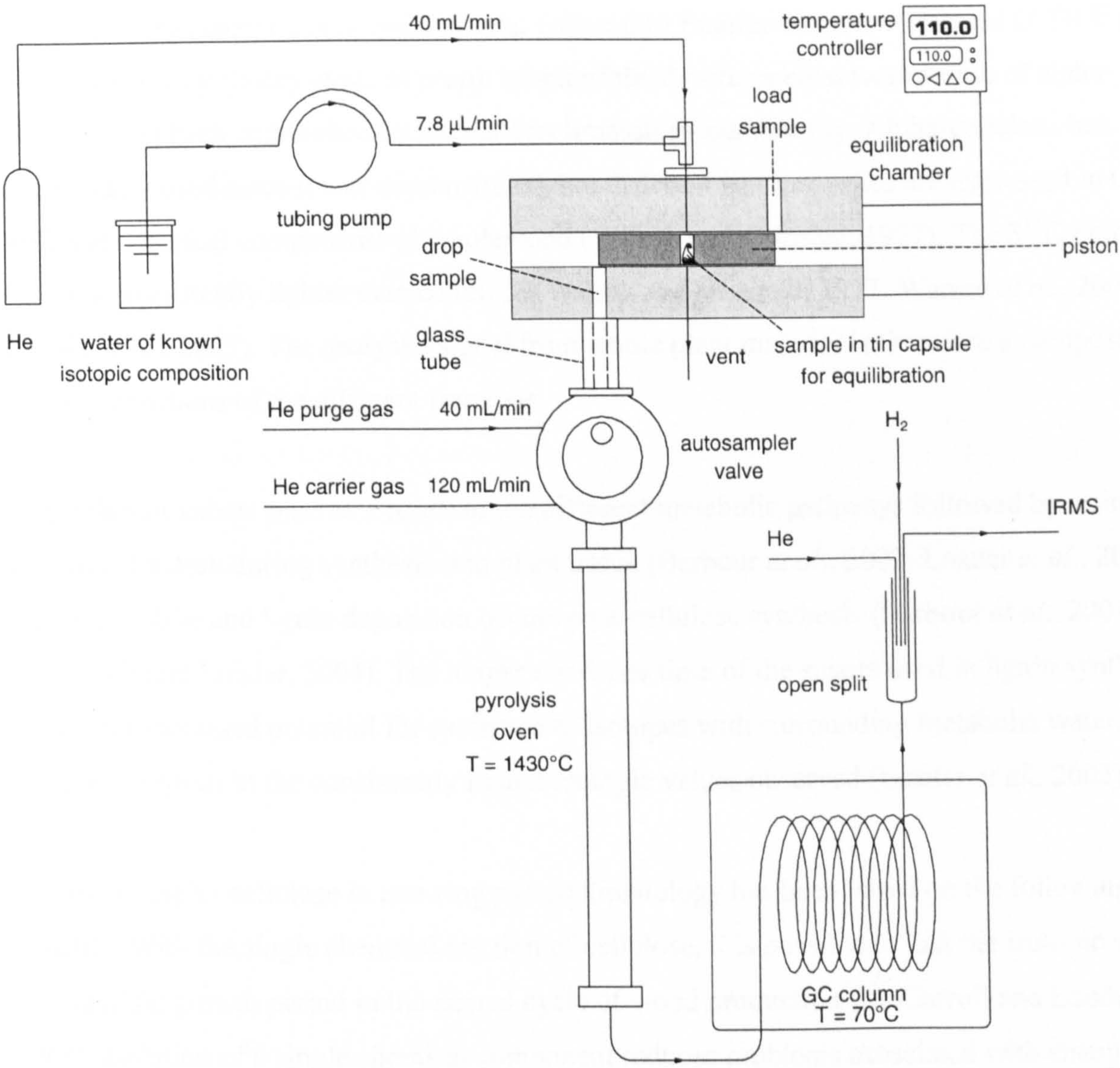

Figure 2.6 Schematic of the new equilibration chamber interfaced with an online pyrolysis IRMS system (Filot *et al.*, 2006).

2.4.3 The need for alpha-cellulose as a precise recorder

Bulk plant tissue is made up of a number of chemical components that differ in their proportions between species. Wholewood, for example, is composed of lignins, cellulose, hemicelluloses, lipids, tannins and resin (McCarroll and Loader, 2004; Rinne *et al.*, 2005). *Sphagnum* is a much simpler construction composed mainly of cellulose, hemicelluloses and galaturonic lipids (van Breemen, 1995). *Sphagnum* is thought not to contain any lignin (van Breemen, 1995), although spectra relating to bonds associated with the presence of this

chemical were observed in attenuated total reflectance Fourier transform infrared (ATR/FT-IR) spectroscopy (Daley et al., *in prep*). Much of the developmental work in use of alpha-cellulose has been undertaken by the dendroclimatology community. Alpha-cellulose has been widely used since it was demonstrated that different isotopic ratios are expressed in the different chemical components of wholewood (Wilson and Grinsted, 1977). The $\delta^{13}C$ ratio of lignin is consistently lighter than cellulose (Wilson and Grinsted, 1977; Warren *et al.*, 2001; Loader *et al.*, 2003). The analysed signal from whole plant material is therefore a composite of the proportions of the different fractions.

The different values arise as a result of the different metabolic pathways followed by a single chemical fraction during synthesis into plant tissue (Barbour *et al.*, 2002; Loader *et al.*, 2003). Resin is mobile and lignin deposition occurs post-cellulose synthesis (Barbour *et al.*, 2001; McCarroll and Loader, 2004). The longer residence time of the sugars used in lignin synthesis allows for increased potential for exchange of isotopes with surrounding metabolic water, believed to result in the consistently lighter isotopic values observed (Loader *et al.*, 2003).

The use of alpha-cellulose in tree-ring palaeoclimatology has been based on the following benefits. With the single chemical fraction of cellulose, it is possible to link the isotopic signal to a specific growth period in the annual cycle of wood production (McCarroll and Loader, 2004). Isolation of a single chemical component reduces problems associated with changes in the relative proportions of chemical constituents either over time or diagenetically (Suberkropp *et al.*, 1976; Spiker and Hatcher, 1987; Schleser *et al.*, 1999). Homogeneity of samples was also increased as a result of the extraction process, improving the estimate of the mean isotopic value for that sample (McCarroll and Loader, 2004; Borella *et al.*, 2004).

The isolation of alpha-cellulose is a laborious process, particularly in *Sphagnum* where the relative structural fragility of moss compared to wood can result in excessive breakdown under chemical treatment (Borella *et al.*, 2004). Furthermore, although isolation of a single chemical fraction removes variation due to changes in the proportion of the chemicals, the influence of that variation is thought to be small compared to other factors (McCarroll and Loader, 2004). Studies have sought to ascertain the importance of alpha-cellulose extraction for the objective of maximising climatic information. The conclusions of these studies have

been mixed. For $\delta^{13}C$ it has been observed that there is both 1) no statistically significant difference between the variability recorded in cellulose and wholewood (Borella *et al.*, 1998) and 2) that cellulose is more strongly correlated with climate than lignin but that the strongest correlation is in the combined wholewood (Loader *et al.*, 2003). For $\delta^{18}O$, conclusions are even more opposed, where it has been suggested that the climate signal is lost by using wholewood rather than cellulose (Borella *et al.*, 1999), whilst conversely there are other studies that report no loss of climate signal from wholewood (Barbour *et al.*, 2001).

The major benefit of the use of alpha-cellulose relates to issues of differential decay of the cellular components. Particularly with regard to palaeo-climatic application over the timescales of the Holocene, differential decay of cellular components could play a role in distorting the signal if whole plant samples are used as cellulose decays more quickly than lignin (Suberkropp and Klug, 1976; Spiker and Hatcher, 1987; Schleser *et al.*, 1999). Whilst this process will not alter the isotopic composition of the cellulose, the change in relative proportions will be reflected in the analysed ratio from whole plant material (McCarroll and Loader, 2004).

Advances in isotopic techniques since the 1980s have provided the opportunity to test the proposition of van Geel & Middledorp (1988) that peat bog isotope data may provide a palaeotemperature indicator if material from a single genus is used in the analysis. Progress in the development of on-line analytical techniques has radically reduced the sample amount required for isotope analysis and the time taken to generate detailed high-resolution records of climate over timescales of the Holocene. These techniques were not available during previous peat-based palaeoclimate investigations when large samples were required and consequently incorporated a mixture of species. The need for genus-specific investigation has been discussed and the potential for genus rather than species specific taxonomic resolution demonstrated. The use of alpha-cellulose for *Sphagnum* analysis eliminates uncertainty that variation in the isotopic signal is associated with the mixture of chemical components from which *Sphagnum* is constructed (van Breemen, 1995).

3 Site selection and description

3.1 *Site selection criteria*

3.1.1 Wide geographical area

As was described in Chapter 2, the research conducted for this thesis was undertaken as part of a nested project within the NERC RAPID thematic programme. That nested project is ISOMAP-UK. The overriding objective of ISOMAP-UK was to undertake data-model comparison as a means of validating model response to the postulated forcing mechanisms of Holocene climate change. This was to be achieved through advances in modelling and also through the compilation of a number of high quality records of the isotopic composition of palaeoprecipitation from a range of archives across northern Europe. One of the aims of this research then, was to provide these isotopic records from a selection of peat bog archives in the ISOMAP-UK research area.

3.1.2 Site characteristics: *Sphagnum* depth maximisation

A principal focus of the wider RAPID thematic programme is the role of the thermohaline circulation in climate change. For those projects with a palaeo-climatic component this inevitably meant a focus on the development of records spanning the early Holocene when evidence is strongest for a link between the thermohaline circulation and climate during the 8200 BP event. The 8200 BP event has assumed some prominence because the cause is believed to be related to meltwater release into the North Atlantic, the size and duration of which is relatively well constrained (section 2.1.1). The event therefore provides an excellent opportunity for model testing (Alley and Agustsdottir, 2005). With limitations over the computational time and resolution achievable in advanced numerical models such as the HADCM3, the modelling component of ISOMAP-UK was focussed on 8200 BP. Given the central role of palaeodata in validating model response in the ISOMAP project, it was necessary to select peatland archives that were most likely to provide either a long *Sphagnum*-

dominant record that might be able to provide a record extending back to this period or records that showed evidence of *Sphagnum* layers at considerable depth that were still considered to be within the ombrotrophic phase of bog development. The importance of *Sphagnum* as the principal substrate has been discussed in section 2.4.1.

Finding European sites with ombrotrophic *Sphagnum* at depth is difficult. Many of the bogs in NW Europe are characterised by a bipartite developmental structure of sedge and heather dominated peat in the early Holocene followed by a sudden switch to dominant *Sphagnum* peat during the mid- to late Holocene through to the present. Many of the dates of *Sphagnum* initiation in NW European records indicate that the *Sphagnum* phase coincides with known periods of climatic fluctuation suggesting a climatic driver for *Sphagnum* peat initiation and dominance. Whilst most peatland archives record climate changes from ~4600-4400 BP to present (Barber and Charman, 2003), only a few are sufficiently long as to record changes prior to these dates (Hughes *et al.*, 2000; Langdon *et al.*, 2003). Those records that are, display early Holocene assemblages dominated by sedges and heathers, lacking, in the most part, the critical *Sphagnum* deposits for isotopic analysis.

Three peat bog archives were chosen from NW Europe that satisfied these selection criteria. They form a broad NW European spread from oceanic to continental settings. All are known to be deep or from previous research have been shown to contain *Sphagnum* peat at depth that was considered to be independent of *Sphagnum* associated with the fen-bog transition. These were Raheenmore in the Irish midlands, Walton Moss in northern England and Dosenmoor in northern Germany (Figure 3.1). As an extension to the original project, an additional site was included from the western side of the Atlantic (Figure 3.2) following the discovery of a strong climatic anomaly at 8200 BP in a peat core from Nordans Pond Bog on the eastern coast of Newfoundland (Hughes *et al.*, 2006).

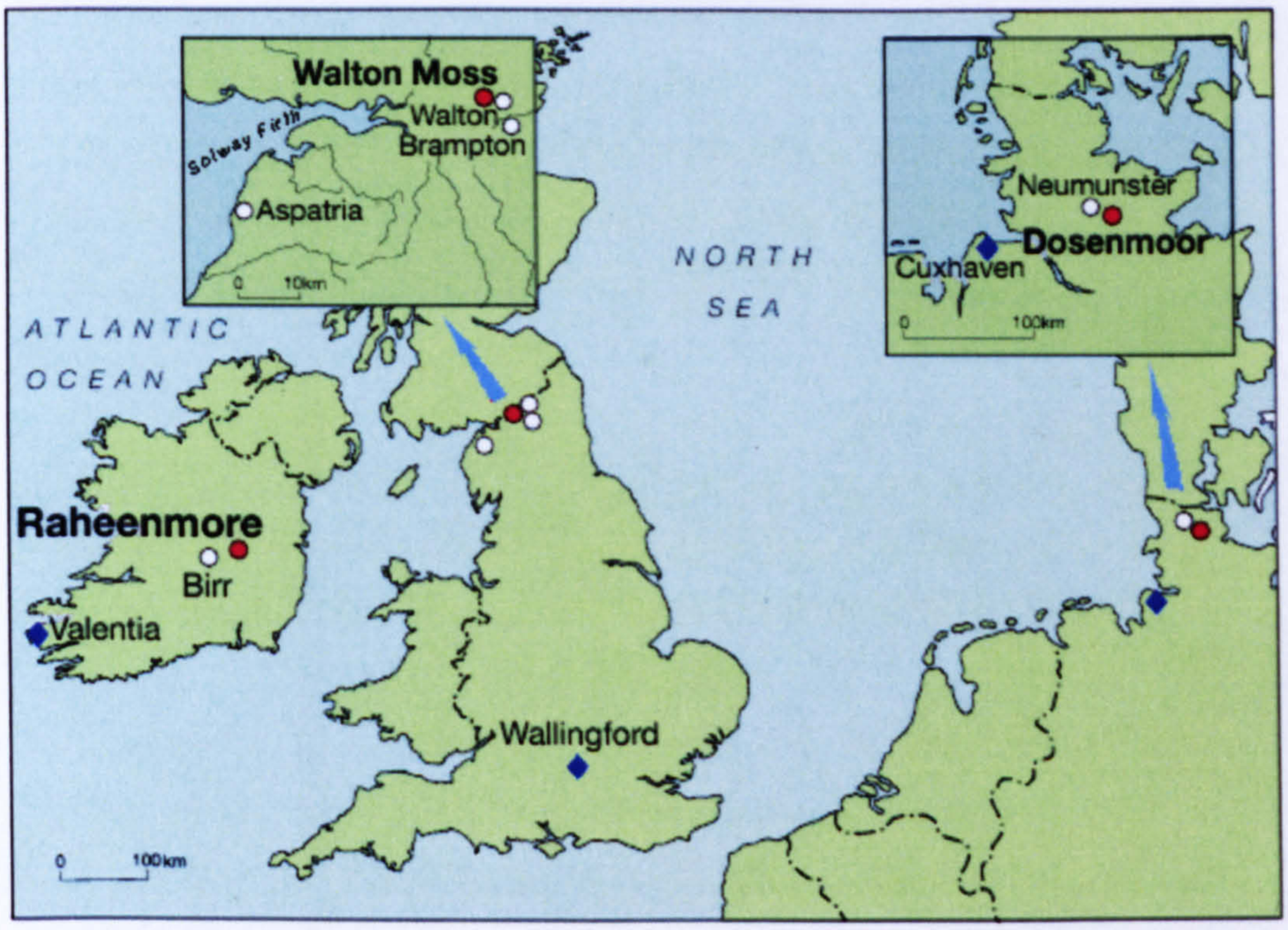

Figure 3.1 Location of study sites (red dots) in relation to meteorological (open dots) and Global Network for Isotopes in Precipitation (GNIP) stations (blue diamonds) for NW Europe

Figure 3.2 Location of Nordans Pond Bog (red dot) in relation to meteorological station at Musgrave Harbour (open circle) and GNIP stations at Goose Bay, Labrador and Truro, Nova Scotia (blue diamonds)

The following sections describe the geographical context of each site, its surface ecology, the modern climatology and isotope climatology of the area, previous research on the site and the results of stratigraphical surveys that were used to identify sub-surface variability and the optimum location for coring.

3.2 *Walton Moss, northern England*

Walton Moss is a large intact lowland raised bog located at 54.993°N, 2.764°W in Cumbria in northern England (altitude 100m AOD; Figure 3.3). The peat complex covers a surface area of 150 ha and comprises more than 10 m of peat in its deepest part (Barber *et al.*, 1998). The vegetation surface is classified as NVC M18 (*sensu* Rodwell, 1991) and represents a comparatively unique site among English lowland raised bogs (Barber *et al.*, 1994; Hughes *et al.*, 2000) owing to its relatively undamaged condition.

The surface is composed of a variety of vascular and non-vascular plant species. *S. magellanicum* and *S. papillosum* are dominant in lawn locations. *S. cuspidatum*, *S. tenellum* and *S. pulcrum* are found extensively in the wetter hollow areas and frequently associated with *Rhynchospora alba* and *Eriophorum angustifolium*. *S. capillifolium var. rubellum* is the dominant hummock forming species, typically associated with relatively restricted abundances of the Ericaceous species, *Erica tetralix, Calluna vulgaris, Andromeda polifolia,* and *Vaccinium oxycoccus* and with the grass species *Eriophorum vaginatum* and *Tricophorum cespitosum*. *Eriophorum vaginatum* dominates the microtopographical zone between lawn and hummock. The carnivorous plant *Drosera rotundifolia* is found frequently across the surface in nearly all microtopographical zones. Occasional scattered *Betula* trees are present.

It is interesting to note that previous descriptions of the site have alluded to wetter surface conditions than has been observed in the period 2003-2006 (Hughes *et al.*, 2000; Barber *et al.*, 2003) and a shift in dominance from *S. cuspidatum* to *S. magellanicum* and *S. papillosum* may reflect drying of the bog surface in the last decade.

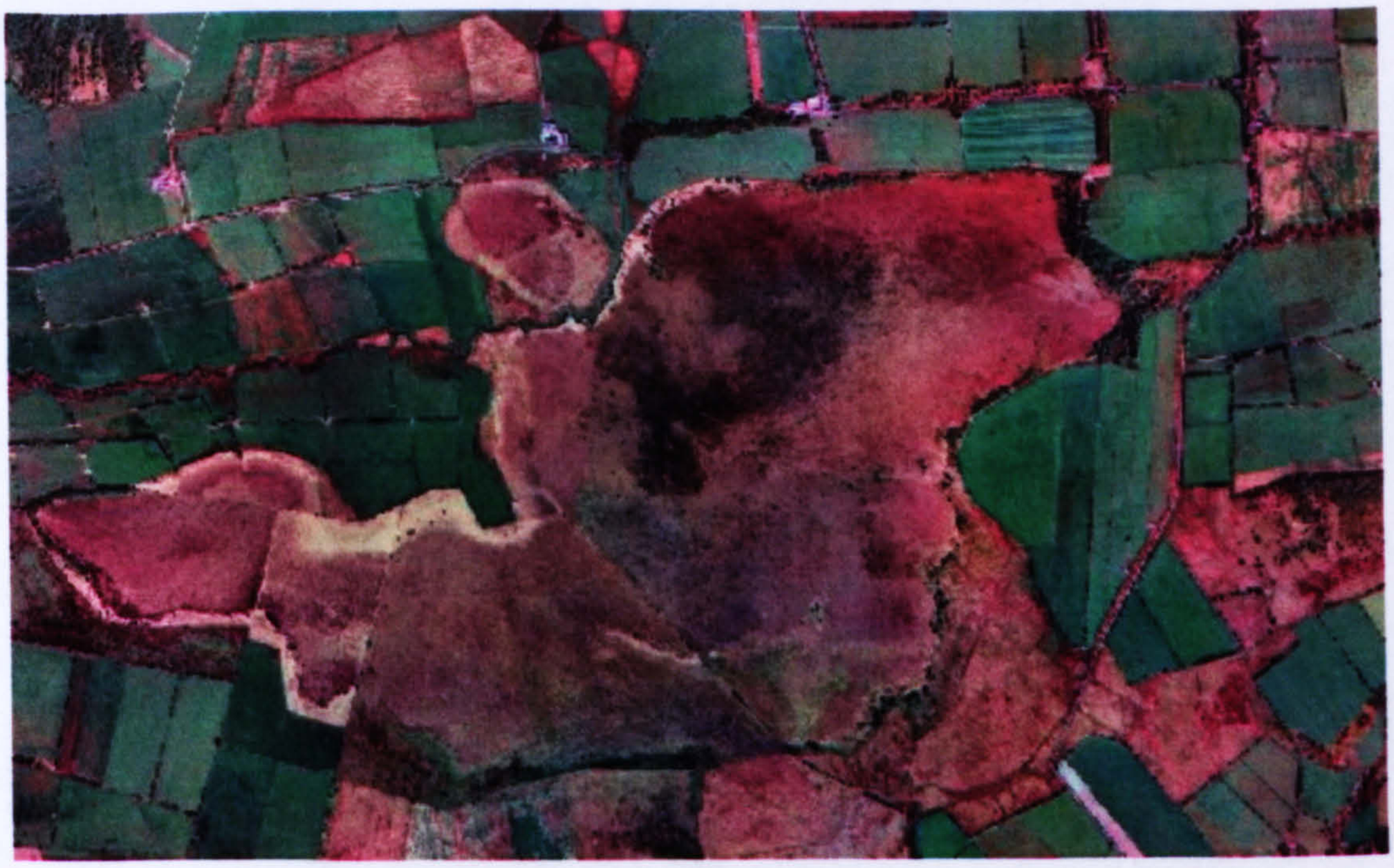

Figure 3.3 Aerial photo of Walton Moss (Getmapping.com, 2007)

Walton Moss falls within the maritime climatic regime of the western British Isles, dominated by the prevailing Northern Hemisphere mid-latitude westerlies, with their associated polar front jet stream. Precipitation is experienced in every month on average although most is associated with Atlantic depressions during the autumn and winter months (October average, 112.7 mm; Figure 3.4). Consequently the prevailing moisture source is water evaporated from the Atlantic Ocean. Temperatures at Aspatria (54.761°N, 3.329°W; altitude 62m AOD; 45km WSW of Walton Moss, Figure 3.4), vary seasonally with an average January minimum of 0.8°C and maximum of 6.1 °C and a July minimum of 10.8 °C and maximum of 18.7 °C.

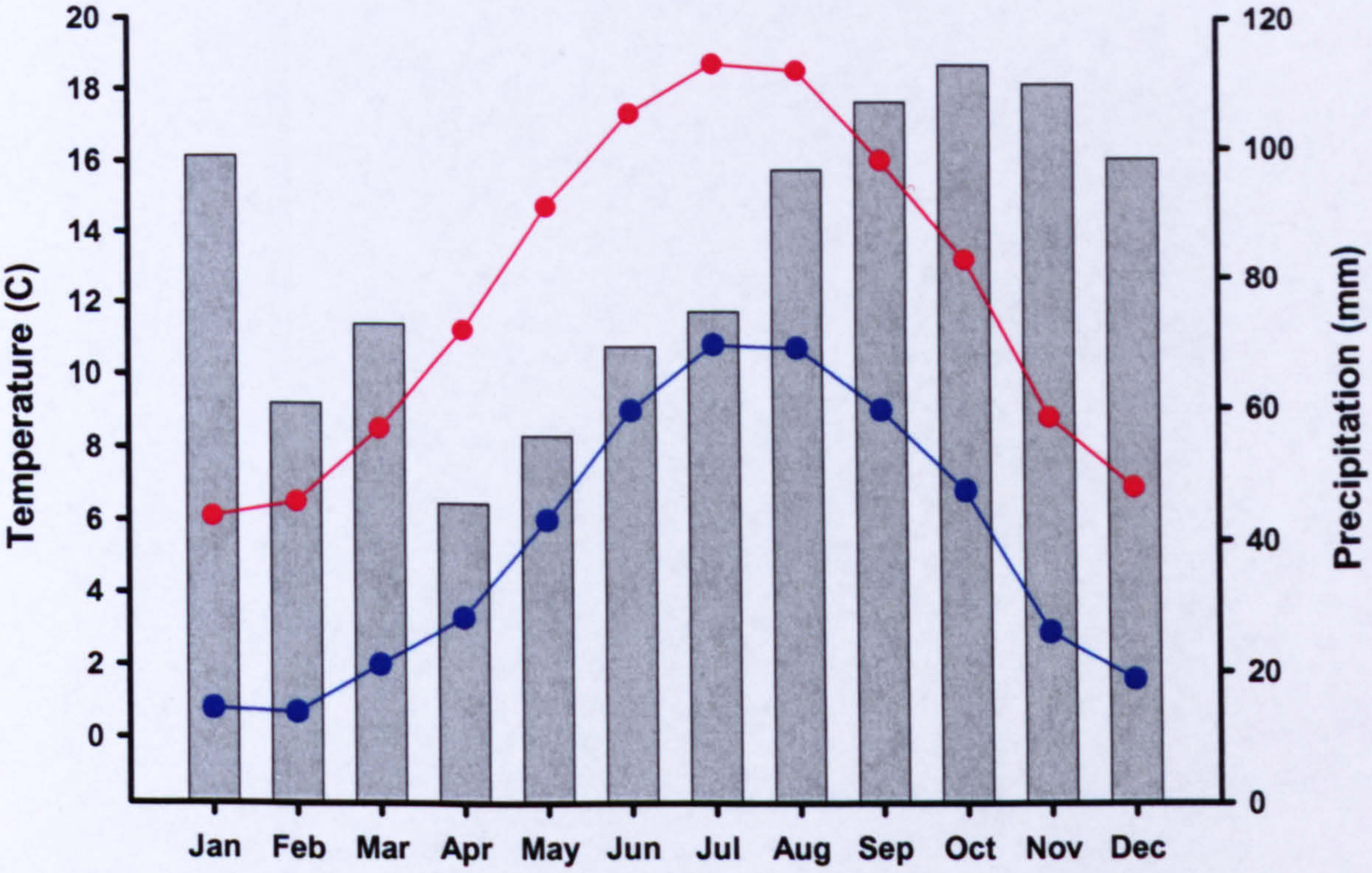

Figure 3.4. Monthly mean maximum and minimum temperature (red and blue dots) and precipitation (grey bars) (1961-1990) for Aspatria, northern England (54.761°N, 3.329°W; 62 m altitude)

Intra-regional variability in precipitation is evident from Figure 3.5 (locations of stations: Figure 3.1). The 1971-2000 average precipitation amount for Walton (54.973°N, 2.742°W; Figure 3.5) is notably less than Aspatria in the winter months when most bog recharge takes place and shows slight differences from the Brampton record (54.946°N, 2.742°W) located 3 km south. Brampton is the site at which data were collected on the isotopic composition of precipitation (2003-2005) for ISOMAP-UK. These are analysed later in this study.

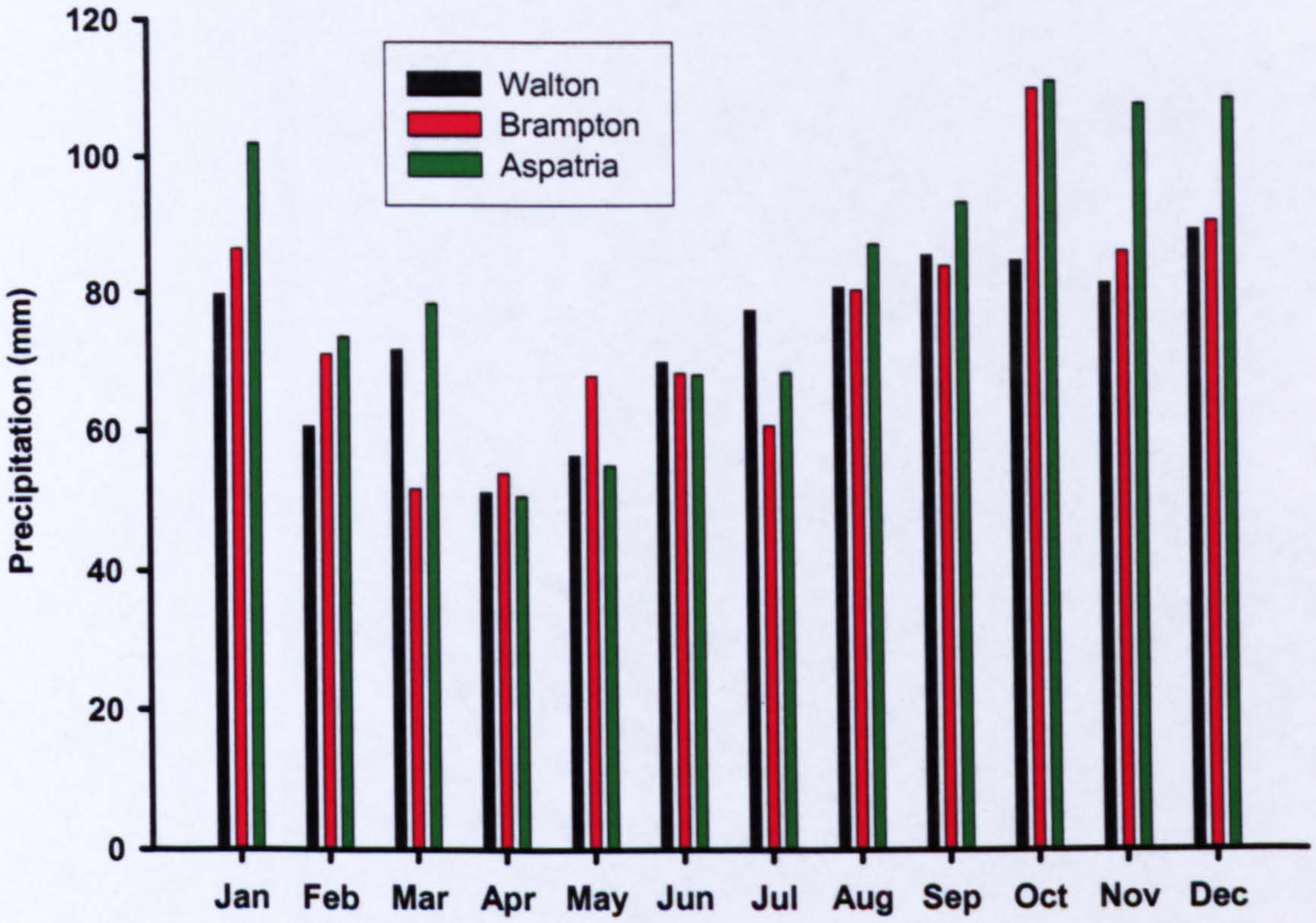

Figure 3.5 Comparison of mean monthly precipitation totals for Aspatria (1971-2000), Walton (1971-2000) and Brampton (1999-2007).

As discussed in Chapter 2, global meteoric waters have a fairly constant relationship between the proportion of hydrogen and oxygen isotopes in their molecules. The relationship is known as the global meteoric water line (GMWL) and takes the form $\delta D = 8 \times \delta^{18}O + 10$ (Craig, 1961a). This relationship is subject to regional variation, which can provide climatological clues for characterising an area.

The longest record from England is the Wallingford series (51.600°N, 1.100°W; altitude 48m AOD; Figure 3.6 & Figure 3.7). This record exhibits a lower slope (7) than that of the GMWL and an intercept of 1.2 (Darling and Talbot, 2003)(Figure 3.6). Comparison with slopes for Valentia, Ireland (6.8; shown later this section) and Groningen, Austria (7.2) (Darling and Talbot, 2003) suggest that the data from Wallingford is consistent with other sites in NW Europe (Darling and Talbot, 2003; Diefendorf and Patterson, 2005).

The relationship between the isotopic composition of precipitation and meteorological variables over both short (annual) and longer-term (1982-2001) timescales from Wallingford has previously been reviewed in detail (Darling and Talbot, 2003), and updated here to 2002 (Figure 3.7). The slope angle of 7 varies seasonally, from 7.4 ± 0.3 (Sep-Feb) to 6.9 ± 0.3 (Mar-Aug) (Darling and Talbot, 2003) which has been attributed to increased opportunity for secondary evaporation of falling raindrops and the dominance of convective precipitation during the summer and a dominance of frontal rainfall sourced by Atlantic depressions during the winter.

Figure 3.7 and Figure 3.8 show the relationship between the oxygen isotopic content of precipitation ($\delta^{18}O_{precipitaiton}$) at Wallingford with surface air temperature and precipitation amount respectively using monthly data for the period 1981-2002. A positive correlation exists with temperature (Figure 3.7, $r^2 = 0.28$, $p<0.001$) and a negative correlation exists with precipitation amount (Figure 3.8, $r^2 = 0.23$, $p<0.001$). It is evident that at monthly resolution the strength of the correlations between temperature and precipitation amount and $\delta^{18}O$ values are very similar.

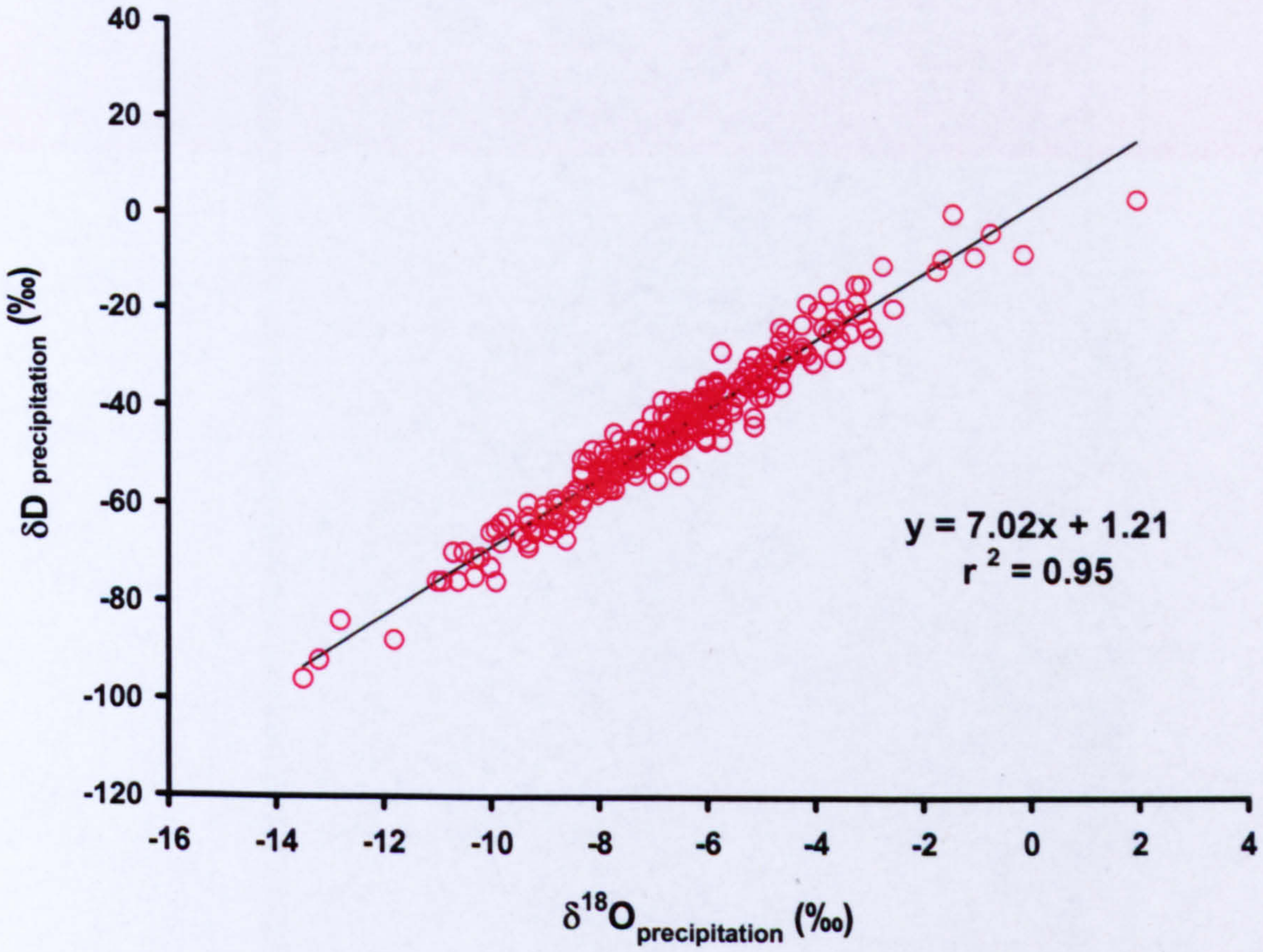

Figure 3.6 Bi-plot of mean monthly δD and δ^{18}O values in precipitation for Wallingford (1981-2002) (IAEA/WMO, 2004)

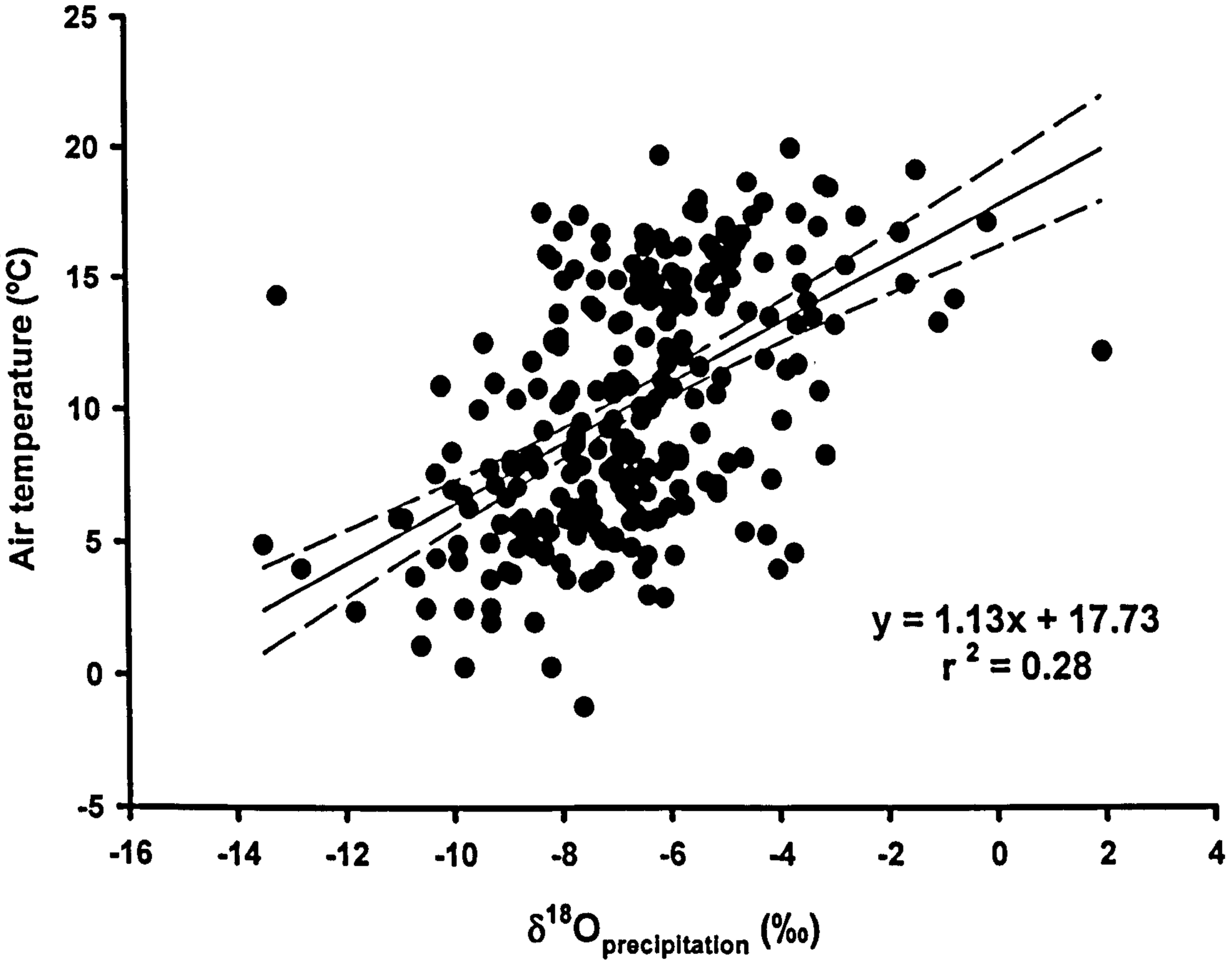

Figure 3.7 Relationship between mean monthly $\delta^{18}O$ values in precipitation and surface air temperature for Wallingford (1981-2002) (IAEA/WMO, 2004) (linear regression in solid line, 95% confidence limits in dashed lines)

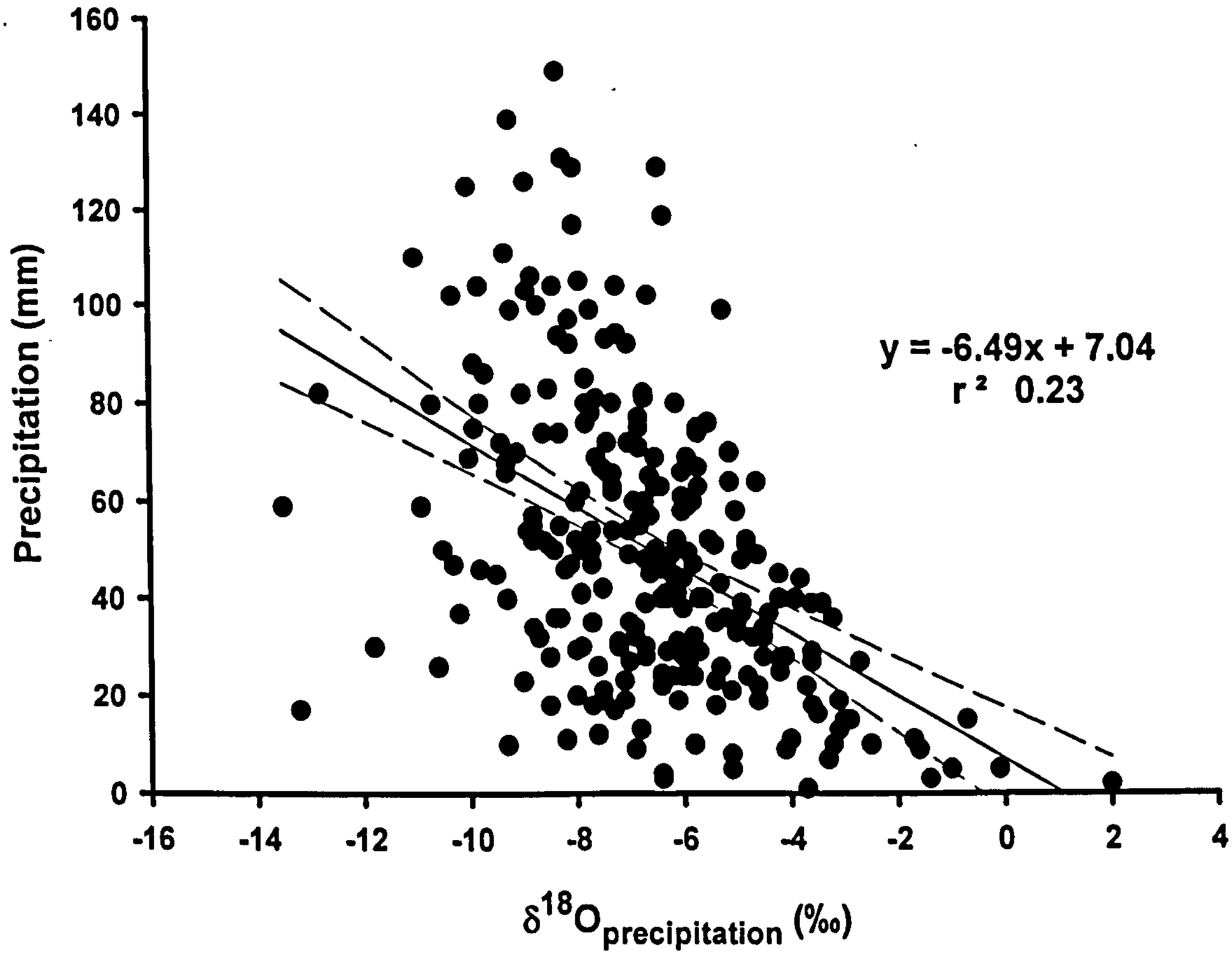

Figure 3.8 Relationship between mean monthly $\delta^{18}O$ values in precipitation and precipitation amount for Wallingford (1981-2002) (IAEA/WMO, 2004) (linear regression in solid line, 95% confidence limits in dashed lines)

Despite the noise in the record, seasonal variation is readily observed (Figure 3.9). Whilst there is significant overlap between the individual monthly means for spring and autumn (Figure 3.9), differences are observed in the clustering of summer and winter isotopic values. Lightest values are observed in the winter and heaviest values in the summer (Table 3.1). Mean values for each month over the period 1981-2002 are presented in Figure 3.10 & Figure 3.11 for the relationship between surface air temperature and precipitation amount respectively. Indication of a seasonal distribution is supported by a strong positive correlation between longer-term monthly mean surface air temperature and $\delta^{18}O$ values (Figure 3.10, $r^2 = 0.85$, $p<0.001$). The regression of $\delta^{18}O$ values against surface air temperature yields the relationship:

Equation 6) $\Delta T = 3.64(\Delta\delta^{18}O)$

The reciprocal of this relationship yields an isotope-temperature coefficient of 0.27 ‰°C^{-1}. This is roughly half the coefficient observed previously in central Europe (0.6 ‰°C^{-1}) (Rozanski *et al.*, 1992) and more globally (Dansgaard, 1964; Gat, 1980; Rozanski *et al.*, 1993).

It is possible this relatively low coefficient results from the influence of amount effects in precipitation. Data in Figure 3.11 indicate that a statistically significant relationship between summer precipitation amount and $\delta^{18}O$ values exists which must inevitably act to distort the relationship with temperature (Figure 3.11, $r^2 = 0.82$, $p<0.05$). This relationship with summer precipitation can be understood as a proxy for rainfall intensity during convective rainfall events (Darling and Talbot, 2003).

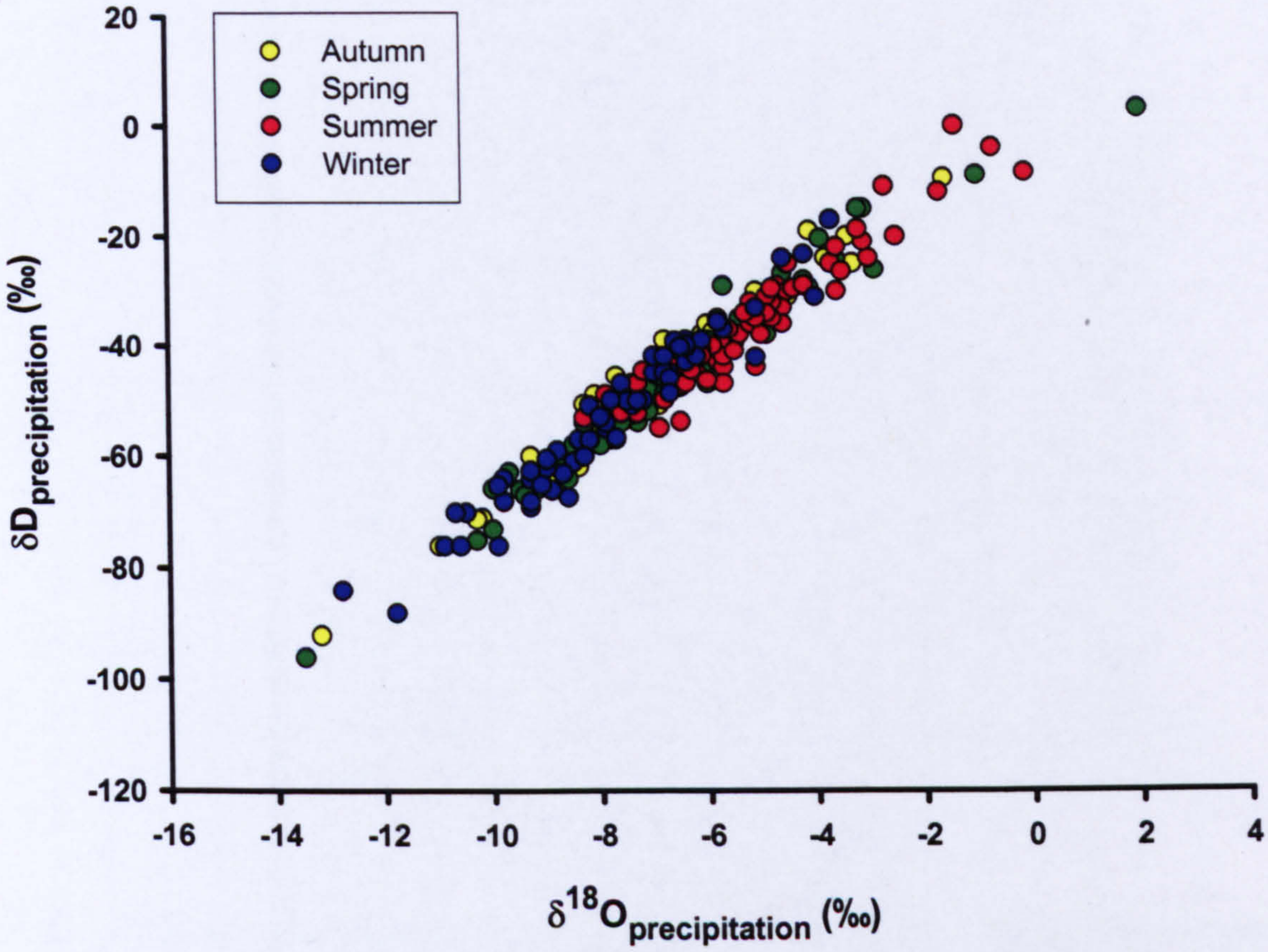

Figure 3.9 Bi-plot of mean monthly isotopic values in precipitation by season for Wallingford (1981-2002) (IAEA/WMO, 2004)

Table 3.1 Seasonal means of monthly mean isotopic data for Wallingford (1981-2002) (IAEA/WMO, 2004)

		Autumn	Winter	Spring	Summer
Wallingford	$\delta^{18}O$	-7.1	-7.9	-6.7	-5.1
	σ	1.9	1.9	2.3	1.7
	δD	-47.2	-53.5	-46.5	-35.8
	σ	14.5	14.5	16.6	12.6

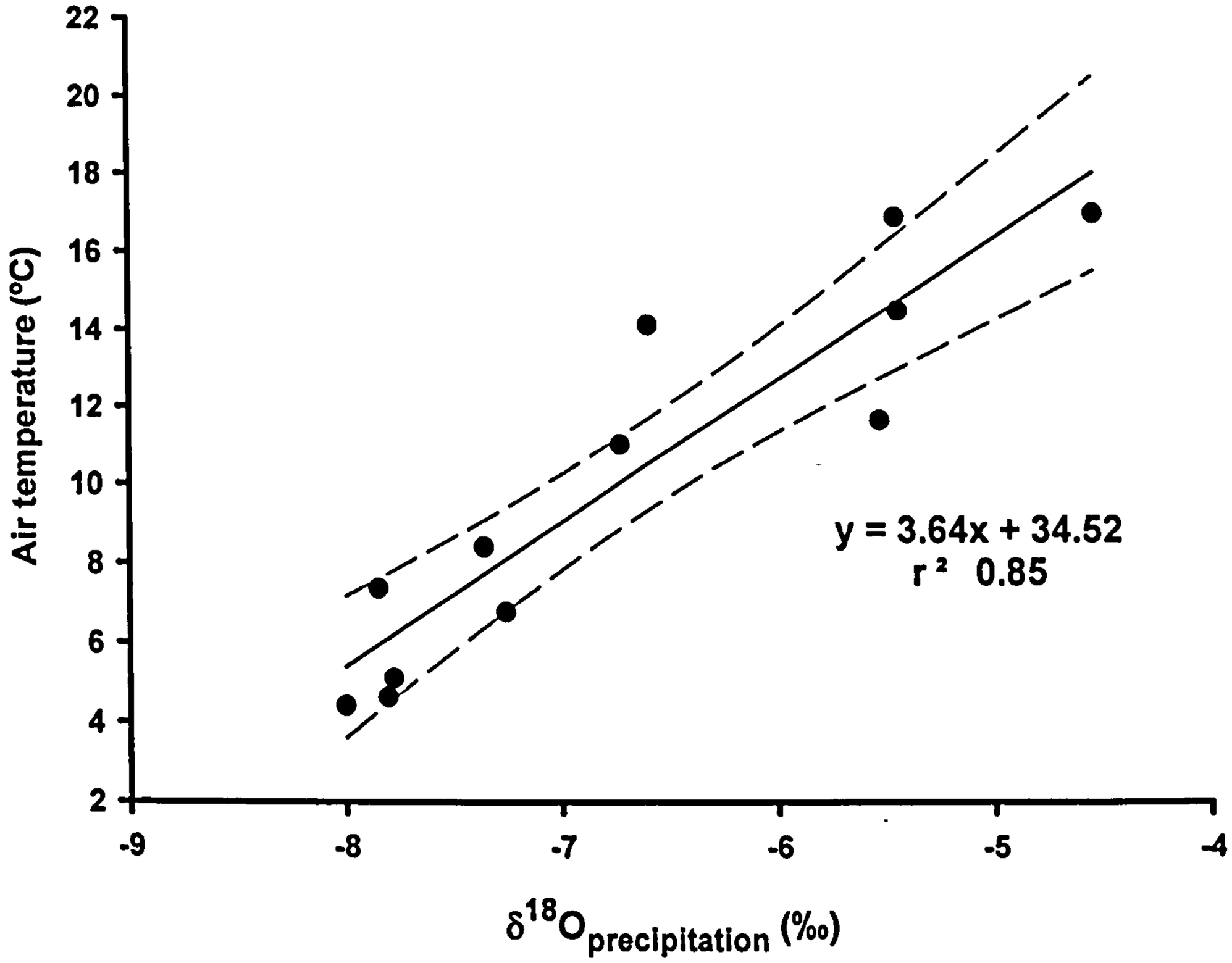

Figure 3.10 Relationship between long-term monthly means of $\delta^{18}O_{precipitaiton}$ and surface air temperature for Wallingford (1981-2002) (linear regression in solid line, 95% confidence limits in dashed lines)

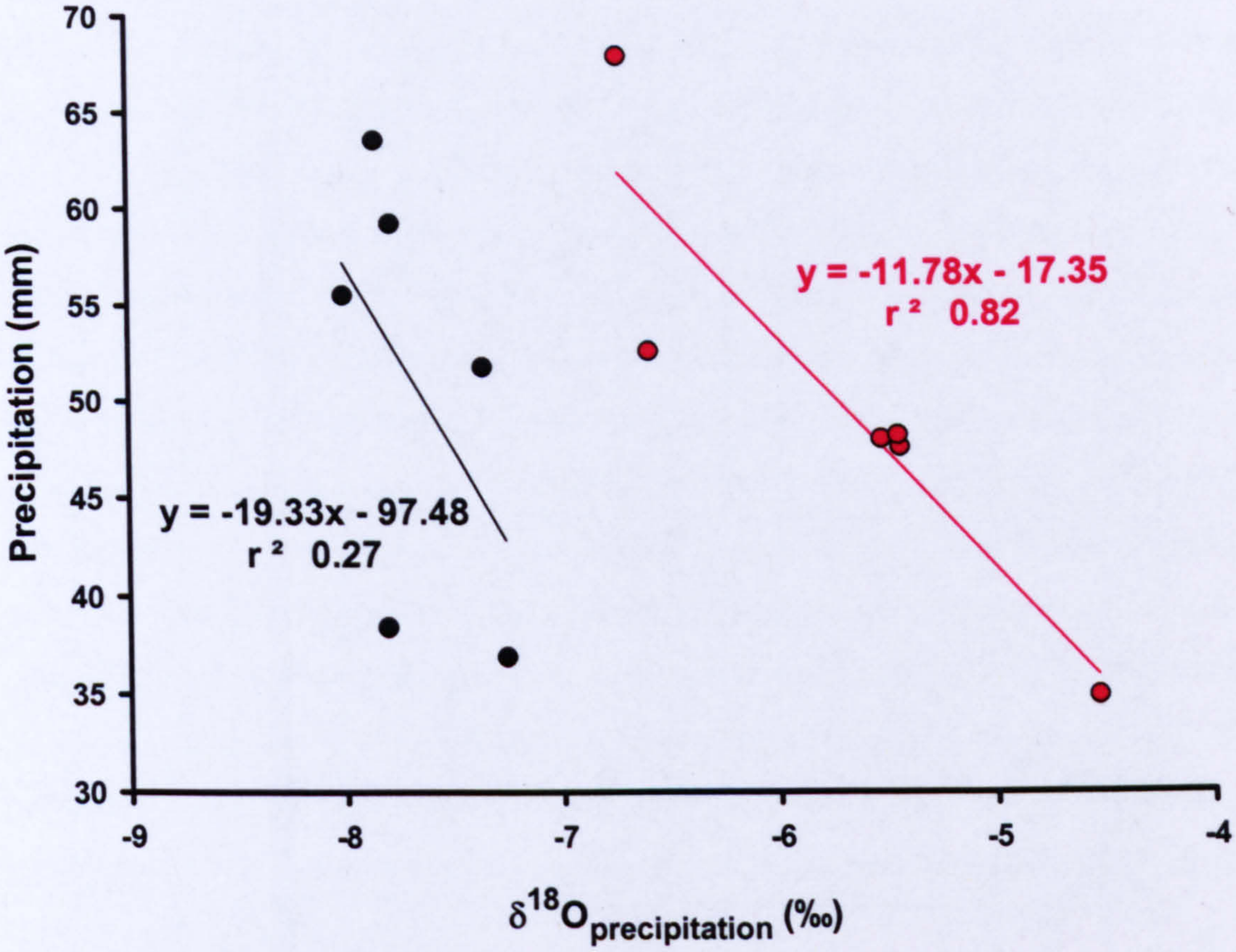

Figure 3.11 Relationship between long-term monthly means of $\delta^{18}O_{precipitaiton}$ and precipitation amount for Wallingford (1981-2002) by season (summer = red dots; winter = black dots)

Previous palaeoclimatic research at Walton Moss has been extensive providing an excellent knowledge of site stratigraphy (Barber *et al*., 1994; Barber *et al*., 1998; Mauquoy and Barber, 1999a; Hughes *et al*., 2000; Mauquoy and Barber, 2002; Barber *et al*., 2003), a long (~9,600 yr) record of climate change (Hughes *et al*., 2000) and demonstration of both within site (Barber *et al*., 1998) and regional scale replicability (Barber *et al*., 2000; Langdon and Barber, 2004). To that end, Walton Moss provided an excellent site for the purposes of answering the research questions that guide this thesis. With detailed stratigraphical work already published, it was possible to identify the optimal location for coring without the need for collection of an additional set of stratigraphical data. Optimal location criteria are described in section 4.2.

3.3 *Dosenmoor, northern Germany*

Dosenmoor is situated centrally in the Bundesländer of Schleswig-Holstein in northern Germany at 54.138ºN, 10.025ºE (Altitude 30m AOD; Figure 3.1). It is a large raised bog approximately 200 ha in area that supports a surface vegetation structure, in undamaged areas, of the NVC M18 classification (*sensu* Rodwell, 1991). These undamaged areas are, however, relatively rare on the bog surface (Plate 3.1). Disturbance associated with downwasting of surface peat with lowering of water levels by drainage and subsequent rising of water tables by the installation of hundreds of dams in drainage ditches has lead to a surface flora dominated by *Tricophorum cespitosum* and the nutrient enriched *Sphagnum* species, *S. fallax, S. subnitens* and *S. fimbriatum*. In special reserve areas (Plate 3.2) *Sphagnum* species common to more intact ombrotrophic bog surfaces still survive. *Betula* trees are common across much of the bog surface, particularly in those areas where cutting had previously been extensive close to the margins. Although the site has been subject to cutting and associated drainage, the peat stratigraphy has been shown to display variation that compares well with changes recorded at other sites on a regional scale and which has been interpreted as a climatic proxy (Barber *et al.*, 2004).

Plate 3.1 Aerial photo of Dosenmoor from the south indicating substantial surface disturbance through peat cutting and drainage (photo: K. Müller)

Plate 3.2 Bog pool development and survival of typical ombrotophic species in restored areas at Dosenmoor (photo: T. Daley)

Dosenmoor is subject to a relatively continental climate in comparison to the other sites in this study (Figure 3.12) with a greater seasonal range in mean monthly temperatures but precipitation amounts and seasonality similar to northern England (Figure 3.4). Despite its more continental location, the site lies at a similar latitude to that of Walton Moss and is consequently influenced by mid-latitude westerlies, Atlantic depressions and the sources of vapour associated with those atmospheric systems. Annual variation in mean monthly temperatures is > 16ºC.

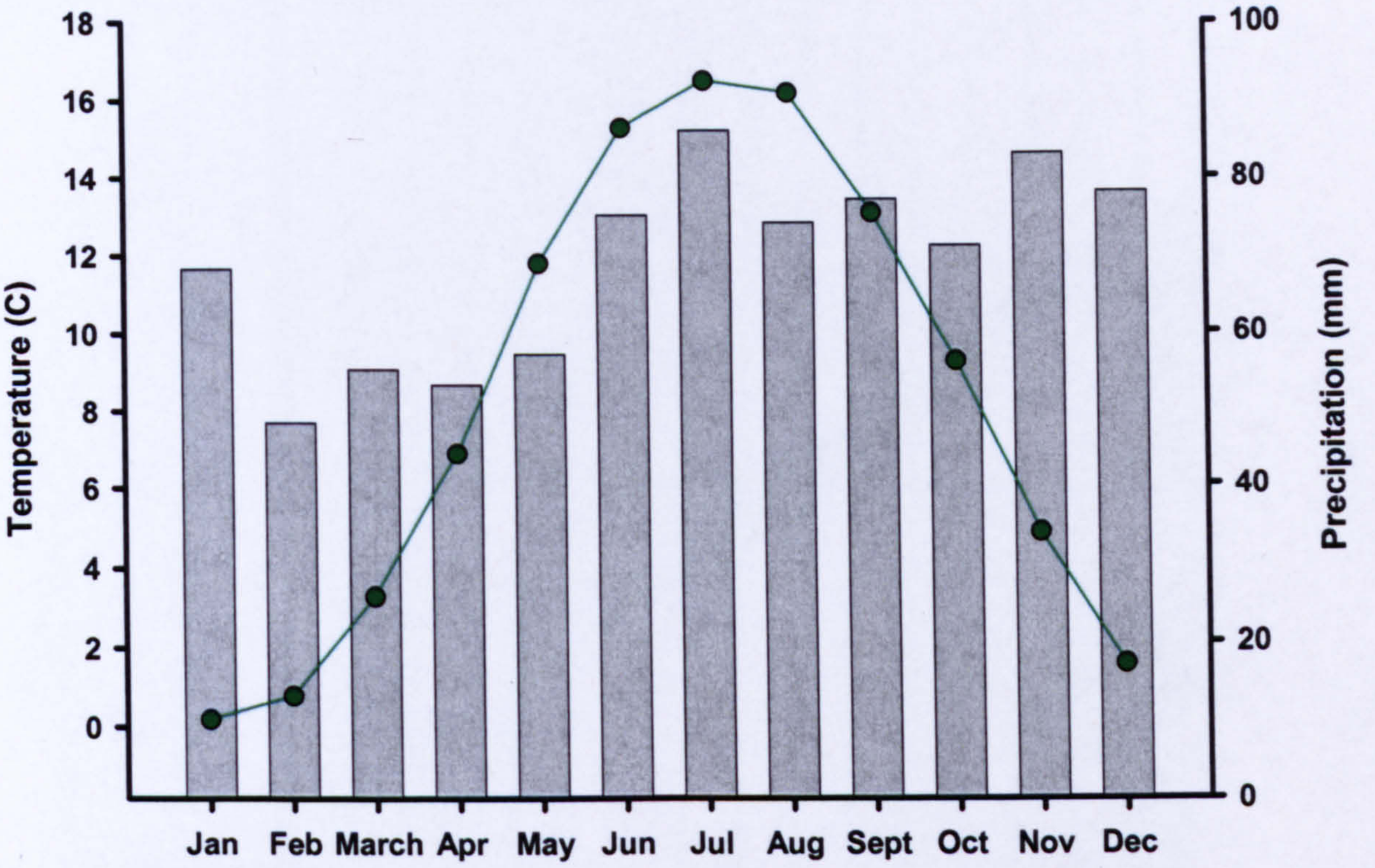

Figure 3.12 Mean monthly temperature (dots) and precipitation (grey bars) (1961-1990) for Neumunster, Schleswig-Holstein, Germany (54.067N, 9.983E; 13 km south of Dosenmoor)

The isotope record most local to Dosenmoor is that of Cuxhaven GNIP station (1978-2001) on the northwest coast of Germany (53.868°N, 8.718°E; altitude 12m AOD; Figure 3.13). Compared to the record from Wallingford, the data for this location suggest a slightly higher deuterium excess and a slope more similar to the GMWL. This can be indicative of a less humid vapour source on average or the evaporation of falling raindrops through air of low relative humidity.

The relationship between monthly oxygen isotopic content of precipitation ($\delta^{18}O_{precipitation}$) at Cuxhaven and surface air temperature (1984-2001; Figure 3.14) indicates that a positive correlation exists with temperature ($r^2 = 0.13$, $p<0.001$) that although weak, is statistically significant. No linear correlation exists with precipitation amount in monthly resolution data (Figure 3.15). It is highly likely that this noise level, in part, reflects synoptic-scale variability. This can be demonstrated by reference to seasonal means extracted from the monthly data (Figure 3.16, Table 3.2). Although the individual monthly data show a high degree of overlap

(Figure 3.16), of the seasonal means, lightest isotopic values are observed in the winter and heaviest values in the summer (Table 3.2).

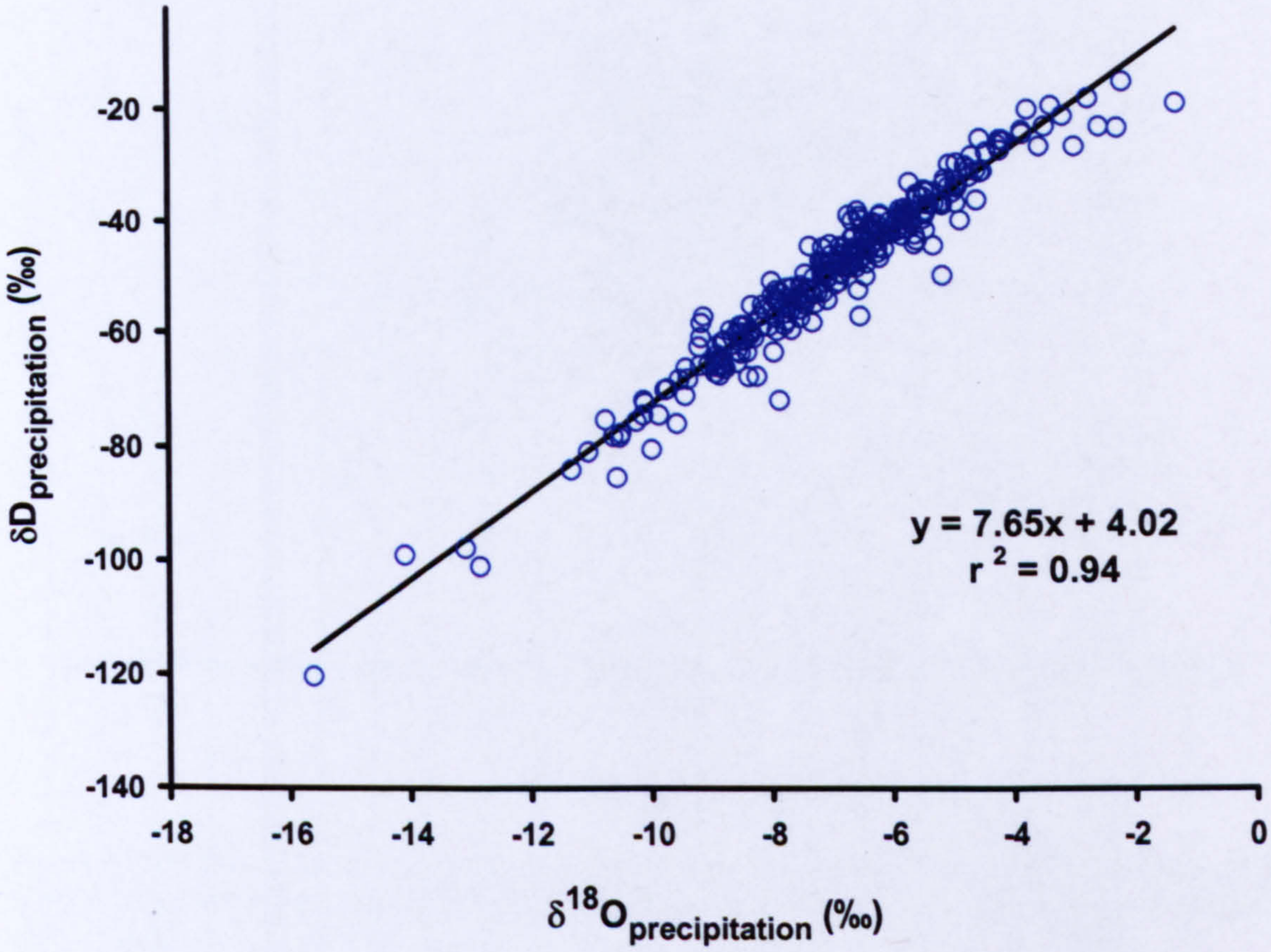

Figure 3.13 Bi-plot of mean monthly δD and δ^{18}O values in precipitation for Cuxhaven (1978-2001) (IAEA/WMO, 2004)

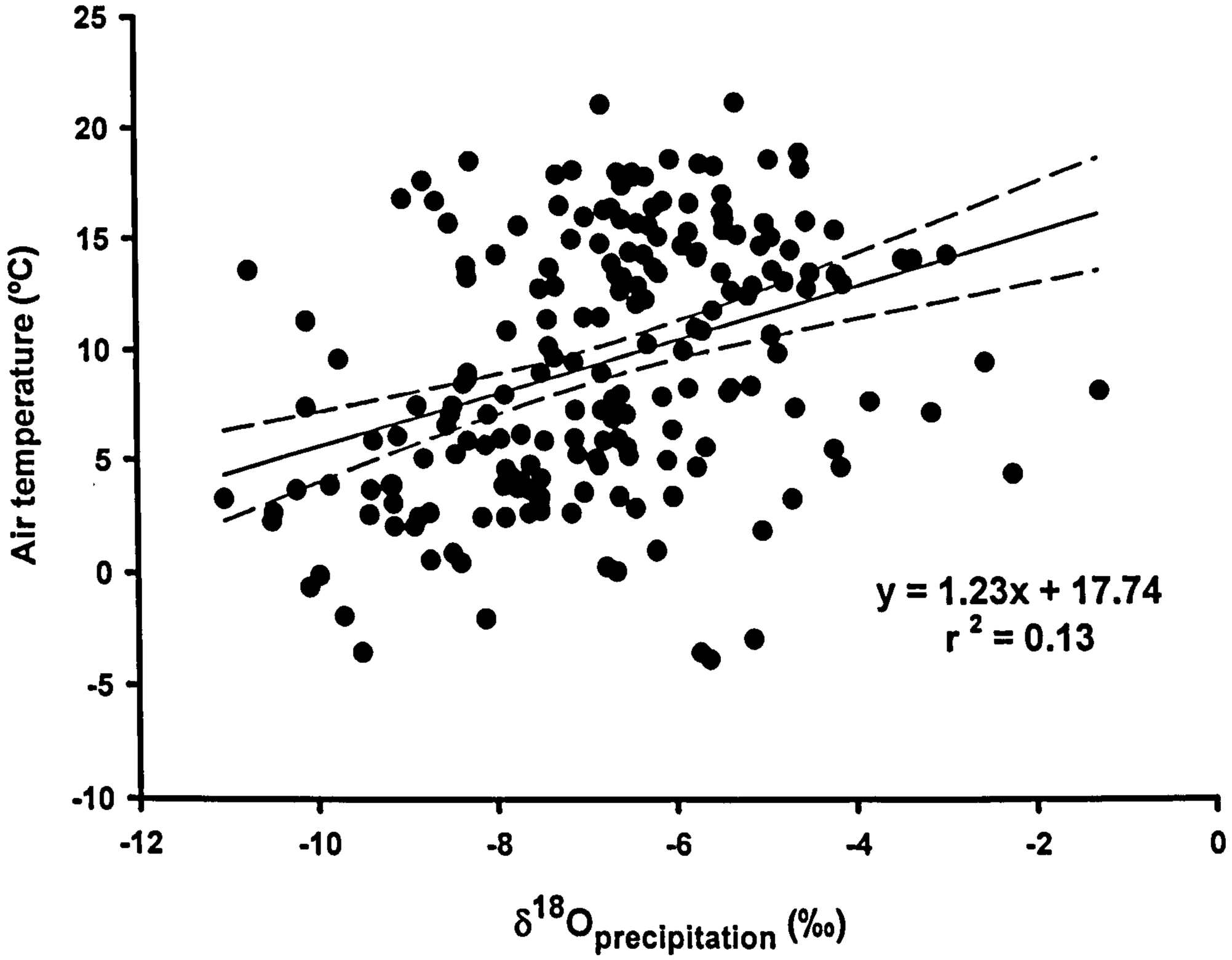

Figure 3.14 Relationship between mean monthly $\delta^{18}O$ values in precipitation and surface air temperature for Cuxhaven (1984-2001) (IAEA/WMO, 2004) (linear regression in solid line, 95% confidence limits in dashed lines)

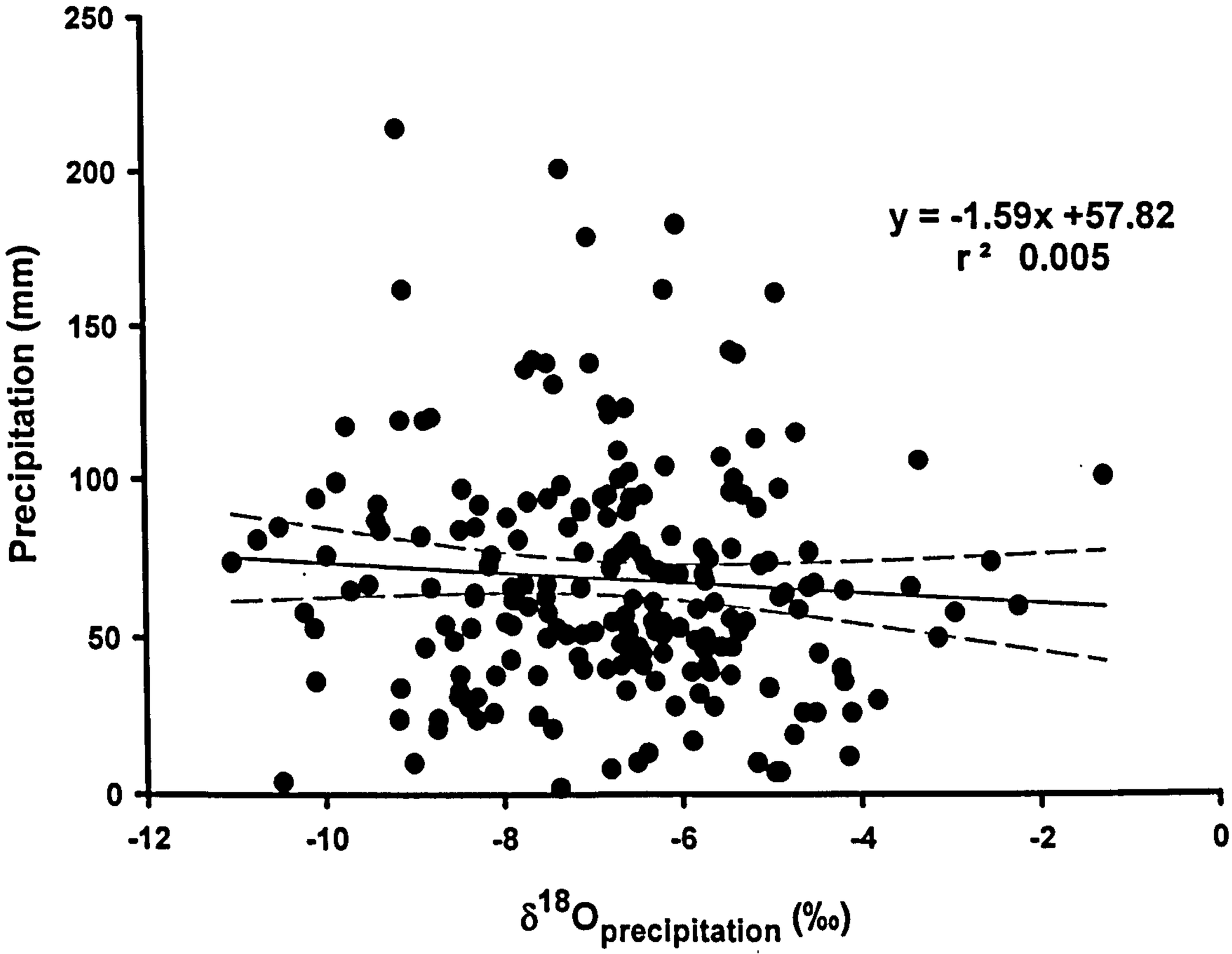

Figure 3.15 Relationship between mean monthly $\delta^{18}O$ values in precipitation and precipitation amount for Cuxhaven (1984-2001) (IAEA/WMO, 2004) (linear regression in solid line, 95% confidence limits in dashed lines)

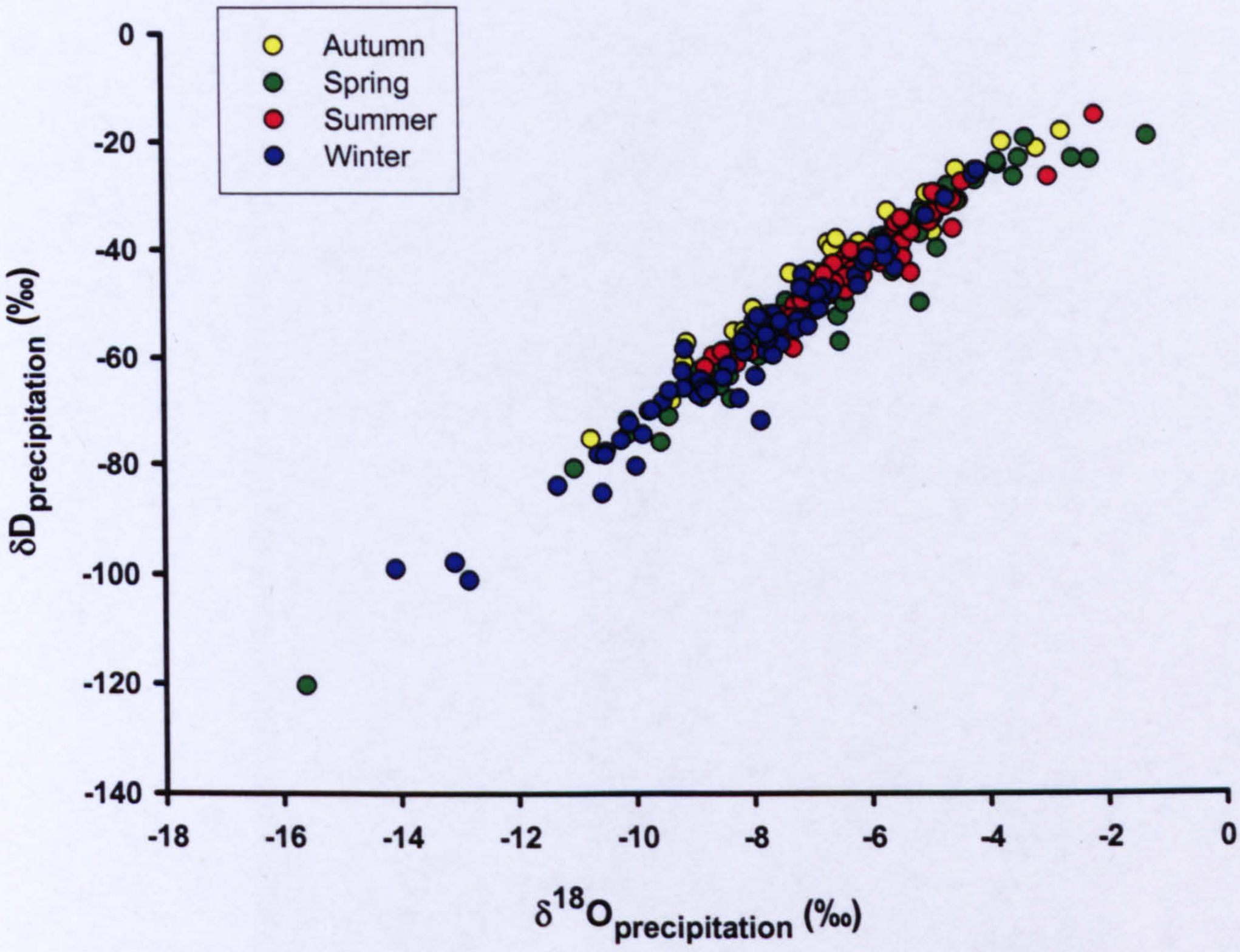

Figure 3.16 Bi-plot of mean monthly isotopic values in precipitation by season for Cuxhaven (1978-2001) (IAEA/WMO, 2004)

Table 3.2 Seasonal means of monthly isotopic data for Cuxhaven (1978-2001) (IAEA/WMO, 2004)

		Autumn	Winter	Spring	Summer
Cuxhaven	$\delta^{18}O$	-6.8	-8.0	-6.6	-6.2
	σ	1.5	1.9	2.2	1.3
	δD	-45.9	-58.3	-48.3	-43.3
	σ	11.9	15.7	17.3	9.6

Mean values for each month over the period 1978-2001 are presented in Figure 3.17 for the relationship between $\delta^{18}O$ values in precipitation and surface air temperature. The relationship with longer-term monthly means is not as strong at Cuxhaven (Figure 3.17, $r^2 = 0.60$, $p < 0.05$) as that observed at Wallingford (Figure 3.10) although the relationship is statistically significant. Linear regression of $\delta^{18}O$ values against surface air temperature yields the relationship:

Equation 7) $\Delta T = 5.93(\Delta\delta^{18}O)$

The reciprocal of Equation 7 yields an isotope-temperature coefficient (0.16 ‰°C^{-1}) that is considerably lower than that observed previously in central Europe (Siegenthaler and Oeschger, 1980; Rozanski *et al.*, 1992). Unlike the data from Wallingford, no clear correlation is observed with precipitation amount over the longer-term at Cuxhaven (Figure 3.18). The marked difference between the coefficient for data from Cuxhaven and previous observation in continental Europe (Siegenthaler and Oeschger, 1980; Rozanski *et al.*, 1992) suggests any palaeotemperature reconstruction using this relationship should be interpreted with caution.

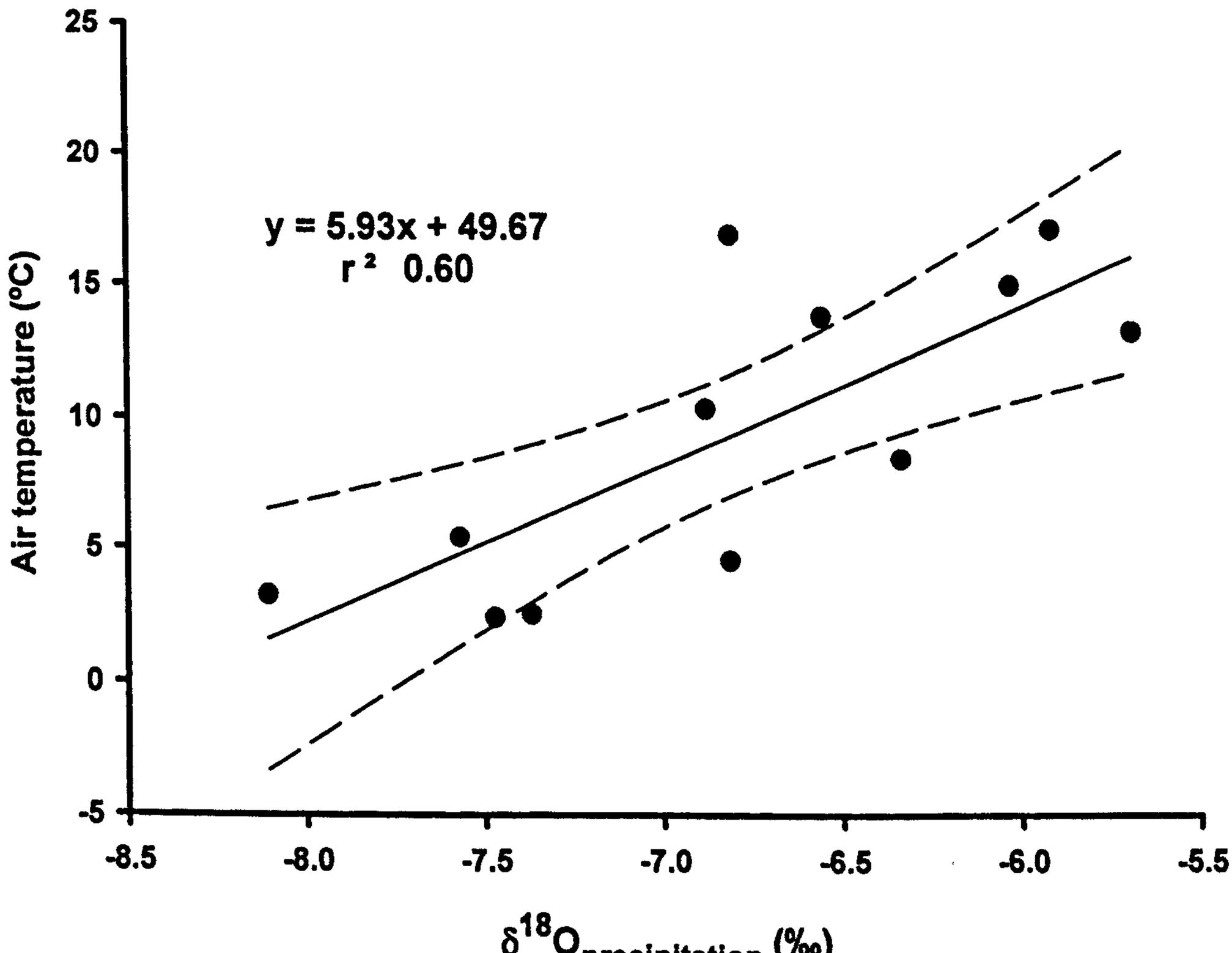

Figure 3.17 Relationship between long-term monthly means of $\delta^{18}O_{precipitaiton}$ and surface air temperature for Cuxhaven (1978-2001) (IAEA/WMO, 2004) (linear regression in solid line, 95% confidence limits in dashed lines)

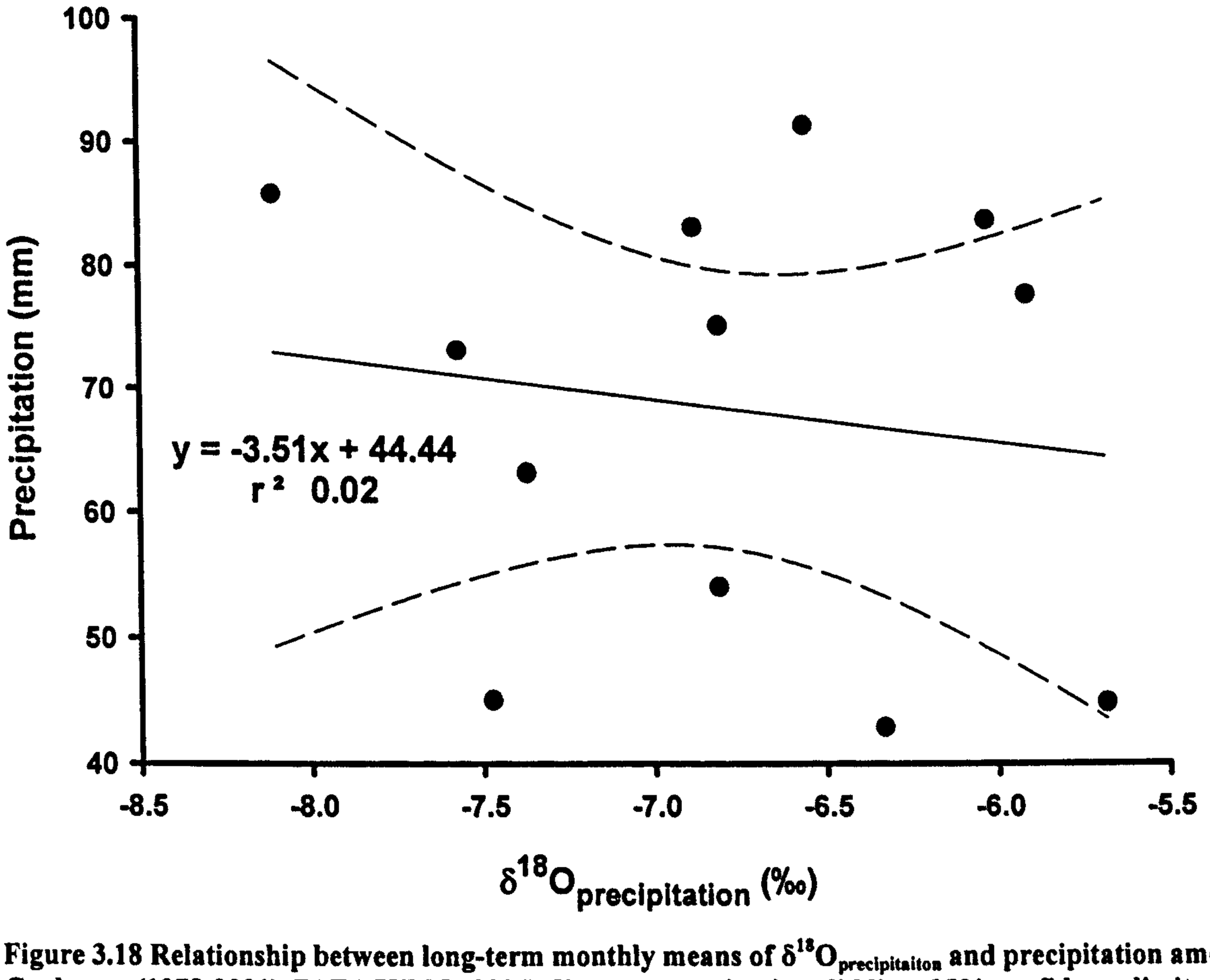

Figure 3.18 Relationship between long-term monthly means of $\delta^{18}O_{precipitaiton}$ and precipitation amount for Cuxhaven (1978-2001) (IAEA/WMO, 2004) (linear regression in solid line, 95% confidence limits in dashed lines)

Previous work at Dosenmoor, whilst not nearly as extensive as that undertaken on Walton Moss, provides both an understanding of the palaeoclimatology of the region (Barber *et al.*, 2004) and also a well constrained tephrochronological framework (Van Den Bogaard and Schmincke, 2002). Both are invaluable for validating the results produced from this study.

Stratigraphical survey work was carried out during fieldwork in May 2004 to develop a better understanding of the sub-surface topography in the area of deepest peat and allow identification of the optimum location for coring. The transect data are presented in Figure 3.21 & Figure 3.22.

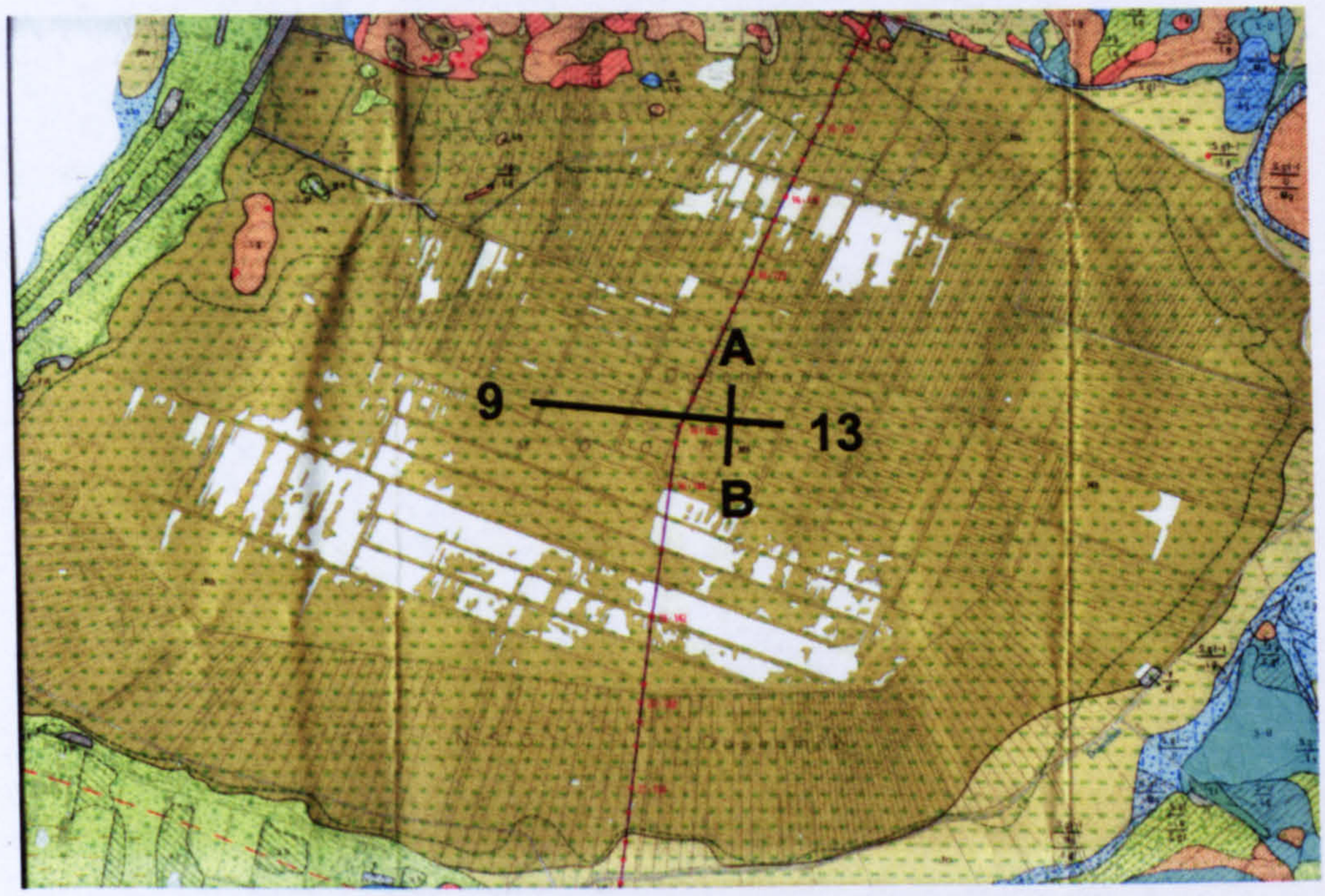

Figure 3.19 Transects used for stratigraphical analysis superimposed on a map of the surface area of Dosenmoor (adapted from Irmler *et al*., 1998). Transect labels refer to stratigraphical cores used in analysis (Figure 3.21, Figure 3.22)

CONTAINS PULLOUTS

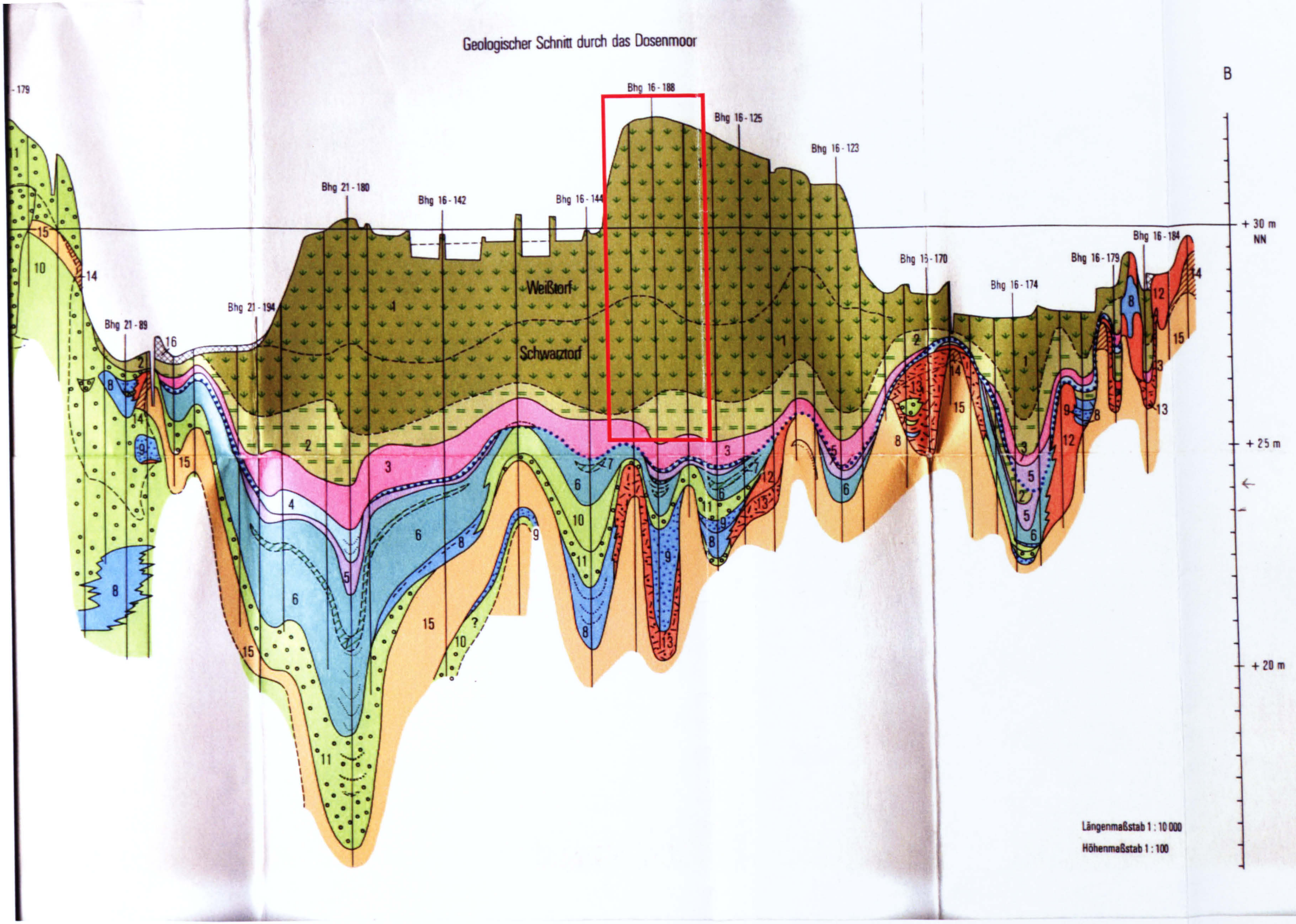

Figure 3.20 Geological cross-section of Dosenmoor along a north-south transect. Top three layers refer to peat deposits. Brighter colours refer to riverine and lacustrine deposits. Cut sections of the bog surface are clearly represented. Red box indicates bog region from which additional stratigraphical survey work was undertaken (adapted from Irmler *et al.*, 1998)

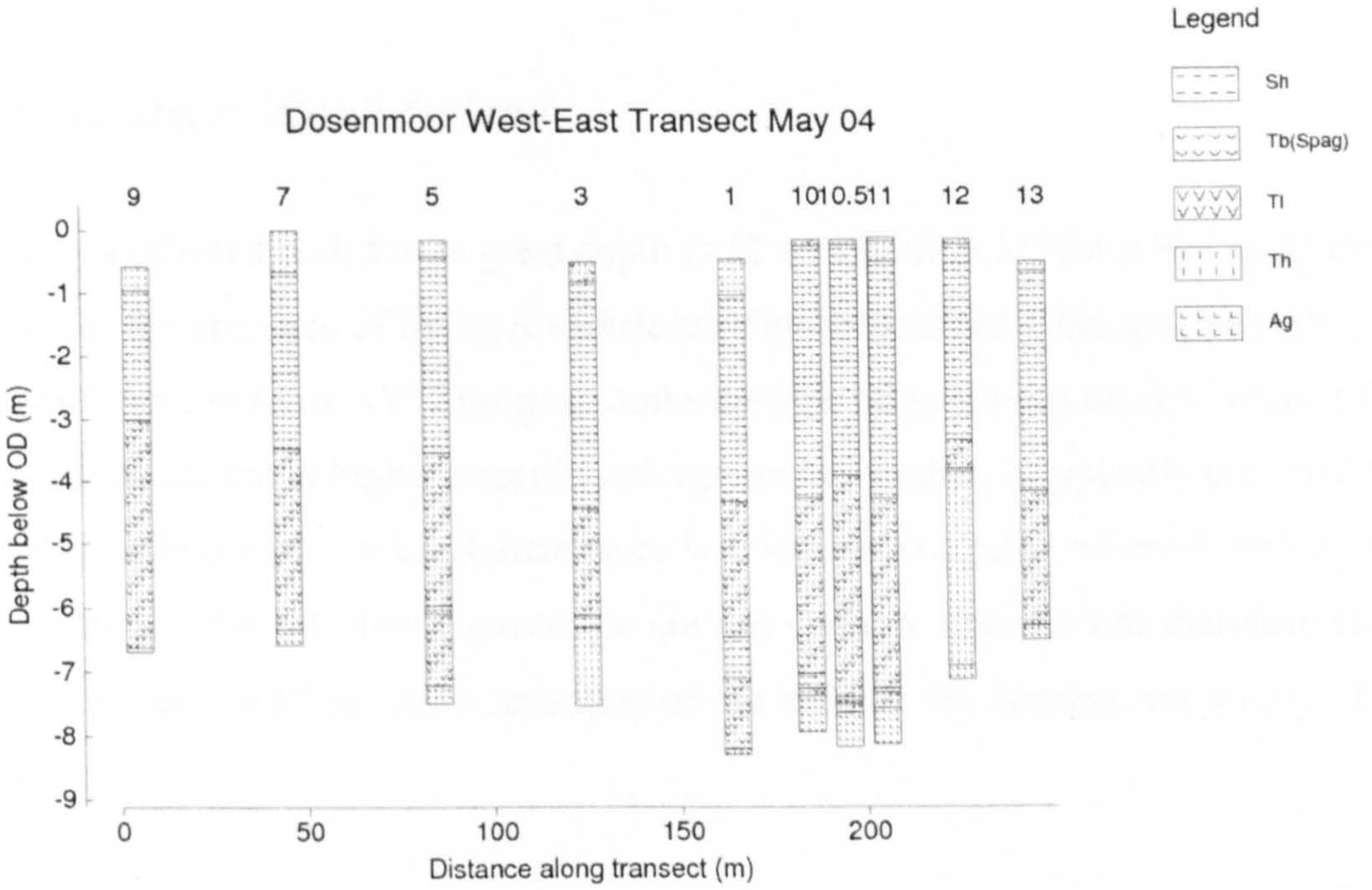

Figure 3.21 Stratigraphical summary for West-East transect of Dosenmoor. Symbol notation follows Troels-Smith (1955)

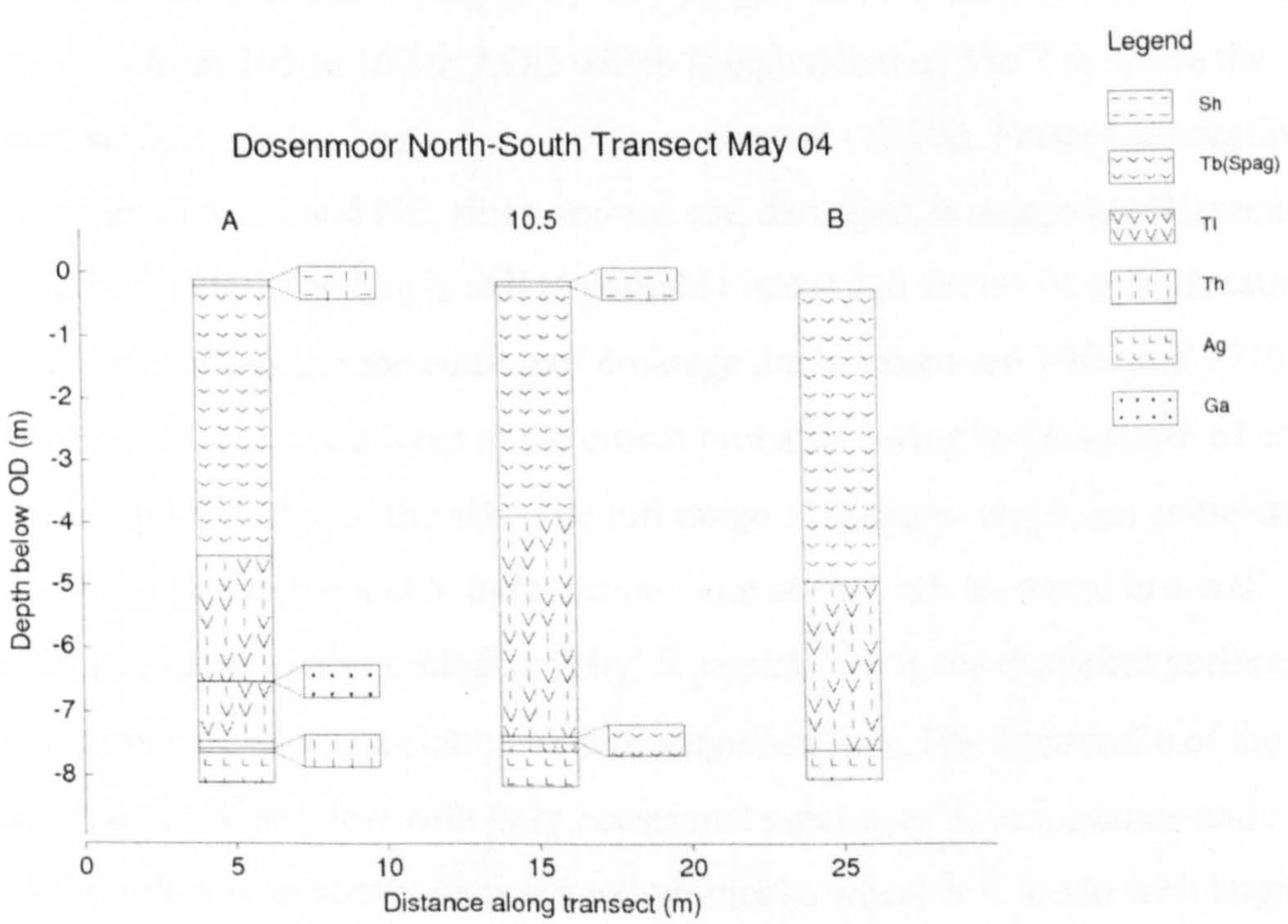

Figure 3.22 Stratigraphical summary for North-South transect of Dosenmoor. Symbol notation follows Troels-Smith (1955).

3.4 *Raheenmore, midland Ireland*

Raheenmore was selected both for its great depth (>12 m; Figure 3.31) for a Holocene raised peat bog, and for the presence of living *S. imbricatum* on the surface. This species is the dominant peat former in most NW European ombrotrophic bogs but has become extinct from much of the region except in highly oceanic settings, and even then is typically confined to rare occurrences in bog hummocks. Raheenmore is a notable exception where *S. imbricatum* can still be found as a lawn forming species on the bog surface. The site was therefore chosen in addition to its depth to allow characterisation of the modern day isotopic variability of *S. imbricatum*.

Raheenmore is a slightly asymmetric and dome shaped raised bog that developed in a small basin in the catchments of the major rivers Brosna and Boyne on the border of counties Offaly and Westmeath in midland Ireland (53.336°N, 7.343°W; altitude 107m AOD). Geological data are scarce but indicate an underlying gritty clay on glacial till (van der Schaaf, 1999).The surface altitude rises from 103 to 107 m AOD which is equivalent to 3 to 7 m above the surrounding land surface and the bog covers a present area of ~130 ha. Former connection to a larger bog complex to the N and NE, since drained and damaged, is suggested (Hammond, 1981; van der Schaaf, 1999).The bog is still remarkably intact and shows little degradation despite marginal peat cutting and the cutting of drainage ditches between 1950 and 1970. Bog pool development is presently restricted to the crown probably owing to the system of arterial drainage works around the edge of the site. The full range of *Sphagnum* species associated with Irish raised bogs (*S. fuscum* and *S. imbricatum*, note above) can be found in a well developed carpet and hummock microtopography. *S. papillosum* is the dominant surface species in lawn/ carpet areas in association with *S. magellanicum*. The abundance of the wetter indicator species is very low with only occasional patches of *S. cuspidatum* and *S. pulchrum*. *S. imbricatum* is generally resticted to hummocks where is it found with large abundances of *S. fuscum* although rare areas exist where *S. imbricatum* is observed as a lawn species. *Eriophorum vaginatum* is the dominant grass and is associated with *Tricophorum*

cespitosum. Occasional *Eriophorum angustifolium* is observed. The depth of peat is exceptional, up to 15 m in places.

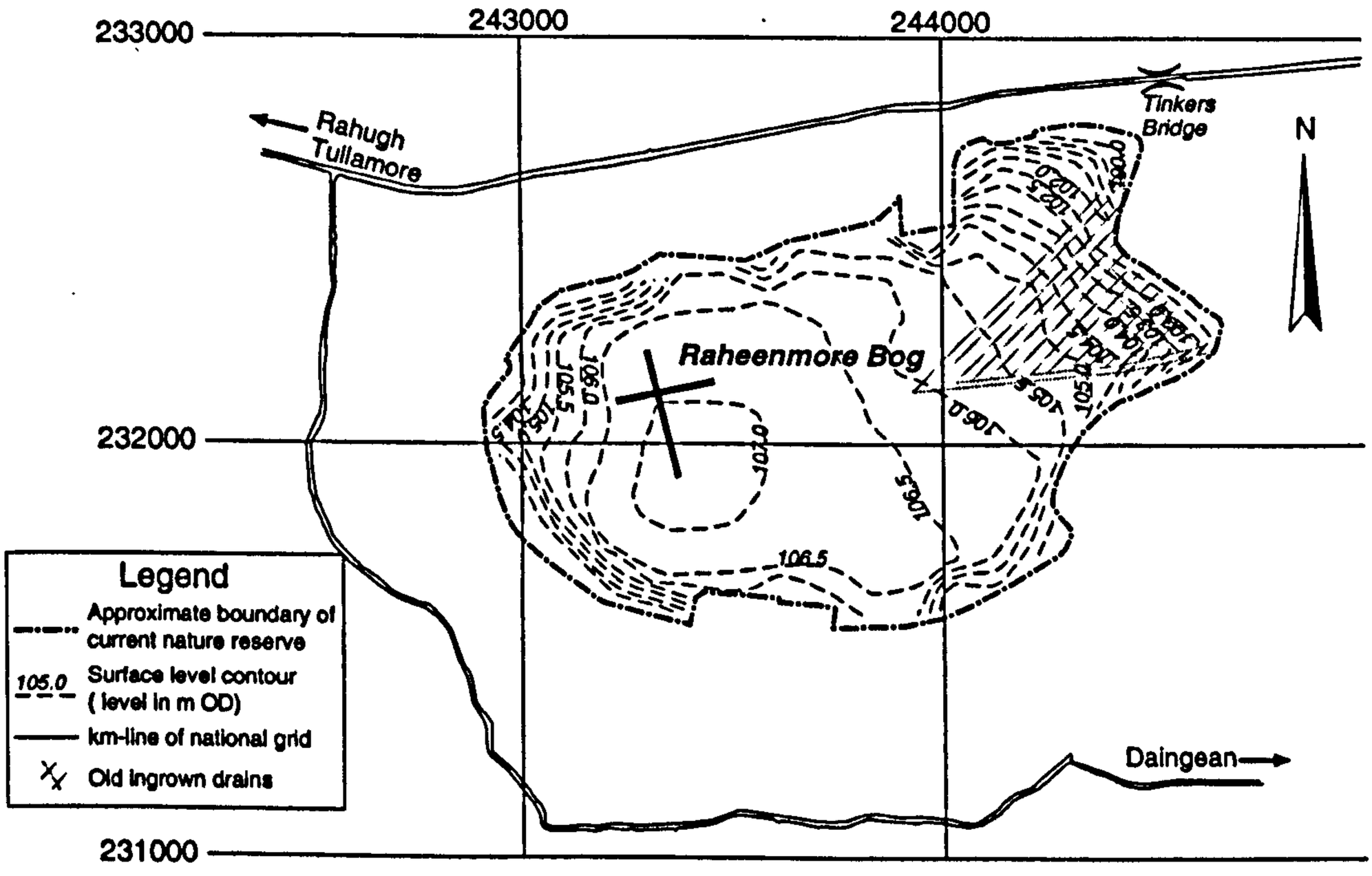

Figure 3.23 Surface level contour map of Raheenmore Bog with stratigraphical transect locations (black cross), former (now ingrown) drainage system in northeast corner and Irish co-ordinate system overlaid (van der Schaaf, 1999).

Restoration work was carried out in the 1990s following a change in ownership of the site from Bord na Mona to Duchas and following the findings of a joint Dutch-Irish project that concluded that >50% of the bog vegetation was dead or dying (van der Schaaf, 1999). The decline was attributed to subsidence at the bog margins and consequent increased drainage resulting from peripheral peat cutting. A series of eight concentric bunds spreading out from the centre of the bog was used to raise the water level artificially in an attempt to re-swell the peat and restore a shallower gradient to the bog surface at <30 cm per 100 m.

Raheenmore experiences a highly oceanic climate sharing the dominant mid-latitude westerly belt of the other NW European sites in this study. The Irish midlands have a mean annual precipitation of 800-1000 mm yr^{-1} (van der Schaaf, 1999).

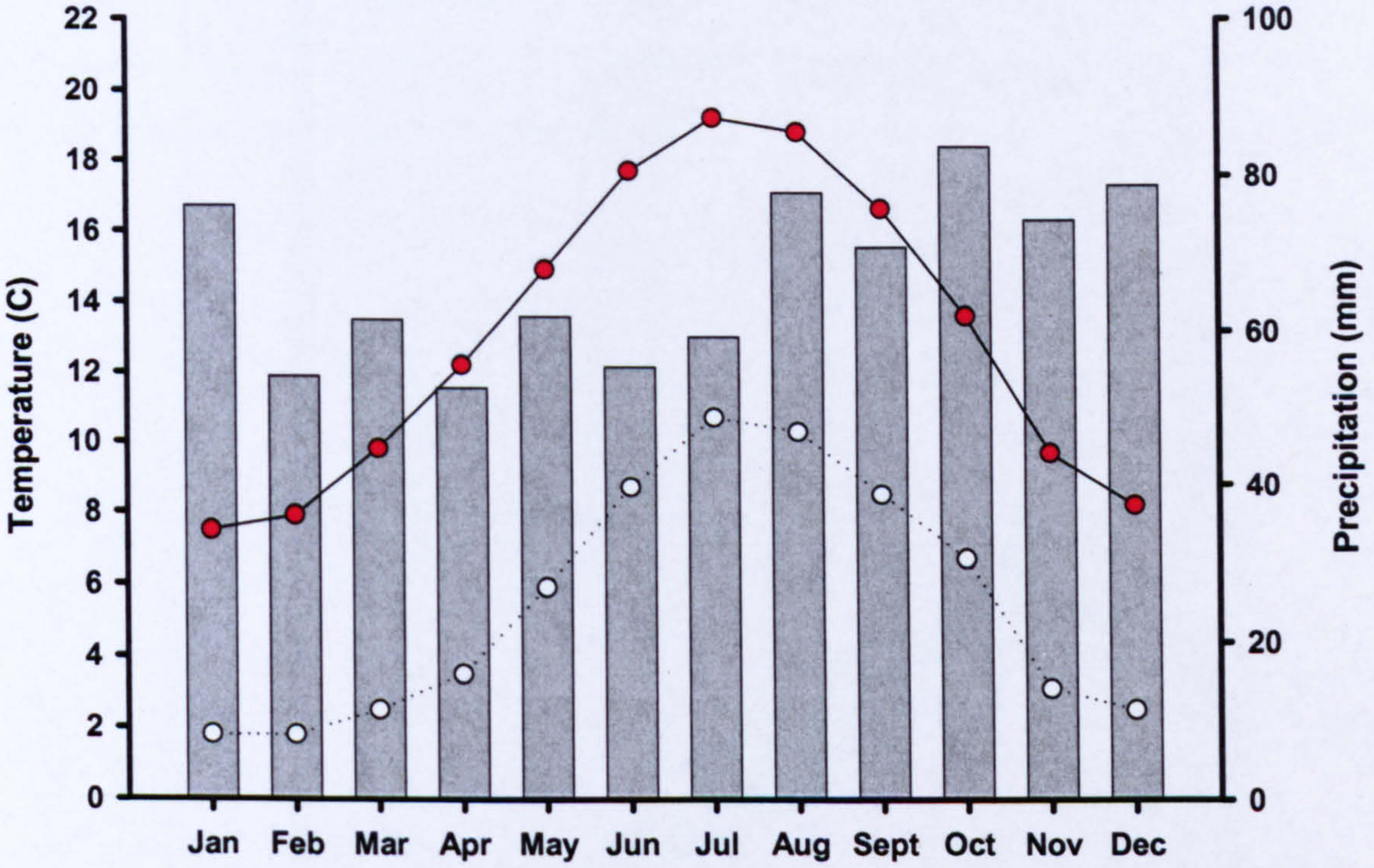

Figure 3.24 Mean monthly maximum and minimum temperature (dots) and precipitation (grey bars) (1961-1990) for Birr, midland Ireland (53.08°N, 7.88°W; 73 m altitude)

Monthly precipitation averages (1961-1990) (Figure 3.24) indicate that whilst seasonality of precipitation exists it is less variable than that at Dosenmoor and Walton Moss. Mean monthly temperatures vary between a January minimum of 1.8ºC and maximum of 7.5ºC to a July minimum of 10.7ºC and maximum of 19.2ºC. Annual variation in the mean monthly temperature is 10.3ºC (~60% of the mean annual variation at Dosenmoor). The reduced mean annual temperature range is a reflection of the oceanic climate experienced at this site.

The GNIP station at Valentia observatory on the SW coast of Ireland (51.93N, 10.25W; 9 m altitude AOD; Figure 3.1) provides one of the longest records of isotopes in precipitation in the world. The shallow slope angle of the bi-plot (Figure 3.25) relative to the GMWL and the low deuterium excess (intercept <10) are indicative of either a relatively humid vapour source or secondary evaporation of falling rain during the summer months. Like the other NW European sites of this study, there is a positive and significant relationship between mean monthly oxygen isotopic composition and surface air temperature values (Figure 3.26, r^2 = 0.23, $p<0.001$) and a negative correlation of similar strength with the amount of precipitation

(Figure 3.27, $r^2 = 0.19$, $p<0.001$). As with the seasonal averages for Wallingford and Cuxhaven, a similar comparison for Valentia demonstrates seasonal variation with the heaviest isotopic values observed in the summer months and lightest isotopic values observed in the winter months (Table 3.3, Figure 3.28).

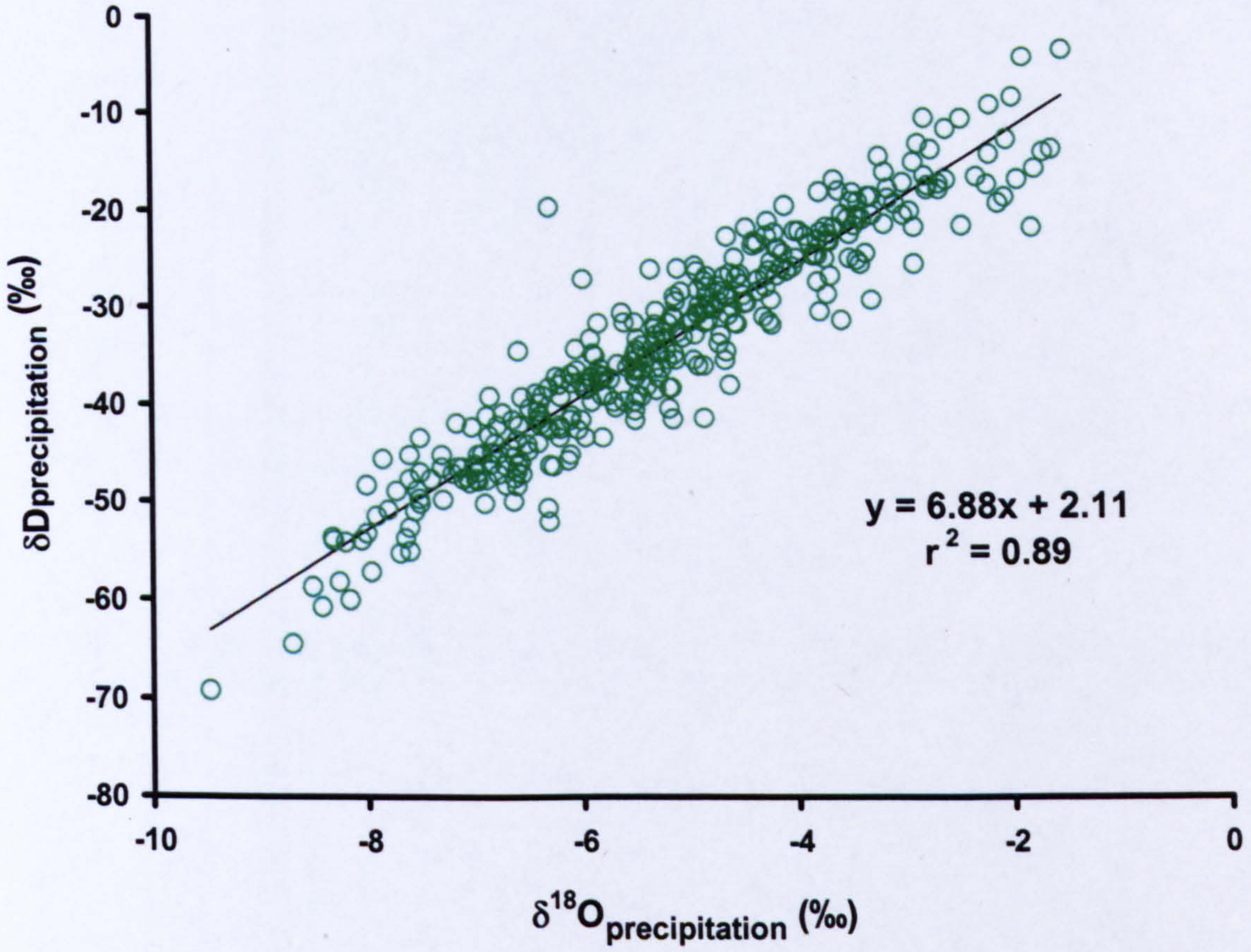

Figure 3.25 Bi-plot of mean monthly δD and δ^{18}O values in precipitation for Valentia (1960-2002) (IAEA/WMO, 2004)

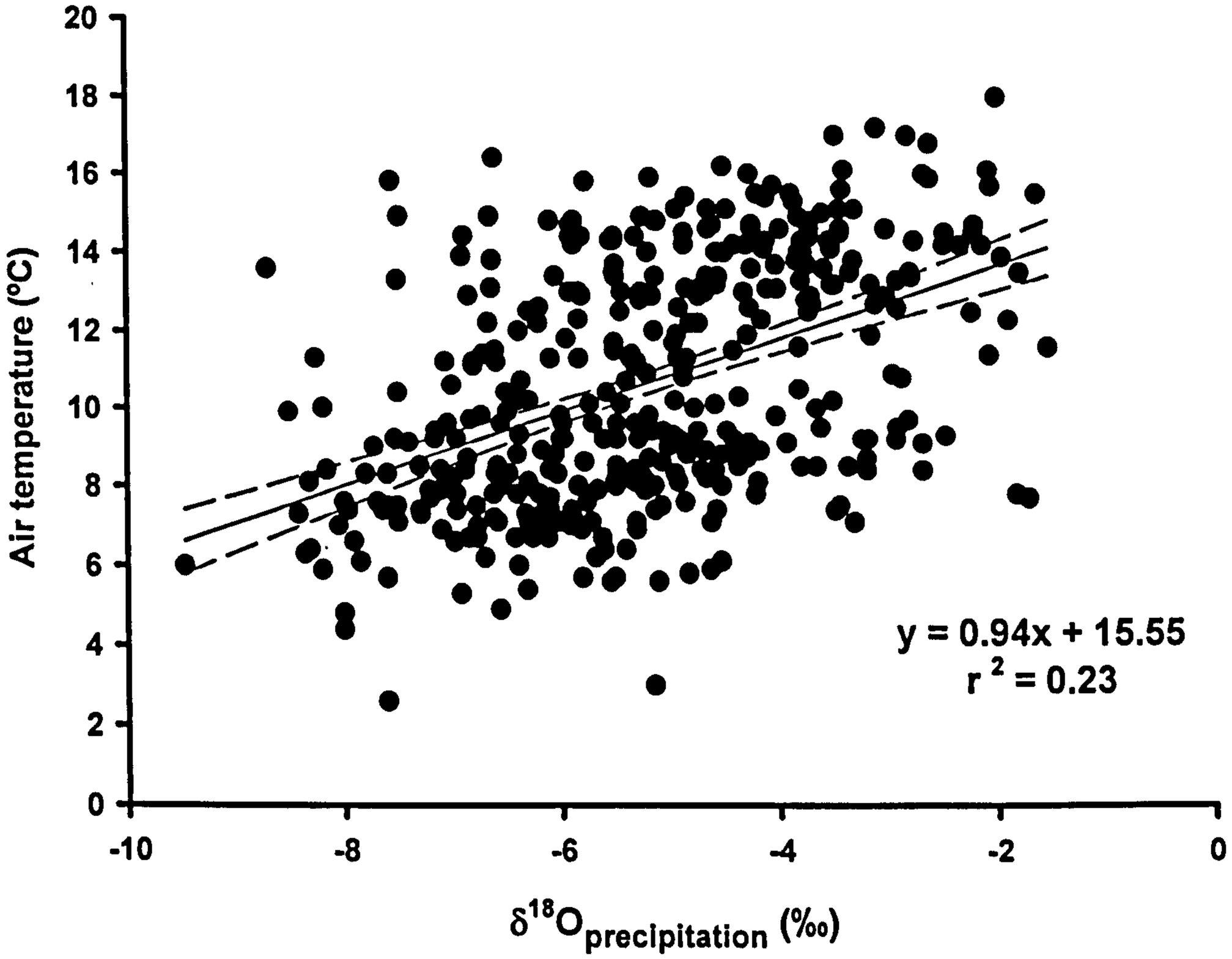

Figure 3.26 Relationship between mean monthly $\delta^{18}O$ values in precipitation and surface air temperature for Valentia (1960-2002) (IAEA/WMO, 2004) (linear regression in solid line, 95% confidence limits in dashed lines)

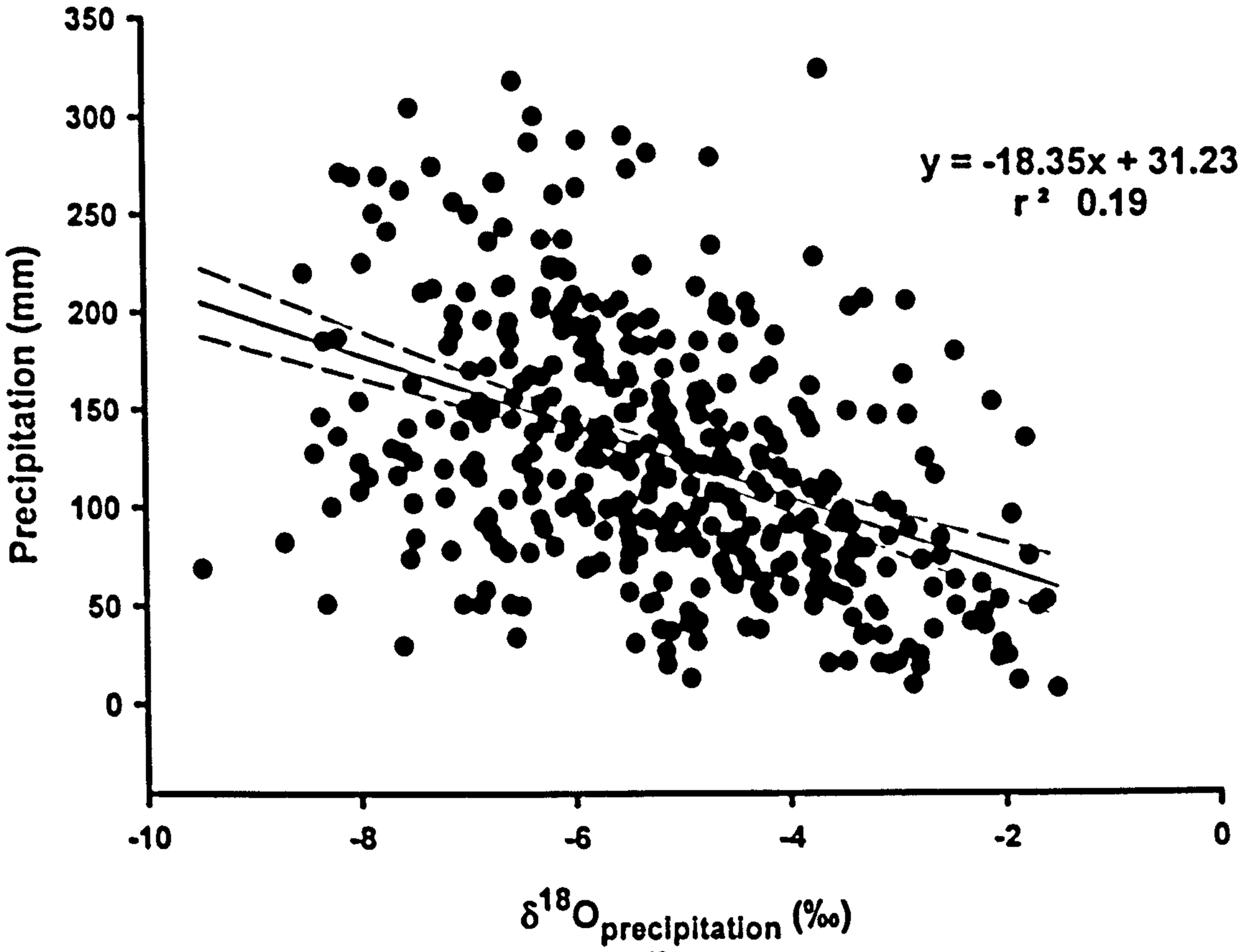

Figure 3.27 Relationship between mean monthly $\delta^{18}O$ values in precipitation and precipitation amount for Valentia (1960-2002) (IAEA/WMO, 2004) (linear regression in solid line, 95% confidence limits in dashed lines)

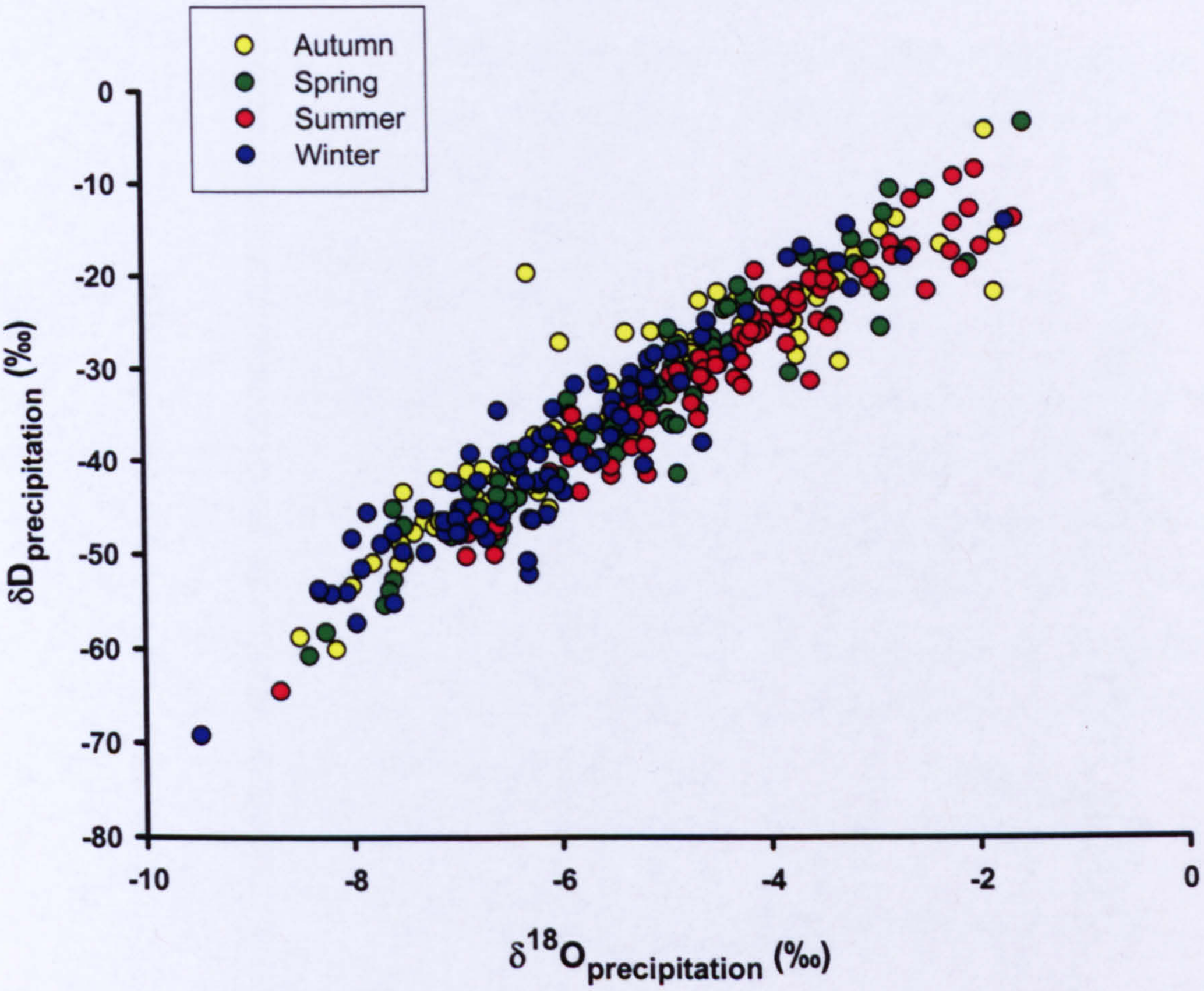

Figure 3.28 Bi-plot of mean monthly isotopic values in precipitation by season for Valentia (1960-2002) (IAEA/WMO, 2004)

Table 3.3 Seasonal means of monthly isotopic data for Valentia (1960-2002)

		Autumn	Winter	Spring	Summer
Valentia	$\delta^{18}O$	-5.4	-6.0	-5.2	-4.3
	σ	1.6	1.3	1.5	1.3
	δD	-33.4	-38.9	-34.1	-28.5
	σ	11.0	10.4	11.3	10.3

Mean values for each month over the period 1960-2002 are presented in Figure 3.29 for the relationship between $\delta^{18}O$ values in precipitation and surface air temperature. The relationship with longer-term monthly values shows a strong and significant positive correlation between the variables (Figure 3.29, $r^2 = 0.87$, $p<0.001$). The correlation found at Valentia over the

longer-term means is the strongest of all three European GNIP stations used in this study, which possibly reflects the increased length of the record (42 year time span, although not every year sampled) at this location. The regression of $\delta^{18}O$ values against surface air temperature yields the relationship:

Equation 8) $$\Delta T = 3.83(\Delta\delta^{18}O)$$

The reciprocal of Equation 8 yields an isotope-temperature coefficient (0.26 ‰°C^{-1}) which is very similar to the coefficient from Wallingford (0.27 ‰°C^{-1}). Further similarity in the isotope climates of both Wallingford and Valentia is demonstrated by the existence of a strong and significant negative relationship between $\delta^{18}O_{precipitaiton}$ and precipitation amount at Valentia over the longer-term (Figure 3.30, $r^2 = 0.50$, $p<0.01$). Inevitably, again, this relationship must act to distort the temperature relationship in Equation 8, implying that any palaeotemperature reconstruction should be interpreted with caution.

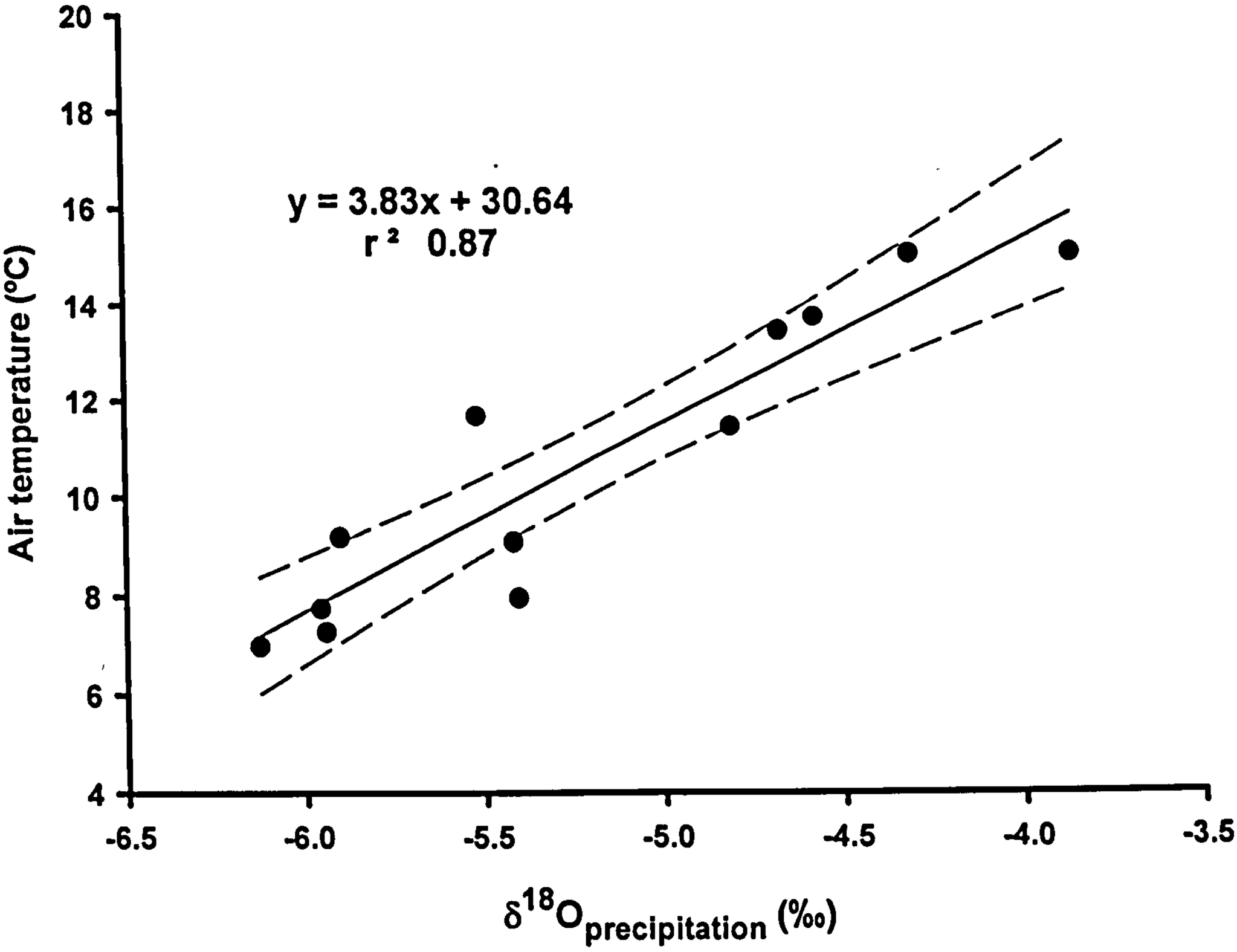

Figure 3.29 Relationship between long-term monthly means of $\delta^{18}O_{precipitation}$ and surface air temperature for Valentia (1960-2002) (IAEA/WMO, 2004) (linear regression in solid line, 95% confidence limits in dashed lines)

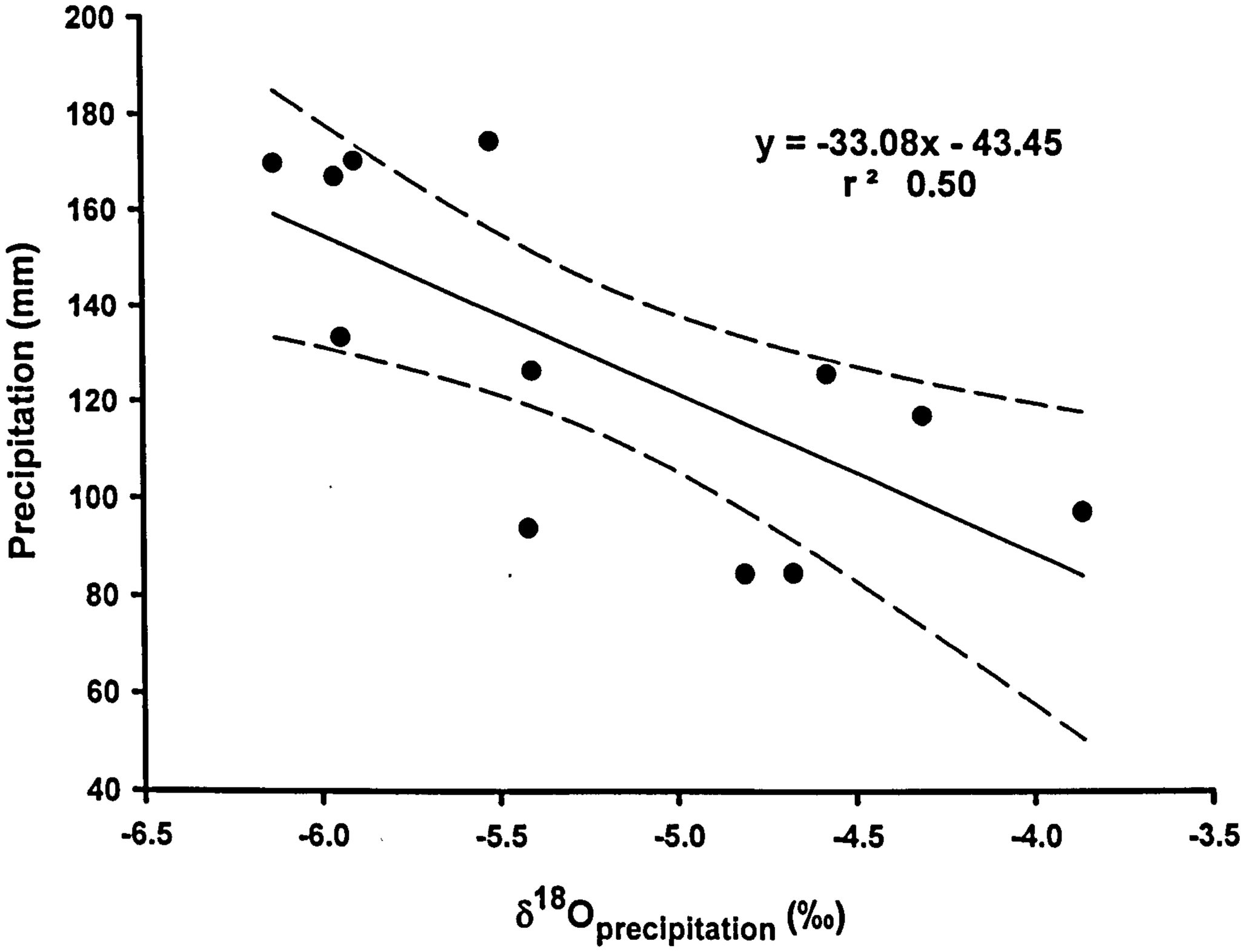

Figure 3.30 Relationship between long-term monthly means of $\delta^{18}O_{precipitaiton}$ and precipitation amount for Valentia (1960-2002) (IAEA/WMO, 2004) (linear regression in solid line, 95% confidence limits in dashed lines)

Previous work at Raheenmore is scarce and limited to one published project (van der Schaaf, 1999) on an analysis of site hydrology. No previous palaeoecological or stratigraphical work is understood to have taken place at the site. Accordingly, a thorough stratigraphical survey was carried out in July 2005 to identify the optimum location for collection of a master core. The data from intersecting transects of cores spaced 50 m apart are presented in Figure 3.31 and Figure 3.32 below.

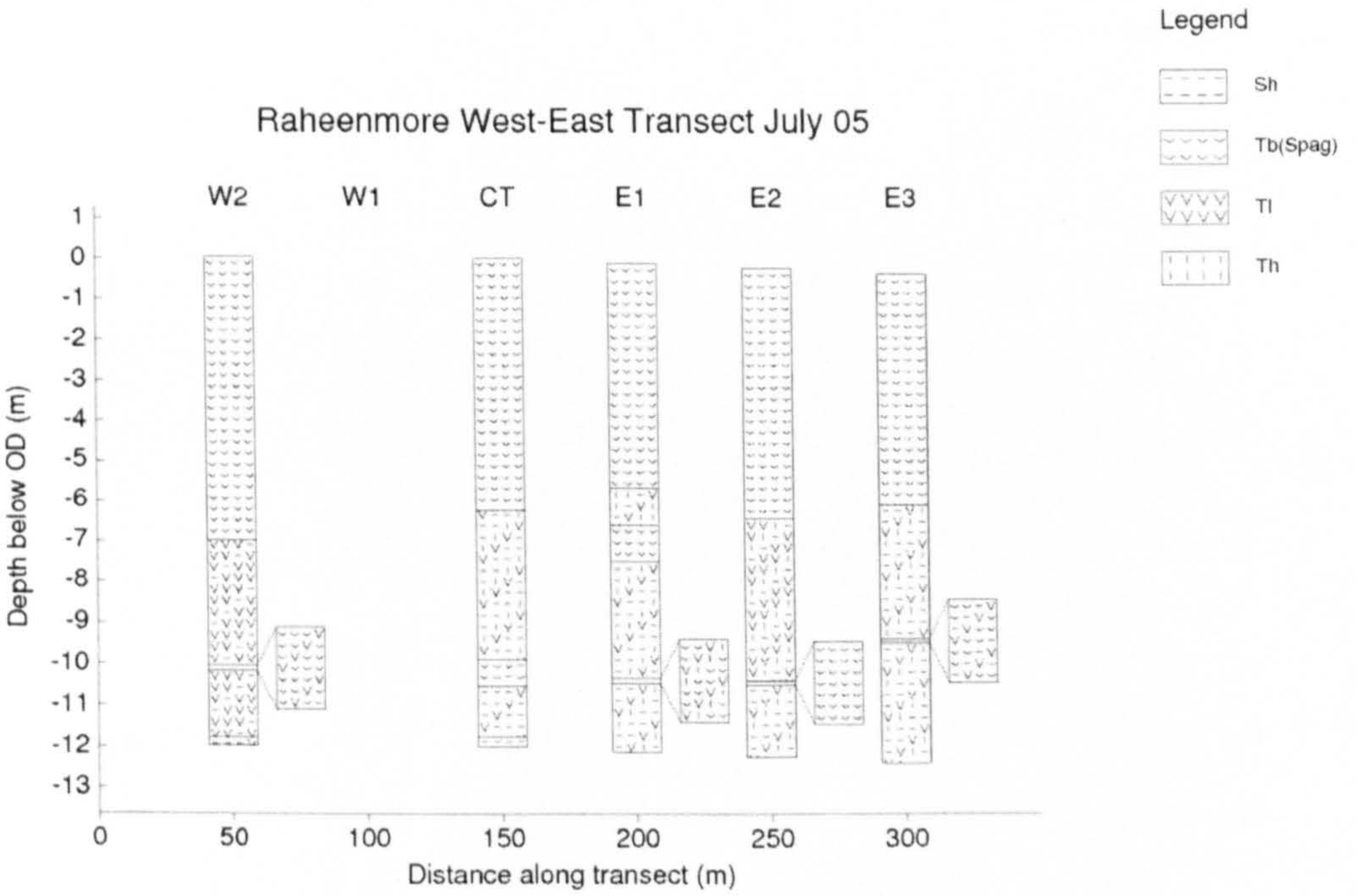

Figure 3.31 Stratigraphical summary for west-east transect of Raheenmore bog. Symbol notation follows Troels-Smith (1955)

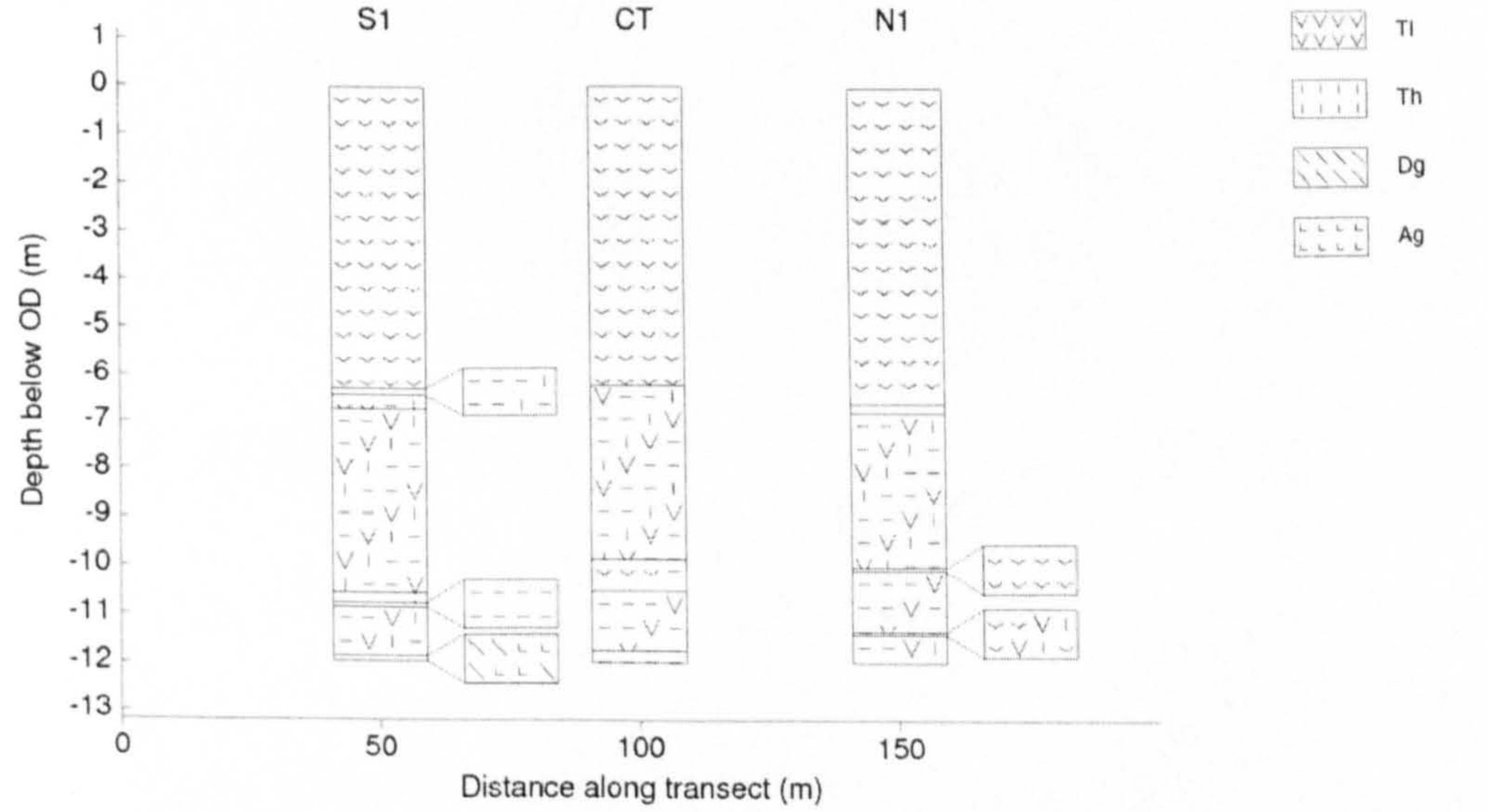

Figure 3.32 Stratigraphical summary for south-north transect of Raheenmore bog. Symbol notation follows Troels-Smith (1955)

3.5 *Nordans Pond Bog, Newfoundland*

In an extension to the original objectives of the ISOMAP-UK project a further site from outside NW Europe was added to this study in a location directly proximal to the hypothesized route of the Lake Agassiz meltwater plume thought to have caused the 8200 BP event (Barber *et al.*, 1999; Keigwin *et al.*, 2005). Previous multi-proxy investigation (Hughes *et al.*, 2006) had revealed a strong climatic anomaly at a date directly coincident with the best estimate of the flood (Barber *et al.*, 1999). The event was characterised by high abundances of a single *Sphagnum* species: *S. cuspidatum*. Unlike European cores, *Sphagnum* remains were also relatively persistent throughout the entire core length, representing a time-span of ~8500 years (Hughes *et al.*, 2006). Investigation of the core for *Sphagnum*-specific isotopic variability offered the ideal opportunity for characterisation of the 8200 BP event from North America where quantitative palaeotemperature records were scarce.

Nordans Pond Bog is an ombrotrophic plateau bog (49.150°N, 53.583°W; altitude 62m AOD) located 1.5 km inland from the present-day east coast of Newfoundland and ~2 km^2 in surface area. In contrast to even the most well preserved bogs in NW Europe, Nordans Pond Bog remains pristine and has not been subject to any peat cutting. The surface comprises extensive *Sphagnum* lawn and a distinctive hummock-hollow microtopography with many hollows occupied by wide bog pools. A detailed site description has been published previously but of particular note is the abundance of *S. imbricatum* in lawn habitats. As described earlier, this speices has declined to extinction from many NW European bog surfaces. Co-existant are a range of *Sphagnum* species including *S. pulchrum, S. tenellum, S. fuscum, S. papillosum, S. magellanicum,* and *S. flavicomens*.

Modern climate data from Musgrave Harbour (49.450°N, 53.967°W; altitude 3m AOD; 43 km NW of Nordans Pond bog) indicate a similar precipitation seasonality to the NW European sites but, by contrast, a much higher temperature seasonality (Figure 3.33). Mean monthly temperatures vary from a January maximum of -2.3°C and minimum of -9.8°C to a July maximum of 19.9°C and minimum of 10.8°C. This equates to an average temperature range of ~20°C, approximately double the equivalent measure observed in Birr, midland Ireland.

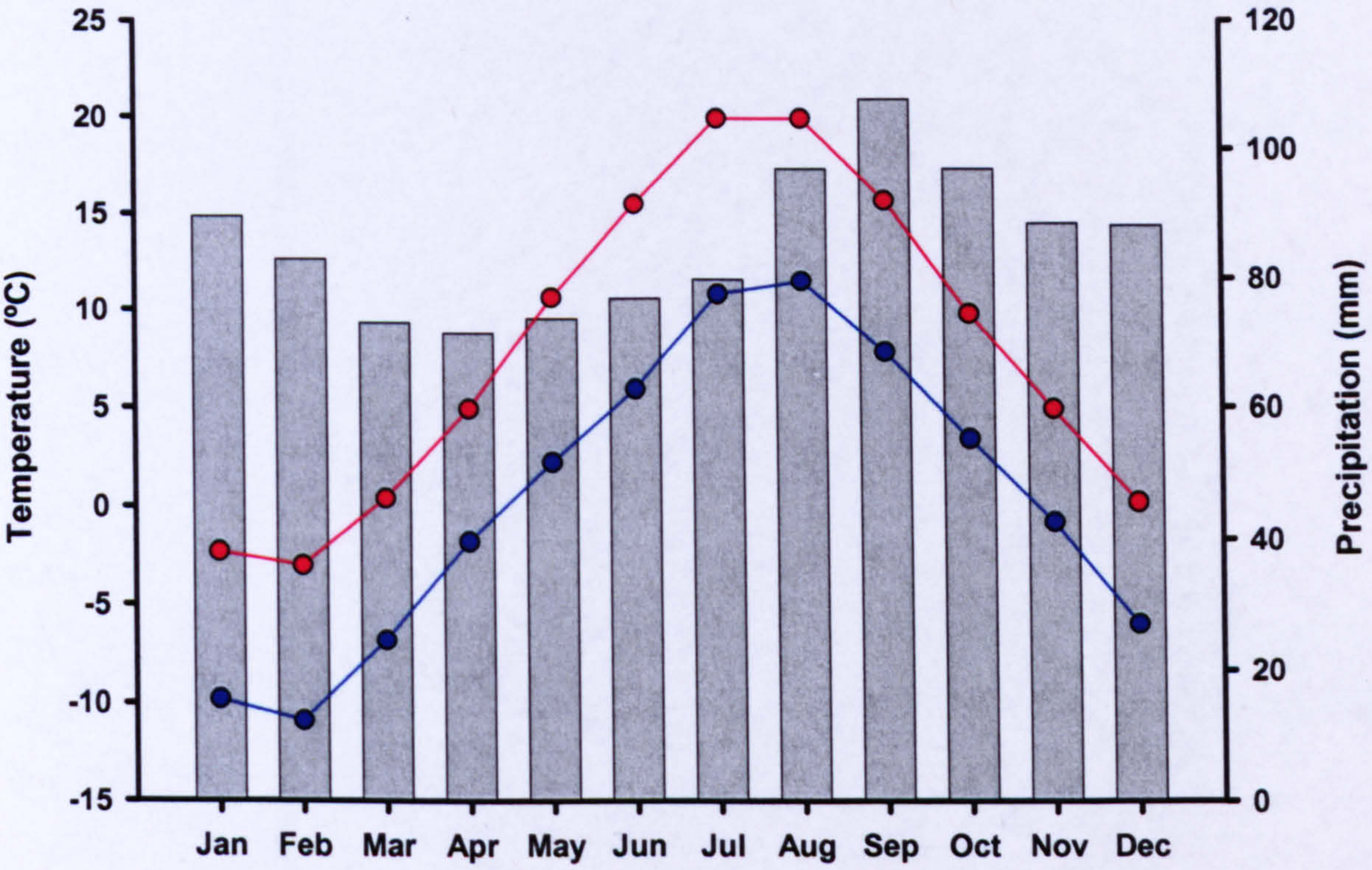

Figure 3.33 Mean monthly maximum and minimum temperature (dots) and precipitation (grey bars) (1971-2000) for Musgrave Harbour (49.450°N, 53.967°W; 43 km NW of Nordans Pond bog)

Whilst no GNIP station exists on Newfoundland itself, the site falls approximately equidistant from two stations: Truro, Nova Scotia (45.370°N, 63.270°W) and Goose Bay, Labrador (53.320°N, 60.420°W). The MWLs for these stations (~1500 km apart) are remarkably similar (Figure 3.34). As expected, $\delta^{18}O_{precipitation}$ values for Nova Scotia are, on average, heavier given the generally warmer conditions at the lower latitude and upstream location in the trajectory of moisture sourced primarily from Atlantic cyclonic activity. In comparison with those GNIP sites in NW Europe, there is a compellingly strong connection between the isotopic values of precipitation and surface air temperature at the monthly timescale (Figure 3.35). It is likely that this stronger link is related to the greater seasonality of temperature experienced by the Atlantic provinces of Canada, which imprints a dominant temperature signal on the isotopic composition of precipitation. There is also strong similarity in the slopes of the relationship between air temperature and $\delta^{18}O_{precipitation}$ values for the two GNIP stations

~1500 miles apart (Figure 3.35). They are identical to 2 decimal places implying a well constrained and consistent temperature-precipitation relationship for the region. No consistent correlation is observed between $\delta^{18}O_{precipitation}$ and precipitation amount (Figure 3.36). The greater seasonality of isotopic values is evidenced by Figure 3.37 where a clear separation is observed between summer (red) and winter (blue) values for both Canadian stations (Table 3.4). This separation is not evident to the same degree in data from GNIP stations close to the NW European peat bog sites.

The slopes of the regressions of $\delta^{18}O$ values against surface air temperature from both GNIP stations yield the relationship:

Equation 9) $$\Delta T = 2.28(\Delta\delta^{18}O)$$

The isotope-temperature coefficient derived from the reciprocal of this relationship (0.44 ‰°C^{-1}) remains less than the ~0.6‰°C^{-1} identified in previous studies yet is the most similar of all the study sites here.

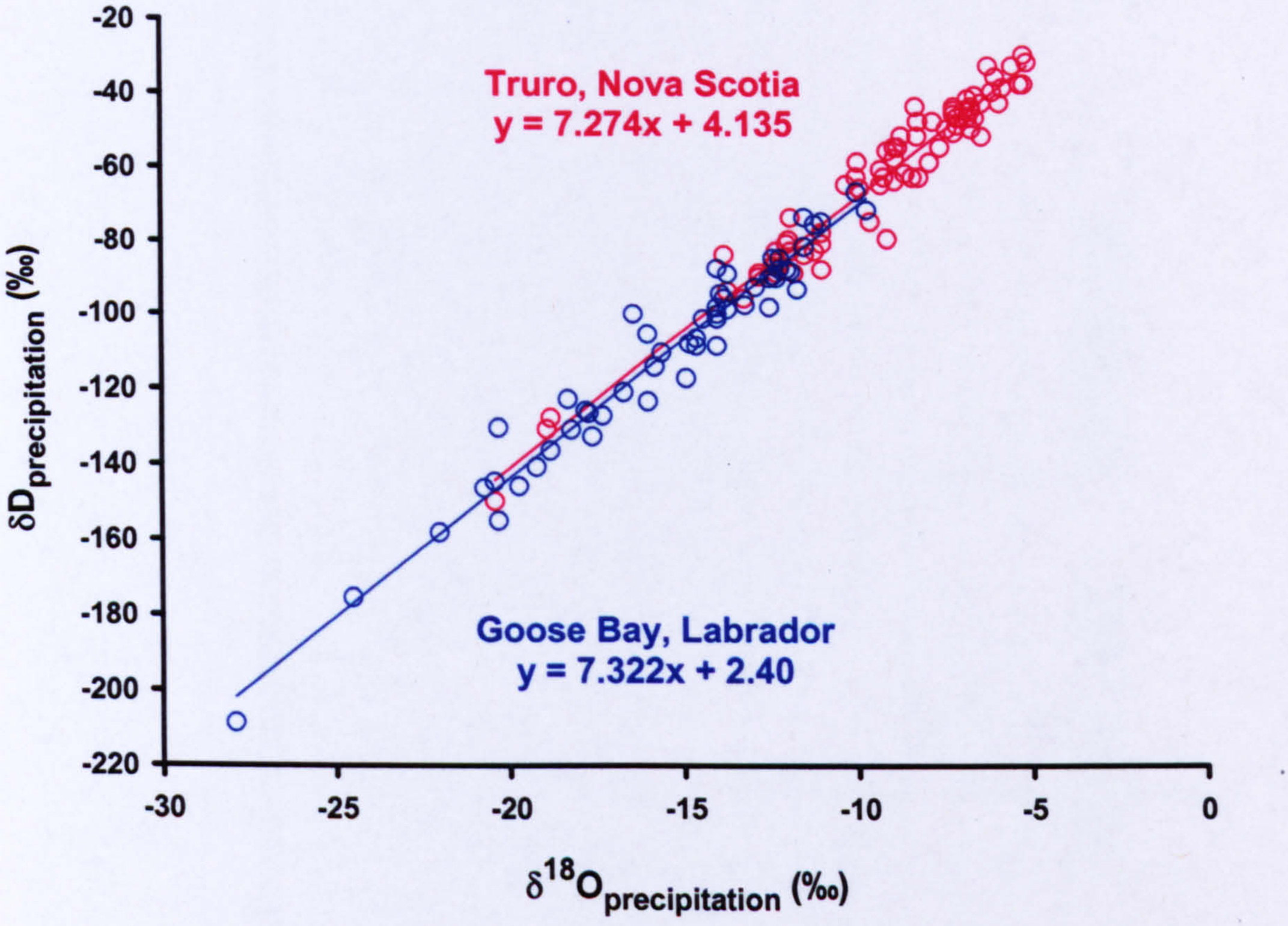

Figure 3.34 Bi-plot of mean monthly δD and $\delta^{18}O$ values in precipitation for Truro, Nova Scotia (1975-1983) and Goose Bay, Labrador (1961-1965) (IAEA/WMO, 2004)

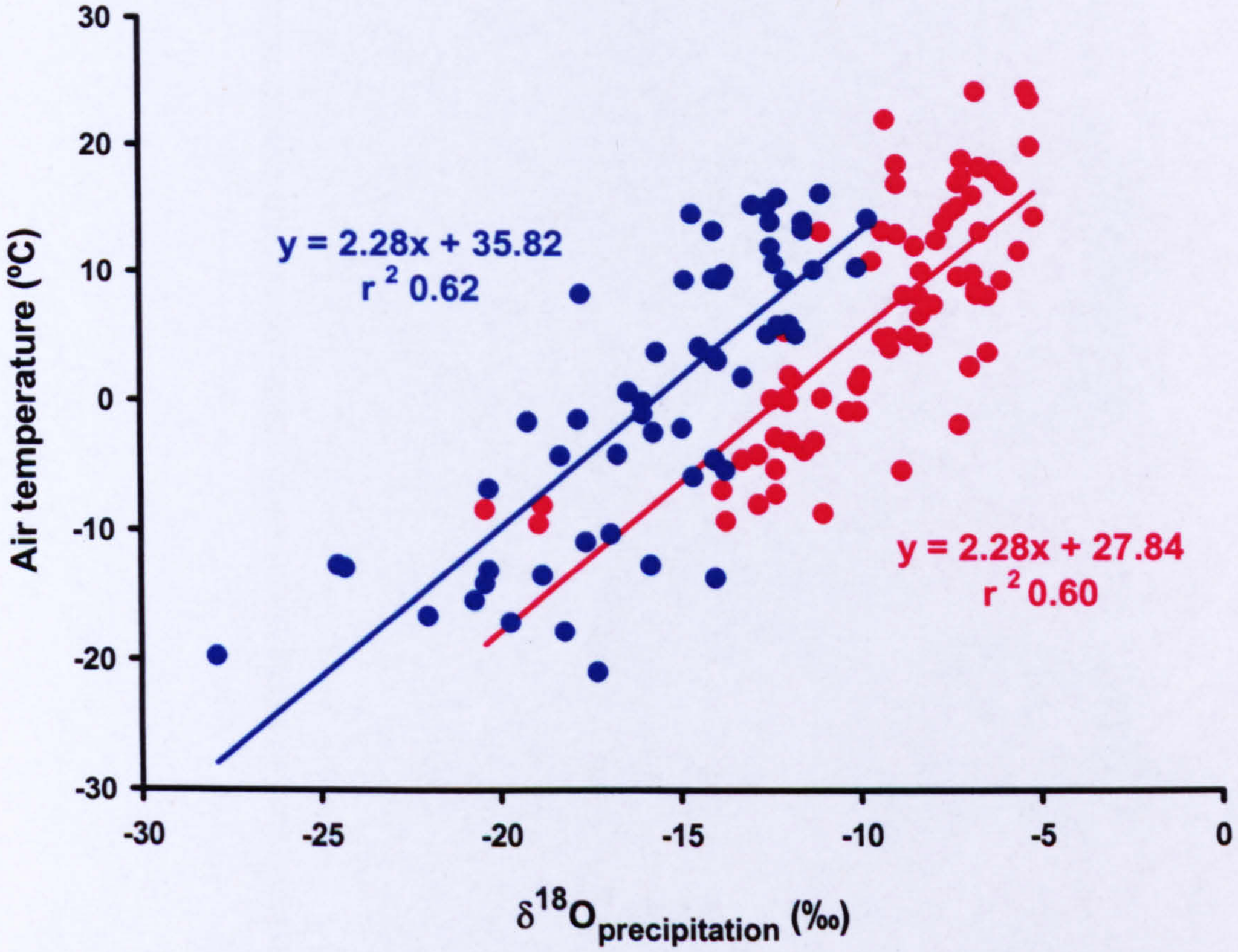

Figure 3.35 Relationship between mean monthly $\delta^{18}O$ values in precipitation and surface air temperature for Truro, NS (1975-1983; red dots) and Goose Bay, Labrador (1961-1965; blue dots) (IAEA/WMO, 2004)

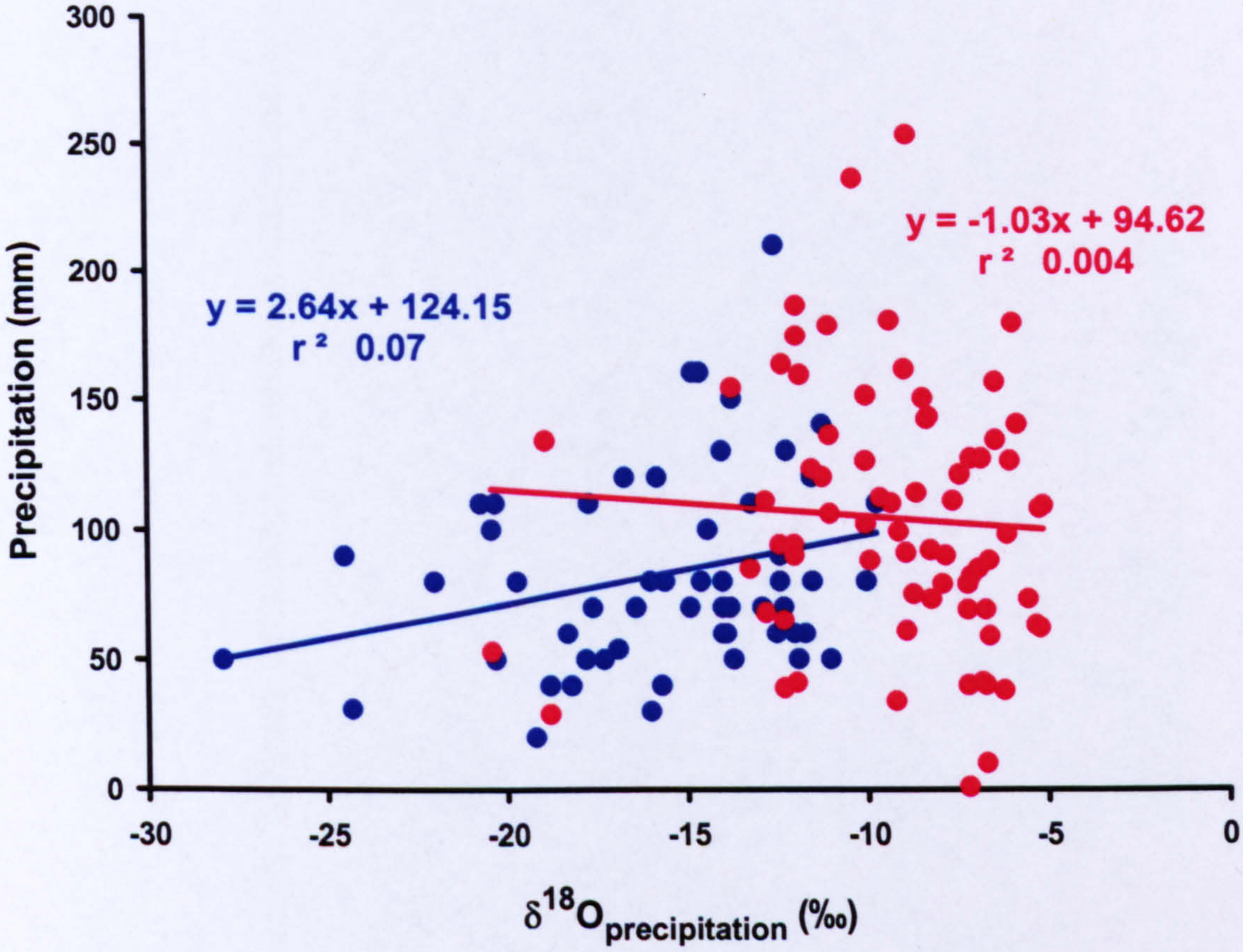

Figure 3.36 Relationship between mean monthly $\delta^{18}O$ values in precipitation and precipitation amount for Truro, NS (1975-1983; red dots) and Goose Bay, Labrador (1961-1965; blue dots) (IAEA/WMO, 2004)

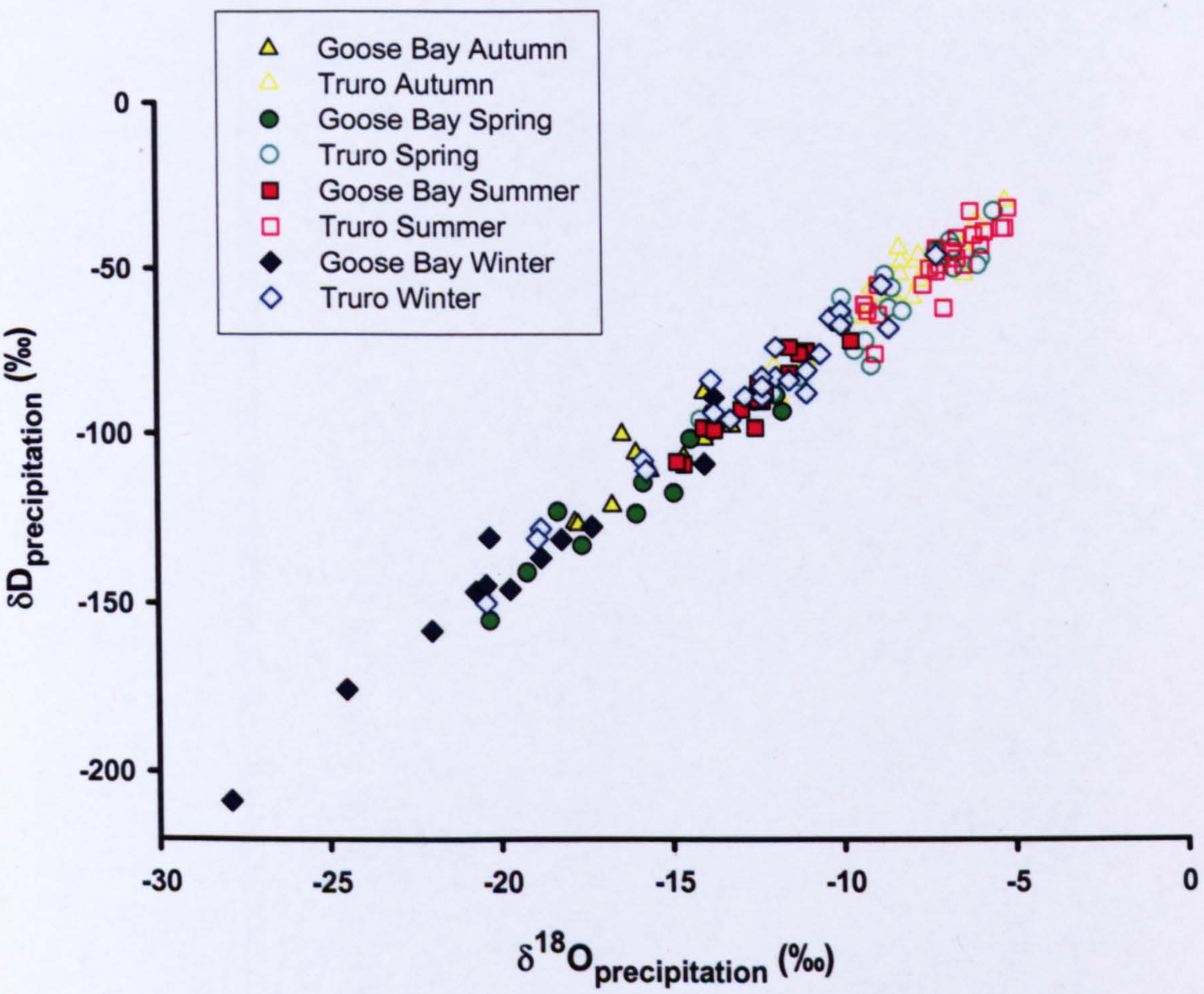

Figure 3.37 Bi-plot of mean monthly isotopic values of precipitation by season for Truro, Nova Scotia (1975-1983) and Goose Bay, Labrador (1961-1965) (IAEA/WMO, 2004)

Table 3.4 Seasonal means of monthly isotopic data for Goose Bay (1961-1965) and Truro (1975-1983) (IAEA/WMO, 2004)

		Autumn	Winter	Spring	Summer
Goose Bay	$\delta^{18}O$	-14.6	-19.8	-15.4	-12.4
	σ	2.1	4.0	3.0	1.4
	δD	-102.0	-142.0	-113.9	-89.2
	σ	15.6	30.5	22.5	12.0
Truro	$\delta^{18}O$	-8.5	-12.6	-8.8	-7.0
	σ	1.9	3.3	2.4	1.3
	δD	-56.7	-87.5	-62.2	-48.9
	σ	15.3	24.4	18.3	11.2

A full stratigraphical survey was undertaken to locate the optimum location for coring and has been published (Hughes *et al.*, 2006). The same core used for their multi-proxy palaeoecological reconstructions was used for isotopic analyses in this study.

3.6 *Comparison of site climatologies*

In order to extract useful quantitative climatic information from the peat core data, it is first necessary to establish that climatic variation can be observed and quantified between sites in the modern day GNIP precipitation data. Figure 3.38 and Table 3.5 summarise the seasonal isotopic variability and Figure 3.39 provides the full $\delta^{18}O_{precipitation}$ time-series for each of the GNIP stations described above and selected for their proximity to the chosen sites.

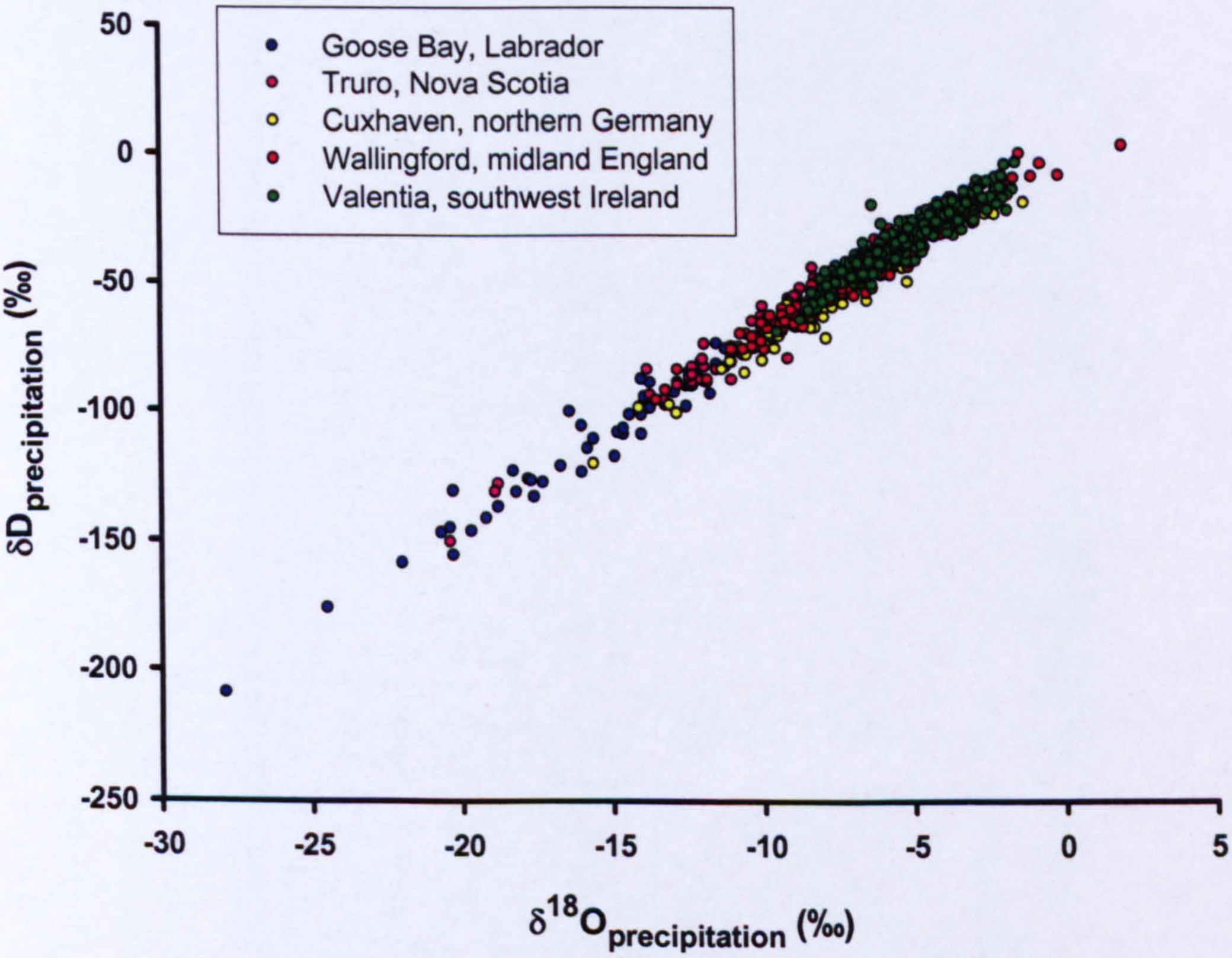

Figure 3.38 Bi-plot of mean monthly δD and δ^{18}O values in precipitation for all GNIP stations (IAEA/WMO, 2004)

Table 3.5 Summary of seasonal means from all GNIP stations (IAEA/WMO, 2004)

		Autumn	Winter	Spring	Summer
Goose Bay	$\delta^{18}O$	-14.6	-19.8	-15.4	-12.4
	σ	2.1	4.0	3.0	1.4
	δD	-102.0	-142.0	-113.9	-89.2
	σ	15.6	30.5	22.5	12.0
Truro	$\delta^{18}O$	-8.5	-12.6	-8.8	-7.0
	σ	1.9	3.3	2.4	1.3
	δD	-56.7	-87.5	-62.2	-48.9
	σ	15.3	24.4	18.3	11.2
Valentia	$\delta^{18}O$	-5.4	-6.0	-5.2	-4.3
	σ	1.6	1.3	1.5	1.3
	δD	-33.4	-38.9	-34.1	-28.5
	σ	11.0	10.4	11.3	10.3
Wallingford	$\delta^{18}O$	-7.1	-7.9	-6.7	-5.1
	σ	1.9	1.9	2.3	1.7
	δD	-47.2	-53.5	-46.5	-35.8
	σ	14.5	14.5	16.6	12.6
Cuxhaven	$\delta^{18}O$	-6.8	-8.0	-6.6	-6.2
	σ	1.5	1.9	2.2	1.3
	δD	-45.9	-58.3	-48.3	-43.3
	σ	11.9	15.7	17.3	9.6

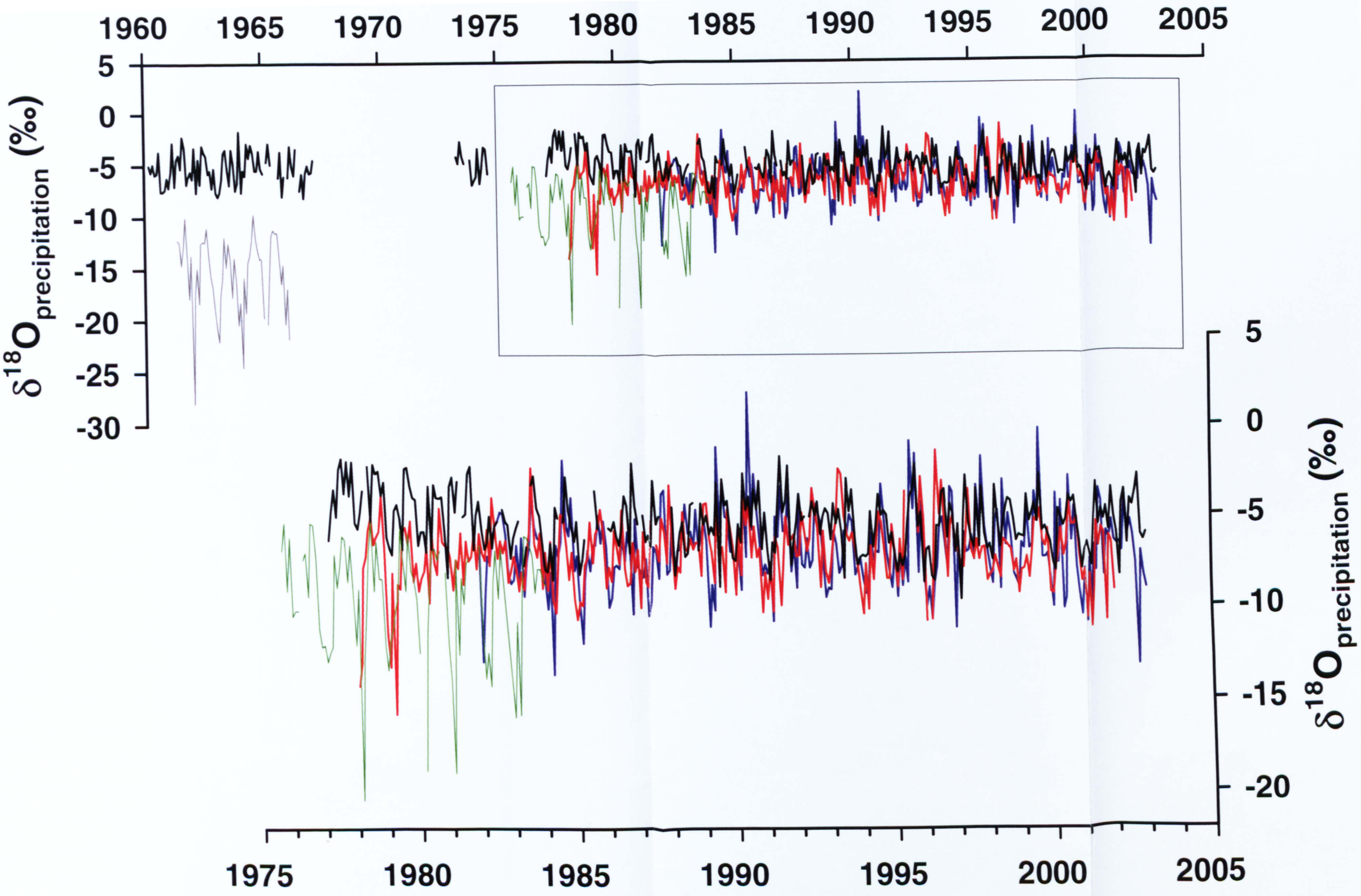

Figure 3.39 Monthly time-series of $\delta^{18}O_{precipitation}$ values for data from all five GNIP stations used in this study (IAEA/WMO, 2004) (dark gray = Goose Bay, light green = Truro, black = Valentia, blue = Wallingford, red = Cuxhaven)

Despite the wide variability observed between individual monthly data and surface air temperature for the European sites, longer-term (decadal) monthly means and seasonal means for these data indicate that there is significant correlation between surface air temperature and $\delta^{18}O_{precipitation}$ values at each of the locations used in this study. At all stations, precipitation is isotopically lighter during winters than summers. Furthermore, the lightest values with the greatest range are observed at Goose Bay where mean annual temperatures are lowest and show most seasonal variation. The site with the least range in isotopic monthly values (Valentia) is the site with the smallest range in mean annual temperature (Diefendorf and Patterson, 2005). Isotope-temperature coefficients have been derived for variability over the decadal timescale that are lower than expected and lower than would be generated using all monthly data. The consequence of these low coefficient values is that large temperature changes are predicted for relatively small changes in isotopic composition.

These empirical relationships with temperature are complicated by the existence of statistically significant correlations between $\delta^{18}O_{precipitation}$ values and the amount of precipitation at Valentia (annual) and Wallingford (summer precipitation amount only). At Cuxhaven and over the Atlantic provinces of Canada, however, no clear correlation is observed between $\delta^{18}O_{precipitation}$ values and the amount of precipitation at either the monthly or longer-term decadal timescale.

The reconstruction of past temperatures from palaeo-isotopic data will therefore be complex. It has been described in Chapter 2 how the isotopic composition of precipitation provides a history of rainout along the trajectory of a moist air mass, which in turns relates to the amount of cooling of that air mass due to advection (both horizontally and vertically) between vapour source region and study site. In the mid-latitudes, correlation has previously been demonstrated with surface air temperature (Dansgaard, 1964; Siegenthaler and Oeschger, 1980; Rozanski *et al.*, 1992; Rozanski *et al.*, 1993) in agreement with analysis of GNIP data here. However, reconstruction of temperature from archives analysed later in this study will be complicated for two reasons. Firstly, there remains a statistically significant relationship with precipitation amount in the modern day at both Wallingford and Valentia despite the link with temperature which must inevitably act to distort the temperature relationship. Secondly,

strong evidence exists for palaeo-atmospheric circulation change through Holocene (Edwards *et al.*, 1996; Magny and Begeot, 2004; Magny *et al.*, 2006) which may have altered the modern ΔT - $\Delta\delta^{18}O_{precipitation}$ relationship over the timescales of interest at any of the study sites. The reliability of any temperature reconstructions derived from the palaeo-data in this project must therefore be interpreted with caution.

4 Methods

4.1 *Introduction*

The following sections detail the methods that were used to collect and analyse the data. Justification for a method is given with particular reference to the aims and objectives of the study. The chapter begins with details on the selection of coring location within the sites previously described (Chapter 3). A large degree of methodological development was undertaken to devise a procedure that could isolate *Sphagnum* cellulose from the peat for isotopic analysis. The rationale behind this developmental work is briefly summarised from the earlier discussion in section 2.4.1. The separation techniques investigated and the final procedure used are documented here. The remainder of the chapter summarises mass spectrometry procedures, sampling procedures for obtaining modern isotopic calibration data, established palaeoecological preparation procedures and the chronological strategy used to develop a chronostratigraphical framework that was sufficiently detailed to answer the research questions of this project.

4.2 *Core location selection, retrieval and storage*

Prior to collection of the main core for laboratory analysis, a stratigraphical survey was carried out in addition to analysis of aerial photography and Ordnance Survey data in order to determine the optimal coring location. The optimal location was required to satisfy a number of criteria relating to broader project objectives. These were

1. Maximisation of *Sphagnum* depth within the core from which isotopic data could be derived.
2. Maximisation of depth of ombrotrophic status in order to maximise the length of the Holocene period from which climatic data could later be extracted.
3. Collection of a core from a lawn-location that showed evidence of sensitivity to changes in past bog surface water tables (Barber *et al.*, 1998).
4. Minimal evidence of surface disturbance.

5. Evidence for rapid and continuous accumulation.

At all sites, the locations that most closely matched these criteria were typically close to the crown or highest point on the present bog surface. In minor modification to the recommendations of Barber *et al.* (1998) final cores were taken from bog surface positions more similar to wet-lawn or pool edge where possible rather than mid-lawn positions. These locations offered a good balance between the sensitivity to change, as detected during the field stratigraphical survey, and conditions suitable for maximised *Sphagnum* presence throughout the core.

At each site, the stratigraphical survey consisted of a spatial array of full depth corings on which sedimentological changes were recorded using standard descriptive systems (von Post, 1924; Troels-Smith, 1955) and plotted using the Troels-Smith Plotting Program (TSPP) (Duller, 1995) (Chapter 3). Stratigraphy cores were taken using a 4cm x 1m bore Russian corer from a single borehole to the base of the peat. Peat bases were identified by the presence of lacustrine clays or silts below layers containing fen peat. Fen peat was identifiable by the distinctive remains of *Phragmites spp* in association with other nutrient demanding species. The pattern of the arrays involved two intersecting transects with cores taken at regular spacing and GPS locations noted. Higher spatial resolution coring took place subsequent to analysis of the initial transect data to determine optimal location. Data from these surveys are presented in the site descriptions in Chapter 3.

Master cores were taken from the optimal location using a 9cm x 30cm large bore Russian corer. Separate 30cm sections were taken alternately from two adjacent bore holes (Barber *et al.*, 1998) < 1 metre apart and overlapped by 5cm to avoid the need to sample disturbed end sections of cores. The master cores were transported with the minimum of disturbance to the laboratory and stored at 4°C in dark conditions in order to prevent bacterial and fungal decomposition.

4.3 *Isotopic methods*

4.3.1 Development of an isotopic preparation method

4.3.1.1 Isolation of *Sphagnum* from the peat matrix

Progress in the use of isotopic proxies from peat has been limited by the need for large sample sizes for mass spectrometry which inevitably meant the use of a mixture of peat plants in any sample. As described in Chapter 2, the difference in isotopic composition between vascular plants and non-vascular plants (Brenninkmeijer *et al.*, 1982; Ménot-Combes *et al.*, 2002) and indeed within a single leaf of a vascular plant (Helliker and Ehleringer, 2002) is typically greater than the variation due to changes in the isotopic composition of the plant source water which is linked to climate. The availability of new technology in the form of continuous flow isotope ratio mass spectrometry (CF-IRMS) has allowed for the analysis of organic samples ~0.3-0.35mg in dry weight for oxygen and with on-line equilibration (Filot *et al.*, 2006), ~0.5-0.7mg dry weight for hydrogen. The possibility of smaller sample sizes has opened up the potential for the generation of species-specific isotopic analyses for oxygen and hydrogen. The influence of mixed species and the case for a *Sphagnum*-specific approach has been discussed in section 2.4.1. Despite the sample size improvement, the practicalities of separating individual species from the mixture of plant components present in the peat matrix and recovering a *Sphagnum*-specific residue remains problematic.

The development of an on-line equilibration method for analysis of the hydrogen isotopic composition of organics is very recent (Filot *et al.*, 2006). In the design stages of this study, it was expected that hydrogen analyses would be undertaken on nitrated *Sphagnum* cellulose. Nitration is a procedure used to replace oxygen-bound exchangeable hydrogen atoms with a Nitrogen unit (section 2.4.2). Using this procedure, it was expected that for each sub-sample 32-33 mg of dry weight *Sphagnum* would be required.

A new method had to be devised that separated *Sphagnum* from the matrix with high enough yields to satisfy this mass requirement on a timescale commensurate with that of the project.

Trial experiments indicated that micromanipulation (or picking) of *Sphagnum* remains from each sub-sample would be ineffective in achieving the desired weight in the timescale available. Conversely, use of bulk sub-samples had been shown to produce misleading results (section 2.4.1). Therefore, a sample-scale separation procedure was required.

Bulk separation procedures are problematic due to similarity in the properties of the various plant remains. The plant remains typically have similar chemical properties. All are composed of plant cell wall structures that include cellulose and hemicelluloses. Many contain more complicated carbohydrates such as lignin. Particularly in the case of sedges and mosses, the density of fragmented remains is frequently similar. Despite clear differences in physical dimensions when alive, fragmented sub-fossil remains are often variable in size, especially with partial decomposition or degradation.

To develop a method that reliably achieved *Sphagnum* separation from the peat matrix experiments were conducted on a number of sub-sample preparation techniques.

The techniques used were:

Separation by grain size differences (sieving)
Rate Zonal Density separation (centrifugation)
Isopycnic sucrose density gradient separation by unit gravity (settling)
Elutriation

Isopycnic density gradient separation is a procedure used frequently in medical sciences for the separation of cellular or sub-cellular material (White, 1995; Moon *et al.*, 1996). For relatively dense materials heavy liquids such as sodium polytungstate are used as a density gradient medium (Dyrkacz *et al.*, 1996) and regularly used in pollen concentration (Regnell and Everitt, 1996). For the purpose of this experiment, sodium polytungstate was prohibitively expensive. An alternative medium used in medical and soil sciences is a sucrose solution. A density gradient of 10ml layers of 10-50% sucrose solution was prepared at 10% increments in a 50ml test tube. Samples were subjected to both separation by unit gravity and accelerated separation by centrifugation. Although some separation of peat components was

achieved, the procedure failed to produce sufficient quantities of material and failed to separate grass remains from *Sphagnum* remains. There was also a potential problem with contamination of the cellulose isotopic signal by the use of sucrose.

Separation by grain size fraction was tested using a stacked sieve system. The mesh sizes were selected based on published data on *Sphagnum* branch leaf size (Daniels and Eddy, 1990). The system consisted of four sieves of 1000, 500, 250 and 125 μm mesh. Subsamples were prepared by washing 4 cm^3 subsamples through the stacked sieves using 5l of tap water. Size fractions were then observed under a stereoscopic binocular microscope and digital photos taken to identify the grain size with the highest proportion of *Sphagnum* remains.

The grain size separation procedure was remarkably effective. Best results were achieved in the upper peats where little degradation of the remains has led to grain sizes similar to modern living plant material. Typically, branch-free *Sphagnum* section *Sphagnum* leaves collect in the 500 μm sieve and section *acutifolia* and *cuspidata* leaves collect in the 250 μm sieve. This distribution is complicated in the preparation of fresh peat layers where branch leaves remain attached to the branches in "bunches". These bunched units typically have similar grain sizes within any stratigraphical level and concentrate in one of the sieve size fractions during preparation. For example, section *acutifolia* bunches frequently collect in the 500 μm mesh sieve, whilst section *Sphagnum* bunches often collect in the 1000 μm mesh sieve. In these upper peats the sieved fraction with the highest concentration of *Sphagnum* remains was often the 1000 μm mesh fraction. These remains could then be picked and washed of non-*Sphagnum* material in an efficient process.

Despite the concentration of *Sphagnum* remains in a particular size fraction which differed depending on the species mixture, non-*Sphagnum* elements inevitably remained. These elements typically fell into two categories. The first was sedge remains. The second was fragments of dicot remains. Separation of heavy particles from light particles by washing (elutriation) was tested at this stage with excellent results. A gold-panning technique or hand-swilling procedure was applied to the sieved fraction with the greatest proportion of free *Sphagnum* leaves in a 4.5cm radius plastic Petri-dish. During elutriation denser elements settled out in the centre of the Petri-dish and less dense elements were carried by the agitated

water to the rim of the Petri-dish. The results of elutriation can be seen in the sample in Figure 4.1 below.

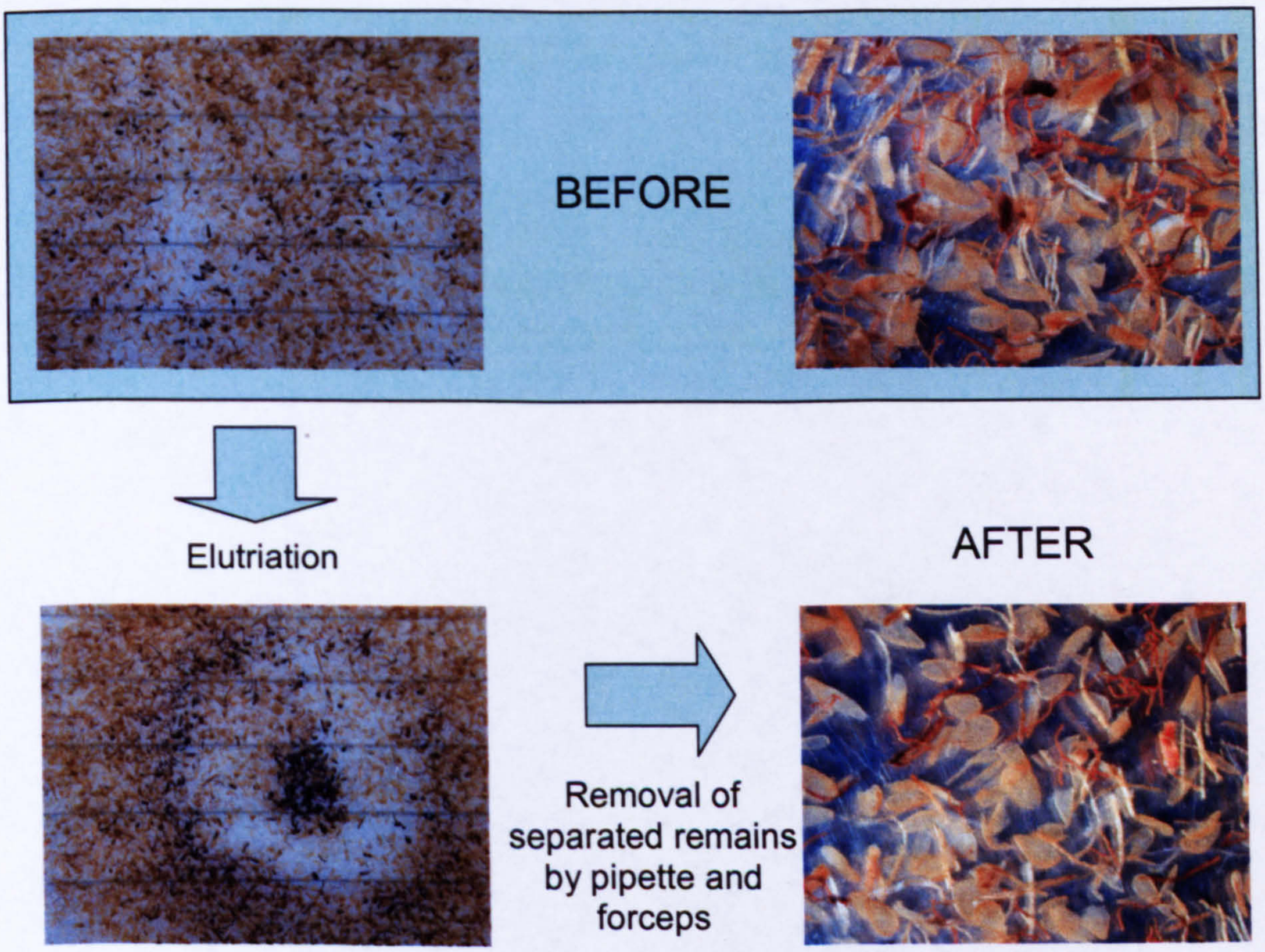

Figure 4.1 Photographic results of the elutriation process at Petri-dish scale and at 10x magnification (before and after). Absence of heavy dicot remains and reduction in fine ericaceous rootlets and sedge roots is observed.

Heavy elements that concentrated in the centre of the dish were removed by pipette. Lighter (sedge) remains and longer ericaceous rootlets were removed from the rim zone using precision forceps. A successful pairing of grain size separation, selection of size fraction with the greatest proportion of free *Sphagnum* leaves and elutriation produced *Sphagnum* concentrate samples of improved purity in comparison to bulk sub-samples.

This chosen technique for the preparation of *Sphagnum* concentrate samples from bulk sub-samples was tested for isotopic composition using 25 levels from core WLM22 against

corresponding preparations of pure *Sphagnum*, bulk alpha-cellulose and raw material. Results are presented below.

4.3.1.1 Preparation test results and discussion

The purpose of the preparation test was to establish the performance of various preparation techniques in their approximation of the *Sphagnum*-specific isotope signal from core samples. The need to perform this test was driven by the impracticality of generating the volumes of material required for analysis by simple picking of pure *Sphagnum*. The results below strongly suggest that *Sphagnum* concentrates represent a considerable improvement in approximating the signal compared with techniques used previously.

$\delta^{18}O$ values for all preparations from core WLM22 and corresponding species mixture index value are presented in Table 4.1. The effect of the isolation of alpha-cellulose on $\delta^{18}O$ values is shown in Figure 4.2. $\delta^{18}O_{bulk\ raw}$ values are consistently depleted with respect to those of $\delta^{18}O_{bulk\ \alpha\text{-}cell}$. Despite this consistency, the extent of depletion is highly variable. Samples in the middle section of the core show greatest separation. Conversely, five samples (144, 148, 152, 156 and 160 cm) all have an isotopic composition that falls within the 0.32 ‰ precision inherent in the analytical technique and so may be considered identical within measurement precision.

Table 4.1 $\delta^{18}O$ values for all preparations from WLM22 including the difference between $\delta^{18}O_{Sphag\text{-pure}}$ and $\delta^{18}O_{Sphag\text{-conc}}$ values ($\delta^{18}O_{Sphag\text{-conc}}$ residuals) and species mixture ranking

Depth	$\delta^{18}O_{Sphag\text{- pure}}$	$\delta^{18}O_{Sphag\text{ -conc}}$	$\delta^{18}O_{bulk\ \alpha\text{-cell}}$	$\delta^{18}O_{bulk\ raw}$	$\delta^{18}O_{Sphag\text{ -conc residuals}}$	1-5 contamination
128	18.83	19.93	19.84	17.90	1.10	1
136	21.38	21.12	21.22	19.81	-0.26	1
144	20.30	21.45	20.70	20.32	1.16	1
328	21.92	22.53	21.57	19.85	0.62	1
132	18.51	20.25	19.99	16.74	1.74	2
148	19.91	21.02	19.77	19.13	1.11	2
152	21.14	21.74	20.36	20.00	0.59	2
176	21.30	21.82	19.87	19.14	0.52	2
112	21.62	21.96	21.58	19.74	0.35	3
124	18.69	20.04	21.05	16.90	1.36	3
140	20.58	21.26	22.18	19.19	0.68	3
156	21.52	22.39	20.61	20.38	0.87	3
160	21.02	21.65	19.76	19.43	0.63	3
336	20.23	22.34	20.67	19.61	2.11	3
344	20.67	21.00	19.93	18.76	0.32	3
120	21.21	21.62	21.41	18.61	0.41	4
224	21.26	21.81	22.12	16.92	0.54	4
288	21.58	22.32	21.35	18.27	0.74	4
216	21.73	22.82	22.07	17.76	1.10	5
232	19.51	21.02	22.01	17.96	1.51	5
240	21.95	22.01		17.08	0.06	5
256	21.16	24.00	22.94	18.40	2.85	5
264	20.88	23.13	23.67	17.81	2.25	5
384	22.33	22.49	26.50	21.10	0.16	5
392	22.03	24.61	24.06	18.74	2.58	5

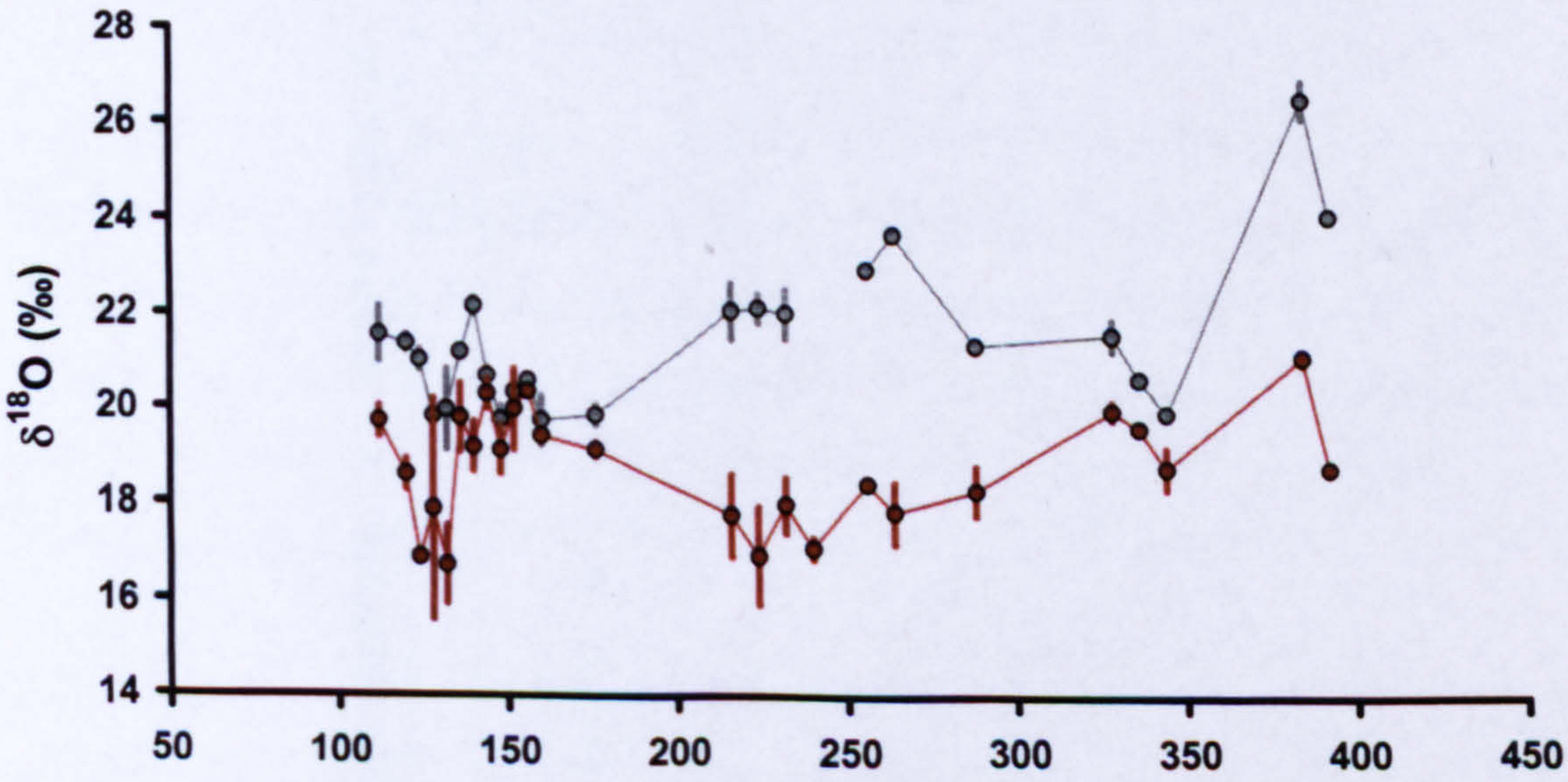

Figure 4.2 $\delta^{18}O_{bulk\ raw}$ (brown line) versus $\delta^{18}O_{bulk\ \alpha\text{-cell}}$ values (grey line). 2σ range on duplicate measurements is given (vertical bars).

The differences observed between bulk plant and cellulose $\delta^{18}O$ values are due to the presence in bulk plant material of lipid and lignin fractions depleted in $\delta^{18}O$ in comparison to cellulose (Green, 1963; Wilson and Grinsted, 1977; Loader *et al.*, 2003). The lack of a constant offset relates to changes in the relative species abundance in each sample. For an individual species the offset should be consistent relating to the proportion of cellulose in the plant type (Green, 1963; Wilson and Grinsted, 1977; Menot and Burns, 2001). In the peat matrix, the mixture of plant species results in a percentage of cellulose that is specific to any particular depth. Because the proportion of lignin and lipid fractions in *Sphagnum* is low (van Breemen, 1995; Menot and Burns, 2001), those bulk samples composed almost exclusively of *Sphagnum* show high similarity between bulk and cellulose $\delta^{18}O$ values. Samples with greater proportions of vascular plants will show increased separation between bulk and cellulose values proportional to cellulose composition.

Figure 4.3 and Figure 4.4 show oxygen isotope values with depth for bulk alpha-cellulose ($\delta^{18}O_{bulk\ \alpha\text{-cell}}$) and *Sphagnum* concentrates ($\delta^{18}O_{Sphag\text{-conc}}$) compared against those of the pure *Sphagnum* preparation ($\delta^{18}O_{Sphag\text{-pure}}$). Whilst both $\delta^{18}O_{bulk\ \alpha\text{-cell}}$ and $\delta^{18}O_{Sphag\text{-conc}}$ values show differences from $\delta^{18}O_{Sphag\text{-pure}}$ values, it should be seen that variance in the pure samples is better preserved in the *Sphagnum* concentrate samples than in bulk alpha-cellulose.

Figure 4.3 provides evidence of similarity in structure between 112cm and 160cm despite variable magnitudes. Samples in the middle section of the core show little correlation. Values within the precision of the analytical technique are found in levels 288, 328 and 336cm. Isotopic depletion is observed in samples 152-176cm and is unexpected. Samples deeper in the core show high variability including a ~6‰ difference in $\delta^{18}O$ value between preparations in sample 384 cm.

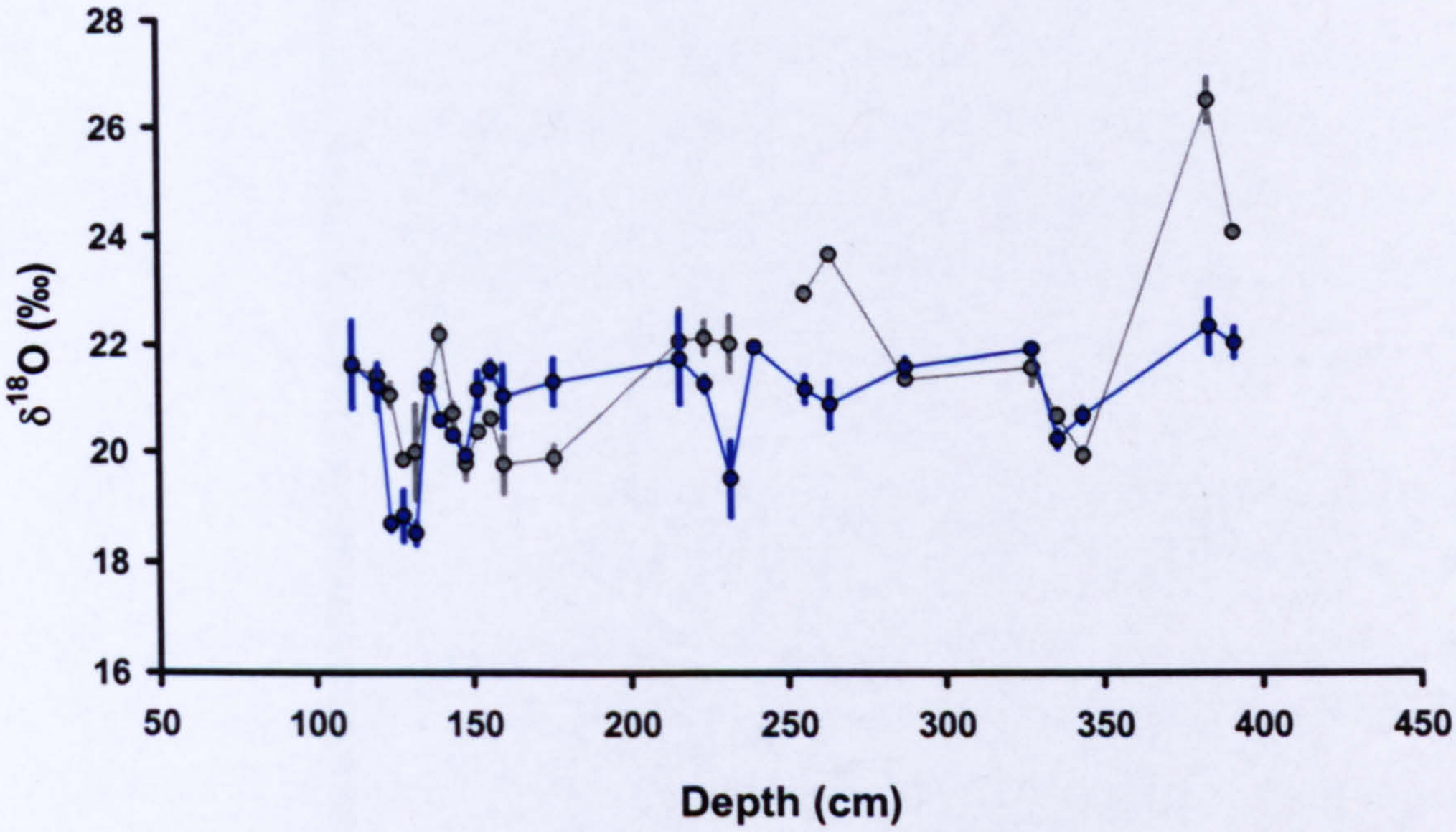

Figure 4.3 $\delta^{18}O_{Sphag\text{-}pure}$ (blue line) versus $\delta^{18}O_{bulk\ \alpha\text{-}cell}$ values (grey line). 2σ range on duplicate measurements is given (vertical bars).

In *Sphagnum* dominant sediments, the bulk alpha-cellulose values approximate the pure signal relatively well (112cm -160 cm). This is because the signal is driven by the dominance of *Sphagnum* species in these levels. The bulk isotopic signal is therefore statistically similar to the pure *Sphagnum* $\delta^{18}O$ values. In those samples where *Sphagnum* comprised only a small component, little agreement is observed. Isotopic depletion in some bulk samples relative to the pure values (152-176cm) is unexpected. Theoretically, *Sphagnum* should provide the least enriched isotopic values as a result of the simple pathway by which water is incorporated as cellulose (Zanazzi and Mora, 2005) assuming the source water is the same for all plants at a given core depth. In vascular plants, the transport and fractionation of water should lead to enriched $\delta^{18}O$ values in cell wall tissues (Epstein *et al.*, 1977; Brenninkmeijer *et al.*, 1982; Sternberg *et al.*, 1984a; Sternberg *et al.*, 1986; Ménot-Combes *et al.*, 2002). The consistent depletion across a range of samples coupled with the low standard deviations from replicate analyses suggests that the signal was not a product of chance analysis of a misrepresentative fraction of cellulose. Analyses of photographs reveal no obvious species percentage based reason for the depletion. It is possible that depleted water, sourced from greater depth by vascular plant roots during cellulose synthesis is responsible for this depletion. With this

argument, isotopic depletion would be proportionally independent of changes in the percentage of vascular roots. Determination of the isotopic composition of vascular roots would therefore rely on the isotopic composition of water at depth during plant growth. The roots of grasses have been shown to extend up to 60 cm in depth (Boggie *et al.*, 1958) which may represent the sourcing of water 100s of years old in vascular plant cellulose synthesis. If this water was isotopically depleted in comparison with the surface water, this could explain the relative enrichment observed in the pure-*Sphagnum* samples at these levels.

Figure 4.4 shows the isotope stratigraphy of the pure samples compared against those using the new concentration technique. Unlike $\delta^{18}O_{bulk\ \alpha\text{-cell}}$ values in Figure 4.3, the structure of variability in pure samples is much more closely preserved in $\delta^{18}O_{Sphag\text{-conc}}$ values across the full depth range of the core samples, not simply in the upper sections. Most transitions are marked by a change of similar magnitude as well as direction despite the apparent enrichment of $\delta^{18}O_{Sphag\text{-conc}}$ values by ~1‰. Slight underestimation of the magnitude of change towards isotopically depleted values is also observed. Anomalously enriched values are constrained to three samples: 256cm, 264cm and 392cm.

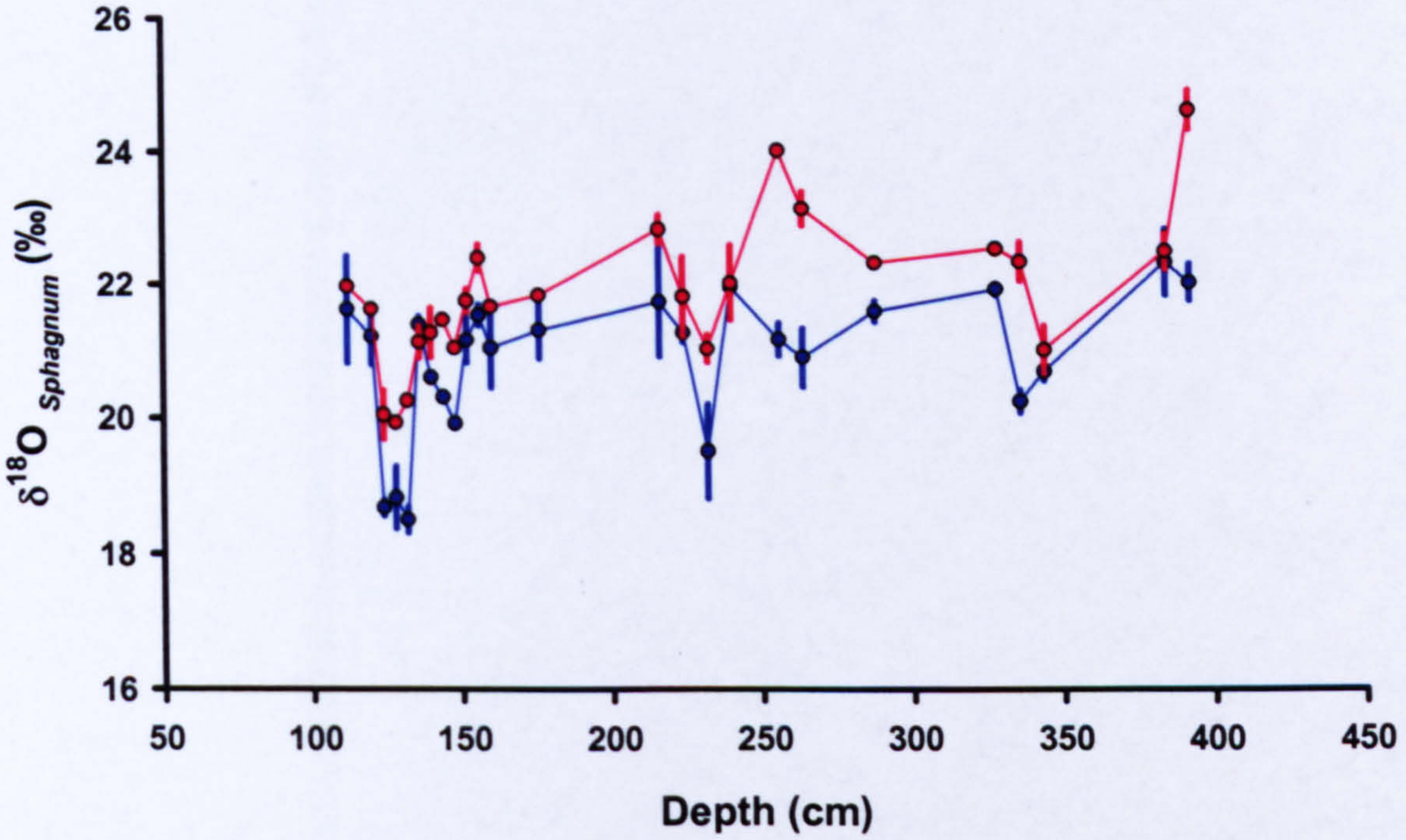

Figure 4.4 $\delta^{18}O_{Sphag\text{-pure}}$ (blue line) versus $\delta^{18}O_{Sphag\text{-conc}}$ values (red line). 2σ range on duplicate measurements is given (vertical bars).

To summarise, where lack of correspondence is noted between bulk cellulose values and pure values, these can be explained by the mixture of species present in the sub-sample, consistent with findings in previous research that demonstrated dominance of a species signal (Brenninkmeijer *et al.*, 1982; Dupont, 1986; Dupont and Mook, 1987; van Geel and Middeldorp, 1988). Data from *Sphagnum* concentrates, however, clearly reveal a marked improvement in the approximation of pure *Sphagnum* isotopic composition. Three data exhibit anomalously enriched values. All three of these samples are ranked 5 in the 5 point scale of source sample component-species mixture indicating a highly mixed peat substrate (Table 4.1). The anomalous enrichment of these samples is consistent with the presence of vascular material which distorted the *Sphagnum* signal in the respective concentrate preparations.

In addition to the records plotted against depth above, the improved performance of *Sphagnum* concentrates over bulk samples is demonstrated in Figure 4.5 and Figure 4.6. They

display the linear regressions of bulk samples and concentrates against pure samples respectively. Measures of correlation and significance show improvement afforded by the *Sphagnum* concentration method (Table 4.2). If two preparations are replicating each other identically the regression takes the form $y = 1x + 0$ with $r^2 = 1$. The coefficient of determination (r^2) shows a marked improvement for the regression of *Sphagnum* concentrates compared to bulk samples (Figure 4.5, $r^2 = 0.25$; Figure 4.6, $r^2 = 0.53$). Pearson correlation coefficient also shows improvement where an integer of 1 equals perfect positive correlation (0.73, pure versus concentrates; 0.50, pure versus bulk alpha cellulose).

Table 4.2 Pearson correlation and r^2 for data from three preparation procedures with $\delta^{18}O_{Sphag\text{-}pure}$ values

	Pearson correlation	r^2
$\delta^{18}O_{Sphag\text{-}conc}$	0.73	0.53
$\delta^{18}O_{bulk\ \alpha\text{-}cell}$	0.50	0.25
$\delta^{18}O_{bulk\ raw}$	0.44	0.19

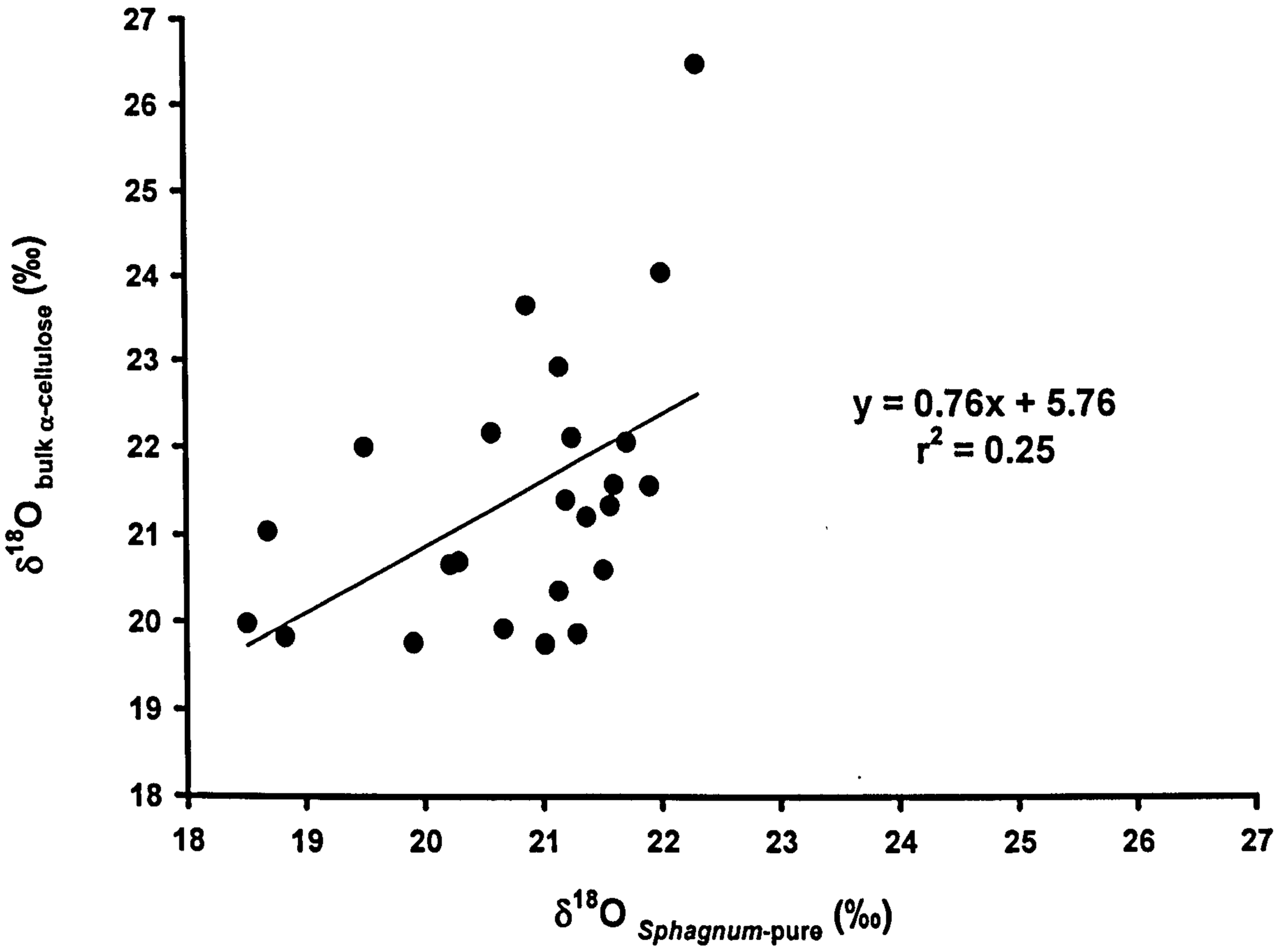

Figure 4.5 Bi-plot of $\delta^{18}O_{Sphag\text{-pure}}$ and $\delta^{18}O_{bulk\ \alpha\text{-cell}}$ values for sample levels in the preparation test

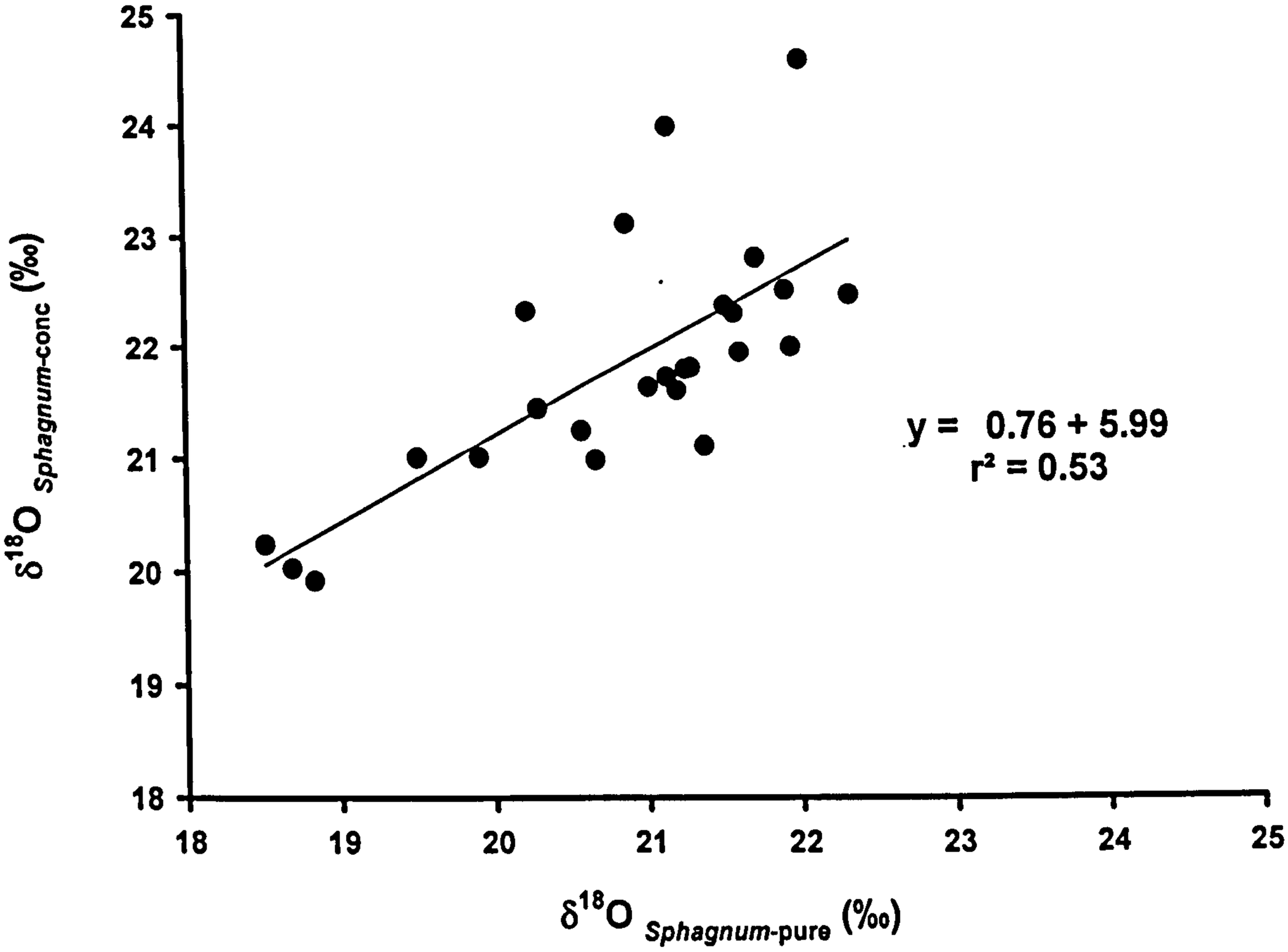

Figure 4.6 Bi-plot of $\delta^{18}O_{Sphag\text{-}pure}$ and $\delta^{18}O_{Sphag\text{-}conc}$ values for sample levels in the preparation test

Figure 4.7 shows a plot of isotopic residuals derived from the arithmetic difference between $\delta^{18}O_{Sphag\text{-}conc}$ values and $\delta^{18}O_{Sphag\text{-}pure}$ values versus the degree of species mixture in the source core sample. There is no linear relationship between pure-concentrate $\delta^{18}O$ residuals and the species mixture of the source bulk sample (Figure 4.7). A single factor ANOVA test of the 5 species mixture populations reveals that the residual means show a small amount of inequality that is fractionally statistically significant ($F = 0.924007$; $p < 0.5$). A repeat of the ANOVA test excluding the samples with an index value of 5 reveals the inequality between the group means to be insignificant ($F = 0.464038$; $p > 0.5$).

The increase in variance with increasing source material species mixture is consistent both with the ANOVA results and with the interpretation of the influence of species mixture in the wide variance of these samples. The small standard deviations in replicate analyses of the

samples indicate that the measured values are representative of the whole sample and typically within analytical error. The variance increase with species mixture is therefore indicative of a real species signal induced by the influence of vascular plant isotopic composition. The lack of a linear relationship suggests that the degree of influence may be species dependent. Whilst variance in the $\delta^{18}O_{Sphag\text{-}conc}$ values is shown to increase with species mixture, 72% of the residuals fall within 1σ of the residual mean (0.99 ‰) for the entire sample population (n = 25).

The general consistency of residual means reflects the performance of the concentrate methodology. The similarity in residual means for a large range of species mixtures indicates that the method is working well to approximate the isotopic composition of *Sphagnum*. The data indicate, however, that samples taken from very mixed core levels should be interpreted with care. The mean ~1‰ enrichment present in those residual means represents the influence of vascular material that persists in *Sphagnum* concentrate preparations. The relatively consistent nature of this offset across a range of species mixtures in source material is promising for the application of the method because it is not introducing a highly variable signal. Rather, contrary to previous peat studies where the signal excessively over-amplified by species variability (Brenninkmeijer *et al.*, 1982; Dupont and Brenninkmeijer, 1984; Dupont and Mook, 1987; van Geel and Middeldorp, 1988), the concentrate method provides a fast and more robust approximation of the climate signal.

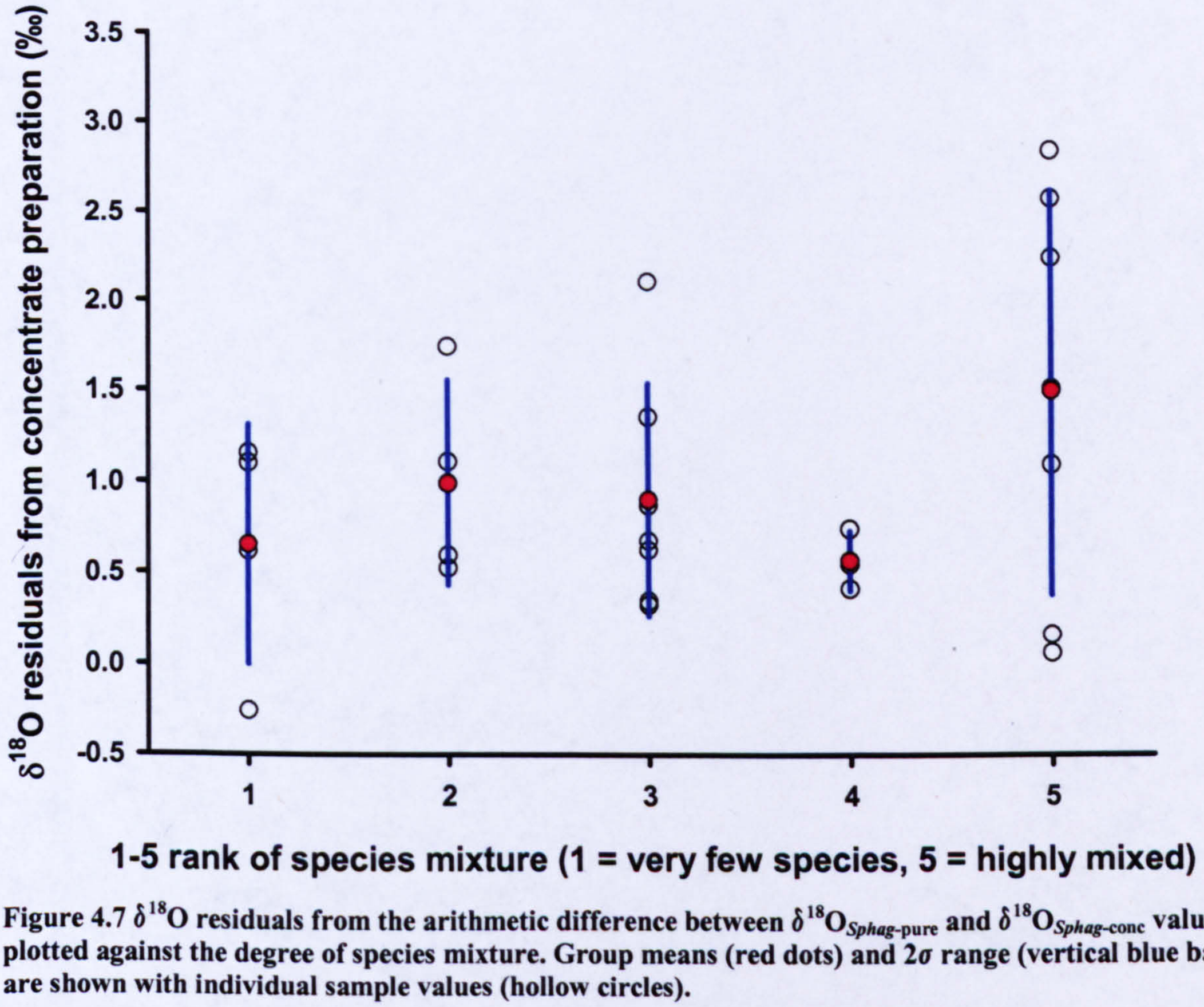

Figure 4.7 $\delta^{18}O$ residuals from the arithmetic difference between $\delta^{18}O_{Sphag\text{-}pure}$ and $\delta^{18}O_{Sphag\text{-}conc}$ values plotted against the degree of species mixture. Group means (red dots) and 2σ range (vertical blue bars) are shown with individual sample values (hollow circles).

4.3.1.2 Quantifying *Sphagnum* concentrate measurement error

Whilst the measurement precision of CF-IRMS is well known through extensively repeated measurement of industry reference cellulose samples (e.g. Sigma & IAEA; see source details below: Table 4.3), the variability attributable to the *Sphagnum* concentrate preparation procedure required quantification. Ten replicate sub-sample preparations were made from the same stratigraphical level and subjected to identical treatment through to measurement. Each sample was measured in triplicate. The results from all 30 measurements and the means of all 10 sub-samples are given in comparison with data for cellulose reference samples run in the same sequence in Table 4.3.

Table 4.3 $\delta^{18}O$ values for replicate measurement data from *Sphagnum* preparation error test (IAEA cellulose: Vienna, IAEA C3 cellulose; Sigma cellulose: Batch No 92F0243, 99.5% α-cellulose)

	All	10 replicates	Sigma	IAEA
Mean	19.22	19.22	27.50	31.58
Stdev	0.32	0.20	0.21	0.41
n	30	10	19	5

The standard deviation of the ten replicates is actually less than the same measure for the reference cellulose samples (0.20‰ versus 0.21‰ for Sigma and 0.41 ‰ for IAEA; Table 4.3), indicating both excellent sample homogeneity and excellent replicability of the *Sphagnum* concentrate technique. Application of the standard deviation of 0.32‰, reflecting the range on all 30 measurements, provides a robust measurement error for the oxygen isotopic measurement of *Sphagnum* concentrates.

4.3.1.3 Alpha-cellulose extraction

The benefits of the use of alpha-cellulose have been discussed in section 2.4.3. The procedure followed for the isolation of alpha-cellulose was based on a modification of the procedure used on wood slivers (Green, 1963; Loader *et al.*, 1997; Rinne *et al.*, 2005). The chemical composition of *Sphagnum* is relatively simple compared with wood cellulose (van Breemen, 1995; Pendall *et al.*, 2001). Filtration during early efforts at cellulose extraction was found to be prohibitively slow due to the breakdown of the simpler cellular material into very fine grained material that formed a gel-like substance. This was particularly the case following a boiled water wash and again during the 17% NaOH treatment stage as found by other workers (Borella *et al.*, 2004).

Tests were conducted on the chemical composition of the organic residue at different stages in the alpha-cellulose isolation procedure by infra-red spectroscopy in collaboration with Anglia Ruskin University, Cambridge. This was done to assess whether the procedure could be improved. Modifications were then able to be made which reduced the length of the extraction procedure and enabled the isolation of fibrous chains of alpha-cellulose from the moss. In addition, new glassware was designed and commissioned specifically for *Sphagnum* filtration

with the sinter placed closer to the mouth of the vessel providing a greater surface area than that used in wood cellulose extraction (Loader *et al.*, 1997)(Figure 4.8). This modified procedure of Rinne *et al.* (2005) for the isolation of alpha-cellulose from *Sphagnum* moss is summarised below. For more detailed description, the reader is referred to Rinne *et al.*, (2005).

Figure 4.8 New chemical extraction glassware

Raw sub-samples were transferred to glass Soxlet vessels (extraction tubes) comprising a material chamber ~2 cm^3 and a p1 porosity glass sinter filter (Figure 4.8) with equal diameter to the material chamber. Extraction tubes containing samples were suspended in a water bath at 70°C. Acidified $NaClO_2$ (aq) was added to each tube and left to react for one hour. Following the hour samples were filtered *in vacuo*. This bleaching treatment was repeated up to a total of 5 times. After the 5^{th} treatment samples were washed with 2 ml boiling double distilled water and filtered *in vacuo* immediately. A further five 2 ml double distilled water washes were made to ensure the removal of bleaching treatment agents from the residue. Samples were then treated to 2 ml of 10% NaOH at 80°C for 45 minutes and filtration *in vacuo*. This was followed by five further 2 ml double distilled water washes, a single 2 ml 1% HCl wash and another five 2 ml double distilled water washes until neutral pH value of 7 was achieved.

Samples were transferred to 2 ml plastic eppendorf tubes and filled with 1ml of 4°C double distilled water. They were then homogenised using an ultrasonic probe for at least 30 seconds until the alpha-cellulose was fully mixed. Samples were then freeze-dried over two days (~ -50°C, ~180mb). Alpha-cellulose material was then ready for analysis by mass spectrometry.

4.3.2 Oxygen isotopic analysis

Mass spectrometric analysis of oxygen stable isotopic composition was undertaken using an online method shown to provide reliable results in analyses of tree-ring cellulose (Werner *et al.*, 1996; Saurer *et al.*, 1998). The procedure is described in detail in Saurer *et al.* (1998). In summary, alpha-cellulose samples were pyrolysed over glassy carbon at 1090°C using an ANCA GSL elemental analyser interfaced with a PDZ Europa 20/20 isotope-ratio mass spectrometer and the results expressed in δ notation (‰) relative to VSMOW. The precision of replicate alpha-cellulose extractions from a single core level was ± 0.32‰ (1σ, n = 10) (section 4.3.1.2).

4.3.3 Hydrogen isotopic analysis

Two methods exist for the preparation and measurement of D/H ratios from cellulose. These are nitration or equilibration. The on-line equilibration method (discussed in section 2.4.2) is used here for the benefits offered in terms of the rapidity of the process, the small sample sizes necessary, the limited fractionation effects and the avoidance of dangerous chemical procedures. The procedure used is described in detail in Filot *et al.*, (2006) and is summarised below.

0.5-0.7mg of dry alpha cellulose was weighed into tin capsules and wrapped loosely to allow water vapour to enter whilst remaining closed enough to prevent sample loss. Samples were then placed into an equilibration chamber and subjected to a continuous flow of 'Meerwasser' water vapour of known isotopic composition (+1‰ vs VSMOW) at 110°C and a flow rate of

7.8μL/min delivered by a helium carrier gas stream at 40 mL/min. After 540 seconds the water supply was stopped and the sample transferred into an AS128 autosampler and then the pyrolysis reactor after only a few seconds. Pyrolytic conversion took place at 1450°C over a glassy carbon granulate on a 2mm layer of silver wool and 20 mm bed of quartz wool in a Thermo-Chemical Elemental Analyser (TC/EA). Pyrolysis products were separated using a 1m GC column then carried by a ConFlow II open split unit to a ThermoFinnigan Delta plus XL isotope ratio mass spectrometer. Results are given in standard delta notation vs Vienna Standard Mean Ocean Water (VSMOW). The D/H ratio of non-exchangeable carbon-bound hydrogen was estimated from the bulk hydrogen isotope data using a mass balance relationship (Filot *et al.*, 2006).

4.3.4 Modern sampling for isotopic calibration

Calibration of palaeo-isotope data is essential for reconstruction of the isotopic composition of palaeo-precipitation source waters and further reconstruction of meteorological variables through knowledge of the processes that modify the measured signal (Leng and Marshall, 2004). The source water used for cellulose synthesis in ombrotrophic bog plants resides in two stores in the pathway from precipitation to cellulose. These are bog water and leaf water. Precipitation can rain onto the plant surface and be absorbed directly into the leaf spaces avoiding the bog water store. Alternatively, leaf water and bog water can be at equilibrium where there is regular wetting of the leaves by close proximity to the bog surface or submergence. Measurement of each of precipitation, bog water, leaf water and *Sphagnum* cellulose allows for the estimation of the fractionation effects during the transition between each stage. Measurement across an annual range of meteorological conditions allows the upper and lower limits of the calibration to be estimated. By inverting this model, palaeo-precipitation can be reconstructed from core *Sphagnum* cellulose data.

Although research in the 1980s and 1990s suggested that there was a difference between the isotopic compositions of *Sphagnum* species along a topographic gradient (Brenninkmeijer *et al.*, 1982; Aravena and Warner, 1992), it has been shown more recently that the isotopic difference is not statistically significant (Ménot-Combes *et al.*, 2002) (section 2.4.1). Whilst variability in bog water shows a relationship with surface topography, the isotopic

composition of the moss "dampens" the signal in bog waters (Ménot-Combes *et al.*, 2002). It is possible, however, that observed variability in water and moss may also relate to the period of sampling. In each of these studies, samples have been taken either once or in summer months only when higher evaporation rates would be expected to have a greater influence on distortion of the precipitation signal through kinetic fractionation. As *Sphagnum* moss grows at >4°C under sufficiently moist conditions (Williams, 1996), in many temperate bogs it is possible that the growing season could be long enough to record a near annual signal.

Regular year-round sampling of precipitation, bog water and *Sphagnum* was undertaken to serve the joint purposes of both testing the fraction of the year for which *Sphagnum* was a recorder and also to cover a range of "climates" (Siegenthaler and Oeschger, 1980) that might be expected through the temporal range of the core. In so doing, the climatic range for the calibration of core data was extended. Leaf water samples were collected using a standard method (Pendall *et al.*, 2001) but budget and time constraints prevented their analysis.

Precipitation and bog water data were analysed at the School of Ocean and Earth Sciences, University of Liverpool by Dr. Elizabeth Fisher as part of the ISOMAP-UK project. For hydrogen isotopic analysis, water samples were analysed using a standard zinc reduction method. Stable isotope ratios were measured on an automated VG Isogas Sira 12 triple collecting mass spectrometer and the results expressed using the conventional delta notation δ per mille (‰) relative to the VSMOW (Vienna Standard Mean Ocean Water) and normalized to the SMOW-SLAP Scale using the international standards (IAEA) OH-1, OH-3 and OH-4.

For oxygen isotopic analysis, water samples were analysed using a standard equilibration method. The samples (~ 5 ml) were loaded into glass vessels and an aliquot of CO_2 transferred to the vessel. The sample was then reacted at constant temperature of 25°C for 1-2 days to allow the isotopic exchange between water oxygen and CO_2 oxygen to reach equilibrium. The exchanged CO_2 was then extracted and analysed on a VG SIRA 12 mass spectrometer and the results expressed using the conventional delta notation (δ per mille (‰). The $\delta^{18}O$ ratios are reported versus VSMOW (Vienna Standard Mean Ocean Water).

Unlike previous studies, *Sphagnum* cellulose data were collected at bi-monthly or quarterly intervals throughout the water measurement periods. Data collection comprised five phases: field microsite selection, field sampling, laboratory sub-sampling, alpha-cellulose extraction and mass spectrometric measurement. The latter four phases were conducted identically between sites. The first phase differed between sites based on the satisfaction of key objectives. At Walton Moss, Dosenmoor and Nordans Pond Bog, field microsite selection was based on the need to collect samples from a range of microtopographical habitats. The most objective solution was the random selection of topographic gradients and the systematic sampling along gradients to cover a range of species and habitats. Raheenmore was chosen as a site for its satisfaction of a number of key objectives described in Chapter 3. One of these was the presence of the key Holocene *Sphagnum* species, *Sphagnum imbricatum*. Despite the presence of the species, its abundance was spatially limited. It was necessary to mark the sites at which it was found by flag and return to those same sites during each successive sampling period in order to ensure that the temporal variation in the isotopic composition of this species was measured.

Sphagnum capitula (or heads) (Plate 4.1) were collected from the field using stainless steel scissors and bagged for transport to the laboratory. Depth to water table was measured to a precision of 1cm as the distance perpendicular to the water table from the site of *Sphagnum* sampling. A vegetation survey of an area 15 cm^2 in which the *Sphagnum* was sampled was taken prior to sampling to give context on the proportion of vascular plants that may be modifying the water isotopic signal. The vegetation survey was conducted by visual estimation of percentage spatial cover.

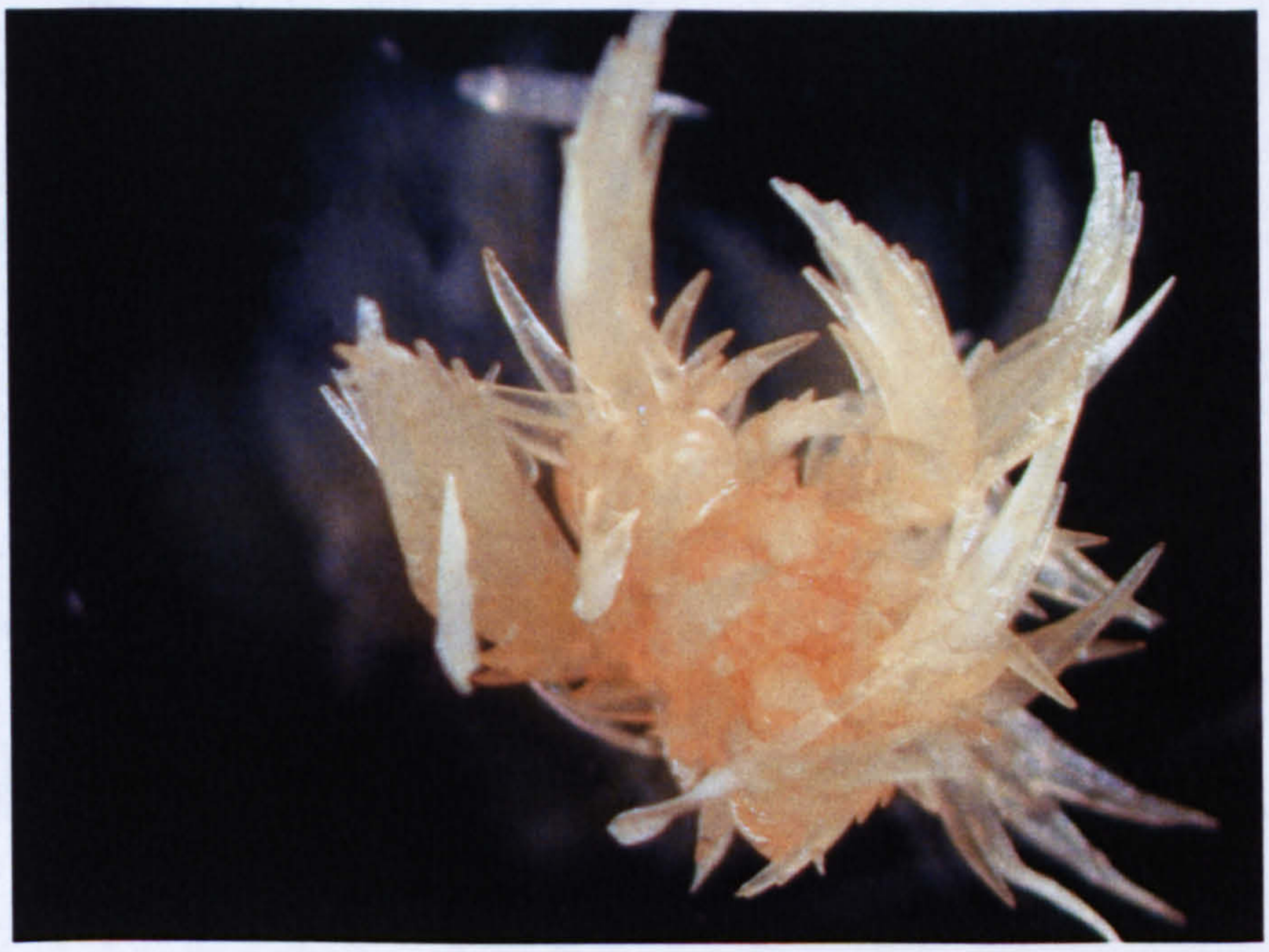

Plate 4.1 Capitulum of *Sphagnum cuspidatum* (photo: T. Daley)

Sphagnum species were identified in the laboratory (Daniels and Eddy, 1990) by the mounting of picked branch and stem leaves under a powerful Nikon 400x magnification microscope. The central capitula, representing the most recent growth, of ≥10 plants were sub-sampled by forceps under a stereoscopic binocular microscope and any non-*Sphagnum* elements removed. Capitula were washed with distilled water and transferred to a glass vial containing distilled water.

Alpha-cellulose was isolated from the modern *Sphagnum* samples using a modification of the standard procedure used for wholewood samples (Green, 1963; Loader *et al.*, 1997), as described above (section 4.3.1.3). Samples were measured for oxygen isotopic composition by an identical procedure to core samples (section 4.3.2). This involved pyrolysis over glassy carbon at 1090°C using an ANCA GSL elemental analyser interfaced with a PDZ Europa 20/20 isotope-ratio mass spectrometer and the results were expressed in δ notation (‰) relative to VSMOW. A selection of samples representing a period of a year from Dosenmoor were also analysed for hydrogen isotopic composition. Samples were subjected to the equilibration and measurement procedure already described for core samples (section 4.3.3).

4.4 *Palaeoecological methods*

4.4.1 Palaeoecological proxy selection

Three main palaeoecological proxy techniques are now routinely used to reconstruct past water table levels from peat cores in multi-proxy studies (Chiverrell, 2001; Blundell and Barber, 2005; Langdon and Barber, 2005). These are plant macrofossil analysis, testate amoebae analysis and peat humification analysis. Due to time constraints and the need to develop, test and implement a new procedure for isotopic analysis, it was not possible to employ all three methods on every core. Selection of the most appropriate indicators for the research questions was required.

Plant macrofossil analysis was considered the most important proxy indicator in addition to *Sphagnum* concentrate isotopic variability because it provides evidence for floral species change. Given that isotopic variability has been previously linked to species change, it was seen as essential that species data be available across the main time periods of interest in the cores. The role of any species-dependent signal in the isotopic variability could then be tested on the core material. Humification data was also ranked in preference to testate amoebae data for the rapidity with which a large dataset could be generated. Despite this rapidity, the interpretative power of humification data has been questioned and variability due to species change suggested (Caseldine *et al.*, 2000; Yeloff and Mauquoy, 2006). The collection of plant macrofossil data in synchrony with humification data allows for direct address of the species issue and hence stronger interpretative power in the resulting palaeo-climate reconstruction. Unlike the two previous proxy measures, testate amoebae data had a more singular role in assessing climate variation with a comparatively reduced role in understanding the isotopic characterisation of *Sphagnum* cellulose. Testate amoebae (TA) analysis was therefore focussed on core WLM22 from Walton Moss only. Walton Moss had previously been investigated for testate amoebae stratigraphy over a 3 metre (~3 ka BP) section (Barber & Langdon, *in press*). Walton Moss was therefore an ideal target site for both testing the replication of TA stratigraphy and extending the record further back in time through lower sediments.

4.4.2 Plant macrofossil preparation

Plant macrofossil analysis has been used routinely in ombrotrophic peatland research for the development of proxy-climate records using changes in the relative abundance of sub-fossil plant remains (Barber *et al.*, 1998; Hughes *et al.*, 2000; Blundell and Barber, 2005; Hughes *et al.*, 2006). The degree of bog surface moisture is the principal driver in the determination of plant and animal distributions. The premise behind the technique is one of uniformitarian ecology in that the ecological preferences of species in the modern day have remained constant over the timescale of interest. The benefits and limitations of the technique have been discussed in Chapter 2.

Sub-samples of core material 4cm^3 were extracted from the core using stainless steel scissors and scalpel and washed through a 125 micron sieve with 5l of tap water. A standard volume of 5l ensured consistency between samples in the removal of fine grained (<125 micron) UOM (Unidentified Organic Matter) (Hughes *et al.*, 2000). Residues were suspended in a plastic trough with a thin layer of distilled water and analysed for the relative abundance of species remains under a stereoscopic binocular microscope (x10). Abundances were estimated using the Quadrat and Leaf Count (QLC) method described by (Barber *et al.*, 1994). Fifteen quadrat counts were made systematically from all parts of the trough and percentage spatial cover for each type of remains was made using a graticule mounted in the microscope lens. Plant macrofossils were identified using reference material collected in the field and using (Grosse-Brauckmann, 1986).

Sphagnum leaf counts were taken by the mounting of >100 leaves picked from randomly chosen sections of the trough and identified by microscopy at 100-400x magnification. If *Sphagnum* remains constituted < 2% of the total percentage cover then no leaves were counted. In some rare cases it was not possible to find 100 leaves or occasionally to identify them with sufficient accuracy due to degradation. In these instances the maximum number of leaves practicable was identified. To avoid bias towards the picking of large leaves that may either be less degraded or more readily identifiable and often easier to pick, areas of the trough were chosen at random and then cleared of the leaves in that section. This procedure assumes that the distribution of leaves in the trough is uniformly mixed but is the least likely

to introduce bias due to the worker. *Sphagnum* leaves were identified using standard taxonomy (Daniels and Eddy, 1990; Smith, 2004).

Completed plant macrofossil datasets were subjected to statistical analyses to assist in climatic interpretation. Weighted averaging (Dupont, 1986) and DCA ordination analyses (Ter Braak and Juggins, 1993; Birks, 1995) were applied to the data and critically compared (section 4.4.5). Dupont reconstruction was selected over DCA ordination owing to a better ability of the method to represent the changes found in the core. This assessment is described in more detail in section 4.4.5 below.

4.4.3 Humification Preparation

The degree of peat humification is linked to bog surface wetness at the time of peat deposition. Where bog surface wetness is directly linked to climate on raised mires measurement of the degree of humification can be used as a palaeoclimatic indicator. The benefits and limitations of the technique have been discussed in Chapter 2. Whilst a number of techniques are available, the procedure of humic substance removal by alkali extraction was chosen. This method offers a robust and replicable record of humification changes in the most quantitative form available (Blackford and Chambers, 1993b). This chemical extraction method has been employed extensively in the determination of the degree of humification for palaeoclimatic studies (Aaby, 1976; Nilssen and Vorren, 1991; Blackford and Chambers, 1995; Mauquoy and Barber, 2002; Langdon *et al.*, 2003; Blundell and Barber, 2005).

The proportion of humic acids increases in peat with decomposition. Alkali extraction allows for the separation of these acids from the peat matrix which can be measured to assess decomposition. The absorption of light from an alkaline extract is proportional to the amount of humic matter dissolved (Aaby and Tauber, 1975). The greater the light absorption, the more decomposed the peat sample from which the acids were derived. Evidence of higher decomposition is taken to relate to lower average water tables during the period of deposition. The procedure followed was that of (Blackford and Chambers, 1993b).

Subsamples ($4cm^3$) were taken from the core and dried under an infra-red lamp. Dry samples were then homogenised with a pestle and mortar. 200 mg of material was weighed into a beaker and 100ml of fresh 8% NaOH added. Samples were brought to the boil and allowed to simmer for one hour to extract humic acids. After cooling, the samples in solution were transferred to a 200ml volumetric flask, filled to 200ml with distilled water and mixed well. To remove suspended solids, samples were filtered through 'Whatman Qualitative 1' paper. Fifty millilitres of the filtrate was then diluted with 50ml of distilled water and mixed well. Four hours after the initial mixing, percentage transmission of 540nm light was measured on a WPA S106 digital spectrophotometer. Raw data were normalised and detrended following a modification of the procedure of (Blundell and Barber, 2005) to allow for more direct comparison between the proxy-techniques used in this study.

4.4.4 Testate Amoebae Preparation

Use of testate amoebae in the production of palaeoclimate records was previously limited by a lack of ecological knowledge on modern distributions and ecological preferences of the single-celled organisms (Warner and Charman, 1994; Charman and Warner, 1997; Woodland *et al.*, 1998; Bobrov *et al.*, 1999; Bobrov *et al.*, 2002). Since the 1990s, there have been numerous studies redressing this gap in knowledge. This work married with the construction of a comprehensive taxonomy (Charman *et al.*, 2000) and a simple and effective preparation procedure (Hendon and Charman, 1997) has allowed for the generation of much more readily interpretable records of surface wetness change. The use of transfer functions based on weighted averaging of the modern distribution data have also allowed for quantitative reconstruction of past bog water tables from the fossil testate amoebae assemblages (Woodland *et al.*, 1998).

Due to time and core material volume constraints and the need to develop detailed isotopic records from the master cores which most directly targeted the main research questions, only one European core was analysed for fossil testate amoebae remains. The reasons for the limited use of this particular technique in this study have been described previously (section 4.4.1).

The standard procedure for preparation of testate amoebae was followed (Hendon and Charman, 1997). Sub-samples of 1cm^3 were measured by displacement of water in a measuring cylinder and transferred into a 250ml beaker. To estimate test concentration two tablets of *Lycopodium* were added as an exotic marker. 100ml of distilled water was added and samples brought to the boil for 10 minutes, stirring occasionally to disaggregate the peat. Coarse detritus was removed by washing each sample through a 250µm mesh sieve into a 10µm mesh to remove the fine fraction detritus. The residue >24µm and <250µm containing the preserved amoebae tests was retained and concentrated by two stages of centrifugation at 3000rpm for 5 minutes. The resulting concentrate was stored in 0.5ml glycerol in stoppered vials.

For microscope analysis, a small drop of concentrate was mounted on a microscope slide. A minimum of 100 tests were counted and identified using a standard taxonomy (Charman *et al.*, 2000).

Testate data were converted to depth to water table estimates using the transfer function developed by (Woodland *et al.*, 1998).

4.4.5 Data Analysis methods: condensation of multivariate data

4.4.5.1 Critical comparison of DCA ordination versus Dupont for plant macrofossil data

It has become established practice to transform multivariate biological data derived from palaeoecological investigation into variation along one axis for ease of interpretation (Hughes *et al.*, 2000; Langdon *et al.*, 2003). The most commonly used technique is that of Detrended Correspondence Analysis (DCA) which assumes each species has a Gaussian distribution in relation to the principal driving variable. DCA is often used in preference to other indices as it allows exploration of the data to extract any latent gradients by an objective approach (Birks, 1995). The axis of maximum variability (axis 1) reflects a gradient of dominant control over species variability. As this is understood to typically relate to depth to water table, DCA is

often used as a means of condensing the multivariate macrofossil data into a univariate distribution that relates the assemblage at any depth in the core to this gradient of wet or dry conditions. The correspondence analysis is objective in so far as it relies solely on natural clustering within the data. But the strength of the interpretation of the final curve relies on the analysis of the axis 1 axis 2 bi-plot where it is determined whether axis one reflects a known ecological gradient. Essentially then, the interpretive relevance of the DCA relies on a judgement of whether the axes represent realistic environmental variables.

Whilst DCA ordination has proven effective in Bog Surface Wetness (BSW) reconstruction from late-Holocene *Sphagnum* dominated peat, its use in records extending back to the early Holocene has been limited. NW European bog records extending back to this period typically display a bipartite division of early to mid- Holocene *Eriophorum / Calluna* peat followed by *Sphagnum* peat in the late Holocene that may bear more relation to bog ontology than climate (Hughes and Barber, 2004). The effect of this division on the DCA ordination is not well known but may represent a crossed gradient, distorting the climatic reconstruction. A crossed gradient describes a situation where the dominant driving variable behind the distribution of samples in axis one is replaced by an alternative driver. In palaeoecology, for example, this would represent a change from water table dominance to inter-specific species competition.

An alternative condensation technique is the Dupont hydroclimatic index (Dupont and Brenninkmeijer, 1984). This is a weighted averaging function and despite reduced use in recent studies has benefits over the DCA option. In DCA, a proportion of the data typically needs to be removed to allow the ordination to perform properly. In Dupont, the full range of data can be used with little distortion of the result. In DCA, the resulting axis may bear no relation to a single environmental variable as is implied from the production of a single axis 1. In Dupont, weightings are assigned based on sound, established ecological knowledge of species response to a particular environmental variable. So despite the apparent subjectivity of the method, it is likely to yield a meaningful result.

In order to determine which data condensation technique to use on data from this project, which covered the early-Holocene period as well as the late-Holocene, the two techniques were applied to plant macrofossil data from Walton Moss. The results of the DCA ordination

are shown in Figure 4.10 and demonstrate the influence of the bipartite division in the DCA reconstruction. The results of the Dupont analysis are presented in Figure 6.2 (Chapter 6).

In the DCA ordination, all species were used with no adjustment to species weighting. The top 56 cm was removed to avoid problems associated with a postulated crossed gradient with the rise to dominance of *S. magellanicum* and the levels below 832 cm removed to avoid a similar crossed gradient associated with proximity to the fen-bog transitional depths. Figure 4.9 shows the bi-plot of the DCA ordination and a key to species labels is given in Table 4.4.

Sample scores based on the weighted average of the species scores and their relative abundances in each sample are presented against depth for WLM22 in Figure 4.10 and displays variation typical of the results achieved from DCA ordination of the long cores used in this study. Whilst axis one appears to represent a hydrological gradient from comparison of the species scores with ecological knowledge of species preferences (Figure 4.9), the specific clustering of the data and sharp contrast between the two major stratigraphical units in the bogs produces a model of variation with depth that is strongly dominated by the bipartite division (Figure 4.10). The strength of this separation confuses the water table signal in the upper *Sphagnum* dominated peat and effectively subdues the amplitude of variation known to exist in these layers (Hughes *et al.*, 2000). By contrast, it is found that the Dupont hydroclimatic index analysis of plant macrofossil data produces a much more consistent result with the other proxy records over the length of cores (and species present) used in this study (Chapter 6).

For the analysis of testate amoebae data, the higher species diversity and more consistent presence of species throughout the length of the core provides the consistency of gradient that allows DCA ordination to perform well in the extraction of a dominant hydrological gradient. For this reason, analysis by the Dupont hydroclimatic index has been favoured for plant macrofossil data and DCA ordination used only for testate amoebae data in this study.

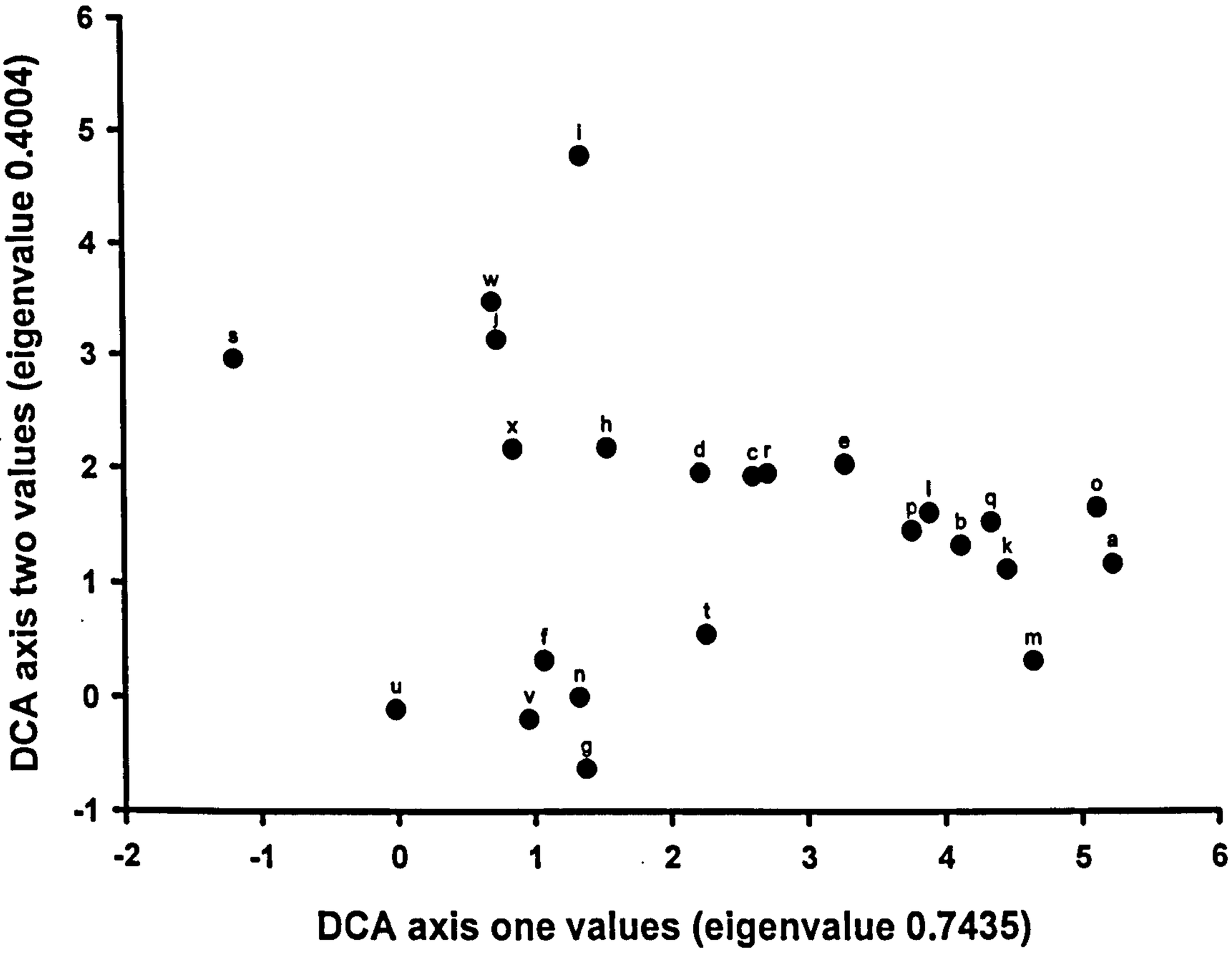

Figure 4.9 Bi-plot of DCA ordination results for WLM22 plant macrofossil data

Table 4.4 Key to species labels in Figure 4.9

Species	Label
Betula sp. Wood	a
Polytrichum alpestre type	b
Wood undif.	c
Calluna vulgaris, leaves and stem	d
Calluna vulgaris, flower / seedbox	e
Erica tetralix, leaves and stem	f
Monocot leaves and stem undif.	g
Monocot roots undif.	h
Monocot node/ root undif.	i
Eriophorum angustifolium, roots	j
Eriophorum vaginatum, leaves and stem	k
Eriophorum vaginatum, roots	l
Eriophorum vaginatum, node / spindles	m
Trichophorum cespitosum, leaves	n
Brown moss undif.	o
Aulacomnium palustre	p
Racomitrium lanuginosum	q
Ericaceae rootlets	r
Algal muds cf.	s
UOM	t
Sphagnum sect. Cuspidata	u
Sphagnum tenellum	v
Sphagnum imbricatum	w
Sphagnum sect. Acutifolia	x

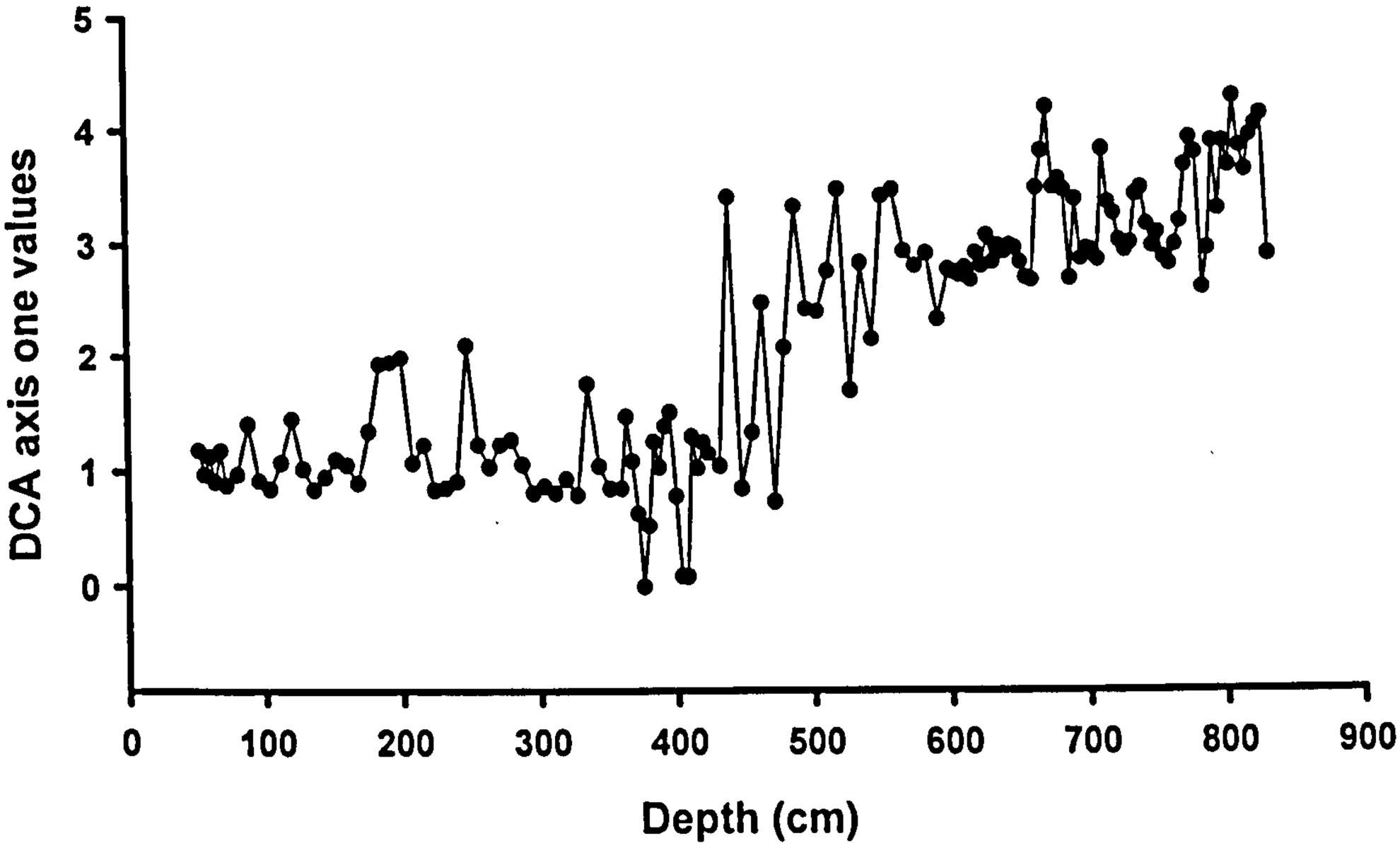

Figure 4.10 WLM22 DCA axis one sample scores with depth

4.4.5.2 Dupont hydroclimatic index

As described above, the Dupont surface wetness index is a weighted averaging method of estimating surface wetness. Weights are given to individual species based on ecological knowledge of their modern relationship to depth to water table. As shown above, the ordination plot from DCA of plant macrofossil data produced a gradient of species in axis one that did not reflect a simple water table gradient (Grosse-Brauckmann, 1986; Daniels and Eddy, 1990). The Dupont wetness index was used as an alternative BSW index for comparison with the other proxy reconstruction techniques. A variant of the Dupont index was used with the inclusion of weighted values for dicot remains. An evaluation of the relative performance of the variants of Dupont index construction is beyond the scope of this study. Rather, the Dupont index is used solely to assist palaeo-hydrological interpretation.

The weightings given to each of the species are shown in

Table 4.5 (Dupont and Brenninkmeijer, 1984; Dupont, 1986; Mauquoy and Barber, 2002) and new inclusions (var. Daley) noted (*).

Table 4.5 Species weightings for the Dupont Hydroclimatic index reconstruction

Taxon	Dupont weighting
Betula sp. Wood*	8
Polytrichum alpestre type	8
Wood*	8
Calluna vulgaris, leaves and stem*	8
Calluna vulgaris, flower / seedbox*	8
Erica tetralix, leaves+stem*	8
Monocot leaves and stem undif	7
Monocot roots, undif	7
Monocot node/ root undif	7
Rhynchospora, propagules	3
Rhynchospora, leaves and node	3
Eriophorum angustifolium, leaves, stem & node	2
Eriophorum angustifolium, roots	2
Eriophorum vaginatum, leaves and stem	7
Eriophorum vaginatum, roots	7
Eriophorum vaginatum, node / spindles	7
Trichophorum cespitosum, leaves+node	6
Brown moss undif.*	6
Aulacomnium palustre	6
Racomitrium lanuginosum	6
Ericaceae rootlets	8
Algal muds cf.*	1
UOM	8
Sphagnum sect. Cuspidata	1
*Sphagnum tenellum**	2
Sphagnum imbricatum	4
Sphagnum sect. Acutifolia	6
Sphagnum magellanicum	3
Sphagnum papillosum	3

4.5 *Dating Methods*

4.5.1 Chronological methodology

Chronological control on core stratigraphy was required to satisfy two objectives: 1) to cover the range of each palaeo-record and 2) to produce high-precision chronological control across phases of abrupt or rapid change. The methodology applied to each of the cores satisfied these complementary objectives using the resources available.

Three factors should be considered in the selection of any dating strategy: applicability, time range and precision/ accuracy of the technique (Smart and Frances, 1991). Applicability relates to the presence of a suitable material for dating in the core. Time range considers whether the technique matches the expected age of the deposits. For example, use of lead-210 dating on material >150 years old would not be constructive (Appleby, 2001). Precision/ accuracy questions whether the technique is capable of resolving the ages of interest. For instance, if annual resolution is required, is the technique capable of delivering that scale of temporal resolution?

A robust chronology for each core was developed using between 14 and 23 ^{14}C AMS dated levels in each core and a suitable age-depth model for interpolation of intervening depths. The objectives of this study and the wider ISOMAP-UK project placed focus on good temporal precision across early Holocene abrupt climate change events and across millennial scale cyclical changes. Consequently, high precision chronological control in the last 200 years was not a top priority in the chronological strategy. Lead-210 and spheriodal carbonaceous particle (SCP) dating are used for generating age estimates for sediments younger than those in the main age of interest for this study and were discounted. It was originally intended that the ^{14}C age depth models could be enhanced by the use of tephra layer pinning points. However, time constraints and the availability of a maximum of 30 ^{14}C dates per core under NERC RAPID allocation 15.64 enabled the construction of age depth models using ^{14}C dates alone that were suitable for answering the key research questions.

Two complementary strategies were used in the selection of levels for dating: regular spacing throughout the core length and finer sampling across key zones. Following a broad-based array of rangefinder dates used to determine coarse temporal structure, additional levels were selected at regular intervals throughout the core length to provide a full core length age-depth model. The precise levels chosen for these dates were decided in reference to the presence of datable remains, climatological significance (e.g. a change in the proxy-indicators) as previously recommended (Telford *et al.*, 2004), and with reference to the predicted slope of the radiocarbon calibration curve (Reimer *et al.*, 2004). Reference to the calibration curve was allowed by the initial array of rangefinder dates for each core. This enabled the construction of basic age-depth models that allowed general estimation of the probable age of particular levels. Levels chosen for addition dates in the main dating array were checked against the initial rangefinder model and against the radiocarbon calibration curve. Stratigraphical levels slightly higher or lower in the core than initially intended were chosen if a steep section of the curve could be targeted.

For any event to be shown to be rapid, the chronology across that shift must be suitably precise. An age estimate in the range of 200 years for example is not sufficient to firstly characterise a shift on a decadal time scale and secondly allow comparison of the record with other archives of rapid climate variability with any great confidence. Particularly where the peat accumulation rates may undergo change as a result of the climatic shift, reference to an age-depth model requiring interpolation between two distant points, may yield reduced information on rapidity. Accordingly, the requirement for a precise chronology across potential rapid events was met by a higher stratigraphical resolution of ^{14}C AMS dates in the section of interest in the core.

The use of this dating strategy, outlined above, most closely satisfied the recommendations of Smart and Frances (1991) and Telford *et al.* (2004). It was similarly the most appropriate method for answering the research questions of this thesis.

4.5.2 Age depth modelling

The age depth model used for each site necessarily varied to reflect the nature of accumulation rate change specific to each site. In general, however, two principles were followed:

1) For the mathematical model with the least number of terms to be used that most appropriately fitted the data available. It is possible to infinitely increase the terms of a model until all dating control points are fitted. This does not necessarily reflect an increase in model accuracy (Telford *et al.*, 2004).
2) For the assumptions in the model to be valid in relation to extrinsic knowledge of the core, past process and other contributing data. For example, where there is no evidence for an accumulation rate change, this should be reflected in the model and similarly if stratigraphic evidence points towards a change in accumulation rate the model should reflect this.

The age depth model used for each site and a justification of use of that model are presented in Chapter 5.

5 Chronological results and age-depth modelling

5.1 *Introduction*

A total of eighty ^{14}C AMS radiocarbon dates were applied to the four cores used in this study. Sixty-seven dates were secured under NERC RAPID allocation 15.64 and analysed by the NERC Radiocarbon Laboratory, East Kilbride. All dates on the European cores were provided exclusively under this allocation. For the Newfoundland core, NDN02/1, four dates were supplied by Gröningen Radiocarbon Laboratory funded by the ACCROTELM project, five dates were analysed by Beta-Analytic Inc. and four further dates were awarded to Dr. Paul Hughes by the NERC radiocarbon steering committee and analysed by the NERC Radiocarbon Laboratory (Hughes *et al.*, 2006).

The results from these eighty ^{14}C AMS dates are presented below. For each core, raw ^{14}C dates have been calibrated using the calibration program CALIB 5.1.0 beta (Stuiver *et al.*, 2005) using the INTCAL04 dataset (Reimer *et al.*, 2004) and are presented as the calibrated range from the 2σ conventional radiocarbon age estimate. The date for each depth has been calculated as the midpoint of the peak of maximum probability from the 1σ range given by CALIB 5.1.0 beta. Age depth models are produced from the dates given and the specific model used is justified.

5.2 *Walton Moss*

5.2.1 ^{14}C dating

Twenty three radiocarbon measurements were undertaken on core WLM22. The rationale behind sample level selection and the material used has been described in Chapter four. The data are summarised in Table 5.1 and Figure 5.1. There have been a number of previous studies that have analysed cores from Walton Moss (Barber *et al.*, 1998; Mauquoy and

Barber, 1999a; Hughes *et al.*, 2000; Langdon *et al.*, 2003) and consequently a rich chronostratigraphical database exists to describe the site. The results of the twenty-three ^{14}C dates presented here are in excellent agreement with those from previous studies and confirm the assertion that the bog has accumulated at a relatively constant rate since the early Holocene. Dating control points are focussed on the mid- to late Holocene period in the core, where significant changes in ecological and isotopic stratigraphy were observed (Chapters 6 & 7). Fewer dates are available for the lower sections of the core due to the insufficient preservation of *Sphagnum* at these depths to allow isotopic analysis (Chapter 6). Dates were necessarily focussed on those sections providing abrupt change in proxy-indicators that could also be isotopically characterised.

Table 5.1 Walton Moss Radiocarbon Measurements and Calibration

Lab. Code	Material	Depth below bog surface (cm)	^{14}C date BP (uncal.)	±1σ	Calibrated Age (BP)	Calibrated range from 2σ error on ^{14}C age (BP)	
SUERC-11176	*Sphagnum* and dicot remains	44	380	35	467	317	508
SUERC-11175	*Sphagnum*	87	1075	35	962	930	1056
SUERC-4157	*Sphagnum*	100	1188	24	1104	1015	1177
SUERC-11174	*Sphagnum* and dicot remains	150	1586	35	1442	1397	1544
SUERC-11173	Sphagnum and Eriophorum node	174	1598	35	1443	1405	1556
SUERC-11172	*Sphagnum* and dicot remains	232	2332	35	2342	2186	2464
SUERC-4158	*Sphagnum*	264	2504	26	2548	2487	2729
SUERC-11171	*Sphagnum* and dicot remains	273	2816	35	2914	2799	3058
SUERC-11170	*Sphagnum*	300	2876	35	3010	2879	3142
SUERC-11169	*Sphagnum*	328	3256	35	3466	3397	3565
SUERC-11168	*Sphagnum*	370	3341	35	3596	3475	3683
SUERC-11165	*Sphagnum*	388	3713	35	4018	3930	4153
SUERC-11163	*Sphagnum*	399	3366	35	3604	3484	3692
SUERC-11162	*Sphagnum* and dicot remains	412	3808	35	4196	4086	4401
SUERC-11161	*Sphagnum* and dicot remains	420	3941	35	4410	4255	4516
SUERC-11160	*Sphagnum* and dicot remains	452	4026	38	4482	4417	4782
SUERC-11159	*Eriophorum* node & *Calluna* stem	482	4201	35	4731	4620	4846
SUERC-11156	*Calluna* stem & flowers	528	4654	35	5415	5310	5566
SUERC-11155	*Calluna* stem, flowers & seed. Charred *Calluna*	642	5782	36	6587	6493	6666
SUERC-11154	Grass node & stem. *Calluna* stem & *Sphagnum*	660	5906	36	6711	6653	6841
SUERC-11153	*Sphagnum* and dicot remains	688	6169	35	7082	6965	7166
SUERC-11152	*Calluna* stem, flowers & seed. Charred *Calluna*	748	6682	35	7527	7488	7609
SUERC-11151	*Sphagnum*	876	8105	38	9017	8818	9239

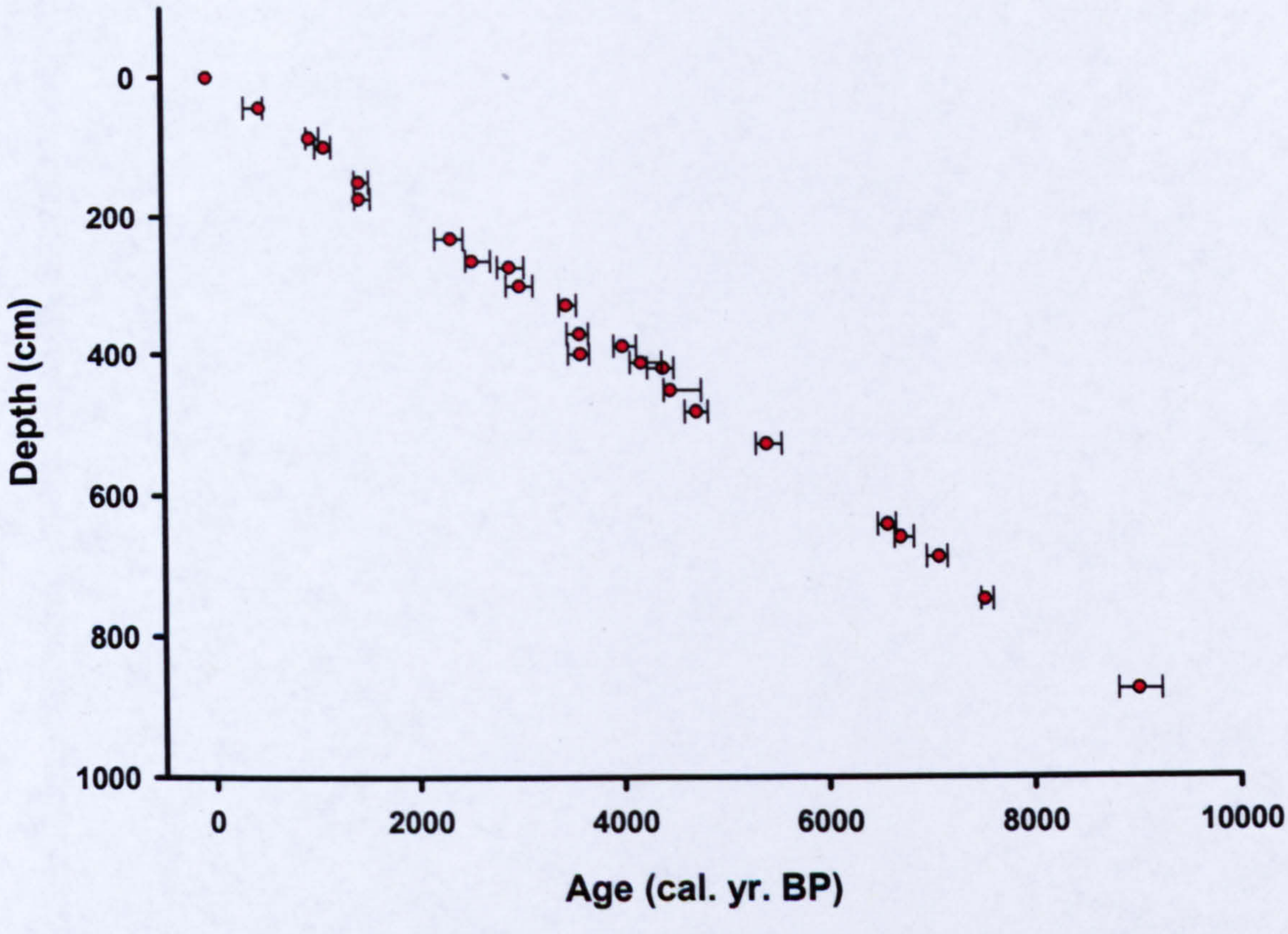

Figure 5.1 Calibrated ^{14}C dates with calibration range from 2σ error on conventional radiocarbon age for WLM22

5.2.2 Age-depth modelling

A linear regression of the sequence of dated levels in core WLM22 and a surface date taken as the year of core retrieval provides a model (Age = 10.24*Depth -57.92) that describes a constant accumulation rate of ~1mm/yr (Figure 5.2). The model is justified on the basis of its close approximation of nearly all dating control points (Figure 5.2). Excellent performance is demonstrated by firstly, close agreement with previous studies and secondly, by the intersection of the y axis at -57.92 which is within 4 years of that in which the core was taken. The model misses the 2σ range of only two dates. These are 174 cm and 399 cm. In both cases the dates are slightly younger than the model predicts based upon all 24 dates. Whilst every care was taken to use only the remains of aerial parts of plants and minimise the presence of small rootlets, it is possible that some may have persisted resulting in a slightly

younger date than reality. The penetration of younger roots into the sample is more plausible than the remaining 21 dates suffering from the interjection of older material.

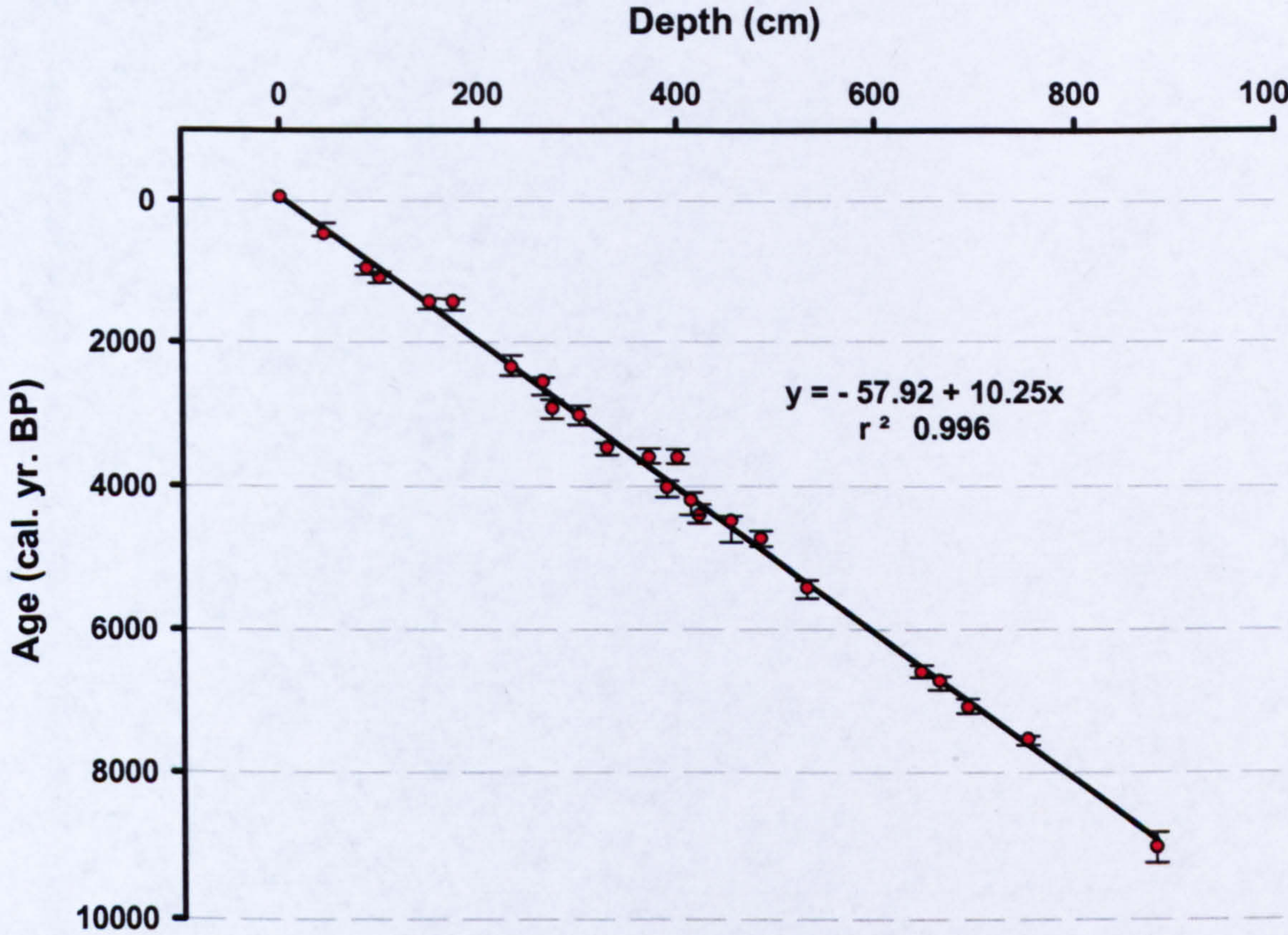

Figure 5.2 Calibrated ^{14}C dates for core WLM22 (red dots) with calibration range from 2σ error on conventional radiocarbon age. Linear regression age depth model (Age = 10.24 x depth – 54) is shown (bold black line)

5.3 *Dosenmoor*

5.3.1 ^{14}C dating

Twenty-one AMS ^{14}C measurements were taken on core DSM3 from Dosenmoor. Raw ^{14}C ages, the 2σ calibrated range and the statistically most probable date are summarised in Table 5.2. Calibrated dates are plotted in Figure 5.3. Despite the depth proximity of several of the dates, stratigraphical order is maintained and no age reversals are evident in the data. There is

a relatively large error margin associated with the date at 388cm which is explained by coincidence with a plateaux in the radiocarbon calibration curve between 2350 and 2700 BP (Reimer *et al.*, 2004). Similar to findings at Walton Moss, excellent agreement is found between the dated levels of DSM3 and the dates published from previous cores taken near to the core site (Van Den Bogaard and Schmincke, 2002; Barber *et al.*, 2004).

Table 5.2 Dosenmoor Radiocarbon Measurements and Calibration

Lab. Code	Material	Depth below bog surface (cm)	^{14}C date BP (uncal.)	±1σ	Calibrated Age (BP)	Calibrated range from 2σ error on ^{14}C age (BP)	
SUERC-10331	*Sphagnum* and dicot remains	72	940	35	834	780	929
SUERC-4239	*Sphagnum*	100	1102	24	988	959	1060
SUERC-10332	*Sphagnum*	128	1291	35	1256	1148	1294
SUERC-10333	*Sphagnum*	158	1297	35	1259	1173	1294
SUERC-10334	*Sphagnum* and dicot remains	178	1495	35	1375	1306	1512
SUERC-4240	*Sphagnum*	200	1711	29	1596	1547	1697
SUERC-10335	*Sphagnum*	212	1700	35	1590	1536	1696
SUERC-10336	*Sphagnum* and dicot remains	220	1786	36	1716	1612	1819
SUERC-10337	Grass seeds, dicot remains and *Sphagnum*	228	1786	35	1716	1614	1818
SUERC-10338	*Sphagnum*	242	1897	35	1854	1731	1922
SUERC-10341	*Sphagnum*	278	1971	35	1915	1830	1994
SUERC-4160	*Sphagnum*	320	2245	25	2209	2157	2338
SUERC-10343	*Sphagnum*	328	2264	35	2323	2157	2346
SUERC-10344	*Sphagnum*, dicot remains, grass remains	388	2488	35	2555	2366	2725
SUERC-10345	*Eriophorum* remains	404	2852	36	2963	2866	3075
SUERC-10346	*Rhyncospora* remains and *Sphagnum*	428	2903	35	3022	2930	3205
SUERC-10347	*Sphagnum* and dicot remains	436	3029	36	3239	3081	3353
SUERC-10348	Ericaceous remains	444	3057	36	3291	3164	3365
SUERC-10351	Ericaceous remains and charcoal	536	3957	37	4426	4291	4522
SUERC-10352	*Sphagnum*	634	4868	36	5602	5485	5660
SUERC-4161	*Sphagnum* and dicot remains	668	5124	31	5906	5751	5933

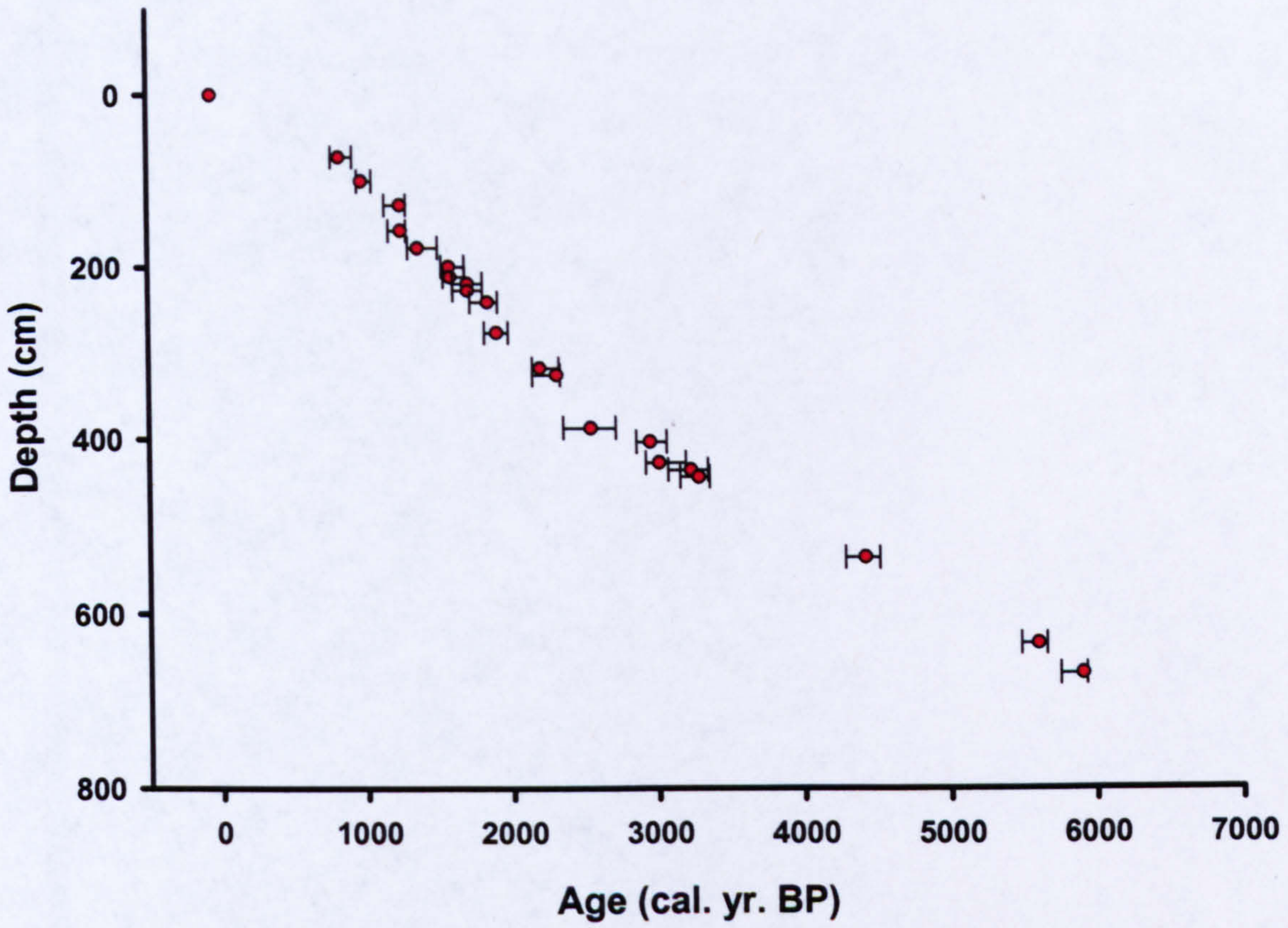

Figure 5.3 Calibrated ^{14}C dates with calibration range from 2σ error on conventional radiocarbon age for DSM3

5.3.2 Age-depth modelling

A 4th order polynomial regression has been used to model the variation of age with depth in core DSM3 (Figure 5.4). The model is given by the equation:

Equation 10) $\mathbf{Age = k + ax + bx^2 + cx^3 + dx^4}$

where x = Depth

k = -58.278972129

a = 15.8529161742

b = -0.0636535274

c = 1.43422885e-4

d = -9.5167874099e-8

The problems associated with the use of polynomial regressions and particularly a focus on r^2 value as a measure of the performance of the model have been documented (Telford *et al.*, 2004). However, it is argued here that this model offers a good approximation for the data available. It has been recommended that where the number of dates available is restricted, the most appropriate course of action is to date levels where stratigraphical evidence suggests a change of accumulation rate and to apply a linear interpolation model (Telford *et al.*, 2004). Linear interpolation has been rejected here as there are no grounds to expect significant changes in accumulation rate at *every* depth at which the dates have been taken and at the frequency afforded by the total of twenty-one dates.

Given enough additional terms, a polynomial will eventually match a set of dates exactly when number of terms ≥ number of dates. For this reason higher order polynomials must be used with care. If the number of dates readily exceeds the number of changes in accumulation rate, a more global model rather than linear interpolation is recommended as more appropriate (Telford *et al.*, 2004).

In the case of DSM3, the 4th order fits well with understanding of the site and stratigraphical results (Chapter 6). For a 4th order polynomial to be a satisfactory model, there need to be reasons to suspect that the core exhibits three points of inflexion in accumulation rate. The dates in Figure 5.3 show a clear tendency towards a slowing accumulation rate in the early Holocene, followed by a period of faster accumulation in the upper peat before a rapid slowing in the upper section of the core (Figure 5.3; Figure 5.4).

Rapid accumulation in the upper *Sphagnum* peat sections of NW European bogs is documented (Barber *et al.*, 2004). Furthermore, Dosenmoor has been subject to extensive surface cutting (Chapter 3) and the surface is composed of disturbance species overlying a highly humified layer (Chapter 6). A rapid slow-down in accumulation rate or indeed a short hiatus would be expected for the near surface sediments. A 4th order satisfies this variability well and correlates very closely with the dating control points. The intersection of the curve with the y-axis at -58 equates to a date of 2008 AD. The core was collected in 2004. Given the typical errors associated with ^{14}C dating, this can be seen as an excellent approximation.

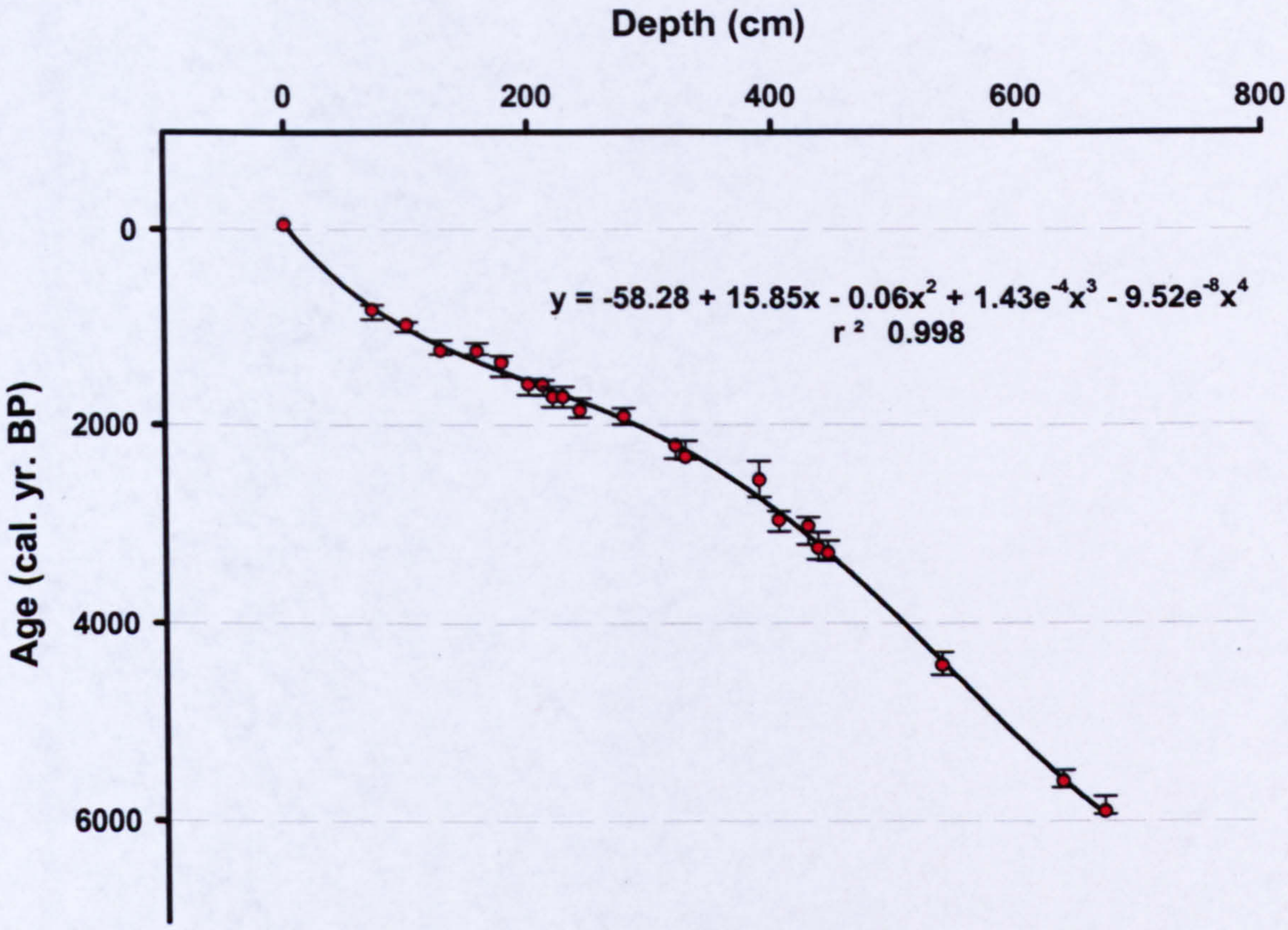

Figure 5.4 Calibrated ^{14}C dates for DSM3 (red dots) with calibration range from 2σ error on conventional radiocarbon age (black bars). A 4th order polynomial age-depth model (Age = k + ax + bx^2 + cx^3 + dx^4) (bold black line) is given as an approximation of accumulation rate with depth.

5.4 *Raheenmore*

5.4.1 ^{14}C dating

Thirteen ^{14}C AMS measurements were applied to core RHM2 from Raheenmore. Samples for dating were spread evenly at one metre intervals to gain a broad idea of accumulation rate change. Additional dates were focussed on a section of the lower part of the core following

discovery of a significant anomaly in the proxy-indicators at a depth resolved by rangefinder dates to correspond with the period around 8200 BP to more finely resolve this area of interest. The ^{14}C dates, calibrated ranges and control points are summarised in Table 5.3 and control points are plotted in Figure 5.5 along with 2σ ranges.

It is evident that a fairly constant accumulation rate persisted throughout the time-span of the core (Figure 5.5). However, subtle variations in accumulation rate are evident and particularly noticeable in the more finely resolved section between ~7800 and ~8500 BP. Currently, no published data exist for this site with which to compare these data.

Table 5.3 Raheenmore Radiocarbon Measurements and Calibration

Lab. Code	Material	Depth below bog surface (cm)	^{14}C date BP (uncal.)	±1σ	Calibrated Age (BP)	Calibrated range from 2σ error on ^{14}C age (BP)	
SUERC-11150	*Sphagnum* and dicot remains	100	192	35	168	-2	304
SUERC-11146	*Sphagnum* and dicot remains	200	1306	35	1263	1177	1293
SUERC-11145	*Rhyncospora* node and *Sphagnum*	300	2118	35	2095	1994	2298
SUERC-11144	*Sphagnum*	400	2877	35	3011	2881	3142
SUERC-11143	*Sphagnum* and dicot remains	500	3875	35	4274	4159	4417
SUERC-11142	*Eriophorum* node and *Calluna* stem	600	4458	35	5228	4962	5290
SUERC-11141	*Calluna, Eriophorum* seed & *Sphagnum*	700	4980	35	5697	5610	5879
SUERC-7764	*Calluna* and *Eriophorum*	800	5867	31	6694	6572	6777
SUERC-7765	*Calluna, Eriophorum and insect remains*	900	6807	37	7644	7584	7690
SUERC-11140	*Calluna* and *Eriophorum* node	932	6986	36	7825	7715	7931
SUERC-11139	*Calluna* and *Eriophorum* seed	968	7342	36	8173	8027	8293
SUERC-7767	*Calluna* and *Eriophorum*	1000	7885	45	8664	8586	8976
SUERC-7700	*Sphagnum* and dicot remains	1100	8769	53	9790	9556	10119

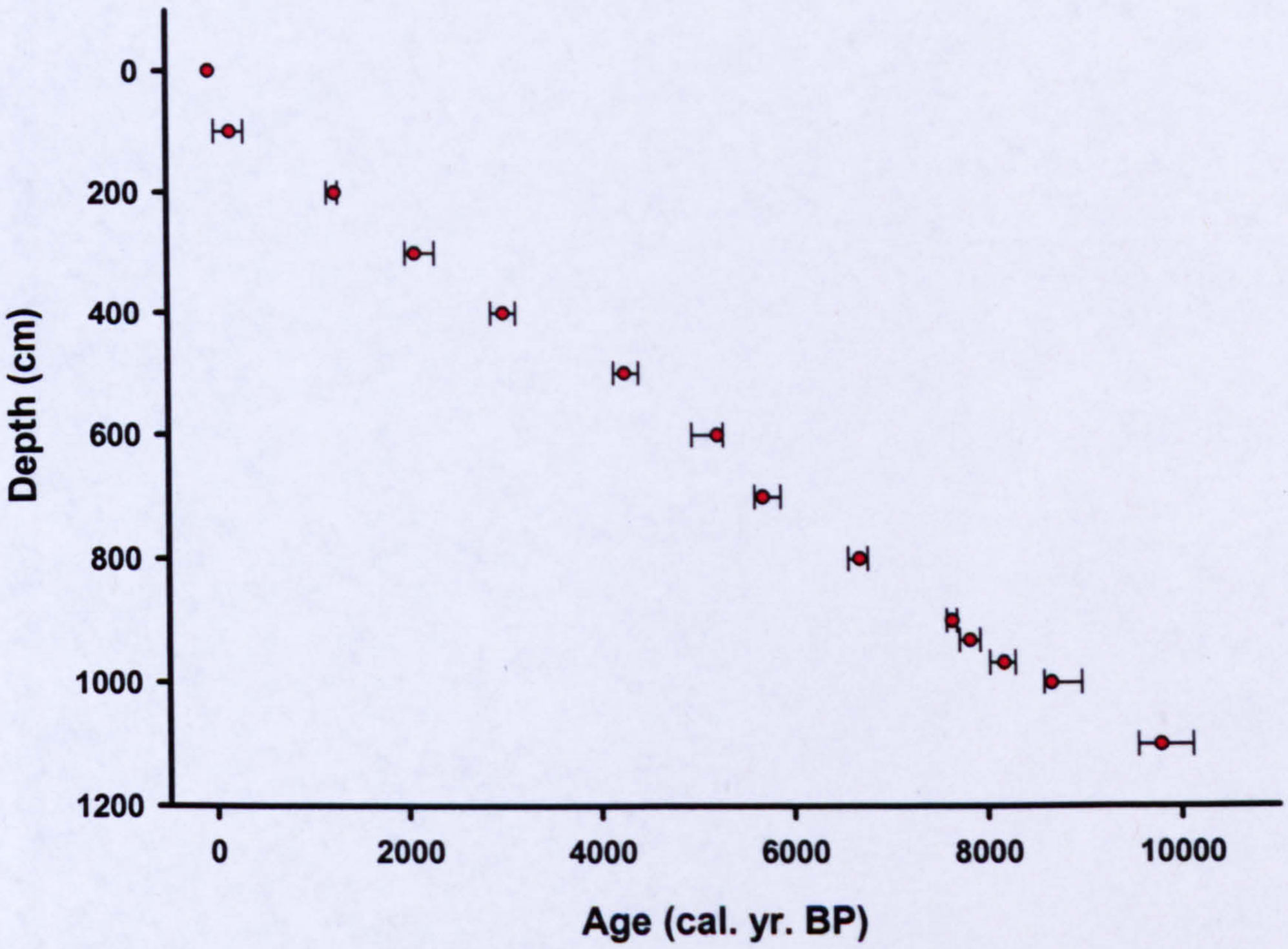

Figure 5.5 Calibrated ^{14}C dates with calibration range from 2σ error on conventional radiocarbon age for RHM2

5.4.2 Age-depth modelling.

The sampling of dated levels at one metre intervals prevents the use of a linear interpolation model because the assumption of a change in accumulation rate at each date is invalid. A more global model of rate change using information throughout the core is more appropriate in this case. The model offering the best degree of fit with the raw data is a 4^{th} order polynomial (Figure 5.6). The model is given by:

Equation 10) $\mathbf{Age = k + ax + bx2 + cx3 + dx4}$

where x = depth
k = -110.8512619536
a = 1.9293747392

b = 0.0282331401

c = -3.872807506e-5

d = 1.7222604775e-8

As has been discussed above for Dosenmoor, a 4th order polynomial necessarily assumes that the accumulation rate underwent three general rate changes. This assumption matches the raw data most closely and provides the most realistic surface value whilst maintaining the simplest model. The increase in accumulation rate in the top metre is consistent with findings during fieldwork for an unusually deep acrotelm layer composed entirely of high-porosity broad-leaved *Sphagnum* peat. The accumulation rate over this low-density peat would be expected to be high in comparison to lower levels. A 4th order polynomial is the simplest model that allows this rate change at the surface to be at least partly represented. The intersection of the curve with the y axis at -110 predicts that the present surface age is ~50 years in the future. Despite this limitation, the model remains the most appropriate for approximating the early to late Holocene peat ages prior to the 20th century and hence most appropriate for the ages of interest to this study (Figure 5.6).

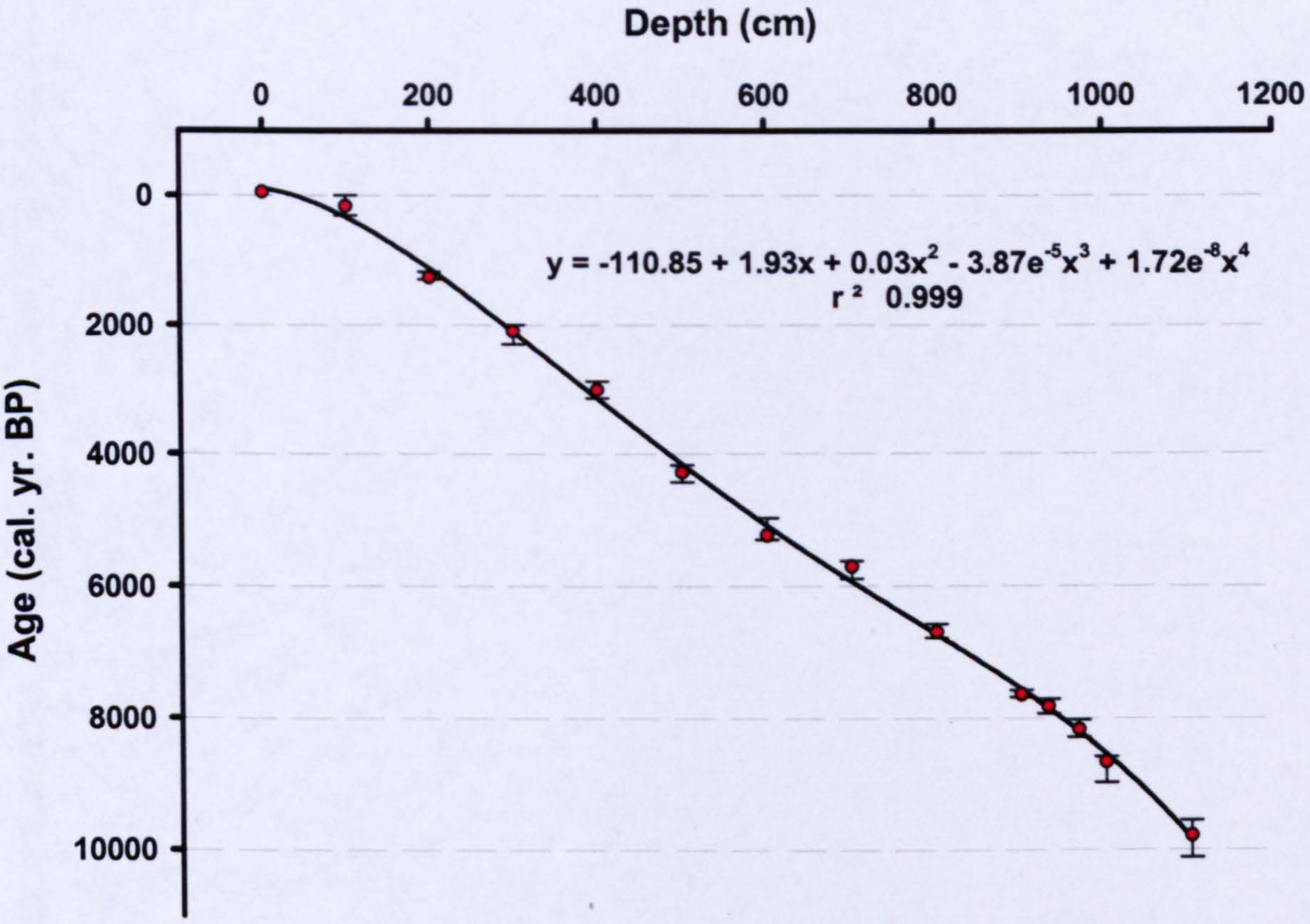

Figure 5.6 Calibrated ^{14}C dates for core RHM2 (red dots) with calibration range from 2σ error on conventional radiocarbon age (black bars). A 4th order polynomial is used as an age-depth model of the accumulation rate (bold black line).

5.5 *Nordans Pond Bog*

5.5.1 ^{14}C dating

The full array of twenty-three ^{14}C dates taken on core NDN02/1 and the date of core collection at the surface are presented in Table 5.4 and plotted in Figure 5.7. The data show a general trend towards decreasing accumulation rate in the lower peat followed by a period of increasing accumulation rate towards the surface. Unlike the data presented from the European cores, several temporal reversals are evident in the Nordans Pond Bog data. The

most noticeable is at 450 cm where a reversal of ~200 years is observed. Smaller magnitude reversals are observed at 652 cm and 616 cm. Data in Table 5.4 indicate that only above ground in situ remains were used for dating in these levels, so their explanation is problematic. The spacing of dates collected under this project is described in Chapter 4.

Table 5.4 Nordans Pond Bog Radiocarbon Measurements and Calibration

Lab. Code	Material	Depth below bog surface (cm)	^{14}C date BP (uncal.)	±1σ	Calibrated Age (BP)	Calibrated range from 2σ error on ^{14}C age (BP)	
SUERC- 508	*Sphagnum*	75	355	35	364	500	310
SUERC-9924	*Sphagnum* and dicot remains	136	912	35	838	920	740
Beta - 182370	*Sphagnum*	204	1790	40	1714	1820	1580
SUERC-9923	*Sphagnum* and dicot remains	232	2279	35	2326	2360	2150
GrA-31483	*Sphagnum*	242	2470	30	2528	2720	2360
GrA-31485	*Sphagnum*	254	2635	30	2758	2800	2720
GrA-31487	*Sphagnum*	259	2855	30	2994	3080	2870
GrA-31488	*Sphagnum*	265	2865	30	2998	3080	2870
Beta - 182371	*Sphagnum*	272	2890	40	3042	3200	2880
SUERC-9922	*Sphagnum* and dicot remains	312	3632	37	3926	4090	3840
SUERC- 538	*Sphagnum*	334	3691	40	4006	4150	3900
SUERC-9919	*Sphagnum*	408	4922	38	5660	5730	5590
SUERC- 539	*Sphagnum*	450	4640	31	5419	5470	5310
SUERC-9918	*Sphagnum*	472	5796	43	6584	6730	6480
Beta - 182373	*Sphagnum*	504	5950	40	6780	6870	6670
SUERC-9917	*Sphagnum*	528	6144	43	7048	7170	6910
SUERC-9915	*Sphagnum*	600	7330	62	8118	8320	8010
SUERC - 540	*Sphagnum*	616	7156	34	7980	8110	7870
SUERC-9914	*Sphagnum*	632	7475	50	8286	8380	8190
Beta - 182374	*Sphagnum*	652	7460	40	8279	8350	8180
SUERC-9913	*Sphagnum*	668	7740	52	8509	8600	8410
SUERC-9912	*Carex* eutricles and seeds	702	7921	52	8711	8980	8600
Beta - 182375	*Sphagnum*	720	7980	40	8850	9010	8650

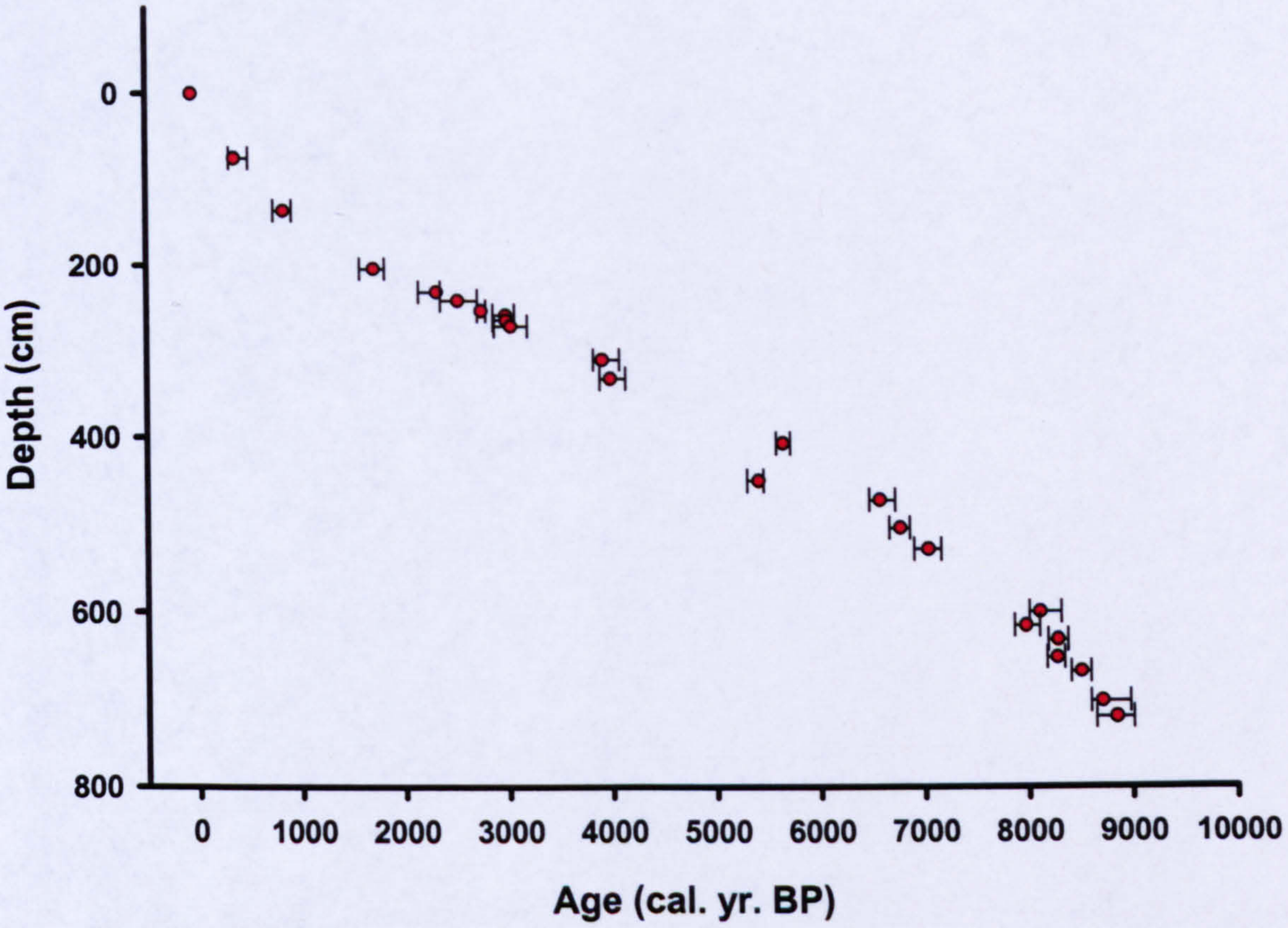

Figure 5.7 Calibrated ^{14}C dates with calibration range from 2σ error on conventional radiocarbon age for NDN02/1

5.5.2 Age-depth modelling

Two options exist for modelling a sequence in which temporal reversals are present. Either a choice needs to be taken to omit one of the two dates that comprise a reversal or a global model needs to be fitted that treats each date as equally probable and avoids the inherent subjectivity of selecting one for omission. The second, more objective option has been used here (Figure 5.8). A third alternative is to replicate the dating. This is, however, a costly and impractical solution within time and financial constraints.

A cubic regression model has been used to approximate the accumulation rate of NDN02/1. This matches the overall trends evident from the calibrated dates well and offers a good approximation across the principal zone of interest between 7800 and 8500 BP (Figure 5.8).

Table 6.1 Assemblage zones and environmental interpretation for WLM22 plant macrofossils

Zone	Depth (cm)	Description	Age (cal. yr. BP)
WLM-a	896-880	This zone contains species characteristic of nutrient enriched and basic environments. The presence of *Phragmites australis*, *Equisetum* and *Carex spp*. along with *Betula spp*. is indicative of poor fen conditions and marks the beginning of the fen-bog transition (Hughes and Barber, 2004). Dominance of heavily degraded Unidentified Organic Matter (UOM) provides further evidence for fen conditions in this zone.	9120 - 8960
WLM-b	880 – 834	Dominance of "ecosystem engineer species" *S. palustre* with smaller percentages of *S. recurvum* and *S. sect. acutifolia*. Disappearance of fen indicator species. *E. vaginatum* appears but abundance variable. The dominance of the *Sphagnum* species indicates water tables were relatively high and stable during the period of transistion from fen to bog.	8960 - 8490
WLM-c	834 – 774	Dominance of *E. vaginatum* remains and undifferentiated wood remains. This reflects a landscape strongly dominated by grasses and some birch trees. Percentages of *E. vaginatum* roots and leaves fluctuate alternately which may reflect a diagenetic process. The presence of *E. vaginatum* is indicative of fluctuating water tables. Short single sample event of *S. sect. acutifolia* occurs at 784cm (~ 8200 BP) and may reflect a very short-lived elevation of bog water table. This event is accommodated by a reduction in the above ground remains of *E. vaginatum*.	8490 - 7870
WLM-d	774 – 464	Major change to assemblage strongly dominated by ericaceous rootlet remains in association with *E. vaginatum* remains, undifferentiated wood and upper parts of the *Calluna vulgaris* heather plant. Occasional remains of the brown mosses *Aulacomnium palustre* and *Rancomitrium lanuginusom* are present along with the grass *Trichophorum cespitosum*. This assemblage is indicative of relatively deep and fluctuating bog water table and relatively dry conditions on the bog surface.	7870 - 4700
WLM-e	464 – 362	Major transition from peat dominated by grasses and heathers to *Sphagnum* peat. Assemblage dominated by *Sphagnum spp*. percentages of different species highly variable but includes *S. cuspidatum, S. imbricatum* and *S. sect. acutifolia*. Ericaceous and *E. vaginatum* remains are substantially lower than in WLM-d contributing only a minor percentage to the assemblage. The floral composition of this zone indicates that bog water tables were higher than in the preceding zone. The presence of periods dominated by *S. cuspidatum* indicate that water tables were high enough to allow bog pool development.	4700 - 3650
WLM-f	362 – 48	*Sphagnum* bog dominated by *S. imbricatum* and *S. sect. acutifolia*. These dominant species are both documented to have a large range of water table tolerances. It is possible that during this period, sensitivity to water table change is low. Two fluctuations are highlighted. At ~200cm *Sphagnum* abundance drops markedly replaced by ericaceous remains and *E. vaginatum* and a substantial increase in UOM. This is indicative of drier bog surface conditions. At ~120cm *S. cuspidatum* and *S. tenellum* briefly replace *S. imbricatum* and *S. sect. acutifolia.* This change is representative of an increase in bog water tables.	3650 - 440
WLM-g	48 – 20	This zone is characterised by high abundance of *S. cuspidatum* and low percentages of *S. imbricatum* and *S. sect. acutifolia*. *Rynchospora alba* remains are also present. Within this zone *S. magellanicum* makes a first appearance. This reflects a prolonged and sustained change to wet bog surface conditions and bog pool development. *S. imbricatum* disappears from the record and is no longer found at this site.	440 - 150
WLM-h	20-0	Dominated by *S. magellanicum* with some *S. cuspidatum*. *Erica tetralix* leaves are associated with the presence of *S. cuspidatum* Low percentages of Ericaceous rootlets and grass remains persist. The floral composition reflects a change towards drier bog surface conditions for the most recent period.	150 - present

6 Palaeoecological results and analysis

6.1 *Introduction*

In this chapter, data from plant macrofossil, testate amoebae and humification analyses are presented from Walton Moss, Dosenmoor and Raheenmore. Multi-proxy analyses have been published previously for Nordans Pond Bog (Hughes *et al.*, 2006). The combination of analyses used and the length and resolution of these records varies depending on the specific research objectives attached to each site and already documented in Chapter 4. Later in the chapter, the data are combined in multi-proxy format and interpreted for changes in the condition of bog surface wetness with depth. Age depth models from Chapter 5 are used to construct time-series from the multi-proxy records. More detailed palaeoclimatic inference and comparison with isotopic data is explored later in Chapter 8. Comparison of time-series from all three sites is given in Chapter 8. Throughout the chapter, species taxonomy is given in full at first description and abbreviated thereafter (e.g. *Amphitrema flavum; A. flavum*).

6.2 *Walton Moss*

6.2.1 WLM22 plant macrofossil data

Plant macrofossil data for core WLM22 are presented in Figure 6.1. The diagram has been divided into zones in which each species assemblage is significantly different from the zones bordering and in which the internal composition is relatively consistent. Although numerical programs exist for the zonation of diagrams e.g. CONSIS, and have been debated in the literature (Bennett, 1996) these groups have been determined by eye. Descriptions of the assemblage characteristics for each zone are given in Table 6.1.

Figure 6.1 WLM22 plant macrofossil diagram (896 - 0 cm; 9120 BP - present)

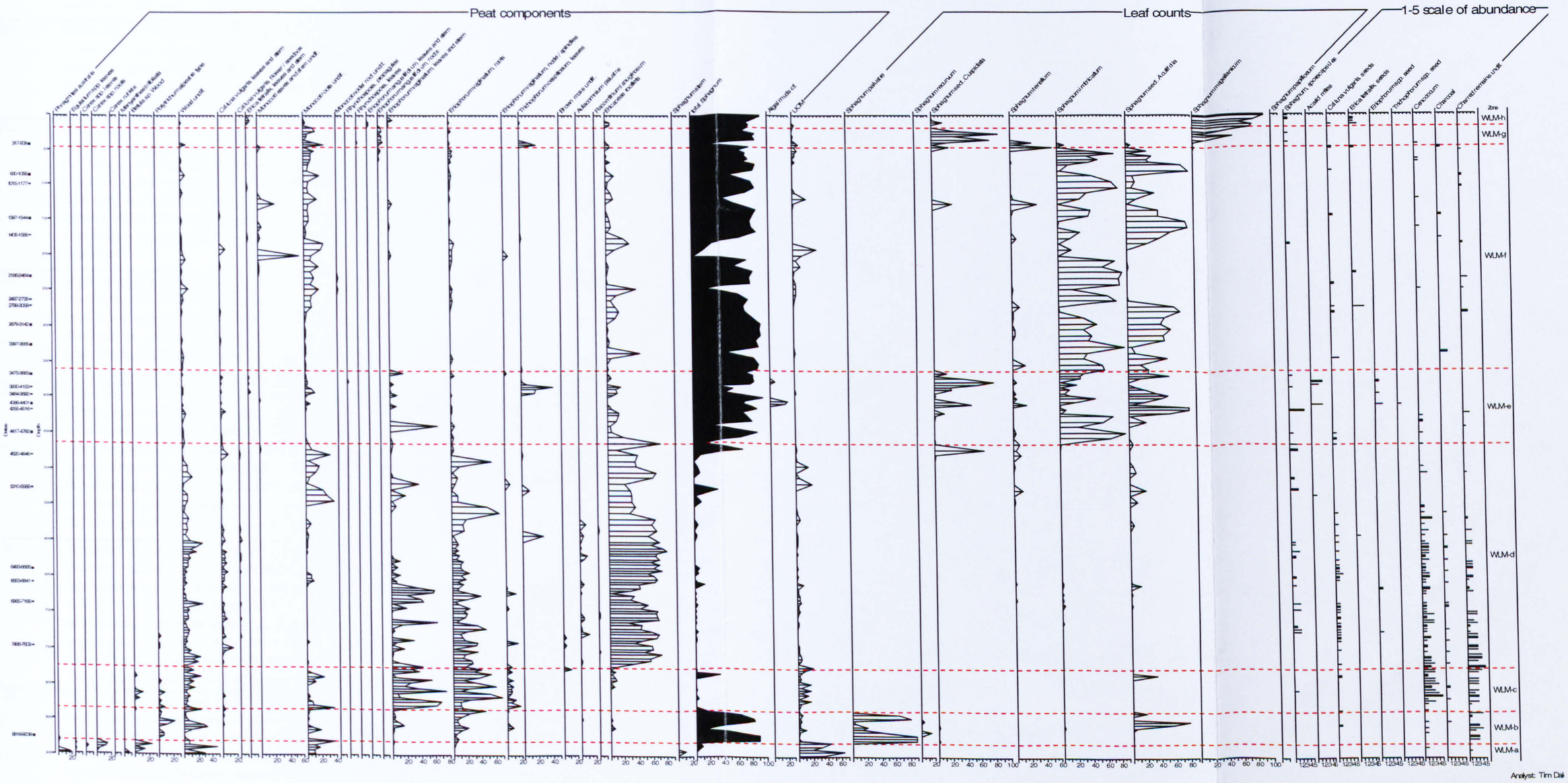

Table 6.1 Assemblage zones and environmental interpretation for WLM22 plant macrofossils

Zone	Depth (cm)	Description	Age (cal. yr. BP)
WLM-a	896-880	This zone contains species characteristic of nutrient enriched and basic environments. The presence of *Phragmites australis*, *Equisetum* and *Carex spp*. along with *Betula spp*. is indicative of poor fen conditions and marks the beginning of the fen-bog transition (Hughes and Barber, 2004). Dominance of heavily degraded Unidentified Organic Matter (UOM) provides further evidence for fen conditions in this zone.	9120 - 8960
WLM-b	880 – 834	Dominance of "ecosystem engineer species" *S. palustre* with smaller percentages of *S. recurvum* and *S. sect. acutifolia*. Disappearance of fen indicator species. *E. vaginatum* appears but abundance variable. The dominance of the *Sphagnum* species indicates water tables were relatively high and stable during the period of transistion from fen to bog.	8960 - 8490
WLM-c	834 – 774	Dominance of *E. vaginatum* remains and undifferentiated wood remains. This reflects a landscape strongly dominated by grasses and some birch trees. Percentages of *E. vaginatum* roots and leaves fluctuate alternately which may reflect a diagenetic process. The presence of *E. vaginatum* is indicative of fluctuating water tables. Short single sample event of *S. sect. acutifolia* occurs at 784cm (~ 8200 BP) and may reflect a very short-lived elevation of bog water table. This event is accommodated by a reduction in the above ground remains of *E. vaginatum*.	8490 - 7870
WLM-d	774 – 464	Major change to assemblage strongly dominated by ericaceous rootlet remains in association with *E. vaginatum* remains, undifferentiated wood and upper parts of the *Calluna vulgaris* heather plant. Occasional remains of the brown mosses *Aulacomnium palustre* and *Rancomitrium lanuginusom* are present along with the grass *Trichophorum cespitosum*. This assemblage is indicative of relatively deep and fluctuating bog water table and relatively dry conditions on the bog surface.	7870 - 4700
WLM-e	464 – 362	Major transition from peat dominated by grasses and heathers to *Sphagnum* peat. Assemblage dominated by *Sphagnum spp*. percentages of different species highly variable but includes *S. cuspidatum, S. imbricatum* and *S. sect. acutifolia*. Ericaceous and *E. vaginatum* remains are substantially lower than in WLM-d contributing only a minor percentage to the assemblage. The floral composition of this zone indicates that bog water tables were higher than in the preceding zone. The presence of periods dominated by *S. cuspidatum* indicate that water tables were high enough to allow bog pool development.	4700 - 3650
WLM-f	362 – 48	*Sphagnum* bog dominated by *S. imbricatum* and *S. sect. acutifolia*. These dominant species are both documented to have a large range of water table tolerances. It is possible that during this period, sensitivity to water table change is low. Two fluctuations are highlighted. At ~200cm *Sphagnum* abundance drops markedly replaced by ericaceous remains and *E. vaginatum* and a substantial increase in UOM. This is indicative of drier bog surface conditions. At ~120cm *S. cuspidatum* and *S. tenellum* briefly replace *S. imbricatum* and *S. sect. acutifolia.* This change is representative of an increase in bog water tables.	3650 - 440
WLM-g	48 – 20	This zone is characterised by high abundance of *S. cuspidatum* and low percentages of *S. imbricatum* and *S. sect. acutifolia*. *Rynchospora alba* remains are also present. Within this zone *S. magellanicum* makes a first appearance. This reflects a prolonged and sustained change to wet bog surface conditions and bog pool development. *S. imbricatum* disappears from the record and is no longer found at this site.	440 - 150
WLM-h	20-0	Dominated by *S. magellanicum* with some *S. cuspidatum*. *Erica tetralix* leaves are associated with the presence of *S. cuspidatum* Low percentages of Ericaceous rootlets and grass remains persist. The floral composition reflects a change towards drier bog surface conditions for the most recent period.	150 - present

The floral community response throughout the length of core WLM22 is very similar to that of WLM11 (Hughes *et al.*, 2000) which is reassuring for the replicability of the plant macrofossil technique and adds credibility to the analyses of both records. Evidence for the fen-bog transition is clearly marked in the levels below 880cm with the presence of fen species such as *Phragmites australis, Equisetum spp., Carex spp.* and *Menyanthes trifoliata.* At 880cm it is evident that the original lake infilled sufficiently for the development of the *Sphagnum* ecosystem engineer species *S. palustre*. A prolonged period of sedge and heather dominated flora succeeds the initial *S. palustre* phase. It has been argued that this may be a necessary factor in the development of sufficient peat thickness to support an ombrotrophic hydrology at several NW European mire sites (Hughes and Barber, 2004).

Part of the selection of this site for analysis and particularly the depth to which analyses were undertaken was the documented presence of a layer of the pool forming species *S. cuspidatum* ~660cm in core WLM11 (Hughes *et al.*, 2000). This layer was dated by pollen correlation with sediments from neighbouring Bolton Fell Moss to a period ~7800 BP (Hughes *et al.*, 2000). This fluctuation has been linked with the circum-North Atlantic climate perturbation at ~8200 BP. Core WLM22 shows little evidence for a wet phase at the depth described in WLM11 despite the near depth-for-depth similarity between the core assemblages in the upper 600 cm. One anomalous increase in *Sphagnum* is present at 784 cm. The increase is found in only one sample and is comprised of *S. sect acutfolia*, typically a drier species but, within the context of surrounding flora, indicative of a short period of wetter conditions. Comparison with the age depth model derived from AMS ^{14}C dates for core WLM22 (Chapter 5) indicates that a depth of 784cm equates to an age of ~7800 BP. Despite this increase in *Sphagnum*, remains are highly degraded and insufficient for preparation for isotopic analysis by the techniques available to this study. At a similar depth to that in which the wet phase is recorded in WLM11, WLM22 provides evidence for a sustained decrease in the proportion of ericaceous rootlet remains. The drop in ericaceous rootlets is replaced by remains of aerial parts of *Eriophorum vaginatum.*

A relatively sudden switch from dry *Eriophorum/Calluna* peat remains to *Sphagnum* peat occurs at 464cm and shows a period of fluctuating water tables from very wet to drier surface

conditions. Unlike many of the raised bogs of NW Europe, Walton Moss is relatively intact and as such does not exhibit the flora of nutrient enrichment and drying of the bog surface characteristic at other bog sites in the top strata. Instead, following a period of bog pool development, the top 36 cm are dominated by *S. magellanicum*, a wet lawn species.

The assemblages present in core WLM22 reflect a dominant surface wetness response with the exception of some levels. Below ~800 cm the presence of *Betula spp.* remains suggest that the bog surface during this period may have been slightly nutrient enriched. Below 834 cm, the dominance of *S. palustre* indicates that ombrotrophic conditions were only beginning to become established. In the top ~36 cm, the emergence of *S. magellanicum* as the dominant peat-former and extinction of *S. imbricatum* remains a contentious issue (Mauquoy and Barber, 1999a). It is widely accepted that this change in flora, whilst possibly triggered by climatic change, reflects a change in the competitive relationship of species (Stoneman *et al.*, 1993).

The multivariate plant macrofossil data were transformed using the Dupont hydroclimatic index (Dupont, 1986) method into a continuous univariate index of BSW changes with depth. Results of the Dupont analysis (var. Daley; Chapter 4) on the plant macrofossil data are given in Figure 6.2. Although macrofossil data are available to a depth of 896 cm, only data from 832 cm to the surface are used in this palaeo-proxy reconstruction. Below 832 cm, the species present indicate possible nutrient enrichment and less climatic influence on assemblage determination.

Between 832 cm and 480 cm, Dupont index values remain high indicating that relatively dry bog surface conditions prevailed with fluctuating water tables. Superimposed on this section of relatively dry conditions are five features where increased surface wetness is observed. The bases of the troughs for these features are found at 784, 712, 672, 592 and 528 cm. The trough at 528 cm appears wetter than those preceding. The switch to *Sphagnum* peat, seen in Figure 6.1 (480 cm), is reflected in a large shift in the Dupont index to lower values indicative of wetter conditions. The index values for the core section between 480 cm and 368 cm are highly variable comprising three major shifts to wet index values at 476 cm, 412 cm and 382 cm. Shift depths are taken as the mid-point between two samples that comprise a $\geq 2\sigma$ shift

towards wetter bog surface conditions. The shift at 382 cm represents the wettest conditions recorded at this site throughout the ombrotrophic section of the core. From 368 cm to 44 cm Dupont values show greater variability than in the deeper sections of the core with values fluctuating between 4.2 and 7.1. This greater fluctuation may in part reflect higher sensitivity of the Dupont index method to shifts in *Sphagnum* species than in the vascular species. The method was originally designed for use in upper, *Sphagnum* dominated sediments (Dupont, 1986). Consequently, the drier vascular species are clustered in the relatively short weighting range of 7 or 8 (Table 4.5) which may not fully represent the range of water tables that existed while these species were dominant.

A period of relatively dry bog surface conditions is observed between 200 cm and 176 cm that is followed by fall to wetter surface conditions, the trough of which is found at 128 cm. Dry conditions prevail ~80 cm and are succeeded by a "saw-tooth" fall to wetter conditions with the base of the trough at 28 cm indicative of very wet bog surface conditions. Evidence for a slight general trend towards wetter conditions is observed between 480 cm and the surface.

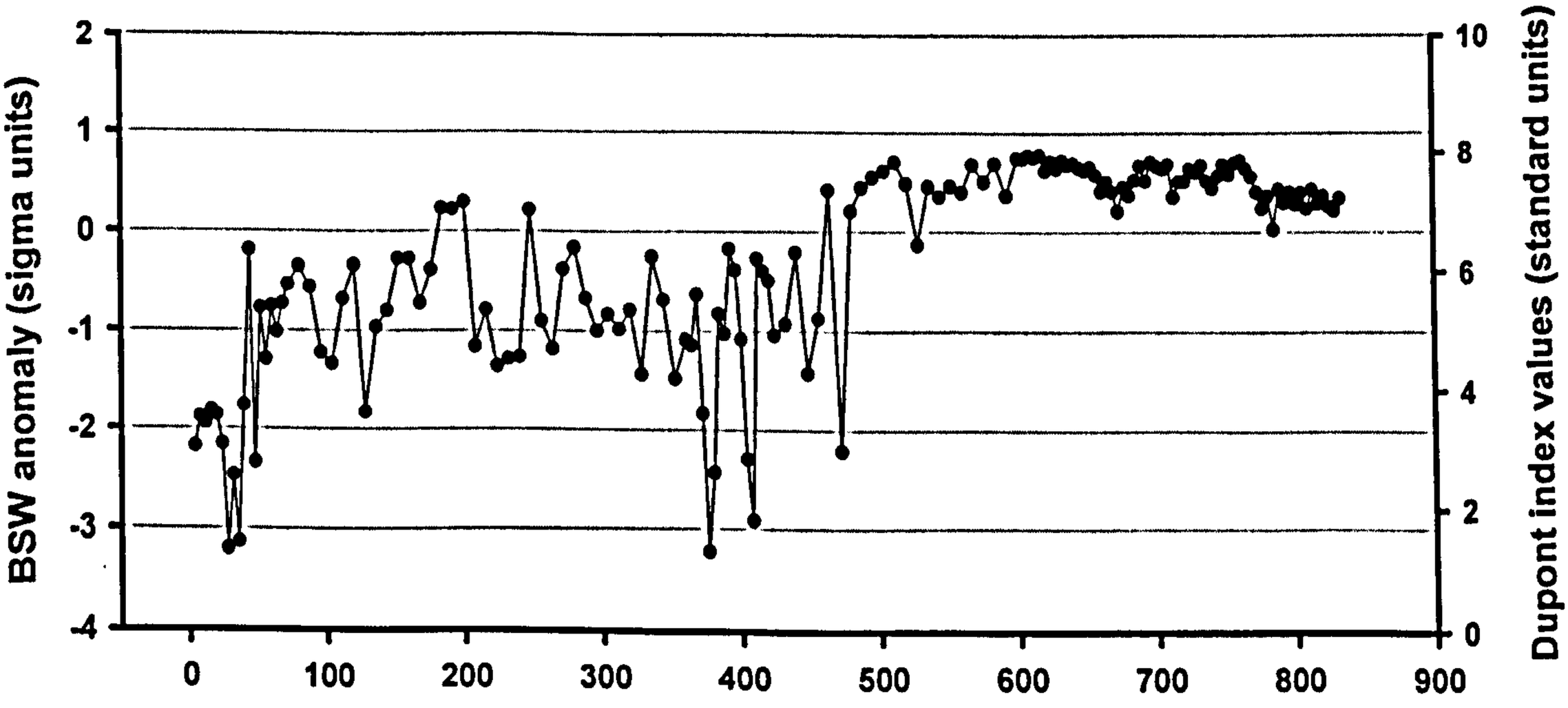

Figure 6.2 WLM22 Dupont wetness index reconstruction for plant macrofossil data; raw values on secondary y-axis, σ anomlies from the mean on primary y-axis

6.2.2 WLM22 testate amoebae data

Core WLM22 from Walton Moss was the only core to be analysed for testate amoebae biostratigraphy. The reasons for this have been outlined in Chapter 4. WLM22 was the principal core used for methodological testing (Chapter 4). Necessarily all proxies available were used on this core. Taxonomy is given according to that published (Charman *et al.*, 2000).

The results of the testate amoebae analysis are shown in Figure 6.3. The diagram has been zoned under the criteria described above and detailed in Chapter 4. Descriptions of each zone and the depths to which they relate are given in Table 6.2. The record extracted from the testate stratigraphy fluctuates between phases dominated by the relatively wet indicators *Amphitrema spp.* and those dominated by *Difflugia pulex* and *Nebela militaris*. Less is known of the water table tolerance of *D. pulex* in relation to many of the other species by virtue of limited presence on modern bog surfaces. Its fossil abundance and recent decline is closely associated with the decline of the *Sphagnum* species *S. imbricatum* which may reflect a host species status for the broad-leaved moss species. The species associated with the *D. pulex* dominated communities are typically relatively dry-tolerant. In the upper parts of the core, the zones dominated by *D. pulex* and *N. militaris* are also associated with significant percentages of *Hyalosphenia subflava* which is known for enduring low water tables and dry surface conditions. Some species exhibit wide hydrological tolerances such as *Assulina muscorum*, *Assulina seminulum* and *Cyclopyxis arcelloides*. *Arcella discoides* is recognised as an intermediate species and shows evidence of highest values in periods of change. It is also more common in the upper peats which may reflect quality of preservation.

Zone WLM-k is significantly more diverse than the lower zones. Taxa such as *Nebela griseola*, *Nebela flabellulum*, *Difflugia leidyi*, and *Euglypha spp.* reach relatively high percentages but are of low abundance or absent from the lower sediments. The poor preservation of *Euglypha spp.* is documented (Charman *et al.*, 2000). Whilst there is little evidence for poor preservation of *N. flabellulum*, *D. leidyi* and *A. discoides* are increasingly documented to be most abundant in upper peats.

Figure 6.3 WLM22 testate amoebae diagram (676 – 0 cm; 6660 BP to present)

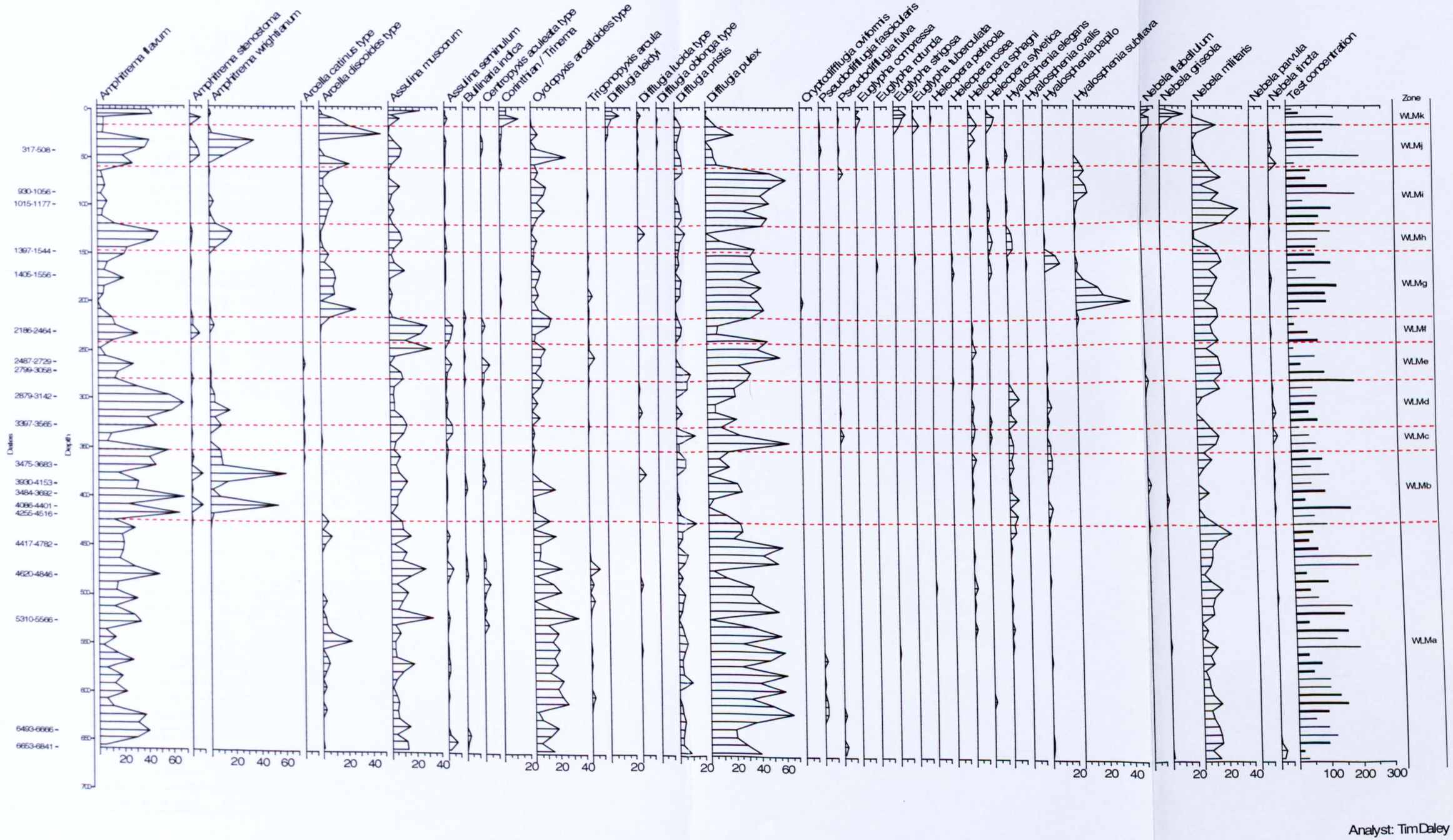

Analyst: Tim Daley

Table 6.2 Assemblage zones and environmental interpretations for WLM22 Testate Amoebae data

Zone	Depth (cm)	Description	Age (cal. yr BP)
WLM-a	656-422	This basal zone is dominated by *Difflugia pulex* with *Amphitrema flavum*, *Assulina muscorum*, *Cyclopyxis arcelloides* and *Nebela militaris* sharing relatively similar percentages. Single sample fluctuations are noted within the zone but no sustained assemblage changes are observed. The composition is indicative of intermediate to dry bog surface conditions. The presence of both *A. flavum* and *N. militaris* are indicative of fluctuating water tables.	6660 - 4290
WLM-b	424-352	Dominated by *Amphitrema spp*. particularly *A. wrightianum* with the presence of *A. stenostoma*. These species reach their greatest percentages in the record in this zone. The composition is indicative of very wet bog surface conditions consistent with bog pool development. Relative percentages fluctuate considerably within the zone indicative of a period of both very wet but also variable water table depths.	4290 - 3550
WLM-c	352-324	This short zone is composed largely of *Difflugia pulex* and *Nebela militaris* and represents an assemblage similar to WLM-a. Indicative of intermediate or dry bog surface conditions. The continued presence of the intermediate to wet indicator species, *Hyalosphenia elegans*, indicates water tables were variable. The increase in *Assulina muscorum* indicates a competitive advantage existed for those species able to resist dessication.	3550 - 3260
WLM-d	324-280	This zone is dominated by *Amphitrema flavum* with a notable presence of *Amphitrema wrightianum*. These species are indicative of bog pool development and wet conditions on the bog surface. The increase in *Hyalosphenia elegans* supports the interpretation of wet conditions.	3260 - 2810
WLM-e	280-242	Dominated by *Difflugia pulex* associated with a consistent percentage of *Nebela militaris*. *Amphitrema flavum* percentages are much lower than in zone WLM-d. The presence of *Trigonopyxis arcula* and *Cyclopyxis arcelloides* in combination with the species above infer drier bog surface conditions than zone WLM-d.	2810 - 2420
WLM-f	242-216	Assemblage is dominated by *Assulina muscorum* ~30% with *Amphitrema flavum* and the presence of wet indicator species *Amphitrema wrightianum* and *Amphitrema stenostoma*. The composition suggests a short period of elevated bog water tables. The dominance of *A. muscorum* is suggestive of fluctuation in the depth to water table.	2420 - 2160
WLM-g	216-148	In this zone, *Difflugia pulex* returns to dominance associated with large percentages of *Hyalosphenia subflava* that increases throughout the zone. There is a consistent presence of *Trigonopyxis arcula* and *Cyclopyxis arcelloides* and relatively low percentages of *Amphitrema flavum*. The assemblage is indicative of dry to very dry bog surface conditions. The return of *Arcella discoides* may reflect periods of intermediate water table.	2160 - 1460
WLM-h	148-120	Assemblage composed of *Amphitrema wrightianum* second in percentage to *Amphitrema flavum* with the presence of *Hyalosphenia elegans*. This reflects a dominance of wet indicator species. *Nebela militaris* percentages drop to zero. Wet bog surface conditions with bog pool development can be inferred for this zone.	1460 - 1180
WLM-i	120-60	*Difflugia pulex* highly dominant associated with large percentages of *Nebela militaris* and significant proportions of *Hyalosphenia subflava* and *Cyclopyxis arcelloides*. *Trigonopyxis arcula* is present. The assemblage in this zone reflects a period of dry bog surface conditions. Despite ability to resist dessication, *Assulina muscorum* percentages are lower than in WLM-h.	1180 - 560
WLM-j	60-16	*Amphitrema spp*. dominate this zone with high percentages of *A. wrightianum* observed in association with *A. flavum* and *A. stenostoma*. *Difflugia pulex* percentages are low as are dry indicator species such as *Nebela militaris* and *Hyalosphenia subflava*. The faunal composition is indicative of wet bog surface conditions with extensive bog-pool development.	560 - 110
WLM-k	16-0	This zone is distinct for the increase in species diversity in the record. Wet indicator species such as *Amphitrema stenostoma* are present and associated with *Difflugia Leidyi*, *Nebela griseola*, *Nebela flabellulum*. These species are rare at depth but all indicative of wet bog surface conditions. *Corinthian/Trinema* and *Euglypha spp*. are also present with significant percentages but rare at depth.	110 BP - present

The greater biodiversity and more continuous presence of species in the testate amoebae data in comparison with the plant macrofossil data allowed for exploration of the testate amoebae data with DCA to search for latent gradients. The increased diversity in the near surface sediments represents either a preservation or anthropogenic signal. In either case, to avoid the documented problems of a crossed gradient (see Chapter 4) the near surface layers were omitted from the DCA ordination. The species scores for axis 1 and axis 2 are given as a bi-plot in Figure 6.4. A key to species labels is given in Table 6.3.

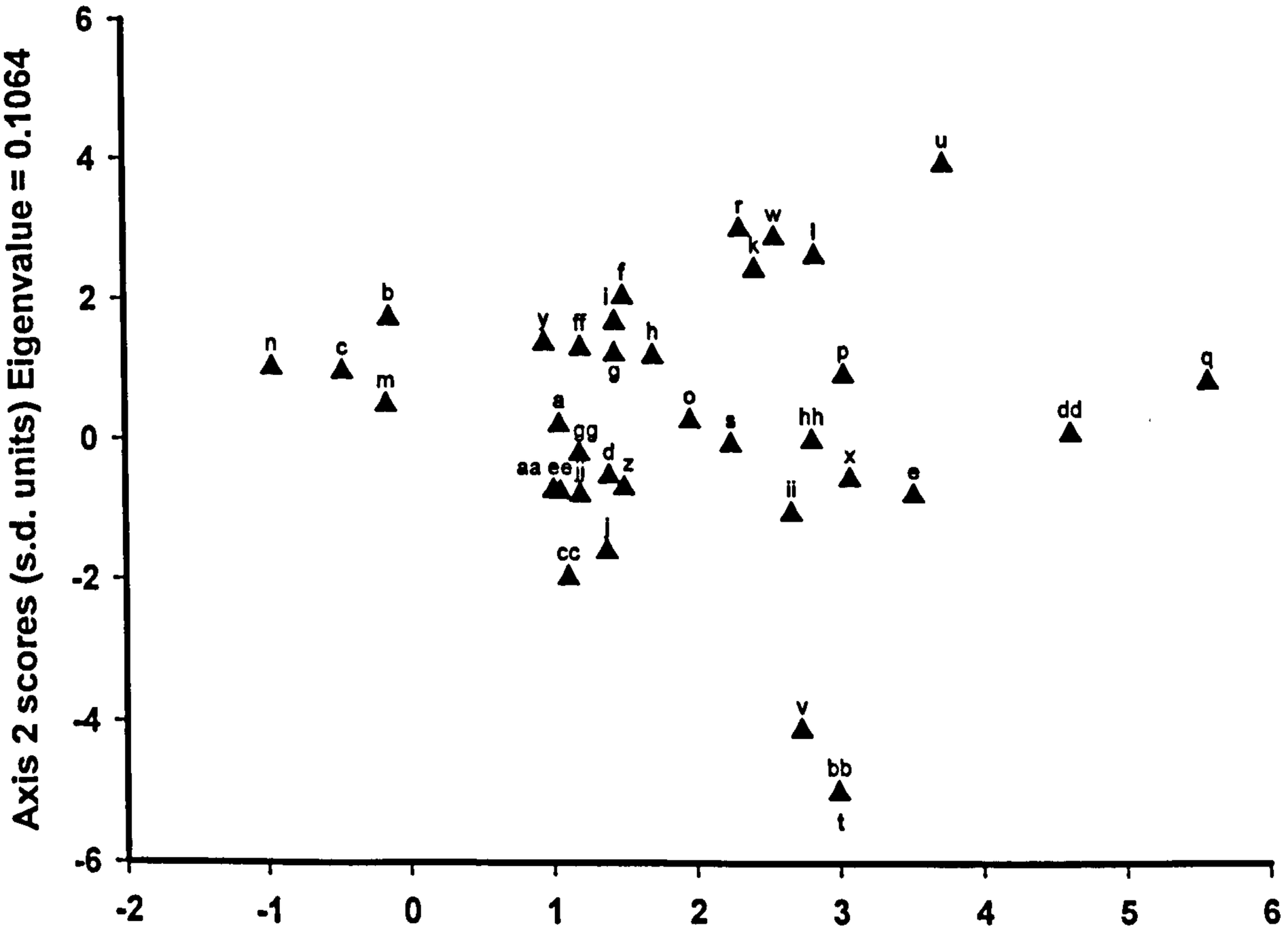

Figure 6.4 Bi-plot of species scores for DCA ordination of WLM22 testate amoebae data (32 -656 cm)

Table 6.3 Species legend for WLM22 Testate Amoebae DCA ordination

Species	Label
Amphitrema flavum	a
Amphitrema stenostoma	b
Amphitrema wrightianum	c
Arcella catinus type	d
Arcella discoides type	e
Assulina muscorum	f
Assulina seminulum	g
Bullinaria indica	h
Centropyxis aculeata type	i
Corinthian / Trinema	j
Cyclopyxis arcelloides type	k
Trigonopyxis arcula	l
Difflugia lucida type	m
Difflugia oblonga type	n
Difflugia pristis	o
Difflugia pulex	p
Cryptodifflugia oviformis	q
Pseudodifflugia fascicularis	r
Pseudodifflugia fulva	s
Euglypha rotunda	t
Euglypha strigosa	u
Euglypha tuberculata	v
Heleopera petricola	w
Heleopera rosea	x
Heleopera sphagni	y
Heleopera sylvetica	z
Hyalosphenia elegans	aa
Hyalosphenia ovalis	bb
Hyalosphenia papilo	cc
Hyalosphenia subflava	dd
Nebela carinata	ee
Nebela flabellulum	ff
Nebela griseola	gg
Nebela militaris	hh
Nebela parvula	ii
Nebela tincta	jj

In Figure 6.4, Axis 1 has an eigenvalue of 0.4232 and covers a range of approximately 7σ units. This indicates that ~ 42% of the variability can be attributed to a dominant driving variable. The eigenvalue for axis 2 is 0.1064 and accounts for approximately 10% of the

variability. Despite the long axis in Axis 2, the low eigenvalue indicates that the gradient in axis 1 dominates the spread of variability.

Species scores suggest that axis 1 represents a hydrological gradient (Figure 6.4). Hygrophilous taxa such as *Amphitrema wrightianum* and *Amphitrema stenostoma* plot at the negative end of axis 1. Taxa that are known to exist in drier conditions, such as *H. subflava* and *N. militaris* are observed to plot at the positive end of axis 1. Certain rare taxa are noted at the extreme positive end of axis one and this is possibly an artefact of their limited abundance throughout much of the core. In general, the scores are in agreement with the interpretation given for the raw testate amoebae diagram.

Sample scores derived from a weighted averaging function of the species scores given in Figure 6.4 are overlaid in Figure 6.5. The position of each open circle is defined by both the species present and their abundance in that sample. Figure 6.6 shows a bi-plot of axis one sample scores versus depth along with results of the transfer function. With reference to Figure 6.4, changes to low or negative values indicate a shift to wetter bog surface conditions. Changes to positive values indicate a drying of the bog surface.

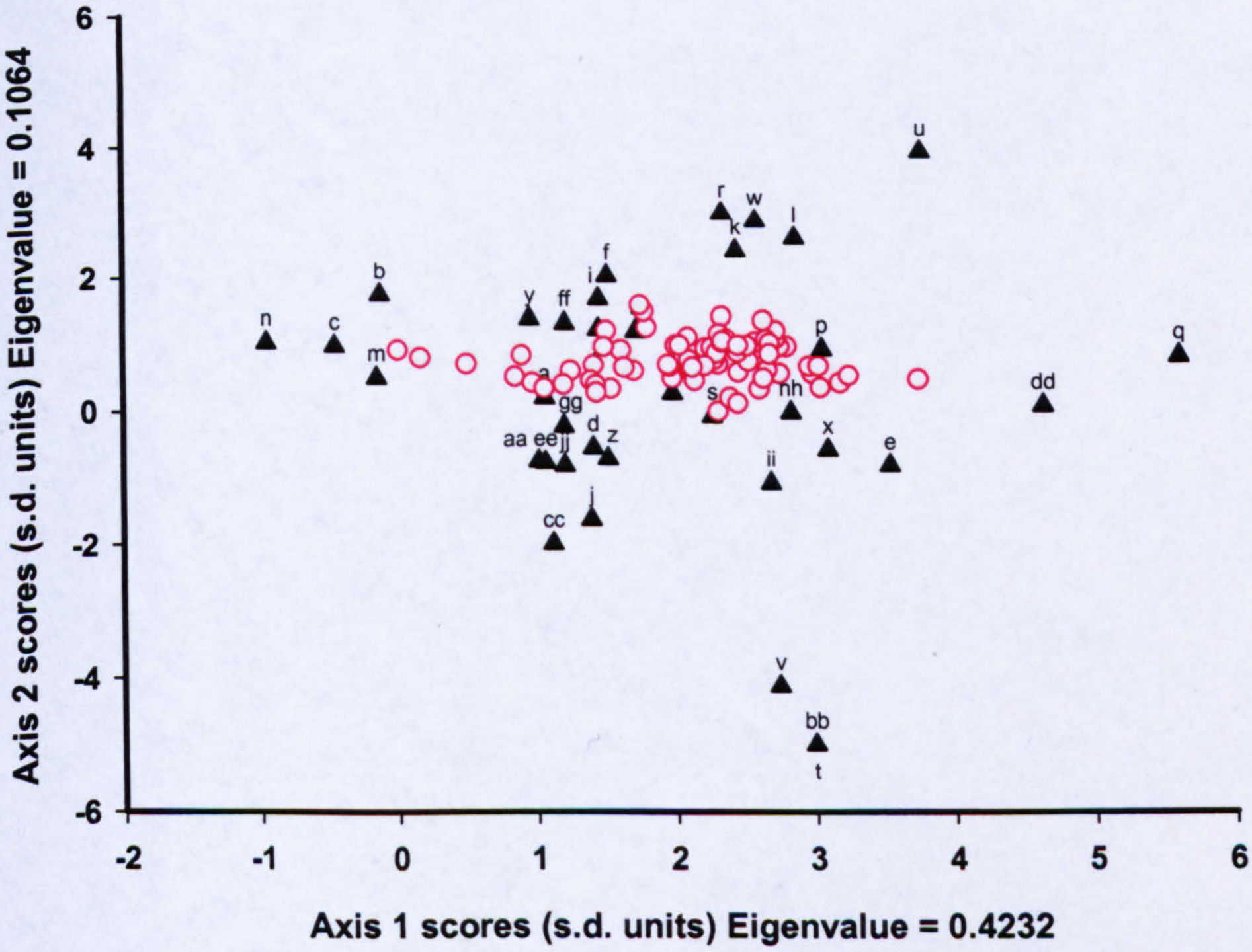

Figure 6.5 Bi-plot of species and sample scores for DCA ordination of WLM22 testate amoebae data

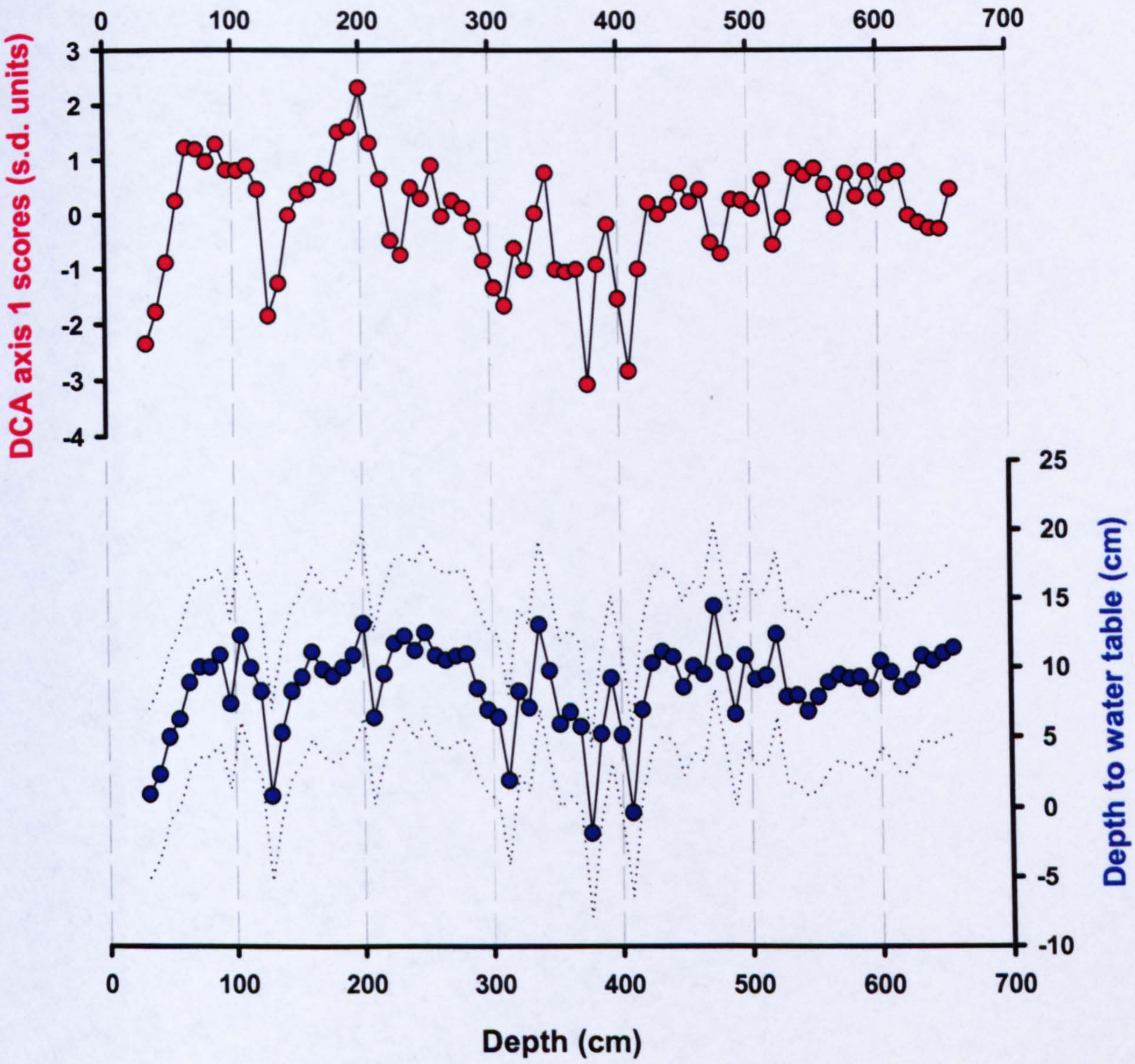

Figure 6.6 WLM22 testate amoebae DCA axis 1 sample scores and transfer function results with depth (32 – 656 cm); dotted lines represent root mean squared error for the transfer function reconstruction.

There is strong agreement between the DCA axis one results and the reconstruction of depth to water table using a WA transfer function (Charman *et al.*, 2007) confirming the interpretation of axis 1 as a hydrological environmental gradient and qualifying the central role of water table in testate amoebae ecology. Minor differences are noted between the structures of the two graphs. At 96 cm the transfer function record reveals a short single sample anomaly towards raised water tables that is not observed in the axis 1 data. The

presence of *A. wrightianum* in this level despite a dominance of drier indicator species is likely to be responsible. The reason the two graphs show difference relates to the water table weightings applied to the species abundances. In this case, the weighting applied in the transfer function is wetter than the weighting derived from the DCA ordination. This explanation can be applied to other discrepancies between the curves, particularly at ~200 cm where the extreme dry values in the axis 1 scores are produced by variation in the abundance of *H. subflava* which is absent from lower parts of the record, despite the likelihood that conditions were similarly dry on the bog surface.

Wet shifts in the testate data are defined as a $\geq 2\sigma$ change towards lower axis 1 values and interpreted as an increase in BSW. These are observed after 424, 392, 344, 240, 200 and 64 cm. Comparison with the transfer function data indicate that water tables rose during these periods by ~10, ~11, ~11, ~5, ~12 and ~9 cm.

Conversely, dry shifts are defined as a $\geq 2\sigma$ change towards higher axis 1 values and interpreted as a decrease in BSW. These are observed after 408, 376, 312, 232 and 128 cm. Comparison with the transfer function data indicate that water tables fell during these periods by ~ 9, ~15, ~10, ~7 and ~11 cm. Comparison of these shifts with the other proxies is given in section 6.2.4 where a stacked record is produced and presented as a time-series using the age depth model developed in Chapter 5.

6.2.3 WLM22 humification data

The degree of decomposition of the peat is used as a measure of the depth of the aerated zone at the time of deposition. The lower the bog water table, the greater the aerated zone and consequently the greater the decomposition of the peat (Blackford and Chambers, 1993a). The rationale for use of this proxy measure is given in Chapter 4. The benefits and limitations of the method are discussed in Chapter 2.

Raw transmission results are presented in Figure 6.7 A. The data are taken at 4 cm stratigraphical resolution throughout the core with higher resolution contiguous 1cm data through 360- 412 cm. Two trends are evident from first inspection, (1) a general trend towards lower transmission values with depth and (2) decreasing amplitude of variation with depth. Both of these factors relate to autogenic processes of diagenesis and do not reflect a sole climatic influence. The second of these factors is considered at the interpretation stage. Previous studies have used linear regression to isolate and remove the diagenetic signal of increased humification with depth (1) (Blundell and Barber, 2005). With the record from WLM22, a linear regression is too simple a model to reflect the influence of depth. Within the *Sphagnum* peat (0-504 cm), a linear model approximates well the trend of freshening towards the surface. In the *Eriophorum/Calluna* peat below 504 cm, the autogenic decay slows to plateaux. It can be seen from Figure 6.7 that where a linear model is used for the entire sequence an artificial freshening with depth would result in the lower layers. Similarly, this is also observed if the linear model is replaced by an exponential model. Accordingly, the humification data are therefore detrended using a linear model for the top 504 cm only and an offset applied to the lower layer raw transmission values to allow synchronisation with the final value at 504 cm. The choice of 504 cm as a hinge point is judged both visually and by cross-reference with the base of the upper core *Sphagnum* peat layer derived from the plant macrofossil record. The independence of the humification record is not compromised by this process as the magnitudes and directions of shifts are not altered. Detrended and normalised humification data are presented in Figure 6.7 B.

Shifts towards higher transmission values reflect a decrease in the degree of decomposition and hence infer a change towards increased BSW. Wet-shifts are observed to occur at 532, 488, 420, 396, 373, 336, 184 and 68 cm. Shifts towards lower transmission levels conversely indicate drier bog surface conditions. Dry-shifts are observed at 522, 474, 404, 376, 350, 292 and 128 cm.

It is possible that the $\geq 2\sigma$ threshold may neglect legimate shifts from the deeper peats using this proxy. The influence of species composition on humification data has been well documented (Caseldine *et al.*, 2000; Yeloff and Mauquoy, 2006). Accordingly, the magnitude of humification response to a change of water table depth may be represented differently in

Sphagnum peat from that dominated by *E. vaginatum* and ericaceous remains which both possess a higher decay rate than *Sphagnum* (Clymo and Hayward, 1982; Scheffer *et al.*, 2001) and which have a wide range of water table tolerance. This higher decay rate may subdue the extent of the wet shift. Whilst the technique is sensitive enough to detect a direction of change, care must be used in comparison of the magnitudes of change. To that end, the presence of shifts <2σ in the lower sections of the core are noted.

The middle section of the core is notable for a period of highly variable, large magnitude shifts in the humification record in both directions indicating highly variable water tables. The highest magnitude change of the record is found in this part of the core with a shift in transmission values from 28.1 to 59.1 % representing a 3.5σ shift from the mean.

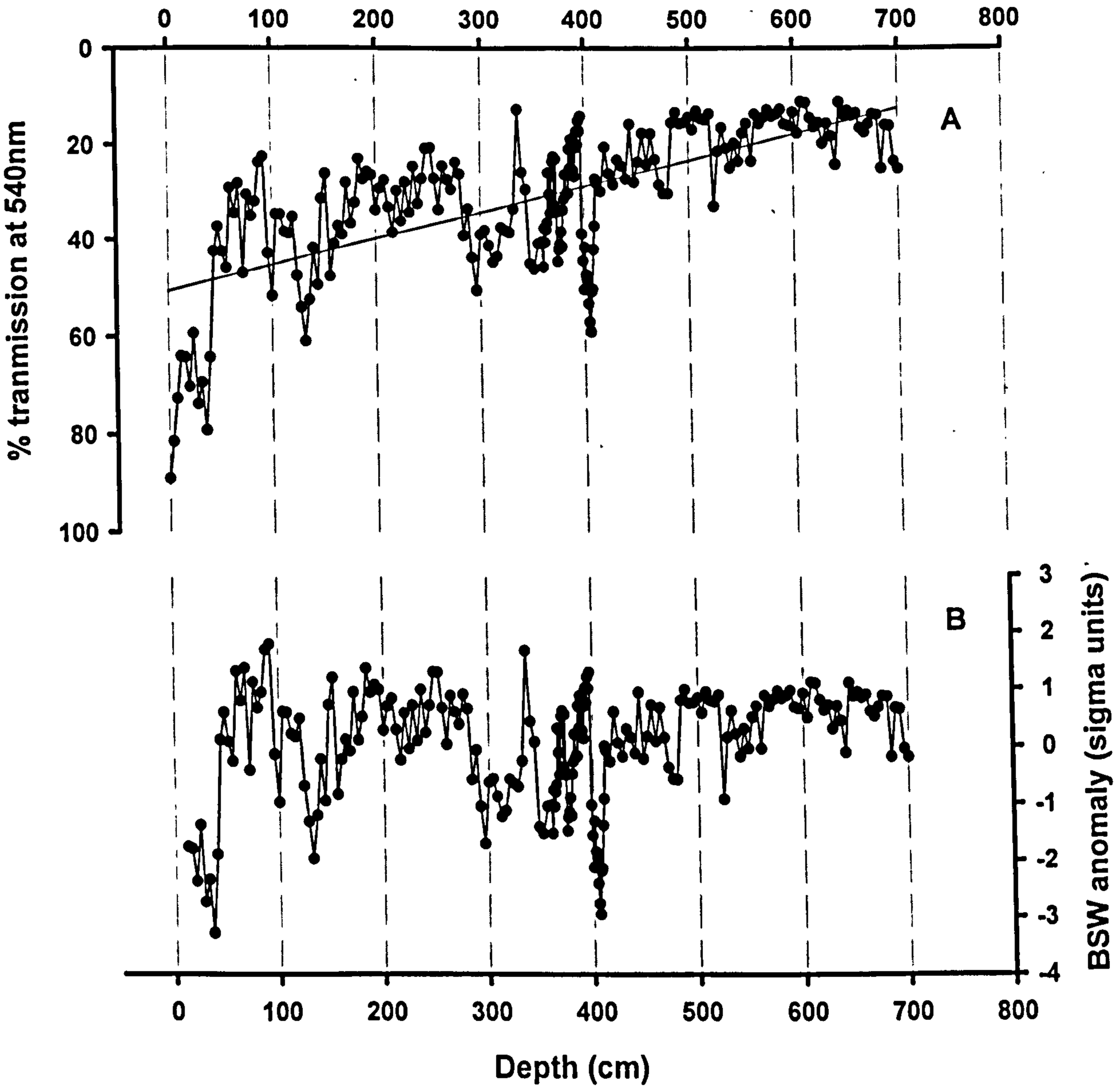

Figure 6.7 WLM22 peat humification data; A) raw transmission values and demonstration of artificial freshening at depth with whole core detrending, B) detrended (16 - 504 cm) and normalised transmission values presented as σ anomalies from the mean

6.2.4 Multiproxy comparison for WLM22

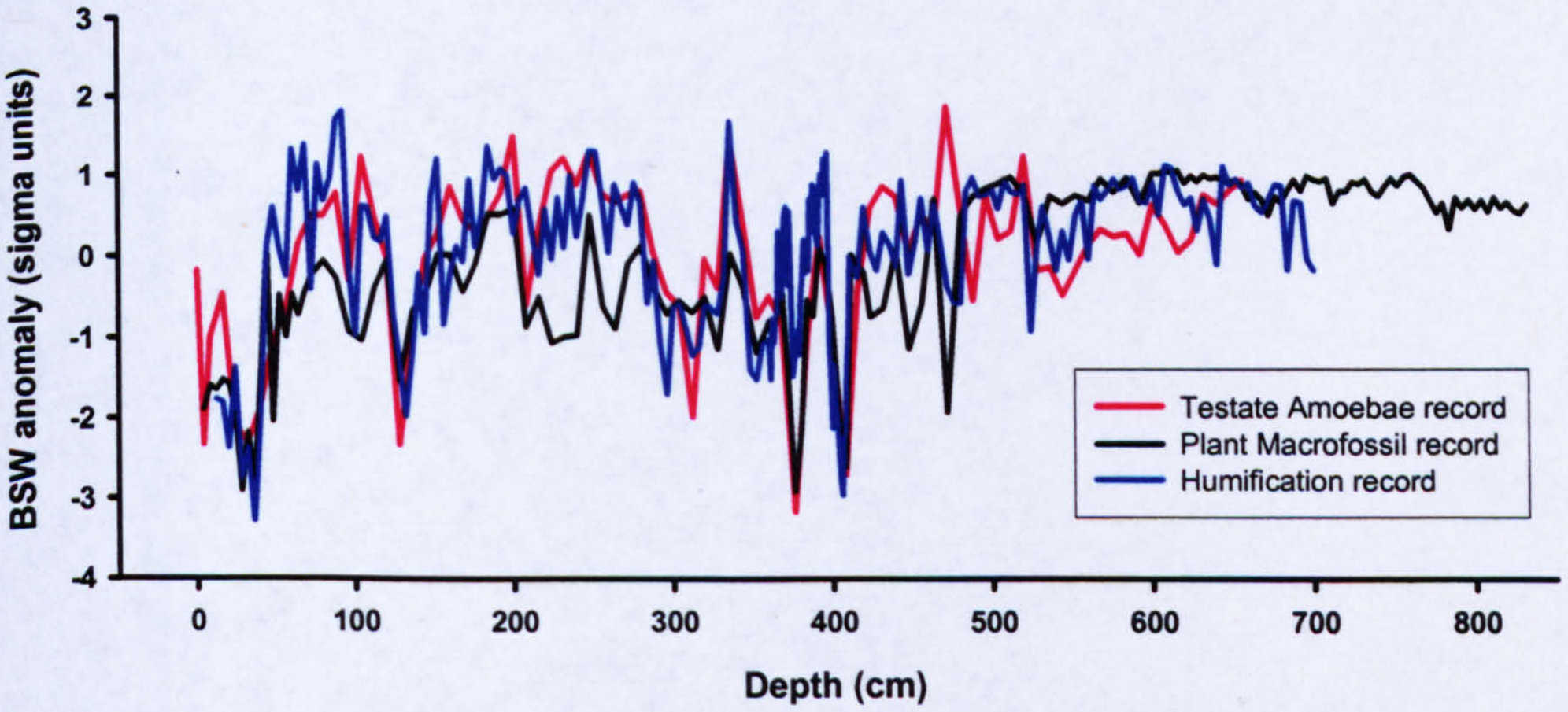

Figure 6.8 WLM22 multi-proxy comparison comprising plant macrofossil data (black line; 4 - 832 cm), testate amoebae transfer function data (red line; 0 - 656 cm) and peat humification data (blue line; 12 - 700 cm)

Normalised variability in all three proxy reconstruction techniques for core WLM22 is presented in Figure 6.8. There is excellent general agreement between the independent proxy records with major shifts in direction, and frequently in the magnitude of change, preserved in all three records. The depths of the major changes and their corresponding ages are reported later in this section. It is noted that no issues of chronological uncertainty are involved in the comparison of these records as all are obtained from samples from the same core and so are directly comparable.

Whilst agreement is excellent, minor differences are noted between the proxy records. Dupont index values derived from the plant macrofossil record suggest consistently wetter bog surface conditions than the other proxies through the upper *Sphagnum* sections of the core (504 cm - surface). This is possibly due to a concentration of data in the lower part of the core (Figure 6.1) and consequential distortion of the mean towards the values represented by the lower section of the core. This slightly non-normal distribution inevitably results in lower

normalised values in the upper (*Sphagnum*) section of the core. It will be noticed that the humification signal is also more variable or noisy than the other proxies and this in part reflects a higher sampling resolution.

Two sections are observed where the macrofossil record is anomalously wetter than the other proxies (270-200 cm and 110-80 cm). Both of these phases coincide directly with periods of dominance of *S. imbricatum*. In the section between 270-200 cm, the short fluctuation to drier conditions is accounted for in all three proxies and in the macrofossil record specifically by an increase in the proportion of ericaceous rootlets and reduction in *S. imbricatum* (Figure 6.1). The structure of change through these phases is very similar to that of the humification and testate amoebae records but magnitudes (σ deviation from the mean) are different. This evidence leads to the suggestion that the weightings applied to species during the Dupont weighted averaging process may not be properly proportional to relative species ecology. This is more plausible than both the humification and testate amoebae signals equally recording anomalously dry values during these periods. The wide water table tolerance of *S. imbricatum* has been shown previously (Green, 1968; Barber, 1981; Stoneman *et al.*, 1993).

The sensitivity of the Dupont index may also explain the higher variability noted in the humification record below 5 m than that in the macrofossil record. The sensitivity of the Dupont technique in peat dominated by vascular species has been discussed previously. It is possible that the humification record through these levels is more responsive to change than the macrofossil record due to the clustering of drier-dwelling (xeric) species with large water table ranges under a narrow range of weightings. The Dupont index still provides a good approximation of the direction of change, however, for these data where low species diversity prevents the use of a macrofossil transfer function.

Testate amoebae data suggest consistently wetter surface conditions than the other proxies through the lower peat sections. The assemblage in this zone is dominated by *D. pulex* which has been assigned a wetter ecology in the most recent transfer function, used here (Charman *et al.*, 2007) compared to that of the earlier British transfer function (Woodland *et al.*, 1998). The ecology of the taxon remains complex however owing to a preference for relatively high water tables whilst also favouring relatively low percentage moisture (Charman *et al.*, 2007).

It is possible that *D. pulex* may have been responding more, in this situation, to percentage moisture, a low value for which would be supported by the other proxies, implying relatively dry bog surface conditions existed during this period.

Direct disagreement between two proxies is found in just one sample. At 472 cm, a strong signal to wetter surface conditions is observed in the plant macrofossil data that is matched by a signal of increased wetness in the humification data. Testate data, conversely, show the deepest water table depth for the record. The testate DCA record, however, shows a shift to wetter conditions in this level. The sample directly preceding 472cm at 480 cm is also relatively wet in the transfer function data.

The discrepancy is explained by the weightings given to the species in the averaging process. The sample is dominated by *A. flavum* with significant percentages of *A. muscorum* and a relatively high (8%) abundance of *T. arcula*. In the DCA bi-plot (Figure 6.4), these species plot as Intermediate-wet, Intermediate-wet and Intermediate-dry, respectively. In the transfer function, the optima for these species are intermediate, intermediate-dry and very dry respectively. *T. arcula* is poorly represented in core WLM22 and hence is poorly represented in terms of its optimum in the DCA ordination. The peak in *T. arcula* and the strongly dry optima in the transfer function produce a dry peak in the testate reconstruction seen in Figure 6.8.

Despite the presence of dry indicator testate amoebae species, it is more plausible that the sample level is indicative of wetter conditions. Charman et al. (2007) state that in drier samples, the presence of wet indicators is more important than the presence of dry indicators as the wet have a narrower range of water table tolerances. The presence of wet indicator species such as *C. aculeata* and dominance of *A. flavum* suggest that the xeric species may have existed on dry microsites whilst intermediate water table conditions prevailed. The presence of a relatively wet-indicating sample directly preceding 472 cm at 480 cm supports this interpretation and may suggest a more rapid response of the testate amoebae to environmental conditions, consistent with the more rapid life-cycle turnover (Tolonen, 1986).

The stacked record of inferred Bog Surface Wetness (BSW) change is presented for all available data (Figure 6.9) and only those samples where two or more proxies are available (Figure 6.10). The stack is derived from the mean of the sigma values for the proxy data presented in Figure 6.8 above. For Figure 6.9, the stacked record is inevitably dominated by the humification signal for which there are nearly double the number of data. However, comparison with the record in Figure 6.10 where sampling resolution has been degraded to allow only those samples where ≥2 proxies are available reveals that the major changes are preserved in the lower resolution stacked record. The effect of incorporation of the higher resolution data in Figure 6.9, in the most part, is to add noise rather than significantly alter the climatic interpretation throughout the record. Two exceptions are noted to this general finding in the enhancement of the size of the wet shifts at 532 and 488 cm. In Figure 6.9, these are comparable in magnitude to the wet shift at 336 cm. In Figure 6.10, the fluctuations are relatively subdued.

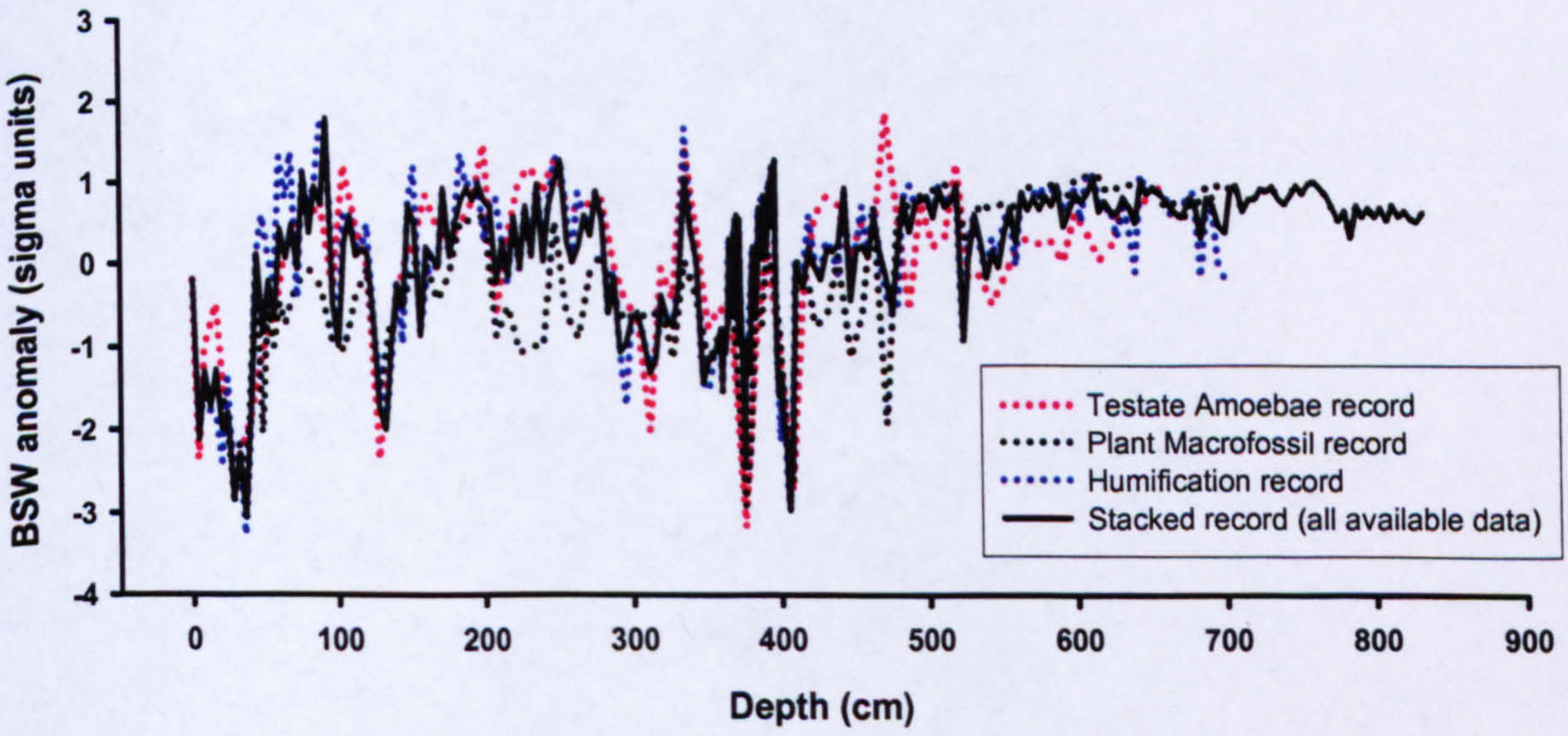

Figure 6.9 WLM22 stacked record of inferred Bog Surface Wetness change using all available data

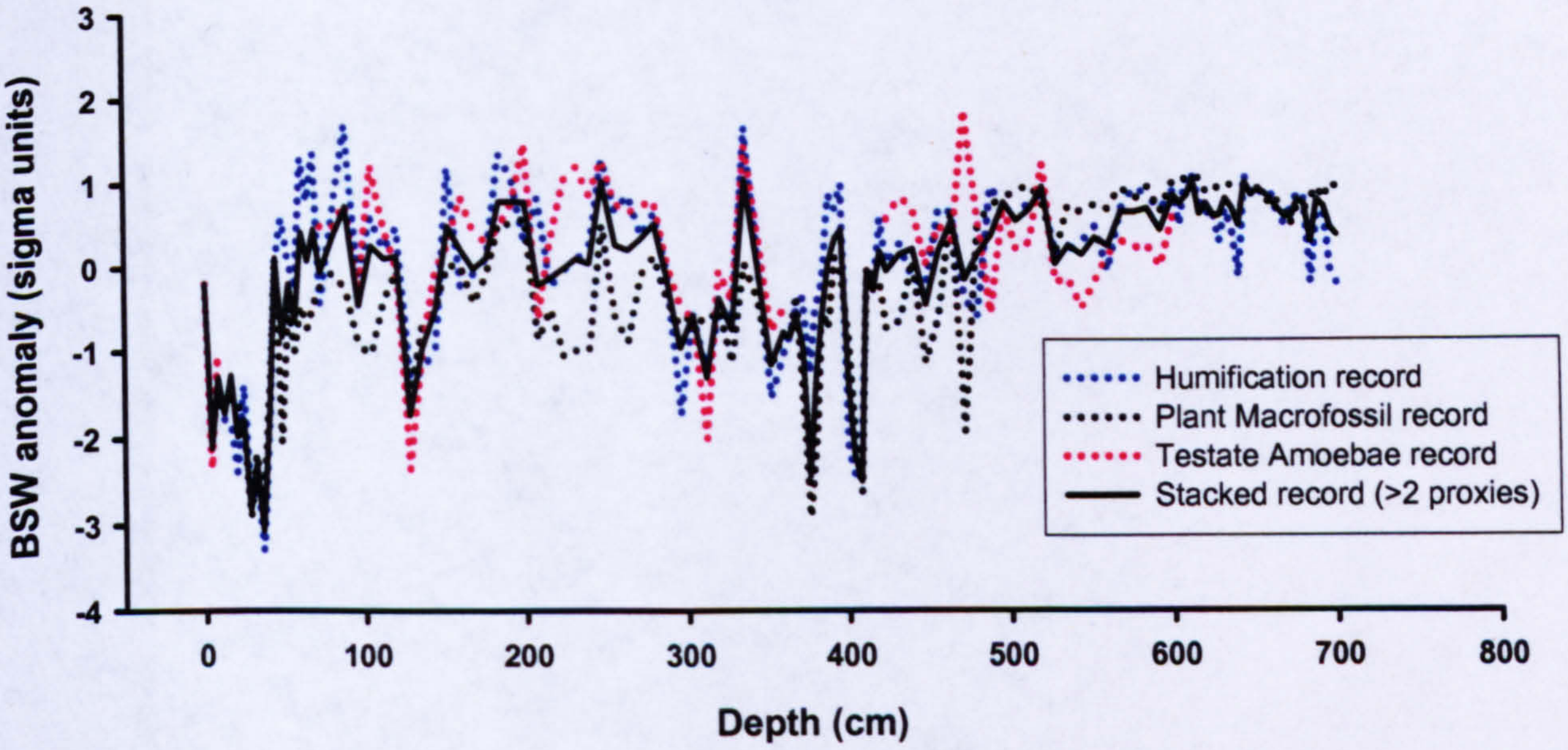

Figure 6.10 WLM22 stacked record of inferred Bog Surface Wetness (BSW) using all samples with ≥2 proxies available

For both records the strength of agreement between proxies noted in the earlier discussion is displayed in the correspondence between the stacked record and the individual proxies. The locations in the core where agreement is less (270 – 200 cm and 472 cm) have already been discussed.

The two stacked records are combined with the age depth model for core WLM22 (Chapter 5) and presented as proxy-climatic time-series for the last ~8,500 years and ~7000 years respectively in Figure 6.11. Clear shifts to wetter bog surface conditions occur at 4200, 3950, 3350, 1450 and 400 BP. Smaller wet shifts are noted at 5700 and 4900 BP. Clear shifts to drier bog surface conditions occur at 4050, 3800, 3500, 2900, 2000, 1200, 200 BP. All shifts are noted here rounded to the nearest 50 years. The most rapid shift in BSW occurred ~ 4200 BP with a switch to very wet bog surface conditions over approximately 40 years, succeeded by an equally rapid shift to dry conditions, which occurred over approximately 80 years. Assuming little variation in the accumulation rate at this time, the duration of the wet period was ~150 years. From 4000 BP to present, the data display evidence of millennial scale cyclicity, most noticeable in the last 2000 years with shifts to wetter conditions occurring at a similar time to known fluctuations in IRD events (Bond *et al.*, 1997; Bond *et al.*, 2001) and

thermohaline circulation (Bianchi and McCave, 1999; Hall *et al.*, 2004). A shift to wetter conditions during the Dark Ages period is well defined at 1450 BP. A further strong wet shift at 400 BP is inferred as contemporaneous with the Little Ice Age (LIA). Whilst the possibility of reduced sensitivity in the humification and macrofossil proxies at depth has been discussed above, there is no indication that the testate amoebae record is any less sensitive in so far as the species present are well-represented in the transfer function. It is therefore with some confidence that it can be inferred from the data that the climatic deterioration contemporaneous with the LIA was the most severe in this region in at least the last 7000 years.

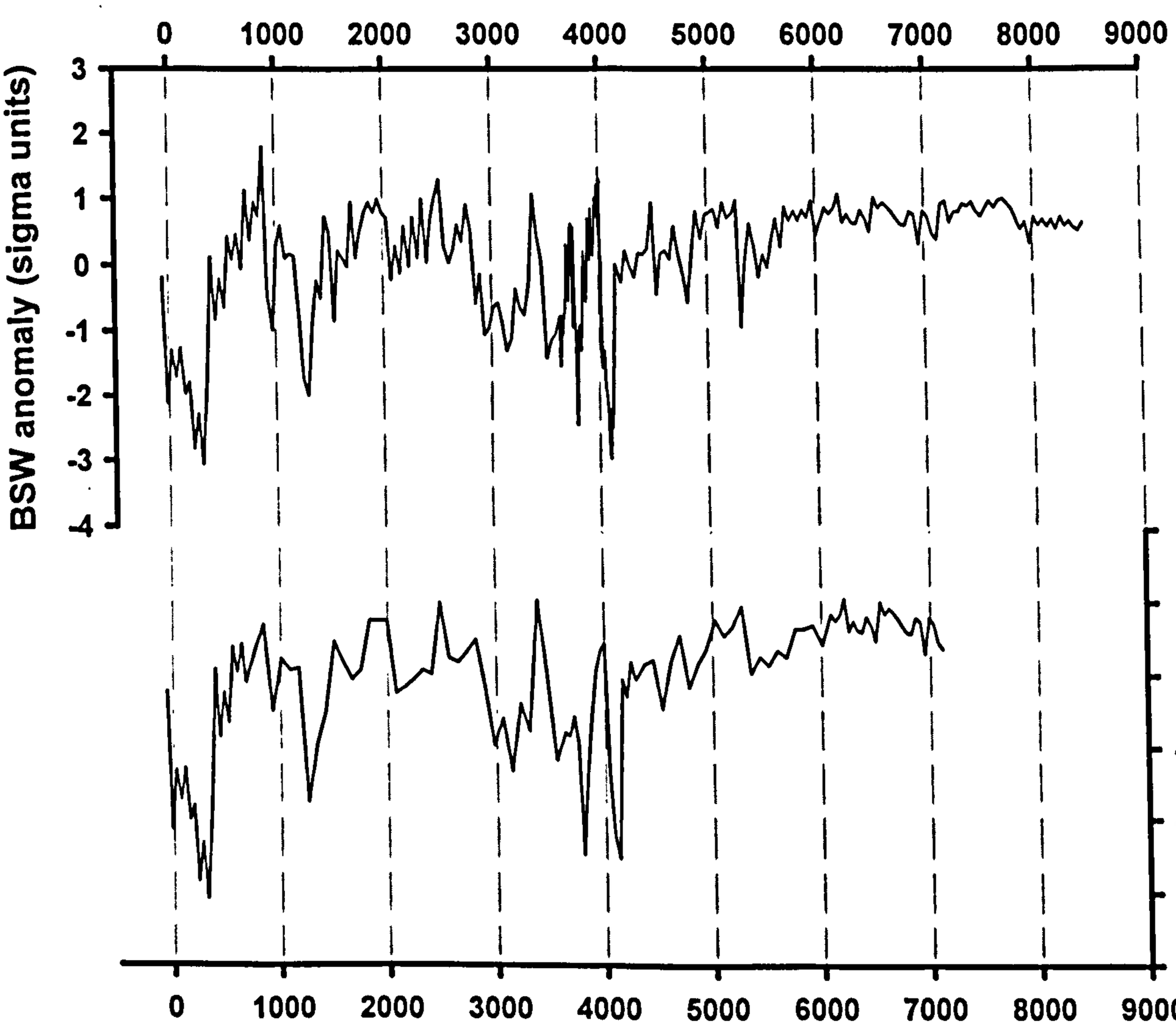

Figure 6.11 WLM22 multi-proxy climatic time-series; A) using all available data, B) using all samples with ≥2 proxies available

6.3 *Dosenmoor*

6.3.1 DSM3 plant macrofossil data

Plant macrofossil data for core DSM3 are presented in Figure 6.12. The diagram has been zoned into units of similar floral assemblage for the purposes of summarising the principal changes in stratigraphy. These zones have been determined by eye, consistent with those records from the other sites in this study. Descriptions of the floral communities of each zone are given in Table 6.4. The plant macrofossil record from DSM3 exhibits a prolonged phase of *Eriophorum/Calluna* peat following transition to ombrotrophic status in common with bogs in NW Europe (Hughes and Barber, 2004) and within this study (Figure 6.1). This phase is ended by a period of highly variable surface wetness conditions reflected in zones DSM-d, DSM-e and DSM-f. During these zones, the floral communities shift dramatically from those associated with very wet conditions and bog pool formation to those associated with dry surface conditions and fluctuating water tables. Thereafter, *Sphagnum* remains the dominant peat former though to the surface. The principal peat forming species is *S. imbricatum*, which fluctuates in abundance with *S. sect. acutifolia*. The dominance of these species is interrupted in zone DSM-h by a shift in assemblage to a community indicative of very wet conditions, indicated especially by the presence of algal muds. Despite the dominance of *S. imbricatum* in DSM-i, there is evidence for increased variability compared with DSM-g. This is demonstrated by the switch from increased percentages of *S. cuspidatum* to drier species and more frequent charred remains before a subsequent rise in *S. cuspidatum*. The top-most zone leading to the surface is composed of species indicative of nutrient enrichment. They are commonly associated with human disturbance. There has been extensive cutting of the peat surface for fuel and drainage and this has altered both the hydrology and nutrient status of the surface sufficiently as to afford competitive advantage to these disturbance species. It is highly unlikely that the assemblage in DSM-j reflects a climatic influence.

Figure 6.12 DSM3 plant macrofossil diagram (672 – 0 cm; 5830 BP to present)

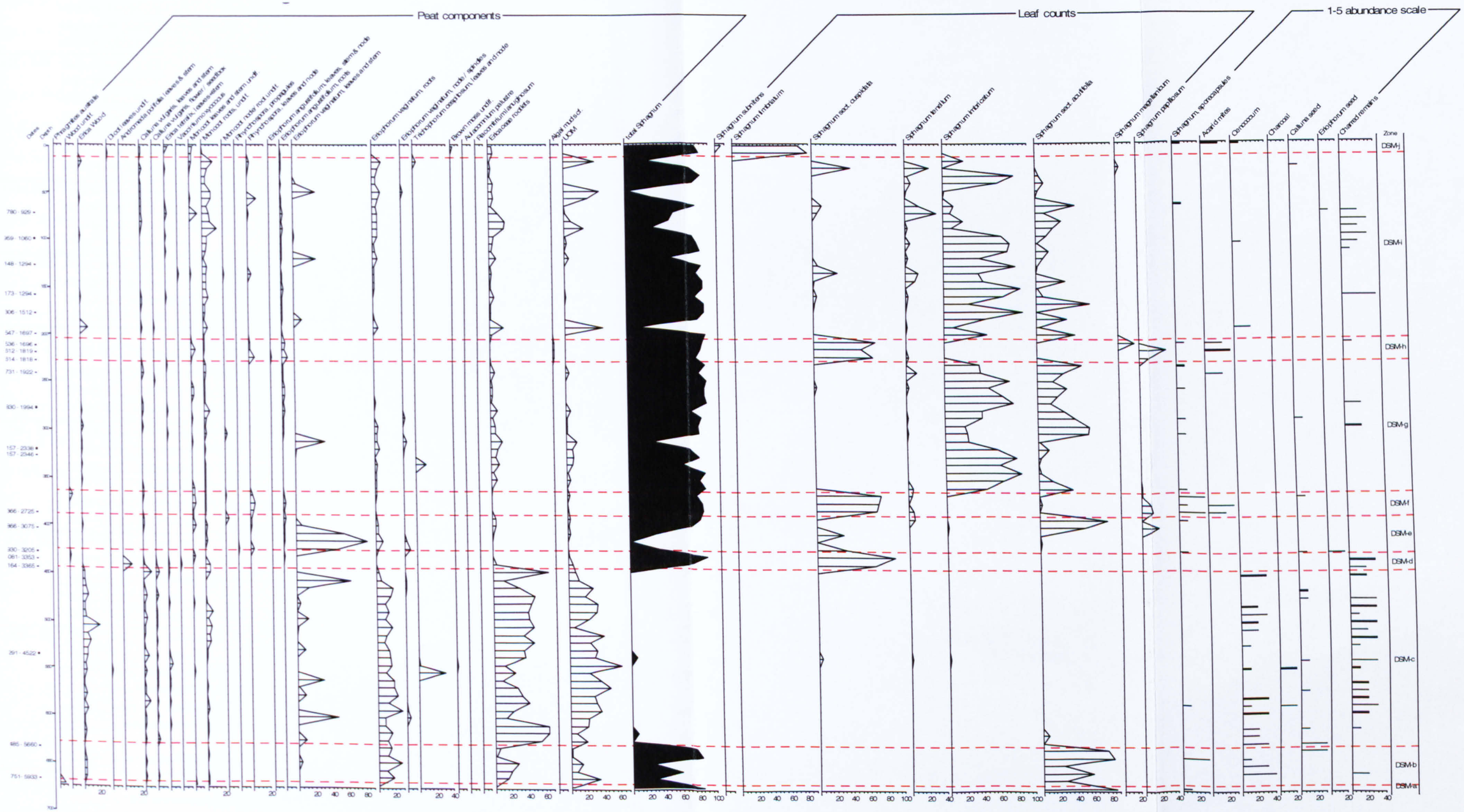

Table 6.4 Assemblage zones for core DSM3 from Dosenmoor

Zone	Depth (cm)	Description	Age (cal. yr. BP)
DSM-a	672 - 668	Basal zone, dominated by *Sphagnum sect. acutifolia* with significant presence of *Phragmites australis*, indicative of nutrient enriched, basic conditions. Lack of characteristic ombrotrophic species. Heathers and grasses absent. The flora in this zone suggests a fen-like environment.	5830 - 5800
DSM-b	668 - 628	Dominated by *S. sect. acutifolia* associated with rising percentages of ericaceous rootlets, Erica wood and *Eriophorum vaginatum* remains. Aerial parts of the *E. vaginatum* plant are found at 592 cm. The assemblage is indicative of an early ombrotrophic community with relatively dry surface conditions.	5800 - 5400
DSM-c	628 - 444	Base of zone characterised by a sharp reduction in *Sphagnum* and replacement by large percentages of UOM and ericaceous rootlets. *E. vaginatum* roots maintain a similar percentage to those in DSM-b with occasional spikes in aerial remains. Aerial parts of *Calluna vulgaris* are observed consistently associated with occasional *Erica tetralix* remains. The assemblage is indicative of dry ombrotrophic conditions. Charred remains and cenococcum are high indicating frequent fire and a dry, well aerated surface.	5400 - 3250
DSM-d	444 - 426	Assemblage dominated by the wet-dwelling taxa *Sphagnum cuspidatum* with the presence of *Rhyncospora alba*. Ericaceous rootlets and *E. vaginatum* remains become absent in the zone. The flora are indicative of very wet surface conditions and bog pool development.	3250 - 3060
DSM-e	426 - 388	Dominated by the aerial remains of *E. vaginatum* and the drier-dwelling *S. sect. acutifolia*. *Trichophorum cespitosum* remains are present along with Erica wood. *S. cuspidatum* percentages are much lower than in DSM-d. This assemblage is indicative of a drier bog surface with lower, more variable water tables.	3060 - 2700
DSM-f	388 - 364	Dominated by *S. cuspidatum* and associated with a variety of wet-dwelling taxa, such as the wet lawn species, *Sphagnum papillosum* and the presence of *Rhyncospora* remains. Acarid mites are frequent and seeds and *Sphagnum* spore capsules readily preserved. Ericaceous rootlets and *E. vaginatum* remains are absent. This community is strongly indicative of wet bog surface conditions with bog pool development.	2700 - 2500
DSM-g	364 - 228	Dominated by *Sphagnum imbricatum* and *S. sect. acutifolia*. *E. vaginatum* and ericaceous rootlets percentages are low but relatively persistent with occasional remains of Erica wood. Occasional charred remains are observed. The assemblage is indicative of intermediate to dry bog surface conditions. Flucatuations in the water table are evidenced by variation between the percentages of *S. imbricatum* and *S. sect. acutifolia*, with drier conditions during phases of *S. sect. acutifolia* dominance.	2500 - 1690
DSM-h	228 - 204	Short phase of very wet bog surface conditions indicated by the dominance of *S. cuspidatum* and the presence of algal muds. Dry indicator species in DSM-g are replaced by *Eriophorum angustifolium* and *R. alba*. Erica wood, ericaceous rootlets and *E. vaginatum* become absent. The proportion of acarid mites is high and the wet lawn species, *S. magellanicum* and *S. papillosum* are present.	1690 -1580
DSM-i	204 - 12	Dominated by *S. imbricatum* which fluctuates with *S. sect acutifolia*. In the upper third of the zone, *Sphagnum* abundance fluctuates with ericaceous rootlets and UOM. Three phases of variation coincide with increased charred remains indicative of drier conditions and fire frequency. Monocot root percentage rises throughout the zone towards the surface. Three short, single or dual sample fluctuations to wetter surface conditions are noted with rises in *S. cuspidatum* and *S. tenellum* at 136, 64 and 24 cm. Overall, this zone is indicative of intermediate conditions of BSW with short fluctations to higher water tables.	1580 - 120
DSM-j	12 - 0	The topmost zone is dominated by *S. fimbriatum* associated with the presence of *S. subnitens* and brown mosses. This community is indicative of nutrient enrichment and disturbance.	120 - present

DSM3 plant macrofossil data were condensed to univariate index using Dupont weighted averaging. The modified index (var. Daley) (Chapter 4; Table 4.5) was used to provide weights for individual species. The lowest levels of core DSM3 were omitted as the assemblages present were indicative of a transitional community that may have received nutrient input from groundwater and hence provided a weaker link to climate. Similarly the upper-most core samples composed of disturbance species were omitted.

The results of the averaging function are presented in Figure 6.13. In the Dupont analysis, a prolonged phase of dry bog surface conditions is observed, ornamented by relatively minor fluctuations in water tables. This prolonged period is succeeded by a sharp change to very wet surface conditions at 448 cm. From this point to the near surface, the record is much more variable and coincides with the onset of *Sphagnum* peat dominance (see above). As noted above, this higher variability may reflect a greater sensitivity of the Dupont technique to *Sphagnum* based variation. Three major shifts to wet conditions are observed at 448, 392 and 232 cm. These shifts are represented strongly owing to the low weights applied to *S. cuspidatum* and algal mud and the high abundance of these taxa in these samples. A less severe shift to wet conditions is noted at 144 cm. The upper part of the record (120 - 32 cm) shows a highly variable but general trend towards drier bog surface conditions with the exception of a strong wet shift observed at 24 cm. A relatively sudden drying of the bog surface is inferred in the top strata (24 – 0 cm).

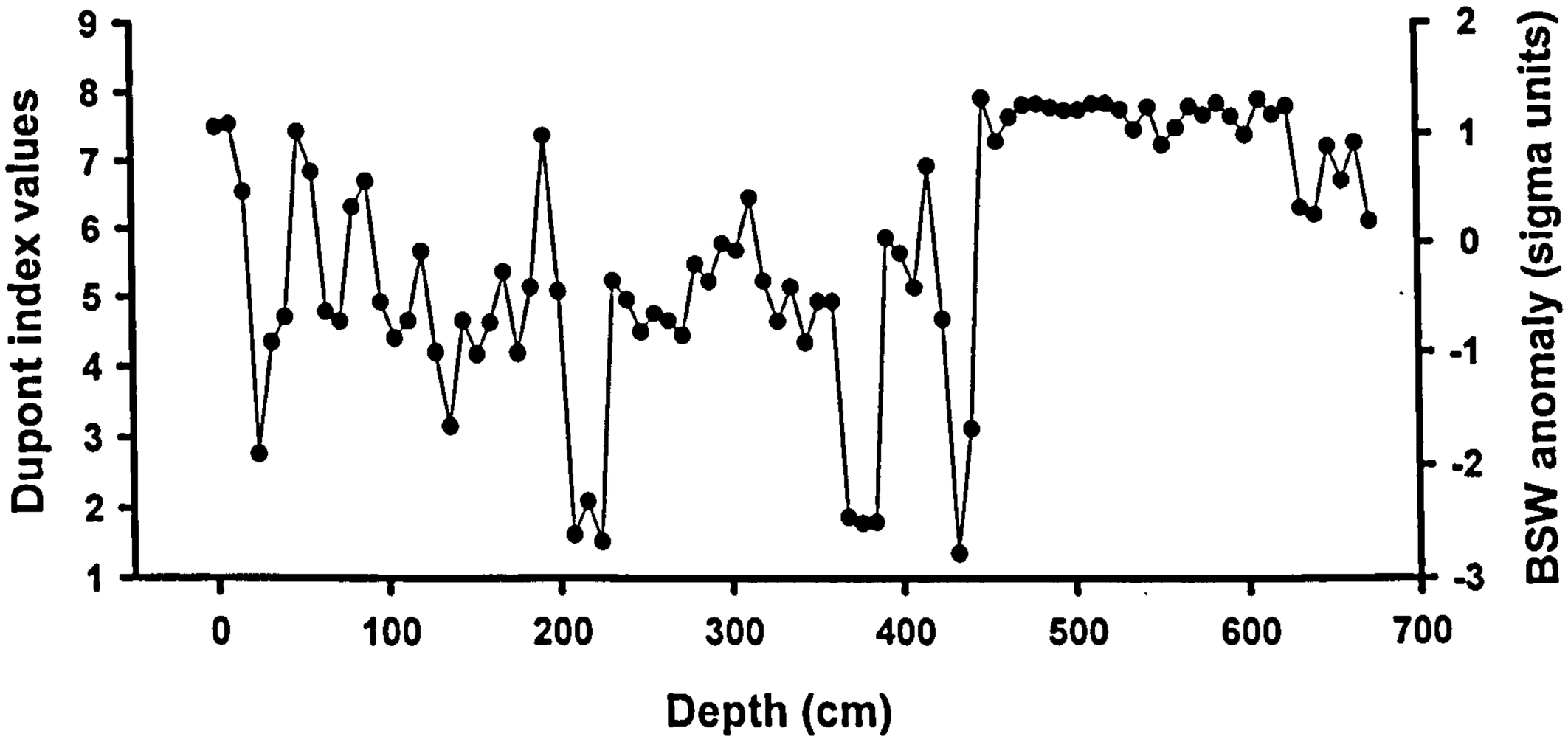

Figure 6.13 DSM3 Dupont wetness index reconstruction using plant macrofossil data; raw values on primary y-axis, σ anomalies from the mean on secondary y-axis

6.3.2 DSM3 humification data

Results of humification analyses on DSM3 at a constant stratigraphical resolution of 4cm are presented in Figure 6.14. The results in Figure 6.14 (A) display a prolonged phase of relatively stable transmission values from the base to 448 cm and then a highly variable stratigraphy with a clear trend towards higher transmission values with decreasing depth. As discussed earlier for Walton Moss and in Chapter 4, this is due to an autogenic response of increasing humification with depth. It is necessary to detrend these data to allow meaningful comparison with the plant macrofossil data for this core. A modified version of the detrending procedure used in (Blundell and Barber, 2005) is used on this core consistent with the approach used on core WLM22 from Walton Moss (Figure 6.7).

In general, bog surface conditions were relatively dry in the lower sections of the core. Above 448 cm, following a period of high variability, the record shows evidence of a sustained

period of wetter conditions before a period of relatively dry conditions in the top ~120 cm. The rapid shift to high transmission values in the top-most samples is a diagenetic artefact. These near-surface samples are consequently omitted from the detrending procedure and the normalised data.

Phases of increased transmission values are representative of reduced decomposition of the peat and can be interpreted as periods of higher bog water tables. Shifts to relatively wet conditions are identified at depths of 448, 412, 276, 228, 178, 78 and 48 cm. Shifts to relatively dry conditions are identified at depths of 424, 342, 200, 144 and 58 cm. Consistent with the analysis of humification shifts in the deeper layers from core WLM22, minor wet shifts are noted at 560 and 640 cm. As discussed earlier, magnitudes of these shifts may be relatively subdued owing to the higher decay rate of the dominant species in these levels.

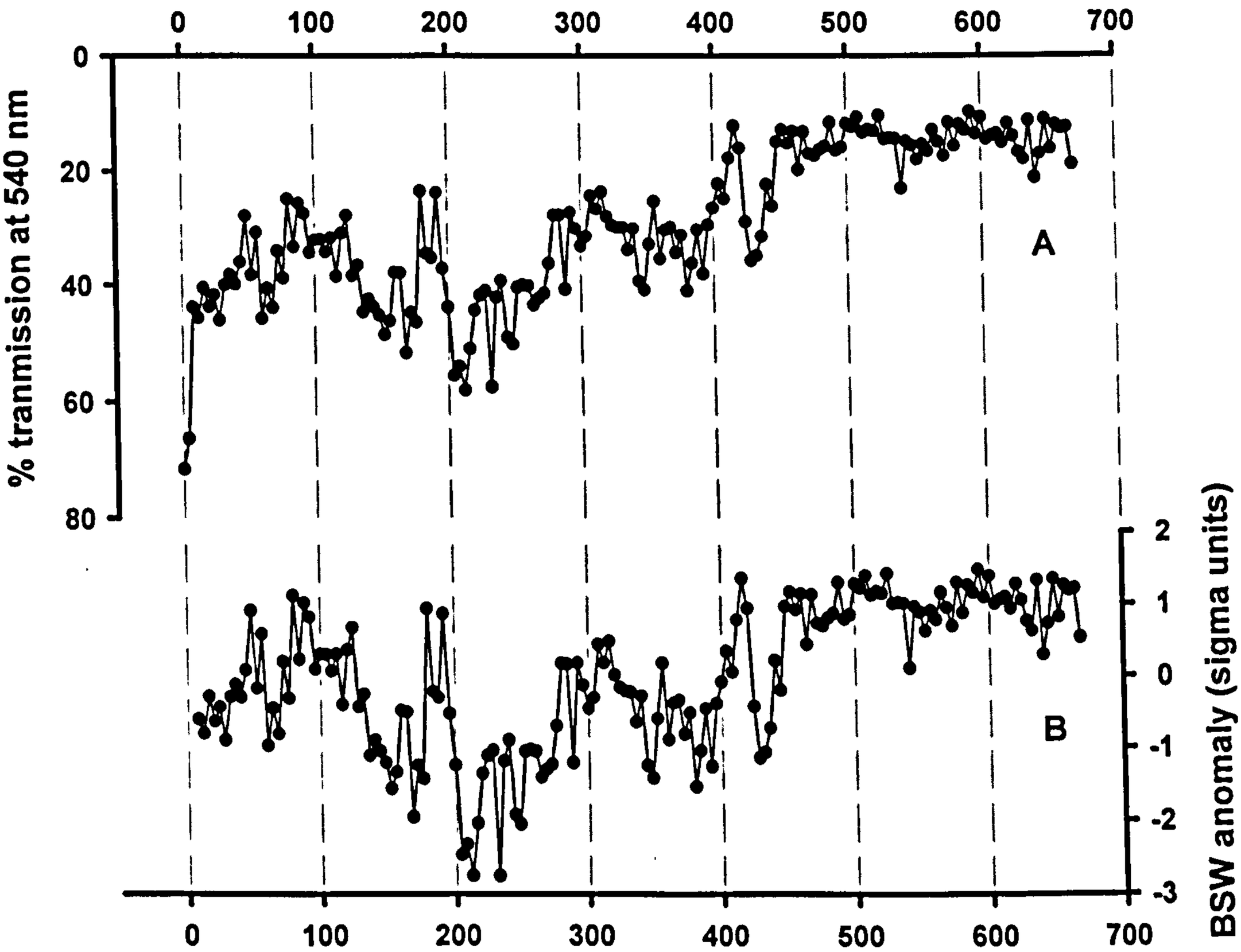

Figure 6.14 DSM3 peat humification data; A) raw transmission values, B) detrended (448 – 0 cm) and normalised transmission values presented as σ anomalies from the mean

6.3.3 Multi-proxy comparison for DSM3

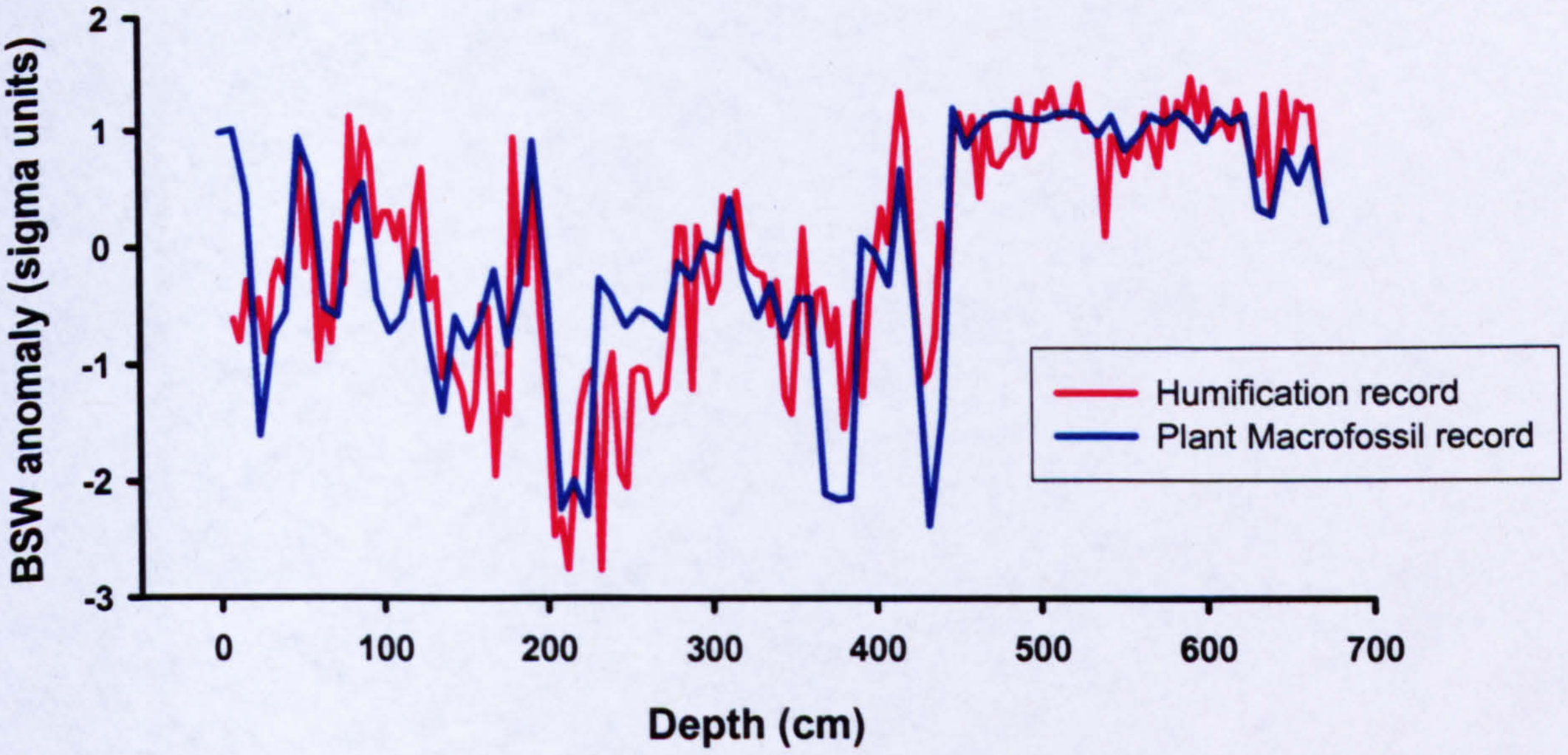

Figure 6.15 DSM3 multi-proxy comparison comprising plant macrofossil data (blue line) and peat humification data (red line)

Normalised variability from both proxy reconstructions in presented in Figure 6.15. There is excellent general agreement between the proxies in both direction and the magnitudes of sigma anomalies. In general, where discrepancies exist, these are in magnitude rather than direction and are probably due to varying sensitivities in the scaling of the two techniques and the weightings applied during the Dupont averaging, as has been discussed above.

Several specific sections in the core are of note. Between 656 and 624 cm both proxies register an increase in bog surface wetness. In the Dupont curve, this is driven by a dominance of *S. sect. acutifolia* (Figure 6.12). Whilst there is no question that water tables during this period were relatively higher than for the succeeding 200 cm, the increase in wetness should be interpreted with care as a climatic inference given the proximity of *Phragmites australis* at 672 and 668 cm. The associated species through the *S. sect .acutifolia* dominated sections do, however, indicate ombrotrophic conditions, which permits the inclusion of these layers in the reconstruction.

At 536cm, the humification decreases by ~1σ whilst the macrofossil reconstruction shows little change. Figure 6.12 indicates a single sample presence of very low percentages of *Sphagnum*, but critically the presence of *S. cuspidatum*, an indicator of wet conditions and water tables close to the surface. Abundances are probably too low to register strongly in the Dupont reconstruction. However, the presence of this species combined with the humification signal provides evidence of a brief increase in BSW in which water tables were at or close to the surface.

Between 272 and 232 cm separation is observed in the two proxy reconstructions. The humification data record a noisy but steady trend towards increased BSW. The plant macrofossil data define this increase later and with a more rapid shift to wetter surface conditions. The relatively stable macrofossil values mirror the abundance of the dominant *S. imbricatum* species (Figure 6.12) and reflect complacency in the macrofossil record due to the wide water table tolerance of this species.

The stacked record of inferred Bog Surface Wetness (BSW) change is presented for all available data in Figure 6.16 and those levels where data from both proxies were available in Figure 6.17. It is noticeable that the effect of a doubling of humification data in Figure 6.16 leads to an increase in the noisyness of the data but does not alter the general climatic interpretation of the record. This signifies the close correspondence found between the two proxy measures (Figure 6.15). The main exception to this finding is the increased magnitude of the wet shift recorded at 532 cm in Figure 6.16. Lower sample resolution precludes the detection of a similar strength signal in Figure 6.17.

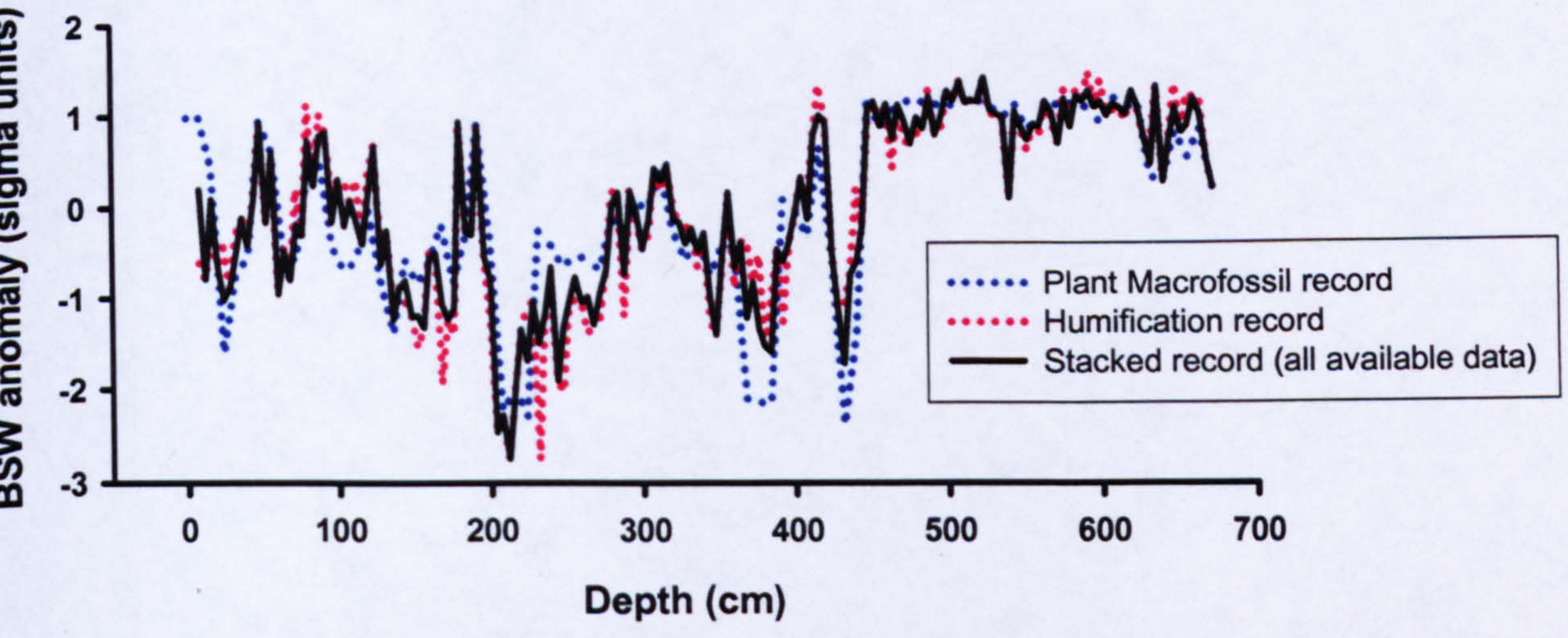

Figure 6.16 DSM3 stacked record of inferred Bog Surface Wetness change using all available data

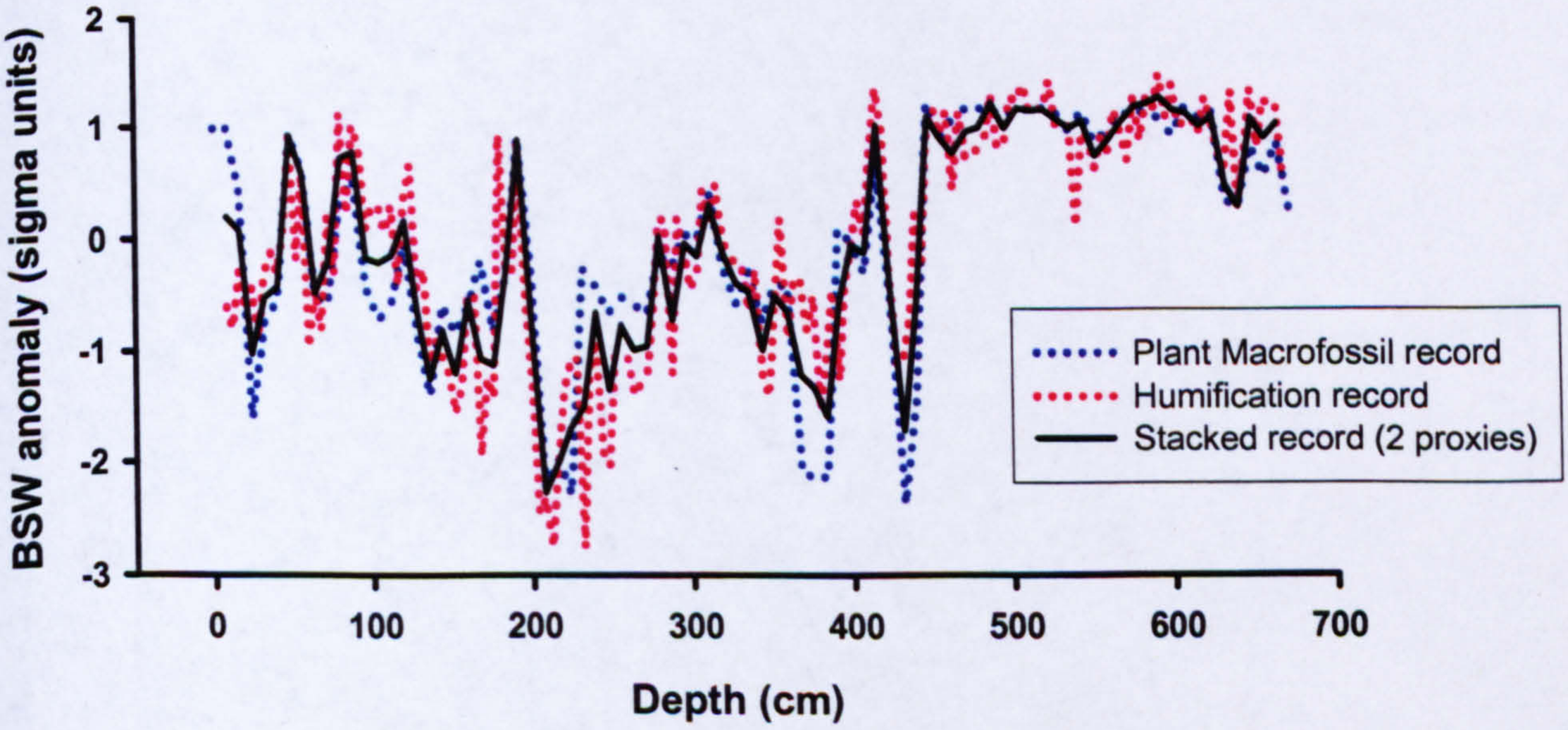

Figure 6.17 DSM3 stacked record of inferred Bog Surface Wetness (BSW) using all samples with 2 proxies

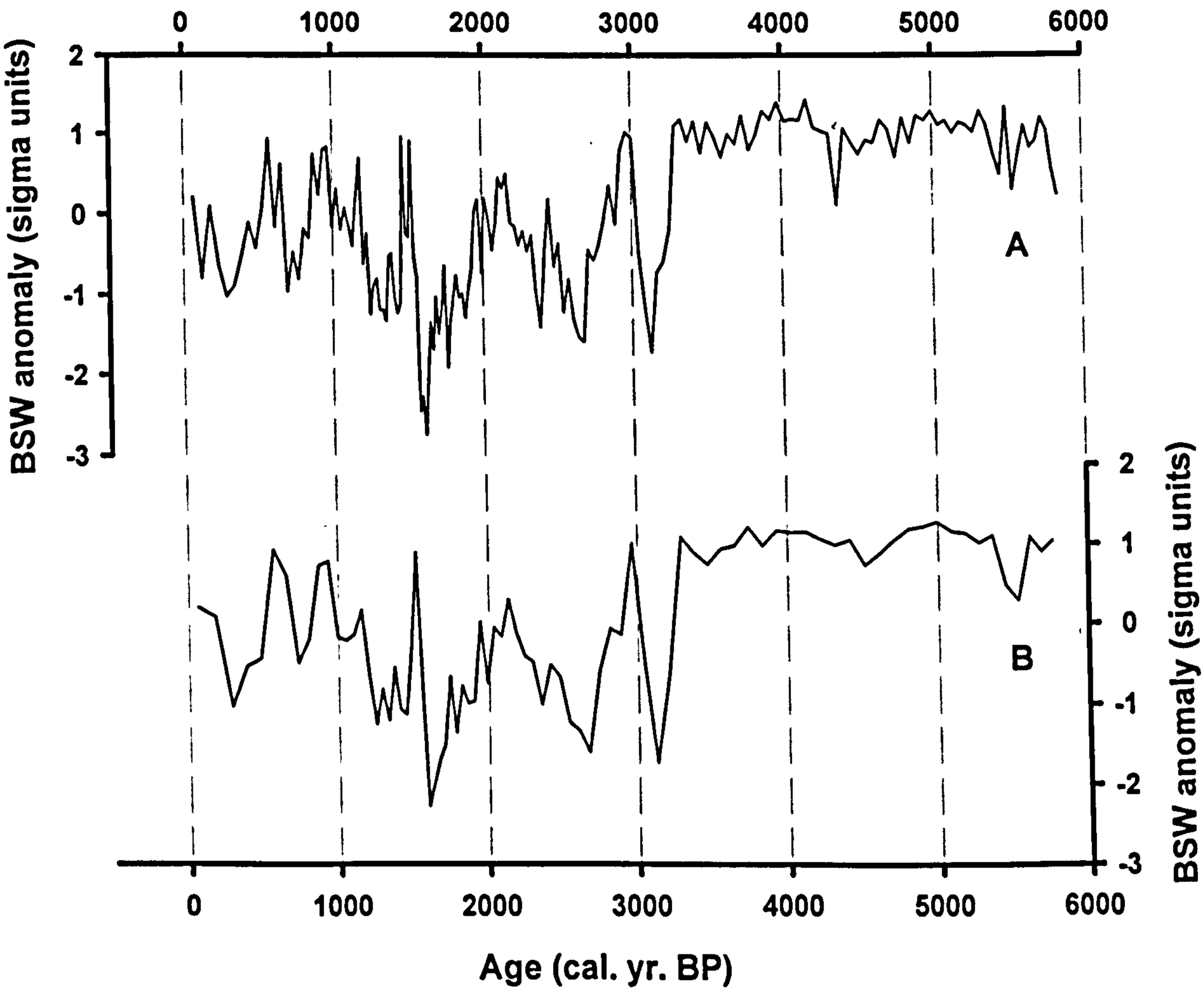

Figure 6.18 DSM3 multi-proxy climatic time-series A) using all available data, B) using samples with 2 proxies available

The two stacked records are combined with the age depth model for core DSM3 (Chapter 5) and presented as proxy-climatic time-series for the last ~5900 years in Figure 6.18. Clear shifts to wetter bog surface conditions occur at 3250, 2900, 2100, 1500 800 and 500 BP. Smaller wet shifts are noted at 5700 and 4300 BP. Clear shifts to drier bog surface conditions occur at 3100, 2600, 1600, 1150, 650 BP. All shifts are noted here rounded to the nearest 50 years.

Similar to the initiation of *Sphagnum* peat in WLM22 (Figure 6.11), the initiation of *Sphagnum* peat is marked by a rapid increase in BSW followed by a rapid decrease to an inferred level similar to the average for the early to mid-holocene (Figure 6.18). This phase begins at 3250 BP in the record from DSM3 with the majority of the climatic deterioration occurring in ~ 80 years. The episode has a duration of ~200 years.

The wet shift at 2900 BP initiates a period of relatively sustained wet conditions. In the higher resolution proxy time-series (Figure 6.18 A) there is evidence for the period comprising two sub-periods of wetter conditions separated by a short-lived fluctuation to drier bog surface conditions. This is captured in the lower resolution curve but appears as noise within a period of general drying of the bog surface. The most severe wet shift in the record from DSM3 is observed beginning at 2100 BP and reaching maximum values ~1600 BP. Following a period of relatively dry conditions 1150 - 800 BP, two shifts to wetter conditions are observed at 800 and 500 BP. These may relate to the two phases of the Little Ice Age (Lamb, 1977).

6.4 *Raheenmore*

6.4.1 RHM2 plant macrofossil data

Plant macrofossil data for core RHM2 from Raheenmore, Offaly, Ireland are presented in Figure 6.19. The data cover the section of the core from 888 to 1112 cm, which rangefinder dates taken soon after core recovery indicated covered a period that encapsulated 8200 BP. The diagram has been zoned by eye with each zone reflecting a relatively consistent floral community that is notably different from neighbouring zones. Descriptions of the assemblages of each zone are given in Table 6.5.

Figure 6.19 RHM2 plant macrofossil diagram (1112 – 888 cm; 10030 – 7460 BP)

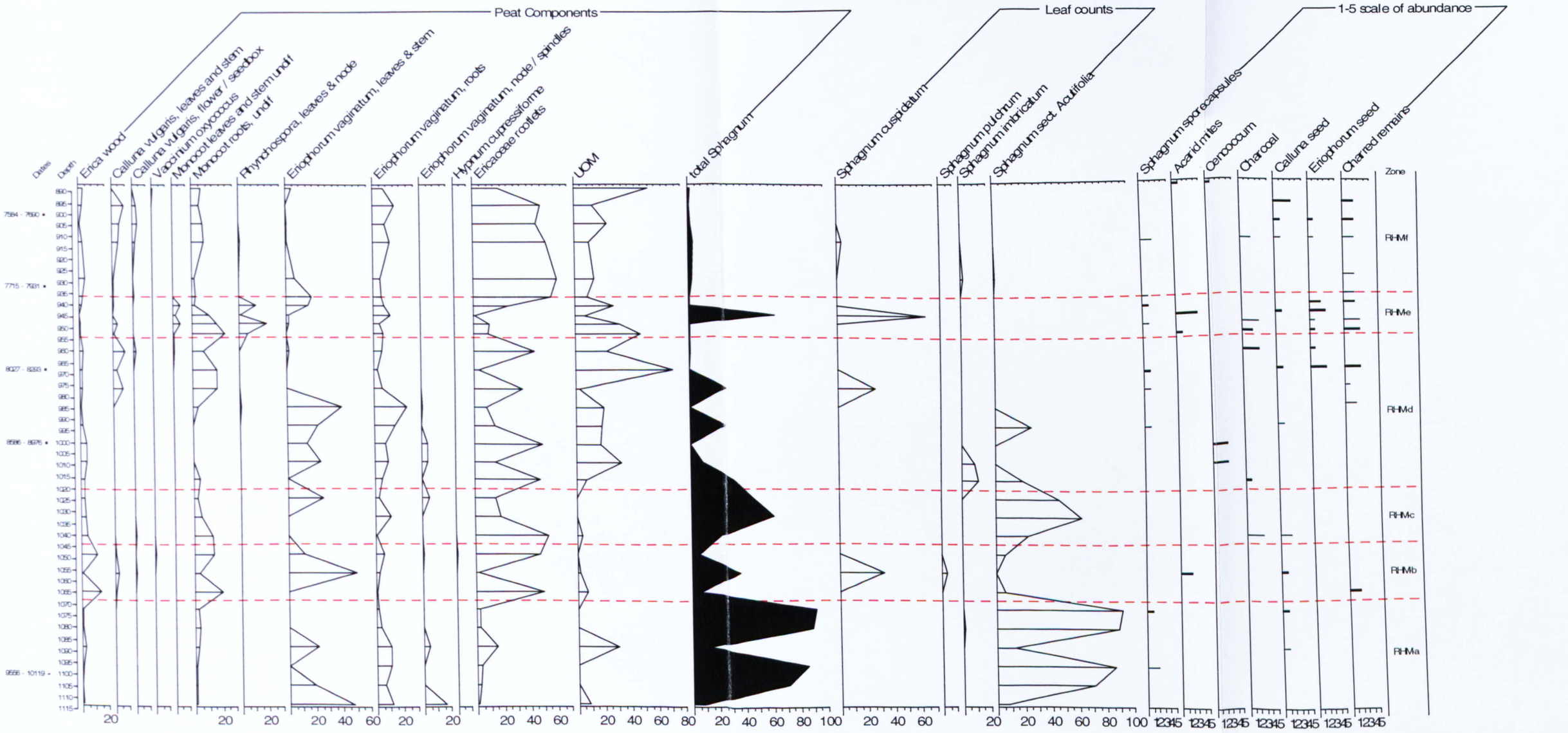

Table 6.5 Assemblage description and interpretation for RHM2 plant macrofossil data

Zone	Depth (cm)	Description	Age (cal. yr. BP)
RHM-a	1112 - 1068	Basal zone of record dominated by *Sphagnum section acutifolia* associated with variable percentages of *Eriophorum vaginatum* (both above and below ground remains) and ericaceous rootlets. Occasional remains of *Calluna vulgaris* and *Erica wood* are present. A single sample fluctuation to increased Unidentified Organic Matter (UOM) indicates brief period of lower water tables. Otherwise, the assemblage is indicative of ombrotrophic status with relatively dry surface conditions.	10030 - 9380
RHM-b	1068 - 1044	*Sphagnum* is replaced in this zone by the above ground remains of *E. vaginatum* which alternate with ericaceous rootlet remains. The peak in *E. vaginatum* remains coincides with a single sample peak in *Sphagnum cuspidatum* and the presence of Acarid mites. This is an unusual association and suggests highly variable water tables whilst indicating that water tables were briefly at or close to the surface.	9380 - 9070
RHM-c	1044 -1020	Dominated by *S. sect. Acutifolia* and associated with ericaceous rootlets, *E. vaginatum* roots and low but persistent percentages of ericaceous wood remains. The presence of charcoal remains is indicative of fire on the bog surface. The assemblage suggests relatively low water tables prevailed through this zone.	9070 - 8820
RHM-d	1020 - 954	UOM and ericaceous rootlets dominate the assmblage in this zone and are associated with increased proportion of *E. vaginatum* remains. Water tables are inferred to be highly variable through this period indicated by a single sample peak in *S. sect. acutifolia* at 992 cm and a single sample peak in *S. cuspidatum* at 976 cm. Towards the top of the zone, UOM and ericaceous rootlets increase along with increases in the percentages of *C. vulgaris* and charred remains. *E. vaginatum* percentages fall. This is indicative of falling water tables and drying of the bog surface.	8820 - 8070
RHM-e	954 - 936	Short and significant change to species indicative of wet bog surface conditions. A rise in *Rhyncospora alba* is succeeded by a peak in *S. cuspidatum* associated with the presence of acarid mites and good preservation of seeds. UOM and ericaceous rootlet percentages reduce and ericaceous wood briefly disappears from the record. The assemblage suggests water tables were at or close to the surface and sustained over this short period.	8070 - 7890
RHM-f	936 - 888	Dominated by ericaceous rootlets with the presence of charred remains associated with stable percentages of *E. vaginatum*, *C. vulgaris*, ericaceoua wood and UOM. The assemblage is indicative of very dry bog surface conditions, low water tables and regular surface desiccation.	7890 - 7460

The species assemblage throughout this record and the age of the sediments as indicated from the array of ^{14}C AMS dates (Chapter 5) indicate that Raheenmore bog contains some of the oldest ombrotrophic sediments in NW Europe. The species assemblage in zone RHM-a contains no diagnostic indictors of nutrient enrichment suggesting that the sediments could be ombrotrophic below the basal zone given here which equates to >10,000 years of proxy-hydrological data where the water table is linked to climate. Whilst no indication is given within the species present of groundwater sourcing, it is noted that a period of *S. sect. acutifolia* dominance is observed in the basal stratigraphy at each of the three NW European sites in this project and may be indicative of proximity to the fen-bog transition in RHM2.

The inferred water table throughout the RHM2 record is highly variable. In the most part, the floral communities observed suggest that low water tables and relatively dry bog surface conditions prevailed. Within this general pattern, short duration and relatively rapid fluctuations to very wet surface conditions are identified where the species data suggest water tables were at or close to the surface and bog pools may have developed. These are identified at 912, 976 and 992 cm.

Two changes in assemblage are noted that differ in character from these brief fluctuations. The shift to *S. cuspidatum* and *S. pulchrum* from *S. sect. acutifolia* at 1054 cm has a more prolonged and gradual character than the shifts higher in the core and is observed within the context of a *Sphagnum* dominant section of the core where a lower magnitude shift would be required to transform the community to *S. cuspidatum* dominant. Zone RHM-e, on the other hand, represents a strong and sustained shift towards wet conditions on the bog surface identified by an initial rise in *R. alba* followed by a large peak in *S. cuspidatum* and a subsequent continuation of *R. alba* before the assemblage becomes very dry in zone RHM-f. The period of inferred wet conditions lasts ~200 years, is dated to occur between 8070 -7890 and is highly likely to represent a floral response to climatically induced hydrological changes that occurred in association with the 8200 yr event.

RHM2 plant macrofossil data were condensed to a univariate index using Dupont weighted averaging. The modified index (var. Daley) (Chapter 4; Table 4.5) was used to provide weights for individual species. The results of the averaging function are presented in Figure 6.20. A variable but general trend towards decreasing bog surface wetness (BSW) from the base of the record to 960 cm is interrupted by two single point excursions to wetter conditions at 1056 and 972 cm. A major excursion to very wet bog surface conditions is observed after 960 cm and highest bog water tables inferred at 944 cm. Although the excursion is represented most strongly by a single point in the Dupont reconstruction, the downward trend visible in the previous data points and comparison with the floral communites present in Figure 6.19 indicate that this excursion was defined by series of data. Following the intense wet period, water tables are inferred to lower to values similar to those preceding the event and remain stable for the remainder of the record.

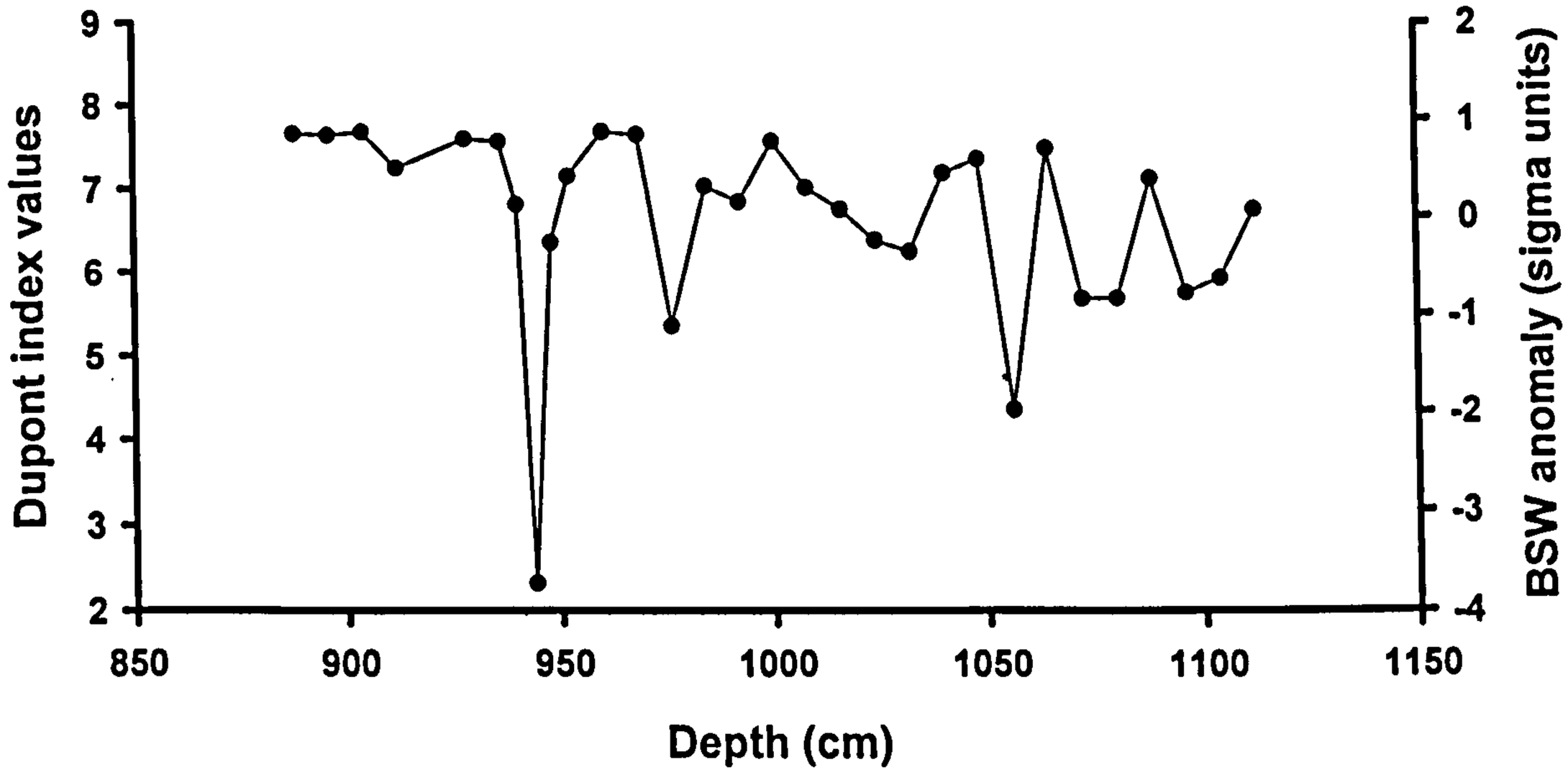

Figure 6.20 RHM2 Dupont wetness index reconstruction for plant macrofossil data; raw values on primary y-axis, σ anomalies from the mean on secondary y-axis

6.4.2 RHM2 humification data

Results of humification analyses on RHM2 at a constant stratigraphical resolution of 8 cm are presented in Figure 6.21. The raw transmission data in Figure 6.21 (A) display the most clearly of any of the humification records in this project the trend towards increasing transmission values with decreasing depth in the upper *Sphagnum* peat dominated layers. Also, clearly evident from these data is the trend for increasing amplitude of variability with decreasing depth.

The record was detrended using an identical method to that applied to the records from Dosenmoor and Walton Moss. Although the RHM2 macrofossil record was focussed on the section 888 – 1112 cm, isotopic sub-sampling involved collection of digital photographs (Chapter 4) from which macrofossil abundance estimation could be visually determined for the whole core. The initiation of sustained *Sphagnum* presence from photographic analysis coincides with a clear point of inflexion at 600 cm. Two linear trends are evident. A plateau in mean values is observed in the deeper peat layers with a linear trend for increasing

transmission values from ~600 cm to the surface. The detrended and normalised curve, Figure 6.21 (B), is therefore produced by the linear regression of data from 0-600 cm and by the application of an offset to the data from 600 cm to the base of the record.

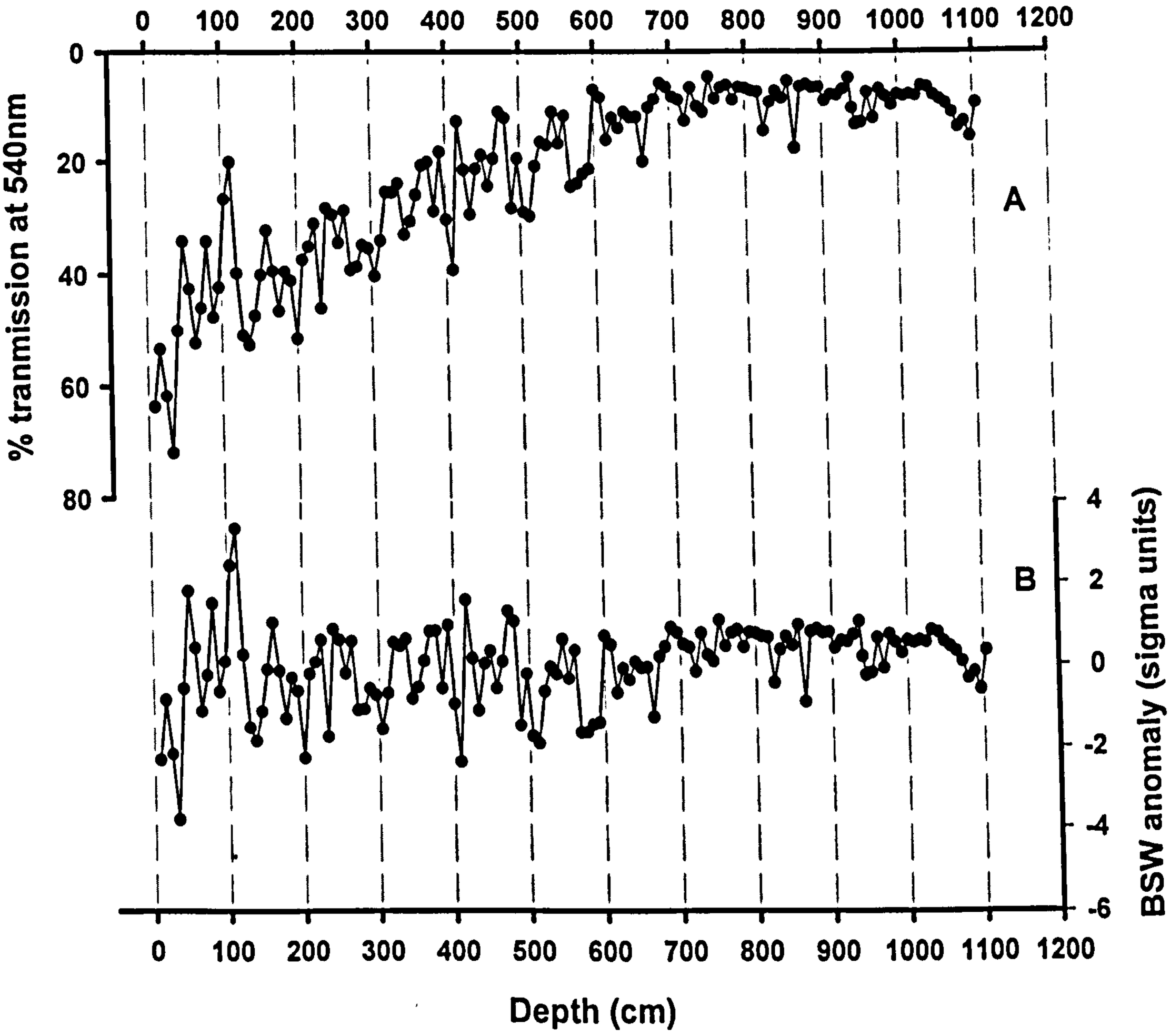

Figure 6.21 RHM2 peat humification data; A) raw transmission values; B) detrended (600 – 0 cm) and normalised transmission values presented as σ anomalies from the mean

The trend towards increasing amplitude of variability with decreasing depth is displayed clearly in Figure 6.21 (B). This apparent sensitivity change through the core is reflected in an increasingly damped response with increasing depth. The data from RHM2 confirm that comparison of magnitudes of change within the humification record must be considered

carefully and in most cases, only directions of change should be used in final palaeo-climatic interpretation. This corroborates the approach used earlier to also note those shifts where $<2\sigma$ change is observed in humification data.

The humification record shows comparatively little variability that is significantly greater than the background noise. However, several clear phases of less humified and more humified layers are noted which are interpreted as phases of wetter or drier conditions on the bog surface. Shifts to wetter conditions are noted at 596, 540, 468, 412, 316, 220, 156, 108 and 44 cm. Shifts to drier conditions are noted at 504, 484, 428, 404, 268, 174, 124 and 60 cm. The corresponding ages for these shifts are described in section 6.4.3 below.

6.4.3 Multi-proxy comparison for RHM2

Normalised variability in the proxy reconstructions from plant macrofossil and humification data are presented in Figure 6.22. Whilst directions of change are similar, magnitudes of change are highly dissimilar reflecting large differences in the sensitivities of the proxies at depth. Both records show relatively dry surface conditions at the base within the context of the whole core but which may be interpreted as relatively moist conditions within the context of the lower 5 metres. Whilst variable, both records show a trend towards drying of the bog surface between 1104 and 1000 cm. Both records show two peaks to wetter conditions at 972 and 956 cm although both peaks are relatively subdued in the humification data. The strong excursion detected in the plant macrofossil record at 944 cm corresponds with the second of the two lows in the humification record exactly. The records are in high correspondence for the remaining 56 cm to 888 cm.

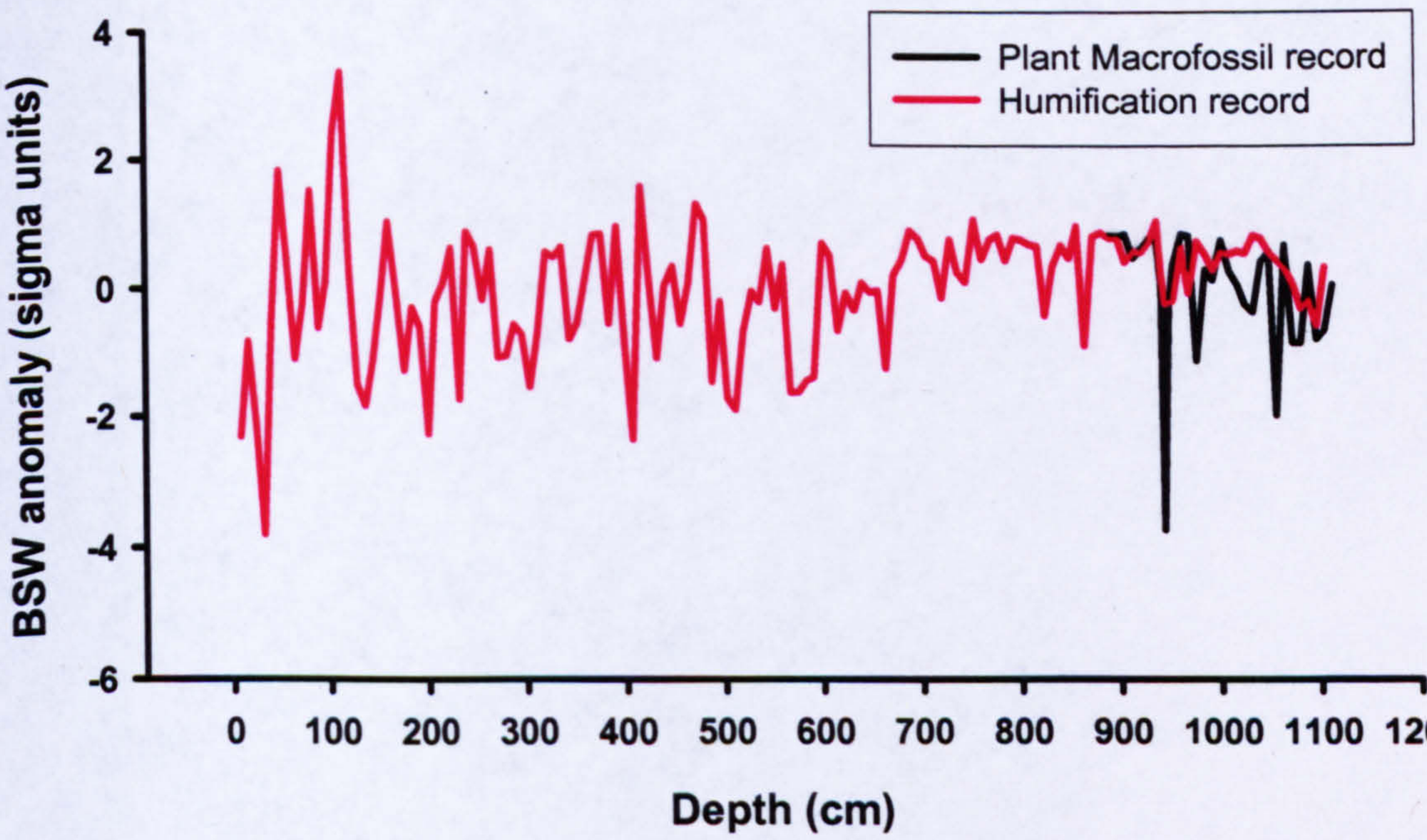

Figure 6.22 RHM2 multi-proxy comparison comprising plant macrofossil data (1112 – 888 cm; black line) and peat humification data (1112 cm – surface; red line)

The stacked record of BSW reconstruction is presented in Figure 6.23. Humification and plant macrofossil data were sampled at identical resolution through 888 - 1104 cm allowing both proxies to be available for every data point. In contrast to the stacked records generated for DSM3 and WLM22, it can be seen that one proxy dominates the signal in the RHM2 stacked record and that is the more variable macrofossil record. The marked differences in magnitude inevitably shorten the magnitudes of change observed in the stack. However, the trend towards general drying of the bog surface from the base of the record and the presence of an excursion towards wet bog surface conditions at 944 cm are both preserved.

Given the evidence presented for the potentially wide ranging sensitivities of the two proxy indicators at depth, it is inappropriate to attempt a tying of the lower stacked record to the humification record as a continuous time-series for RHM2. To that end, the stacked record and the humification record are presented as separate time-series in Figure 6.24. As detailed earlier (Chapter 3), one of the principal reasons for the selection of Raheenmore as a site in

this project was the potential for discovering old ombrotrophic peat that might preserve a signal from the period surrounding 8200 BP and contain sufficient *Sphagnum* remains to characterise this period isotopically. It is clear from the macrofossil and humification evidence that a shift towards higher water tables and wetter bog surface conditions occurred ~8120 BP with wettest conditions observed at 7970 BP. The total duration of the event was ~ 200 years. The implications of this finding and correlation with other records of a climate event ~8200 BP are discussed in Chapter 8.

Shifts to wetter conditions in the humification record, previously noted by depth, are now recognised at 5040, 4530, 3830, 3260, 2270, 1310, 740, and 380 BP. Shifts to dry conditions are identified at 4190, 3990, 3430, 3180, 1780, 890, 490 and 100 BP. In addition, shifts are also noted in the lower section of the core at 9250, 8120, 7300 and 6950 BP. All dates are rounded to the nearest 10 years.

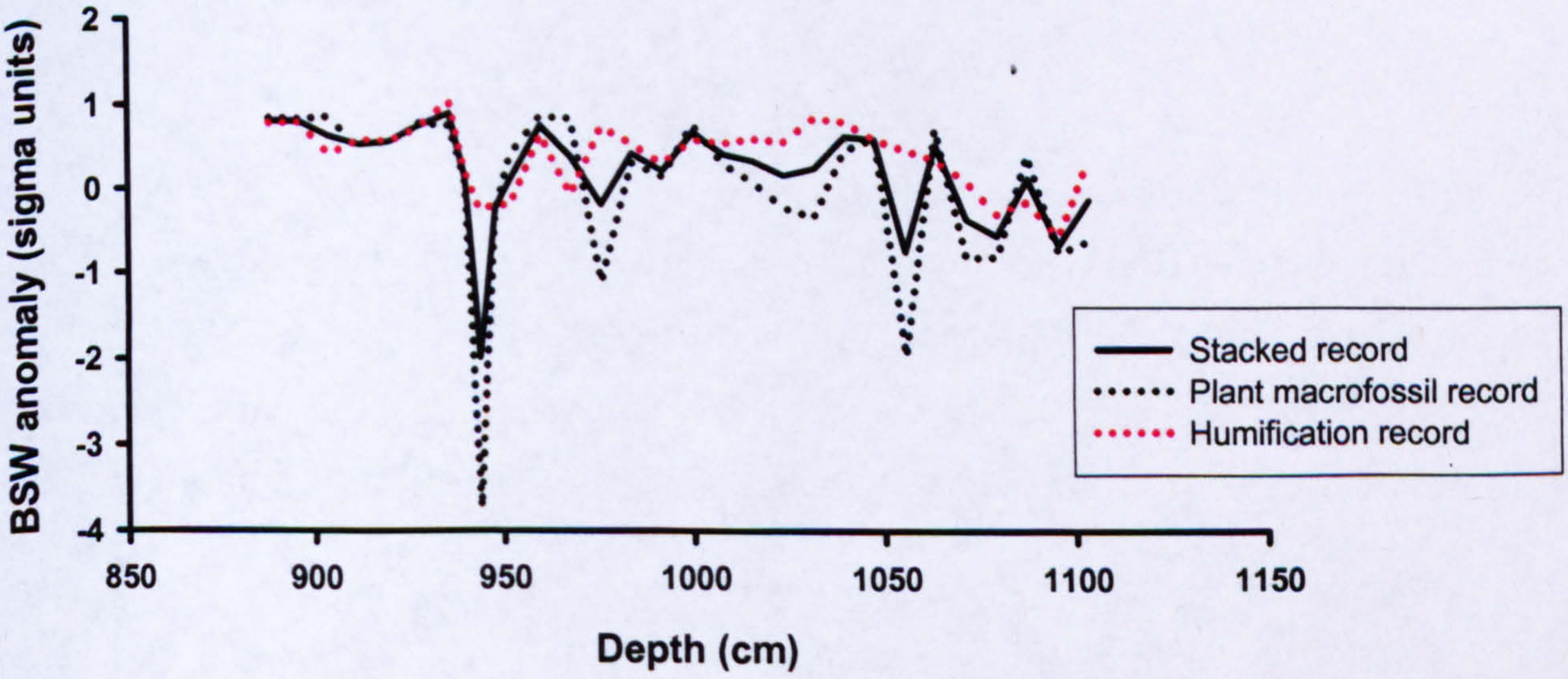

Figure 6.23 RHM2 stacked record of inferred Bog Surface Wetness (BSW)

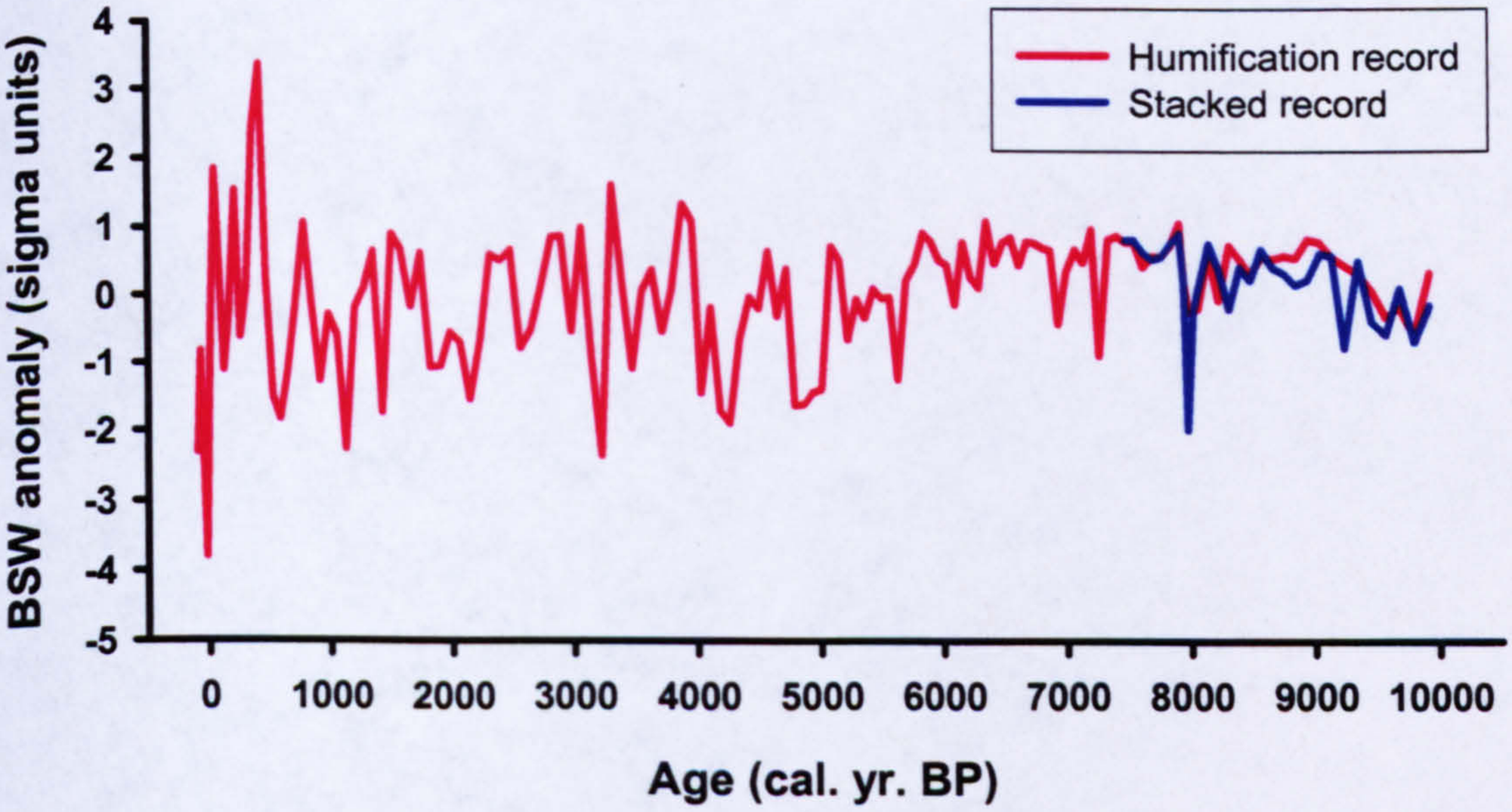

Figure 6.24 RHM2 multi-proxy climatic time-series (10030 – 7460 BP; blue line) and full core peat humification time-series (10030 BP – present; red line)

7 Isotopic results and analysis

7.1 *Introduction*

In this chapter, isotopic results from modern surface sample analyses and modern precipitation and bog surface water samples (section 7.2) are presented prior to palaeo-sequence reconstructions (section 7.3). Precipitation and bog water data were analysed in collaboration with Dr. Elizabeth Fisher of the University of Liverpool as part of the ISOMAP-UK project. In section 7.3, raw *Sphagnum* isotopic data are presented for each of the four cores and plotted both as records and time-series using the age-depth models constructed from data in Chapter 5.

The production of both oxygen and hydrogen *Sphagnum*-specific stable isotope records combined with the ability to calibrate these values and generate estimates of palaeo-source water composition represents a significant advance in the field (Chapter 2). Accordingly, analyses of $\delta D_{Sphagnum}$ values form a central component of this study. The majority of the data in this chapter are measurements of oxygen isotopic composition. Resources for hydrogen isotope analyses were limited by virtue of the need to undertake these measurements in Berne, Switzerland within a short time-window. Cellulose samples were prioritised based on the $\delta^{18}O$ results from core data and the need to generate a calibration training data set of modern samples. $\delta D_{Sphagnum}$ values for these prioritised cellulose samples are presented with oxygen data where analyses were undertaken on those samples.

7.2 *Modern monitoring results*

7.2.1 Introduction

Central to understanding the core isotopic values and particularly how they relate to the isotopic composition of precipitation is the development of modern calibration datasets. Modern measurement of the isotopic values of water in a number of stores on its path from precipitation to cellulose allows for estimation of the fractionation that occurs between each stage and enables functions to be empirically derived that estimate palaeotemperature from the core isotopic values. Collection and measurement of modern isotopic data was undertaken in collaboration with Dr. Elizabeth Fisher of the University of Liverpool (Chapter 4) for ISOMAP-UK. Whilst studies have previously attempted to characterise the variability in bog water, precipitation and *Sphagnum* cellulose over individual months or seasons, this remains the only study undertaken on modern bog surfaces in which regular monitoring was conducted for periods of at least one year at each NW European site. This temporal span allows for a range of climatic conditions (Siegenthaler and Oeschger, 1980) to be observed and for estimation of the fraction of the yearly isotopic signal recorded by the growth of *Sphagnum*. Whilst no such regular monitoring was possible for Nordans Pond Bog, eight surface bog water samples and twelve *Sphagnum* cellulose samples were collected in June 2004 and are presented here.

7.2.2 $\delta^{18}O$ and δD in precipitation and bog water

Results of $\delta^{18}O$ and δD analyses of precipitation and bog water over the sampling period are shown in Figure 7.1 - Figure 7.4. A high noise element is observed in precipitation data which masks any potential seasonal signal. Conversely, periodic seasonal variation is detected in both $\delta^{18}O$ and δD values of bog water samples at all sites. The range of $\delta^{18}O$ and δD values in precipitation is approximately double that in bog water values reflecting the strong influence of synoptic scale variability on the isotopic composition of precipitation. This synoptic scale variability appears to be dampened in bog water values as judged from the lower range of

values and more consistent seasonal signal. The most enriched values are observed in summer months and the lightest values in winter months. Whilst there is variability between replicate samples from the same site, reflecting microtopographical conditions, the seasonal signal amplitude overshadows this variability. This is in agreement with findings from other studies (Ménot-Combes *et al.*, 2002).

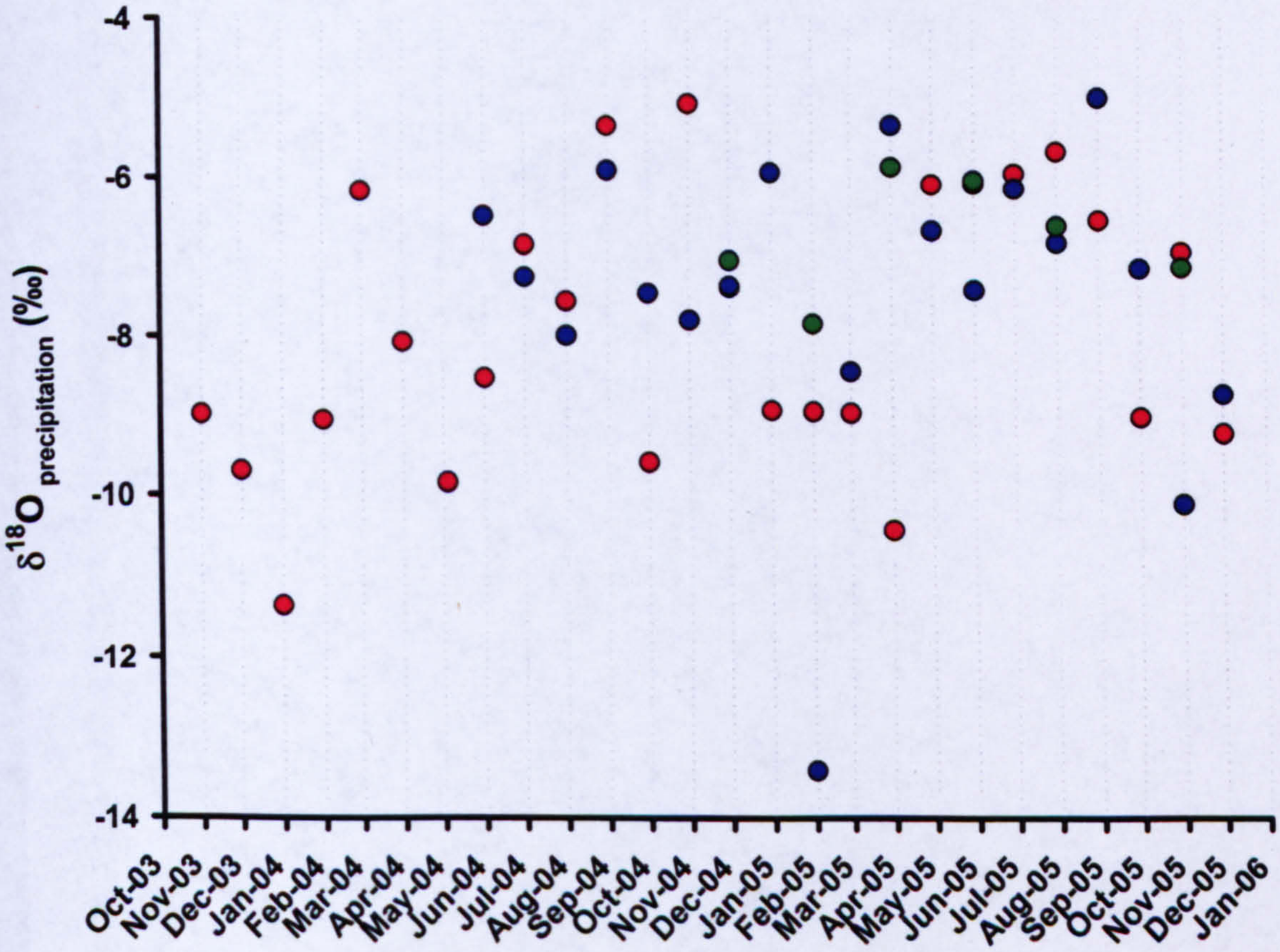

Figure 7.1 $\delta^{18}O_{precipitation}$ values for all sites for the period November 2003 – December 2005; Brampton weather station 3 km south of Walton Moss (red dots), Dosenmoor centre of bog surface (blue dots) and Raheenmore centre of bog surface (green dots)

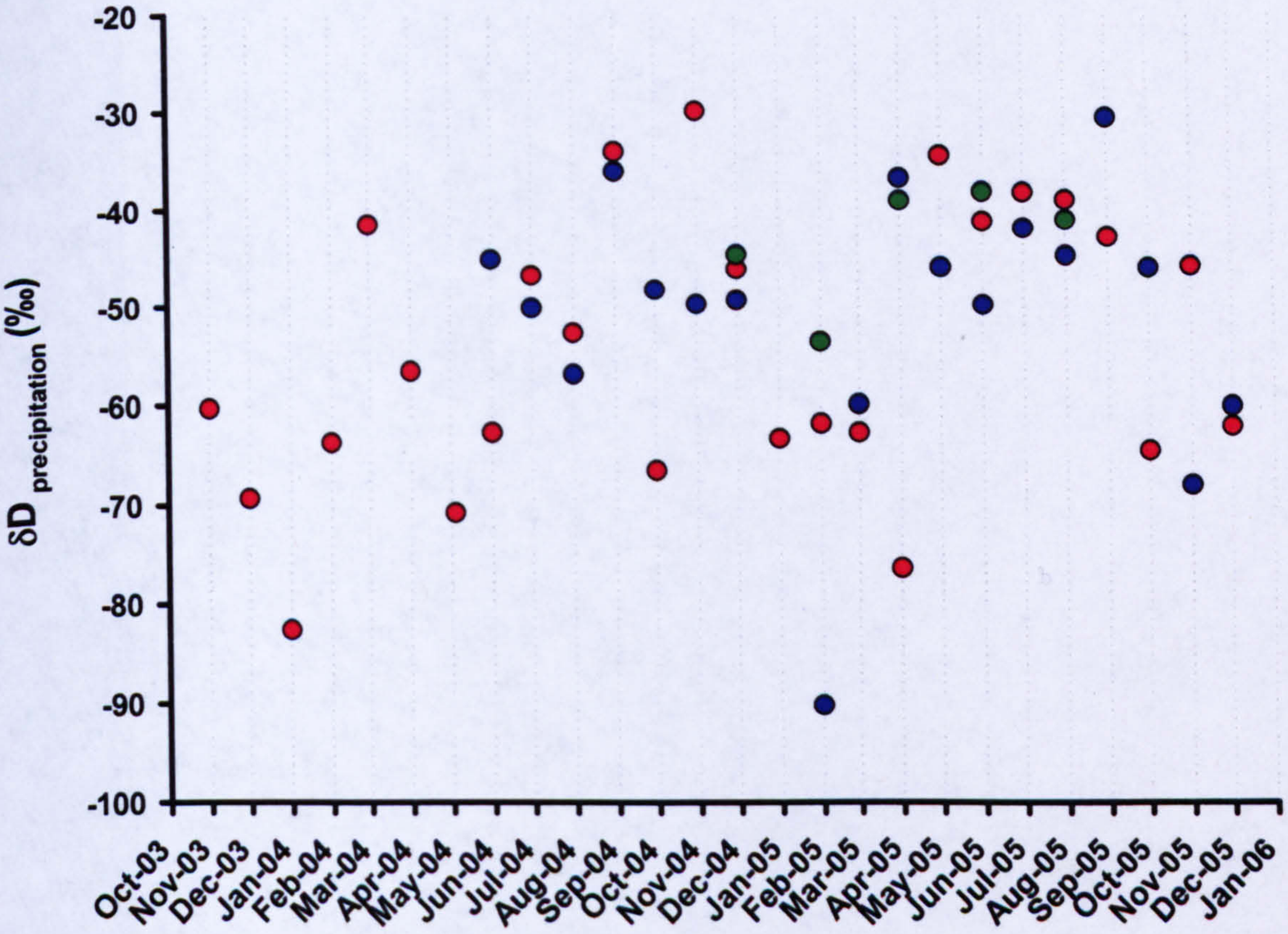

Figure 7.2 $\delta D_{precipitation}$ values for all sites for the period November 2003 – December 2005; Brampton weather station 3 km south of Walton Moss (red dots), Dosenmoor centre of bog surface (blue dots) and Raheenmore centre of bog surface (green dots)

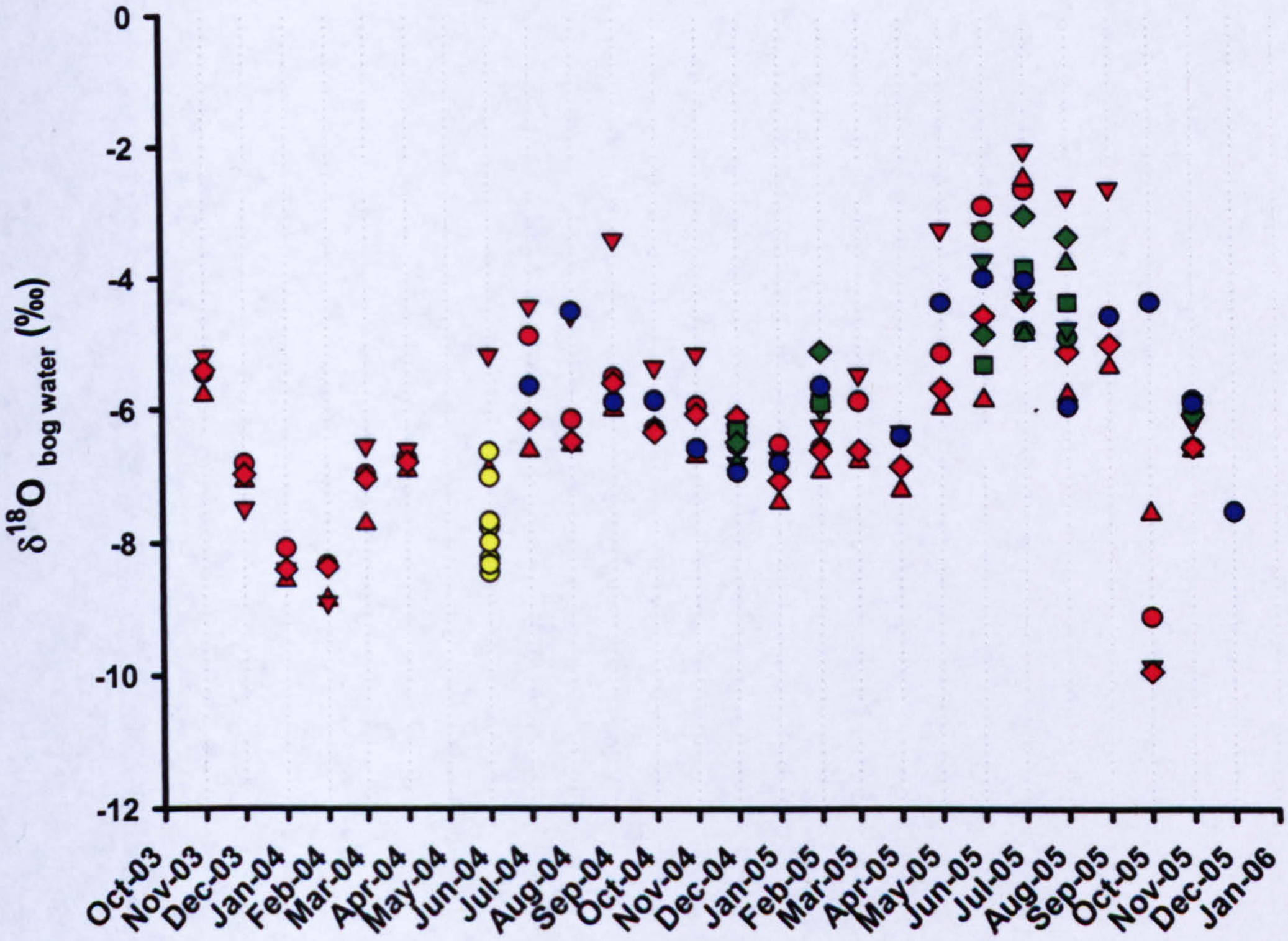

Figure 7.3 $\delta^{18}O_{bog\ water}$ values for all sites for the period November 2003 – December 2005; replicate measurements are indicated by different symbols (Walton Moss, red symbols; Dosenmoor, blue dots; Raheenmore, green symbols; Nordans Pond Bog, yellow dots)

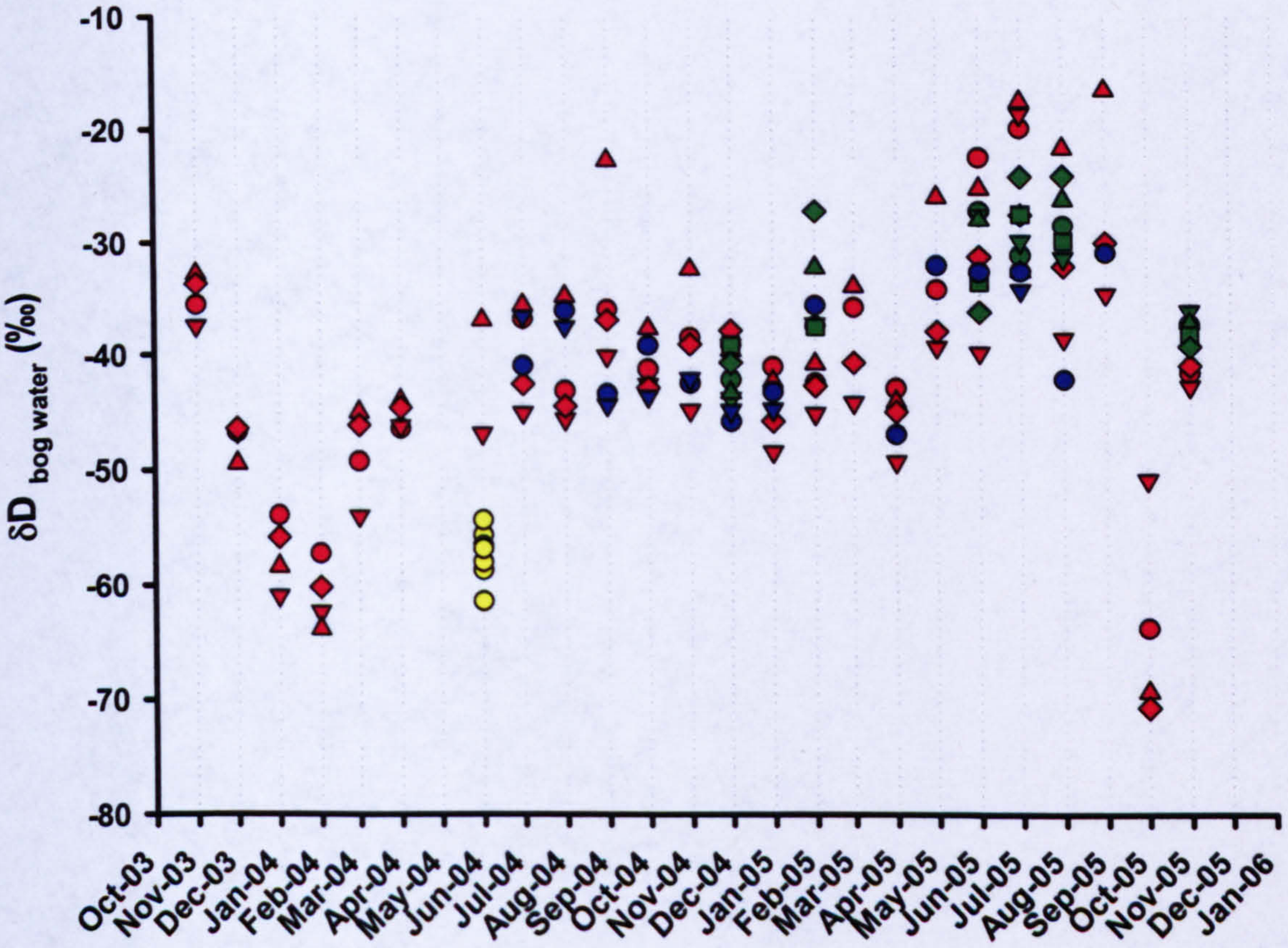

Figure 7.4 $\delta D_{bog\ water}$ values for all sites for the period November 2003 – December 2005; replicate measurements are indicated by different symbols (Walton Moss, red symbols; Dosenmoor, blue symbols; Raheenmore, green symbols; Nordans Pond Bog, yellow dots)

Bi-plots of precipitation and bog water data for each of the European sites in this study make it possible to see how the isotopic composition of waters evolve once precipitated on the bog surface (Figure 7.5 - Figure 7.7). There is a notable difference between the slopes of the precipitation values and the bog water data. At all sites, bog waters follow evaporative water lines which are identified by a shallower slope angle and increasing separation between the lines with increasing enrichment of isotopic values. The strongest evaporation signal is detected in the Raheenmore bog waters (Figure 7.7) and the least severe in the Dosenmoor bog waters (Figure 7.6).

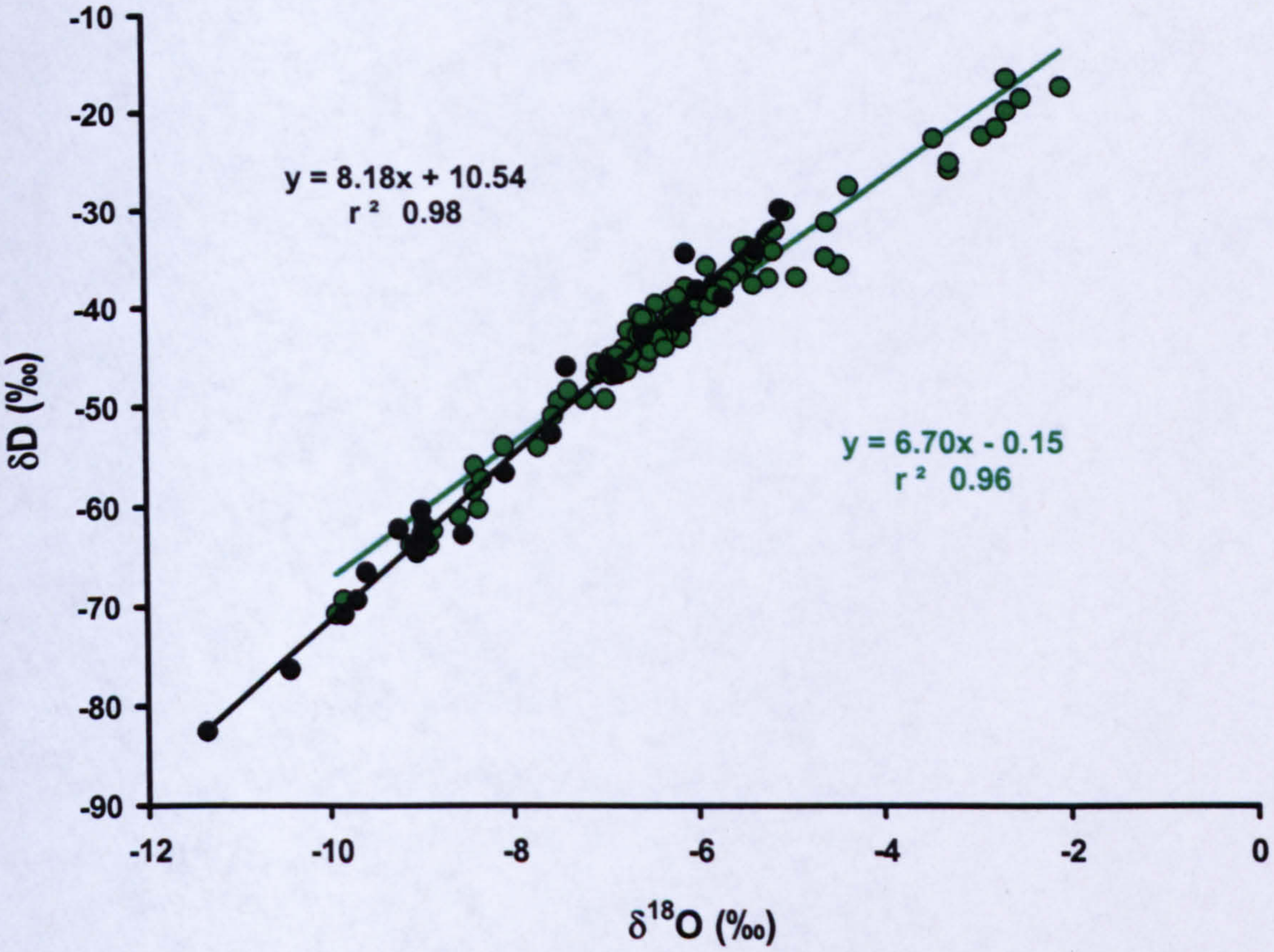

Figure 7.5 Bi-plot of mean monthly δD and $\delta^{18}O$ values in precipitation (black dots; from Brampton weather station 3 km south of Walton Moss) and bog water (green dots) from the surface of Walton Moss

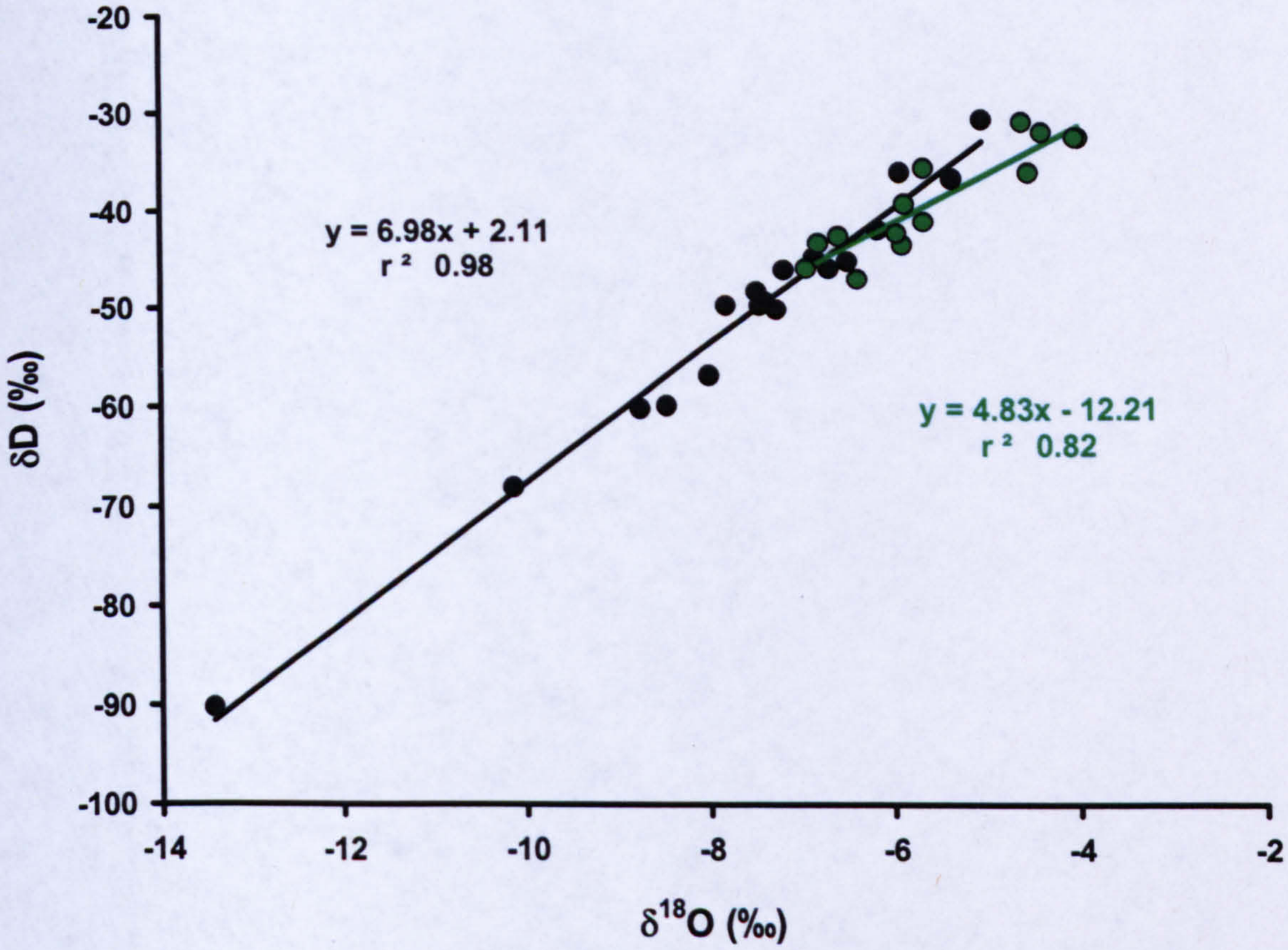

Figure 7.6 Bi-plot of mean monthly δD and δ^{18}O values in precipitation (black dots) and bog water (green dots) from the surface of Dosenmoor

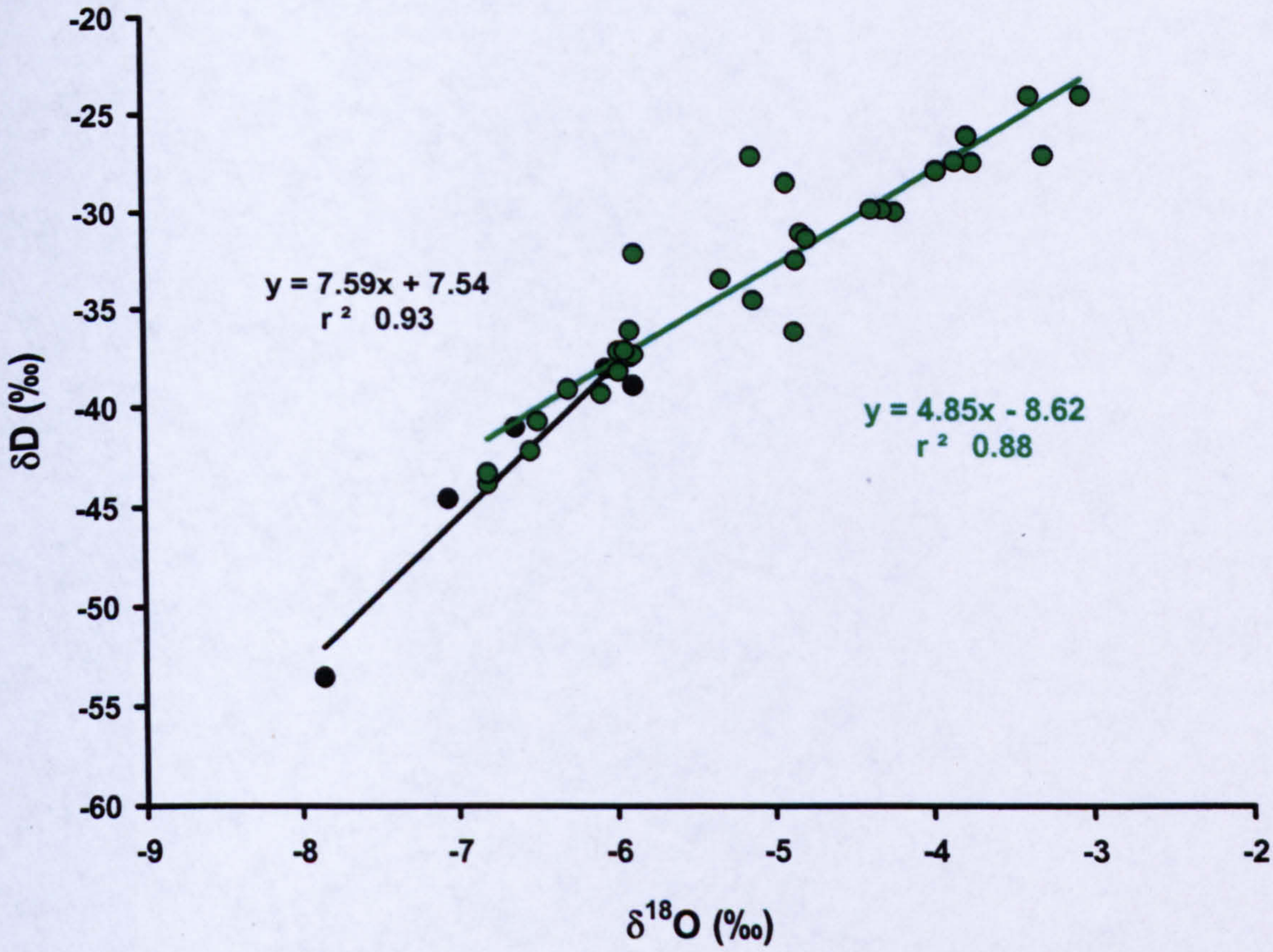

Figure 7.7 Bi-plot of mean monthly δD and δ^{18}O values in precipitation (black dots) and bog water (green dots) from the surface of Raheenmore

Seasonal separation of the data reveals evidence that at all sites much of the evaporation responsible for evolution of the bog water from the isotopic values of precipitation occurs during summer months (March – August). At Walton Moss, the winter bog water slope (8.1) (September – February) is identical to that of precipitation and absolute values are also similar (Figure 7.8). Summer bog water values show a clear evaporative enrichment in slope (6.12) and absolute values from the source precipitation (Figure 7.8).

The least difference between summer and winter values of bog water is observed at Dosenmoor (Figure 7.9), which explains the least severe evaporation signal in Figure 7.6 above. Winter values are within the scatter of precipitation values. Summer values are only slightly enriched. The restored area on Dosenmoor from which data were taken is relatively sheltered compared to the other sites in this study. The area is surrounded by wind-breaking

birch trees in close proximity and wide bog pools have developed. The large volume of water from which samples were taken and reduced wind speeds will have contributed to the reduced evaporation signal from this site.

The largest difference between summer and winter bog water values is detected in data from Raheenmore (Figure 7.10). Winter bog waters and precipitation are equivalent in slope and absolute values with the exception of two data points that are relatively enriched but which do not show the reduced slope angle consistent with kinetic fractionation effects associated with evaporation. These data may reflect an equilibrium fractionation with atmospheric vapour under high humidity or a mixing of waters of different ages in the bog surface reservoir. The summer data are strongly enriched with a markedly reduced slope angle characteristic of the influence of evaporation (Figure 7.10). These data are unexpected for the most oceanic of the three NW European sites and possibly reflect greatest wind exposure at Raheenmore.

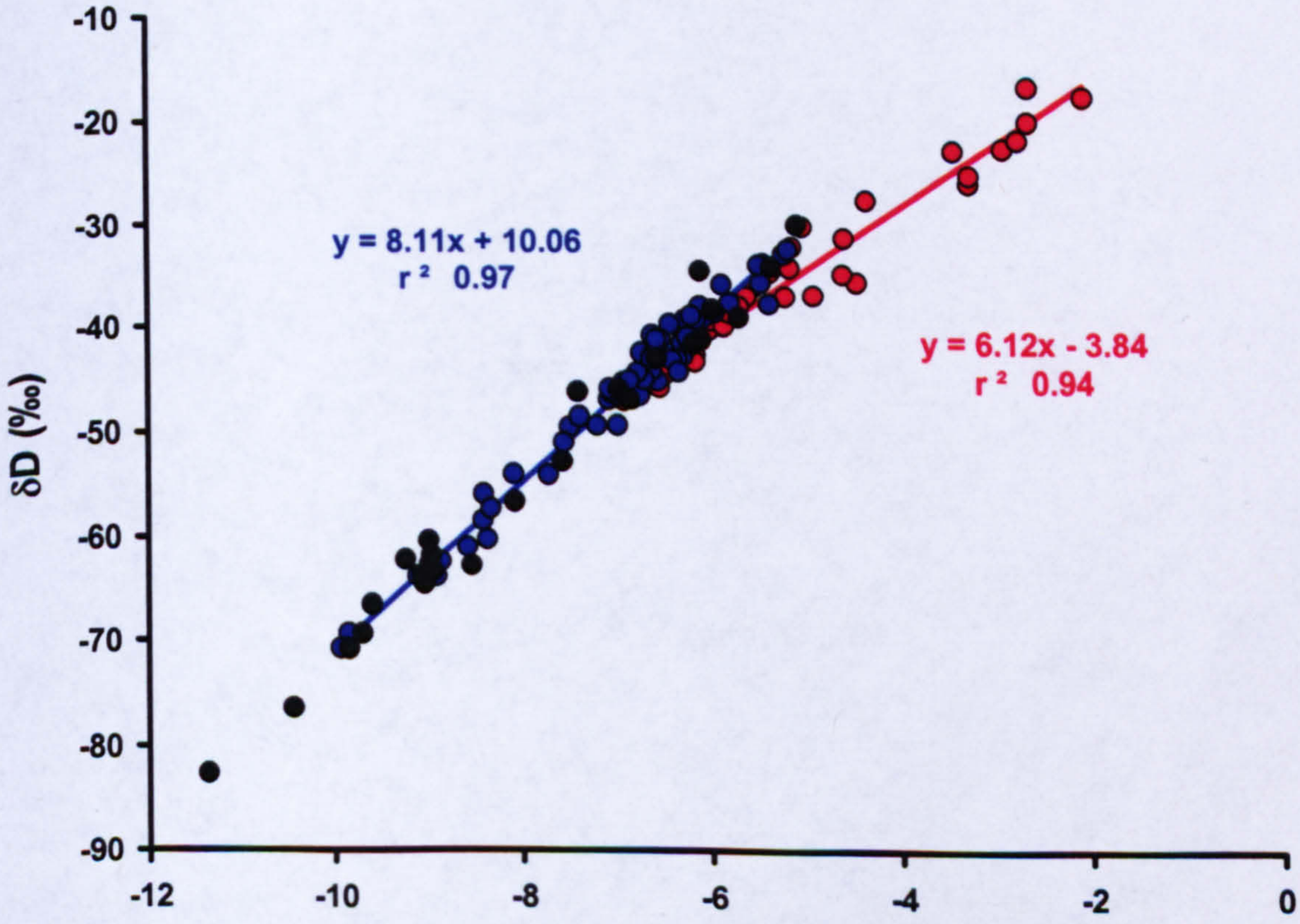

Figure 7.8 Bi-plot of mean monthly δD and δ^{18}O values in precipitation (black dots; from Brampton weather station 3 km south of Walton Moss) and bog water separated by season (blue dots = September to February, red dots = March to August) from the surface of Walton Moss

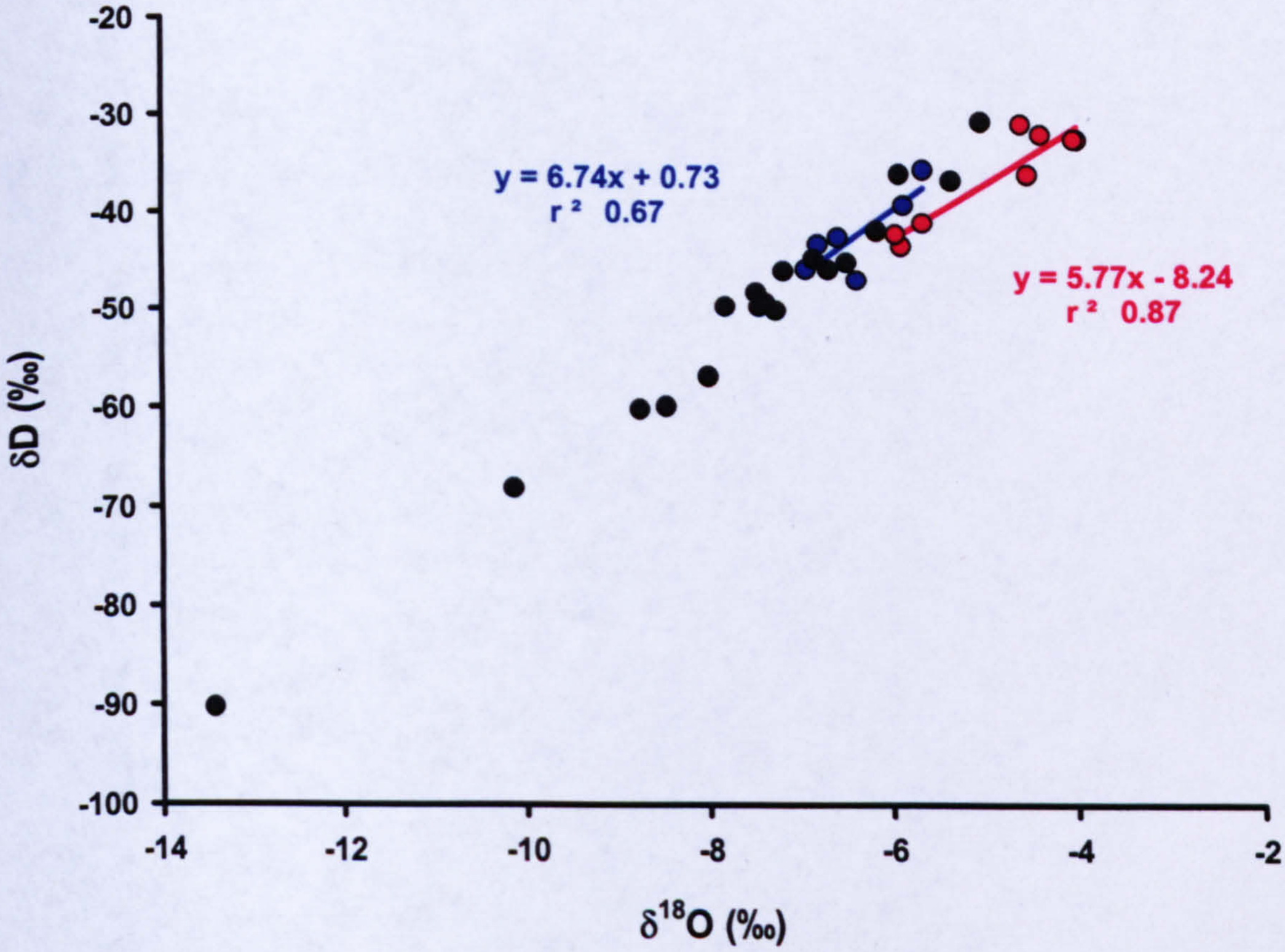

Figure 7.9 Bi-plot of mean monthly δD and δ^{18}O values in precipitation (black dots) and bog water separated by season (blue dots = September to February, red dots = March to August) from the surface of Dosenmoor

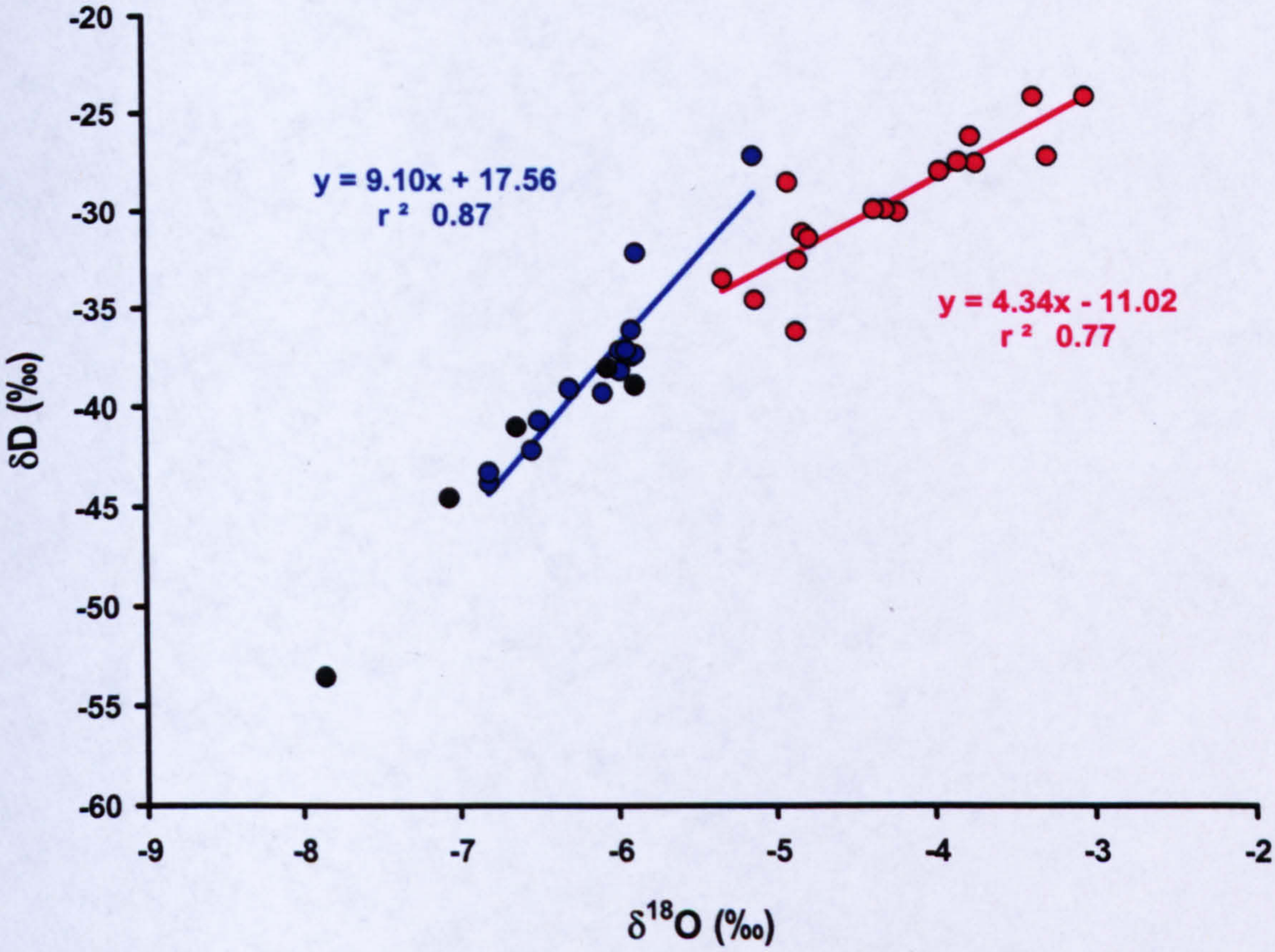

Figure 7.10 Bi-plot of mean monthly δD and $\delta^{18}O$ values in precipitation (black dots) and bog water separated by season (blue dots = September to February, red dots = March to August) from the surface of Raheenmore

Comparisons with GNIP data from the stations most local to each site (Chapter 3; Figure 7.11 - Figure 7.14) reveals that much of the variability in both precipitation and bog water data is contained within that of the longer term isotopic composition of meteoric water. The meteoric water line (MWL) at Walton is more similar to the GMWL than the MWL for Wallingford. The Wallingford MWL, conversely, is more similar in slope to the Walton Moss bog water line, which is shown in Figure 7.5 to be consistent with an evaporative influence. The comparison provides perspective, however, on the severity of the evaporative evolution of bog waters from Walton Moss. Although evaporation is detected in the Walton Moss bog waters, that evaporation is minimal compared to the scatter of meteoric waters over the extended time-range of the Wallingford series. The same is true at Dosenmoor, where both bog water and precipitation values fall within the scatter of data from Cuxhaven GNIP station

(Figure 7.12). A slightly shallower slope angle of precipitation waters is detected for Dosenmoor than Cuxhaven.

Despite the apparent strong evaporation signal detected in bog waters from the surface of Raheenmore, both precipitation and bog water data also fall within the scatter of the GNIP precipitation series from Valentia. There is a comparatively large scatter in the series from Valentia (Chapter 3; Figure 7.13) which may reflect local conditions. Unlike other sites in this study, precipitation data from Raheenmore span a very narrow range of relatively depleted isotopic values in comparison with the GNIP data. This may reflect a real difference in range due to location or an artefact of the short length of the record, for example, if 2005 was a year in which the seasonal range in delta values was unusually low at Raheenmore and relatively depleted precipitation persisted throughout the year.

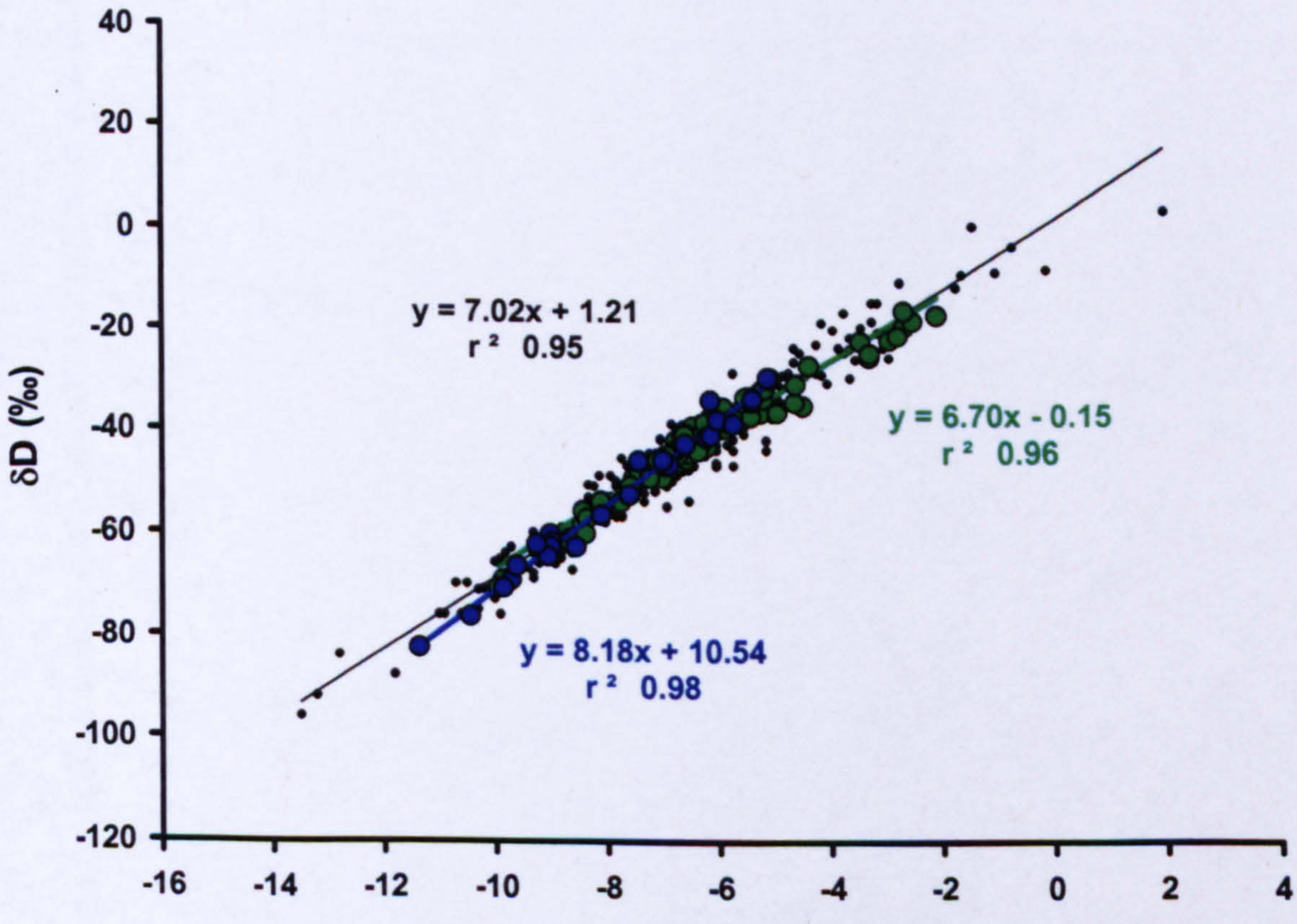

Figure 7.11 Bi-plot of mean monthly δD and $\delta^{18}O$ values in precipitation from Wallingford (GNIP; 1981-2002) (black dots) compared against precipitation at Brampton weather station 3 km south of Walton Moss (blue dots) and bog water (green dots) from the surface of Walton Moss (November 2003 – December 2005)

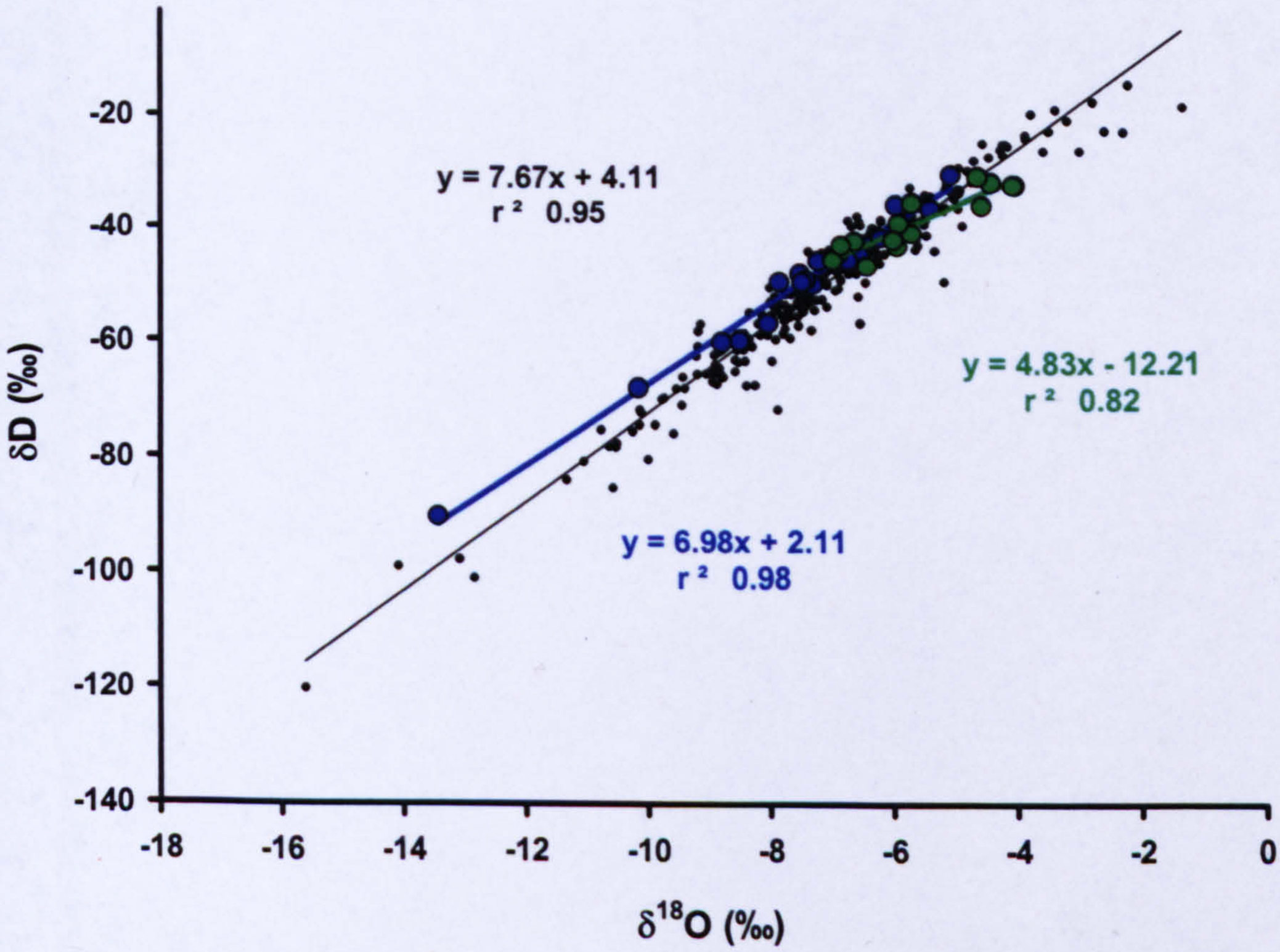

Figure 7.12 Bi-plot of mean monthly δD and δ^{18}O values in precipitation from Cuxhaven (GNIP; 1978-2001) (black dots) compared against precipitation (blue dots) and bog water (green dots) from the surface of Dosenmoor (June 2004 – December 2005)

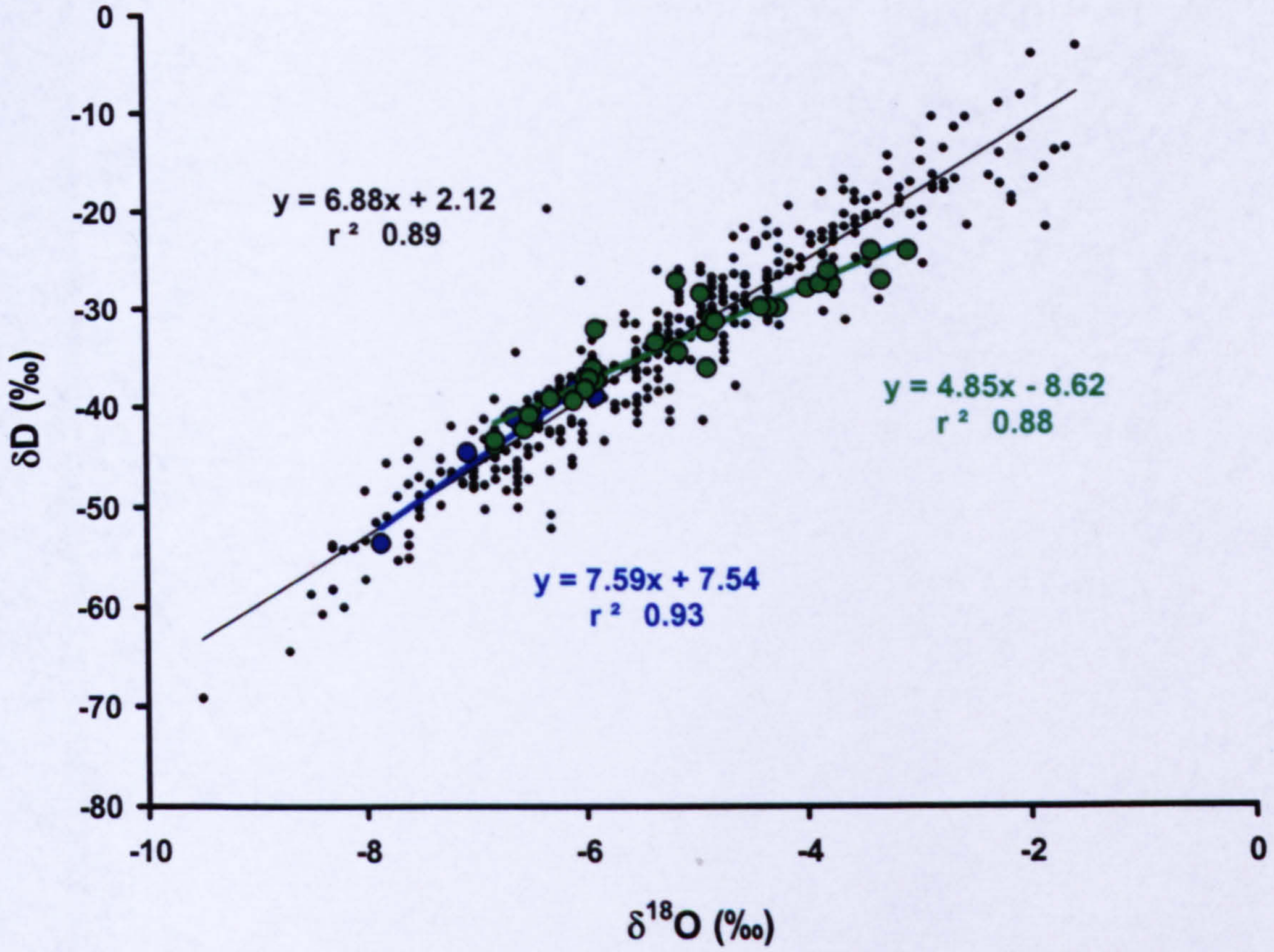

Figure 7.13 Bi-plot of mean monthly δD and $\delta^{18}O$ values in precipitation from Valentia (GNIP; 1960-2002) (black dots) compared against precipitation (blue dots) and bog water (green dots) from the surface of Raheenmore (December 2004 – November 2005)

Whilst regular monitoring of precipitation and bog water isotopic values was not possible for Nordans Pond Bog, eight surface samples of bog water were collected for analysis following fieldwork in late June 2004. The results are compared with precipitation data from GNIP stations at Truro, Nova Scotia and Goose Bay, Labrador (Figure 7.14). The bog water data display a relatively short range of values in comparison to the NW European sites reflecting sampling over a single period. Whilst the slope of the bog water line is shallow suggesting slight evaporative enrichment of meteoric source waters, all the bog water data plot within the scatter of the GNIP precipitation data suggesting that bog water values and precipitation are not significantly different.

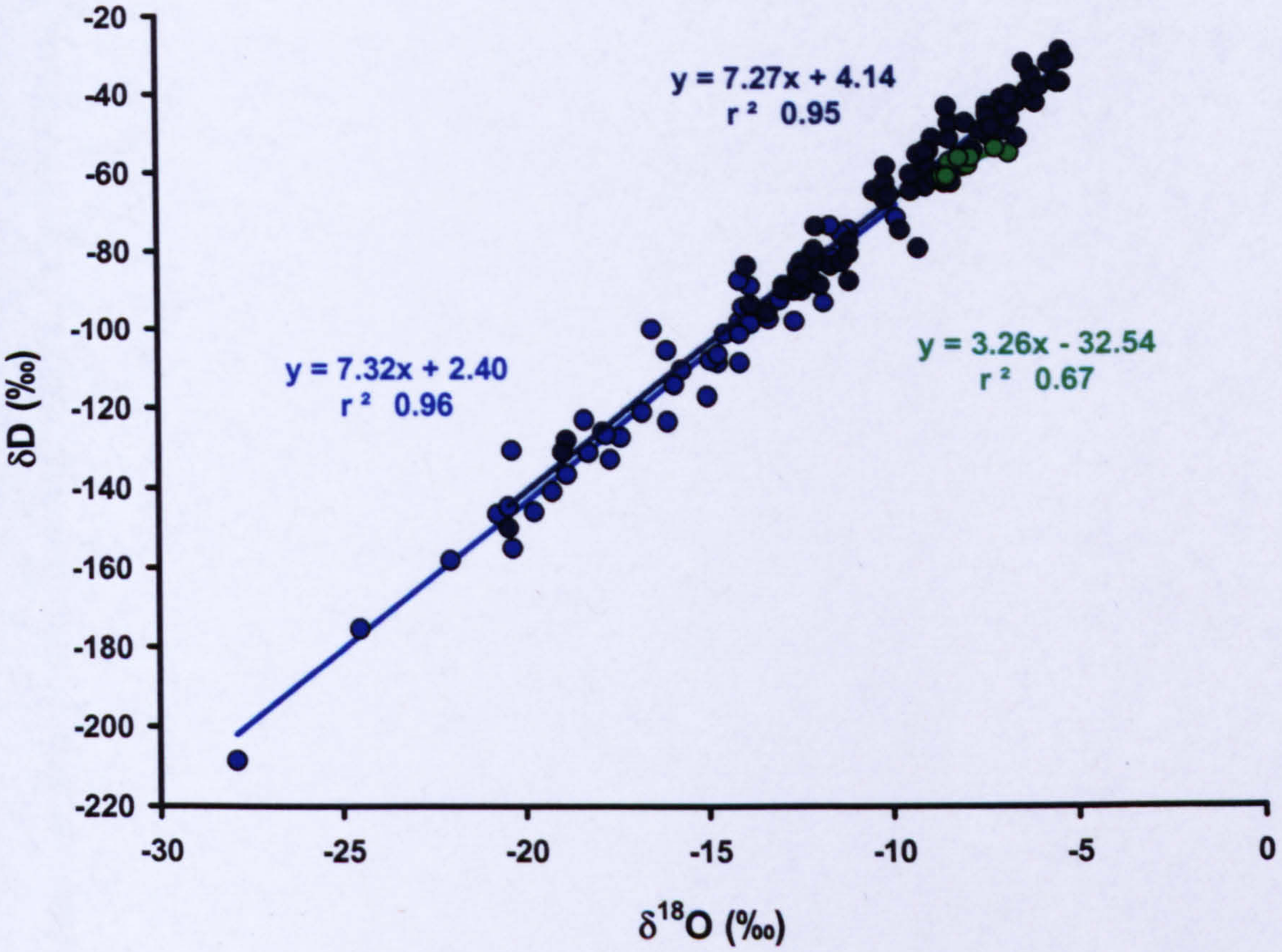

Figure 7.14 Bi-plot of δD and δ^{18}O values in bog water from the surface of Nordans Pond Bog (green dots; June 2004) compared against mean monthly precipitation from Goose Bay (light blue dots; GNIP, 1961-1965) and Truro (dark blue dots; GNIP, 1975-1983)

7.2.3 $\delta^{18}O_{Sphagnum}$ values

Results of δ^{18}O analyses of *Sphagnum* cellulose are presented from each of the sites in Figure 7.15 - Figure 7.17 and tabulated in Table 7.1 - Table 7.3. Seasonal variation is observed in the $\delta^{18}O_{Sphagnum}$ values from Walton Moss. Lightest values were observed in October 2004. The heaviest single species delta value was recorded in *S. magellanicum* in April 2004 although the heaviest combined $\delta^{18}O_{Sphagnum}$ value was found in July 2005. No consistent difference between species means or standard deviation was observed and ranges indicated by standard deviation showed high incidence of overlap. High σ variability was noted in April 2004 which

may reflect source water variability during spring conditions of varying temperature and precipitation. Crucially, each sampled month was significantly different from the next, implying that new growth occurred between each of the periods and that the growing season for Walton Moss was at least April to October. The possibility that the moss was growing and hence recording isotopic composition of source water into the winter months cannot be discounted using these data.

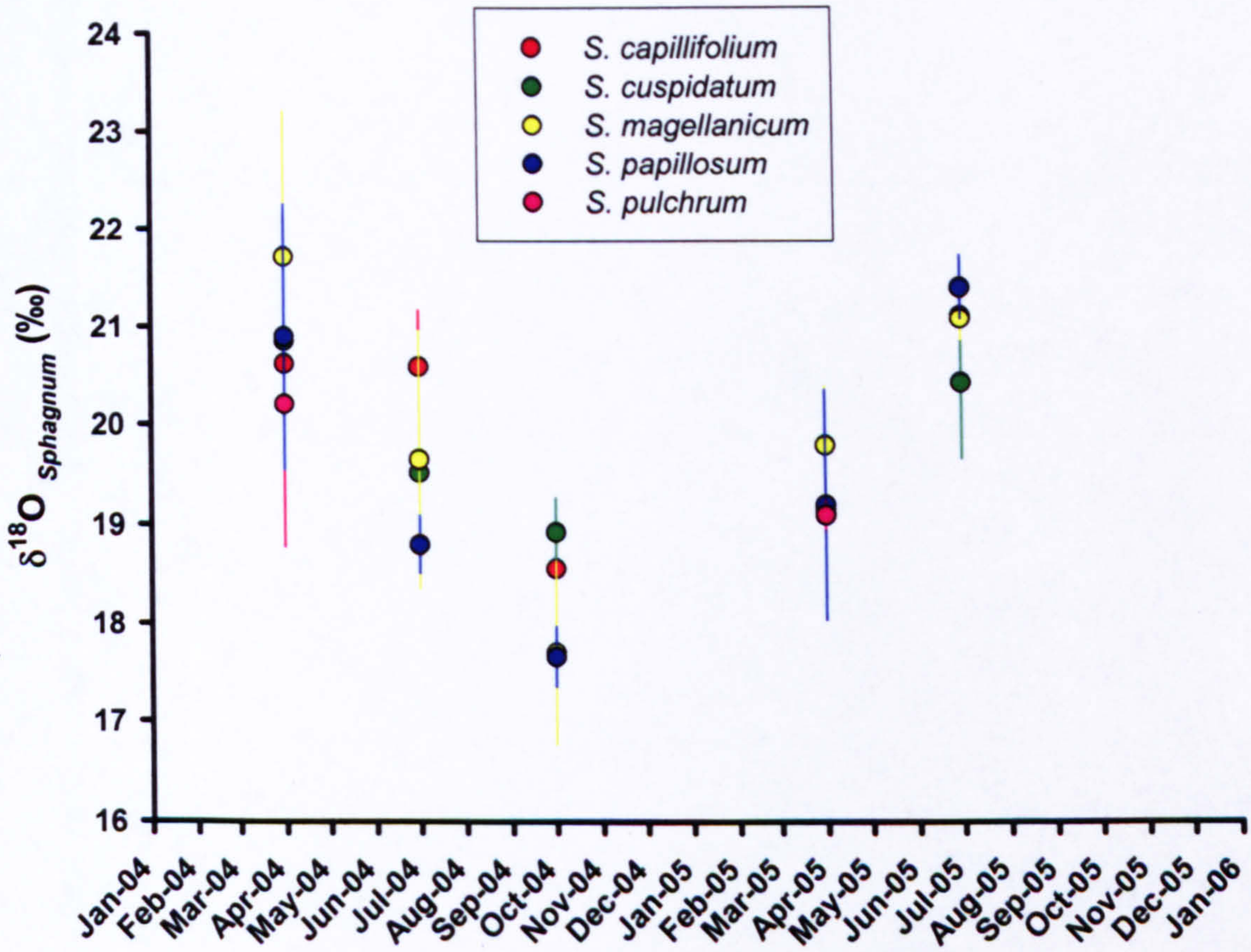

Figure 7.15 Species mean $\delta^{18}O_{Sphagnum}$ values (dots) and 2σ range (bars) for modern surface samples from Walton Moss (April 2004 – July 2005)

Table 7.1 $\delta^{18}O_{Sphagnum}$ species means and σ range for Walton Moss (April 2004 – July 2005)

		Apr-04	Jul-04	Oct-04	Apr-05	Jul-05	Mean
S. capillifolium	*n*	9	5	4	5	5	
	mean	20.62	20.59	18.55	19.14	21.10	**20.00**
	σ	1.84	0.57	0.64	0.30	0.47	**1.09**
S. cuspidatum	*n*	8	6	2	3	5	
	mean	20.85	19.52	18.92	19.11	20.43	**19.76**
	σ	0.95	0.54	0.34	0.02	0.78	**0.84**
S. magellanicum	*n*	8	2	4	3	2	
	mean	21.72	19.65	17.69	19.79	21.08	**19.98**
	σ	1.49	1.31	0.94	0.59	0.22	**1.55**
S. papillosum	*n*	3	2	2	2	3	
	mean	20.90	18.80	17.65	19.19	21.39	**19.59**
	σ	1.35	0.29	0.31	1.16	0.32	**1.54**
S. pulchrum	*n*	1			2		
	mean	20.21			19.09		**19.65**
	σ				0.14		**0.79**
S. tenellum	*n*	1					
	mean	20.49					

Reduced seasonal variation is observed at Dosenmoor in comparison with the amplitude of that at Walton Moss (Figure 7.16; Table 7.2). Heaviest delta values were detected in June 2005 and the lightest average $\delta^{18}O_{Sphagnum}$ values found in September 2004. As with Walton Moss, there is no evidence for a consistent offset between species means in the data from Dosenmoor. Separation beyond the 2σ range was noted in August 2005 with anomalous enrichment of the semi-submergent species *S. cuspidatum* (Figure 7.16). It has been previously reported that submergent species exhibit less enriched values during single sample analyses in peak summer months (Brenninkmeijer *et al.*, 1982; Aravena and Warner, 1992). So the relatively enriched status of this species is unexpected. It is possible that the pool surface waters become more enriched than the water residing in *Sphagnum* lawn and hummock areas during through enhanced evaporation on exposed open water surfaces. This is in agreement with data from Nordans Pond Bog (below) and may explain the comparative enrichment of *S. cuspidatum* at Dosenmoor in this month.

Enriched cellulose values were detected at Dosenmoor during the winter of 2004-2005 and relatively depleted values observed during September 2004 and April 2005 (Figure 7.16). This is the opposite of the expected seasonal signal and contradicts variation observed in the bog waters (Figure 7.3). Precipitation waters showed high noise with little seasonal signal (Figure 7.1). The difference between the $\delta^{18}O_{Sphagnum}$ means of November 2004 and January 2005 was small suggesting that the moss may have suspended growth over December and January and that January data were replicating analyses of cellulose growth during the previous autumn. Given that significant differences in the means were observed in each of the other months, the data suggest that the growing season extends at least from April to November. Alternatively, the cellulose data could reflect real differences in source water or evaporation signal during the sampled months. Whilst the source water (precipitation) does not appear to have varied comparably with either the cellulose or bog water data, more enriched values of bog water would be expected in November 2004 and January 2005 if the moss was growing and evaporation was the driver of high cellulose values over these months. Clearly this is not the case.

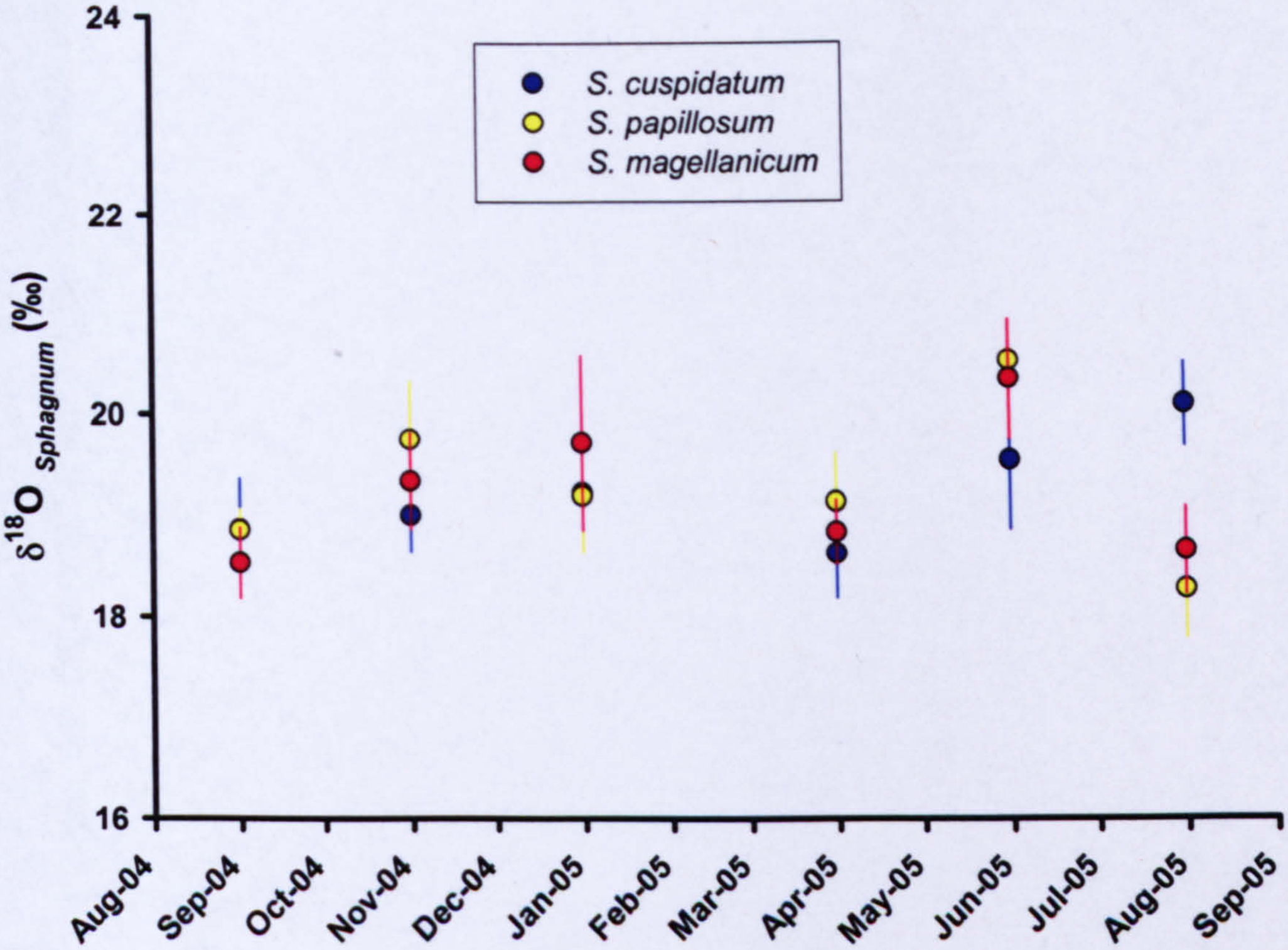

Figure 7.16 Species mean $\delta^{18}O_{Sphagnum}$ values (dots) and 2σ range (bars) for modern surface samples from Dosenmoor (September 2004 – August 2005)

Table 7.2 $\delta^{18}O_{Sphagnum}$ species means and σ range for Dosenmoor (September 2004 – August 2005)

		Sep-04	Nov-04	Jan-05	Apr-05	Jun-05	Aug-05	Mean
S. cuspidatum	***n***	4	5	2	4	8	7	
	Mean	18.86	19.01	19.22	18.62	19.53	20.07	**19.22**
	σ	0.50	0.36	0.06	0.44	0.68	0.41	**0.52**
S. papillosum	***n***	2	8	10	9	2	3	
	Mean	18.86	19.74	19.19	19.13	20.51	18.26	**19.28**
	σ	0.21	0.57	0.55	0.48	0.08	0.49	**0.77**
S. magellanicum	***n***	6	5	2	2	4	5	
	Mean	18.53	19.34	19.71	18.83	20.33	18.64	**19.23**
	σ	0.35	0.47	0.86	0.31	0.59	0.43	**0.70**

In similarity with data from Walton Moss and Dosenmooor, seasonal variation was observed in the *Sphagnum* cellulose data from Raheenmore with heaviest values detected in July 2005 and lightest values in December 2004 (Figure 7.17). Again, there was no evidence for a consistent offset between species means. Unlike the data from Dosenmoor, significant differences were observed in the combined means for each month indicating that new *Sphagnum* growth is laid down in every month sampled (i.e. *Sphagnum* is preserving an annual record). The presence of year-round *Sphagnum* growth probably reflects the reduced seasonality of the site afforded by its oceanic location and the lowest seasonal temperature range of any of the study sites. Whilst annual recording cannot be discounted for Walton Moss, a record of growth at Raheenmore in the coldest months confirms an annual mean signal in the *Sphagnum* cellulose from this site under modern conditions.

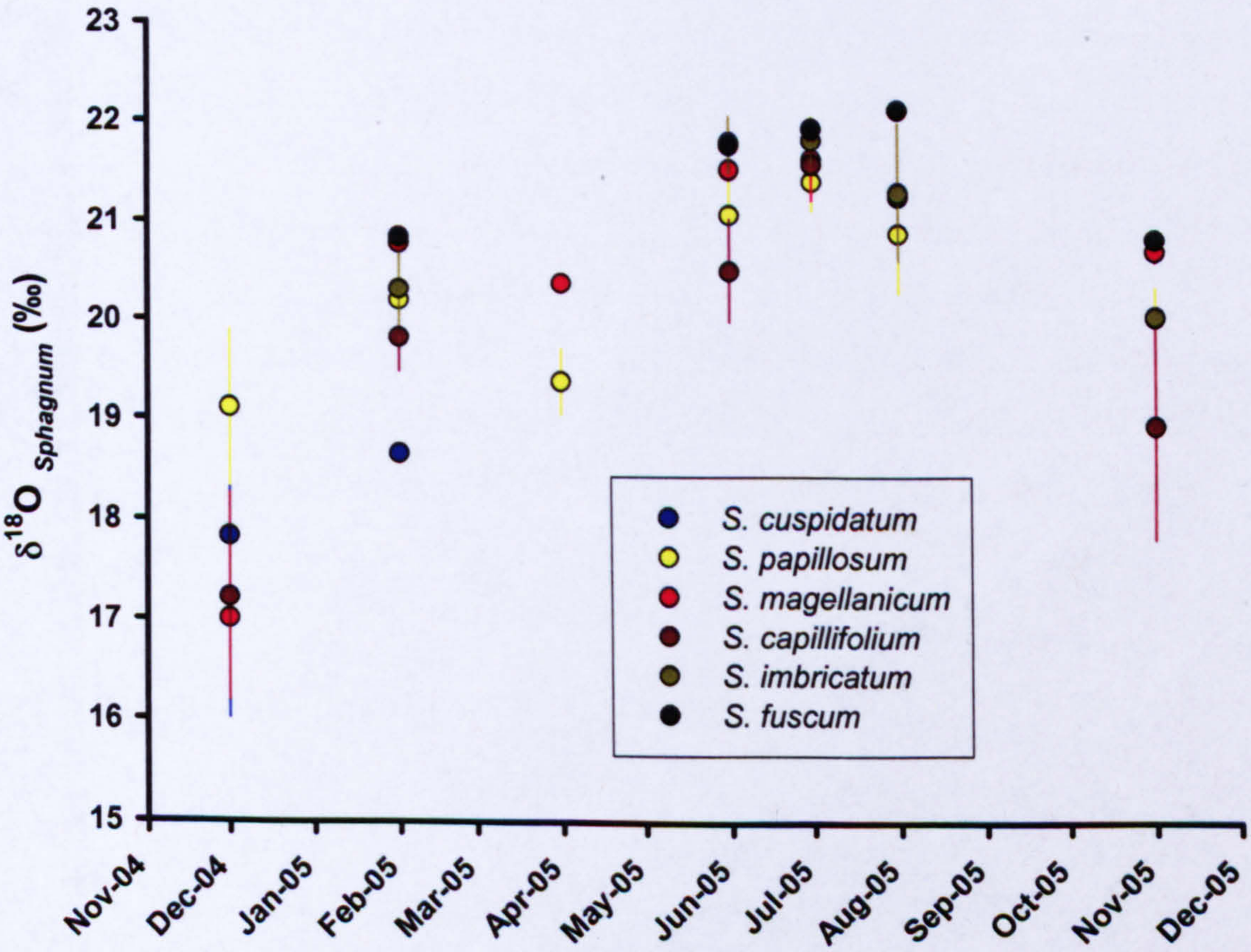

Figure 7.17 Species mean $\delta^{18}O_{Sphagnum}$ values (dots) and 2σ range (bars) for modern surface samples from Raheenmore (December 2004 – November 2005)

Table 7.3 $\delta^{18}O_{Sphagnum}$ species means and σ range for Raheenmore (December 2004 – November 2005)

		Dec-04	Feb-05	Apr-05	Jun-05	Jul-05	Aug-05	Nov-05	Mean
S. cuspidatum	*n*	4	1						
	Mean	17.83	18.66						
	σ	1.82							
S. papillosum	*n*	3	9	2	5	4	6	7	
	Mean	19.11	20.20	19.37	21.08	21.41	20.89	20.04	**20.30**
	σ	0.78	0.59	0.33	0.39	0.29	0.60	0.30	**0.87**
S. magellanicum	*n*	5	1	1	2	3	3	2	
	Mean	17.01	20.78	20.38	21.53	21.63	21.26	20.71	**20.47**
	σ	0.48		0.01	0.41	0.35	0.11		**1.59**
S. fuscum	*n*		1	1	1	1	1		
	Mean		20.84	21.80	21.94	22.12	20.83		**21.51**
	σ								**0.62**
S. capillifolium	*n*	3	2	3	2	2	4		
	Mean	17.22	19.82	20.51	21.58	21.27	18.93		**19.89**
	σ	1.04	0.35	0.52	0.03	0.20	1.12		**1.62**
S. Imbricatum	*n*		6	5	4	3	1		
	Mean		20.31	21.77	21.82	21.30	20.05		**21.05**
	σ		0.37	0.28	0.22	0.69			**0.83**

Twelve surface samples of *Sphagnum* moss from five species were collected from Nordans Pond bog in late June 2004 and were analysed for $\delta^{18}O_{Sphagnum}$ values. The results are presented in Figure 7.18 below. Whilst data on the annual variation in $\delta^{18}O_{Sphagnum}$ values and hence the length of the growing season and seasonal variability are not available, the data contradict earlier studies of species signals (Brenninkmeijer *et al.*, 1982; Aravena and Warner, 1992). As has been mentioned previously, much of the earlier work on modern *Sphagnum* isotopic characterisation involved sampling in a single month or season (Brenninkmeijer *et al.*, 1982; Aravena and Warner, 1992; Ménot-Combes *et al.*, 2002). Data in Figure 7.18 demonstrate how this single sampling can suggest a clear difference between species means. Interestingly, the pattern observed in other studies for increasing $\delta^{18}O_{Sphagnum}$ values with increasing elevation in the microtopographical habitat is reversed in these data. The data here suggest that *Sphagnum* closer to the water table was more enriched than those specimens inhabiting hummocks. *S. fuscum* is known (Daniels and Eddy, 1990) and was observed in this study to inhabit hummock zones. The mean of the *S. fuscum* data is not statistically different from the mean of *S. magellanicum* in which the least enriched $\delta^{18}O_{Sphagnum}$ values are

observed. The pool species *S. pulchrum* exhibit a $\delta^{18}O_{Sphagnum}$ value similar to the more enriched values of *S. fuscum* within the range sampled. There is a wide range of scatter in the data which is larger than the scatter observed in data from NW Europe. This may reflect the strong contrast in seasonality that exists at this location or differences in the timing of new *Sphagnum* growth following the spring snow melt.

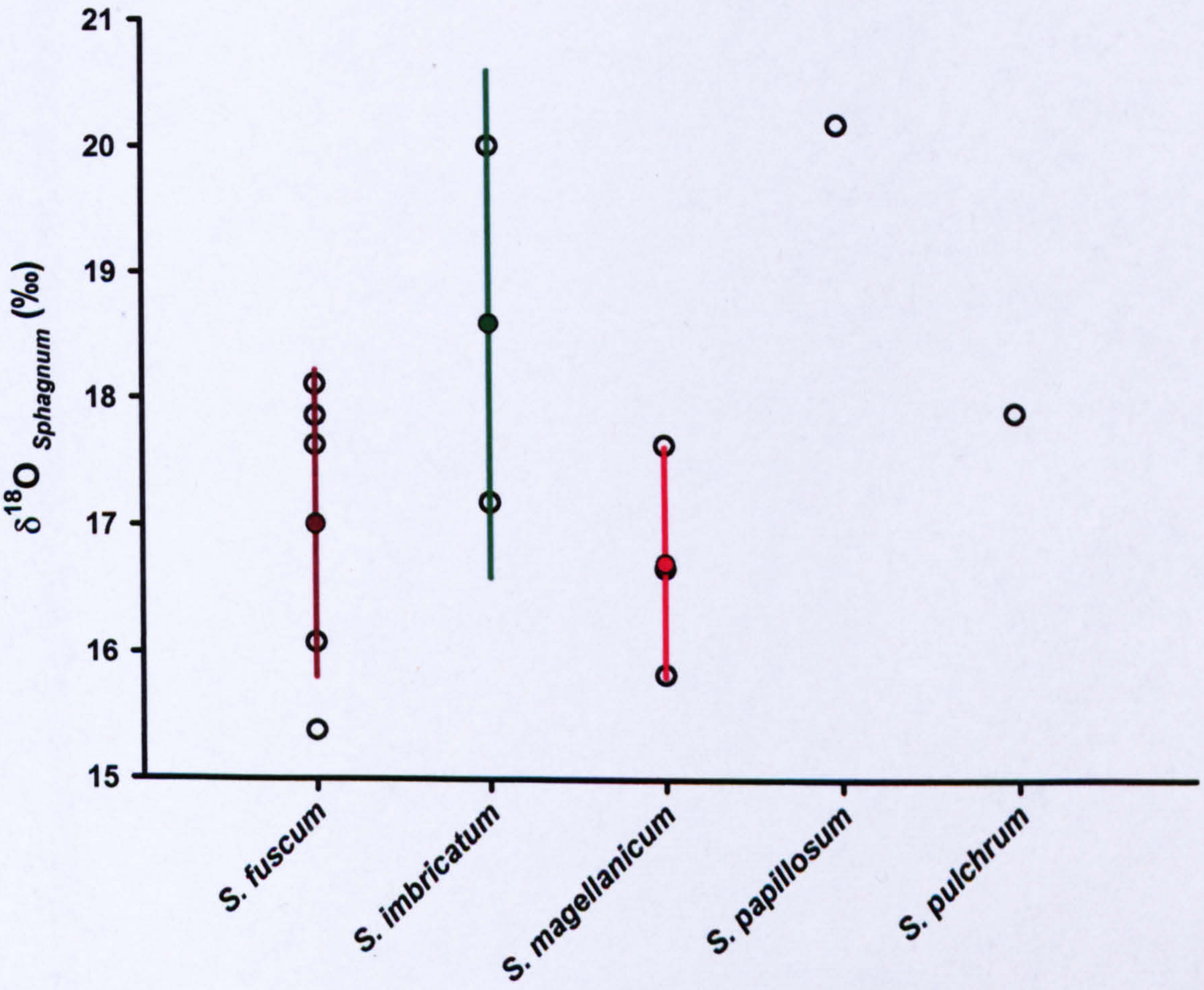

Figure 7.18 Species mean $\delta^{18}O_{Sphagnum}$ values (solid dots) and 2σ range (bars) for modern surface samples from Nordans Pond Bog (June 2004). Individual samples are shown in open circles.

7.2.4 $\delta D_{Sphagnum}$ values

Results of the δD analysis of 36 modern cellulose samples selected from Dosenmoor are given in Figure 7.19. Samples from Dosenmoor were selected for δD analysis because of the

regular spacing between sample periods allowing characterisation of variability within a year and because $\delta^{18}O$ values had indicated excellent agreement between species means. With a limited number of hydrogen analyses available, samples were prioritised under the following scheme. Two samples for each of the three species present were selected for each month (n = 6). The two samples chosen from each species group were selected for proximity to the mean $\delta^{18}O_{Sphagnum}$ value for the species group and for a low standard deviation between replicate analyses.

A bi-plot of $\delta D_{Sphagnum}$ and $\delta^{18}O_{Sphagnum}$ values (Figure 7.19) displays a high degree of scatter in the more depleted values and a strong linear feature in the more enriched values. The slope (10.23) is also steeper than that expected for a meteoric signal. Species labelling of the data reveals that this pattern is not forced by any one species (Figure 7.20), although least scatter is observed in the *S. cuspidatum* data. The parallel slopes for the three sampled species (*S. cuspidatum, S. magellanicum* and *S. papillosum*) (Figure 7.20) indicate that the magnitude of change in source water is replicated relatively equally in all species. The difference in the intercept of each of the regressions is not statistically significant in relation to the range of scatter in the cellulose values. Monthly separation of the data reveals that scatter is not confined to any one month (Figure 7.21) although scatter towards anomalously enriched hydrogen values is found in the months of September 2004 and August 2005 and scatter towards anomalously depleted hydrogen values is found in January 2005. The monthly data reveal that the linear feature towards enriched values is composed of a mix of data from autumn and winter months as well as summer months with the exception of the two data plotted on the far right of the graph (Figure 7.21). This suggests that the feature is not associated solely with summer evaporation as might be expected.

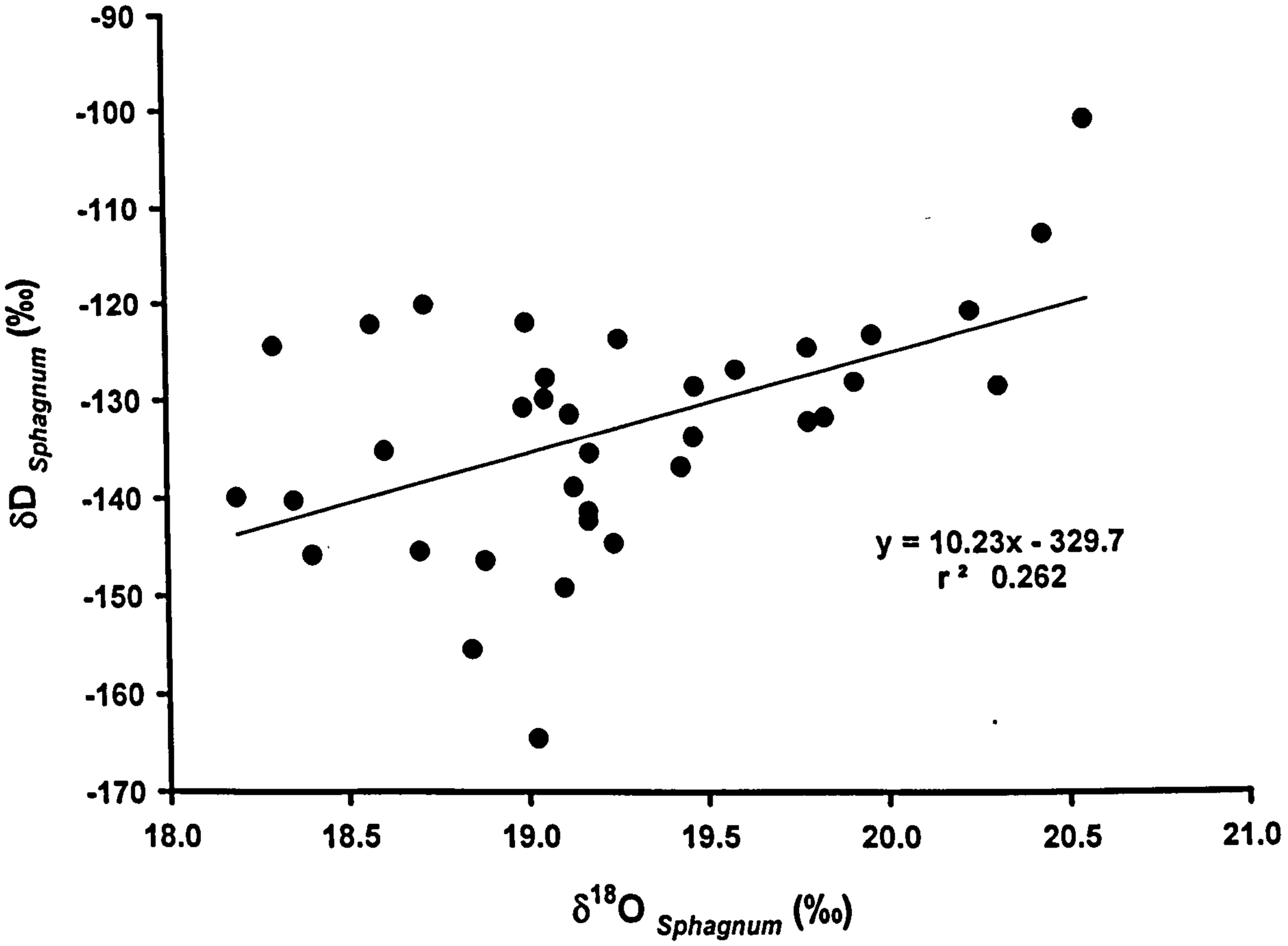

Figure 7.19 Bi-plot of δD and $\delta^{18}O$ values in *Sphagnum* cellulose from the surface of Dosenmoor (September 2004 – August 2005)

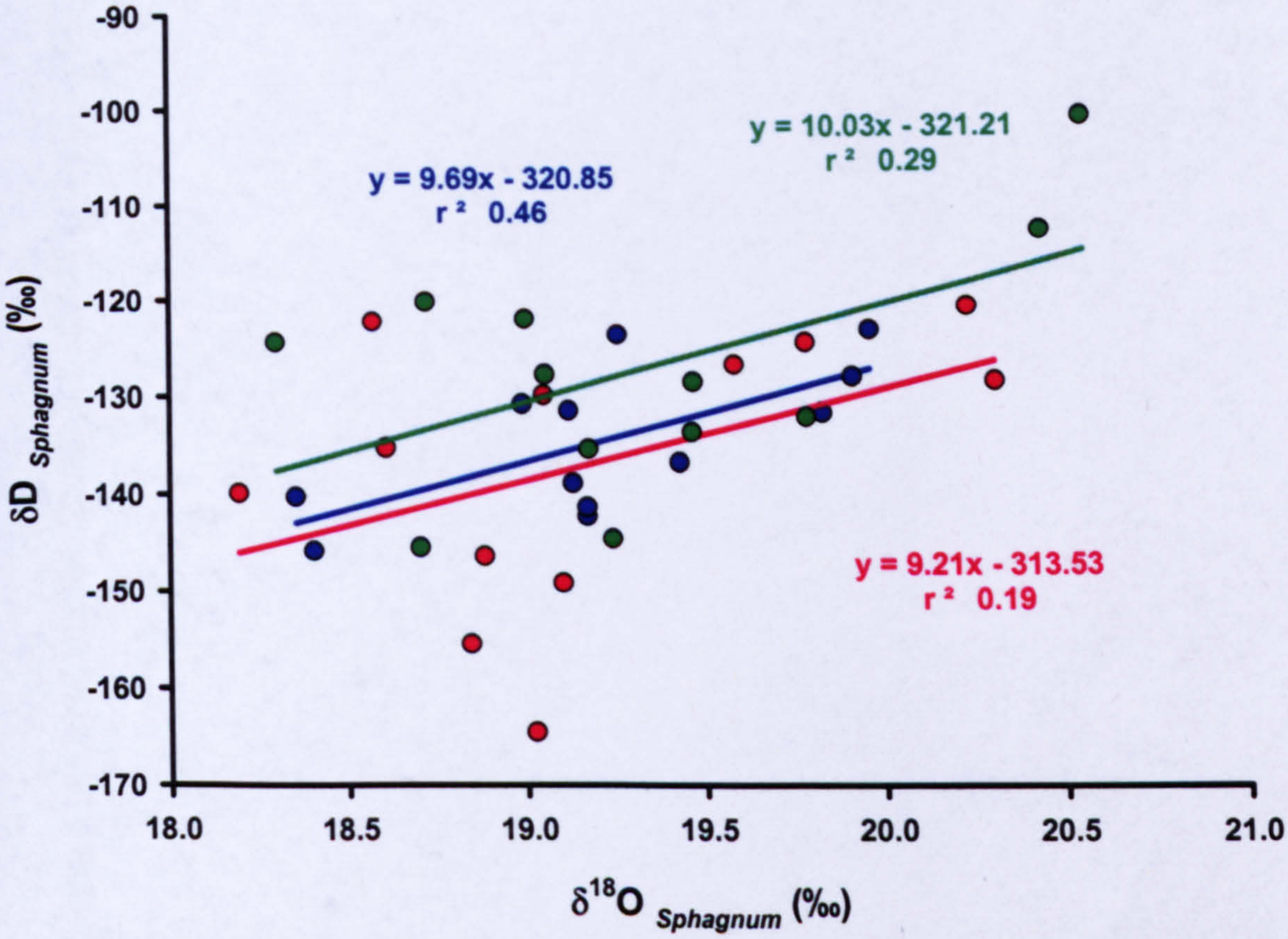

Figure 7.20 Bi-plot of δD and δ^{18}O values in *Sphagnum* cellulose from the surface of Dosenmoor (September 2004 – August 2005) by taxon (*S. cuspidatum*, blue dots; *S. magellanicum*, red dots; *S. papillosum*, green dots)

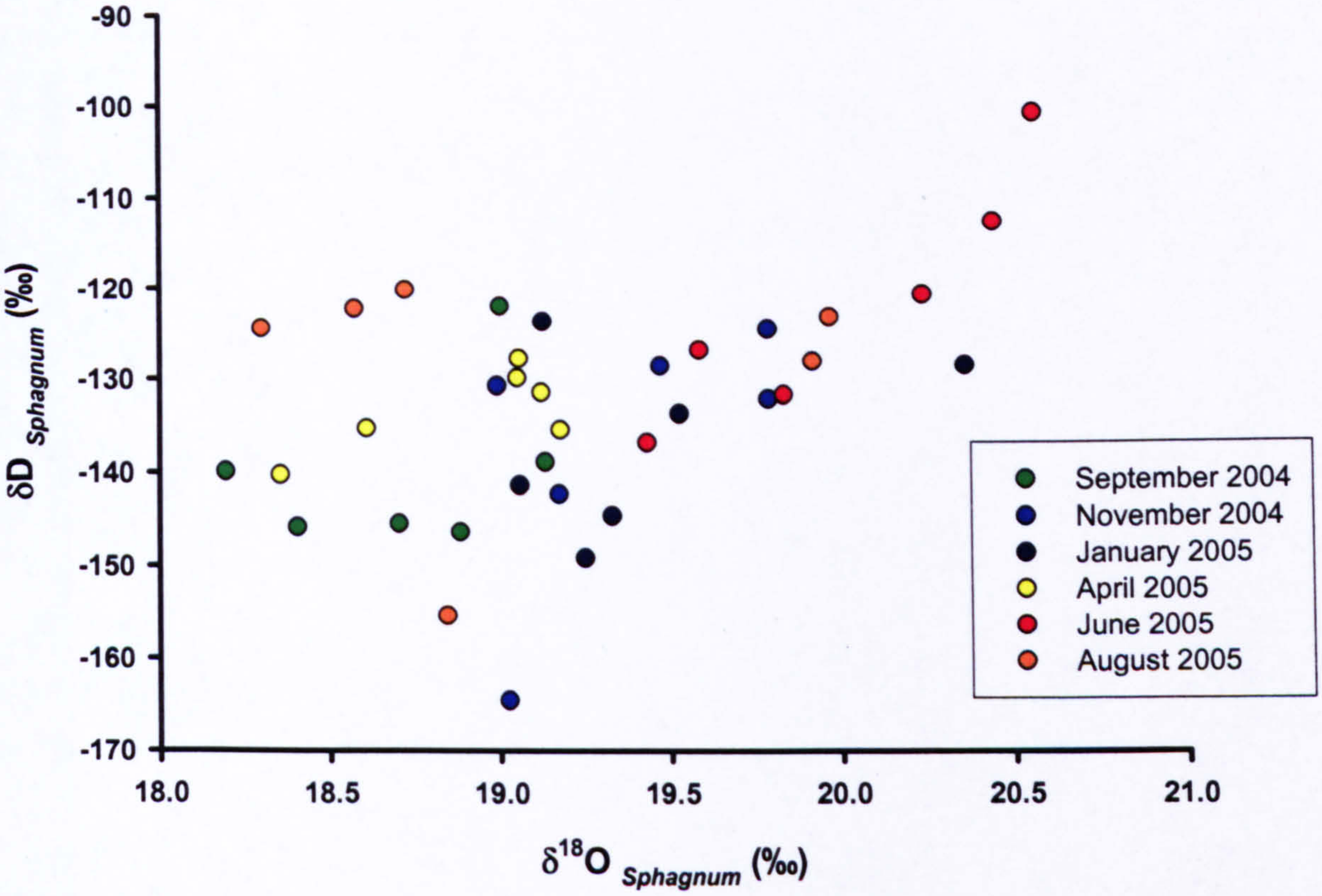

Figure 7.21 Bi-plot of δD and δ^{18}O values in *Sphagnum* cellulose from the surface of Dosenmoor (September 2004 – August 2005) by month of sampling

Enough funds were available to permit the measurement of hydrogen isotopic values on three of the twelve samples of surface *Sphagnum* cellulose collected in June 2004 from Nordans Pond Bog. These are summarised in Table 7.4 in which each cellulose sample is referenced against the closest of the eight bog water samples. The difference between replicates is represented by the standard deviation (σ). Two of the three samples are within published measurement precision (± 4 ‰) (Filot *et al.*, 2006). The σ range on replicates from sample NDB0604-5 is outside measurement precision indicating either heterogeneity in the isotopic composition of the cellulose or incomplete equilibration of one of the replicates. The former is the more likely explanation.

Table 7.4 Summary of Nordans Pond Bog surface cellulose and bog water isotopic data

Lab. Code	Species	mean $\delta^{18}O$	s.d.	mean δD	s.d.	$\delta^{18}O$ (bw)	δD (bw)	d xs (bw)
NDB0604-3b	*S. fuscum*	17.86	0.04	-109.13	3.50	-7.01	-54.35	1.72
NDB0604-4b	*S. fuscum*	18.11	0.20			-8.24	-57.98	7.94
NDB0604-6	*S. fuscum*	17.63	0.43			-8.32	-61.41	5.19
NDB0604-7	*S. fuscum*	16.08	0.27			-7.68	-56.58	4.82
NDB0604-9	*S. fuscum*	15.38	0.26			-7.99	-56.84	7.10
NDB0604-4	*S. imbricatum*	20.02	0.52			-8.24	-57.98	7.94
NDB0604-5	*S. imbricatum*	17.18	0.51	-127.57	6.25	-8.44	-61.43	6.12
NDB0604-2	*S. magellanicum*	16.68	0.91			-7.75	-58.69	3.34
NDB0604-8	*S. magellanicum*	15.83	0.42			-7.99	-56.84	7.10
NDB0604-10	*S. magellanicum*	17.63	0.14			-7.75	-58.69	3.34
NDB0604-3a	*S. papillosum*	20.17	0.00			-7.01	-54.35	1.72
NDB0604-1	*S. pulchrum*	17.87	0.25	-127.65	1.47	-6.64	-55.67	-2.56

7.3 *Sphagnum cellulose palaeo-isotopic results*

7.3.1 WLM22 $\delta^{18}O_{Sphagnum}$ record

$\delta^{18}O$ values analysed from concentrated *Sphagnum* alpha-cellulose samples are presented for core WLM22 against depth in Figure 7.22 and as a time-series in Figure 7.23. Error bars refer to the 2σ range on duplicate measurements of the same sample. The stratigraphical resolution of the data is variable depending on the availability of *Sphagnum* in sufficient abundance to allow isotopic analysis by the concentration method, as is the total depth of the record which is limited to 428 cm (~ 4300 years) due to the absence of sufficient *Sphagnum* remains below this depth. Despite the presence of a small *Sphagnum* spike at 784 cm (Figure 6.1), which dates to ~7900 BP and may relate to climatic changes ~8200 BP, remains were insufficient to allow isotopic analysis.

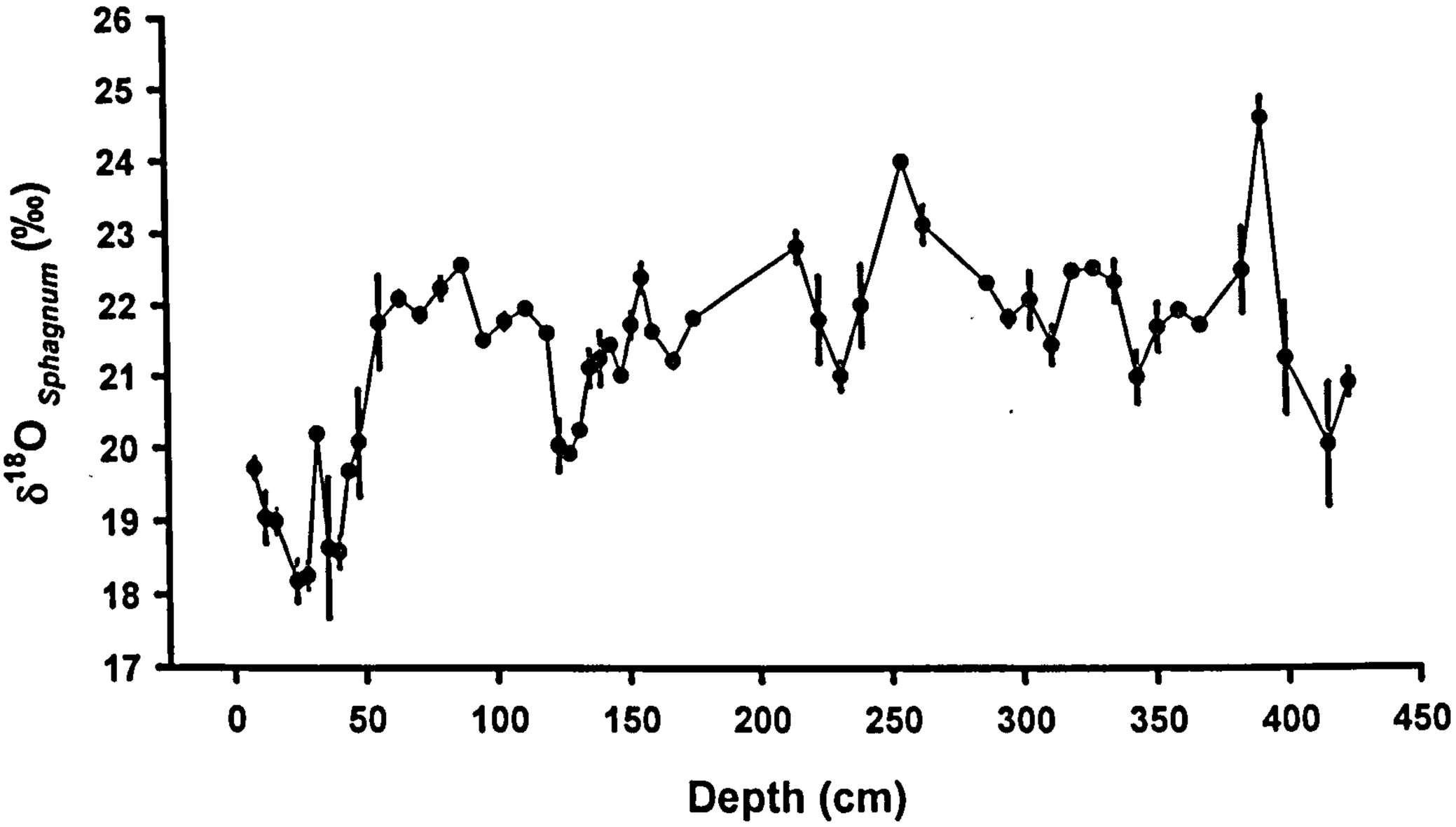

Figure 7.22 WLM22 $\delta^{18}O_{Sphagnum}$ record

Over the period of the record there is a slight downward trend in $\delta^{18}O_{Sphagnum}$ values with the highest value for the record observed at 396 cm (~3950 BP; Figure 7.23) and the lowest observed at 24 cm (~250 BP; Figure 7.23). For the majority of the record, $\delta^{18}O_{Sphagnum}$ values vary within ± 1‰ of 22‰. Rarely do values exceed this level. Many of the larger magnitude changes (those >1‰ deviation) are towards isotopically depleted conditions which may reflect differences in *Sphagnum* abundance, i.e. *Sphagnum* is more frequently present during isotopic depletions than during enriched periods. Isotopic excursions towards depleted $\delta^{18}O_{Sphagnum}$ values are clearly identified in the record. Points of inflexion for these excursions occur at 425, 392, 352, 312, 256, 156 and 56 cm (Figure 7.22). These correspond to ages of ~ 4300, 3950, 3550, 3200, 2550, 1550, 500 BP (Figure 7.23) rounded to the nearest 50 years. The apparent spacing of ~100 cm (~1000 years) between several of the key changes towards lighter $\delta^{18}O_{Sphagnum}$ values is of note. The total range of isotopic variation in the record is 6.8‰.

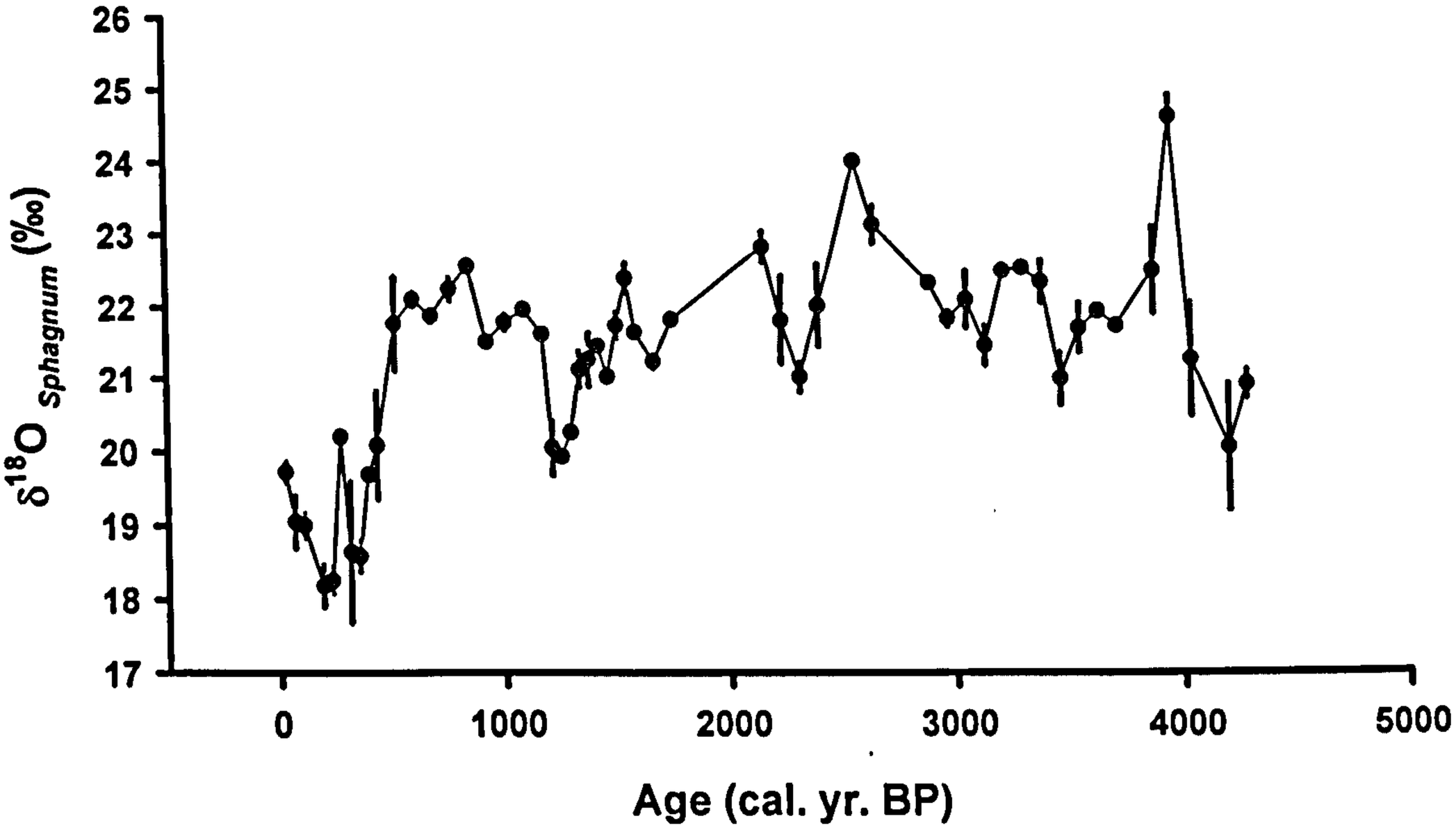

Figure 7.23 WLM22 $\delta^{18}O_{Sphagnum}$ time-series

7.3.2 WLM22 $\delta D_{Sphagnum}$ record

$\delta D_{Sphagnum}$ results from a short section (112 – 160cm) of WLM22 in which a strong $\delta^{18}O$ decline was observed in *Sphagnum* rich sediment are presented in Figure 7.24 for comparison with the $\delta^{18}O$ excursion. The structure of variation through the short section of record is highly similar. Both records begin with relatively enriched values followed by a low magnitude fluctuation to lighter isotopic values between 152 and 140 cm (~1500 – 1380 BP). After 136 cm, both records show a steep isotopic decline which, for both records, is centred on 128 cm (~1250 BP). The magnitude of the decline in δD is 37‰ and for $\delta^{18}O$ is 2.8‰. The principal difference between the two records is in the duration of the main negative excursion where the $\delta^{18}O$ anomaly is observed to persist for longer than that observed in δD values. Notwithstanding, the agreement between these two records is exceptional.

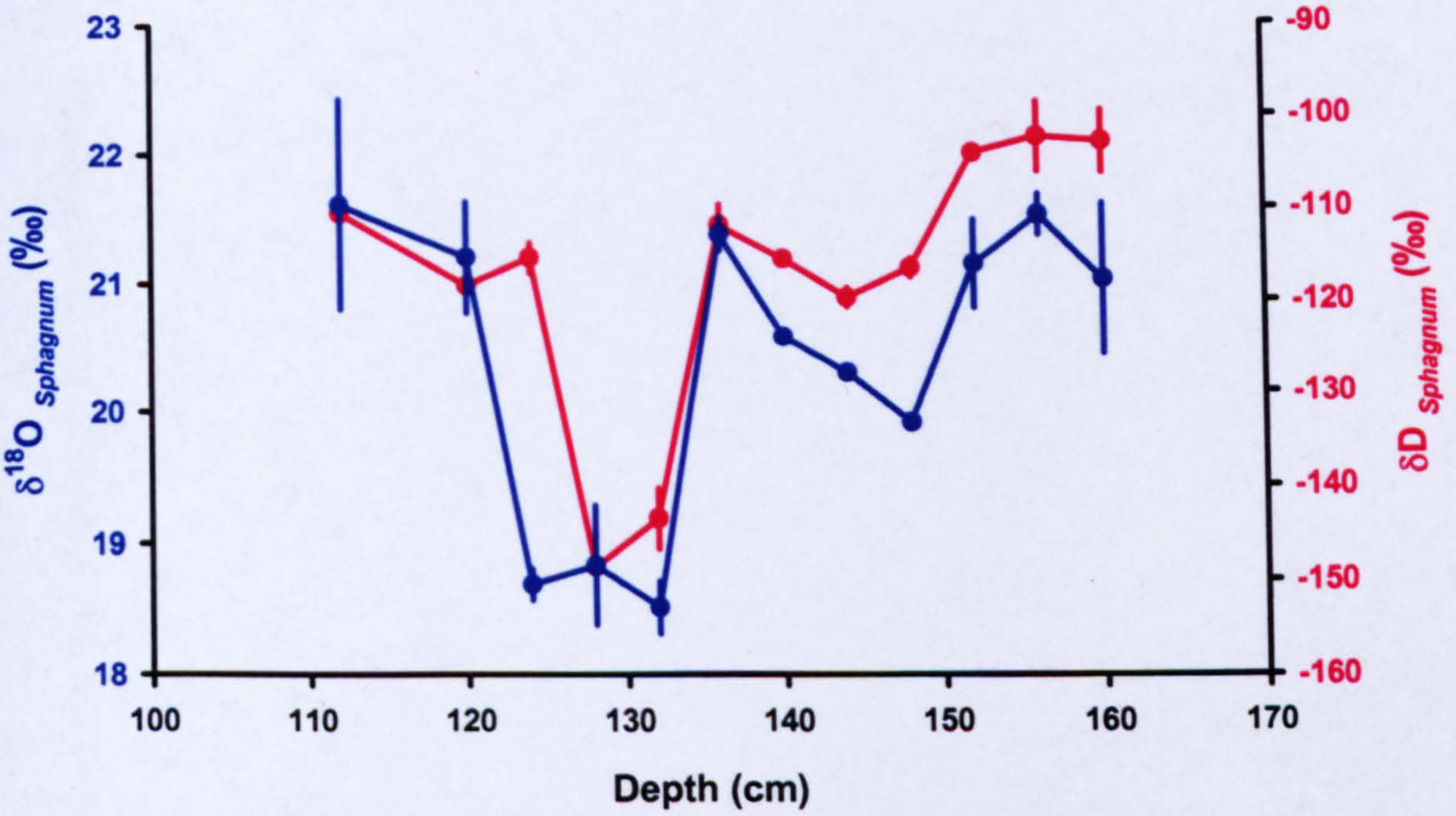

Figure 7.24 Comparison of $\delta D_{Sphagnum}$ values (red line) and $\delta^{18}O_{Sphagnum}$ values (blue line) from WLM22 (160 – 110 cm; ~1580 – 1090 BP)

The strength of the agreement between the two isotope signals is further demonstrated by a bi-plot of these data in Figure 7.25. The linear regression of these data (slope = 9.88, $r^2 = 0.60$) and the 95% confidence limits are also presented. The slope angle is slightly steeper than that of modern precipitation at Walton Moss (8.11), which is equal to the GMWL (Figure 7.5). With only twelve data, however, the correspondence between the modern MWL for Walton Moss and the slope of the palaeodata is impressive and suggests that in northern England, over this short period at least (~500 years, 1580-1090 BP), the source water for cellulose synthesis undergoes little fractionation from meteoric waters prior to assimilation and subsequent cellulose synthesis.

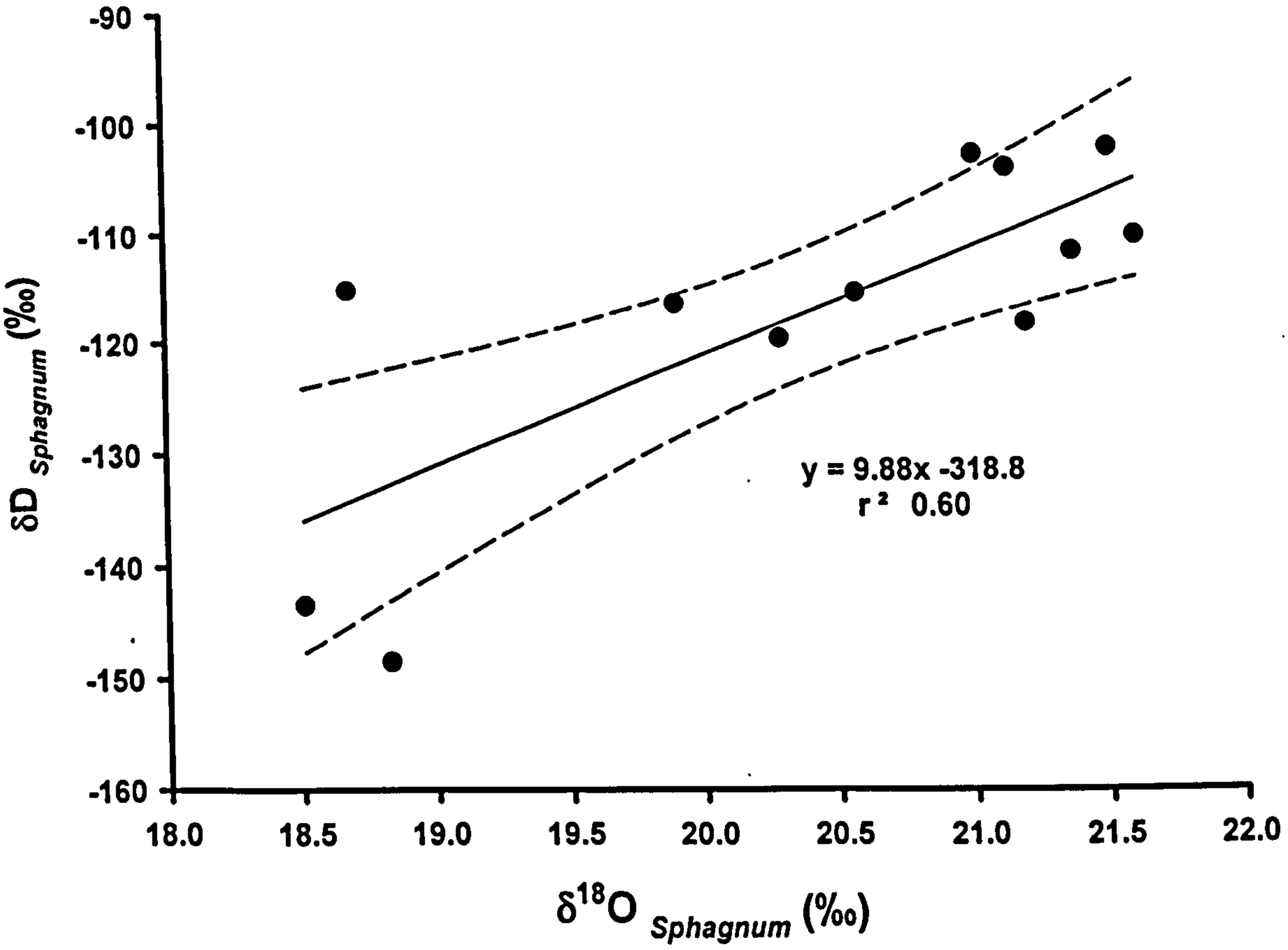

Figure 7.25 WLM22 δD - $\delta^{18}O$ palaeo-cellulose bi-plot; linear regression (solid line) and 95% confidence limits (dashed lines) are shown

7.3.3 DSM3 $\delta^{18}O_{Sphagnum}$ record

$\delta^{18}O_{Sphagnum}$ values for DSM3 are presented against depth in Figure 7.26 and as a time-series in Figure 7.27. Error bars represent the 2σ range on duplicate sample measurements. Unlike the record from WLM22, there is a general trend towards increasing $\delta^{18}O_{Sphagnum}$ values through time. In similar fashion to WLM22, the record is limited to the upper *Sphagnum* peat of the core where the abundance of material was sufficient to allow isotopic analysis.

The record displays a cyclical behaviour of highs and lows sequenced approximately every 1000 years. Early in the record there is a steady decrease in $\delta^{18}O_{Sphagnum}$ values of 2.8‰ over ~350 years to an isotopic minimum at 2600 BP prior to a more rapid rise in $\delta^{18}O_{Sphagnum}$

values to 21.5‰ over 200 years. There follows a noisy period of relatively enriched $\delta^{18}O_{Sphagnum}$ values prior to a fall of 3.4‰ over ~70 years which begins ~1700 BP. The isotopic minimum occurs at ~1630 BP. A subsequent longer term (~700 yrs) trend towards increasing $\delta^{18}O_{Sphagnum}$ values is interrupted by a single sample minimum at 192 cm (~1520 BP) and an isotopic excursion to lighter $\delta^{18}O_{Sphagnum}$ values beginning ~1480 BP with a minimum at ~1370 BP. $\delta^{18}O_{Sphagnum}$ values remain relatively enriched from ~1200 BP to ~870 BP prior to an isotopic decline of 1.4‰ over ~70 years. In the peat layers above this depth the isotopic variability becomes very high which may relate to the influence of physical disturbance of surface layers by human activity. The data suggest that the isotopic minima observed at ~2600 BP and ~1630 BP are relatively equal in magnitude although the excursion at ~1630 BP is more rapid. The lowest $\delta^{18}O_{Sphagnum}$ values are recorded during these two climatic anomalies. The total range in isotopic variation for the record is 5.2‰.

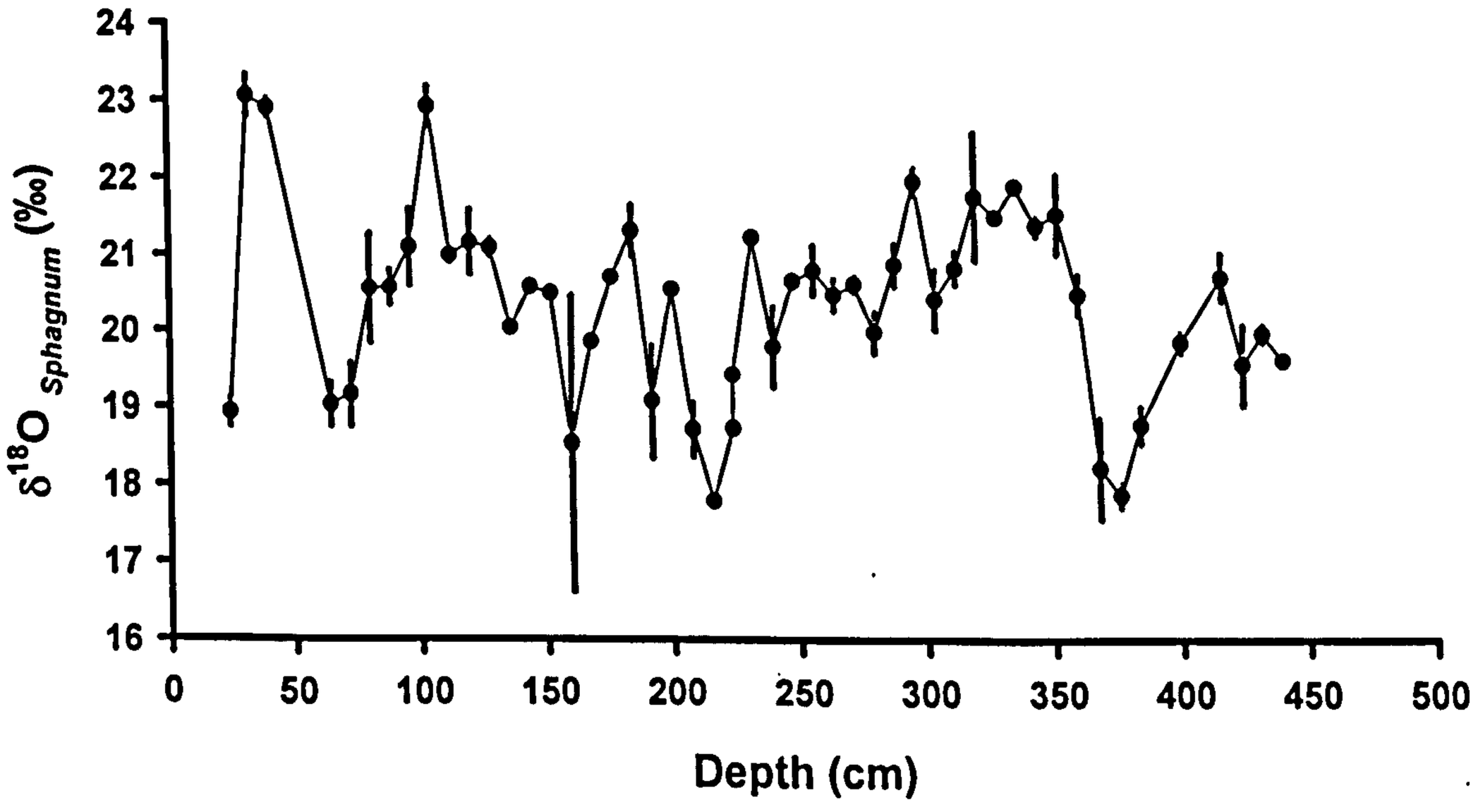

Figure 7.26 DSM3 $\delta^{18}O_{Sphagnum}$ record

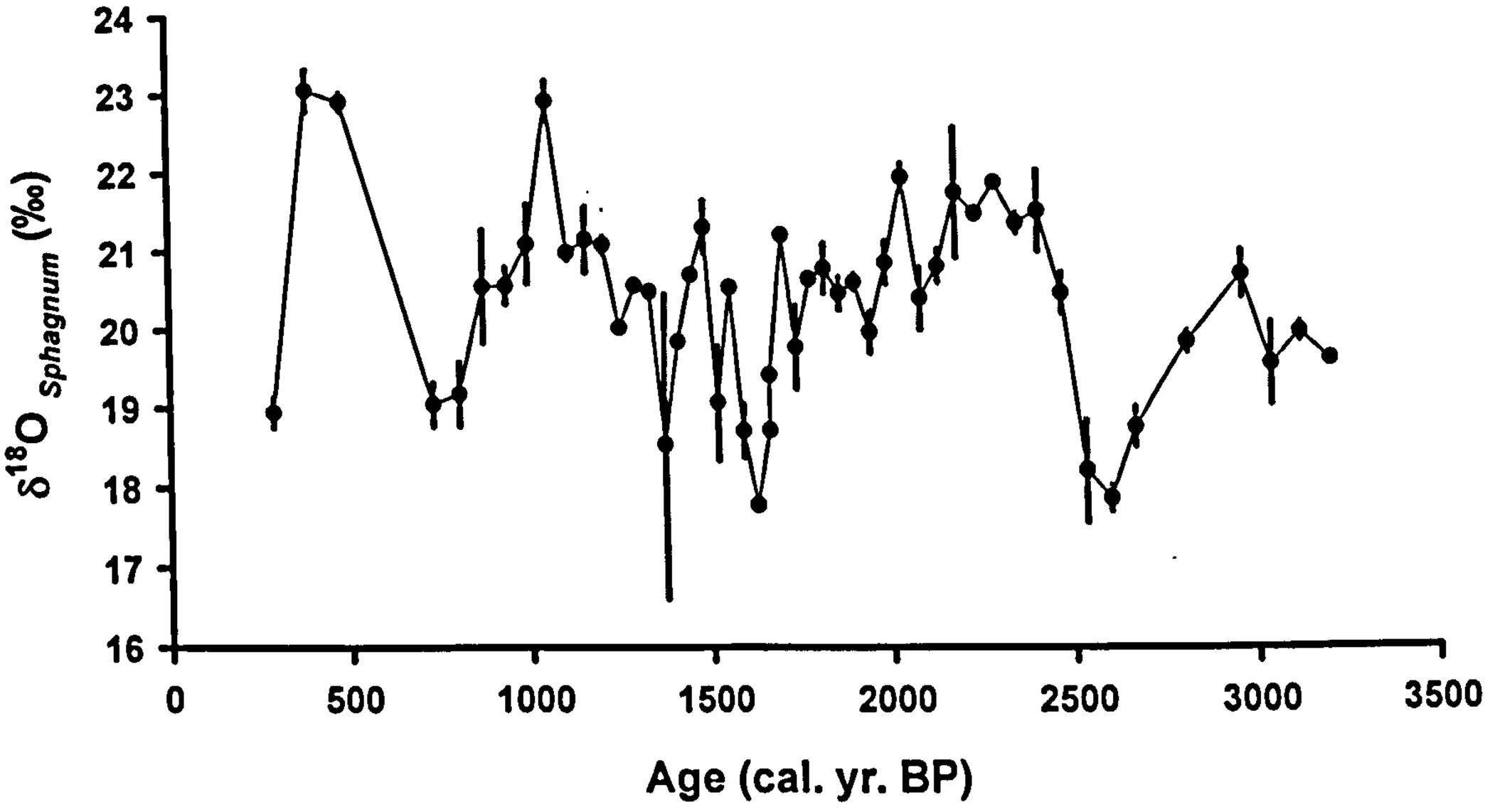

Figure 7.27 DSM3 $\delta^{18}O_{Sphagnum}$ timeseries

7.3.4 RHM2 $\delta^{18}O_{Sphagnum}$ record

$\delta^{18}O_{Sphagnum}$ values for core RHM2 from Raheenmore bog are presented against depth in Figure 7.28 and as a timeseries in Figure 7.29. Error bars represent the 2σ range on duplicate sample measurements. The record from Raheenmore is visibly different from those of Walton Moss and Dosenmoor by virtue of its length. The maximum sampled depth was 1104cm which corresponds to an age of ~ 9900 yr BP. The upper 664 cm are characterised by relatively continuous *Sphagnum* peat. Below 664 cm, the record is restricted to occasional data from isolated levels containing *Sphagnum* remains in sufficient quantities to allow isotopic analysis.

The two sections of core divided by this *Sphagnum* threshold exhibit very different patterns of variability. The lower section is highly variable with $\delta^{18}O_{Sphagnum}$ values predominantly more enriched than the mid- to late Holocene average and sharp single- sample excursions noted at

1056 and 944 cm (~9300 and ~7950 BP). Relatively depleted $\delta^{18}O_{Sphagnum}$ values are also observed at 880 and 830 cm corresponding to ~7200 and 6950 BP.

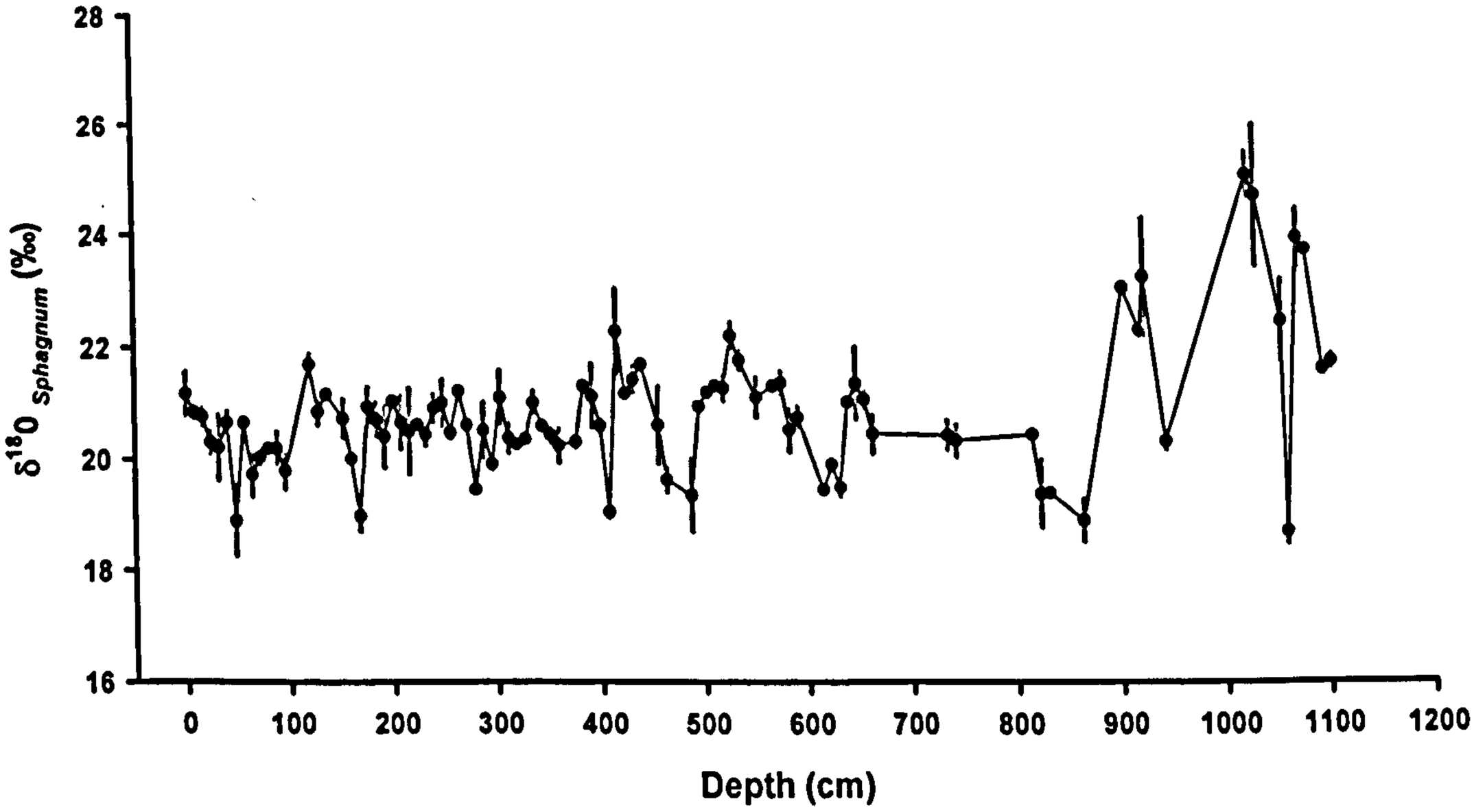

Figure 7.28 RHM2 $\delta^{18}O_{Sphagnum}$ record

In the upper sections of the core (664 cm – surface), a near-continuous presence of abundant *Sphagnum* remains affords the construction of a ~5700 year time-series of oxygen isotopic variability from this site (see expansion, Figure 7.29). The majority of the data oscillate within ± 1‰ of the 664-0 cm mean of 20.6‰.

There are several exceptions to this pattern throughout the length of the record and similar to the findings at Walton Moss, most of the larger excursions are towards depleted $\delta^{18}O_{Sphagnum}$ values. A 1.9‰ shift to lighter $\delta^{18}O_{Sphagnum}$ values is observed at 640 cm (~5400 BP) that is estimated to have lasted approximately 300 years followed by a steady rise in $\delta^{18}O_{Sphagnum}$ values to peak at 528 cm (~4400 BP). A subsequent decline of 2.9‰ in $\delta^{18}O_{Sphagnum}$ values is observed from 528 cm to a minimum at 488 cm which is estimated to have taken ~400 years. The minimum centred between 488 cm and 464 cm (~4000 to 3800 BP) is followed by a rise of 2.1‰ which is estimated to have occurred over approximately 250 years. The largest fall in the record occurs between 416 cm and 408 cm where $\delta^{18}O_{Sphagnum}$ values fall by 3.3‰.

Timeseries data suggest that this isotopic decline occurred after ~3300 BP and was completed in ~75 years. This abrupt excursion is followed by a similarly abrupt recovery to begin a period of noisy but relatively stable $\delta^{18}O_{Sphagnum}$ values between 400 to 170 cm (corresponding to ~3000 BP and ~1000 BP). This stable period is noticeably interrupted by a short phase of lower $\delta^{18}O_{Sphagnum}$ values between 304 and 272 cm (~2100 and ~1900 BP). The majority of values through this section fall close to the mean. A rapid depletion of $\delta^{18}O_{Sphagnum}$ values occurs after 170cm (~900 BP). A fall of 1.9‰ is estimated to have occurred over ~70 years, followed by a more gradual rise to enriched $\delta^{18}O_{Sphagnum}$ values at 120 cm (~460 BP). Relatively low $\delta^{18}O_{Sphagnum}$ values are observed between 120 and 56 cm (~300 to 120 BP) prior to a trend for isotopic enrichment in the upper levels of the record (~120 BP through to the present day). The total range of isotopic variation in the record over the mid- to late Holocene period, for comparison with the other European sites, is 3.5‰. This is the smallest range of the three European sites in this study.

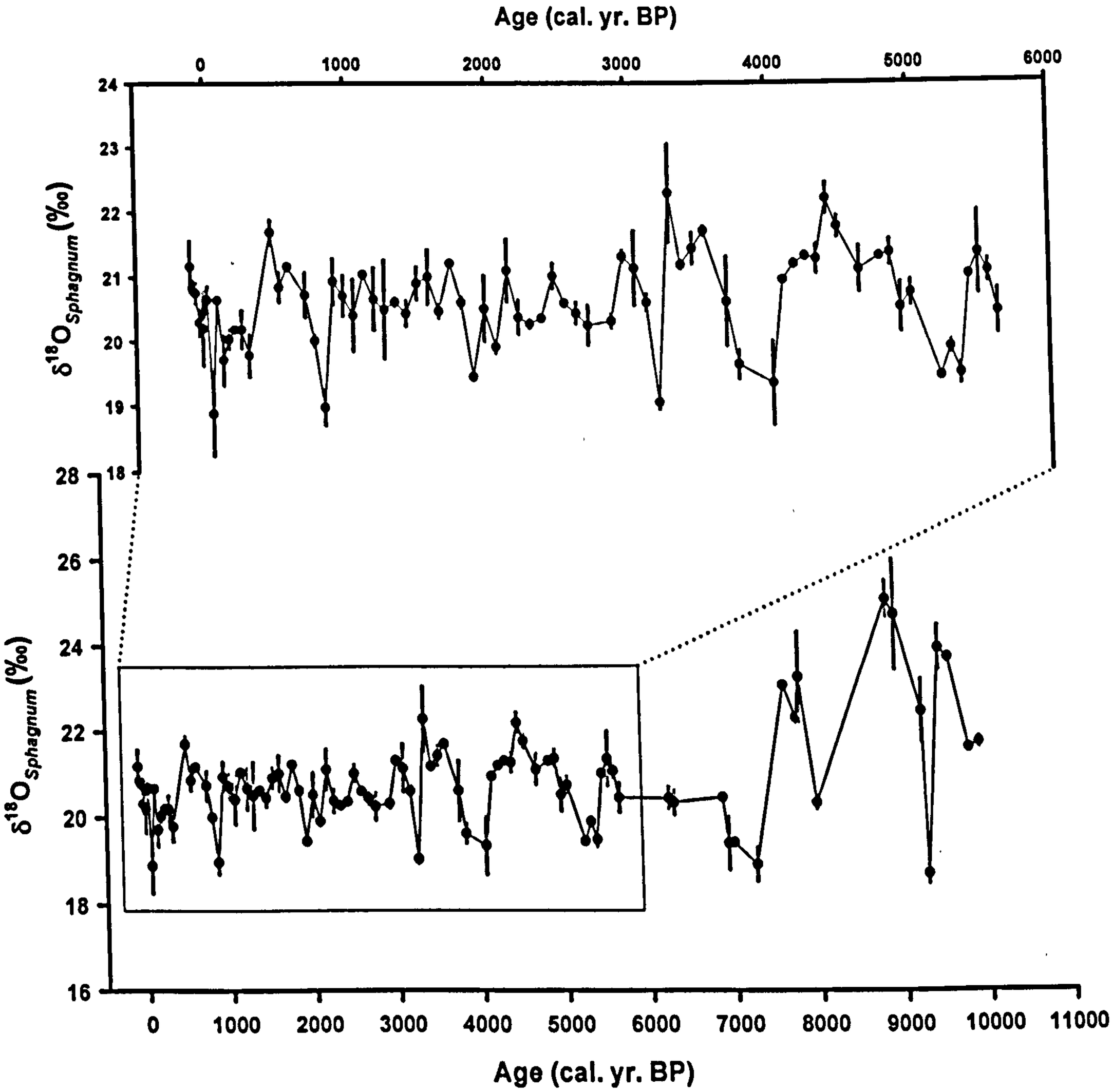

Figure 7.29 RHM2 $\delta^{18}O_{Sphagnum}$ time-series

7.3.5 NDN02/1 $\delta^{18}O_{Sphagnum}$ record

Oxygen isotopic analyses were undertaken on core NDN02/1 from Nordans Pond Bog, Newfoundland at a stratigraphical resolution of 8 cm throughout the full length of the core. Higher resolution (4 cm) analyses were undertaken across 600- 636 cm and contiguous 1 cm samples, providing sub-decadal temporal resolution, were undertaken over the section 636 – 649 cm (8300 - 8400 BP), following discovery of a high magnitude isotopic anomaly in this stratigraphical range. Results of these analyses are presented in Figure 7.30 against depth and

as a timeseries in Figure 7.31. Error bars are the 2σ range on duplicate analyses. Core NDN02/1 was dissimilar to the other NW European cores in this study in so far as *Sphagnum* was persistent throughout much of its depth and there is little evidence for the bipartite assemblage division observed in NW European cores (Hughes *et al.*, 2006). Despite this more consistent presence, small gaps are observed in the oxygen isotopic record where remains were insufficient for isotopic analysis.

Following an abrupt isotopic decrease in the base of the record, $\delta^{18}O_{Sphagnum}$ values exhibit an overall trend towards lightening of isotopic values through time. Enriched cellulose isotopic values (~22‰ ± 1‰), similar to the mean value in the base of the record are observed from 576 cm through to 336 cm (~7000 - 4000 yr BP). Lower average values of $\delta^{18}O_{Sphagnum}$, with considerable superimposed centennial-scale variability, are registered from 256 cm (~3000 yr BP) to the surface. Separating these two isotopic periods is a phase of higher variability that begins after 336 cm (~4100 BP) and comprises a steep fall in $\delta^{18}O_{Sphagnum}$ values from 22.4‰ to 19.0‰ between 320 and 308 cm (3830 - 3630 BP). The steep fall is followed by a short sustained period of light $\delta^{18}O_{Sphagnum}$ values prior to a relatively gradual recovery.

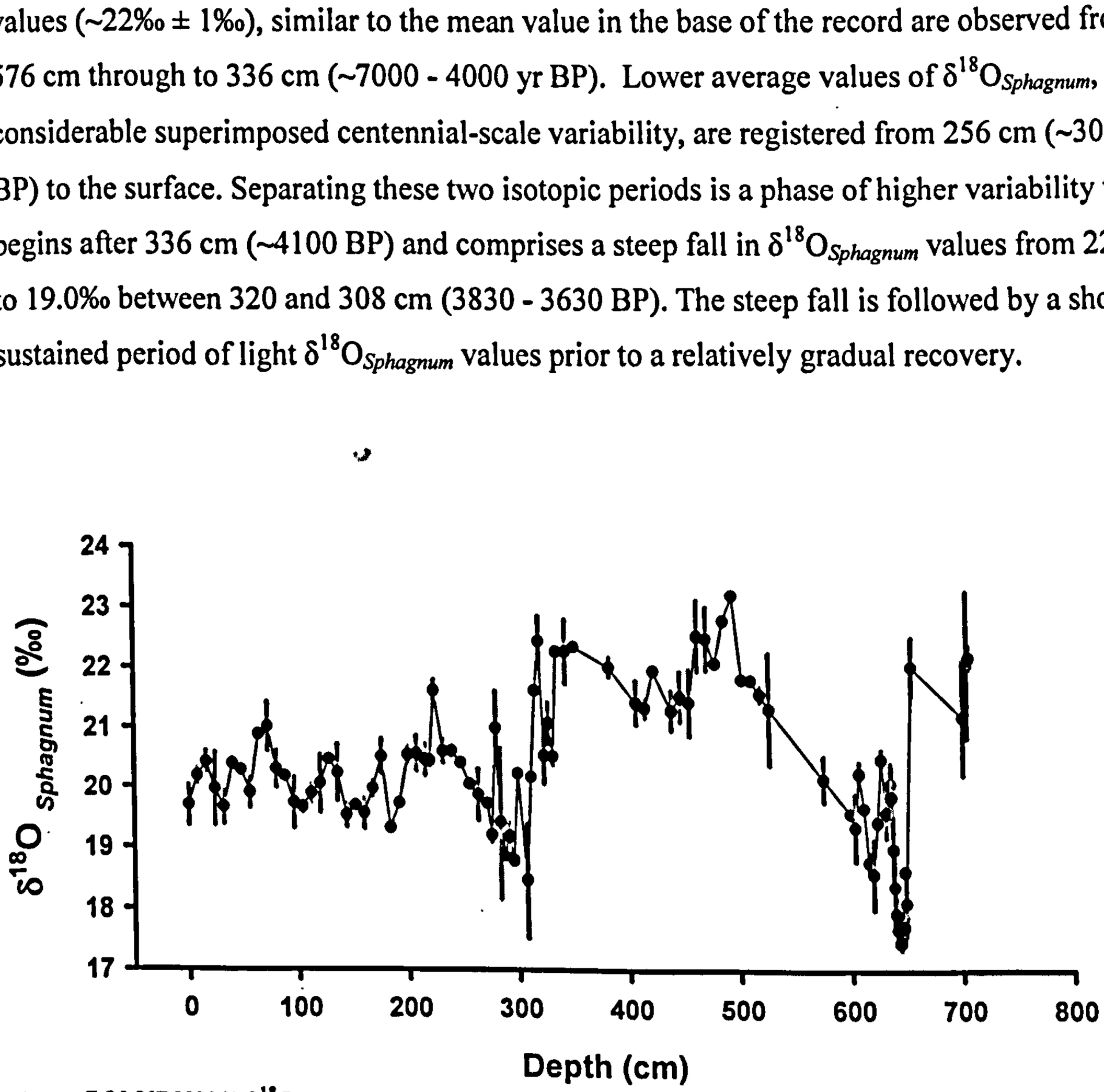

Figure 7.30 NDN02/1 $\delta^{18}O_{Sphagnum}$ record

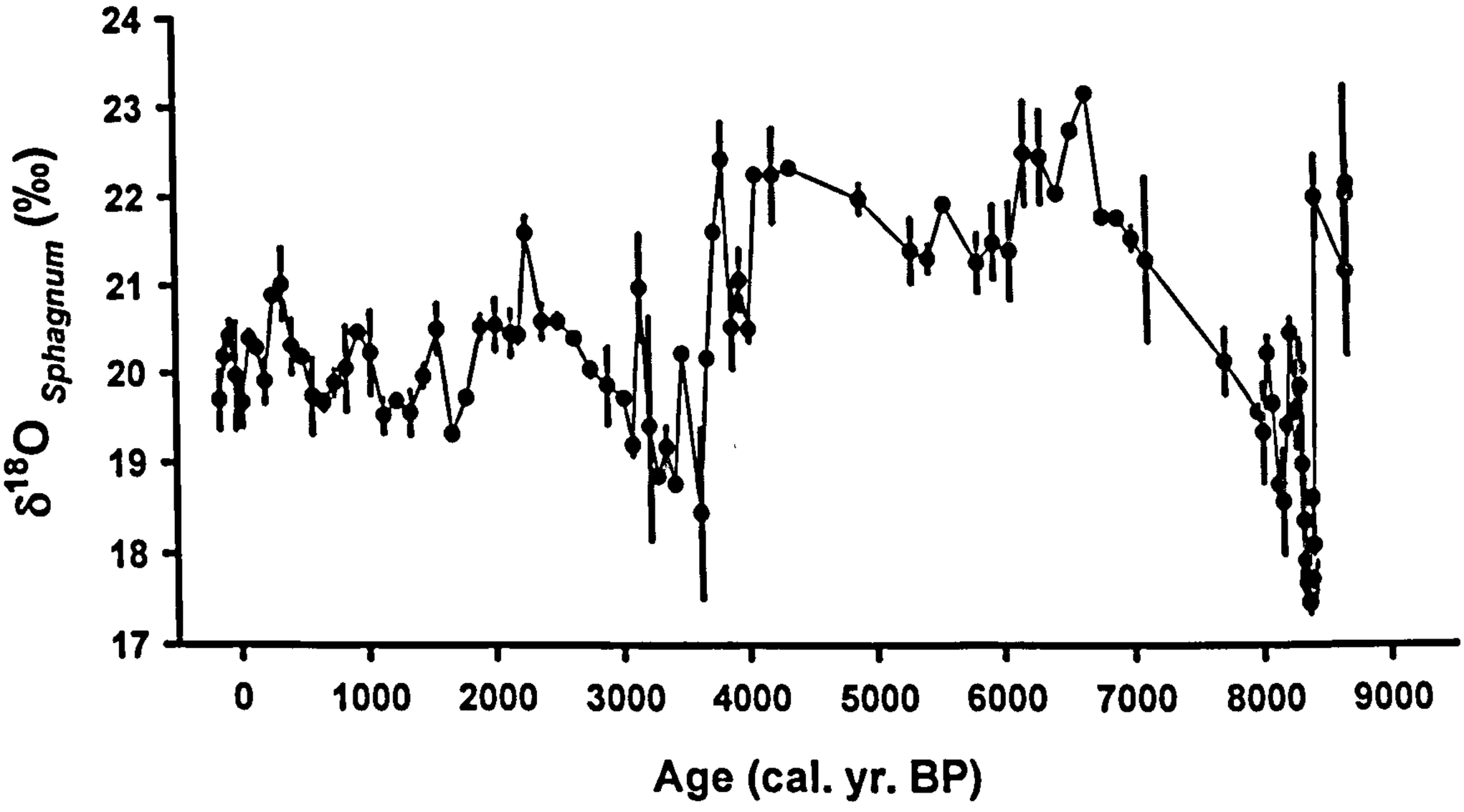

Figure 7.31 NDN02/1 $\delta^{18}O_{Sphagnum}$ time-series

Closer examination of the large negative excursion in $\delta^{18}O_{Sphagnum}$ values during the early Holocene reveals a two phase climatic deterioration (Figure 7.32). A primary isotopic decline beginning at 649 cm (~8450 yr BP) is followed by a smaller negative excursion at 628cm (~200 yr later). From higher than modern values before 8450 ± 90 yr BP, $\delta^{18}O_{Sphagnum}$ values fall abruptly by 3‰ in ≤ 55 yr. The isotopic minimum is centred on 8350 yr BP, representing a total decrease of 4.63‰ in ~100 yr. The duration of the primary event is ~150 yr. A rapid recovery to $\delta^{18}O_{Sphagnum}$ values similar to the average for the last 4000 yr precede a secondary negative excursion with an amplitude of just under 2‰, beginning ~8250 yr BP and culminating ~8170 yr BP. Recovery to values similar to the mid- to late Holocene average is complete by ~8060 yr BP, giving a total duration for the secondary isotopic excursion of ~200 yr.

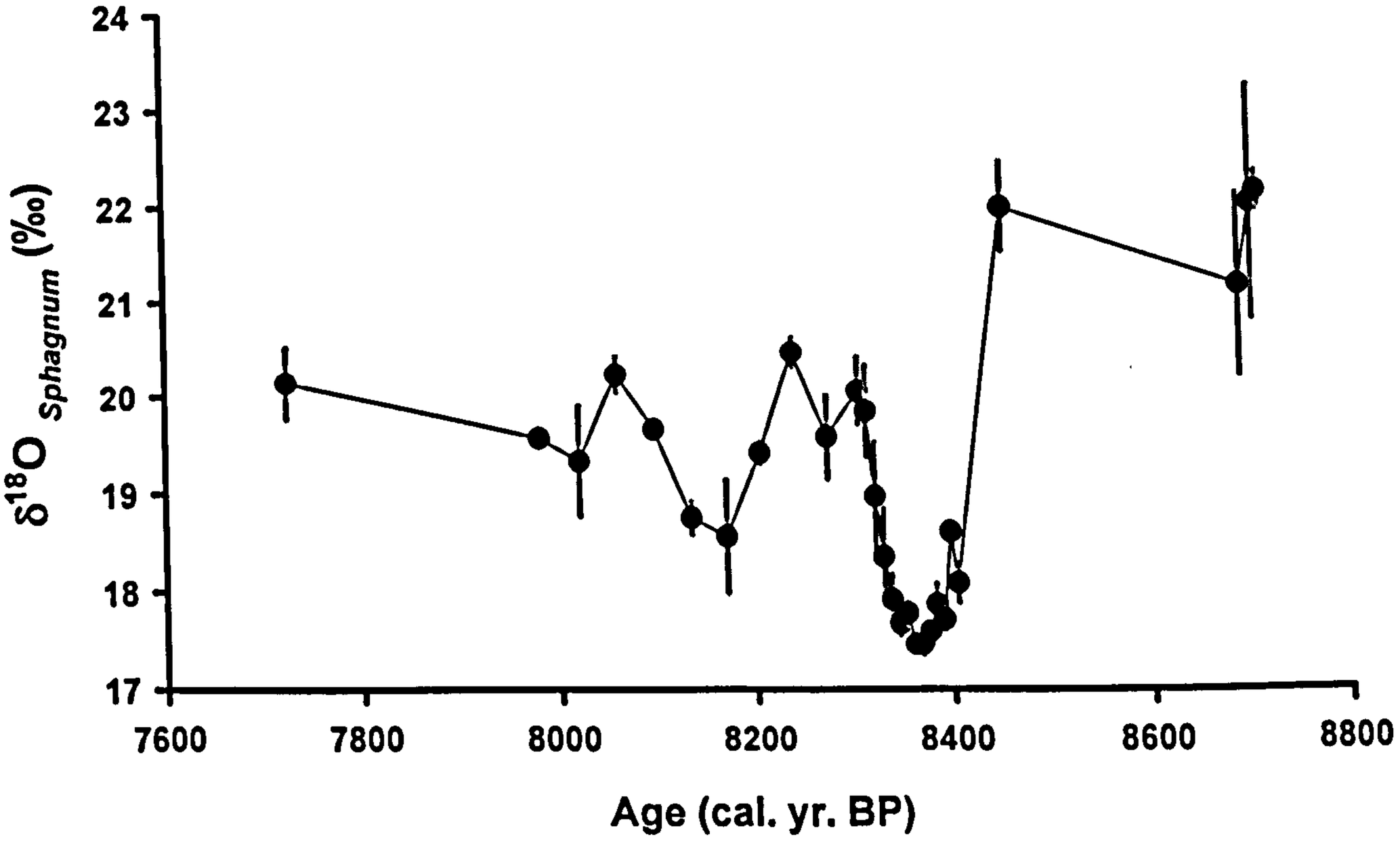

Figure 7.32 NDN02/1 $\delta^{18}O_{Sphagnum}$ time-series (8750 – 7720 BP)

7.3.6 NDN02/1 $\delta D_{Sphagnum}$ record

$\delta D_{Sphagnum}$ values for core NDN02/1 from Nordans Pond Bog are presented against depth (Figure 7.33) and as a time-series (Figure 7.34) using the age-depth model from Chapter 5. Grey bars represent the 2σ range on repeat sample measurements. Groups of four adjacent samples from the oxygen record were selected every ~1000 years for hydrogen analysis to allow the best possible estimate of variation between the two proxies over the length of the record with the number of analyses available. Sampling resolution was increased to equal that of oxygen through 576 - 708 cm in order to characterise the early Holocene isotopic anomaly with detail. With the equilibration procedure, measurement error was limited to ~5‰. With the exception of the early Holocene event, $\delta D_{Sphagnum}$ values show variation centred on ~120‰ ± 10‰ with no general increasing or decreasing trend. Although sample resolution increases substantially through the early Holocene event, the values found during this section of the core exceed the range of variability found throughout the rest of the record.

Closer examination of $\delta D_{Sphagnum}$ values through the early-Holocene event (Figure 7.35) reveals high variability in values at the base of the record that is within the range of variability found higher up in the core. At ~8450 BP, $\delta D_{Sphagnum}$ values fall ~15‰ in ≤ 55 years, stabilise for ~40 years then drop a further ~22‰ in approximately 10 years to an isotopic minimum ~8350 BP. The subsequent recovery is very rapid (~30‰ in ~20 years) and is followed by a second isotopic excursion of lower magnitude with a minimum centred on ~8250 BP. Following this second minimum, $\delta D_{Sphagnum}$ values recover to 130‰ ± 5‰ for the next 200 years.

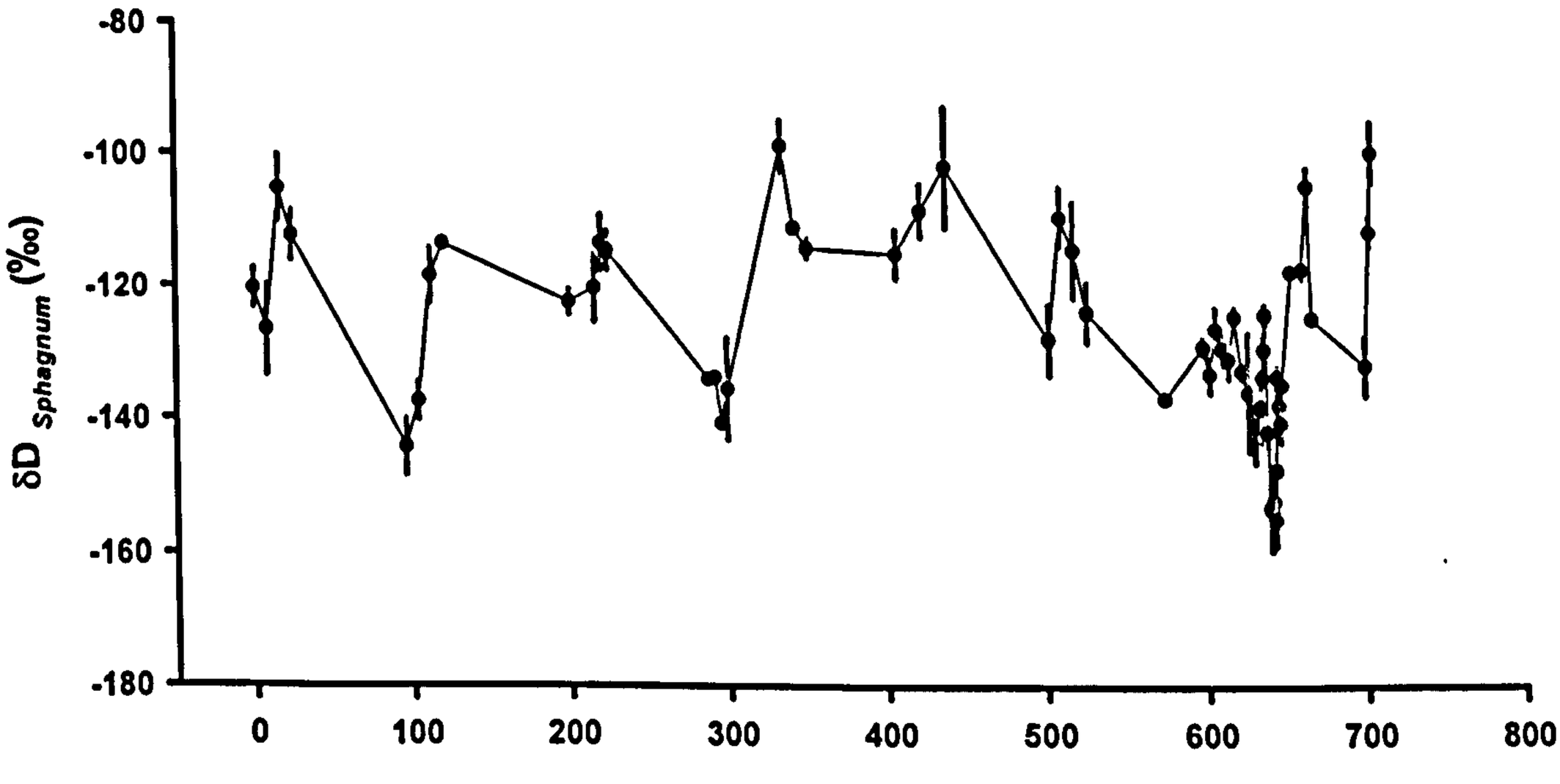

Figure 7.33 NDN02/1 $\delta D_{Sphagnum}$ record

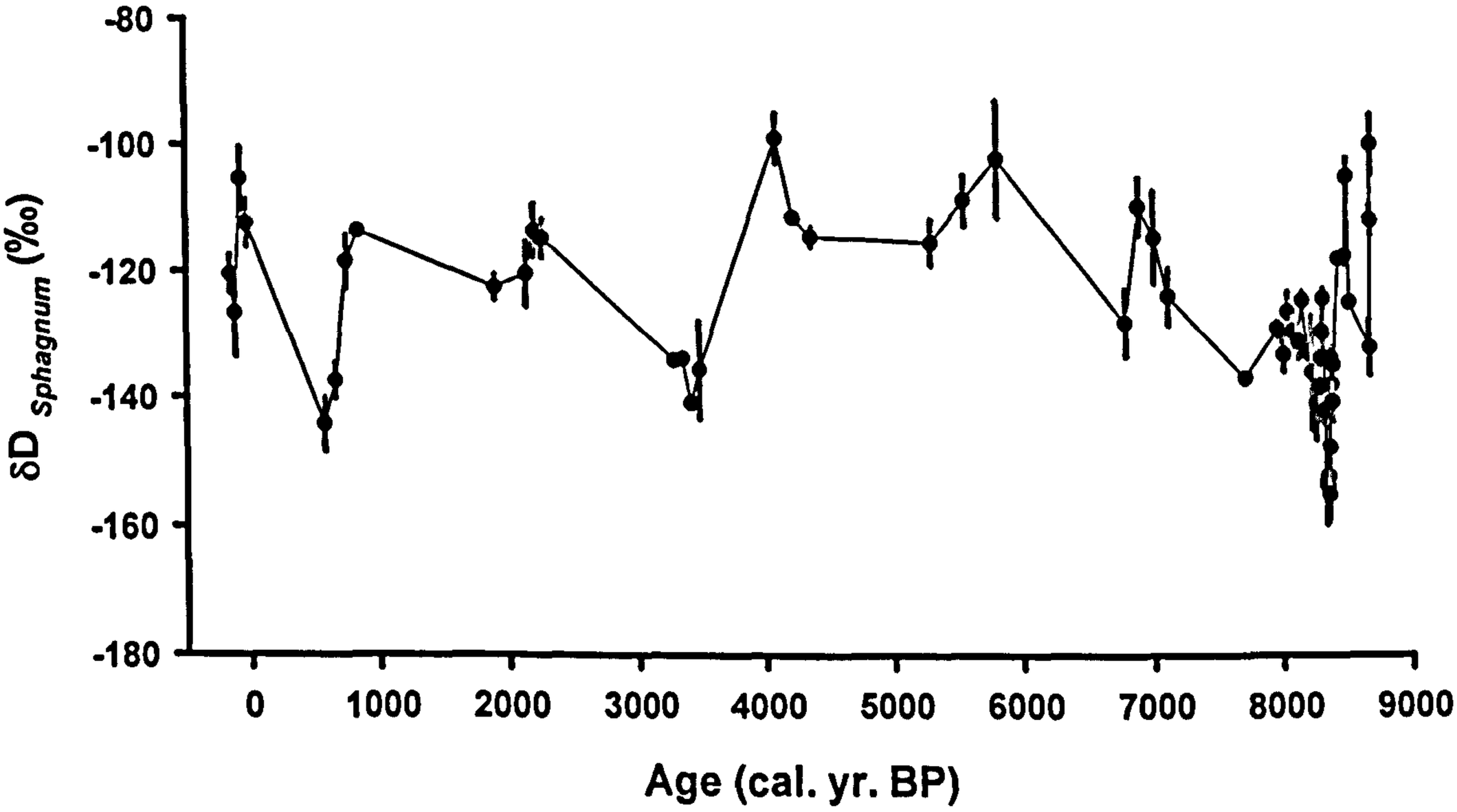

Figure 7.34 NDN02/1 $\delta D_{Sphagnum}$ time-series

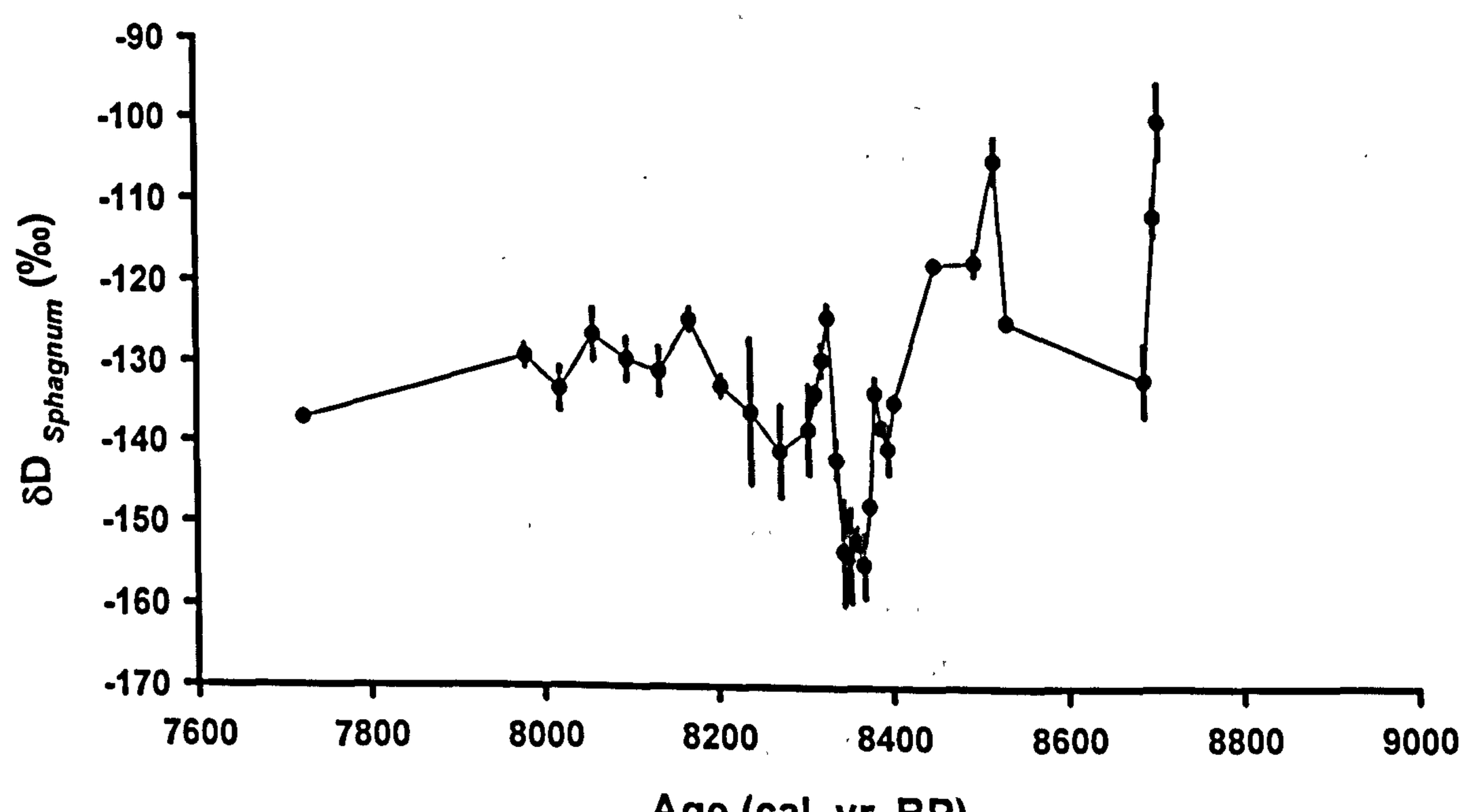

Figure 7.35 NDN02/1 $\delta D_{Sphagnum}$ time-series (8750 – 7720 BP)

Results of oxygen and hydrogen isotope analyses of NDN02/1 are overlaid in Figure 7.36. Good correspondence between the two isotopic records is observed. Both datasets show relatively enriched values at the base of the record, a strong isotopic depletion with a minimum at 644 cm, enriched and generally rising values between 576 cm and 336 cm, and a fall to depleted values centred on 300 cm rising to more enriched values between 200 and 224 cm. Least correspondence between the two records is observed in the upper section of the core. Between 120 and 100 cm $\delta^{18}O_{Sphagnum}$ values show a relatively low magnitude isotopic decline. This corresponds to a large decline in the $\delta D_{Sphagnum}$ data. In the top four samples from depths 0, 8, 16 and 24 cm, $\delta D_{Sphagnum}$ values again show higher variability than the equivalent $\delta^{18}O_{Sphagnum}$ values for these levels.

Expansion of the section covering the early-Holocene isotopic event (Figure 7.37) reveals both strong similarities and significant differences between the records from the two isotopes. Whilst both records show evidence of dual stage decline within the primary isotopic event, much of the decline to depleted values in $\delta^{18}O_{Sphagnum}$ values occurs between samples within the first stage between 656 and 649 cm (~8450 – 8390 BP). The $\delta D_{Sphagnum}$ decline, conversely, takes place over two stages of similar magnitude. The duration of the primary event for both records is similar if the primary event is considered to be initiated from the point of inflexion in both records at 656 cm (~8450 BP). The most notable difference between the two records is in the timing of a second isotopic minimum that succeeds the primary event. In the $\delta^{18}O_{Sphagnum}$ data, this second minimum is centred on ~8150 BP, is of roughly half the magnitude of the primary event and has a duration of ~200 years. In the $\delta D_{Sphagnum}$ data, a second excursion is also observed with a similar duration and relative magnitude, but which starts immediately after the primary event with a minimum observed ~100 years earlier. During the period in which $\delta^{18}O_{Sphagnum}$ values are observed to fall, $\delta D_{Sphagnum}$ values show a general trend towards enrichment. Comparison of the two isotopic tracers therefore suggests that a high magnitude isotopic event is observed beginning ~8450 BP with a minimum centred on ~ 8350 BP and a total duration of ~150 years. The presence of a co-registered secondary minimum is less clear.

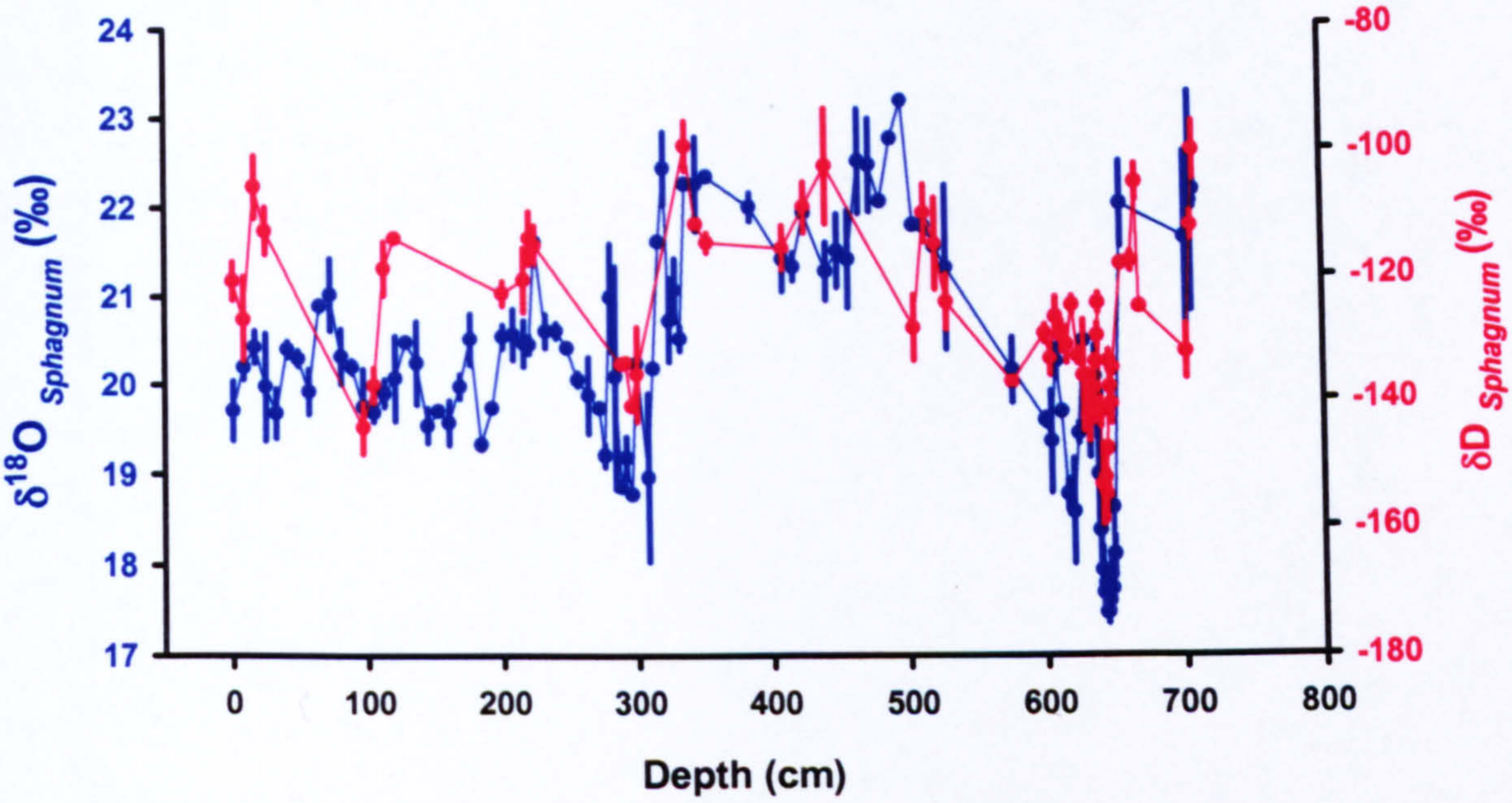

Figure 7.36 Comparison of records of δD values (red line) and $\delta^{18}O$ values (blue line) from NDN02/1

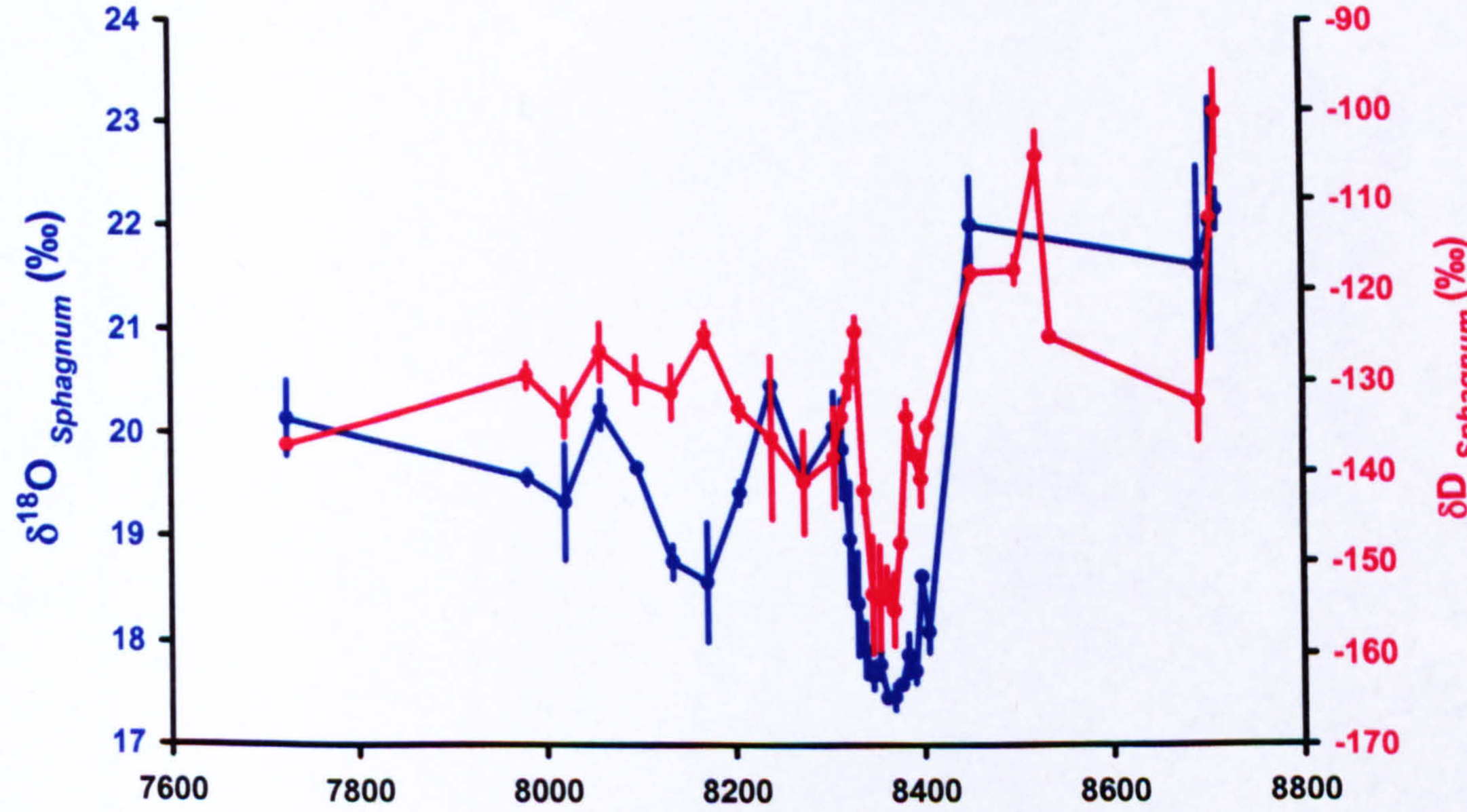

Figure 7.37 Comparison of records of δD values (red line) and $\delta^{18}O$ values (blue line) from NDN02/1 (8750 – 7720 BP)

A bi-plot of the palaeo-cellulose data from NDN02/1 is given in Figure 7.38 with a linear regression of the data (slope = 7.56, $r^2 = 0.61$) and 95% confidence limits on the slope presented. The slope of the regression in cellulose values is highly similar to the slope of regional modern precipitation (7.35) derived by amalgamating the GNIP data from Truro and Goose Bay (Chapter 3). Cellulose has the advantage over other materials used for palaeoclimate analysis such as calcite that fractionation of isotopes between water and cellulose is not believed to be temperature dependent (Sternberg *et al.*, 1986; Yakir and DeNiro, 1990) and so should be relatively constant under different climate conditions. The highly similar slope in the bi-plot of cellulose data with that of modern precipitation confirms that the source water used for cellulose synthesis undergoes little fractionation from the meteoric water that supplies the bog and also suggests that the regional MWL for the Atlantic provinces of Canada has remained relatively stable over the period spanned by the palaeo-record.

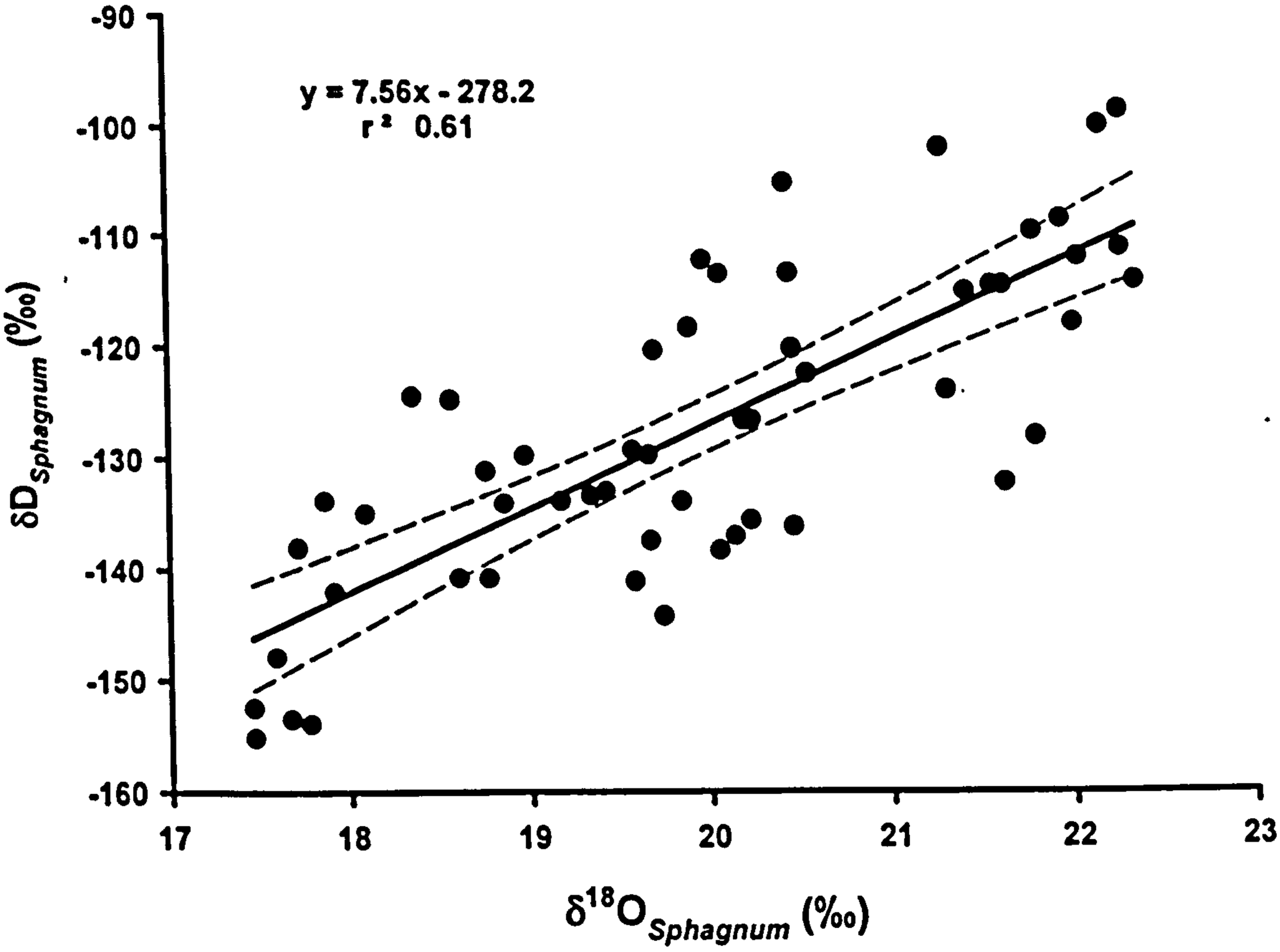

Figure 7.38 NDN02/1 palaeo-cellulose bi-plot; linear regression (solid line) and 95% confidence limits (dashed lines) are shown

8 Discussion

8.1 *Introduction*

In Chapters 1 and 2 the case was made for stable isotopic analysis of *Sphagnum* cellulose for two clear purposes. The first was the derivation of isotopic data, with a particular focus on the early-Holocene where possible, which may be used for tracking the magnitudes of climate change and hypothesis testing by data-model validation within ISOMAP-UK. The second was to derive isotopic records for use in testing the role of temperature or precipitation in forcing BSW. It was also recognised that significant investigation was required to determine exactly how the isotopic signal from precipitation is captured and archived in *Sphagnum* prior to palaeoclimatic application.

Consequently five research questions were proposed:

1) How does the isotopic composition of *Sphagnum* cellulose relate to the isotopic composition of precipitation?
2) How does variability in the isotopic composition of palaeo-*Sphagnum* cellulose relate to variation in past bog surface wetness?
3) How have spatial isotopic gradients varied in the past and what information do these provide on the mechanisms of change throughout the Holocene?
4) How have palaeotemperatures varied during key Holocene climatic changes?
5) Is temperature the primary driver of variation in BSW?

These are addressed in turn through the following sections using data presented in the previous chapters. The answer to question 5 relies on those previous. With specific reference to the raised bog system, for temperature to have played the major role in forcing the bog records recovered here, the following statements must hold true:

1) *Sphagnum* isotopic composition must relate directly to the isotopic composition of precipitation
2) BSW records must co-vary with directions and durations of change recorded in *Sphagnum* cellulose isotopic composition
3) The isotopic composition of precipitation must be driven primarily by temperature

Therefore if it can be established that variation in the stable isotope records of oxygen and hydrogen in raised bog *Sphagnum* moss primarily reflects a past temperature signal, then where isotopic records are shown to co-vary with conventional bog surface wetness records, it can be argued that temperature is driving the bog surface wetness signal over the same timescales.

As was reviewed in Chapter 2, a number of methods have been developed previously to establish the principal driver of BSW change using independent temperature reconstructions from nearby lakes (Barber and Langdon, 2007), and using instrumental comparison over relatively short timescales (Hendon and Charman, 2004; Schoning *et al.*, 2005; Charman, 2007). With both of these approaches, the accuracy of chronological control assumes high importance. In this project, similar issues with chronological control are avoided as the isotopic records which provide the link to quantitative measures of climate and temperature are derived from the same core.

In parallel with the developing discussion on the primary driver of BSW, the isotopic data are used to explore postulated mechanisms for Holocene climate change at those scales in which changes in circulation of the North Atlantic Ocean have been observed. Discussion focuses on possible mechanisms for the explanation of the strong negative isotopic excursion observed in Newfoundland beginning ~8450 BP and on possible mechanisms for the explanation of the increasing magnitude of isotopic depletion with continentality in Europe in the mid- to late Holocene.

8.2 *Validation of the climatic driver of BSW*

If the climatic driver of BSW is to be tested, it is necessary to independently determine whether the BSW records recovered here preserve a climatic signal through comparison with other BSW records from the surrounding region. Despite considerable evidence in support of the climatic determination of raised bog stratigraphy, it is accepted that there is inevitable "noise" in the record from any core. This non-climatic noise can arise from the sampling of hummock zones rather than lawn areas where plant species are relatively insensitive in response to climatic forcing (Barber *et al.*, 1998) or can arise from the influence of ecological factors other than climate such as changes in the nutrient loading of the bog surface with land clearance in the recent past (van Geel and Middeldorp, 1988) or changes in species inter-specific competition (Rydin, 1993; Mauquoy and Barber, 1999a). Some testate amoebae species are shown to respond in alternate directions to changes in water table versus changes in percentage moisture (Charman *et al.*, 2007). This multi-directional response to hydrological change produces added noise in any reconstruction.

Difficulties with chronological linking of distant records are well documented and command the resources of a separate research field in themselves. Much has been achieved in the generation of more accurate age-depth modelling through the use of tephra layer pinning points (Pilcher and Hall, 1996; Hall and Pilcher, 2002; Langdon and Barber, 2004) and wiggle-match dating of peat sediments throughout Holocene layers (Blaauw *et al.*, 2004) and lead-210 (Appleby and Oldfield, 1992; Oldfield *et al.*, 1995) dating for sediments in the last 150 years. Other workers have attempted to exploit that uncertainty to "tune" the chronologies of the records and match climatic changes across wide geographical areas (Charman *et al.*, 2006). This assumes, of course, that those chronologies require tuning and that the differences in timing do not reflect real spatial and temporal transgression of climatic events across the region.

Despite these difficulties of correlation due to both core noise and chronology, published syntheses of the dates of readily detected regional climatic changes reveal coherent age ranges against which the data here can be validated for detection of a climatic signal (Table 8.1;

Barber, 2006). To some degree, this process also allows the identification of regional versus local changes. Those that are observed regionally are interpreted as climatic. Those that are observed locally may also be climatic but are treated with caution.

Table 8.1 (Barber, 2006) reveals periods of major inferred climatic change that are replicated within chronological error across a wide area of northern Europe. Whilst the list of sites here is by no means exhaustive, it provides evidence of contemporaneous climate variation across a broad region. Not all cores pick up every change which may reflect complacency in the individual records, differences in proxy sensitivities, problems of chronological comparison or real climatic differences between the sites listed.

It is noted that the format of tabulation adopted by other workers and reproduced here, when presented on its own, gives no precise details on any dating uncertainty and lacks information on the relative magnitude of these wet shifts which would be necessary for a signal to noise assessment. In part, this arises from the lack of magnitude information from the traditional techniques such as plant macrofossil and humification analysis. The table does, however, serve as a useful device for initial comparison between sites within a region.

Nearly all sites record major climatic change at ~4600-4000 BP (Aaby, 1976; Dupont, 1986; Hughes *et al.*, 2000; Barber *et al.*, 2003; Langdon *et al.*, 2003; Langdon and Barber, 2005), ~3500-3100 BP (Aaby, 1976; Dupont, 1986; Chambers *et al.*, 1997; Hughes *et al.*, 2000; Ellis and Tallis, 2000; Barber *et al.*, 2003; Langdon *et al.*, 2003; Barber *et al.*, 2004; Blundell and Barber, 2005; Langdon and Barber, 2005) and ~2900- 2500 BP (van Geel *et al.*, 1996; Chambers *et al.*, 1997; van Geel and Renssen, 1998; Ellis and Tallis, 2000; Barber *et al.*, 2003; Langdon *et al.*, 2003; Barber *et al.*, 2004; Blundell and Barber, 2005; Langdon and Barber, 2005). The next most well represented change is recorded regionally at ~1500-1350 BP in all tabulated sites with the exception of Mongan bog (Barber *et al.*, 2003). At least one of the two phases of the Little Ice Age (LIA) is detected in most published studies (Barber, 2006).

The ranges of these broad periods are superimposed as shaded bars on the BSW records from each of the European sites in this study in Figure 8.1. All three sites show increases in BSW

inferred as climatic deterioration within the broad periods 3500-3100 BP and 1500-1350 BP. At least two of the three time-series provide evidence for climatic deterioration within the zones 4600-4000 BP, 2900-2500 BP and across the LIA period.

Table 8.1 Climatic fluctuation dates for European raised and blanket peat proxy data. Adapted from Barber (2006). For full references see Barber et al. (2004). All ages are given in calendar years before present (BP) and represent the onset of a shift in proxy-records towards increased BSW.

Abbeyknockmoy	Co. Galway, Ireland	Barber *et al.* (2003)		700	1050	1400	1750		2200	2750	3150	4000
Mongan Bog	Co. Offaly, Ireland	Barber *et al.* (2003)	450	600 850			1600 1800		2250 2350	2450 2750	3200	
Kentra Moss	western Scotland	Ellis and Talllis (2000)	330	600 880	1150	1400			2150	2550	3250	
Tore Hill Moss	north central Scotland	Blundell and Barber (2005)	310	860	1250	1380 1520			2010	2510		
Temple Hill Moss	southeast Scotland	Langdon *et al.* (2003)	250			1450				2800	3400 3850	4500
Seven Scottish bogs		Langdon and Barber (2005)	250- 150	600- 400	1050- 850	1450- 1350	1800- 1650	2000	2600- 2200	2900- 2700	3500- 3200	4450- 4150
Talla Moss	Borders, Scotland	Chambers *et al.* (1997)	540		1100		1700	1930	2270	2600	3460	
Border Mires	northern England	Mauquoy and Barber (1999a;1999b)	180 550	850	1030	1400	1740	1980	2130	2540 2710		
Bolton Fell Moss	Cumbria, England	Barber (1981), Barber *et al.* (1994; 2003)	210 500	620 720	1000	1400			2200	2350 2440 2580	3020 3200 3600	4020 4280 4420
Walton Moss	Cumbria, England	Hughes *et al.* (2000)	100 350			1450	1750		2320- 2040	2900	3750 3170- 2860 3500	4620 4410- 3990
British and Irish blanket bogs		Blackford and Chambers (1991; 1995)	490		1150	1310 1330		1910				
Engbertsdijksveen	The Netherlands	Van Geel (1978), Van Geel *et al.* (1996)								2850 2750- 2450	3020 3750	4350
Bourtangerveen	The Netherlands	Dupont (1984)						1950			3650- 3300	4450
Draved Mose	Jutland, Denmark	Aaby (1976)	450	660 860		1500	1700		2250		3000 3400	4000 4300 4600
Dosenmoor	northern Germany	Barber *et al.* (2004)		600		1400		1950		2750- 2600	3350	
Svanemose	Denmark	Barber *et al.* (2004)		700	1080	1350	1800	1950		2650	3500	

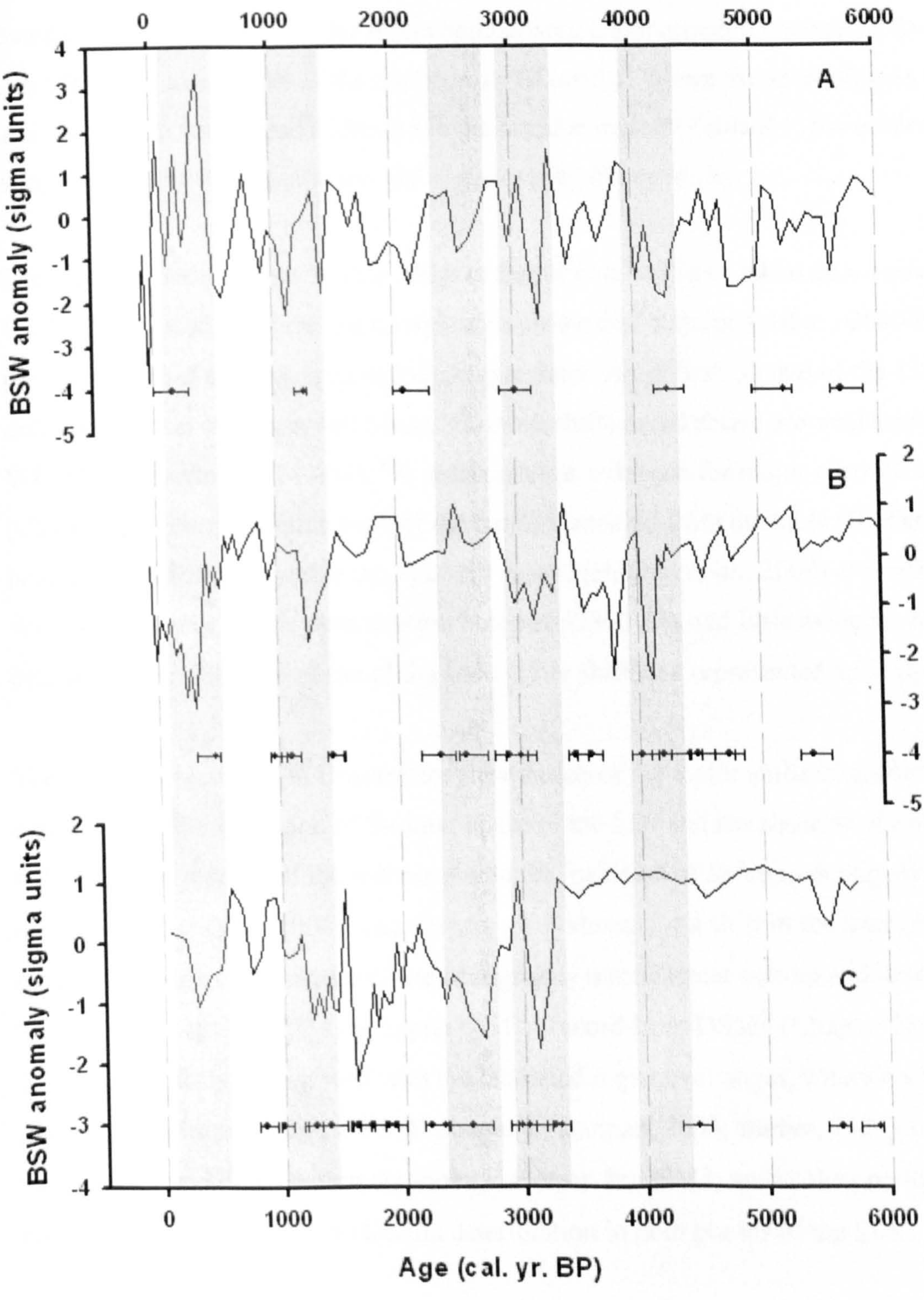

Figure 8.1 Comparison of BSW records from the three NW European raised bog sites investigated in this project: A) Raheenmore B) Walton Moss C) Dosenmoor. Dating control points and calibrated ranges (from ^{14}C 2σ error) are shown beneath each record. Grey bars represent periods of regionally identified wet shifts (Barber, 2006).

It is fortunate that two of the four sites analysed for this project have replicate cores that are listed in Table 8.1 and allow for direct comparison. Comparison with records from the same site allows for assessment of the replicability of results. Where the same signals are replicated and correspond with signals detected in the broader region (Table 8.1) the evidence for allogenic forcing is strengthened and suggests climatic causality.

The tabulated record from Walton Moss is that of core WLM11 taken 20 metres NW of WLM22 (this study). There is a conspicuous absence of a major shift at ~2800 BP and only the later phase of the LIA is recorded, despite detection of both phases of the LIA only 2 miles north-west at Bolton Fell Moss. All other shifts noted above are well represented. Core WLM22, supported by 24 AMS ^{14}C dates exhibits evidence for major climatic changes (Chapter 6) occurring within each of the bands identified from the table (Barber, 2006). Notable absences observed in the WLM11 record (Hughes *et al.*, 2000) are replicated in WLM22 with no climatic deterioration noted at ~2800 BP, and little evidence for a major deterioration in the early phase of the LIA. Other shifts are represented strongly.

The tabulated record from Dosenmoor shows each of the major shifts identified above are detected with the exception of the later phase of the LIA and the absence of a shift earlier than 4000 BP. The absence of the latter is due to the initiation of *Sphagnum* bog after this event at this site (Barber *et al.*, 2004). The absence of evidence for a shift in the later phase of the LIA may well relate to disturbance of the stratigraphy through peat cutting and drainage (Chapter 3), as is noted in core DSM3 (Chapter 6). The record from DSM3 (Chapter 6), supported by 21 AMS ^{14}C dates, agrees well with the tabulated regional changes, where each of the climatic deteriorations noted in Table 8.1 (Barber and Charman, 2003; Barber, 2006) are replicated in the record from DSM3 within chronological error. In DSM3, unlike the previously published record, evidence exists for a climatic deterioration in both phases of the LIA.

Palaeoecological study of the stratigraphy of Raheenmore is very limited. Two nearby bogs, however, provide inferred palaeo-climatic records with which the data from RHM2 can be compared. Major climatic changes at Abbeyknockmoy bog (95 km from Raheenmore) and Mongan bog (40 km from Raheenmore) are reported in Table 8.1. Detection of a major climatic change is observed from the stratigraphy of Abbeyknockmoy at each of the dates

noted above, with the exception of the later phase of the LIA. Mongan bog, on the other hand, records most of the changes with the exception of that at ~1400 BP and any change prior to 4000 BP. Both phases of the LIA are detected at Mongan bog. The record from Raheenmore, supported by 13 AMS ^{14}C dating control points, reveals evidence of climatic change at ~4250 BP and ~3200 BP in agreement with the records from Abbeyknockmoy and Mongan bog (Chapter 6). The record from RHM2 then becomes relatively stable. Despite this relative stability, minor oscillations are detected at similar times to those of the regional shifts at ~2250 BP and ~1400 BP. Photographs taken for isotopic sub-sample preparation reveal the dominance of broad-leaved *Sphagnum* moss through much of this section of core. The dominance of a single-species should act to increase the accuracy of the humification analyses on which the comparison is based through minimisation of the influence of species change on the humification signal (Caseldine *et al.*, 2000; Yeloff and Mauquoy, 2006). The relative stability is therefore likely to represent real climatic variation rather than a decrease in the sensitivity of this record. The general agreement in timing of the fluctuations observed in core RHM2 to those tabulated records suggests that the record is detecting broader-scale climatic change.

Although there are limitations to the comparison offered by the tabulated format, the close correspondence of the data generated for this project with that from widely varying regions of northern Europe indicates externally driven variation in the bog proxy reconstructions. This is most likely climatic. Traditionally, further inference has been restricted from BSW records at this stage due to chronological constraints and/or the limited interpretive power of the magnitudes of change from the semi-quantitative techniques applied. There may however, be real differences in timing and or magnitude and in some cases direction that could provide new insight into the drivers of climatic change. Potential differences in timing, within chronological limitations, and magnitude are discussed in the context of isotopic data from these cores later in this chapter (section 8.6).

8.3 *BSW-isotopic variability comparison*

If the principal driver of variability in the stable isotopic composition of precipitation is temperature, and if that variability is incorporated with little distortion in the cellulose of *Sphagnum* moss, then if temperature is driving the BSW record over long timescales, variability in *Sphagnum* isotopic values should co-vary with BSW values. Comparison of the inferred curve of BSW change for each of the European sites (Chapter 6) in this project with $\delta^{18}O_{Sphagnum}$ records from the same stratigraphical levels (Chapter 7) (Figure 8.2) reveals strong correspondence at two sites and lower correspondence at the Irish site. Visual assessment suggests strong correlation is observed for both Walton Moss (A) and Dosenmoor (B) with markedly reduced correlation at Raheenmore. Statistical analysis using Pearson Product Moment Correlation (PMCC) reveals strong positive correlation is observed in the records from Walton Moss (PMCC = 0.723) (A). Good positive correlation is observed in the records from Dosenmoor (PMCC = 0.386) (B). Low positive correlation is observed for Raheenmore (PMCC = 0.186) (C). PPMC is favoured in this instance for its flexibility in returning the correlation between two variables that are measured on different scales. It is of note that variations in correlation are not due to chronology as records are taken from the same core.

Despite the differences in statistical point-for-point correlation, from visual assessment, much of the major structure in the BSW reconstructions from both Walton Moss and Dosenmoor is replicated in the oxygen isotopic stratigraphy. Whilst variation in the isotopes is represented on a linear scale, the BSW reconstructions provide evidence of direction of change. Magnitudes of change must be interpreted with caution, as has been discussed previously. Noise will be pervasive throughout both records. In the calculation of PPMC coefficients, the directions of change from point-to point are required to be similar to yield a highly positive outcome. Therefore, variation due to noise will inevitably be incorporated into the assessment of correlation. If the proportion of low magnitude variations due to noise is relatively high compared to the proportion of higher magnitude shifts and the correlation in the noisy sections is low, this will influence the final value for correlation. This potentially explains why visual correlation appears better than PMCC values.

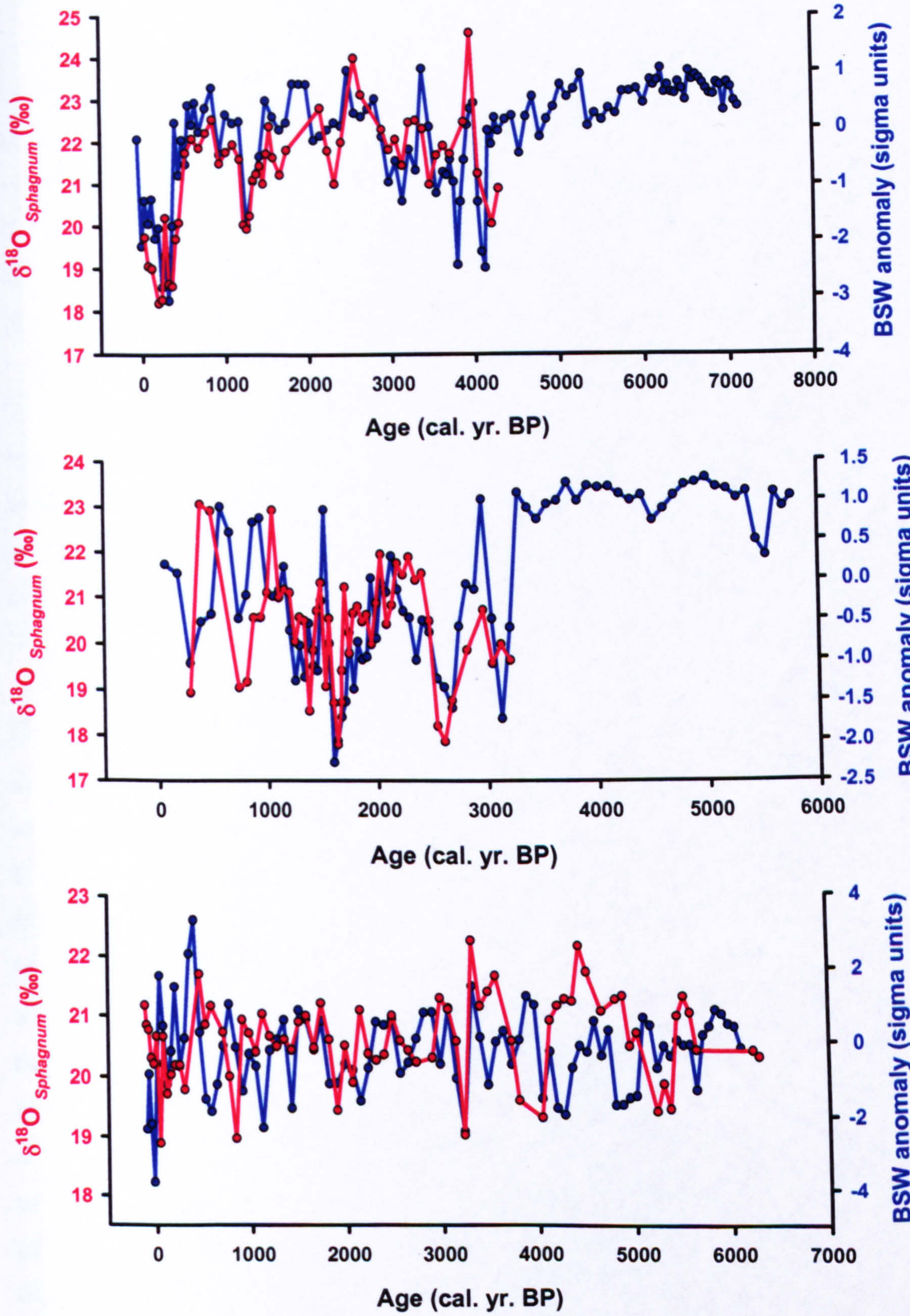

Figure 8.2 Comparison of BSW records (blue lines) and $\delta^{18}O_{Sphagnum}$ values (red lines) from A) Walton Moss B) Dosenmoor C) Raheenmore

Correlation may also relate to the number of proxies used to derive the BSW signal. Multi-proxy palaeoecological investigation has been demonstrated to enhance the surface wetness signal (Blundell and Barber, 2005). It is interesting to note that the core on which the most proxies have been used shows the best correlation. At Dosenmoor, the BSW signal is reconstructed using two proxies and at Raheenmore, only humification data are presented. The visibly close relationship observed for Walton Moss and Dosenmoor suggests variation in the BSW records is replicated closely by variation in the oxygen isotopic composition of *Sphagnum* cellulose, suggesting a common driver exists.

The reduced correlation both visually and statistically between BSW and bog isotopes at Raheenmore suggests either that alternate drivers are influencing the respective signals or that increased non-climatic noise is prevalent in the BSW reconstruction due to the use of only one proxy. The data reveal periods when the variation is in phase and periods when the data are out of phase. Three sections are identified where variation between the records is in phase: 3300 – 3060 BP, 2140 – 1820 BP and 300 – 80 BP.

Between 3300 – 3060 BP, the records show a sharp shift towards increased BSW and more depleted $\delta^{18}O$ values respectively. Reference to Figure 8.1 reveals that this shift is replicated in all three cores from this study and many cores across the northern European region (Table 8.1), within the errors inherent in the respective chronologies. The sharp, 3.3‰ shift to lighter $\delta^{18}O_{Sphagnum}$ values contemporaneous with this widespread climatic fluctuation suggests that the driver of isotopic variation during this period was also the driver of climatic change across a wide area of northern Europe. The section of in-phase variation between 2140 – 1820 BP is defined by a period of variable but generally increased BSW and variable but lighter $\delta^{18}O_{Sphagnum}$ values. Similar variation is found in Abbeyknockmoy and Mongan bog (Barber *et al.*, 2003) throughout the same period. Whilst the magnitude of the increase in BSW is relatively subdued at Raheenmore, the isotopic depletion registered in the core and correspondence with inference of regional climatic deterioration suggests a common allogenic driver. The section of in-phase variation between 300 – 80 BP is shown to coincide, within the constraints of chronological error, with the period associated with the LIA. Indeed, both

records show evidence for simultaneous BSW increase and lightening of $\delta^{18}O$ values as the two curves enter in-phase variation.

The absence of *Sphagnum* in sections where relatively dry BSW conditions are inferred may promote a misleading lack of correlation that is simply an artefact of sample resolution. Samples at 472 cm (~3870 BP) and 480 cm (~3950 BP) are absent from the isotopic record due to the absence or insufficient presence of *Sphagnum* remains in these levels. In the BSW record, these samples are represented by values indicative of relatively dry bog surface conditions. If a positive correlation exists between BSW and oxygen isotopic values, enriched values would be predicted for these levels had the data been obtainable. Consequently, the absence of data and the graph display style selected suggest that a period of depleted values persisted across this period. The data do not allow this assumption to be made. If it is accepted that the section in which an anti-phase relationship is most obviously represented may be a misleading representation of sample resolution, many of the discrepancies that are detected visually can be evaluated as discrepancies arising from large differences in the magnitudes of change between the two curves and the sensitivities of the techniques used to derive them. Whilst the data cannot confirm that there is a consistent commonality of driver of both BSW and isotopic variation at Raheenmore, they do confirm that at certain periods, which correspond to periods of regional deterioration in climate, BSW and $\delta^{18}O_{Sphagnum}$ values vary in phase.

Previous $\delta^{18}O$ studies on peat have used mixtures of species, some using vascular plants (Brenninkmeijer *et al.*, 1982; Dupont and Brenninkmeijer, 1984; Dupont and Mook, 1987; Aucour *et al.*, 1996). These previous studies concluded that much of the observed isotopic variability was caused by changes in the relative proportions of species that comprised the peat matrix. In the data presented here, the bulk source sample plant composition has been shown to have little effect on the magnitudes of change recorded in *Sphagnum* concentrates (Chapter 4). Instead, *Sphagnum* concentrates have been demonstrated to approximate *Sphagnum*-specific oxygen isotopic variability (Chapter 4). Results from Chapter 7 on the modern isotopic composition of *Sphagnum* moss through seasonal monitoring periods revealed that contrary to a number of studies in which data were collected in either a single summer season or summer day (Brenninkmeijer *et al.*, 1982; Aravena and Warner, 1992) but

in agreement with a more recent study (Ménot-Combes *et al.*, 2002) there is no consistent difference between species mean isotopic composition throughout the growing season (section 7.2.3). Therefore, the variation observed in the core *Sphagnum* cellulose isotopic values presented here is independent of variation in the relative proportions of *Sphagnum* species and is not related to the abundance of vascular material in the core source sample. By elimination, control on the palaeo-cellulose signal must be derived from the isotopic composition of the water used for cellulose synthesis. It can be concluded that the palaeo-*Sphagnum* cellulose signal reflects the isotopic composition of the source water used in cellulose synthesis and that for at least two of the European sites and significant periods in the record from the third, there is a common driver of that source water signal and BSW over centennial timescales.

8.4 *What drives the isotopic signal in cellulose?*

It has been demonstrated that the isotopic composition of source water is the primary control on core $\delta^{18}O_{Sphagnum}$ values derived from *Sphagnum* concentrates (section 8.3 above). This source water is the moss leaf water. Fundamental, however, to understanding the signal in palaeo-*Sphagnum* cellulose is establishing how this leaf water relates to meteoric water. Once water is precipitated onto the bog surface, leaf water can arise from either direct input by precipitation or through mixing with the bog water reservoir. Its composition can therefore either, 1) follow precipitation directly, 2) reflect evaporative enrichment of water received directly by precipitation or 3) reflect a mix of precipitation and bog water which may be subject to evaporation. If evaporation of leaf water significantly alters the isotopic composition, this will be reflected in the cellulose, weaken the link to palaeo-precipitation and cloud any relationship between meteoric waters and temperature in this region.

The character of the leaf water composition can be tested using a deterministic model that allows prediction of source water from cellulose values. Several models have been developed that relate cellulose isotopic composition to that of the source water and a series of thermo- and fluid dynamic properties that quantify the potential for fractionation (Chapter 2) (Yapp and Epstein, 1982a; Buhay *et al.*, 1996; Roden *et al.*, 2000; Pendall *et al.*, 2001; Waterhouse

et al., 2002; Anderson *et al.*, 2002; Zanazzi and Mora, 2005). Most are based on Craig and Gordon's (1965) model for steady-state evaporation from a closed reservoir and have been adapted to account for the complexity of processes occurring during cellulose synthesis in vascular plants (Dongmann *et al.*, 1974; Roden *et al.*, 2000; Waterhouse *et al.*, 2002). Whilst these adaptations have lead to variations between the models, the general terms of each can be summarised in the form below (Equation 4; section 2.3.2):

Equation 4) $\delta cell = \delta sw + \varepsilon b + (\varepsilon e + \varepsilon k)(1-h)$

where δ_{cell} = the isotopic composition of cellulose,

δ_{sw} = the isotopic composition of the source water,

ε_b = the biochemical enrichment factor,

ε_e = the liquid vapour equilibrium enrichment factor,

ε_k = the liquid –vapour kinetic enrichment factor due to evaporation,

h = relative humidity (value from 0 to 1).

This can be simplified as $\varepsilon_b + (\varepsilon_e + \varepsilon_k)(1-h) = \Delta$ = net biochemical enrichment factor so that

Equation 11) $\delta_{cell} = \delta_{sw} + \Delta$

The simpler physiological water use strategy of mosses and lack of vascular tissues and functioning guard cells means that the mosses are unable to control water loss through transpiration regulation. Consequently, *Sphagnum* inhabits moist environments where the relative humidity is close to 100% (Vitt *et al.*, 1975; Clymo and Hayward, 1982). Zanazzi & Mora (2005) demonstrate that the model can be simplified to account for this habitation of moist environments where h is close to 1, leaving the residual expression:

$\Delta = \varepsilon_b$,

Therefore,

Equation 12) $\delta_{cell} = \delta_{sw} + \varepsilon_b$

ε_b has been determined by experimental and observational measurements as 27 ± 3 ‰ for oxygen (Epstein *et al.*, 1977; Deniro and Epstein, 1981; Wolfe *et al.*, 2001). The enrichment is produced during the hydration of carbonyl groups that takes place during the biosynthesis of carbohydrates (Yakir and DeNiro, 1990). It is understood to be insensitive to temperature (Sternberg and DeNiro, 1983; Wolfe *et al.*, 2001).

Therefore the approach here is to assume relative humidity in the atmospheric boundary layer directly above the moss leaves is ~100% (h = 1) and predict ε_b using cellulose data and by substituting bog water (δ_{bw}) and precipitation ($\delta_{precipitation}$) values for the isotopic composition of the source water (δ_{sw}) respectively.

$$\delta_{cell} - \delta_{sw} = \varepsilon_b$$

$\delta_{cell} - \delta_{sw}$ should equal 27 ± 3 ‰ if the source water $\delta^{18}O$ values approximate the leaf water $\delta^{18}O$ values used in cellulose synthesis. It is fair to make this assumption as it has been shown that h = 1 in the atmospheric layers directly above bog moss (Vitt *et al.*, 1975; Brenninkmeijer, 1983) and because *Sphagnum* has been demonstrated to suspend photosynthesis in the absence of sufficient moisture, i.e. under conditions when the evaporative signature would be reflected most strongly (Williams, 1996). The analysis also relies on the occurrence of *Sphagnum* growth contemporaneous with the period of water sampling. Results in Chapter 7 indicated significant differences between monthly $\delta^{18}O_{Sphagnum}$ means consistent with the occurrence of such growth. Indeed, results suggested that at Raheenmore, *Sphagnum* moss growth occurred throughout the annual monitoring period implying preservation of an annual signal in the stratigraphy. The high temporal sensitivity of *Sphagnum* to variation in source water composition has been noted previously (Ménot-Combes *et al.*, 2002).

Table 8.2 shows results of annually averaged α- values for each of the species at each of the European sites. α- values allow for expression of the enrichment as a coefficient (Yapp and Epstein, 1982a) (Equation 5, below). Values greater than 1 indicate enrichment. Values less than 1 indicate depletion.

Equation 5) $$\alpha = ((\delta cellulose / 1000) + 1) / ((\delta source_{water} / 1000) + 1)$$

If fractionation from source water is entirely ε_b with little or no evaporative enrichment, $\alpha = 1.027$.

Table 8.2 Mean biochemical enrichment coefficients for species and sites

Bog Site	Species	Annual α cell-bw	σ	Annual α cell-precip	σ
Dosenmoor	*S. cuspidatum*	1.025	0.0010	1.026	0.0013
	S. papillosum	1.025	0.0009	1.026	0.0015
	S. magellanicum	1.025	0.0009	1.026	0.0015
Walton	*S. capillifolium*	1.026	0.0014	1.028	0.0011
	S. cuspidatum	1.025	0.0016	1.028	0.0015
	S. magellanicum	1.026	0.0020	1.028	0.0018
	S. papillosum	1.025	0.0016	1.028	0.0016
Raheenmore	*S. capillifolium*	1.025	0.0008	1.027	0.0015
	S. imbricatum	1.026	0.0002	1.028	0.0004
	S. papillosum	1.026	0.0004	1.027	0.0007
	S. magellanicum	1.026	0.0012	1.027	0.0018
	S. fuscum	1.027	0.0004	1.029	0.0005
All sites	**All species**	**1.0256**	**0.0004**	**1.0274**	**0.0010**

In general, α values are very similar across all species and all sites for a particular water source confirming findings from Chapter 7 that there is no statistically significant difference between the isotopic compositions of *Sphagnum* celluloses. A clear difference is observed, however, in α coefficients derived using $\delta_{sw} = \delta_{bw}$ (1.0256) compared to those using $\delta_{precipitation}$ (1.0274). Values < 1.027 indicate underestimation of the published biochemical enrichment factor associated with cellulose synthesis by the C3 photosynthetic pathway. It is evident that where δ_{bw} is used as source water, ε_b is underestimated. Where $\delta_{precipitation}$ is used as δ_{sw}, ε_b is fractionally overestimated. Both however, are within the published ± of 3 ‰ (~0.003). Underestimation can be expected if the leaf water is less enriched than the substituted source water. Overestimation results when the leaf water is more enriched than the substituted source water.

Two hypotheses can explain these observations. 1) ε_b in *Sphagnum* is ~25 ‰, leaf water composition is similar to δ_{bw} and undergoes similar evaporative evolution from meteoric waters prior to cellulose synthesis. 2) ε_b in *Sphagnum* is consistent with plants following a C3 photosynthetic pathway at 27 ± 3 ‰; source water is largely precipitation. Leaf water may undergo some slight evaporative enrichment but when this gradient is large, *Sphagnum* dries out and photosynthesis is suspended preserving a dominant meteoric source signal in *Sphagnum* cellulose. The annual data alone are not sufficient to eliminate either of these hypotheses as a value of 1.0256 is within the value of 27 ± 3 ‰, on annual average it is shown to be similar in locations across NW Europe and agrees well with other field observations (Aucour *et al.*, 1996; Wolfe *et al.*, 2001).

Monthly separation of the data, however, allows clarification of the provenance of leaf water. Monthly mean $\alpha_{cellulose\text{-}bog\ water}$ coefficients are shown in Table 8.3 and $\alpha_{cellulose\text{-}precipitation}$ values in Table 8.4. Figure 8.3 has been complied using data from all the European sites in this study. The structure of the ε_b α-values modelled using bog water as source water follows an apparent seasonal variation (Figure 8.3). Values closest to 1.027 (~27 ‰) are observed in winter months and coefficients representing $\delta^{18}O$ values 2-3 ‰ lower are observed in summer months. Given that ε_b is not temperature dependent, variation must be related to real differences in the isotopic composition of leaf water relative to that of δ_{bw}. The data indicate that δ_{bw} is considerably enriched compared to cellulose source water in the summer months and closer to leaf water in the winter months. The inference of evaporative enrichment of bog water over and above that of the source water is consistent with results in Chapter 7 which showed clear evaporative effects in the isotopic composition of bog waters from each of the sites with strongest evaporative influence in summer months. This is consistent with findings from previous studies for considerable variability and enrichment of bog surface waters during summer months (Aravena and Warner, 1992; Ménot-Combes *et al.*, 2002).

Table 8.3 Monthly mean $\alpha_{cellulose\text{-}bog\ water}$ (bw) coefficients

	Walton				Dosenmoor			Raheenmore						All sites
	S. capillifolium	*S. cuspidatum*	*S. magellanicum*	*S. papillosum*	*S. cuspidatum*	*S. papillosum*	*S. magellanicum*	*S. capillifolium*	*S. cuspidatum*	*S. fuscum*	*S. imbricatum*	*S. magellanicum*	*S. papillosum*	
Apr-04	1.0276	1.0278	1.0287	1.0278										1.0280
May-04														
Jun-04														
Jul-04	1.0263	1.0252	1.0253	1.0245										1.0253
Aug-04														
Sep-04					1.0249	1.0249	1.0246							1.0248
Oct-04	1.0248	1.0251	1.0239	1.0239										1.0244
Nov-04					1.0258	1.0265	1.0261							1.0261
Dec-04								1.0240	1.0247			1.0238	1.0259	1.0246
Jan-05					1.0262	1.0262	1.0267							1.0263
Feb-05								1.0261	1.0249	1.0271	1.0266	1.0270	1.0265	1.0264
Mar-05														
Apr-05	1.0260	1.0260	1.0267	1.0261	1.0252	1.0257	1.0254							1.0258
May-05														
Jun-05					1.0236	1.0246	1.0244	1.0252		1.0265	1.0265	1.0262	1.0258	1.0253
Jul-05	1.0240	1.0234	1.0240	1.0243				1.0259		1.0262	1.0261	1.0259	1.0257	1.0251
Aug-05					1.0262	1.0244	1.0247	1.0260		1.0269	1.0261	1.0260	1.0256	1.0257
Sep-05														
Oct-05														
Nov-05								1.0252		1.0271	1.0264	1.0270	1.0264	1.0264
Dec-05														
	1.0257	1.0255	1.0257	1.0253	1.0253	1.0254	1.0253	1.0254		1.0268	1.0263	1.0260	1.0260	1.0257

Table 8.4 Monthly mean $\alpha_{cellulose\text{-}precipitation}$ coefficients

	Walton				Dosenmoor			Raheenmore						All sites
	S. capillifolium	*S. cuspidatum*	*S. magellanicum*	*S. papillosum*	*S. cuspidatum*	*S. papillosum*	*S. magellanicum*	*S. capillifolium*	*S. cuspidatum*	*S. fuscum*	*S. imbricatum*	*S. magellanicum*	*S. papillosum*	
Apr-04	1.0289	1.0292	1.0300	1.0292										1.0293
May-04														
Jun-04														
Jul-04	1.0276	1.0265	1.0267	1.0258										1.0267
Aug-04														
Sep-04					1.0249	1.0249	1.0246							1.0248
Oct-04	1.0284	1.0288	1.0276	1.0275										1.0281
Nov-04					1.0270	1.0278	1.0274							1.0274
Dec-04								1.0244	1.0251			1.0242	1.0263	1.0250
Jan-05					1.0253	1.0253	1.0258							1.0255
Feb-05								1.0279	1.0267	1.0289	1.0284	1.0289	1.0283	1.0282
Mar-05														
Apr-05	1.0299	1.0299	1.0305	1.0299	1.0241	1.0246	1.0243							1.0276
May-05														
Jun-05					1.0272	1.0281	1.0280	1.0267		1.0280	1.0280	1.0278	1.0273	1.0276
Jul-05	1.0272	1.0266	1.0272	1.0275										1.0271
Aug-05					1.0271	1.0253	1.0257	1.0281		1.0289	1.0281	1.0281	1.0277	1.0274
Sep-05														
Oct-05														
Nov-05								1.0263		1.0282	1.0274	1.0281	1.0274	1.0275
Dec-05														
	1.0284	1.0282	1.0284	1.0280	1.0259	1.0260	1.0259	1.0267		1.0285	1.0280	1.0274	1.0274	1.0271

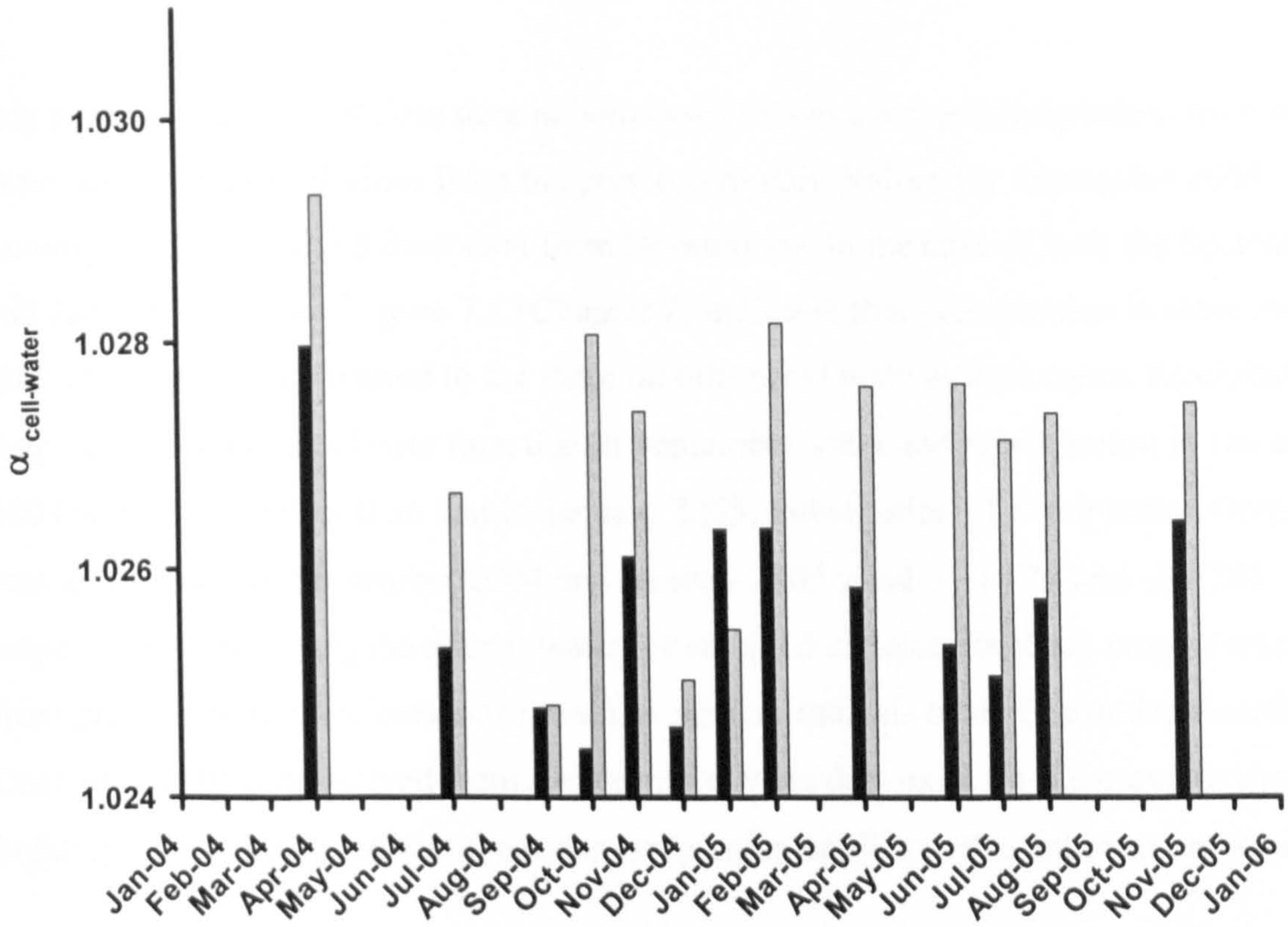

Figure 8.3 Monthly α coefficients for the three European study sites modelled using precipitation as source water (grey bars) and bog water as source water (black bars).

Prediction of ε_b using precipitation as the source water produces much more stable results, with only limited evidence for seasonal variation and a mean value of 1.0271 (~ 27 ‰) in direct agreement with the published value (Sternberg and DeNiro, 1983; Sternberg *et al.*, 1986). Evidence for minor oscillation in the same direction as that observed in ε_b prediction using δ_{bw} reflects limited fractionation due to leaf water evaporation.

Three months are identified where α-coefficients derived from $\delta_{precipitation}$ are unusually low. Where these values are low it indicates that the source water for cellulose synthesis was less enriched than the measured $\delta_{precipitation}$ waters in that month. The data represent two different sites and hence are not specific to just one site. For the January 2005 data, Figure 8.3 indicates that δ_{bw} more closely approximates ε_b. Comparison of variability in bog water, precipitation

and cellulose records (Chapter 7) reveal that the anomalous values in Figure 8.3 are due more to relative depletion in cellulose values than anomalous enrichment in measured water values.

It is possible that the cellulose data in both cases reflect average precipitation from the month previous and hence cellulose from the previous month. Values for September 2004 and January 2005 are derived from data from Dosenmoor. In the case of both the September 2004 and January 2005 data, Figure 7.1 (Chapter 7) indicates that precipitation in these months was relatively enriched compared to the three months previously in both cases. Precipitation in August 2004 was ~2‰ lower than that in September 2004 and precipitation in December 2004 was ~1.5‰ lower than that in January 2005. Substitution of precipitation from the previous month for September 2004 and January 2005 yield α ~1.027 and ~1.0265 respectively, suggesting the source water for sampled cellulose in these months was derived from precipitation in the previous month. A similar analysis cannot be undertaken for the December 2005 data derived from Raheenmore as no data exist for the previous month. It is highly possible, however, that the same explanation applies to the Raheenmore data.

The results from Figure 8.3 support hypothesis 2) that $\delta_{precipitation}$ approximates δ_{sw} more closely than δ_{bw}. Where anomalous deviation is observed from an alpha value of ~1.027, the discrepancy can be explained by the cellulose reflecting precipitation from the previous month. These data therefore support the assertion that variation in the *Sphagnum* cellulose isotopic signal approximates variation in $\delta_{precipitation}$ values.

Although the data are too few (n = 5) to describe a significant relationship, indications as to the validity of this assertion are given with the regression of Walton Moss modern cellulose data against $\delta^{18}O_{precipitation}$ measurements for the same months. The regression of these data provides a line which approximates the equation: $\delta_{cell} = \delta_{sw} + \Delta$. The regression exhibits a slope of ~1 with an intercept of 28.7 relating to Δ (net biochemical enrichment). Δ is reassuringly close to the published value of ε_b.

Comparison of the variation in α-ε_b predictions using $\delta_{sw} = \delta_{bw}$ indicates that the magnitude of seasonal separation between bog water values and leaf water values varies between sites (Figure 8.4). Relatively strong seasonal differences are observed for Walton Moss and

Dosenmoor and a much lower seasonal variation is observed at Raheenmore. Results in Chapter 7 have already demonstrated strong evaporative enrichment of bog surface water at Raheenmore. These data suggest that the leaf water used for cellulose synthesis undergoes similarly strong evaporative enrichment at Raheenmore. This could result from regular exchange with bog water or from continued photosynthesis under evaporative conditions resulting from the high relative humidity at this oceanic site.

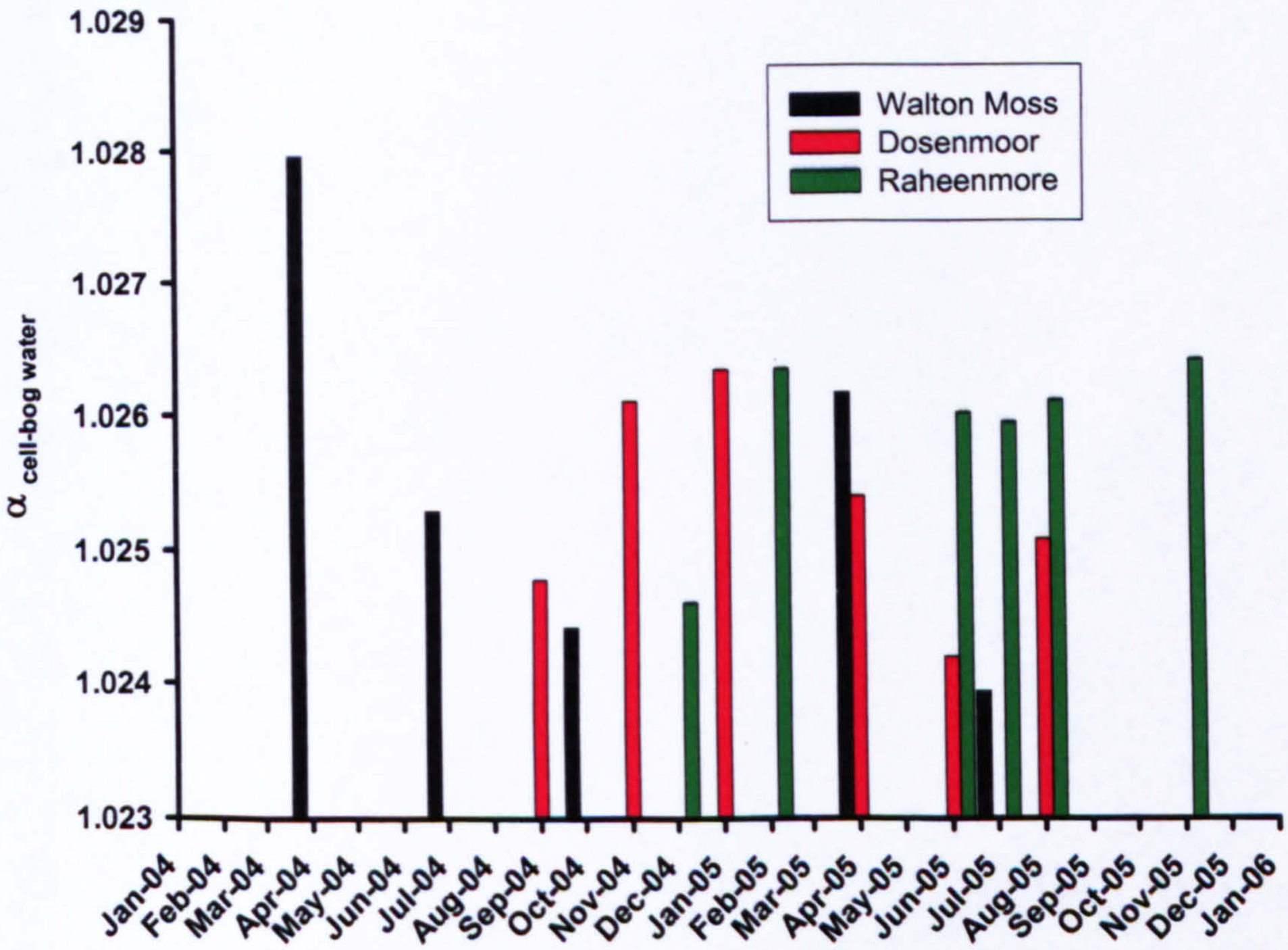

Figure 8.4 Monthly alpha coefficients for each European site where $\delta_{sw} = \delta_{bw}$

Whilst only a handful of studies have been undertaken to ascertain the relationship between modern *Sphagnum* cellulose, bog water and precipitation, each has shown high variability in bog surface water values that is dampened or averaged out by the cellulose values, in agreement with the data presented here. Other authors have concluded that cellulose values of bog plants follow the values of average precipitation (Ménot-Combes *et al.*, 2002). Three

hypotheses have previously been proposed to explain this property; 1) that cellulose is a integrator of source water variability over the monthly timescale, 2) that water is sourced from the well homogenised sub-surface bog water reservoir and 3) that reduced photosynthesis occurs in periods of highly evaporative conditions so as not to record the heavily enriched signal observed in bog surface waters (Ménot-Combes *et al.*, 2002; Zanazzi and Mora, 2005). These hypotheses were founded on data from all bog plants both vascular and non-vascular. Hypothesis 2 is less applicable to *Sphagnum* as the moss does not possess the necessary water transport mechanisms to source deep water for photosynthesis. The most plausible explanation is a combination of both hypothesis 1 and 3. *Sphagnum* cellulose reflects average precipitation $\delta^{18}O$ values as the leaf water used for cellulose synthesis is sourced principally from direct precipitation (this study) and because under conditions of moisture deficit, typically associated with high evaporation, photosynthesis is suspended (Williams, 1996). Relative enrichment and scatter in bog water values is consequently not recorded in *Sphagnum* cellulose. For those *Sphagnum* species that inhabit pool environments, regular mixing with bog water is inevitable. Where pools persist during periods of overall moisture deficit, it would be expected that the species growing in these locations would record an enriched bog water signal. The consistency both of cellulose $\delta^{18}O$ values between species and annual alpha coefficients for cellulose-water enrichment suggest that any distortive effect is minimal.

8.5 *Estimation of isotopic values of Palaeo-precipitation*

The finding that $\delta_{precipitation}$ approximates δ_{sw} more closely than δ_{bw} allows for estimation of $\delta^{18}O_{precipitation}$ from $\delta^{18}O_{\textit{Sphagnum}}$ values using $\alpha\text{-}\delta^{18}O_{cellulose\text{-}precipitation}$ coefficients. The mean $\alpha\text{-}\delta^{18}O_{cellulose\text{-}precipitation}$ coefficient derived from all the European study sites (1.0274 ± 0.0010, 1σ) is applied universally to the palaeo-sequences (Figure 8.5 to Figure 8.7) to yield estimates of the change in $\delta^{18}O_{precipitation}$ through the mid- to late Holocene. In all three NW European cores, mean palaeo-$\delta^{18}O_{precipitation}$ for the mid- to late Holocene period is comparable with modern $\delta^{18}O_{precipitation}$ values that lie towards the more enriched end of the 2004-2005 data range (Chapter 7). Comparison of estimated palaeo-$\delta^{18}O_{precipitation}$ with the longer GNIP datasets from the stations most local to the study sites indicates that values from all sites lie

within the range of variability observed over these longer timescales (Figure 3.39). The mid- to late Holocene mean for Walton Moss lies approximately centrally in the range of $\delta^{18}O_{precipitation}$ values observed at Wallingford (1981-2002) (Figure 3.9) overlapping with data collected for each of the four seasons. The mid- to late Holocene mean for Dosenmoor also falls within an overlapping range of data measured in all seasons in Cuxhaven (1978-2001) (Figure 3.16). Conversely, the mid- to late Holocene average for Raheenmore is relatively depleted in comparison with the >30 year long record from Valentia (Figure 3.28). This may reflect underestimation of the fractionation due to evaporative enrichment of moss leaf water.

Two hypotheses could explain the relatively enriched palaeo-$\delta^{18}O_{precipitation}$ values for the mid- to late Holocene mean at all sites. Enrichment could either 1) relate to inaccuracies of calibration or 2) may instead reflect an amount effect in the seasonality of moss production. Although evidence has been presented here for the occurrence of *Sphagnum* growth throughout the year, the data give no indication as to the seasonal distribution of that growth. Under conditions of sufficient moisture, it is highly likely that much of the biomass production occurs during an optimal growing season (Clymo, 1984). Given that the palaeo-samples reflect an approximate decadal mean, it is possible that much of the cellulose synthesised in that period is derived from summer precipitation and consequently reflects relatively enriched values compared to the range of $\delta^{18}O_{precipitation}$ values collected over the comparably short 2004-2005 period.

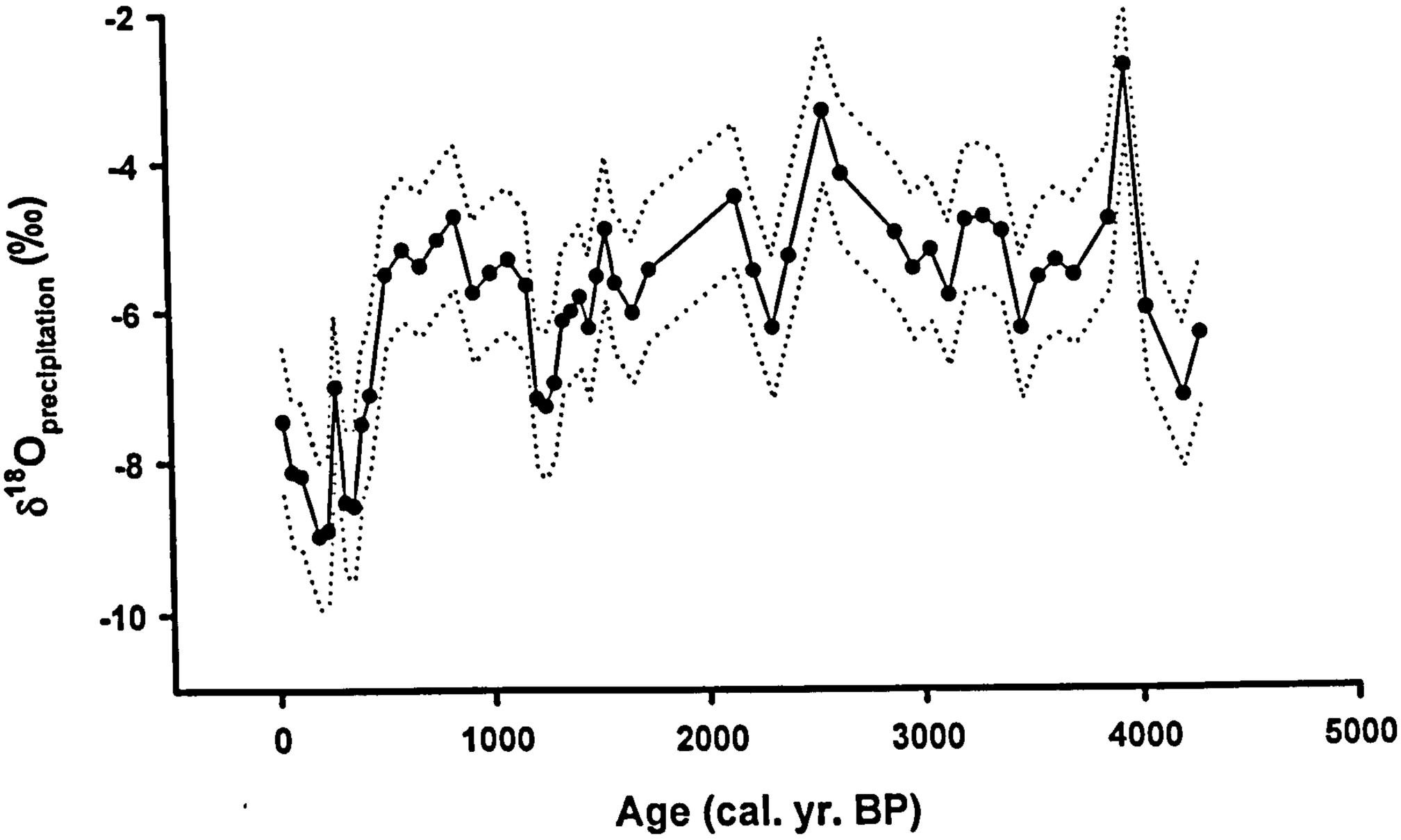

Figure 8.5 WLM22 palaeo- $\delta^{18}O_{precipitation}$ estimate using $\alpha = 1.0274 \pm 0.0010$ (1σ).

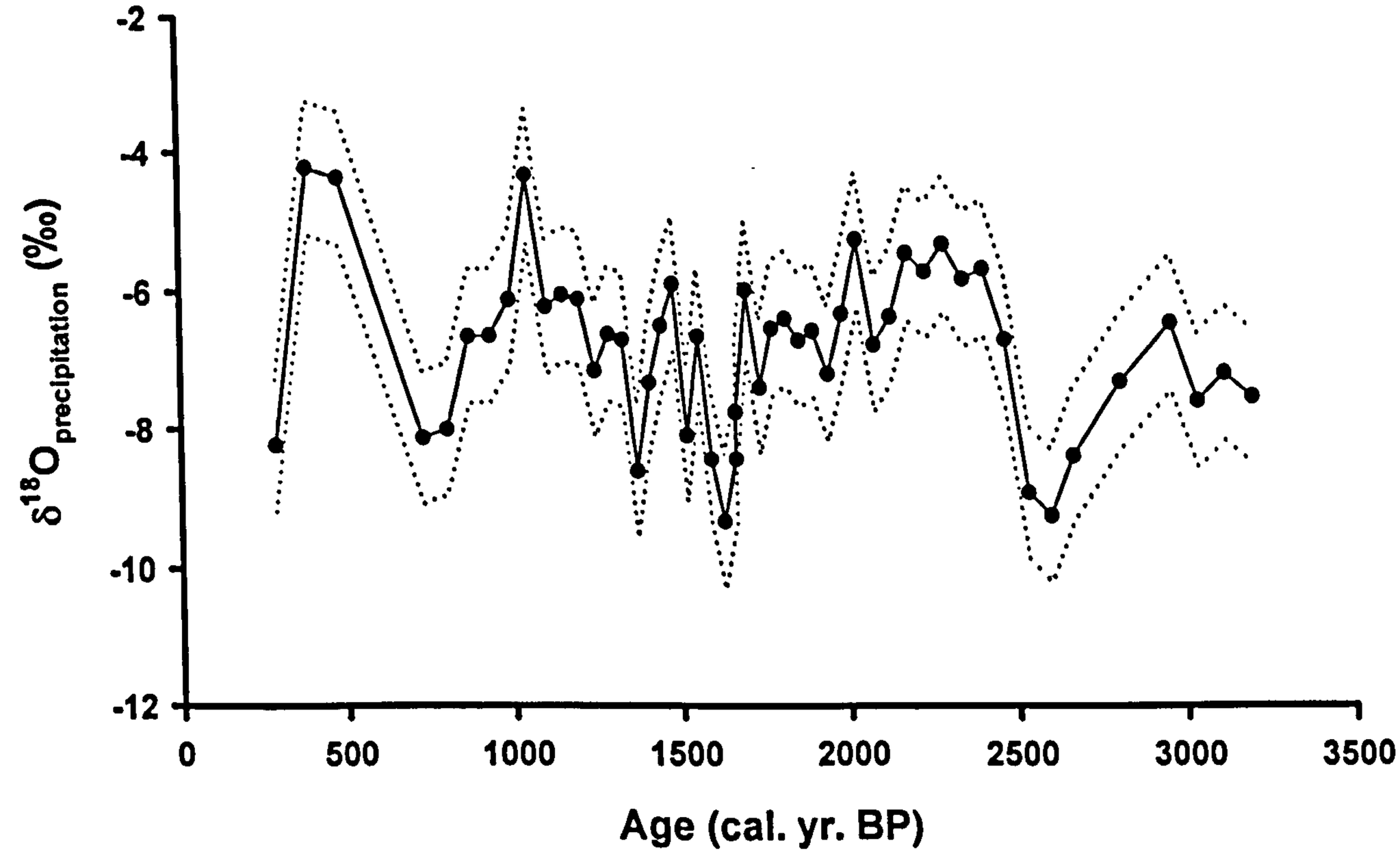

Figure 8.6 DSM3 palaeo- $\delta^{18}O_{precipitation}$ estimate using $\alpha = 1.0274 \pm 0.0010$ (1σ). Dotted lines refer to 2σ error range on biochemical enrichment estimate.

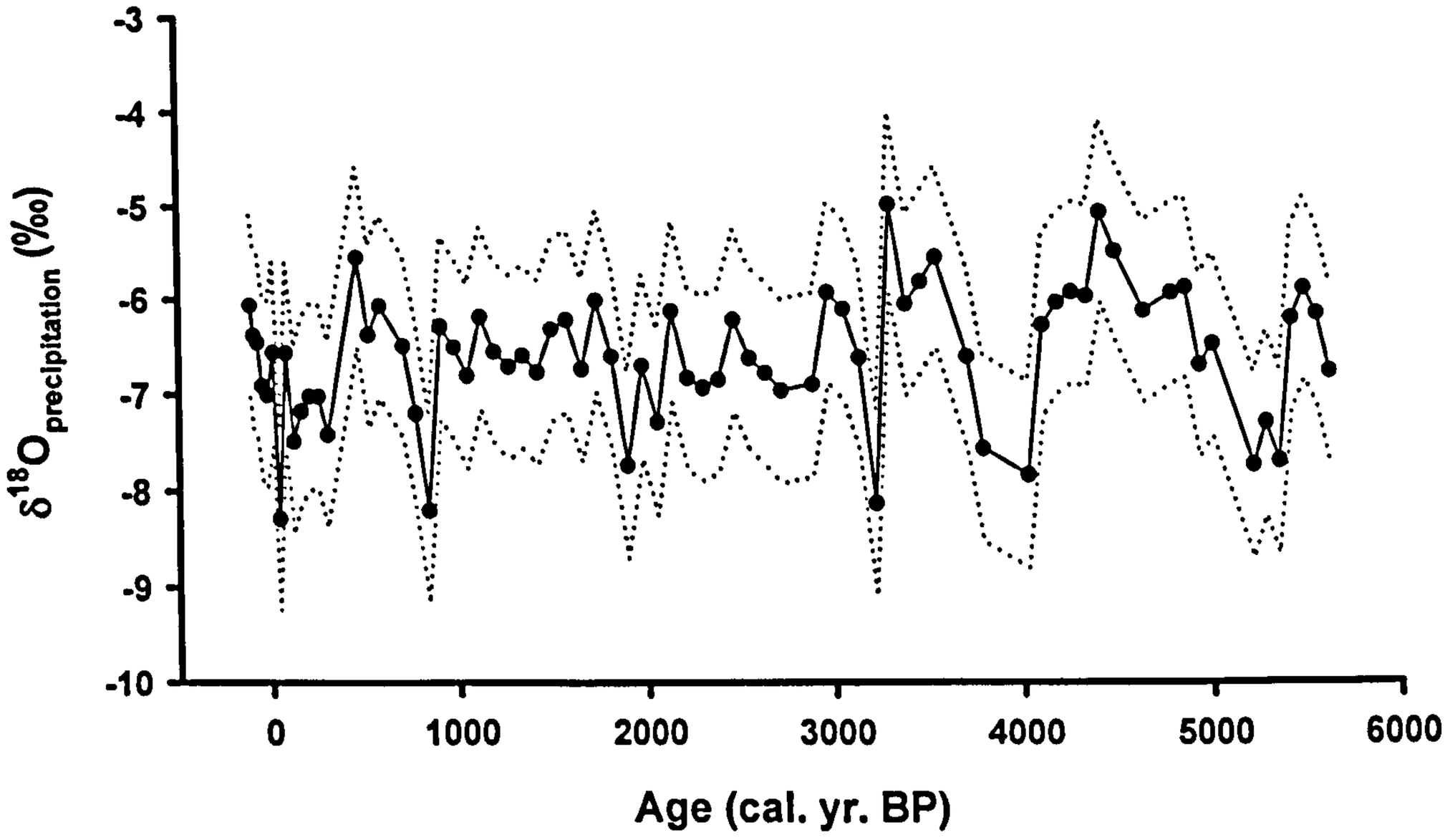

Figure 8.7 RHM2 palaeo- $\delta^{18}O_{precipitation}$ estimate using $\alpha = 1.0274 \pm 0.0010$ (1σ). Dotted lines refer to 2σ error range on biochemical enrichment estimate.

No modern precipitation data exist for Nordans Pond Bog. However, the collection of 8 surface samples of bog water and 12 cellulose samples in June 2004 allows some comparison and tentative calibration with GNIP precipitation data. As described in Chapter 3, Newfoundland has no GNIP station, although the bog site is relatively equidistant from two stations in Goose Bay, Labrador to the north and Truro, Nova Scotia to the south. Figure 8.8 shows a bi-plot of GNIP precipitation data separated by season from the two stations, with June 2004 bog waters superimposed. It is evident that the bog waters plot within the scatter of regional precipitation data over the temporal range of the GNIP data. α-$\delta^{18}O_{cellulose\text{-}bog\ water}$ (1.0255) at Nordans Pond Bog has a very value similar to that of α-$\delta^{18}O_{cellulose\text{-}bog\ water}$ in Europe (1.0256). The slope of the bog water data (~3) also suggests evaporative enrichment of the bog waters relative to the regional MWL (Figure 3.34). Using $\alpha = 1.0253$, it is likely that $\delta^{18}O$ source water estimates for NDN02/1 will be slightly more enriched than real δ_{sw} if the system works similarly to sites in NW Europe (section 8.4). Reconstructed magnitudes of change, however, will be representative.

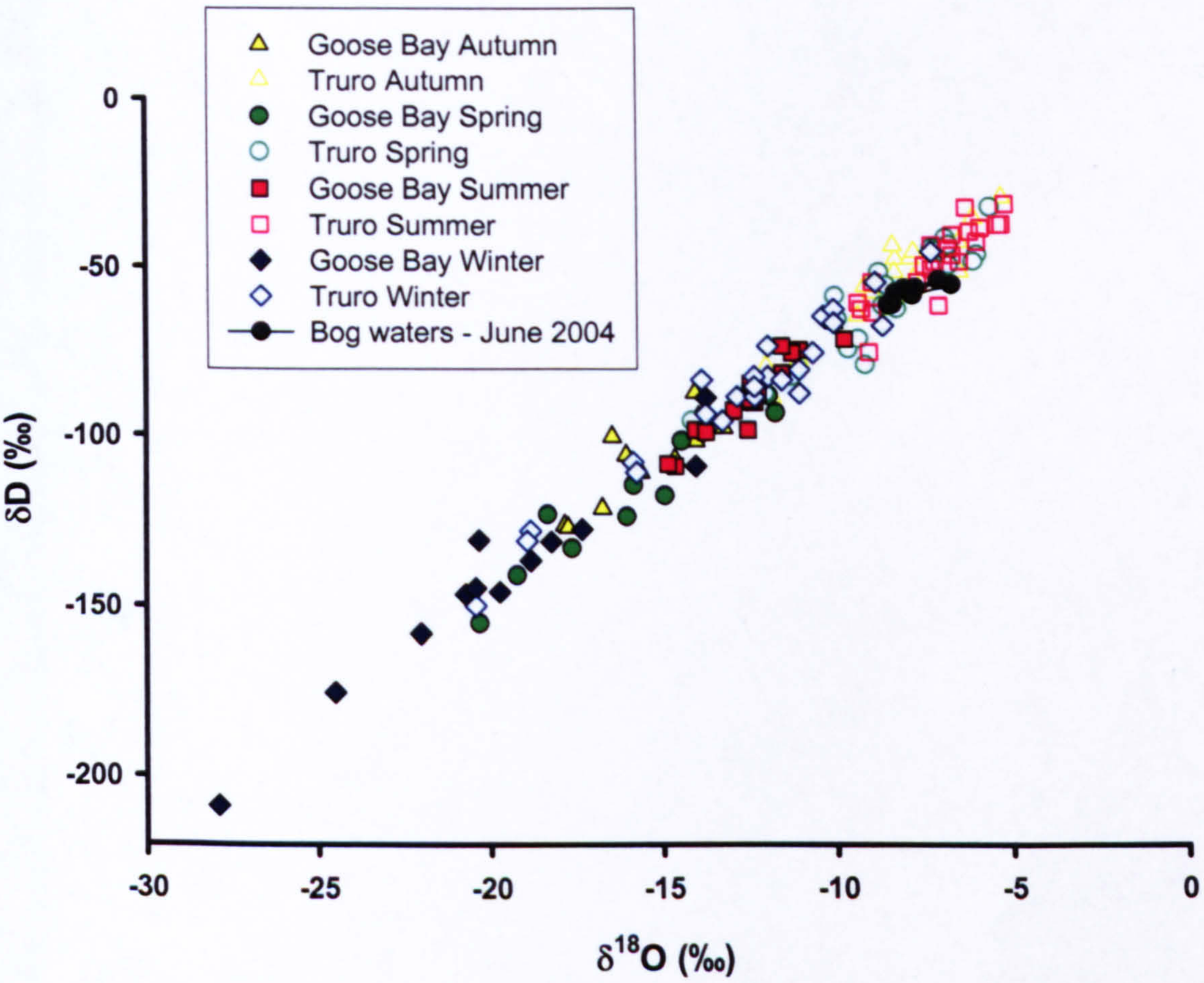

Figure 8.8 Nordans bog water values compared with GNIP precipitation data by season. Closed symbols = Truro. Open symbols = Goose Bay. Bog waters = black dots.

δD values for three of the twelve modern cellulose samples from Nordans Pond Bog were presented in Chapter 7 (Table 7.4). Whilst three samples offers only limited confidence in any resulting calibration, comparison with thirty δD measurements taken on modern cellulose samples from Dosenmoor (Chapter 7) allows basic assessment of the estimation of the net biochemical fractionation factor (ϵ_b) occurring during the cellulose synthesis of non-exchangeable hydrogen atoms. The synthesis of hydrogen atoms follows a different pathway to that of oxygen (Chapter 2) and is subject to a biochemical fractionation that leads to depletion of deuterium in the cellulose relative to the source water (Epstein *et al.*, 1977; Brenninkmeijer *et al.*, 1982; Yakir and DeNiro, 1990; Pendall *et al.*, 2001).

Again, Equation 4 can be used:

Equation 4) $\delta cell = \delta sw + \varepsilon b + (\varepsilon e + \varepsilon k)(1-h)$

with the same humidity parameters as those used for oxygen to generate Equation 11 where Δ in this case refers to the net biochemical depletion due to the operation of NADPH during cellulose synthesis.

Equation 11) $\delta cell = \delta sw + \Delta$

α-$\delta D_{cellulose\text{-}water}$ coefficients are derived using Equation 5 from $\delta D_{\textit{Sphagnum}}$ values:

Equation 5) $\alpha = ((\delta cellulose / 1000) + 1) / ((\delta source_{water} / 1000) + 1).$

The mean α-$\delta D_{cellulose\text{-}water}$ for Nordans Pond Bog (0.9318 ± 0.0094, 1σ) is similar to the value for modern Patagonian *Sphagnum* moss (0.922 ± 0.006, 1σ) (Pendall *et al.*, 2001). For the thirty surface data from Dosenmoor this value is 0.9073 ± 0.0158 (1σ). The surface data from Dosenmoor show highly variable values in $\delta D_{\textit{Sphagnum}}$ which is responsible for producing the relatively large σ error documented here (Figure 7.19). Use of Equation 5 from Nordans Pond Bog enables calibration of both $\delta^{18}O_{sw}$ and δD_{sw} values for the three samples. These are plotted against the GNIP data and bog waters in Figure 8.9.

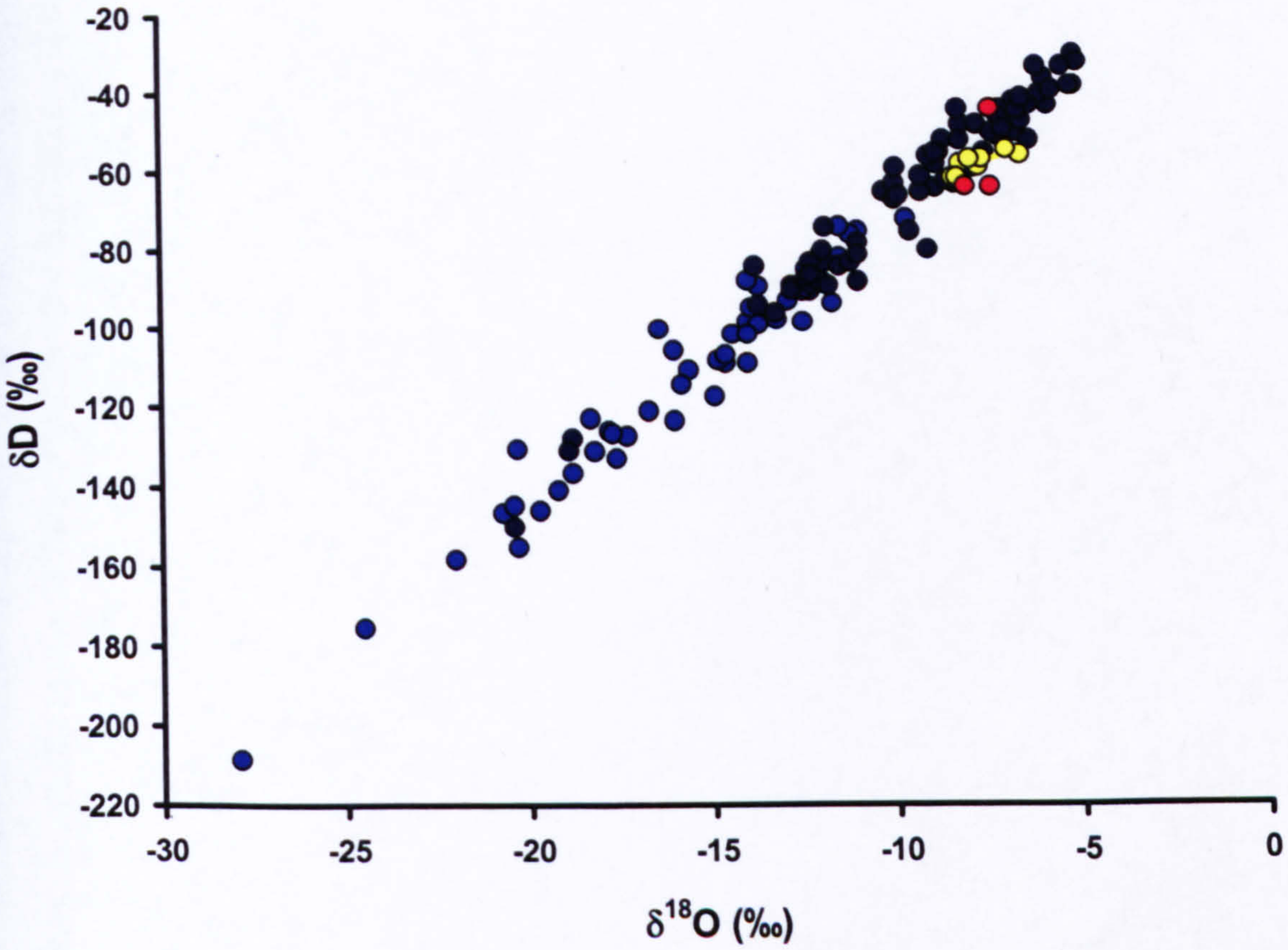

Figure 8.9 Source water estimates for modern *Sphagnum* cellulose from Nordans Pond Bog (red dots). Yellow dots are bog waters used for calibration. Blue dots are GNIP precipitation data from Truro, NS (1975-1983; dark blue dots) and Goose Bay, Labrador (1961-1965; light blue dots) (IAEA/WMO, 2004).

Using $\alpha_{\text{cellulose-bog water}}$ coefficients for both $\delta^{18}O$ (1.0255 ± 0.0015) and δD (0.9318 ± 0.0094) it is possible to estimate palaeo-bog water δ values from Nordans Pond Bog with the caveat that estimated $\delta^{18}O$ values may show greater enrichment than δD values if the conditions of bog water evaporative enrichment are similar to those observed in NW Europe. Calibrated palaeo-*Sphagnum* data are plotted against GNIP data in Figure 8.10. The slope of palaeo-source water estimates is very similar to that of the regional MWL, suggesting that the Holocene data are reflecting shifts along a precipitation-isotope gradient.

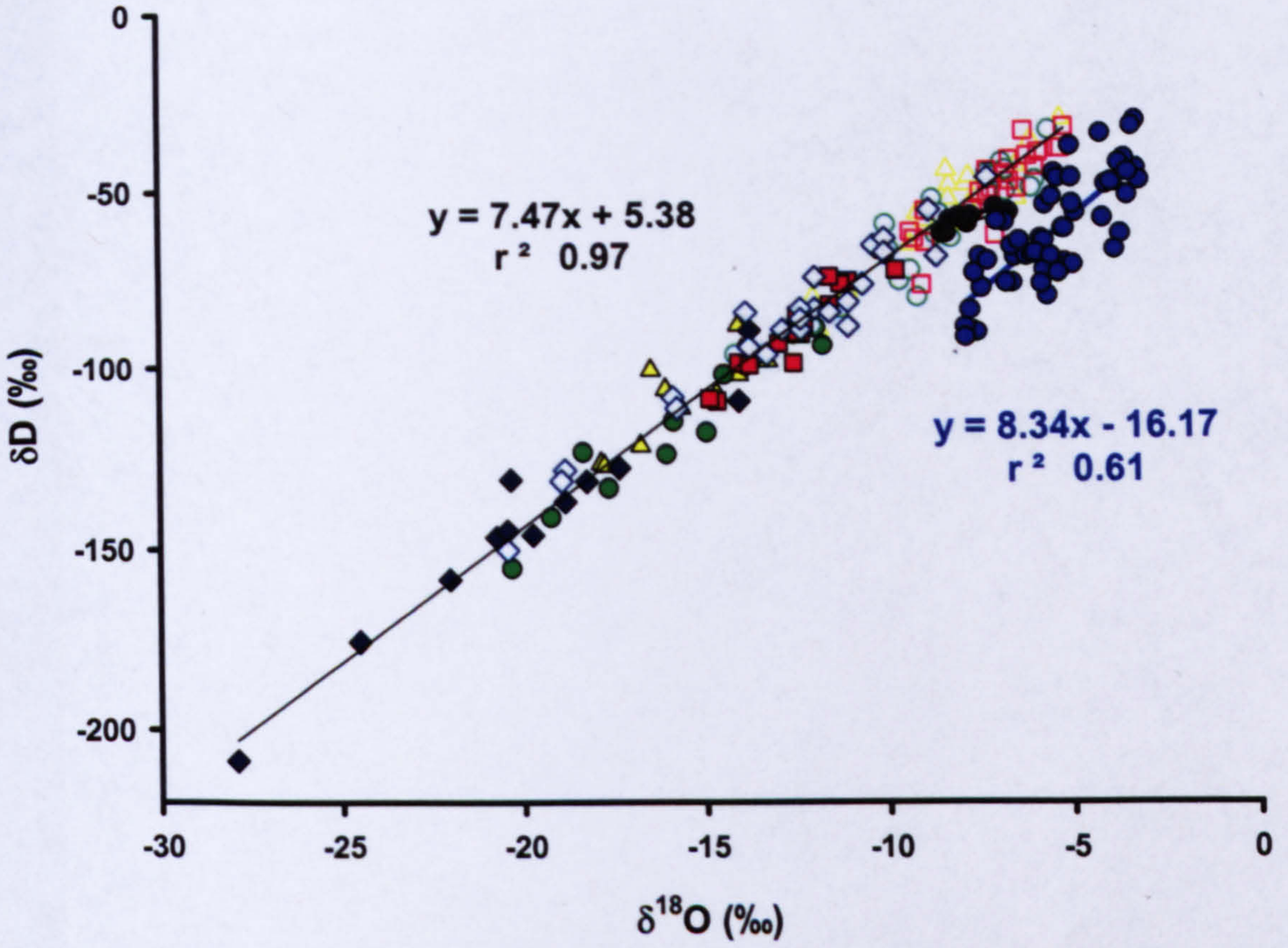

Figure 8.10 Comparison of Holocene *Sphagnum* source water reconstruction from NDN02/1 with modern GNIP precipitation data (IAEA/WMO, 2004). GNIP variation in the isotopic composition of meteoric waters is given by season. Closed symbols = Truro. Open symbols = Goose Bay. Bog water used for calibration = black dots. NDN02/1 cellulose palaeo-source water estimates = bold blue dots.

Source-water estimates do not, however, overlie data from modern precipitation. As the slopes of the regressions are not identical this apparent offset is variable, yet it can be partly quantified by the difference between the intercepts of the x and y axes by the two curves. Palaeo-precipitation values are 21.55‰ more depleted in deuterium at x = 0, and 2.66‰ more enriched in oxygen-18 at y = 0 than modern precipitation.

With only three data for hydrogen calibration, it is possible that the separation of palaeo-estimates from modern data is due to use of such a small training dataset. However, it is also possible that this separation results from inaccuracies in the oxygen calibration. The inaccuracy comprises two components. One relates to the ability of cellulose laid down in

June to represent the annual average source water signal archived over time. The other relates to the use of bog water as a proxy for leaf water. It is argued that these two components are together responsible for the offset observed. Whilst cellulose values from June 2004 inevitably calibrate close to the bog water values (Figure 8.9), those cellulose values were, on average, 2.16‰ depleted in $\delta^{18}O$ relative to the top core sample from NDN02/1 collected in September 2002. The mean palaeo- $\delta^{18}O$ cellulose values are consistently more enriched than the modern calibration cellulose.

The 2.16‰ difference in the June 2004 cellulose oxygen values from the top of core cellulose oxygen values suggests that the data for that month are not characteristic of the average annual source water signal that is recorded in the archived cellulose. The summer season in Newfoundland is short compared to the same latitude in Europe by virtue of proximity to the cold Labrador Current which maintains cool surface air temperatures throughout the year. June represents the beginning of the summer season in which temperatures rise considerably through July and August before falling again during September (Figure 3.33). Cellulose growth during this longer period is then likely to preserve a more enriched isotopic composition than the cellulose from June alone. It is the mean value from this longer period that is archived in core cellulose values. If cellulose laid down in June is comparatively depleted in relation to the annual signal, this explains at least part of the offset observed.

However, it cannot be the whole story, if, like European sites, the leaf water signal reflects precipitation rather than bog water. If June 2004 represented a depleted month within the annual archived signal, the palaeo-cellulose data would plot in a more enriched position *along* the regional MWL. It does not. Instead the position below the regional MWL is indicative of the effect of kinetic fractionation. This can arise from one of two sources. Either 1) palaeo-source water was persistently enriched in oxygen by a similar value throughout the Holocene and throughout changing climatic conditions compared to modern precipitation, consistent with kinetic fractionation effects occurring within leaf water, or 2) the calibration involves a consistent underestimation of ε_b due to the kinetic fractionation affecting bog waters used for calibration.

The data suggest that an underestimation of ε_b is the more likely explanation. The differential transmissivities of hydrogen and oxygen isotopes means that they fractionate at different rates under kinetic conditions (evaporation). The liquid phase enriches more rapidly in ^{18}O than ^{2}H during evaporation resulting in water lines for evaporating waters that have a lower slope than the GMWL (Craig, 1961a). Whilst the modern bog water data from Nordans Pond Bog appear to plot within the scatter of regional precipitation in the later half of the 20th Century, the slope angle of measured bog waters indicate that the bog water was kinetically enriched at the time of sampling and hence had evolved from its precipitation source water. This is consistent with findings from the NW European sites where the α_{18} value for Nordans bog waters exhibited a very similar value to the bog waters of NW Europe (above). It has been demonstrated in Europe that the enrichment of bog waters is greater than that occurring in the moss leaf water used for cellulose synthesis. If leaf water approximates precipitation in Newfoundland as found in the NW European sites, underestimation of ε_b will result from calibration against bog water values. Less underestimation is observed in δD values due to the differential transmissivities under kinetic conditions. This is consistent with the offset of reconstructed source water to the right of the regional MWL as seen in Figure 8.10.

The combined effect of the two sources of potential offset are to shift the cellulose source water estimation data firstly to more enriched values *along* the MWL and secondly to shift them right of the MWL by ~2‰ in oxygen. Use of $\alpha_{18} = 1.0274$ obtained for European sites substantially reduces the separation between the curves and produces close conformity between palaeo-precipitation estimates and modern precipitation values (Figure 8.11). The new difference in y axis intercept (6.0‰) is of similar size to the analytical precision of deuterium measurement (± 4‰; Chapter 4).

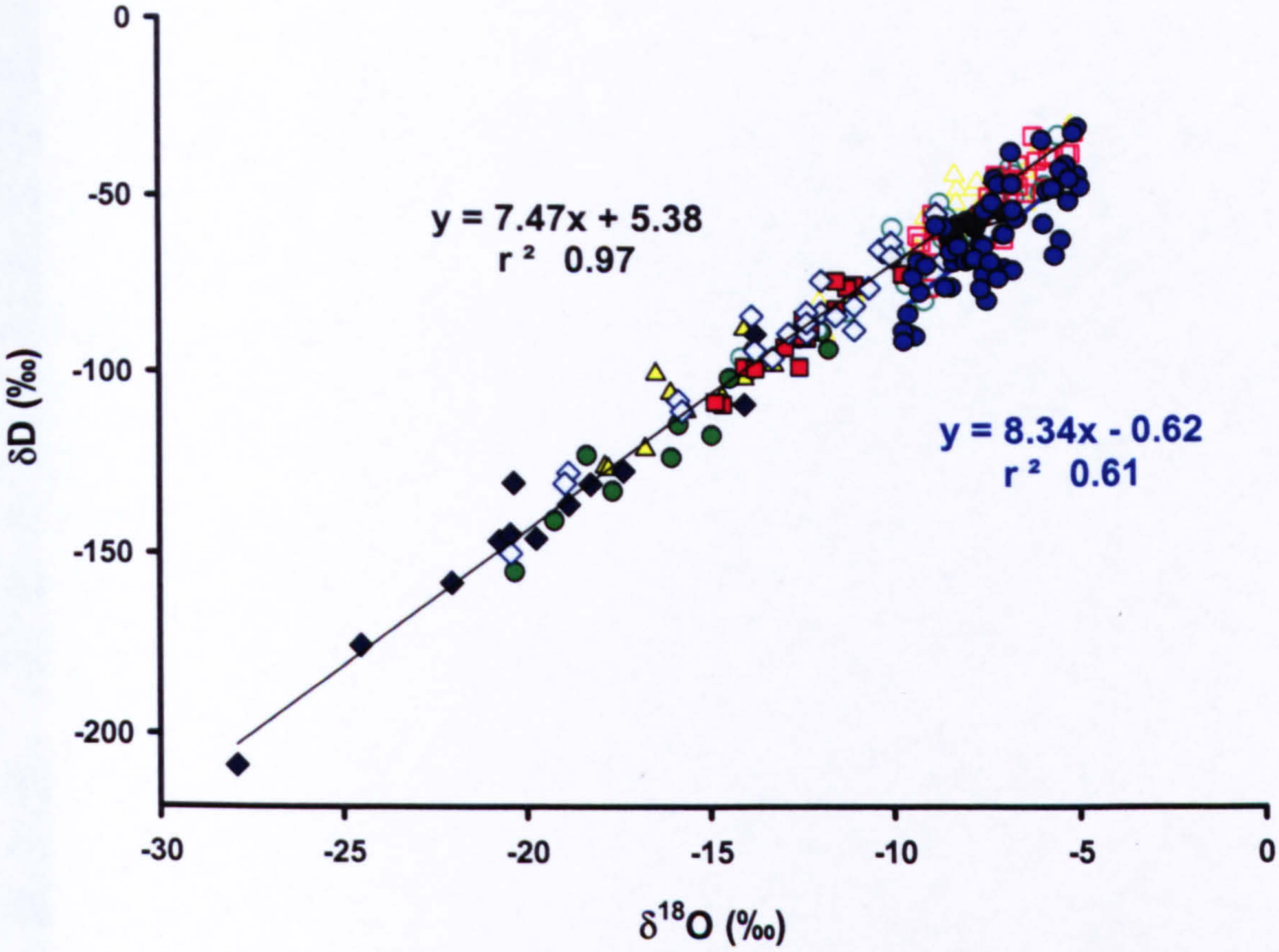

Figure 8.11 Comparison of Holocene *Sphagnum* source water reconstruction from NDN02/1 with modern GNIP precipitation data (IAEA/WMO, 2004) *using $\alpha = 1.0274$ for $\delta^{18}O$ cellulose-water enrichment*. GNIP variation in the isotopic composition of meteoric waters is given by season. Closed symbols = Truro. Open symbols = Goose Bay. Bog water used for calibration = black dots. Cellulose palaeo-source water estimates = bold blue dots.

If this feature of the offset is then understood as a calibration product, it suggests that palaeo-cellulose δD and $\delta^{18}O$ values in core NDN02/1 preserve a record closely approximating the isotopic composition of precipitation over the Holocene. It also suggests that over the average of that period, the deuterium excess has been relatively constant. Whilst it is theoretically possible to deduce changes in deuterium excess from scatter of the data above and below the cellulose regression line presented in Figure 8.10 and Figure 8.11, the uncertainty associated with calibration and the scatter evident in hydrogen data from the modern environment (Figure 7.19) reduces the extent to which firm conclusions can be drawn from this approach.

8.6 *Improved understanding of change through the mid- to late Holocene*

Understanding of the isotopic record from *Sphagnum* moss as a record closely approximating the isotopic composition of palaeo-precipitation has considerable implications for interpretation of past changes in climate in the mid- to late Holocene, where *Sphagnum* preservation is abundant. With sufficient chronological control and a suitable density of palaeo-data locations, it is possible to map spatial variation in palaeo-precipitation. This essentially encompasses the role of the wider ISOMAP-UK research for which this study was part. With regard to the contribution of this study alone, whilst only four sites are insufficient to attempt such a mapping exercise, the data are still sufficient to explore changes in isotopic gradients throughout the mid- to late Holocene from which changes in circulation and hence processes may be inferred.

In general, mean isotopic gradients from Newfoundland to northern Germany during the mid to late Holocene (Figure 8.12) were similar to the modern day (Chapter 3; Figure 3.39). During periods of change towards conditions of isotopic depletion in precipitation, however, the data suggest that these gradients altered so that the magnitude of change was greater with increasing continentality (Figure 8.12). In general, the mean isotopic composition of precipitation over Newfoundland was most depleted. The means from Raheenmore and Dosenmoor were fairly similar, although Dosenmoor showed greater variability. $\delta^{18}O_{precipitation}$ at Walton Moss was the most enriched of any of the study sites through the mid- to late Holocene. In the modern day, Valentia and Raheenmore exhibit the most enriched average values (Figure 3.39 and Figure 7.1, respectively). In general, more enriched values reflect oceanic location, lower altitude, warmer temperatures or upstream location on a rainout trajectory. Over the timescale of the mid- to late Holocene it is unlikely that any of these conditions described the relative difference between midland Ireland and northern England, suggesting that the relative enrichment observed at Walton Moss is a product of calibration.

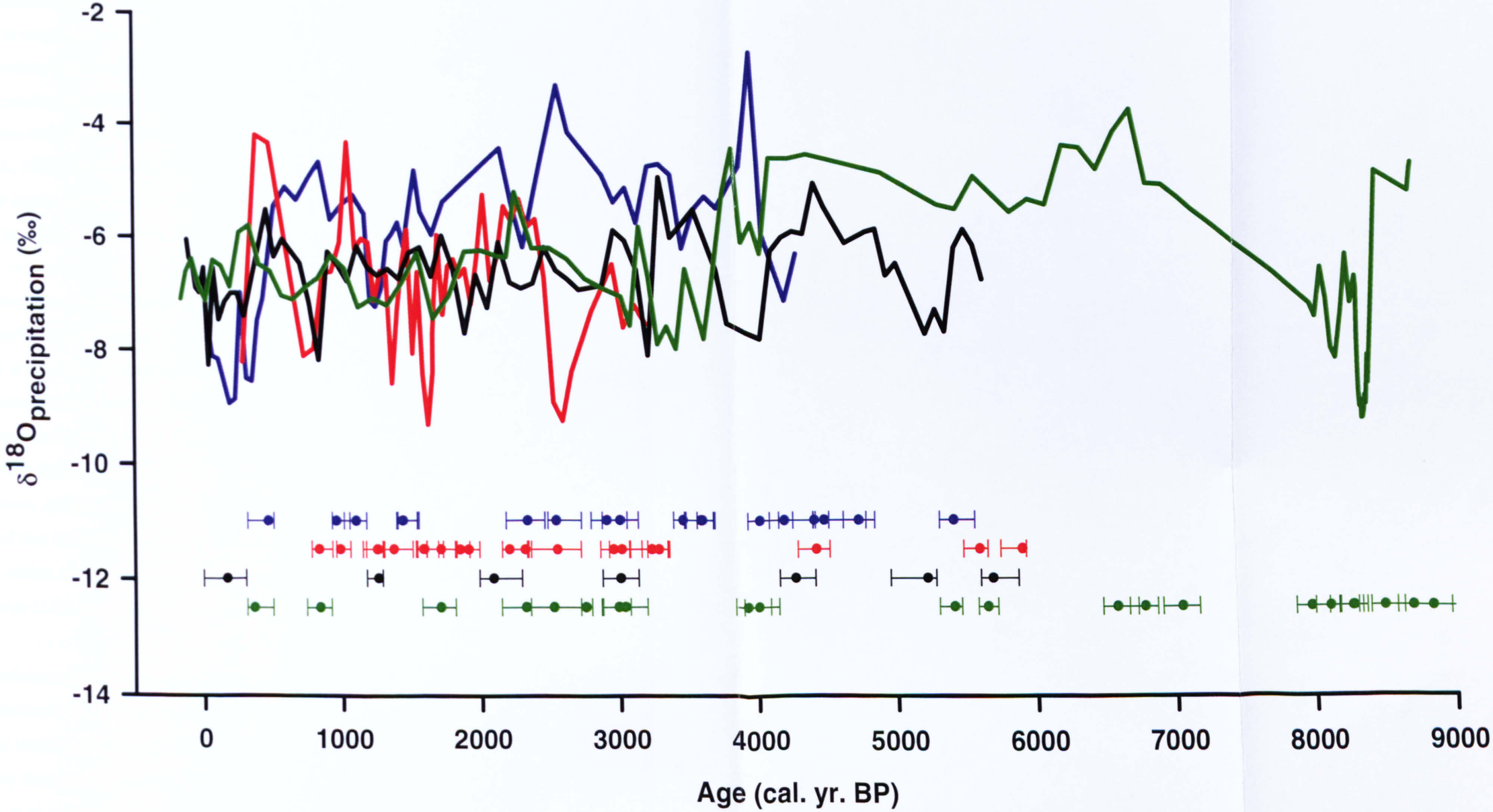

Figure 8.12 $\delta^{18}O$ precipitation estimates for four study sites (Red line = Dosenmoor; Blue line = Walton Moss; Black line = Raheenmore; Green line = Nordans Pond Bog). Error bars refer to the upper and lower calibrated ranges from the 2σ error on AMS ^{14}C dates

Mechanisms of climatic change in the mid- to late Holocene can be explored with specific reference to two regional climatic events at ~2700-2300 BP and ~1800-1200 BP. The nature of these events, records of their distribution and theories proposed for their cause have been reviewed previously (Chapter 2). Both periods coincide with known phases of climatic deterioration associated with millennial cycles of Holocene climate (O'Brien *et al.*, 1995; Bond *et al.*, 1997; Bond *et al.*, 2001). Consequently, their explanation must in part relate to postulated mechanisms involved in millennial cyclicity or the events themselves must be shown to be different from that of cyclical behaviour.

Climate change ~2700-2300 BP has been detected in peat records both in the North Atlantic region (van Geel and Renssen, 1998; Speranza *et al.*, 2003) and in the Southern Hemisphere (van Geel *et al.*, 2000; Chambers *et al.*, 2007). An isotopic excursion is observed in the record from Dosenmoor beginning ~2950 BP with a minimum at ~2550 BP. In Walton Moss, a similar magnitude excursion is observed beginning ~2550 BP with a minimum observed at ~2350 BP. In Raheenmore, a minor fluctuation is noted with similar duration to that in Walton Moss. At first inspection it appears as though the event in Dosenmoor occurs in advance of that in Walton Moss despite their similarities in magnitude. Both events are, however, within the 2σ range of dating uncertainty which would allow these to be synchronous if the chronologies were "tuned" (Charman *et al.*, 2006).

Two hypotheses can be proposed to explain the data around this period. Either 1) the events are not synchronous but may instead reflect a time and space transgressive response to latitudinal shifting of storm track trajectories in association with a global climatic downturn induced by changes in solar forcing (van Geel and Renssen, 1998; van Geel *et al.*, 2000; Speranza *et al.*, 2003; Magny *et al.*, 2003b; Dergachev *et al.*, 2004; van Geel *et al.*, 2004; Chambers *et al.*, 2007) or 2) the events are synchronous and reflect similar responses in both northern England and northern Germany to a single climatic event possibly modulated through changes in the thermohaline circulation (Bianchi and McCave, 1999; Chapman and Shackleton, 2000; Hall *et al.*, 2004; Andersen *et al.*, 2004).

Given the chronological control available on the cores, both hypotheses are plausible. The direct influence of solar reduction is suggested to be minimal given changes of only 0.24% in solar irradiance (Beer *et al.*, 2000) so any isotopic response will probably have been modulated through additional feedbacks, including changes in the THC. The later isotopic decline experienced in Walton Moss at the same time as a minor oscillation in Raheenmore could reflect increased precipitation due to the return of storm-tracks to a more northerly latitude. The difference in magnitude between the responses in Walton Moss from that in Raheenmore could reflect mitigation of temperature change with proximity to the Atlantic.

Equally, the similarity in magnitude, if the events were considered synchronous, would imply a common driver of change. Evidence for slow-down in the rate of Iceland-Scotland Overflow Water (ISOW) across this period (Bianchi and McCave, 1999; Hall *et al.*, 2004) and latitudinal extension of polar waters into the sub-polar North Atlantic (Andersen *et al.*, 2004) indicate reduction in the strength of heat transport by meridional overturning of the North Atlantic conveyor. Subsequent resumption of THC overturning as indicated by the strength of ISOW within the timescale of the isotopic recoveries observed in both records makes hypothesis two also plausible.

The data cannot be used to determine which of these hypotheses is true without greater chronological control. If thermohaline circulation change played a significant causal role, a strong response would be expected in Raheenmore since its oceanic location should be reflected in greater sensitivity to THC change. Although chronological control does not allow these hypotheses to be separated, the availability of data on magnitude of change is highly influential here as it suggests a mechanistic association between the two records of isotopic excursion which would not exist to such a degree with directional data alone. It is noted also that with BSW records only, the limited response in WLM22 (Figure 8.1) would allow this climatic episode to appear more minor than in combination with the isotopic evidence.

Climatic deterioration observed in the period ~1800-1200 BP has been relatively understudied in comparison to the Little Ice Age (LIA) and ~2700 BP events. Whilst atmospheric changes at this time (O'Brien *et al.*, 1995) have been linked to changes in the transport of ice-rafted debris (IRD) (Bond *et al.*, 2001) and the speed of ISOW (Bianchi and McCave, 1999), these

records have not been explored with the same intensity of investigation as other millennial scale changes (Chapter 2). Climatic fluctuation between ~1800-1200 BP at the three European sites is seen to occur at different times in different places since it occurs outside the 2σ range of chronological uncertainty from ^{14}C AMS dating. Variation in BSW records from all three sites provides evidence for two increases in surface wetness over the period, one typically more severe than the other (Figure 8.1). Isotopic variation at Raheenmore is remarkably stable during this period, despite variation towards increased BSW (Figure 8.2). In the record from Walton Moss, the later shift is expressed more strongly both in BSW (Figure 8.1) and isotopic variability (Figure 8.2). At Dosenmoor, the earlier shift is expressed most strongly in both BSW and isotopic variability (Figure 8.2). This earlier shift at Dosenmoor is outside the 2σ range of ^{14}C AMS dating of the later shifts recorded at all three sites. Of the later of the two shifts, the magnitude of change increases with distance from the Atlantic Ocean (Figure 8.12).

It is possible that the detection of two shifts in BSW within the period 1800-1200 BP is in fact the detection of noise in the palaeo-hydrological reconstruction. Indeed, it is also possible that the detection of minor fluctuation in isotopic records relates to analytical noise. However, the likelihood of these signals originating from non-climatic noise is decreased 1) by the presence of similar signals in three BSW records spread across northern Europe 2) by changes in the oxygen isotope stratigraphy of similar relative magnitude and direction to that in BSW and 3) by the replication of variation in oxygen stratigraphy by variation in deuterium stratigraphy across the period of interest at Walton Moss (Chapter 7; Figure 7.24). The slope of the δD-$\delta^{18}O$ bi-plot for this section of WLM22 (~1580-1090 BP; Figure 7.25) is similar to that of the modern MWL for this site, reflecting limited change in the average humidity, temperature and wind speed characteristics of the vapour source region of precipitation over this period. This strengthens the case for the detection of two phases of climatic change of different magnitude that were induced by changes in the amount of air mass cooling taking place between an oceanic vapour source and the bog site.

As with climate change ~2700 BP, shifting storm-track trajectories have been proposed for explaining differences in timing of climatic change between latitudinal zones (Magny *et al.*, 2003b; Magny *et al.*, 2006) and as a mechanism that allows amplification of solar forcing (van Geel *et al.*, 2000). The presence of two climatic episodes in this period, with both

replicated regionally (Aaby, 1976; Mauquoy and Barber, 1999b; Hughes *et al.*, 2000; Barber *et al.*, 2003; Barber *et al.*, 2004; Magny, 2004; Nesje *et al.*, 2004) is suggestive of two separate events rather than one time and space-transgressive event, which may identify processes different from those involved in change ~2700 BP.

The key questions here are why should a moisture balance response be detected regionally and an isotopic response increase in magnitude with distance from the ocean? The isotopic data suggest an enhanced continentality effect during the period ~1800 – 1200 BP. A hypothesis can be proposed related to changes in the penetration of advected warm and moist air masses which may be due to long term changes in the NAO index (White *et al.*, 1997; Dawson *et al.*, 2003; Vinther *et al.*, 2003; Jones and Mann, 2004; Witak *et al.*, 2005; Chapron *et al.*, 2005). Again the initial driver may be solar variability. Prolonged periods of reduced solar activity such as the Maunder Minimum are associated with overall cooler conditions that are more pronounced over mid- to high latitude continental interiors than over oceanic locations (Bradley, 2003), characteristic of sustained shifts in the NAO to lower index values. Reduced zonal penetration of air masses would reduce the delivery of warm moist air to the European continental interior and consequently result in larger isotopic responses in central and eastern Europe than in the west due to enhanced rainout upstream. This model explains the increasing magnitude of response with distance from the ocean observed in the bog isotopic records. In support, storminess indices from Greenland (sea salt ions) show increase throughout the period consistent with sustained negative NAO (O'Brien *et al.*, 1995). Changes in the NAO typically occur over sub-decadal timescales (Hurrell, 1995). The resolution of the bog isotope data here is therefore not sufficient to extract variability over these timescales prohibiting a test of the role of NAO variability. However, the data do suggest that widespread climatic deterioration occurred, coincident with the timing of events in both the ocean and the atmospheric response over Greenland, which was expressed in Europe with a greater change in the isotopic composition of precipitation with distance from the Atlantic.

If variation in the NAO is the mechanism through which climate change is manifest in the second of the two climatic fluctuations, the trigger behind that variation may relate to short-timescale perturbations such as volcanic eruptions or extra-terrestrial interactions with either the atmosphere or surface (Baillie, 2007). The data presented here are not sufficiently

resolved either stratigraphically or in terms of dating control to clearly distinguish such short term changes. Although the later phase of change in all cores, expressed as the larger change in Walton Moss and Raheenmore in BSW coincides with the global AD 536-542 event represented clearly in tree-ring climate time-series (Scuderi, 1990; Baillie, 1994; Keys, 1999; Baillie and Brown, 2003; Baillie, 2007).

8.7 *Palaeotemperature reconstruction*

Variation in the stable isotopic composition of precipitation in the mid-latitudes over the last three decades has been shown to correlate with variation in the condensation temperature of precipitation. Calibration functions have been empirically derived from monthly mean GNIP data over decadal timescales from stations nearby the peat bog study sites (Chapter 3) and are used here to estimate palaeotemperature anomalies relative to the mean of each of the records (Figure 8.13). The derivation of a temperature relationship using monthly means has been advocated previously (Darling and Talbot, 2003).

For all three European sites the magnitudes of the temperature changes are approximately four to five times larger than expected (Figure 8.13). Estimates of change in other archives for the Holocene period indicate that temperatures were 1.5-3.5°C higher than present in northern Europe and the North Atlantic region between 8000 and 4500 BP (Johnsen *et al.*, 1995; Dahl-jensen *et al.*, 1998; Seppa and Birks, 2001; Johnsen *et al.*, 2001; Heikkila and Seppa, 2003; Seppa and Poska, 2004; Burman and Schmitz, 2005). The dates of this Holocene Thermal Maximum (HTM) period vary for different locations, but its existence is well recognised (Kaufman *et al.*, 2004). After ~4500 BP, temperatures are observed to fall by ~3°C through the mid- to late Holocene (Johnsen *et al.*, 2001; Heikkila and Seppa, 2003; Seppa and Poska, 2004). Whilst some records demonstrate gradual cooling through the late Holocene (Palmer *et al.*, 2002), others register greater variability. Between ~2000 BP and present, Greenland temperatures are estimated to have varied from 0.5°C lower than present at ~2000 BP to 1°C higher than present ~1000 BP followed by a further fall to 0.7°C lower than present during the LIA (Johnsen *et al.*, 1995; Johnsen *et al.*, 2001).

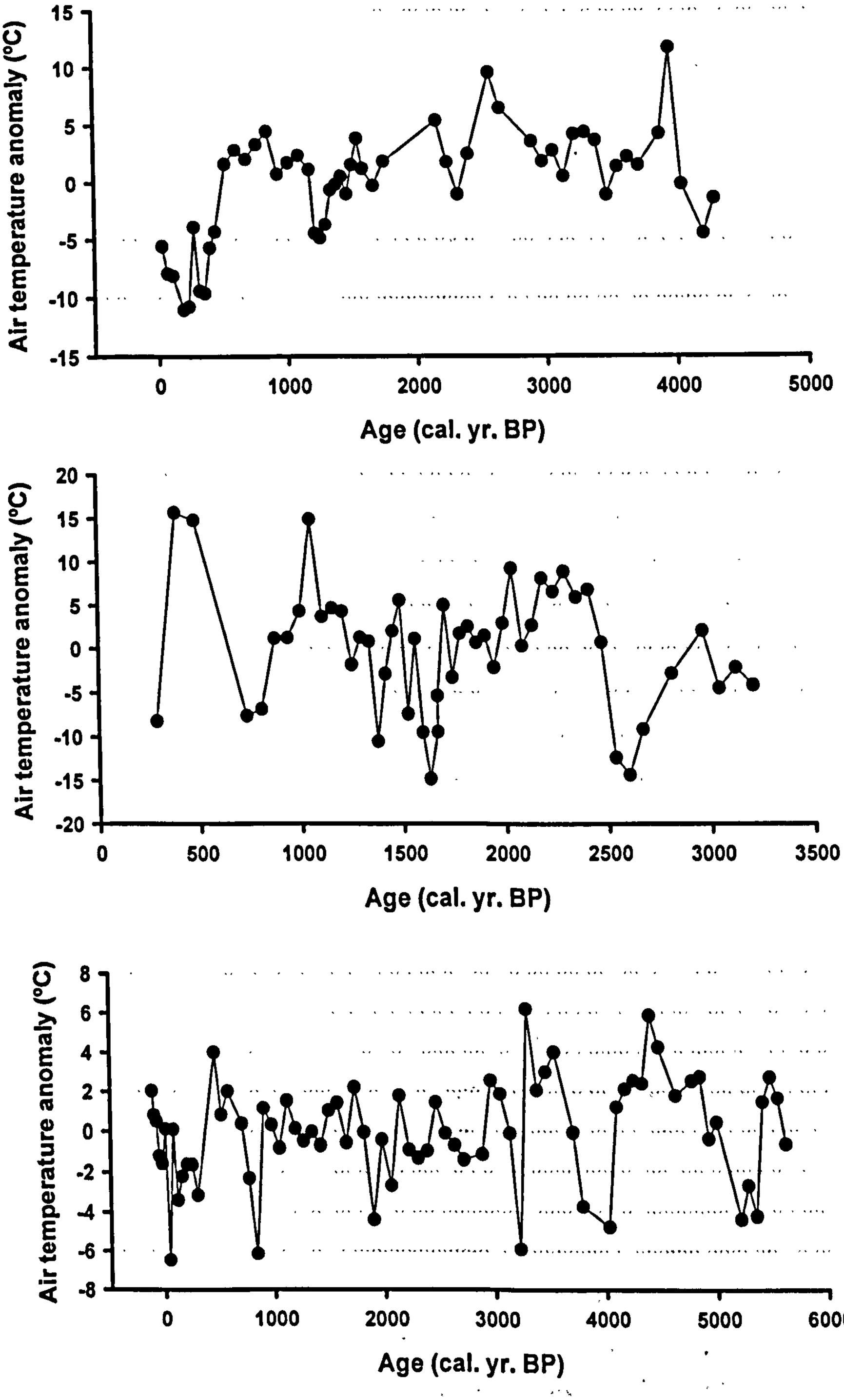

Figure 8.13 Reconstructed surface air temperature anomalies for each of the European sites using *decadal scale* $\delta^{18}O_{precipitation}$ -temperature coefficients derived from modern GNIP data (chapter 3) (Walton Moss = A, Dosenmoor = B, Raheenmore = C)

Magnitudes of isotopic change four to five times larger than expected were observed in peat isotopic analysis in studies in the 1980s and were attributed to climate signal amplification by changes in the proportion of vascular plant remains in the analysed peat samples (Brenninkmeijer *et al.*, 1982; Dupont and Brenninkmeijer, 1984; Dupont and Mook, 1987; van Geel and Middeldorp, 1988). The signal here is not related to species-based amplification. *Sphagnum* concentrates have been demonstrated to approximate pure *Sphagnum* isotopic variability closely (Chapter 4). Indeed, data from the method preparation test in Chapter four indicated that *Sphagnum* concentrates underestimated the magnitude of isotopic change in pure *Sphagnum* during shifts to conditions associated with $\delta^{18}O$ depletion. The signal from *Sphagnum* concentrates has also been shown to reflect a leaf water isotopic composition that more closely approximates the isotopic composition of precipitation than the evaporatively influenced bog surface water (section 8.4). Hence, the large magnitude variation is not a function of amplification by evaporative enrichment.

The estimation of change in the isotopic composition of precipitation would therefore seem robust. Consequently, the source of the large magnitude temperature anomalies may well relate to inadequacies in the modern characterisation of ΔT - $\Delta\delta^{18}O$ relationships, variation in these relationships over time or variation in the seasonality of *Sphagnum* growth with climate change.

Each of these explanations is plausible. For instance, at Valentia and Wallingford, statistically significant correlations between $\delta^{18}O_{precipitation}$ and precipitation amount are observed over the same timescales as the relationships with temperature. The distortive effect of this association on the ΔT - $\Delta\delta^{18}O$ relationship has already been addressed (Chapter 3). The temperature coefficients derived from the site specific data (Chapter 3) were uniformly lower than the average estimate previously derived from coastal stations (0.6 ‰ $°C^{-1}$) (Dansgaard, 1964), leading to large temperature change estimates for only small changes in isotopic composition. This is reflected most clearly in the reconstruction from Dosenmoor where a coefficient of 0.16 ‰ $°C^{-1}$ is derived from monthly means, which is approximately four times smaller than the published average (Dansgaard, 1964; Rozanski *et al.*, 1992). As a result, temperature variation at Dosenmoor of ~30°C throughout the Holocene is estimated (Figure 8.13), well outside the range of estimates from other archives. There is also evidence for considerable

variability in atmospheric circulation over Holocene timescales which must inevitably call into question the assumption of uniformitarianism of the ΔT - $\Delta\delta^{18}O$ relationship when the isotopic composition of precipitation is understood to reflect rainout history along a given trajectory of a moist air mass (Chapter 2).

Variation in the seasonality of optimal *Sphagnum* growth is a less likely candidate for explanation of the large magnitudes observed. During periods of cooler climate, it would be expected that *Sphagnum* growth would concentrate in summer periods due to unfavourable conditions through winter periods, a shift towards a summer precipitation signal may be observed. During periods of warmer climate, *Sphagnum* growth may persist throughout the year, as observed at Raheenmore (Chapter 7), incorporating more of a winter signal in the preserved cellulose. Consequently, it would be expected that variation in *Sphagnum* growth seasonality would dampen the magnitudes of isotopic change in precipitation.

Although each are plausible, the data suggest that the most likely source of the high magnitude temp reconstructions results from inadequacies in the modern characterisation of ΔT - $\Delta\delta^{18}O$ relationships. Relationships for the longer-term decadal monthly means of $\delta^{18}O_{precipitation}$ consistently exhibit much steeper slopes than those derived from the higher temporal resolution raw monthly data (Chapter 3). Although the strength of the correlation is notably stronger and highly statistically significant in the monthly means, this steeper slope is reflected in the lower temperature coefficients and consequently in the large magnitude palaeotemperature reconstructions. Despite the increased noise in the data and lower strength of correlation, use of the relationships observed between temperature and isotopic composition in the full raw monthly datasets from each of the sites produces much more realistic palaeotemperature estimates from the *Sphagnum* cellulose data (Figure 8.14).

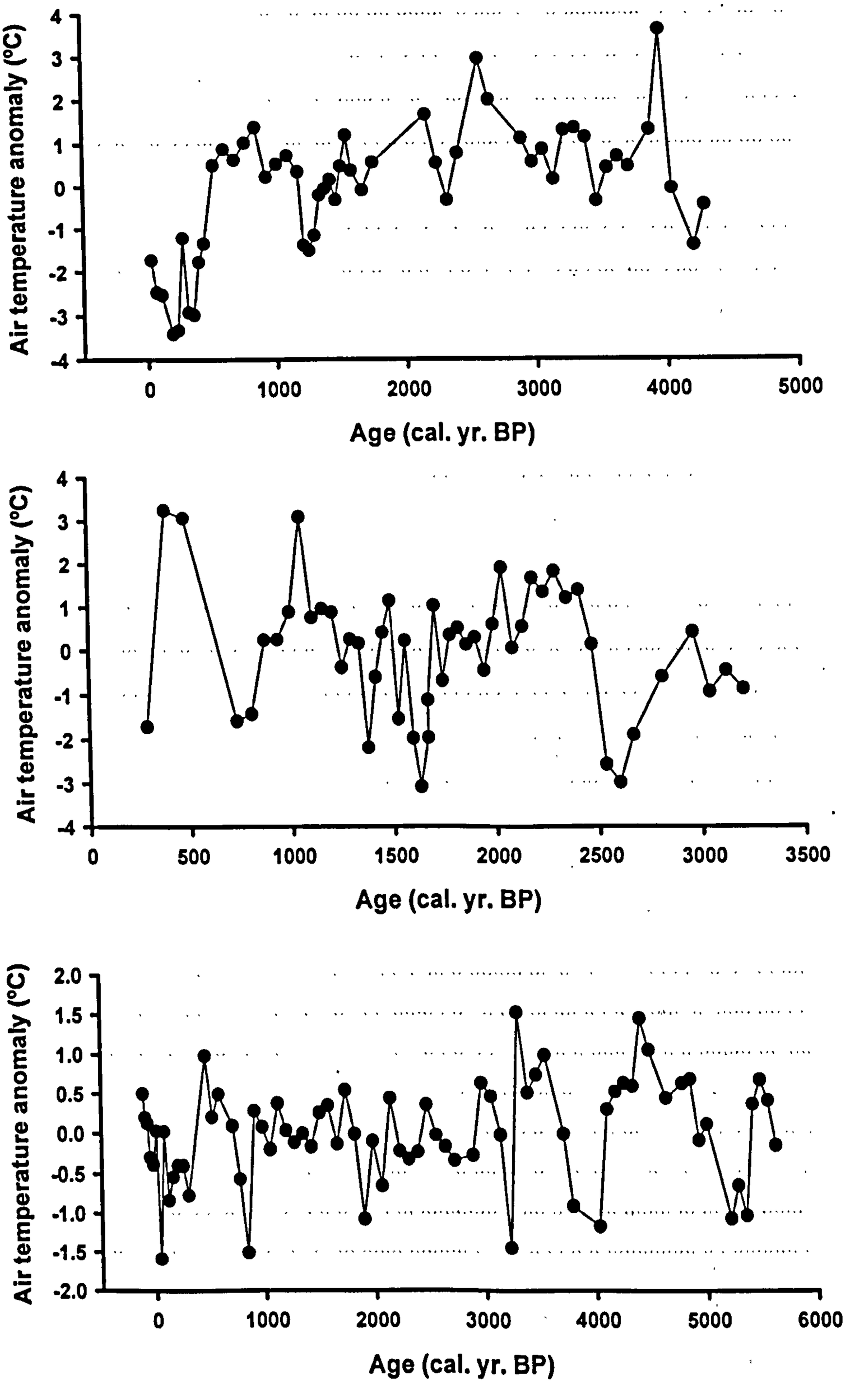

Figure 8.14 Reconstructed surface air temperature anomalies for each of the European sites using $\delta^{18}O_{precipitation}$ -temperature coefficients derived from *raw monthly resolution* modern GNIP data (Chapter 3) (Walton Moss = A, Dosenmoor = B, Raheenmore = C)

Whilst confidence remains in the reconstruction of palaeo-precipitation from *Sphagnum* concentrate isotopic composition, it is less clear how this relates to variation in surface air temperature from sites in northern Europe at least. Despite evidence from both empirical and model-based studies that temperature plays a key role in control of the isotopic composition of precipitation in the mid-latitudes, GNIP data from the sites used here demonstrate that the method used to derive a linear relationship can produce varying results. Whilst regression using monthly resolution data provides a linear relationship that is less well correlated than that for monthly means, the temperature change estimates at all sites are more realistic in comparison with a wealth of other studies. The likelihood that any relationship will have varied over time with changing atmospheric circulation patterns also draws into question the application of relationships based on comparatively short-term datasets.

8.8 *Modelling the 8200 BP cold event*

8.8.1 Newfoundland

In Newfoundland, the dominant temperature signal in the raw monthly resolution GNIP data allows for more confident palaeotemperature reconstruction than that in Europe, without the need to define a relationship based on monthly means (Chapter 3; Figure 3.35). The temperature estimation here is focussed on the 8200 BP event. The 8200 BP event has assumed a position of importance owing to it being the largest climatic change recorded in the northern hemisphere in the last 10,000 years and because the cause is thought to be known, hence offering the ideal opportunity for the testing of climate models (Chapter 2). Temperature estimation across the 8200 BP event requires not only data on variation in the isotopic composition of *Sphagnum* cellulose but also knowledge of past variation in the isotopic composition of the oceanic source water. The latter arose due to the influx of 163,000 km^3 of isotopically depleted meltwater from glacial Lake Agassiz (Teller *et al.*, 2002). Results in Chapter 7 revealed that the climatic response over Newfoundland during this period was characterised by a double episode isotopic excursion, with a primary decline of larger magnitude than a secondary decline ~200 years later (Chapter 7).

The decrease in surface air temperature during the primary event (Figure 7.32) is calculated using the modern relationship $\Delta T = 2.28\ \Delta\delta^{18}O_{precipitation}$ (Figure 3.35), correcting for the isotopic decrease in oceanic source water. Deep-sea cores with an accumulation rate sufficient to resolve the change in oceanic $\delta^{18}O$ composition are scarce. One study from the Gardar drift southwest of Iceland provides a suitable record of change in $\delta^{18}O_{seawater}$ (Ellison *et al.*, 2006) (Figure 8.15). Alignment of the $\delta^{18}O_{seawater}$ curve for marine core MD99-2251 (Ellison *et al.*, 2006) with NDN02/1 (Figure 8.16) suggests a maximum source-water correction of 0.75‰. Alignment is made possible by the imposition of an offset to the $\delta^{18}O_{seawater}$ of minus 100 years. This offset is consistent with that applied in Ellison *et al.* (2006), lies within the dating uncertainties of both NDN02/1 and MD99-2251, and yields good agreement between ocean-freshening events and cooling over Newfoundland. Hence, it is estimated that for the recorded change of 4.63‰ in core NDN02/1 during the primary event, the average temperature during the *Sphagnum* growing season fell by 8.9 ± 3.5°C (1σ; obtained by application of $\Delta T = 2.28\ \Delta\delta^{18}O_{precipitation}$ to the upper and lower limits of palaeo-precipitation reconstruction). Estimates of the temperature depression over Greenland during the 8200 BP event, by comparison, are 5.4-11.7°C, with a best estimate of 7.4°C (Leuenberger *et al.*, 1999).

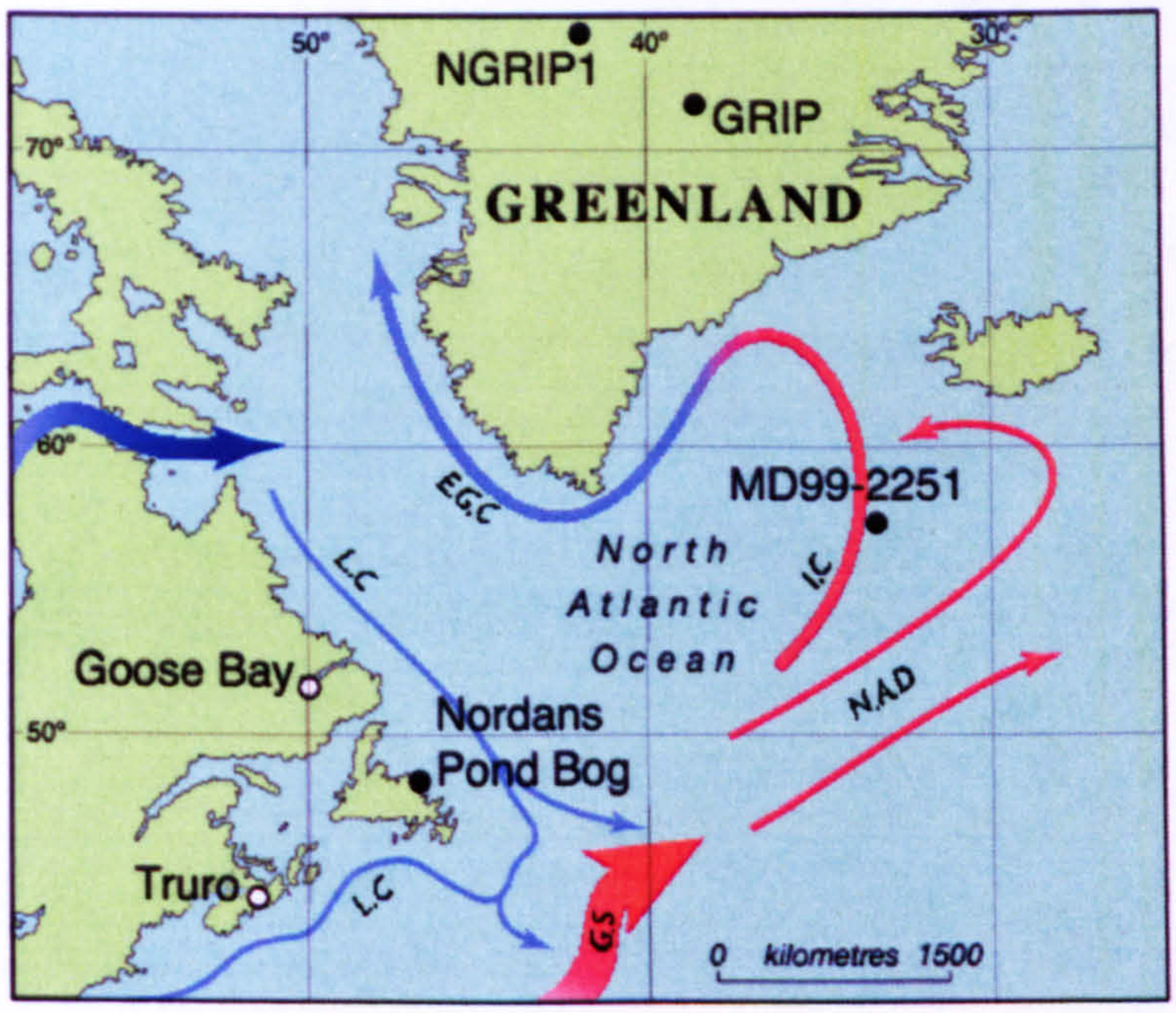

Figure 8.15 Map of the Northwest Atlantic showing modern ocean-surface currents, Glacial Lake Agassiz outflow and site locations. Shown are the core locations (solid circles), GNIP monitoring stations at Goose Bay, Labrador and Truro, Nova Scotia (open circles), modern ocean-surface currents (red lines = warm currents; blue lines = cold currents; L.C. = Labrador Current, G.S. = Gulf Stream, N.A.D. = North Atlantic Drift, E.G.C = East Greenland Current, I.C. = Irminger Current) and routing of the final drainage from Glacial Lake Agassiz ~8450 years ago (Barber *et al.*, 1999) (bold blue arrow).

The possibility that the observed decrease in $\delta^{18}O_{precipitation}$ reflected a change in source-water composition without any temperature change is discounted given that the response was too large and too protracted merely to reflect the evaporating meltwater plume from the initial megaflood. Similarly, the signal is not derived from a change in source water to represent sublimation from an extended perennial ice pack. Ocean cores from the Labrador Sea and the Grand Banks indicate that phytoplankton continued to flourish throughout the event and hence demonstrate that the ocean was free of perennial ice (de Vernal and Hillaire-Marcel, 2006).

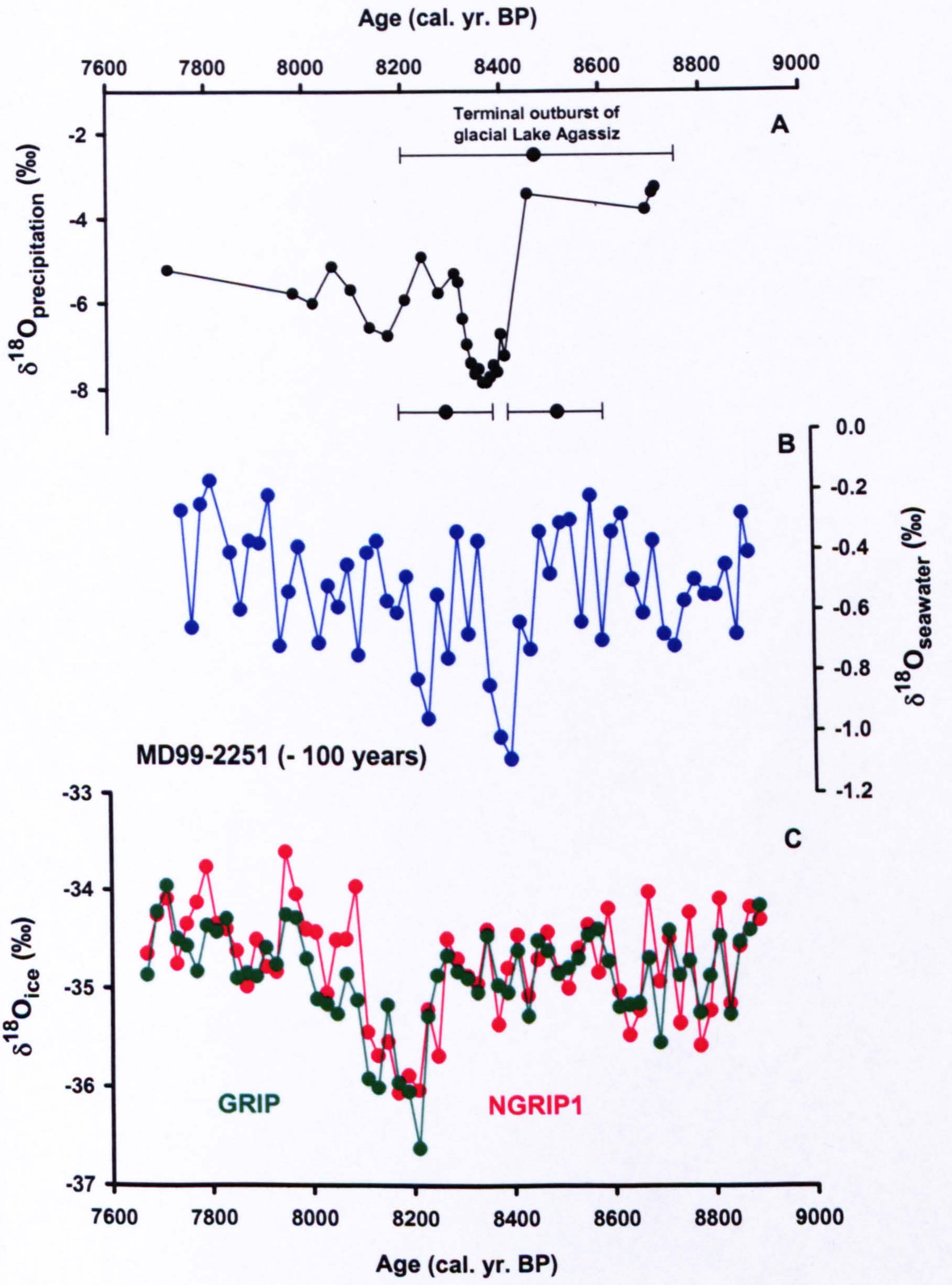

Figure 8.16 Atmospheric response over Newfoundland (A) compared with North Atlantic seawater freshening (Ellison *et al.*, 2006) offset by minus 100 years (B) and two recently synchronised isotope records (C) from Greenland ice cores (Vinther *et al.*, 2006; Rasmussen *et al.*, 2006) covering the period 9000 to 7600 BP. Chronological uncertainty in (C) assumes a layer-counting error of 47 yr throughout this time period (Vinther *et al.*, 2006).

It is not possible to perform the same temperature reconstruction using the deuterium data as no ocean correction is available. Ocean data are typically derived from foraminiferal calcite that only yields information on variations in $\delta^{18}O_{seawater}$. Uncorrected estimates of temperature change from core NDN02/1 are, however, very similar ($\delta^{18}O$ = 10.6°C; δD = 11.1°C, using $\Delta T = 0.30\ \Delta\delta D_{precipitation}$), firstly supporting the assertion that the isotopic record in *Sphagnum* cellulose reflects the isotopic composition of precipitation and secondly supporting the magnitude of the change.

The estimate of cooling in surface air temperatures during the primary event is the largest robust cooling estimate for the "8200-yr event" from the entire circum-North Atlantic region (Alley *et al.*, 1997; Klitgaard-Kristensen *et al.*, 1998; von Grafenstein *et al.*, 1998), but not outside the ranges of temperature change estimated for Greenland (Leuenberger *et al.*, 1999). Recent simulations with earth-system models (Wiersma and Renssen, 2006; LeGrande *et al.*, 2006) exhibit strong cooling and decreased $\delta^{18}O_{precipitation}$ over the study area in response to catastrophic drainage of Glacial Lake Agassiz. The magnitude of the isotopic and temperature changes recorded in core NDN02/1, however, greatly exceeds that predicted by state-of-the-art numerical models.

The double cooling response observed in the oxygen record (Figure 7.32) offers an appealing chance to speculate on the cause of the atmospheric response observed. It has already been argued that the response cannot have been caused solely by a change in $\delta^{18}O_{seawater}$. Variability in solar output (Bond *et al.*, 2001; Muscheler *et al.*, 2004) is discounted as the sole cause of the temperature decrease since the observed 207-yr cyclicity of ^{10}Be and ^{14}C is too long to account for the abrupt variations found in core NDN02/1. If solar variability is not the dominating factor, the only other viable contender for driving and sustaining change over centennial time-scales is variation in the MOC of the North Atlantic (Maslin *et al.*, 2003).

Considering the $\delta^{18}O$ data alone, two mechanisms can be proposed to account for the double cooling event in Newfoundland. The first involves a direct response of the coupled ocean-atmosphere system to a postulated two-stage drawdown of Glacial Lake Agassiz (Teller *et al.*, 2002; Clarke *et al.*, 2004). According to this model, 163,000 km^3 of freshwater were released in two discrete jökulhlaups of ~1-yr duration, with discharges of 3.6 Sv and 1.6 Sv,

respectively, separated by an interval of ~10-50 yr. Whilst it remains unclear whether these two outbursts would have followed the same pathway, there is good evidence for flooding through the Hudson Strait (Kerwin, 1996; Barber *et al.*, 1999). Pulsed meltwater release (Teller *et al.*, 2002; Clarke *et al.*, 2004) was invoked to explain a double minimum in $\delta^{18}O_{seawater}$ reconstructed from marine core MD99-2251 (Ellison *et al.*, 2006). The ages of the two isotopic excursions in core NDN02/1 fall within the chronological error of this two-phase reduction in sea-surface salinity (Ellison *et al.*, 2006) (Figure 8.16). The ~200 yr spacing between the $\delta^{18}O$ minima in both records also implies synchroneity, but is significantly longer than the interval between the two postulated flood pulses.

The second mechanism involves a non-linear response of the MOC, either to a single megaflood (Manabe and Stouffer, 1995) or to sustained re-routing of glacial meltwater through the Hudson Strait (Barber *et al.*, 1999; Teller *et al.*, 2002; Meissner and Clark, 2006). Two-phase weakening of the MOC in response to a single massive meltwater injection has been reported previously (Manabe and Stouffer, 1995). In this simulation, the initial slowdown of the MOC was associated with a maximum cooling of sea-surface temperatures (SSTs) 10-20 years after the imposed freshwater perturbation. The second cooling was less severe and involved a more gradual recovery of both SSTs and MOC. This structure resembles the air-temperature response found in NDN02/1. On the other hand, the prolonged change in meltwater routing after 8450 BP may have had a much greater impact on the MOC than the short-lived flood event itself (Meissner and Clark, 2006). It can be speculated that the MOC responded to the catastrophic drainage of Glacial Lake Agassiz and the subsequent increase in freshwater flux through the Hudson Strait with a complex oscillation that led to a two-phase decrease in air temperatures over Newfoundland.

Deuterium data from the same core (Figure 7.37) suggest that atmospheric circulation may have altered between the two $\delta^{18}O$ minima. Whilst both tracers provide evidence for a primary anomaly of similar magnitude and duration, a second anomaly in δD is not observed at the same time as that in $\delta^{18}O$. This may represent a change in the deuterium excess indicative of a change in mean vapour source. δD values remain stable relative to falling $\delta^{18}O$ values during the second oxygen excursion, reflecting an increase in the deuterium excess. It has been noted previously that deuterium excess estimates from these data must be interpreted

with caution as the excess is effectively represented by scatter either side of the regression line (Figure 8.10). Where a series of data show a prolonged anomaly in one direction, it is more likely that the change reflects variation in the deuterium excess than analytical noise. High values of deuterium excess are observed in areas where precipitation is derived from a relatively arid source region (Chapter 2). Re-evaporation of moisture from continental interiors is an arid source region relative to the ocean and consequently the source vapour precipitated from these regions exhibits high deuterium excess. More generally, however, high deuterium excess indicates a vapour source with low relative humidity and occasionally low temperature. The data suggest then that the second anomaly may have been coincident with an increase in moisture sourced from a more arid vapour source. It seems likely that the second $\delta^{18}O$ minimum therefore represents a secondary atmospheric anomaly possibly induced by oceanic circulation changes of the first.

If the processes responsible for producing both minima in the Newfoundland record (Figure 8.16) were different this might explain the >200 yr gap between the megaflood and the detection of a cooling signal in Greenland. A cluster of five ^{14}C AMS dates in NDN02/1 places the start of the primary isotopic event occurring ~8450 BP in close agreement with best estimates of the date of the megaflood. This response may have been forced by the direct impact of reduced heat transport due to a slowdown of the MOC. The second minimum may reflect atmospheric circulation changes involving alteration of the atmospheric conditions overlying the main moisture source for precipitation over Newfoundland. This would be consistent with a reduction in the sourcing of low-latitude moist air masses to Greenland resulting in the cooling observed in multiple ice core records (Thomas *et al.*, 2007) corresponding to the second cooling in Newfoundland.

With limited confidence in the deuterium excess data it is impossible to say for certain whether the two $\delta^{18}O$ minima reflect different atmospheric processes or a direct response to non-linear forcing of climate by the coupled ocean-atmosphere. If the second response was transmitted through changes in atmospheric circulation and represents the wider circum-North Atlantic signal, the primary response in Newfoundland seems too large to reflect purely a local signal. More plausible in the absence of additional evidence is that the primary event in

Newfoundland is coincident with the event in Greenland and that the apparent age difference relates to limitations in chronological control.

8.8.2 Europe

The absence of *Sphagnum* in sufficient quantities in all of the early-Holocene European cores was a limiting factor on isotopic characterisation of this period. Whilst the record from Dosenmoor is ombrotrophic only as far as 5800 BP, the records from Walton Moss and Raheenmore were explored to significant depth and higher resolution (4cm) in the sections dated by ^{14}C AMS measurements to correspond to the period surrounding the event.

Both European records show evidence of increasing BSW consistent with an atmospheric response during this period. This is expressed more readily in the plant macrofossil record from Raheenmore. Although sub-fossil *Sphagnum* remains indicative of bog pool development are found in only a single sample, the macrofossil record reveals a distinct phase of increasing BSW through increasing *Rhyncospora alba* and lowering ericaceous remains over a ~200 year period (~8070-7890 BP) that is interpreted as a floral response to climatically induced hydrological change(section 6.4.1). The duration of the response and its magnitude relative to proximal sediments in the core (Figure 6.20) strongly suggest causal association with responses observed across the circum-North Atlantic region at this time.

The response in Walton Moss is relatively subdued compared with that at Raheenmore which may reflect higher water transport rates from the surface due to insufficiently developed catatelmic peat in this early-stage of ombrotrophic peat growth (Hughes and Barber, 2004). A response towards increased BSW is, however, observed in the record at ~7800 BP by an anomalous appearance of *Sphagnum*, consistent with a previous record from the site (Hughes *et al.*, 2000). The detection of a signal in both Ireland and northern England after 8000 BP questions the nature of the association with other circum-North Atlantic changes. BSW is an indicator of water balance. Previous studies suggest colder and drier conditions prevailed over NW Europe in response to forcing by slow down of MOC (Alley and Agustsdottir, 2005; Wiersma and Renssen, 2006; LeGrande *et al.*, 2006). The detection of an increased water

balance regionally ~7800-8000 BP may be indicative of the return of moisture transport to these latitudes coincident with re-invigoration of the THC in a process that allowed moisture transport to increase in advance of temperature rise and consequently express as a wet shift in the bog records.

8.9 *Is BSW forced by temperature?*

It has been demonstrated that variation in raised bog *Sphagnum* cellulose approximates variation in the isotopic composition of precipitation from sites both in NW Europe and Newfoundland (section 8.5). It has also been demonstrated that there is significant covariance of BSW records and isotopic records suggesting a common climatic driver (section 8.3). So for BSW to be driven by temperature, the isotopic composition of precipitation must also be driven by temperature.

The strong relationship between isotopic composition of precipitation and temperature in the modern day in Newfoundland suggests that a link between bog isotopic records and temperature can be established (section 8.8.1). However, it is evident that more research is required to establish the link between temperature and the isotopic composition of precipitation in the modern day from sites in Europe. Considerable uncertainty associated with palaeotemperature estimation from sites in Europe arises due to the estimation of unrealistic temperature changes during the Holocene using modern relationships based on long term monthly means in GNIP datasets (section 8.7). Unlike previous studies using the stable isotopic analyses of peat material, the amplitude of these palaeotemperature estimates cannot be due to signal amplification by variation in the proportions of vascular to non-vascular plant remains. Rather, it is associated with uncertainty in the applicability of modern ΔT- $\Delta\delta^{18}O_{precipitation}$ relationships (section 8.7).

The difficulty in establishing the relationship between the isotopic composition of precipitation and temperature for application over Holocene timescales should not be seen as a shortfall in the information provided by the palaeodata. Arguably, the pursuit of functions to predict a single variable may distract from the added information contained in the raw

isotopic data on palaeo-atmospheric circulation which may itself provide clearer insight on the causes of change than any one variable alone. It is evident from the data in this study that location plays a key role in interpretation of the link between isotopes and climate. Differences observed at Raheenmore for example may reflect real differences between water balance and the drivers of isotopic change in precipitation. Conversely, if temperature is the principle driver of centennial variation in $\delta_{palaeo\text{-}precipitation}$ in northern England and northern Germany, then the records suggest a very direct relationship between these variables. With the short timescale of calibration data, it is not possible to confirm or reject the hypothesis that variation in bog surface wetness (BSW) records reflects variation in mean growing season temperatures. However, the data do strongly support the conclusion that variation in BSW records reflects variation in the isotopic composition of palaeo-precipitation, representing a significant advance on previous understanding of the isotopic record preserved in raised peat.

9 Conclusions and future research

9.1 *Specific conclusions from the research*

The central questions of this research were proposed in Chapter 1 and were as follows:

1) How does the isotopic composition of *Sphagnum* cellulose relate to the isotopic composition of precipitation?
2) How does variability in the isotopic composition of palaeo-*Sphagnum* cellulose relate to variation in past bog surface wetness?
3) How have spatial isotopic gradients varied in the past and what information do these provide on the mechanisms of change throughout the Holocene?
4) How have palaeotemperatures varied during key Holocene climatic changes?
5) Is temperature the primary driver of BSW?

From the findings in this study it is now possible to conclude the following:

1) Variation in the stable isotopic composition of *Sphagnum* cellulose derived from *Sphagnum* concentrates closely approximates that of precipitation. The signal preserved in palaeo-*Sphagnum* cellulose therefore approximates a record of past variation in the isotopic composition of precipitation with an isotopic clarity closer to that of ice core data than is presently available in other terrestrial archives.
2) The isotopic signal in palaeo-*Sphagnum* cellulose largely co-varies with BSW. Although the strength of the correlation shows variability, the data suggest that the driver of isotopic composition in precipitation over centennial to millennial timescales in mid-latitude Holocene peatlands is also the primary driver of change in BSW.
3) There is evidence that climatic changes reproduced regionally in records of past bog surface wetness and isotopic variability, and associated with millennial cyclicity, were expressed with increasing magnitude with distance from the North Atlantic Ocean.

During climatic deterioration ~2700 BP, it is possible that a deterioration of similar magnitude was observed in northern England later than in northern Germany suggesting a spatially transgressive mechanism. Records from Ireland, northern England and Newfoundland reveal evidence for centennial scale deterioration in climate in the early Holocene. In the European sites, the climatic response occurs between ~8000 – 7800 BP. In Newfoundland, a complex two-phase climatic response is observed beginning ~8450 BP which may have been the product both of the direct effects of THC variation and secondary effects due to changes in atmospheric circulation. Estimation of the temperature depression over land due to THC weakening represents a significant advance both in the nature of the palaeoclimatic information derived from peatlands and in understanding of the mechanisms responsible for the 8200 BP event.

4) Using ΔT- $\Delta\delta^{18}O_{precipitation}$ relationships based on longer term monthly mean GNIP data, palaeotemperature estimates from *Sphagnum* cellulose isotopic data yield temperature anomalies that are unrealistic for the Holocene. The use of raw monthly GNIP data provides much more realistic estimates from all study sites. Whilst modern ΔT- $\Delta\delta^{18}O_{precipitation}$ relationships have been employed with success from polar locations, the applicability of these approaches in the European study areas requires more research.
5) It has been demonstrated that the primary driver of change in the isotopic composition of precipitation is the dominant driver of change in BSW (conclusion 2) and that over the modern timescales of measurement, the correlation with temperature is stronger than that with precipitation (Chapter 3) (IAEA/WMO, 2004). However, it is not possible to conclude that either temperature or precipitation is the primary driver of BSW change using *Sphagnum* isotopic data due to the absence of a robust modern linear correspondence between these variables that is likely to have prevailed throughout the Holocene.

9.2 *Methodological appraisal and future directions*

At the start of this project, a new technique for the on-line stable isotopic analysis of hydrogen had not yet been developed (Filot *et al.*, 2006). Consequently, there was a requirement for a preparation procedure able to isolate *Sphagnum* from the peat matrix in sufficient quantities to allow analysis of both oxygen and hydrogen stable isotopes using existing methods. This led to testing of the *Sphagnum* concentrate preparation procedure (Chapter 4). With the significant reduction in material now required for analysis through the development of the new on-line equilibration procedure for hydrogen analysis, *both* oxygen and hydrogen can now be analysed on only a few mg of dry alpha-cellulose. This low mass requirement offers new potential for the use of picked samples and even the possibility for discrimination against *Sphagnum* stems or leaves from a core sample. Whilst *Sphagnum* concentrates have been demonstrated to approximate closely pure *Sphagnum* isotopic variability, use of pure *Sphagnum* would eliminate a potential source of uncertainty in the palaeoclimatic reconstruction. Much greater quantitative control of error margins could be achieved through combined modern and palaeo investigation. Comparison of the variability between modern and palaeo samples, for example, in *n* number of modern plants, then *n* number of picked plants from a core would allow for comparison of palaeo versus modern noise estimates and improved understanding of the nature of the isotopic signal in *Sphagnum* moss.

In this study, resources were not sufficient to allow for leaf water analysis of modern *Sphagnum* samples. It has been demonstrated in this project that the isotopic composition of leaf water used for cellulose synthesis approximates that of precipitation more closely than bog surface water and furthermore that *Sphagnum* does not reflect evaporative enrichment during summer months to the same degree as that observed in surface waters. A crucial next step for future research is to explore variability in moss water and precipitation data and in particular assess processes taking place during dry phases when moss has been observed to suspend photosynthesis (Williams, 1996). Such investigation will yield data on the seasonality of the preserved signal and allow palaeo-variation to be attributed to either annual change, or summer/winter change. The case for the importance of such information on seasonality has been described previously (Denton *et al.*, 2005).

It has been demonstrated that isotopic analysis of *Sphagnum* moss has the potential to provide palaeotemperature estimates through the Holocene. The major limiting factor on the reliability of these estimates resides with understanding of the relationship between temperature and the isotopic composition of precipitation. This has two elements. Firstly, there is uncertainty associated with the prevalence of any relationship over time. Secondly, the modern relationships constructed over short timescales can yield unrealistic palaeoestimates. The first source of uncertainty can be approached through the combined analysis of both oxygen and hydrogen data from core *Sphagnum* samples. If variation in both isotopic tracers follows a line of slope similar to the modern MWL, confidence is gained that the reconstruction is of the isotopic composition of palaeoprecipitation and also that the prevailing moisture trajectory has not significantly changed over time. If moisture trajectory has not significantly changed, variation should be due to changes in the temperature of condensation or ocean water isotopic composition. The second source of uncertainty requires improved clarification of the link between temperature and isotopic composition of precipitation, particularly for sites in Europe. Indefinite extension of modern records of the isotopic composition of precipitation and meteorological variables under the IAEA/WMO GNIP programme will assist greatly by lengthening the records used for calibration.

References

Aaby,B. and Tauber,H., 1975. Rates of peat formation in relation to degree of humification and local environment, as shown by studies of a raised bog in Denmark. Boreas, 4: 1-14.

Aaby,B., 1976. Cyclic climatic variations in climate over the past 5,500 yr reflected in raised bogs. Nature, 263(5575): 281-284.

Alley,R.B. and Agustsdottir,A.M., 2005. The 8k event: cause and consequences of a major Holocene abrupt climate change. Quat. Sci. Rev., 24(10-11): 1123-1149.

Alley,R.B., Marotzke,J., Nordhaus,W.D., Overpeck,J.T., Peteet,D.M., Pielke,R.A., Pierrehumbert,R.T., Rhines,P.B., Stocker,T.F., Talley,L.D., and Wallace,J.M., 2003. Abrupt climate change. Science, 299(5615): 2005-2010.

Alley,R.B., Mayewski,P.A., Sowers,T., Stuiver,M., Taylor,K.C., and Clark,P.U., 1997. Holocene climatic instability: A prominent, widespread event 8200 yr ago. Geology, 25(6): 483-486.

Andersen,C., Koc,N., and Moros,M., 2004. A highly unstable Holocene climate in the subpolar North Atlantic: evidence from diatoms. Quat. Sci. Rev., 23(20-22): 2155-2166.

Anderson,W.T., Bernasconi,S.M., McKenzie,J.A., Saurer,M., and Schweingruber,F., 2002. Model evaluation for reconstructing the oxygen isotopic composition in precipitation from tree ring cellulose over the last century. Chem. Geol., 182(2-4): 121-137.

Appleby, P.G., 2001. Chronostratigraphic techniques in recent sediments. In: W.M.Last and J.P.Smol (Editors), Tracking Environmental Change Using Lake Sediments; Basin Analysis, Coring, and chronological techniques. Kluwer Academic.

Appleby, P.G. and Oldfield, F., 1992. Application of lead-210 to sedimentation rate studies. In: M.Ivanovich and R.S.Harman (Editors), Uranium-series disequilibrium: applications to earth, marine and environmental sciences. Clarendon Press, Oxford.

Araguas-Araguas,L., Froehlich,K., and Rozanski,K., 1998. Stable isotope composition of precipitation over southeast Asia. J. Geophys. Res. Atmos., 103(D22): 28721-28742.

Araguas-Araguas,L., Froehlich,K., and Rozanski,K., 2000. Deuterium and oxygen-18 isotope composition of precipitation and atmospheric moisture. Hydrological Processes, 14(8): 1341-1355.

Aravena,R., Suzuki,O., Pena,H., Pollastri,A., Fuenzalida,H., and Grilli,A., 1999. Isotopic composition and origin of the precipitation in Northern Chile. Applied Geochemistry, 14(4): 411-422.

Aravena,R. and Warner,B.G., 1992. O-18 Composition of Sphagnum, and Microenvironmental Water Relations. Bryologist, 95(4): 445-448.

Aucour,A.M., HillaireMarcel,C., and Bonnefille,R., 1996. Oxygen isotopes in cellulose from modern and quaternary intertropical peatbogs: Implications for palaeohydrology. Chem. Geol., 129(3-4): 341-359.

Baertschi,P., 1976. Absolute O-18 Content of Standard Mean Ocean Water. Earth Planet. Sci. Lett., 31(3): 341-344.

Baillie,M.G.L., 1994. Dendrochronology raises questions about the nature of the AD 536 dust-veil event. Holocene, 4: 212-217.

Baillie,M.G.L., 2007. The case for significant numbers of extraterrestrial impacts through the late Holocene. J. Quat. Sci, 22(2): 101-109.

Baillie, M.G.L. and Brown, D.M., 2003. Dendrochronology and the reconstruction of fine-resolution environmental change in the Holocene. In: A.Mackay, R.W.Battarbee, J.Birks, and F.Oldfield (Editors), Global Change in the Holocene. Arnold, London, pp. 75-91.

Barbante,C., Barnola,J.M., Becagli,S., Beer,J., Bigler,M., Boutron,C., Blunier,T., Castellano,E., Cattani,O., Chappellaz,J., hl-Jensen,D., Debret,M., Delmonte,B., Dick,D., Falourd,S., Faria,S., Federer,U., Fischer,H., Freitag,J., Frenzel,A., Fritzsche,D., Fundel,F., Gabrielli,P., Gaspari,V., Gersonde,R., Graf,W., Grigoriev,D., Hamann,I., Hansson,M., Hoffmann,G., Hutterli,M.A., Huybrechts,P., Isaksson,E., Johnsen,S., Jouzel,J., Kaczmarska,M., Karlin,T., Kaufmann,P., Kipfstuhl,S., Kohno,M., Lambert,F., Lambrecht,A., Lambrecht,A., Landais,A., Lawer,G., Leuenberger,M., Littot,G., Loulergue,L., Luthi,D., Maggi,V., Marino,F., Masson-Delmotte,V., Meyer,H., Miller,H., Mulvaney,R., Narcisi,B., Oerlemans,J., Oerter,H., Parrenin,F., Petit,J.R., Raisbeck,G., Raynaud,D., Rothlisberger,R., Ruth,U., Rybak,O., Severi,M., Schmitt,J., Schwander,J., Siegenthaler,U., Siggaard-Andersen,M.L., Spahni,R., Steffensen,J.P., Stenni,B., Stocker,T.F., Tison,J.L., Traversi,R., Udisti,R., Valero-Delgado,F., van den Broeke,M.R., van de Wal,R.S.W., Wagenbach,D., Wegner,A., Weiler,K., Wilhelms,F., Winther,J.G., and Wolff,E., 2006. One-to-one coupling of glacial climate variability in Greenland and Antarctica. Nature, 444(7116): 195-198.

Barber,D.C., Dyke,A., Hillaire-Marcel,C., Jennings,A.E., Andrews,J.T., Kerwin,M.W., Bilodeau,G., McNeely,R., Southon,J., Morehead,M.D., and Gagnon,J.M., 1999. Forcing of the cold event of 8,200 years ago by catastrophic drainage of Laurentide lakes. Nature, 400(6742): 344-348.

Barber,K.E., 1981. Peat stratigraphy and climate change. A palaeoecological test of the theory of cyclic peat bog regeneration. Balkema, Rotterdam.

Barber, K.E., 2006. Peatland records of Holocene climate change. In: S.Elias (Editor), Encyclopedia of Quaternary Science. Elsevier, Oxford, pp. 1883-1894.

Barber, K.E., 2007. Peatland records of Holocene climate change. In: S.Elias (Editor), Encyclopedia of Quaternary Science. Elsevier, Oxford, pp. 1883-1894.

Barber,K.E., Chambers,F.A., Maddy,D., Stoneman,R.E., and Brew,J.S., 1994. A sensitive high-resolution record of Late Holocene climatic change from a raised bog in Northern England. Holocene, 4: 198-205.

Barber,K.E., Chambers,F.M., and Maddy,D., 2003. Holocene palaeoclimates from peat stratigraphy: macrofossil proxy climate records from three oceanic raised bogs in England and Ireland. Quat. Sci. Rev., 22(5-7): 521-539.

Barber,K.E., Chambers,F.M., and Maddy,D., 2004. Late Holocene climatic history of northern Germany and Denmark: peat macrofossil investigations at Dosenmoor, Schleswig-Holstein, and Svanemose, Jutland. Boreas, 33(2): 132-144.

Barber, K.E. and Charman, D.J., 2003. Holocene palaeoclimate records from peatlands. In: A.Mackay, R.W.Battarbee, H.J.B.Birks, and F.Oldfield (Editors), Global Change in the Holocene. Arnold, London, pp. 210-226.

Barber,K.E., Dumayne-Peaty,L., Hughes,P., Mauquoy,D., and Scaife,R., 1998. Replicability and variability of the recent macrofossil and proxy-climate record from raised bogs: field stratigraphy and macrofossil data from Bolton Fell Moss and Walton Moss, Cumbria, England. J. Quat. Sci, 13(6): 515-528.

Barber,K.E. and Langdon,P.G., 2007. What drives the peat-based palaeoclimate record? A critical test using multi-proxy records from northern Britain. Quat. Sci. Rev., *in review*.

Barber,K.E., Maddy,D., Rose,N., Stevenson,A.C., Stoneman,R., and Thompson,R., 2000. Replicated proxy-climate signals over the last 2000 yr from two distant UK peat bogs: new evidence for regional palaeoclimate teleconnections. Quat. Sci. Rev., 19(6): 481-487.

Barbour,M.M., 2007. Stable oxygen isotope composition of plant tissue: a review. Functional Plant Biology, 34(2): 83-94.

Barbour,M.M., Andrews,T.J., and Farquhar,G.D., 2001. Correlations between oxygen isotope ratios of wood constituents of Quercus and Pinus samples from around the world. Australian Journal of Plant Physiology, 28(5): 335-348.

Barbour,M.M., Roden,J.S., Farquhar,G.D., and Ehleringer,J.R., 2004. Expressing leaf water and cellulose oxygen isotope ratios as enrichment above source water reveals evidence of a Peclet effect. Oecologia, 138(3): 426-435.

Barbour,M.M., Walcroft,A.S., and Farquhar,G.D., 2002. Seasonal variation in delta C-13 and delta O-18 of cellulose from growth rings of Pinus radiata. Plant Cell and Environment, 25(11): 1483-1499.

Beck,J.W., Richards,D.A., Edwards,R.L., Silverman,B.W., Smart,P.L., Donahue,D.J., Hererra-Osterheld,S., Burr,G.S., Calsoyas,L., Jull,A.J.T., and Biddulph,D., 2001. Extremely large variations of atmospheric C-14 concentration during the last glacial period. Science, 292(5526): 2453-2458.

Beer,J., Mende,W., and Stellmacher,R., 2000. The role of the sun in climate forcing. Quat. Sci. Rev., 19(1-5): 403-415.

Bennett,C.F. and Timmell,T.E., 1955. Preparation of cellulose trinitrate. Svensk Papperstidning, 58: 281-286.

Bennett,K.D., 1996. Determination of the number of zones in a biostratigraphical sequence. New Phytologist, 132(1).

Beveridge,N.A.S., Elderfield,H., and Shackleton,N.J., 1995. Deep Thermohaline Circulation in the Low-Latitude Atlantic During the Last Glacial. Paleoceanography, 10(3): 643-660.

Bianchi,G.G. and McCave,I.N., 1999. Holocene periodicity in North Atlantic climate and deep-ocean flow south of Iceland. Nature, 397(6719): 515-517.

Birks, H.J.B., 1995. Quantitative palaeoenvironmental reconstructions. In: D.Maddy and J.S.Brew (Editors), Statistical modelling of quaternary science data. QRA Technical guide 5. Quaternary Research Association, Cambridge.

Blaauw,M., van Geel,B., Mauquoy,D., and van der Plicht,J., 2004. Carbon-14 wiggle-match dating of peat deposits: advantages and limitations. J. Quat. Sci, 19(2).

Blackford,J.J. and Chambers,F.C., 1991. Proxy records of climate change from blanket mires: Evidence for a Dark Age (1400BP) climatic deterioration in the British Isles. The Holocene, 1.

Blackford, J.J. and Chambers, F.C., 1993a. Peat bogs as sources of proxy climatic data: past approaches and future research. In: Climate change and human impact on the landscape. Chapman & Hall.

Blackford,J.J. and Chambers,F.M., 1993b. Determining the degree of peat decomposition for peat-based palaeoclimatic studies. International Peat Journal, 5: 7-24.

Blackford,J.J. and Chambers,F.M., 1995. Proxy Climate Record for the Last 1000 Years from Irish Blanket Peat and A Possible Link to Solar Variability. Earth Planet. Sci. Lett., 133(1-2): 145-150.

Blundell,A. and Barber,K., 2005. A 2800-year palaeoclimatic record from Tore Hill Moss, Strathspey, Scotland: the need for a multi-proxy approach to peat-based climate reconstructions. Quat. Sci. Rev., 24(10-11): 1261-1277.

Blunier,T., Chappellaz,J., Schwander,J., Dallenbach,A., Stauffer,B., Stocker,T.F., Raynaud,D., Jouzel,J., Clausen,H.B., Hammer,C.U., and Johnsen,S.J., 1998. Asynchrony of Antarctic and Greenland climate change during the last glacial period. Nature, 394(6695): 739-743.

Bobrov,A.A., Charman,D.J., and Warner,B.G., 1999. Ecology of testate amoebae (Protozoa : Rhizopoda) on peatlands in western Russia with special attention to niche separation in closely related taxa. Protist, 150(2): 125-136.

Bobrov,A.A., Charman,D.J., and Warner,B.G., 2002. Ecology of testate amoebae from oligotrophic peatlands: Specific features of polytypic and polymorphic species. Biology Bulletin, 29(6): 605-617.

Boggie,R., Knight,A.H., and Hunter,R.F., 1958. Studies of the root development of plants in the field using radioactive tracers. J. Ecol., 46.

Bond,G., Kromer,B., Beer,J., Muscheler,R., Evans,M.N., Showers,W., Hoffmann,S., Lotti-Bond,R., Hajdas,I., and Bonani,G., 2001. Persistent solar influence on north Atlantic climate during the Holocene. Science, 294(5549): 2130-2136.

Bond,G., Showers,W., Cheseby,M., Lotti,R., Almasi,P., deMenocal,P., Priore,P., Cullen,H., Hajdas,I., and Bonani,G., 1997. A pervasive millennial-scale cycle in North Atlantic Holocene and glacial climates. Science, 278(5341): 1257-1266.

Borella,S., Leuenberger,M., and Saurer,M., 1999. Analysis of delta O-18 in tree rings: Wood-cellulose comparison and method dependent sensitivity. J. Geophys. Res. Atmos., 104(D16): 19267-19273.

Borella,S., Leuenberger,M., Saurer,M., and Siegwolf,R., 1998. Reducing uncertainties in delta C-13 analysis of tree rings: Pooling, milling, and cellulose extraction. J. Geophys. Res. Atmos., 103(D16): 19519-19526.

Borella, S., Menot, G., and Leuenberger, M., 2004. Sample Homogeneity and Cellulose Extraction from Plant Tissue for Stable Isotope Analyses. In: P.A.de Groot (Editor), Handbook of Stable Isotope Analytical Techniques, Volume 1. Elsevier B.V., pp. 507-522.

Bradley, R.S., 2003. Climate forcing during the Holocene. In: A.Mackay, R.W.Battarbee, J.Birks, and F.Oldfield (Editors), Global Change in the Holocene. Arnold, London, pp. 10-19.

Brenninkmeijer,C.A.M., 1983. Deuterium, Oxygen-18 and Carbon-13 in Tree Rings and Peat Deposits in Relation to Climate. Groningen.

Brenninkmeijer,C.A.M., van Geel,B., and Mook,W.G., 1982. Variations in the D/H and $^{18}O/^{16}O$ ratio in cellulose extracted from a peat core. Earth Planet. Sci. Lett., 61(2): 283-290.

Briffa,K.R., Osborn,T.J., and Schweingruber,F.H., 2004. Large-scale temperature inferences from tree rings: a review. Global and Planetary Change, 40(1-2).

Broecker,W.S., 1994. Massive iceberg discharges as triggers for global climate change. Nature, 372.

Broecker,W.S., 1998. Paleocean circulation during the last deglaciation: a bipolar seesaw? Palaeoceanography, 13.

Broecker,W.S., Clark,E., McCorkle,D.C., Peng,T.H., Hajdas,I., and Bonani,G., 1999. Evidence for a reduction in the carbonate ion content of the deep sea during the course of the Holocene. Paleoceanography, 14(6): 744-752.

Brooks,S.J., 1996. Three thousand years of environmental history in a Cairngorms lochan revealed by analysis of non-biting midges Insecta: Diptera: Chironomidae. Botanical Journal of Scotland, 48.

Brooks,S.J. and Birks,H.J.B., 2001. Chironomid-inferred air temperatures from Lateglacial and Holocene sites in north-west Europe: progress and problems. Quat. Sci. Rev., 20.

Buhay,W.M. and Edwards,T.W.D., 1995. Climate in southwestern Ontario, Canada, between AD 1610 and 1885 inferred from oxygen and hydrogen isotopic measurements of wood cellulose from trees in different hydrologic settings. Quat. Res., 44(3): 438-446.

Buhay,W.M., Edwards,T.W.D., and Aravena,R., 1996. Evaluating kinetic fractionation factors used for ecologic and paleoclimatic reconstructions from oxygen and hydrogen isotope ratios in plant water and cellulose. Geochem. Cosmochim. Acta, 60(12): 2209-2218.

Burk,R.L. and Stuiver,M., 1981. Oxygen Isotope Ratios in Trees Reflect Mean Annual Temperature and Humidity. Science, 211(4489): 1417-1419.

Burman,J. and Schmitz,B., 2005. Periwinkle (Littorina littorea) intrashell delta O-18 and delta C-13 records from the mid-Holocene Limfjord region, Denmark: a new high-resolution palaeoenvironmental proxy approach. Holocene, 15(4): 567-575.

Caseldine,C.J., Baker,A., Charman,D.J., and Hendon,D., 2000. A comparative study of optical properties of NaOH peat extracts: implications for humification studies. Holocene, 10(5): 649-658.

Chambers,F.A. and Charman,D.J., 2004. Holocene environmental change: contributions from the peatland archive. Holocene, 14(1): 1-6.

Chambers,F.M., Barber,K.E., Maddy,D., and Brew,J., 1997. A 5500-year proxy-climate and vegetation record from blanket mire at Talla Moss, Borders, Scotland. Holocene, 7(4): 391-399.

Chambers,F.M., Mauquoy,D., Brain,S.A., Blaauw,M., and Daniell,J.R.G., 2007. Globally synchronous climate change 2800 years ago: Proxy data from peat in South America. Earth Planet. Sci. Lett., 253(3-4): 439-444.

Chapman,M.R. and Shackleton,N.J., 2000. Evidence of 550-year and 1000-year cyclicities in North Atlantic circulation patterns during the Holocene. Holocene, 10(3): 287-291.

Chapron,E., Arnaud,F., Noel,H., Revel,M., Desmet,M., and Perdereau,L., 2005. Rhone river flood deposits in Lake Le Bourget: a proxy for Holocene environmental changes in the NW Alps, France. Boreas, 34(4): 404-416.

Charman,D.J., 2001. Biostratigraphic and palaeoenvironmental applications of testate amoebae. Quat. Sci. Rev., 20(16-17): 1753-1764.

Charman,D.J., 2002. Peatlands and environmental change. Wiley.

Charman,D.J., 2007. Summer water deficit variability controls on peatland water-table changes: implications for Holocene palaeoclimate reconstructions. The Holocene, 17(2): 217-227.

Charman,D.J., Blundell,A., Chiverrell,R.C., Hendon,D., and Langdon,P.G., 2006. Compilation of non-annually resolved Holocene proxy climate records: stacked Holocene peatland palaeo-water table reconstructions from northern Britain. Quat. Sci. Rev., 25(3-4): 336-350.

Charman,D.J., Blundell,A., and Members,A., 2007. A new European testate amoebae transfer function for palaeohydrological reconstruction on ombrotrophic peatlands. J. Quat. Sci, 22(3): 209-221.

Charman,D.J., Brown,A.D., Hendon,D., and Karofeld,E., 2004. Testing the relationship between Holocene peatland palaeoclimate reconstructions and instrumental data at two European sites. Quat. Sci. Rev., 23(1-2): 137-143.

Charman,D.J., Hendon,D., and Packman,S., 1999. Multiproxy surface wetness records from replicate cores on an ombrotrophic mire: implications for Holocene palaeoclimate records. J. Quat. Sci, 14(5): 451-463.

Charman,D.J., Hendon,D., and Woodland,W.A., 2000. The identification of testate amoebae (Protozoa: Rhizopoda) in peats. Quaternary Research Association Technical Guide no. 9.

Charman,D.J. and Warner,B.G., 1992. Relationship Between Testate Amebas (Protozoa, Rhizopoda) and Microenvironmental Parameters on A Forested Peatland in Northeastern Ontario. Canadian Journal of Zoology-Revue Canadienne de Zoologie, 70(12): 2474-2482.

Charman,D.J. and Warner,B.G., 1997. The ecology of testate amoebae (Protozoa : Rhizopoda) in oceanic peatlands in Newfoundland, Canada: Modelling hydrological relationships for palaeoenvironmental reconstruction. Ecoscience, 4(4): 555-562.

Chen,J.L., Wilson,C.R., and Tapley,B.D., 2006. Satellite gravity measurements confirm accelerated melting of Greenland ice sheet. Science, 313(5795): 1958-1960.

Chiverrell,R.C., 2001. A proxy record of late Holocene climate change from May Moss, northeast England. J. Quat. Sci, 16.

Ciais,P., White,J.W.C., Jouzel,J., and Petit,J.R., 1995. The Origin of Present-Day Antarctic Precipitation from Surface Snow Deuterium Excess Data. J. Geophys. Res. Atmos., 100(D9): 18917-18927.

Clague,J.J., Wohlfarth,B., Ayotte,J., Eriksson,M., Hutchinson,I., Mathewes,R.W., Walker,I.R., and Walker,L., 2004. Late Holocene environmental change at treeline in the Northern Coast Mountains, British Columbia, Canada. Quat. Sci. Rev., 23(23-24): 2413-2431.

Clark,I. and Fritz,P., 1997. Environmental Isotopes in Hydrogeology. Lewis Publishers, Boca Raton.

Clark,P.U., Marshall,S.J., Clarke,G.K.C., Hostetler,S.W., Licciardi,J.M., and Teller,J.T., 2001. Freshwater forcing of abrupt climate change during the last glaciation. Science, 293(5528): 283-287.

Clark,P.U., Pisias,N.G., Stocker,T.F., and Weaver,A.J., 2002. The role of the thermohaline circulation in abrupt climate change. Nature, 415(6874): 863-869.

Clarke,G.K.C., Leverington,D.W., Teller,J.T., and Dyke,A.S., 2004. Paleohydraulics of the last outburst flood from glacial Lake Agassiz and the 8200 BP cold event. Quat. Sci. Rev., 23(3-4): 389-407.

Clymo,R.S., 1984. The Limits to Peat Bog Growth. Philosophical Transactions of the Royal Society of London Series B-Biological Sciences, 303-1117.

Clymo, R.S. and Hayward, P.M., 1982. The ecology of *Sphagnum*. In: A.J.E.Smith (Editor), Bryophyte Ecology. Chapman Hall, London, pp. 229-291.

Cole,J.E., Rind,D., Webb,R.S., Jouzel,J., and Healy,R., 1999. Climatic controls on interannual variability of precipitation delta O-18: Simulated influence of temperature, precipitation amount, and vapor source region. J. Geophys. Res. Atmos., 104(D12): 14223-14235.

Coplen,T.B., 1995. New Iupac Guidelines for the Reporting of Stable Hydrogen, Carbon, and Oxygen Isotope-Ratio Data. Journal of Research of the National Institute of Standards and Technology, 100(3): 285.

Coulson,J.C. and Butterfield,J., 1978. Investigation of Biotic Factors Determining Rates of Plant Decomposition on Blanket Bog. J. Ecol., 66(2): 631-650.

Craig,H., 1961a. Isotopic Variations in Meteoric Waters. Science, 133: 1702-1703.

Craig,H., 1961b. Standard for reporting concentrations of deuterium and oxygen-18 in natural waters. Science, 133: 1833-1934.

Craig, H. and Gordon, L., 1965. Deuterium and oxygen 18 variation in the ocean and marine atmosphere. In: E.Tongiorgi (Editor), Stable Isotopes in Oceanographic Studies and Palaeotemperatures, Spoleto 1965. Consiglio Nazionale della Ricerca; Piza, Italy, pp. 9-130.

Criss,R.E., 1999. Principles of Stable Isotope Distribution. Oxford University Press, Oxford.

Curry,R. and Mauritzen,C., 2005. Dilution of the northern North Atlantic Ocean in recent decades. Science, 308(5729): 1772-1774.

Curry,R.G., McCartney,M.S., and Joyce,T.M., 1998. Oceanic transport of subpolar climate signals to mid-depth subtropical waters. Nature, 391(6667): 575-577.

Dahl-jensen,D., Mosegaard,K., Gundestrup,N., Clow,G.D., Johnsen,S.J., Hansen,A.W., and Balling,N., 1998. Past temperatures directly from the Greenland Ice Sheet. Science, 282(5387): 268-271.

Daniels,R.E. and Eddy,A., 1990. A Handbook of European Sphagna. Natural Environment Research Council, Swindon.

Dansgaard,W., 1964. Stable isotopes in precipitation. Tellus, 16: 436-468.

Dansgaard,W., Johnsen,S.J., Clausen,H.B., Dahljensen,D., Gundestrup,N.S., Hammer,C.U., Hvidberg,C.S., Steffensen,J.P., Sveinbjornsdottir,A.E., Jouzel,J., and Bond,G., 1993. Evidence for General Instability of Past Climate from A 250-Kyr Ice-Core Record. Nature, 364(6434): 218-220.

Dansgaard,W., 1954. The O18-abundance in fresh water. Geochem. Cosmochim. Acta, 6(5-6): 241-260.

Darling,W.G., 2004. Hydrological factors in the interpretation of stable isotopic proxy data present and past: a European perspective. Quat. Sci. Rev., 23(7-8): 743-770.

Darling,W.G., Bath,A.H., and Talbot,J.C., 2003. The O & H stable isotopic composition of fresh waters in the British Isles. 2. Surface waters and groundwater. Hydrology and Earth System Sciences, 7(2): 183-195.

Darling,W.G. and Talbot,J.C., 2003. The O & H stable isotopic composition of fresh waters in the British Isles. 1. Rainfall. Hydrology and Earth System Sciences, 7(2): 163-181.

Dawson,A.G., Elliott,L., Mayewski,P., Lockett,P., Noone,S., Hickey,K., Holt,T., Wadhams,P., and Foster,I., 2003. Late-Holocene North Atlantic climate 'seesaws', storminess changes and Greenland ice sheet (GISP2) palaeoclimates. Holocene, 13(3): 381-392.

Dawson, T.E., 1993. Water sources of plants as determined from xylem-water isotopic composition: perspectives on plant competition, distribution and water relations. In: J.R.Ehleringer, A.E.Happ, and G.D.Farquhar (Editors), Stable Isotopes and Plant Carbon-Water Relations. Academic Press, New York, pp. 465-496.

Dawson,T.E. and Pate,J.S., 1996. Seasonal water uptake and movement in root systems of Australian phraeatophytic plants of dimorphic root morphology: A stable isotope investigation. Oecologia, 107(1): 13-20.

De Jong,R., Bjorck,S., Bjorkman,L., and Clemmensen,L.B., 2006. Storminess variation during the last 6500 years as reconstructed from an ombrotrophic peat bog in Halland, southwest Sweden. J. Quat. Sci, 21(8): 905-919.

de Vernal,A. and Hillaire-Marcel,C., 2006. Provincialism in trends and high frequency changes in the northwest North Atlantic during the Holocene. Global and Planetary Change, 54(3-4): 263-290.

De Witt,J.C., Van der Straaten,C.M., and Mook,W.G., 1980. Determination of the absolute hydrogen isotopic ratio of V-SMOW and SLAP. Geostandards Newsletter, 4: 33-36.

Dean,W.E., Forester,R.M., and Bradbury,J.P., 2002. Early Holocene change in atmospheric circulation in the Northern Great Plains: an upstream view of the 8.2 ka cold event. Quat. Sci. Rev., 21(16-17): 1763-1775.

DeNiro,M.J. and Cooper,L.W., 1989. Post-Photosynthetic Modification of Oxygen Isotope Ratios of Carbohydrates in the Potato - Implications for Paleoclimatic Reconstruction Based Upon Isotopic Analysis of Wood Cellulose. Geochem. Cosmochim. Acta, 53(10): 2573-2580.

DeNiro,M.J. and Epstein,S., 1979. Relationship Between the Oxygen Isotope Ratios of Terrestrial Plant Cellulose, Carbon-Dioxide, and Water. Science, 204(4388): 51-53.

DeNiro,M.J. and Epstein,S., 1981. Isotopic Composition of Cellulose from Aquatic Organisms. Geochem. Cosmochim. Acta, 45(10): 1885-1894.

Deniro,M.J. and Epstein,S., 1981. Isotopic Composition of Cellulose from Aquatic Organisms. Geochem. Cosmochim. Acta, 45(10): 1885-1894.

Denton,G.H., Alley,R.B., Comer,G.C., and Broecker,W.S., 2005. The role of seasonality in abrupt climate change. Quat. Sci. Rev., 24(10-11): 1159-1182.

Dergachev,V.A., Raspopov,O.M., van Geel,B., and Zaitseva,G.I., 2004. The 'Sterno-Etrussia' geomagnetic excursion around 2700 BP and changes of solar activity, cosmic ray intensity, and climate. Radiocarbon, 46(2): 661-681.

Diefendorf,A.F. and Patterson,W.P., 2005. Survey of stable isotope values in Irish surface waters. Journal of Paleolimnology, 34(2): 257-269.

Dongmann,G., Nurnberg,H.W., Forstel,H., and Wagener,K., 1974. Enrichment of $H_2{}^{18}O$ in Leaves of Transpiring Plants. Radiation and Environmental Biophysics, 11(1): 41-52.

Duller,G., 1995. Troels-Smith plotting program. Kingston: Kingston University..

Dupont,L.M., 1986. Temperature and Rainfall Variation in the Holocene Based on Comparative Paleoecology and Isotope Geology of A Hummock and A Hollow (Bourtangerveen, the Netherlands). Review of Palaeobotany and Palynology, 48(1-3): 71-159.

Dupont,L.M. and Brenninkmeijer,C.A.M., 1984. Palaeobotanic and Isotopic Analysis of Late Subboreal and Early Subatlantic Peat from Engbertsdijksveen-Vii, the Netherlands. Review of Palaeobotany and Palynology, 41(3-4): 241-&.

Dupont,L.M. and Mook,W.G., 1987. Paleoclimate Analysis of H-2/H-1 Ratios in Peat Sequences with Variable Plant Composition. Chem. Geol., 66(3-4): 323-333.

Dyrkacz,G.R., Ruscic,L., Marshall,C.L., and Reagan,W., 1996. Separation and characterization of FCC catalysts using density gradient separation. Energy & Fuels, 10(3): 849-854.

Edwards,T.W.D. and Fritz,P., 1986. Assessing meteoric water composition and relative humidity from 18O and 2H in wood cellulose: paleoclimatic implications for southern Ontario, Canada. Applied Geochemistry, 1(6): 715-723.

Edwards,T.W.D., Wolfe,B.B., and MacDonald,G.M., 1996. Influence of changing atmospheric circulation on precipitation delta O-18-temperature relations in Canada during the Holocene. Quat. Res., 46(3): 211-218.

Ehhalt,D.H., 1974. Vertical profiles of HTO, HDO and H_20 in the troposhphere. National Center for Atmospheric Research Technical Note, NCAR-TN/STR-100, Boulder, Co.

Ekman,R. and Karunen,P., 1982. Esterified Long-Chain Hydroxy-Acids in Green and Senescent Parts of the Peat Moss Sphagnum-Fuscum. Phytochemistry, 21(1): 121-123.

Ellis,C.J. and Tallis,J.H., 2000. Climatic control of blanket mire development at Kantra Moss, north-west Scotland. J. Ecol., 88.

Ellison,C.R.W., Chapman,M.R., and Hall,I.R., 2006. Surface and deep ocean interactions during the cold climate event 8200 years ago. Science, 312(5782): 1929-1932.

Epstein,S. and Mayeda,T., 1953. Variation of O18 content of waters from natural sources. Geochem. Cosmochim. Acta, 4(5): 213-224.

Epstein,S., Thompson,P., and Yapp,C.J., 1977. Oxygen and Hydrogen Isotopic Ratios in Plant Cellulose. Science, 198(4323): 1209-1215.

Epstein,S. and Yapp,C., 1977. Isotope Tree Thermometers. Nature, 266(5601): 477-478.

Estep,M.F. and Hoering,T.C., 1980. Biogeochemistry of the Stable Hydrogen Isotopes. Geochem. Cosmochim. Acta, 44(8): 1197-1206.

Estep,M.F. and Hoering,T.C., 1981. Stable Hydrogen Isotope Fractionations During Autotrophic and Mixotrophic Growth of Microalgae. Plant Physiol., 67(3): 474-477.

Farquhar,G.D. and Gan,K.S., 2003. On the progressive enrichment of the oxygen isotopic composition of water along a leaf (Reprinted from Plant, Cell and Environment, vol 26, pg 801-819, 2003). Plant Cell and Environment, 26(9): 1579-1597.

Farquhar,G.D., Henry,B.K., and Styles,J.M., 1997. A rapid on-line technique for determination of oxygen isotope composition of nitrogen-containing organic matter and water. Rapid Communications in Mass Spectrometry, 11(14): 1554-1560.

Faure,H., Manguin,E., and Nydal,R., 1963. Formations lacustres du Quaternaire supérieur du Niger oriental: diatomites et âges absolus. Bulletin du Bureau de Recherches de Géologie et Minières, 3: 41-63.

Feng,X.H. and Epstein,S., 1994. Climatic Implications of An 8000-Year Hydrogen Isotope Time-Series from Bristlecone-Pine Trees. Science, 265(5175): 1079-1081.

Feng,X., Krishnamurthy,R.V., and Epstein,S., 1993. Determination of D/H ratios of nonexchangeable hydrogen in cellulose: A method based on the cellulose-water exchange reaction. Geochem. Cosmochim. Acta, 57(17): 4249-4256.

Filot,M.S., Leuenberger,M., Pazdur,A., and Boettger,T., 2006. Rapid online equilibration method to determine the D/H ratios of non-exchangeable hydrogen in cellulose. Rapid Communications in Mass Spectrometry, 20(22): 3337-3344.

Finkel,R.C. and Nishiizumi,K., 1997. Beryllium 10 concentrations in the Greenland Ice Sheet Project 2 ice core from 3-40 ka. Journal of Geophysical Research-Oceans, 102(C12): 26699-26706.

Garcia, M., Villalba, F., Araguas-Araguas, L., and Rozanski, K., 1998. The role of atmospheric circulation patterns in controlling the regional distribution of stable isotopes in precipitation. Preliminary results from two transects in the Ecuadorian Andes. In: Isotope Techniques in the Study of Past and Current Environmental Changes in the Hydrosphere and the Atmosphere. International Atomic Energy Agency, Vienna, pp. 127-140.

Gat, J.R., 1980. The isotopes of oxygen and hydrogen in precipitation. In: P.Fritz and J.C.Fontes (Editors), Handbook of Environmental Isotope Geochemistry. Elsevier, Amsterdam, pp. 21-47.

Gat,J.R., Bowser,C.J., and Kendall,C., 1994. The Contribution of Evaporation from the Great-Lakes to the Continental Atmosphere - Estimate Based on Stable-Isotope Data. Geophys. Res. Lett., 21(7): 557-560.

Gat,J.R. and Carmi,I., 1970. Evolution of Isotopic Composition of Atmospheric Waters in Mediterranean-Sea Area. Journal of Geophysical Research, 75(15): 3039.

Gat,J.R. and Matsui,E., 1991. Atmospheric Water-Balance in the Amazon Basin - An Isotopic Evapotranspiration Model. J. Geophys. Res. Atmos., 96(D7): 13179-13188.

Gedzelman,S.D., 1988. Deuterium in water vapor above the atmospheric boundary layer. Tellus, 40B: 134-147.

Glasser,N.F., Harrison,S., Winchester,V., and Aniya,M., 2004. Late Pleistocene and Holocene palaeoclimate and glacier fluctuations in Patagonia. Global and Planetary Change, 43(1-2): 79-101.

Gonfiantini,R., Roche,M.A., Olivry,J.C., Fontes,J.C., and Zuppi,G.M., 2001. The altitude effect on the isotopic composition of tropical rains. Chem. Geol., 181(1-4): 147-167.

Gore,A.J.P., 1983. Ecosystems of the world. 4A. Mires: swamp, bog, fen, and moor: general studies. Elsevier, New York.

Gray,J. and Thompson,P., 1976. Climatic Information from 18O/16O Ratios of Cellulose in Tree Rings. Nature, 262(5568): 481-482.

Green,B.H., 1968. Factors influencing the spatial and temporal distribution of *S. imbricatum Hornsch Ex. Russ.* in the British Isles. J. Ecol., 56: 47-58.

Green, J.W., 1963. Wood Cellulose. In: R.L.Whistler (Editor), Methods in Carbohydrate Chemistry. Academic Press: New York, pp. 9-21.

Grosse-Brauckmann, G., 1986. Analysis of vegetative plant macrofossils. In: B.E.Berglund (Editor), Handbook of Holocene palaeoecology and palaeohydrology.

Hall,I.R., Bianchi,G.G., and Evans,J.R., 2004. Centennial to millennial scale Holocene climate-deep water linkage in the North Atlantic. Quat. Sci. Rev., 23(14-15): 1529-1536.

Hall,V.A. and Pilcher,J.R., 2002. Late-Quaternary Iclandic tephras in Ireland and Great Britain: detection, characterisation and usefulness. The Holocene, 12(2).

Hammarlund,D., Barnekow,L., Birks,H.J.B., Buchardt,B., and Edwards,T.W.D., 2002. Holocene changes in atmospheric circulation recorded in the oxygen-isotope stratigraphy of lacustrine carbonates from northern Sweden. Holocene, 12(3): 339-351.

Hammond, R. F., 1981, The Peatlands of Ireland. 35, *An Foras Talúntais*, Dublin. 59

Haslam,C.J., 1987. Late Holocene peat stratigraphy and climate change - a macrofossil investigation from the raised mires of north-western Europe.

Heikkila,M. and Seppa,H., 2003. A 11,000 yr palaeotemperature reconstruction from the southern boreal zone in Finland. Quat. Sci. Rev., 22(5-7).

Heiri,O., Lotter,A.F., Hausmann,S., and Kienast,F., 2003. A chironomid-based Holocene summer air temperature reconstruction from the Swiss Alps. Holocene, 13(4): 477-484.

Heiri,O., Tinner,W., and Lotter,A.F., 2004. Evidence for cooler European summers during periods of changing meltwater flux to the North Atlantic. Proc. Natl. Acad. Sci. USA, 101(43): 15285-15288.

Helliker,B.R. and Ehleringer,J.R., 2002. Grass blades as tree rings: environmentally induced changes in the oxygen isotope ratio of cellulose along the length of grass blades. New Phytologist, 155(3): 417-424.

Hendon,D. and Charman,D.J., 1997. The preparation of testate amoebae (Protozoa: Rhizopoda) samples from peat. Holocene, 7(2): 199-205.

Hendon,D. and Charman,D.J., 2004. High-resolution peatland water-table changes for the past 200 years: the influence of climate and implications for management. Holocene, 14(1): 125-134.

Hoefs,J., 1997. Stable Isotope Geochemistry. Springer-Verlag, Berlin.

Holdsworth,G., Fogarasi,S., and Krouse,H.R., 1991. Variation of the Stable Isotopes of Water with Altitude in the Saint Elias Mountains of Canada. J. Geophys. Res. Atmos., 96(D4): 7483-7494.

Horita,J. and Wesolowski,D.J., 1994. Liquid-Vapor Fractionation of Oxygen and Hydrogen Isotopes of Water from the Freezing to the Critical-Temperature. Geochem. Cosmochim. Acta, 58(16): 3425-3437.

Hughen,K.A., Overpeck,J.T., Peterson,L.C., and Trumbore,S., 1996. Rapid climate changes in the tropical Atlantic region during the last deglaciation. Nature, 380(6569): 51-54.

Hughes,P.D.M. and Barber,K.E., 2004. Contrasting pathways to ombrotrophy in three raised bogs from Ireland and Cumbria, England. Holocene, 14(1): 65-77.

Hughes,P.D.M., Blundell,A., Charman,D.J., Bartlett,S., Daniell,J.R.G., Wojatschke,A., and Chambers,F.M., 2006. An 8500 cal. year multi-proxy climate record from a bog in eastern Newfoundland: contributions of meltwater discharge and solar forcing. Quat. Sci. Rev., 25(11-12): 1208-1227.

Hughes,P.D.M., Mauquoy,D., Barber,K.E., and Langdon,P.G., 2000. Mire-development pathways and palaeoclimatic records from a full Holocene peat archive at Walton Moss, Cumbria, England. Holocene, 10(4): 465-479.

Hurrell,J.W., 1995. Decadal Trends in the North-Atlantic Oscillation - Regional Temperatures and Precipitation. Science, 269(5224): 676-679.

IAEA/WMO, 2004, Global Network of Isotopes in Precipitation, the GNIP database, http://isohis.iaea.org.

Ingraham,N.L. and Taylor,B.E., 1986. Hydrogen isotope study of large-scale meteoric water transport in Northern California and Nevada. Journal of Hydrology, 85(1-2): 183-197.

Ingram, H.A.P., 1983. Hydrology. In: A.J.P.Gore (Editor), Ecosystems of the world.4A.Mires: swamp, bog, fen, and moor: general studies. Elsevier.

Jacob,H. and Sonntag,C., 1991. An 8-Year Record of the Seasonal-Variation of H-2 and O-18 in Atmospheric Water-Vapor and Precipitation at Heidelberg, Germany. Tellus Series B-Chemical and Physical Meteorology, 43(3): 291-300.

Johnsen,S.J., Dahljensen,D., Dansgaard,W., and Gundestrup,N., 1995. Greenland Paleotemperatures Derived from Grip Bore Hole Temperature and Ice Core Isotope Profiles. Tellus Series B-Chemical and Physical Meteorology, 47(5): 624-629.

Johnsen,S.J., Dahljensen,D., Gundestrup,N.S., Steffensen,J.P., Clausen,H.B., Miller,H., Masson-Delmotte,V., Sveinbjornsdottir,A.E., and White,J., 2001. Oxygen isotope and palaeotemperature records from six Greenland ice-core stations: Camp Century, Dye-3, GRIP, GISP2, Renland and NorthGRIP. J. Quat. Sci, 16(4).

Johnson,L.C. and Damman,A.W.H., 1991. Species-Controlled Sphagnum Decay on A South Swedish Raised Bog. Oikos, 61(2): 234-242.

Jones,G.A. and Johnson,D.A., 1984. Displaced Antarctic Diatoms in Vema Channel Sediments - Late Pleistocene Holocene Fluctuations in Aabw Flow. Marine Geology, 58(1-2): 165-186.

Jones,P.D. and Conway,D., 1997. Precipitation in the British Isles: An analysis of area-average data updated to 1995. International Journal of Climatology, 17(4).

Jones,P.D. and Mann,M.E., 2004. Climate over past millennia. Reviews of Geophysics, 42(2).

Jouzel,J., Alley,R.B., Cuffey,K.M., Dansgaard,W., Grootes,P., Hoffmann,G., Johnsen,S.J., Koster,R.D., Peel,D., Shuman,C.A., Stievenard,M., Stuiver,M., and White,J., 1997. Validity of the temperature reconstruction from water isotopes in ice cores. Journal of Geophysical Research-Oceans, 102(C12): 26471-26487.

Jouzel,J., Hoffmann,G., Koster,R.D., and Masson,V., 2000. Water isotopes in precipitation: data/model comparison for present-day and past climates. Quat. Sci. Rev., 19(1-5): 363-379.

Jouzel,J., Koster,R.D., Suozzo,R.J., Russell,G.L., White,J.W.C., and Broecker,W.S., 1991. Simulations of the Hdo and (H2O)-O-18 Atmospheric Cycles Using the Nasa Giss General-

Circulation Model - Sensitivity Experiments for Present-Day Conditions. J. Geophys. Res. Atmos., 96(D4): 7495-7507.

Karunen,P. and Ekman,R., 1982. Age-Dependent Content of Polymerized Lipids in Sphagnum Fuscum. Physiologia Plantarum, 54(2): 162-166.

Kaufman,D.S., Ager,T.A., Anderson,N.J., Anderson,P.M., Andrews,J.T., Bartlein,P.T., Brubaker,L.B., Coats,L.L., Cwynar,L.C., Duvall,M.L., Dyke,A.S., Edwards,M.E., Eisner,W.R., Gajewski,K., Geirsdottir,A., Hu,F.S., Jennings,A.E., Kaplan,M.R., Kerwin,M.W., Lozhkin,A.V., MacDonald,G.M., Miller,G.H., Mock,C.J., Oswald,W.W., Otto-Bliesner,B.L., Porinchu,D.F., Ruhland,K., Smol,J.P., Steig,E.J., and Wolfe,B.B. Holocene thermal maximum in the western Arctic (0-180 degrees W). Quaternary Science Reviews 23[18-19]. 2004.
Ref Type: Map

Keigwin,L.D., Sachs,J.P., Rosenthal,Y., and Boyle,E.A., 2005. The 8200 year BP event in the slope water system, western subpolar North Atlantic. Paleoceanography, 20(2): PA2003-10.1029/2004PA001074.

Kelly,S.D., Parker,I.G., Sharman,M., and Dennis,M.J., 1998. On-line quantitative determination of H-2/H-1 isotope ratios in organic and water samples using an elemental analyser coupled to an isotope ratio mass spectrometer. Journal of Mass Spectrometry, 33(8): 735-738.

Kerwin,M.W., 1996. A regional stratigraphic isochron (ca 8000 C-14 yr BP) from final deglaciation of Hudson Strait. Quat. Res., 46(2): 89-98.

Keys,D., 1999. Catastrophe: an investigation into the origins of the modern world. Century, London.

Klitgaard-Kristensen,D., Sejrup,H.P., Haflidason,H., Johnsen,S., and Spurk,M., 1998. A regional 8200 cal. yr BP cooling event in northwest Europe, induced by final stages of the Laurentide ice-sheet deglaciation? J. Quat. Sci, 13(2): 165-169.

Kurek,J., Cwynar,L.C., and Spear,R.W., 2004. The 8200 cal yr BP cooling event in eastern North America and the utility of midge analysis for Holocene temperature reconstructions. Quat. Sci. Rev., 23(5-6): 627-639.

Kurita,N., Yoshida,N., Inoue,G., and Chayanova,E.A., 2004. Modern isotope climatology of Russia: A first assessment. J. Geophys. Res. Atmos., 109(D3).

Lachniet,M.S., Asmerom,Y., Burns,S.J., Patterson,W.P., Polyak,V.J., and Seltzer,G.O., 2004. Tropical response to the 8200 yr BP cold event? Speleothem isotopes indicate a weakened early Holocene monsoon in Costa Rica. Geology, 32(11): 957-960.

Lamb,H.H., 1977. Climate: Past, Present and Future. Methuen, London.

Langdon,P.G. and Barber,K.E., 2004. Snapshots in time: precise correlations of peat-based proxy climate records in Scotland using mid-Holocene tephras. Holocene, 14(1): 21-33.

Langdon,P.G. and Barber,K.E., 2005. The climate of Scotland over the last 5000 years inferred from multiproxy peatland records: inter-site correlations and regional variability. J. Quat. Sci, 20(6).

Langdon,P.G., Barber,K.E., and Hughes,P.D.M., 2003. A 7500-year peat-based palaeoclimatic reconstruction and evidence for an 1100-year cyclicity in bog surface wetness from Temple Hill Moss, Pentland Hills, southeast Scotland. Quat. Sci. Rev., 22(2-4): 259-274.

Langdon,P.G., Barber,K.E., and Lomas-Clarke,S.H., 2004. Reconstructing climate and environmental change in northern England through chironomid and pollen analyses: evidence from Talkin Tarn, Cumbria. Journal of Paleolimnology, 32(2): 197-213.

LeGrande,A.N., Schmidt,G.A., Shindell,D.T., Field,C.V., Miller,R.L., Koch,D.M., Faluvegi,G., and Hoffmann,G., 2006. Consistent simulations of multiple proxy responses to an abrupt climate change event. Proc. Natl. Acad. Sci. USA, 103(4): 837-842.

Leng,M.J. and Marshall,J.D., 2004. Palaeoclimate interpretation of stable isotope data from lake sediment archives. Quat. Sci. Rev., 23(7-8): 811-831.

Leuenberger,M.C., Lang,C., and Schwander,J., 1999. Delta(15)N measurements as a calibration tool for the paleothermometer and gas-ice age differences: A case study for the 8200 BP event on GRIP ice. J. Geophys. Res. Atmos., 104(D18): 22163-22170.

Libby,L.M. and Pandolfi,L.J., 1974. Temperature-Dependence of Isotope Ratios in Tree Rings. Proc. Natl. Acad. Sci. USA, 71(6): 2482-2486.

Libby,L.M., Pandolfi,L.J., Payton,P.H., Marshall,J., Becker,B., and Giertzsienbenlist,V., 1976. Isotopic Tree Thermometers. Nature, 261(5558): 284-288.

Liljequist,G.H. and Cehak,K., 1979. Allgemeine Meteorlogie. Braunschweig, Wiesbaden.

Loader,N.J., Robertson,I., Barker,A.C., Switsur,V.R., and Waterhouse,J.S., 1997. An improved technique for the batch processing of small wholewood samples to alpha-cellulose. Chem. Geol., 136(3-4): 313-317.

Loader,N.J., Robertson,I., and McCarroll,D., 2003. Comparison of stable carbon isotope ratios in the whole wood, cellulose and lignin of oak tree-rings. Palaeogeography Palaeoclimatology Palaeoecology, 196(3-4): 395-407.

Lund,D.C., Lynch-Stieglitz,J., and Curry,W.B., 2006. Gulf Stream density structure and transport during the past millennium. Nature, 444(7119): 601-604.

Luo,Y.H. and Sternberg,L., 1991. Deuterium Heterogeneity in Starch and Cellulose Nitrate of Cam and C3 Plants. Phytochemistry, 30(4): 1095-1098.

Luo,Y.H., Sternberg,L., Suda,S., Kumazawa,S., and Mitsui,A., 1991. Extremely Low D/H Ratios of Photoproduced Hydrogen by Cyanobacteria. Plant and Cell Physiology, 32(6): 897-900.

Luo,Y.H. and Sternberg,L.D.L., 1992. Hydrogen and Oxygen Isotopic Fractionation During Heterotrophic Cellulose Synthesis. Journal of Experimental Botany, 43(246): 47-50.

Lynch-Stieglitz,J., 2004. Hemispheric asynchrony of abrupt climate change. Science, 304(5679): 1919-1920.

Madden,R.A. and Williams,J., 1978. The Correlation between Temperature and Precipitation in the United States and Europe. Monthly Weather Review, 106(1).

Magny,M., 2004. Holocene climate variability as reflected by mid-European lake- level fluctuations and its probable impact on prehistoric human settlements. Quaternary International, 113: 65-79.

Magny,M. and Begeot,C., 2004. Hydrological changes in the European midlatitudes associated with freshwater outbursts from Lake Agassiz during the Younger Dryas event and the early Holocene. Quat. Res., 61(2): 181-192.

Magny,M., Begeot,C., Guiot,J., Marguet,A., and Billaud,Y., 2003a. Reconstruction and palaeoclimatic interpretation of mid- Holocene vegetation and lake-level changes at Saint-Jorioz, Lake Annecy, French Pre-Alps. Holocene, 13(2): 265-275.

Magny,M., Begeot,C., Guiot,J., and Peyron,O., 2003b. Contrasting patterns of hydrological changes in Europe in response to Holocene climate cooling phases. Quat. Sci. Rev., 22(15-17): 1589-1596.

Magny,M., Leuzinger,U., Bortenschlager,S., and Haas,J.N., 2006. Tripartite climate reversal in Central Europe 5600-5300 years ago. Quat. Res., 65(1): 3-19.

Majoube,M., 1971a. Fractionation in O-18 Between Ice and Water Vapor. Journal de Chimie Physique et de Physico-Chimie Biologique, 68(4): 625.

Majoube,M., 1971b. Oxygen-18 and Deuterium Fractionation Between Water and Steam. Journal de Chimie Physique et de Physico-Chimie Biologique, 68(10): 1423.

Manabe,S. and Stouffer,R.J., 1995. Simulation of Abrupt Climate-Change Induced by Fresh-Water Input to the North-Atlantic Ocean. Nature, 378(6553): 165-167.

Marchal,O., Cacho,I., Stocker,T.F., Grimalt,J.O., Calvo,E., Martrat,B., Shackleton,N., Vautravers,M., Cortijo,E., van Kreveld,S., Andersson,C., Koc,N., Chapman,M., Sbaffi,L., Duplessy,J.C., Sarnthein,M., Turon,J.L., Duprat,J., and Jansen,E., 2002. Apparent long-term cooling of the sea surface in the northeast Atlantic and Mediterranean during the Holocene. Quat. Sci. Rev., 21(4-6): 455-483.

Marchitto,T.M., Curry,W.B., and Oppo,D.W., 1998. Millenial-scale changes in North Atlantic circulation since the last glaciation. Nature, 393.

Maslin, M., Pike, J., Stickley, C., and Ettwein, V., 2003. Evidence of Holocene Climate variability in Marine Sediments. In: A.Mackay, R.W.Battarbee, J.Birks, and F.Oldfield (Editors), Global Change in the Holocene. Arnold, London, pp. 185-209.

Maslin, M., Seidov, D., and Lowe, J., 2001. Synthesis of the nature and causes of sudden climate transitions during the Quaternary. In: Seidov, D., Haupt, B., and Maslin, M., The oceans and rapid climate change: past, present and future, AGU Geophysical Monograph Series, 126, 9-52.

Mauquoy,D. and Barber,K., 1999a. Evidence for climatic deteriorations associated with the decline of Sphagnum imbricatum Hornsch ex Russ. in six ombrotrophic mires from northern England and the Scottish Borders. Holocene, 9(4): 423-437.

Mauquoy,D. and Barber,K., 2002. Testing the sensitivity of the palaeoclimatic signal from ombrotrophic peat bogs in northern England and the Scottish Borders. Review of Palaeobotany and Palynology, 119(3-4): 219-240.

Mauquoy,D. and Barber,K.E., 1999b. A replicated 3000 year proxy-record from Coom Rigg Moss and Felecia Moss, The Border Mires, northern England. J. Quat. Sci, 14.

Mauquoy,D., Blaauw,M., van Geel,B., Borromei,A., Quattrocchio,M., Chambers,F.M., and Possnert,G., 2004. Late Holocene climatic changes in Tierra del Fuego based on multiproxy analyses of peat deposits. Quat. Res., 61(2).

Mayewski,P.A., Rohling,E.E., Stager,J.C., Karlen,W., Maasch,K.A., Meeker,L.D., Meyerson,E.A., Gasse,F., van Kreveld,S., Holmgren,K., Lee-Thorp,J., Rosqvist,G., Rack,F., Staubwasser,M., Schneider,R.R., and Steig,E.J., 2004. Holocene climate variability. Quat. Res., 62(3).

Mayr,C., Lucke,A., Stichler,W., Trimborn,P., Ercolano,B., Oliva,G., Ohlendorf,C., Soto,J., Fey,M., Haberzettl,T., Janssen,S., Schabitz,F., Schleser,G.H., Wille,M., and Zolitschka,B., 2007. Precipitation origin and evaporation of lakes in semi-arid Patagonia (Argentina) inferred from stable isotopes (delta O-18, delta H-2). Journal of Hydrology, 334(1-2): 53-63.

McCarroll,D. and Loader,N.J., 2004. Stable isotopes in tree rings. Quat. Sci. Rev., 23(7-8): 771-801.

Meese,D.A., Gow,A.J., Grootes,P., Mayewski,P.A., Ram,M., Stuiver,M., Taylor,K.C., Waddington,E.D., and Zielinski,G.A., 1994. The Accumulation Record from the Gisp2 Core As An Indicator of Climate-Change Throughout the Holocene. Science, 266(5191): 1680-1682.

Meissner,K.J. and Clark,P.U., 2006. Impact of floods versus routing events on the thermohaline circulation. Geophys. Res. Lett., 33(15): L15704-10.1029/2006GL026705.

Menot,G. and Burns,S.J., 2001. Carbon isotopes in ombrogenic peat bog plants as climatic indicators: calibration from an altitudinal transect in Switzerland. Organic Geochemistry, 32(2): 233-245.

Ménot-Combes,G., Burns,S.J., and Leuenberger,M., 2002. Variations of O-18/O-16 in plants from temperate peat bogs (Switzerland): implications for paleoclimatic studies. Earth Planet. Sci. Lett., 202(2): 419-434.

Merlivat,L., 1978. Molecular Diffusivities of (H2O)-O-1 6 Hd16O, and (H2O)-O-18 in Gases. Journal of Chemical Physics, 69(6): 2864-2871.

Merlivat,L. and Coantic,M., 1975. Study of Mass-Transfer at Air-Water-Interface by An Isotopic Method. Journal of Geophysical Research-Oceans and Atmospheres, 80(24): 3455-3464.

Merlivat,L. and Jouzel,J., 1979. Global Climatic Interpretation of the Deuterium-Oxygen-18 Relationship for Precipitation. Journal of Geophysical Research-Oceans and Atmospheres, 84(NC8): 5029-5033.

Moon,D.G., GoodmanSnitkoff,G., and Wetmore,G.A., 1996. Blood cell separation using isopycnic centrifugation: A comparative study of commercial density gradient materials. Molecular Biology of the Cell, 7: 850.

Morgan,V.I., 1982. Antarctic Ice-Sheet Surface Oxygen Isotope Values. Journal of Glaciology, 28(99): 315-323.

Muscheler,R., Beer,J., and Vonmoos,M., 2004. Causes and timing of the 8200 yr BP event inferred from the comparison of the GRIP Be-10 and the tree ring Delta C-14 record. Quat. Sci. Rev., 23(20-22): 2101-2111.

Nesje,A., Bjune,A.E., Bakke,J., Dahl,S.O., Lie,O., and Birks,H.J.B., 2006. Holocene palaeoclimate reconstructions at Vanndalsvatnet, western Norway, with particular reference to the 8200 cal. yr BP event. Holocene, 16(5): 717-729.

Nesje,A., Dahl,S.O., and Lie,O., 2004. Holocene millennial-scale summer temperature variability inferred from sediment parameters in a non-glacial mountain lake: Danntjorn, Jotunheimen central southern Norway. Quat. Sci. Rev., 23(20-22): 2183-2205.

Nilssen,E. and Vorren,K.D., 1991. Peat Humification and Climate History. Norsk Geologisk Tidsskrift, 71(3): 215-217.

O'Brien,S.R., Mayewski,P., Meeker,L.D., Meese,D.A., Twickler,M.S., and Witlow,S.I., 1995. Complexity of Holocene climate as reconstructed from a Greenland ice core. Science, 270.

Oldfield, F., 2003. Introduction: the Holocene, a special time. In: A.Mackay, R.W.Battarbee, J.Birks, and F.Oldfield (Editors), Global Change in the Holocene. Arnold, London, pp. 1-9.

Oldfield,F., Richardson,N., and Appleby,P.G., 1995. Radiometric dating (210 Pb, 137 Cs, 241 Am) of recent ombrotrophic peat accumulation and evidance for changes in mass balance. The Holocene, 5(2).

Oppo,D.W., McManus,J.F., and Cullen,J.L., 2003. Deepwater variability in the Holocene epoch (vol 422, pg 277, 2003). Nature, 423(6938): 400.

Osvald,H., 1923. Die Vegetation des Hochmoores Komosse. Svenska Vaxtsociol Sallsk Handl., 1: 1-266.

Palmer,S., Walker,I., Heinrichs,M., Hebda,R., and Scudder,G., 2002. Postglacial midge community change and Holocene palaeotemperature reconstructions near treeline, southern British Columbia (Canada). Journal of Paleolimnology, 28(4): 469-490.

Pang,H.X., He,Y.Q., Lu,A.G., Zhao,J.D., Ning,B.Y., Yuan,L.L., and Song,B., 2006. Synoptic-scale variation of delta O-18 in summer monsoon rainfall at Lijiang, China. Chinese Science Bulletin, 51(23): 2897-2904.

Parker,D.E., Legg,T.P., and Folland,C.K., 1992. A new dailey Central England temperature series, 1772-1991. International Journal of Climatology, 12.

Pendall,E., Markgraf,V., White,J.W.C., Dreier,M., and Kenny,R., 2001. Multiproxy record of late Pleistocene-Holocene climate and vegetation changes from a peat bog in Patagonia. Quat. Res., 55(2): 168-178.

Petit,J.R., White,J.W.C., Young,N.W., Jouzel,J., and Korotkevich,Y.S., 1991. Deuterium Excess in Recent Antarctic Snow. J. Geophys. Res. Atmos., 96(D3): 5113-5122.

Pilcher,J.R. and Hall,V.A., 1996. Tephrochronological studies in northern England. The Holocene, 6.

Pisias,N., Dauphin,J.P., and Sancetta,C., 1973. Spectral analysis of late Pleistocene-Holocene sediments. Quat. Res., 33: 108-116.

Preston,T. and Owens,N.J.P., 1983. Interfacing An Automatic Elemental Analyzer with An Isotope Ratio Mass-Spectrometer - the Potential for Fully Automated Total Nitrogen and N-15 Analysis. Analyst, 108(1289): 971-977.

Preston,T. and Owens,N.J.P., 1985. Preliminary C-13 Measurements Using A Gas-Chromatograph Interfaced to An Isotope Ratio Mass-Spectrometer. Biomedical Mass Spectrometry, 12(9): 510-513.

Rahmstorf,S., 2000. The thermohaline ocean circulation: A system with dangerous thresholds? An editorial comment. Climatic Change, 46(3): 247-256.

Rahmstorf, S., 2006. Thermohaline Ocean Circulation. In: S.Elias (Editor), Encyclopedia of Quaternary Sciences. Elsevier, Amsterdam.

Rasmussen,S.O., Andersen,K.K., Svensson,A.M., Steffensen,J.P., Vinther,B.M., Clausen,H.B., Siggaard-Andersen,M.L., Johnsen,S.J., Larsen,L.B., hl-Jensen,D., Bigler,M., Rothlisberger,R., Fischer,H., Goto-Azuma,K., Hansson,M.E., and Ruth,U., 2006. A new Greenland ice core chronology for the last glacial termination. J. Geophys. Res. Atmos., 111(D6): D06102-10.1029/2005JD006079.

Regnell,J. and Everitt,E., 1996. Preparative centrifugation - A new method for preparing pollen concentrates suitable for radiocarbon dating by AMS. Vegetation History and Archaeobotany, 5(3): 201-205.

Reimer,P.J., Baillie,M.G.L., Bard,E., Bayliss,A., Beck,J.W., Bertrand,C.J.H., Blackwell,P.G., Buck,C.E., Burr,G.S., Cutler,K.B., Damon,P.E., Edwards,R.L., Fairbanks,R.G., Friedrich,M., Guilderson,T.P., Hogg,A.G., Hughen,K.A., Kromer,B., McCormac,G., Manning,S., Ramsey,C.B., Reimer,R.W., Remmele,S., Southon,J.R., Stuiver,M., Talamo,S., Taylor,F.W., van der Plicht,J., and Weyhenmeyer,C.E., 2004. IntCal04 terrestrial radiocarbon age calibration, 0-26 cal kyr BP. Radiocarbon, 46(3): 1029-1058.

Rhodes,A.L., Guswa,A.J., and Newell,S.E., 2006. Seasonal variation in the stable isotopic composition of precipitation in the tropical montane forests of Monteverde, Costa Rica. Water Resources Research, 42(11).

Richards,D.A. and Beck,J.W., 2001. Dramatic shifts in atmospheric radiocarbon during the last glacial period. Antiquity, 75(289): 482-485.

Rinne,K.T., Boettger,T., Loader,N.J., Robertson,I., Switsur,V.R., and Waterhouse,J.S., 2005. On the purification of alpha-cellulose from resinous wood for stable isotope (H, C and O) analysis. Chem. Geol., 222(1-2): 75-82.

Rochefort,L., Vitt,D.H., and Bayley,S.E., 1990. Growth, Production, and Decomposition Dynamics of Sphagnum Under Natural and Experimentally Acidified Conditions. Ecology, 71(5): 1986-2000.

Roden,J.S., Lin,G.G., and Ehleringer,J.R., 2000. A mechanistic model for interpretation of hydrogen and oxygen isotope ratios in tree-ring cellulose. Geochem. Cosmochim. Acta, 64(1): 21-35.

Rohling,E.J. and Pälike,H., 2005. Centennial-scale climate cooling with a sudden cold event around 8,200 years ago. Nature, 434(7036): 975-979.

Rozanski,K., Araguas-Araguas,L., and Gonfiantini,R., 1992. Relation Between Long-Term Trends of O-18 Isotope Composition of Precipitation and Climate. Science, 258(5084): 981-985.

Rozanski, K., Araguas-Araguas, L., and Gonfiantini, R., 1993. Isotopic patterns in modern global precipitation. In: Swart, P. K., Lohmann, K. C., McKensie, J. A., and Savin, S., Climate Change in Continental Isotopic Records, American Geophysical Union Geophysical Monograph, 78, 1-36.

Rozanski,K. and Sonntag,C., 1982. Vertical-Distribution of Deuterium in Atmospheric Water-Vapor. Tellus, 34(2): 135-141.

Rydin,H., 1993. Interspecific competition between *Sphagnum* mosses on a raised bog. Oikos, 66: 413-423.

Salati,E., Dallolio,A., Matsui,E., and Gat,J.R., 1979. Recycling of Water in the Amazon Basin - Isotopic Study. Water Resources Research, 15(5): 1250-1258.

Sarnthein,M., van Kreveld,S., Erlenkeuser,H., Grootes,P.M., Kucera,M., Pflaumann,U., and Schulz,M., 2003. Centennial-to-millennial-scale periodicities of Holocene climate and sediment injections off the western Barents shelf, 75 degrees N. Boreas, 32(3).

Sarnthein,M., Winn,K., Jung,S.J.A., Duplessy,J.C., Labeyrie,L., Erlenkeuser,H., and Ganssen,G., 1994. Changes in East Atlantic Deep-Water Circulation Over the Last 30,000 Years - 8 Time Slice Reconstructions. Paleoceanography, 9(2): 209-267.

Saurer,M., Robertson,I., Siegwolf,R., and Leuenberger,M., 1998. Oxygen isotope analysis of cellulose: An interlaboratory comparison. Analytical Chemistry, 70(10): 2074-2080.

Saurer, M. and Siegwolf, R., 2004. Pyrolysis Techniques for Oxygen Isotope Analysis of Cellulose. In: P.A.de Groot (Editor), Handbook of Stable Isotope Analytical Techniques. Elsevier B.V., pp. 497-506.

Scheffer,R.A., van Logtestijn,R.S.P., and Verhoeven,J.T.A., 2001. Decomposition of *Carex* and *Sphagnum* litter in two mesotrophic fens differing in dominant plant species. Oikos, 92: 44-54.

Schiegl,W.E., 1972. Deuterium Content of Peat As A Paleoclimatic Recorder. Science, 175(4021): 512-&.

Schimmelmann,A., 1991. Determination of the Concentration and Stable Isotopic Composition of Nonexchangeable Hydrogen in Organic-Matter. Analytical Chemistry, 63(21): 2456-2459.

Schleser,G.H., Frielingsdorf,J., and Blair,A., 1999. Carbon isotope behaviour in wood and cellulose during artificial aging. Chem. Geol., 158(1-2): 121-130.

Schoning,K., Charman,D.J., and Wastegard,S., 2005. Reconstructed water tables from two ombrotrophic mires in eastern central Sweden compared with instrumental meteorological data. Holocene, 15(1): 111-118.

Scuderi,L.A., 1990. Tree-Ring Evidence for Climatically Effective Volcanic-Eruptions. Quat. Res., 34(1): 67-85.

Seidov,D. and Maslin,M., 2001. Atlantic Ocean heat piracy and the bipolar climate see-saw during Heinrich and Dansgaard-Oeschger events. Journal of Quaternary Science, 16(4): 321-328.

Sengupta,S. and Sarkar,A., 2006. Stable isotope evidence of dual (Arabian Sea and Bay of Bengal) vapour sources in monsoonal precipitation over north India. Earth Planet. Sci. Lett., 250(3-4): 511-521.

Seppa,H. and Birks,H.J.B., 2001. July mean temperature and annual precipitation trends during the Holocene in the Fennoscandian tree-line area: pollen-based climate reconstructions. Holocene, 11(5): 527-539.

Seppa,H. and Poska,A., 2004. Holocene annual mean temperature changes in Estonia and their relationship to solar insolation and atmospheric circulation patterns. Quat. Res., 61(1): 22-31.

Serreze,M.C., Maslanik,J.A., Barry,R.G., and Demaria,T.L., 1992. Winter Atmospheric Circulation in the Arctic Basin and Possible Relationships to the Great Salinity Anomaly in the Northern North-Atlantic. Geophys. Res. Lett., 19(3): 293-296.

Siegenthaler,U. and Oeschger,H., 1980. Correlation of O-18 in Precipitation with Temperature and Altitude. Nature, 285(5763): 314-317.

Slater,F.M. and Slater,E.J., 1978. Changing Status of Sphagnum-Imbricatum Hornsch Ex Russ, on Borth-Bog, Wales. Journal of Bryology, 10: 155-161.

Smart,P.L. and Frances,P.D., 1991. Quaternary Dating Methods - a users guide. QRA Technical guide no. 4. Quaternary Research Association, London.

Smith,A.J.E., 2004. The Moss Flora of Britain and Ireland. Cambridge University Press, Cambridge.

Sonntag, C., Rozanski, K., Munnich, K.O., and Jacob, H., 1983. Variations of deuterium and oxygen-18 in continental precipitation and groundwater and their causes. In: F.A.Street-Perrott (Editor), Variations in the Global Water Budget. D. Reidel Publishing Company, Dordrecht, pp. 107-124.

Speranza,A., van Geel,B., and van der Plicht,J., 2003. Evidence for solar forcing of climate change at ca. 850 cal BC from a Czech peat sequence. Global and Planetary Change, 35(1-2).

Spiker,E.C. and Hatcher,P.G., 1987. The Effects of Early Diagenesis on the Chemical and Stable Carbon Isotopic Composition of Wood. Geochem. Cosmochim. Acta, 51(6): 1385-1391.

Spooner,I., Douglas,M.S.V., and Terrusi,L., 2002. Multiproxy evidence of an early Holocene (8.2 kyr) climate oscillation in central Nova Scotia, Canada. J. Quat. Sci, 17(7): 639-645.

Stern,L.A. and Blisniuk,P.M., 2002. Stable isotope composition of precipitation across the southern Patagonian Andes. Journal of Geophysical Research, 107(D23): 4667-doi:10.1029/2002JD002509.

Sternberg,L.D.L. and DeNiro,M.J., 1983. Biochemical implications of the isotopic equilibrium fractionation factor between the oxygen atoms of acetone and water. Geochem. Cosmochim. Acta, 47: 2271-2274.

Sternberg,L.D.L., DeNiro,M.J., and Savidge,R.A., 1986. Oxygen Isotope Exchange Between Metabolites and Water During Biochemical Reactions Leading to Cellulose Synthesis. Plant Physiol., 82(2): 423-427.

Sternberg,L.D.L.O. and Deniro,M.J.D., 1983. Biogeochemical Implications of the Isotopic Equilibrium Fractionation Factor Between the Oxygen-Atoms of Acetone and Water. Geochem. Cosmochim. Acta, 47(12): 2271-2274.

Sternberg,L.O., DeNiro,M.J., and Johnson,H.B., 1984a. Isotope Ratios of Cellulose from Plants Having Different Photosynthetic Pathways. Plant Physiol., 74(3): 557-561.

Sternberg,L.O., DeNiro,M.J., and Ting,I.P., 1984b. Carbon, Hydrogen, and Oxygen Isotope Ratios of Cellulose from Plants Having Intermediary Photosynthetic Modes. Plant Physiol., 74(1): 104-107.

Stocker,T.F. and Johnsen,S.J., 2003. A minimum thermodynamic model for the bipolar seesaw. Paleoceanography, 18(4).

Stoneman,R.E., Barber,K.E., and Maddy,D., 1993. Present and past ecology of *Sphagnum imbricatum* and its significance in raised peat-climate modelling. Quaternary Newsletter, 70: 14-22.

Street,F.A. and Grove,A.T., 1979. Global Maps of Lake-Level Fluctuations Since 30,000 Yr Bp. Quat. Res., 12(1): 83-118.

Street-Perrott,F.A. and Perrott,R.A., 1990. Abrupt Climate Fluctuations in the Tropics - the Influence of Atlantic-Ocean Circulation. Nature, 343(6259): 607-612.

Stuiver,M., Reimer,P.J., and Reimer,R.W., 2005. CALIB 5.0. [WWW program and documentation].

Suberkropp,K., Godshalk,G.L., and Klug,M.J., 1976. Changes in Chemical Composition of Leaves During Processing in A Woodland Stream. Ecology, 57(4): 720-727.

Suberkropp,K. and Klug,M.J., 1976. Fungi and Bacteria Associated with Leaves During Processing in A Woodland Stream. Ecology, 57(4): 707-719.

Taylor, C. B., 1972, The vertical variations of the isotopic concentrations of tropospheric water vapour over continental Europe and their relationship to tropospheric structure. DSIR Report INS-R-107, Lower Hutt. New Zealand. 44

Telford,R.J., Heegaard,E., and Birks,H.J.B., 2004. All age-depth models are wrong: but how badly? Quat. Sci. Rev., 23(1-2): 1-5.

Teller,J.T., Leverington,D.W., and Mann,J.D., 2002. Freshwater outbursts to the oceans from glacial Lake Agassiz and their role in climate change during the last deglaciation. Quat. Sci. Rev., 21(8-9): 879-887.

Ter Braak,C.J.F. and Juggins,S., 1993. Weighted averaging partial least squares regression (WA-PLS): an improved method for reconstructing environmental variables from species assemblages. Hydrobiologia, 269/270.

Thomas,E.R., Wolff,E.W., Mulvaney,R., Steffensen,J.P., Johnsen,S.J., Arrowsmith,C., White,J.W.C., Vaughn,B., and Popp,T., 2007. The 8.2 ka event from Greenland ice cores. Quat. Sci. Rev., 26(1-2): 70-81.

Tinner,W. and Lotter,A.F., 2001. Central European vegetation response to abrupt climate change at 8.2 ka. Geology, 29(6).

Tolonen, K., 1986. Rhizopod analysis. In: B.E.Berglund (Editor), Handbook of Holocene palaeoecology and palaeohydrology. John Wiley, Chichester.

Troels-Smith,J., 1955. Karakterisaring af Lose jordarter. Danmarks Geologiska Undersoegelsa IV Reakke, 3: 1-73.

van Breemen,N., 1995. How Sphagnum bogs down other plants. TREE, 10: 270-275.

Van Den Bogaard,C. and Schmincke,H.U., 2002. Linking the North Atlantic to central Europe: a high-resolution Holocene tephrochronological record from northern Germany. J. Quat. Sci, 17(1): 3-20.

van der Schaaf,S., 1999. Analysis of the hydrology of raised bogs in the Irish midlands: a case study of Raheenmore and Clara Bog. Wageningen Agricultural University.

van Geel,B., Bokovenko,N.A., Burova,N.D., Chugunov,K.V., Dergachev,V.A., Dirksen,V.G., Kulkova,M., Nagler,A., Parzinger,H., van der Plicht,J., Vasiliev,S.S., and Zaitseva,G.I., 2004. Climate change and the expansion of the Scythian culture after 850 BC: a hypothesis. Journal of Archaeological Science, 31(12): 1735-1742.

van Geel,B., Buurman,J., and Waterbolk,H.T., 1996. Archaeological and palaeoecological indications of an abrupt climate change in The Netherlands, and evidence for climatological teleconnections around 2650 BP. J. Quat. Sci, 11.

van Geel,B., Heusser,C.J., Renssen,H., and Schuurmans,C.J.E., 2000. Climatic change in Chile at around 2700 BP and global evidence for solar forcing: a hypothesis. Holocene, 10(5): 659-664.

van Geel,B. and Middeldorp,A.A., 1988. Vegetational History of Carbury Bog (Co. Kildare, Ireland) During the Last 850 Years and a Test of the Temperature Indicator Value of $^{2}H/^{1}H$ Measurements of Peat Samples in Relation to Historical Sources and Meteorological Data. New Phytologist, 109(3): 377-392.

van Geel, B. and Renssen, H., 1998. Abrupt climatic change around 2,650 BP in north-west Europe: Evidence for climatic teleconnections and a tentative explanation. In: A.S.Issar and N.Brown (Editors), Water, environment and society in times of climatic change. Kluwer.

Velle,G., Larsen,J., Eide,W., Peglar,S.M., and Birks,H.J.B., 2005. Holocene environmental history and climate of Ratasjoen, a low- alpine lake in south-central Norway. Journal of Paleolimnology, 33(2): 129-153.

Veski,S., Seppa,H., and Ojala,A.E.K., 2004. Cold event at 8200 yr BP recorded in annually laminated lake sediments in eastern Europe. Geology, 32(8): 681-684.

Victoria,R.L., Martinelli,L.A., Mortatti,J., and Richey,J., 1991. Mechanisms of water recycling in the Amazon Basin: isotopic insights. Ambio, 20: 384-387.

Vinther,B.M., Clausen,H.B., Johnsen,S.J., Rasmussen,S.O., Andersen,K.K., Buchardt,S.L., hl-Jensen,D., Seierstad,I.K., Siggaard-Andersen,M.L., Steffensen,J.P., Svensson,A., Olsen,J., and Heinemeier,J., 2006. A synchronized dating of three Greenland ice cores throughout the Holocene. J. Geophys. Res. Atmos., 111: D13102-10.1029/2005JD006921.

Vinther,B.M., Johnsen,S.J., Andersen,K.K., Clausen,H.B., and Hansen,A.W., 2003. NAO signal recorded in the stable isotopes of Greenland ice cores. Geophys. Res. Lett., 30(7).

Vitt,D.H., Crum,H., and Snider,A.J., 1975. The vertical zonation of Sphagnum species in hummock-hollow complexes in northern Michigan. Michigan Botany, 14: 190-200.

von Grafenstein,U., Erlenkeuser,H., Muller,J., Jouzel,J., and Johnsen,S., 1998. The cold event 8200 years ago documented in oxygen isotope records of precipitation in Europe and Greenland. Clim. Dynam., 14(2): 73-81.

von Post, L., 1924, Das genetishe System der organogenen Bildungen Schwedens. 22, Comite International de Pedologie.

Walker,F.W., Parrington,J.R., and Feiner,F., 1989. Nuclides and Isotopes. General Electric Company, San Jose, California.

Wang,X.F. and Yakir,D., 1995. Temporal and spatial variations in the oxygen-18 content of leaf water in different plant species. Plant Cell and Environment, 18(12): 1377-1385.

Wang,X.-F., Yakir,D., and Avishai,M., 1998. Non-climatic variations in the oxygen isotopic composition of plants. Global Change Biology, 4: 835-849.

Warner,B.G. and Charman,D.J., 1994. Holocene Changes on A Peatland in Northwestern Ontario Interpreted from Testate Amebas (Protozoa) Analysis. Boreas, 23(3): 270-279.

Warren,C.R., McGrath,J.F., and Adams,M.A., 2001. Water availability and carbon isotope discrimination in conifers. Oecologia, 127(4): 476-486.

Waterhouse,J.S., Switsur,V.R., Barker,A.C., Carter,A.H.C., and Robertson,I., 2002. Oxygen and hydrogen isotope ratios in tree rings: how well do models predict observed values? Earth Planet. Sci. Lett., 201(2): 421-430.

Werner,R.A., Kornexl,B.E., Rossmann,A., and Schmidt,H.L., 1996. On-line determination of delta O-18 values of organic substances. Analytica Chimica Acta, 319(1-2): 159-164.

Wershaw, R.L., Friedman, I., and Heller, S.J., 1966. Hydrogen isotope fractionation in water passing through trees. In: F.Hobson and M.Speers (Editors), Advances in Organic Geochemistry. Pergamon, New York, pp. 55-67.

White,J.W.C., Barlow,L.K., Fisher,D., Grootes,P., Jouzel,J., Johnsen,S.J., Stuiver,M., and Clausen,H., 1997. The climate signal in the stable isotopes of snow from Summit, Greenland: Results of comparisons with modern climate observations. Journal of Geophysical Research-Oceans, 102(C12): 26425-26439.

White,J.W.C., Lawrence,J.R., and Broecker,W.S., 1994. Modeling and interpreting D/H ratios in tree rings: A test case of white pine in the northeastern United States. Geochem. Cosmochim. Acta, 58(2): 851-862.

White,P.J., 1995. Separation of K+-Selective and Cl(-)Selective Ion Channels from Rye Roots on A Continuous Sucrose Density Gradient. Journal of Experimental Botany, 46(285): 361-376.

Wiersma,A.P. and Renssen,H., 2006. Model-data comparison for the 8.2 ka BP event: confirmation of a forcing mechanism by catastrophic drainage of Laurentide Lakes. Quat. Sci. Rev., 25(1-2): 63-88.

Wigley,T.M.L., Lough,J.M., and Jones,P.D., 1984. Spatial patterns of precipitation in England and Wales and a revised, homogeneous England and Wales precipitation series. International Journal of Climatology, 4.

Williams,T.G., 1996. Effect of changes in water content on photosynthesis, transpiration and discrimination against $^{13}CO_2$ and $C^{18}O^{16}O$ in *Pleurozium* and *Sphagnum*. Oecologia, 108: 38-46.

Wilson,A.T. and Grinsted,M.J., 1977. C-12-C-13 in Cellulose and Lignin As Palaeothermometers. Nature, 265(5590): 133-135.

Witak,M., Wachnicka,A., Kuijpers,A., Troelstra,S., Prins,M.A., and Witkowski,A., 2005. Holocene North Atlantic surface circulation and climatic variability: evidence from diatom records. Holocene, 15(1): 85-96.

Wolfe, B.B., Edwards, T.W.D., Beuning, K.R.M., and Elgood, R.J., 2001. Carbon and oxygen isotope analysis of lake sediment cellulose: methods and applications. In: W.M.Last and J.P.Smol (Editors), Tracking Environmental Change Using Lake Sediments. Volume 2: Physical and Geochemical Methods. Kluwer Academic Publishers, Dordrecht, The Netherlands, pp. 373-400.

Woodland,W.A., Charman,D.J., and Sims,P.C., 1998. Quantitative estimates of water tables and soil moisture in Holocene peatlands from testate amoebae. Holocene, 8(3): 261-273.

Worden,J., Noone,D., and Bowman,K., 2007. Importance of rain evaporation and continental convection in the tropical water cycle. Nature, 445(7127): 528-532.

Yakir,D. and DeNiro,M.J., 1990. Oxygen and Hydrogen Isotope Fractionation During Cellulose Metabolism in Lemna-Gibba l. Plant Physiol., 93(1): 325-332.

Yamanaka,T., Tsujimura,M., Oyunbaatar,D., and Davaa,G., 2007. Isotopic variation of precipitation over eastern Mongolia and its implication for the atmospheric water cycle. Journal of Hydrology, 333(1): 21-34.

Yapp,C.J. and Epstein,S., 1982a. A reexamination of cellulose carbon-bound hydrogen δD measurements and some factors affecting plant-water D/H relationships. Geochem. Cosmochim. Acta, 46(6): 955-965.

Yapp,C.J. and Epstein,S., 1982b. Climatic significance of the hydrogen isotope ratios in tree cellulose. Nature, 297(5868): 636-639.

Yeloff,D. and Mauquoy,D., 2006. The influence of vegetation composition on peat humification: implications for palaeoclimatic studies. Boreas, 35(4): 662-673.

Yonge,C.J., Goldenberg,L., and Krouse,H.R., 1989. An Isotope Study of Water Bodies Along A Traverse of Southwestern Canada. Journal of Hydrology, 106(3-4): 245-255.

Yurtsever, Y. and Gat, J. R., 1981. Atmospheric waters. In: Stable Isotope Hydrology: Deuterium and Oxygen-18 in the Water Cycle, International Atomic Energy Agency Technical Report Series 210, 103-142.

Zanazzi,A. and Mora,G., 2005. Paleoclimatic implications of the relationship between oxygen isotope ratios of moss cellulose and source water in wetlands of Lake Superior. Chem. Geol., 222(3-4): 281-291.